To the Graduate Council:

I am submitting herewith a thesis written by Douglas A. Lombardi entitled "A Protocol for Modeling Atmospheric Transport and Deposition of Acidic Species in East Tennessee Using MESOPUFF II." I have examined the final copy of this thesis for form and content and recommend that it be accepted in partial fulfillment of the requirement for the degree of Master of Science, with a major in Environmental Engineering.

Terry Miller, Major Professor

We have read this thesis
and recommend its acceptance:

Accepted for the Council:

Associate Vice Chancellor and
Dean of the Graduate School

A PROTOCOL FOR MODELING ATMOSPHERIC TRANSPORT AND DEPOSITION OF ACIDIC SPECIES IN EAST TENNESSEE USING MESOPUFF II

A Thesis
Presented for the Master of Science
Degree
The University of Tennessee, Knoxville

Douglas Adler Lombardi
May 1996

VOLUME 1

DEDICATION

This thesis is dedicated to my best friend and wife

Elizabeth Adler Lombardi

ACKNOWLEDGMENTS

I would like to thank my thesis committee, Dr. Terry Miller, Dr. Wayne Davis, and Dr. T. J. Blasing for the opportunity to conduct this research and the guidance they provided while the thesis was being prepared. Thanks also go to four individuals who provided data instrumental for completion of this research activity: Dr. William Pendergrass of the Atmospheric Turbulence and Diffusion Division, National Oceanic and Atmospheric Administration; Dr. Sally Horn, Department of Geography, The University of Tennessee; Dr. Kaushik Deb, Department of Civil and Environmental Engineering, The University of Tennessee; and Mr. Dennis Yankee, Tennessee Valley Authority.

I am grateful for support received from Oak Ridge National Laboratory's Energy Division. I would like to specifically recognize two members from that organization: Dr. Robert Reed and Mr. Robert Miller. Special thanks to the technical editors who contributed to this thesis: Mr. John Fackenthal, Ms. Martha Adler, Ms. Erin Adler, and Ms. Elizabeth Adler Lombardi.

ABSTRACT

A modeling protocol for estimating atmospheric concentrations and deposition of acidic species resulting from new emission sources or major modifications to existing sources located in East Tennessee has been developed and demonstrated. The protocol is based on the MESOPUFF II air dispersion model and was developed primarily for evaluating acidic deposition in areas that have special protection from the adverse impacts caused by air pollution (i.e., the Great Smoky Mountains National Park, Joyce Kilmer Wilderness Area, and Cohutta Wilderness Area).

Wind fields were created over the modeling domain using 1990 meteorological data from multiple stations. Adjustments were made to the model's meteorological preprocessor to simulate the up- and down-valley wind flow in the mixed layer over East Tennessee. The preprocessor was also modified to smooth an otherwise discontinuous wind field.

Model runs simulating emissions from a 28.8 g/s (1000 tpy) source were made. The hypothetical source was sited at four locations: (1) Knoxville/McGhee Tyson Airport, (2) Bristol/Tri Cities Airport, (3) Chattanooga/Lovell Field, and (4) Crossville. The Knoxville source resulted in the highest concentration and deposition values in the Great Smoky Mountains National Park and Joyce Kilmer Wilderness Area. The Chattanooga source resulted in the highest concentration and deposition values in Cohutta Wilderness Area.

Sensitivity runs made for August 1990 show that estimated concentration and deposition values are linearly proportional to emission rate. These runs also show that changes in stack height result in relatively minor differences in maximum deposition estimates. Based on these results, maps of deposition potential were constructed. These maps may be used as screening tools to provide a first approximation of maximum deposition on the Great Smoky Mountains National Park, Joyce Kilmer Wilderness Area, and Cohutta Wilderness area from any location in East Tennessee.

TABLE OF CONTENTS

1. INTRODUCTION 1

2. BACKGROUND 3
   - 2.1 INTRODUCTION 3
   - 2.2 FORMATION AND DEPOSITION OF ACIDIC PARTICLES AND VAPORS 4
     - 2.2.1 Emissions of Acidic Precursor Species 6
     - 2.2.2 Transformation and Transport of Acidic Precursor Species and Compounds 6
     - 2.2.3 Monitoring of Acidic Deposition 10
   - 2.3 IMPACTS OF ACIDIC DEPOSITION ON CLASS I ECOSYSTEMS IN EAST TENNESSEE 16
   - 2.4 PHASE I OF THE IWAQM WORKPLAN 18
   - 2.5 PHASE II OF THE IWAQM WORKPLAN 20
   - 2.6 REGIONAL TRANSPORT MODEL SELECTED FOR THIS STUDY 22

3. MODELING METHOD 23
   - 3.1 INTRODUCTION 23
   - 3.2 INPUTS TO MESOPAC 24
     - 3.2.1 Extent of the Meteorological Grid 24
     - 3.2.2 Selection of Meteorological Stations 26
     - 3.2.3 Meteorological Grid Construction 29
     - 3.2.4 Land Use/Land Cover Data 30
   - 3.3 IMPLEMENTING MESOPAC 31
     - 3.3.1 Wind Direction in the East Tennessee Modeling Domain 33
     - 3.3.2 Smoothing of Wind Speeds 36
   - 3.4 DEVELOPMENT OF HYPOTHETICAL EMISSION SOURCES 40

4. MODELING RESULTS 43
   - 4.1 INTRODUCTION 43
   - 4.2 BASELINE SCENARIO RESULTS 43
     - 4.2.1 Mass Balance 44
     - 4.2.2 Monthly Variations 47
     - 4.2.3 Maximum Annual Deposition Estimated for the Target Class I Areas 54
     - 4.2.4 Maximum Concentrations Estimated for the Target Class I areas 61
   - 4.3 SENSITIVITY SCENARIOS 65
   - 4.4 DEPOSITION POTENTIAL 69

5. RECOMMENDATIONS AND CONCLUSIONS 78

REFERENCES 80

APPENDICES 84

APPENDIX A. GUIDE FOR USING MESOPUFF II IN THE EAST TENNESSEE MODELING DOMAIN 85
A.1 INTRODUCTION 86
A.2 BACKGROUND 86
A.3 COMPUTER SYSTEM REQUIREMENTS 91
A.4 SETTING UP THE MESOPUFF RUN CONTROL FILE 93
A.5 PERFORMING A MESOPUFF RUN 104
A.6 RUNNING THE POSTPROCESSORS 105
A.6.1 READDEP 105
A.6.2 READCON 108
A.6.3 MAXPARK 111

APPENDIX B. ANNUAL DEPOSITION CONTOUR MAPS 112

APPENDIX C. MONTHLY SO_2 DEPOSITION CONTOUR MAPS 129

APPENDIX D. MONTHLY SO_4^{2-} DEPOSITION CONTOUR MAPS 178

APPENDIX E. MONTHLY NO_x DEPOSITION CONTOUR MAPS 227

APPENDIX F. MONTHLY HNO_3 DEPOSITION CONTOUR MAPS 276

APPENDIX G. MONTHLY NO_3^- DEPOSITION CONTOUR MAPS 325

APPENDIX H. MAXIMUM AND ANNUAL CONCENTRATION CONTOUR MAPS 374

APPENDIX I. READDEP CODE LISTING 391

APPENDIX J. READCON CODE LISTING 398

APPENDIX K. MAXPARK CODE LISTING 405

APPENDIX L. CODE MODIFICATIONS MADE TO MESOPAC SUBROUTINE VERTAV 409

VITA 414

LIST OF TABLES

TABLE **PAGE**

2.1 Major emissions source categories in the United States and their contribution to total emissions of each pollutant in 1992 7

3.1 Locations of surface and rawinsonde stations and surface roughnesses and anemometer heights for surface stations 28

3.2 Land use/land cover data categories used in Tennessee Valley Authority (TVA) maps made using Landsat satellite imagery to corresponding categories and roughness lengths used by MESOPAC/ MESOPUFF 30

3.3 Emission and stack exit parameters of a hypothetical baseline scenario source to be used in the SO_2 and NO_x modeling study performed as part of the Development and Demonstration of Modeling protocols for East Tennessee 41

4.1 Sulfur and nitrogen mass balance (percent of emitted pollutant that is deposited) from a hypothetical source located in the East Tennessee modeling domain 45

4.2 Maximum concentrations estimated in the Great Smoky Mountains National Park from a hypothetical 28.8 g/s (1000 tpy) SO_2 and NO_x emission source 62

4.3 Maximum concentrations estimated in Joyce Kilmer Wilderness Area from a hypothetical 28.8 g/s (1000 tpy) (1000 tpy) SO_2 and NO_x emission source 63

4.4 Maximum concentrations estimated in Cohutta Wilderness Area from a hypothetical 28.8 g/s (1000 tpy) (1000 tpy) SO_2 and NO_x emission source 64

A.1 Files developed to use with MESOPUFF II for studies in the East Tennessee modeling domain 92

A.2 Computer system requirements to run MESOPUFF II for the East Tennessee modeling domain 93

TABLE **PAGE**

A.3 MESOPUFF II inputs specific for the East Tennessee modeling domain - title 95

A.4 MESOPUFF II inputs specific for the East Tennessee modeling domain - general run information 96

A.5 MESOPUFF II inputs specific for the East Tennessee modeling domain - computational variables 97

A.6 MESOPUFF II inputs specific for the East Tennessee modeling domain - grid information 99

A.7 MESOPUFF II inputs specific for the East Tennessee modeling domain - technical options 100

A.8 MESOPUFF II inputs specific for the East Tennessee modeling domain - output options 101

A.9 MESOPUFF II inputs specific for the East Tennessee modeling domain - default override options 102

A.10 MESOPUFF II inputs specific for the East Tennessee modeling domain - point source data 103

A.11 Inputs specified in the READDEP run control file, READEP.IN 107

A.12 Inputs specified in the READCON run control file, REACON.IN 110

LIST OF FIGURES

FIGURE		PAGE
2.1	Sulfur budget for the United States and Canada showing percentage of mass for each pathway	5
2.2	SO_2 oxidation pathways	8
2.3	NO_x oxidation pathways	9
2.4	1991 wet SO_4^{2-} deposition (kilograms per hectare)	11
2.5	1991 wet NO_3^- deposition (kilograms per hectare)	12
2.6	1991 mean annual SO_2 dry deposition fluxes (kilograms per hectare)	14
2.7	1991 mean annual HNO_3 dry deposition fluxes (kilograms per hectare)	15
3.1	The MESOPUFF II meteorological grid defining the East Tennessee modeling domain	25
3.2	Location of rawinsonde and surface data stations used to construct the East Tennesee meteorological grid	27
3.3	Lower-layer wind field generated using MESOPAC II for 2100 ET, May 18, 1990 before smoothing routine was implemented	37
3.4	Lower-layer wind field generated using MESOPAC II for 2100 ET, May 18, 1990 after smoothing routine was implemented	39
4.1	Maximum monthly deposition (kg/ha) for five species estimated for 1990 from a hypothetical 65 m (210 ft) tall point source located at Knoxville/Tyson McGhee Airport emitting 28.8 g/s (1000 tpy) each of SO_2 and NO_x	49
4.2	Maximum monthly deposition (kg/ha) for five species estimated for 1990 from a hypothetical 65 m (210 ft) tall point source located at Bristol/Tri Cities Airport emitting 28.8 g/s (1000 tpy) each of SO_2 and NO_x	50

FIGURE PAGE

4.3 Maximum monthly deposition (kg/ha) for five species estimated for 1990 from a hypothetical 65 m (210 ft) tall point source located at Chattanooga/Lovell Field emitting 28.8 g/s (1000 tpy) each of SO_2 and NO_x 51

4.4 Maximum monthly deposition (kg/ha) for five species estimated for 1990 from a hypothetical 65 m (210 ft) tall point source located in Crossville emitting 28.8 g/s each of SO_2 and NO_x 52

4.5 Comparison of annual average (1990) concentrations from a hypothetical source located at Knoxville/Tyson McGhee Airport emitting 28.8 g/s (1000 tpy) each of SO_2 and NO_x 53

4.6 Annual average (1990) SO_2 concentrations versus the ratio of the sum of nitrogen gas species ($HNO_3 + NO_x$) annual concentrations to SO_2 annual concentrations 55

4.7 Maximum annual dry sulfur deposition estimated for 1990 on Class I areas in the East Tennessee modeling domain from a 65 m (210 ft), 28.8 g/s (1000 tpy) SO_2 emission source 56

4.8 Maximum annual wet sulfur deposition estimated for 1990 on Class I areas in the East Tennessee modeling domain from a 65 m (210 ft), 28.8 g/s (1000 tpy) SO_2 emission source 57

4.9 Maximum annual dry nitrogen deposition estimated for 1990 on Class I areas in the East Tennessee modeling domain from a 65 m (210 ft), 28.8 g/s (1000 tpy) NO_x emission source 58

4.10 Maximum annual wet nitrogen deposition estimated for 1990 on Class I areas in the East Tennessee modeling domain from a 65 m (210 ft), 28.8 g/s (1000 tpy) NO_x emission source 59

4.11 Comparison of maximum annual (1990) total sulfur (wet + dry) deposition estimated for Class I areas in East Tennessee from a hypothetical 28.8 g/s SO_2 source with a stack height of 65 m (210 ft) versus the same source with a stack height of 200 m (660 ft). 67

FIGURE PAGE

4.12 Comparison of maximum annual (1990) total nitrogen (wet + dry) deposition estimated for Class I areas in East Tennessee from a hypothetical 28.8 g/s NO_x source with a stack height of 65 m (210 ft) versus the same source with a stack height of 200 m (660 ft). 68

4.13 Annual deposition potential (kg/ha) of sulfur at the nearest boundary of the Great Smoky Mountains National Park corresponding to a continuous emission of 28.8 g/s (1000 tpy) of SO_2 from a 65 m (210 ft) tall point source 70

4.14 Annual deposition potential (kg/ha) of nitrogen at the nearest boundary of the Great Smoky Mountains National Park corresponding to a continuous emission of 28.8 g/s (1000 tpy) of NO_x from a 65 m (210 ft) tall point source 71

4.15 Annual deposition potential (kg/ha) of sulfur at the nearest boundary of Joyce Kilmer Wilderness Area corresponding to a continuous emission of 28.8 g/s (1000 tpy) of SO_2 from a 65 m (210 ft) tall point source 72

4.16 Annual deposition potential (kg/ha) of nitrogen at the nearest boundary of Joyce Kilmer Wilderness Area corresponding to a continuous emission of 28.8 g/s (1000 tpy) of NO_x from a 65 m (210 ft) tall point source 73

4.17 Annual deposition potential (kg/ha) of sulfur at the nearest boundary of Cohutta Wilderness Area corresponding to a continuous emission of 28.8 g/s (1000 tpy) of SO_2 from a 65 m (210 ft) tall point source 74

4.18 Annual deposition potential (kg/ha) of nitrogen at the nearest boundary of Cohutta Wilderness Area corresponding to a continuous emission of 28.8 g/s (1000 tpy) of NO_x from a 65 m (210 ft) tall point source 75

A.1 Location of the East Tennessee modeling domain 87

FIGURE PAGE

A.2 The MESOPUFF II meteorological grid defining the East Tennessee modeling domain 89

A.3 Location of rawinsonde and surface data stations used to construct the East Tennesee meteorological grid 90

A.4 Example run control file, PUFF.INP, to MESOPUFF II for the studies in the East Tennesee modeling domain 94

A.5 Example run control file to READDEP, called READDEP.IN 106

A.6 Example run control file to READCON, called READCON.IN 109

B.1 Total annual dry sulfur deposition estimated for 1990 resulting from a hypothetical 28.8 g/s (1000 tpy) SO_2 emission source located at Knoxville/McGhee Tyson Airport 113

B.2 Total annual dry sulfur deposition estimated for 1990 resulting from a hypothetical 28.8 g/s (1000 tpy) SO_2 emission source located at Bristol/Tri Cities Airport 114

B.3 Total annual dry sulfur deposition estimated for 1990 resulting from a hypothetical 28.8 g/s (1000 tpy) SO_2 emission source located at Chattanooga/Lovell Field 115

B.4 Total annual dry sulfur deposition estimated for 1990 resulting from a hypothetical 28.8 g/s (1000 tpy) SO_2 emission source located in Crossville 116

B.5 Total annual dry sulfur deposition estimated for 1990 resulting from a hypothetical 28.8 g/s (1000 tpy) SO_2 emission source located at Knoxville/McGhee Tyson Airport 117

B.6 Total annual wet sulfur deposition estimated for 1990 resulting from a hypothetical 28.8 g/s (1000 tpy) SO_2 emission source located at Bristol/Tri Cities Airport 118

B.7 Total annual wet sulfur deposition estimated for 1990 resulting from a hypothetical 28.8 g/s (1000 tpy) SO_2 emission source located at Chattanooga/Lovell Field 119

FIGURE PAGE

B.8 Total annual wet sulfur deposition estimated for 1990 resulting from a hypothetical 28.8 g/s (1000 tpy) SO_2 emission source located in Crossville 120

B.9 Total annual dry nitrogen deposition estimated for 1990 resulting from a hypothetical 28.8 g/s (1000 tpy) NO_x emission source located at Knoxville/McGhee Tyson Airport 121

B.10 Total annual dry nitrogen deposition estimated for 1990 resulting from a hypothetical 28.8 g/s (1000 tpy) NO_x emission source located at Chattanooga/Lovell Field 122

B.11 Total annual dry nitrogen deposition estimated for 1990 resulting from a hypothetical 28.8 g/s (1000 tpy) NO_x emission source located at Bristol/Tri Cities Airport 123

B.12 Total annual dry nitrogen deposition estimated for 1990 resulting from a hypothetical 28.8 g/s (1000 tpy) NO_x emission source located in Crossville 124

B.13 Total annual wet nitrogen deposition estimated for 1990 resulting from a hypothetical 28.8 g/s (1000 tpy) NO_x emission source located at Knoxville/McGhee Tyson Airport 125

B.14 Total annual wet nitrogen deposition estimated for 1990 resulting from a hypothetical 28.8 g/s (1000 tpy) NO_x emission source located at Chattanooga/Lovell Field 126

B.15 Total annual wet nitrogen deposition estimated for 1990 resulting from a hypothetical 28.8 g/s (1000 tpy) NO_x emission source located at Bristol/Tri Cities Airport 127

B.16 Total annual wet nitrogen deposition estimated for 1990 resulting from a hypothetical 28.8 g/s (1000 tpy) NO_x emission source located in Crossville 128

C.1 Total (wet+dry) SO_2 deposition estimated for January 1990 resulting from a 28.8 g/s (1000 tpy) hypothetical SO_2 emission source located at Knoxville/McGhee Tyson Airport 130

C.2 Total (wet+dry) SO_2 deposition estimated for January 1990 resulting from a 28.8 g/s (1000 tpy) hypothetical SO_2 emission source located at Bristol/Tri Cities Airport 131

FIGURE **PAGE**

C.3 Total (wet+dry) SO_2 deposition estimated for January 1990 resulting from a 28.8 g/s (1000 tpy) hypothetical SO_2 emission source located at Chattanooga/Lovell Field 132

C.4 Total (wet+dry) SO_2 deposition estimated for January 1990 resulting from a 28.8 g/s (1000 tpy) hypothetical SO_2 emission source located in Crossville 133

C.5 Total (wet+dry) SO_2 deposition estimated for February 1990 resulting from a 28.8 g/s (1000 tpy) hypothetical SO_2 emission source located at Knoxville/McGhee Tyson Airport 134

C.6 Total (wet+dry) SO_2 deposition estimated for February 1990 resulting from a 28.8 g/s (1000 tpy) hypothetical SO_2 emission source located at Bristol/Tri Cities Airport 135

C.7 Total (wet+dry) SO_2 deposition estimated for February 1990 resulting from a 28.8 g/s (1000 tpy) hypothetical SO_2 emission source located at Chattanooga/Lovell Field 136

C.8 Total (wet+dry) SO_2 deposition estimated for February 1990 resulting from a 28.8 g/s (1000 tpy) hypothetical SO_2 emission source located in Crossville 137

C.9 Total (wet+dry) SO_2 deposition estimated for March 1990 resulting from a 28.8 g/s (1000 tpy) hypothetical SO_2 emission source located at Knoxville/McGhee Tyson Airport 138

C.10 Total (wet+dry) SO_2 deposition estimated for March 1990 resulting from a 28.8 g/s (1000 tpy) hypothetical SO_2 emission source located at Bristol/Tri Cities Airport 139

C.11 Total (wet+dry) SO_2 deposition estimated for March 1990 resulting from a 28.8 g/s (1000 tpy) hypothetical SO_2 emission source located at Chattanooga/Lovell Field 140

FIGURE **PAGE**

C.12 Total (wet+dry) SO_2 deposition estimated for March 1990 resulting from a 28.8 g/s (1000 tpy) hypothetical SO_2 emission source located in Crossville 141

C.13 Total (wet+dry) SO_2 deposition estimated for April 1990 resulting from a 28.8 g/s (1000 tpy) hypothetical SO_2 emission source located at Knoxville/McGhee Tyson Airport 142

C.14 Total (wet+dry) SO_2 deposition estimated for April 1990 resulting from a 28.8 g/s (1000 tpy) hypothetical SO_2 emission source located at Bristol/Tri Cities Airport 143

C.15 Total (wet+dry) SO_2 deposition estimated for April 1990 resulting from a 28.8 g/s (1000 tpy) hypothetical SO_2 emission source located at Chattanooga/Lovell Field 144

C.16 Total (wet+dry) SO_2 deposition estimated for April 1990 resulting from a 28.8 g/s (1000 tpy) hypothetical SO_2 emission source located in Crossville 145

C.17 Total (wet+dry) SO_2 deposition estimated for May 1990 resulting from a 28.8 g/s (1000 tpy) hypothetical SO_2 emission source located at Knoxville/McGhee Tyson Airport 146

C.18 Total (wet+dry) SO_2 deposition estimated for May 1990 resulting from a 28.8 g/s (1000 tpy) hypothetical SO_2 emission source located at Bristol/Tri Cities Airport 147

C.19 Total (wet+dry) SO_2 deposition estimated for May 1990 resulting from a 28.8 g/s (1000 tpy) hypothetical SO_2 emission source located at Chattanooga/Lovell Field 148

C.20 Total (wet+dry) SO_2 deposition estimated for May 1990 resulting from a 28.8 g/s (1000 tpy) hypothetical SO_2 emission source located in Crossville 149

FIGURE PAGE

C.21 Total (wet+dry) SO_2 deposition estimated for June 1990 resulting from a 28.8 g/s (1000 tpy) hypothetical SO_2 emission source located at Knoxville/McGhee Tyson Airport 150

C.22 Total (wet+dry) SO_2 deposition estimated for June 1990 resulting from a 28.8 g/s (1000 tpy) hypothetical SO_2 emission source located at Bristol/Tri Cities Airport 151

C.23 Total (wet+dry) SO_2 deposition estimated for June 1990 resulting from a 28.8 g/s (1000 tpy) hypothetical SO_2 emission source located at Chattanooga/Lovell Field 152

C.24 Total (wet+dry) SO_2 deposition estimated for June 1990 resulting from a 28.8 g/s (1000 tpy) hypothetical SO_2 emission source located in Crossville 153

C.25 Total (wet+dry) SO_2 deposition estimated for July 1990 resulting from a 28.8 g/s (1000 tpy) hypothetical SO_2 emission source located at Knoxville/McGhee Tyson Airport 154

C.26 Total (wet+dry) SO_2 deposition estimated for July 1990 resulting from a 28.8 g/s (1000 tpy) hypothetical SO_2 emission source located at Bristol/Tri Cities Airport 155

C.27 Total (wet+dry) SO_2 deposition estimated for July 1990 resulting from a 28.8 g/s (1000 tpy) hypothetical SO_2 emission source located at Chattanooga/Lovell Field 156

C.28 Total (wet+dry) SO_2 deposition estimated for July 1990 resulting from a 28.8 g/s (1000 tpy) hypothetical SO_2 emission source located in Crossville 157

C.29 Total (wet+dry) SO_2 deposition estimated for August 1990 resulting from a 28.8 g/s (1000 tpy) hypothetical SO_2 emission source located at Knoxville/McGhee Tyson Airport 158

FIGURE PAGE

C.30 Total (wet+dry) SO_2 deposition estimated for August 1990 resulting from a 28.8 g/s (1000 tpy) hypothetical SO_2 emission source located at Bristol/Tri Cities Airport 159

C.31 Total (wet+dry) SO_2 deposition estimated for August 1990 resulting from a 28.8 g/s (1000 tpy) hypothetical SO_2 emission source located at Chattanooga/Lovell Field 160

C.32 Total (wet+dry) SO_2 deposition estimated for August 1990 resulting from a 28.8 g/s (1000 tpy) hypothetical SO_2 emission source located in Crossville 161

C.33 Total (wet+dry) SO_2 deposition estimated for September 1990 resulting from a 28.8 g/s (1000 tpy) hypothetical SO_2 emission source located at Knoxville/McGhee Tyson Airport 162

C.34 Total (wet+dry) SO_2 deposition estimated for September 1990 resulting from a 28.8 g/s (1000 tpy) hypothetical SO_2 emission source located at Bristol/Tri Cities Airport 163

C.35 Total (wet+dry) SO_2 deposition estimated for September 1990 resulting from a 28.8 g/s (1000 tpy) hypothetical SO_2 emission source located at Chattanooga/Lovell Field 164

C.36 Total (wet+dry) SO_2 deposition estimated for September 1990 resulting from a 28.8 g/s (1000 tpy) hypothetical SO_2 emission source located in Crossville 165

C.37 Total (wet+dry) SO_2 deposition estimated for October 1990 resulting from a 28.8 g/s (1000 tpy) hypothetical SO_2 emission source located at Knoxville/McGhee Tyson Airport 166

C.38 Total (wet+dry) SO_2 deposition estimated for October 1990 resulting from a 28.8 g/s (1000 tpy) hypothetical SO_2 emission source located at Bristol/Tri Cities Airport 167

FIGURE PAGE

C.39 Total (wet+dry) SO_2 deposition estimated for October 1990 resulting from a 28.8 g/s (1000 tpy) hypothetical SO_2 emission source located at Chattanooga/Lovell Field 168

C.40 Total (wet+dry) SO_2 deposition estimated for October 1990 resulting from a 28.8 g/s (1000 tpy) hypothetical SO_2 emission source located in Crossville 169

C.41 Total (wet+dry) SO_2 deposition estimated for November 1990 resulting from a 28.8 g/s (1000 tpy) hypothetical SO_2 emission source located at Knoxville/McGhee Tyson Airport 170

C.42 Total (wet+dry) SO_2 deposition estimated for November 1990 resulting from a 28.8 g/s (1000 tpy) hypothetical SO_2 emission source located at Bristol/Tri Cities Airport 171

C.43 Total (wet+dry) SO_2 deposition estimated for November 1990 resulting from a 28.8 g/s (1000 tpy) hypothetical SO_2 emission source located at Chattanooga/Lovell Field 172

C.44 Total (wet+dry) SO_2 deposition estimated for November 1990 resulting from a 28.8 g/s (1000 tpy) hypothetical SO_2 emission source located in Crossville 173

C.45 Total (wet+dry) SO_2 deposition estimated for December 1990 resulting from a 28.8 g/s (1000 tpy) hypothetical SO_2 emission source located at Knoxville/McGhee Tyson Airport 174

C.46 Total (wet+dry) SO_2 deposition estimated for December 1990 resulting from a 28.8 g/s (1000 tpy) hypothetical SO_2 emission source located at Bristol/Tri Cities Airport 175

C.47 Total (wet+dry) SO_2 deposition estimated for December 1990 resulting from a 28.8 g/s (1000 tpy) hypothetical SO_2 emission source located at Chattanooga/Lovell Field 176

FIGURE PAGE

C.48 Total (wet+dry) SO_2 deposition estimated for December 1990 resulting from a 28.8 g/s (1000 tpy) hypothetical SO_2 emission source located in Crossville 177

D.1 Total (wet+dry) SO_4^{2-} deposition estimated for January 1990 resulting from a 28.8 g/s (1000 tpy) hypothetical SO_2 emission source located at Knoxville/McGhee Tyson Airport 179

D.2 Total (wet+dry) SO_4^{2-} deposition estimated for January 1990 resulting from a 28.8 g/s (1000 tpy) hypothetical SO_2 emission source located at Bristol/Tri Cities Airport 180

D.3 Total (wet+dry) SO_4^{2-} deposition estimated for January 1990 resulting from a 28.8 g/s (1000 tpy) hypothetical SO_2 emission source located at Chattanooga/Lovell Field 181

D.4 Total (wet+dry) SO_4^{2-} deposition estimated for January 1990 resulting from a 28.8 g/s (1000 tpy) hypothetical SO_2 emission source located in Crossville 182

D.5 Total (wet+dry) SO_4^{2-} deposition estimated for February 1990 resulting from a 28.8 g/s (1000 tpy) hypothetical SO_2 emission source located at Knoxville/McGhee Tyson Airport 183

D.6 Total (wet+dry) SO_4^{2-} deposition estimated for February 1990 resulting from a 28.8 g/s (1000 tpy) hypothetical SO_2 emission source located at Bristol/Tri Cities Airport 184

D.7 Total (wet+dry) SO_4^{2-} deposition estimated for February 1990 resulting from a 28.8 g/s (1000 tpy) hypothetical SO_2 emission source located at Chattanooga/Lovell Field 185

D.8 Total (wet+dry) SO_4^{2-} deposition estimated for February 1990 resulting from a 28.8 g/s (1000 tpy) hypothetical SO_2 emission source located in Crossville 186

FIGURE **PAGE**

D.9 Total (wet+dry) SO_4^{2-} deposition estimated for March 1990 resulting from a 28.8 g/s (1000 tpy) hypothetical SO_2 emission source located at Knoxville/McGhee Tyson Airport 187

D.10 Total (wet+dry) SO_4^{2-} deposition estimated for March 1990 resulting from a 28.8 g/s (1000 tpy) hypothetical SO_2 emission source located at Bristol/Tri Cities Airport 188

D.11 Total (wet+dry) SO_4^{2-} deposition estimated for March 1990 resulting from a 28.8 g/s (1000 tpy) hypothetical SO_2 emission source located at Chattanooga/Lovell Field 189

D.12 Total (wet+dry) SO_4^{2-} deposition estimated for March 1990 resulting from a 28.8 g/s (1000 tpy) hypothetical SO_2 emission source located in Crossville 190

D.13 Total (wet+dry) SO_4^{2-} deposition estimated for April 1990 resulting from a 28.8 g/s (1000 tpy) hypothetical SO_2 emission source located at Knoxville/McGhee Tyson Airport 191

D.14 Total (wet+dry) SO_4^{2-} deposition estimated for April 1990 resulting from a 28.8 g/s (1000 tpy) hypothetical SO_2 emission source located at Bristol/Tri Cities Airport 192

D.15 Total (wet+dry) SO_4^{2-} deposition estimated for April 1990 resulting from a 28.8 g/s (1000 tpy) hypothetical SO_2 emission source located at Chattanooga/Lovell Field 193

D.16 Total (wet+dry) SO_4^{2-} deposition estimated for April 1990 resulting from a 28.8 g/s (1000 tpy) hypothetical SO_2 emission source located in Crossville 194

D.17 Total (wet+dry) SO_4^{2-} deposition estimated for May 1990 resulting from a 28.8 g/s (1000 tpy) hypothetical SO_2 emission source located at Knoxville/McGhee Tyson Airport 195

FIGURE **PAGE**

D.18 Total (wet+dry) SO_4^{2-} deposition estimated for May 1990 resulting from a 28.8 g/s (1000 tpy) hypothetical SO_2 emission source located at Bristol/Tri Cities Airport 196

D.19 Total (wet+dry) SO_4^{2-} deposition estimated for May 1990 resulting from a 28.8 g/s (1000 tpy) hypothetical SO_2 emission source located at Chattanooga/Lovell Field 197

D.20 Total (wet+dry) SO_4^{2-} deposition estimated for May 1990 resulting from a 28.8 g/s (1000 tpy) hypothetical SO_2 emission source located in Crossville 198

D.21 Total (wet+dry) SO_4^{2-} deposition estimated for June 1990 resulting from a 28.8 g/s (1000 tpy) hypothetical SO_2 emission source located at Knoxville/McGhee Tyson Airport 199

D.22 Total (wet+dry) SO_4^{2-} deposition estimated for June 1990 resulting from a 28.8 g/s (1000 tpy) hypothetical SO_2 emission source located at Bristol/Tri Cities Airport 200

D.23 Total (wet+dry) SO_4^{2-} deposition estimated for June 1990 resulting from a 28.8 g/s (1000 tpy) hypothetical SO_2 emission source located at Chattanooga/Lovell Field 201

D.24 Total (wet+dry) SO_4^{2-} deposition estimated for June 1990 resulting from a 28.8 g/s (1000 tpy) hypothetical SO_2 emission source located in Crossville 202

D.25 Total (wet+dry) SO_4^{2-} deposition estimated for July 1990 resulting from a 28.8 g/s (1000 tpy) hypothetical SO_2 emission source located at Knoxville/McGhee Tyson Airport 203

D.26 Total (wet+dry) SO_4^{2-} deposition estimated for July 1990 resulting from a 28.8 g/s (1000 tpy) hypothetical SO_2 emission source located at Bristol/Tri Cities Airport 204

FIGURE **PAGE**

D.27 Total (wet+dry) SO_4^{2-} deposition estimated for July 1990 resulting from a 28.8 g/s (1000 tpy) hypothetical SO_2 emission source located at Chattanooga/Lovell Field 205

D.28 Total (wet+dry) SO_4^{2-} deposition estimated for July 1990 resulting from a 28.8 g/s (1000 tpy) hypothetical SO_2 emission source located in Crossville 206

D.29 Total (wet+dry) SO_4^{2-} deposition estimated for August 1990 resulting from a 28.8 g/s (1000 tpy) hypothetical SO_2 emission source located at Knoxville/McGhee Tyson Airport 207

D.30 Total (wet+dry) SO_4^{2-} deposition estimated for August 1990 resulting from a 28.8 g/s (1000 tpy) hypothetical SO_2 emission source located at Bristol/Tri Cities Airport 208

D.31 Total (wet+dry) SO_4^{2-} deposition estimated for August 1990 resulting from a 28.8 g/s (1000 tpy) hypothetical SO_2 emission source located at Chattanooga/Lovell Field 209

D.32 Total (wet+dry) SO_4^{2-} deposition estimated for August 1990 resulting from a 28.8 g/s (1000 tpy) hypothetical SO_2 emission source located in Crossville 210

D.33 Total (wet+dry) SO_4^{2-} deposition estimated for September 1990 resulting from a 28.8 g/s (1000 tpy) hypothetical SO_2 emission source located at Knoxville/McGhee Tyson Airport 211

D.34 Total (wet+dry) SO_4^{2-} deposition estimated for September 1990 resulting from a 28.8 g/s (1000 tpy) hypothetical SO_2 emission source located at Bristol/Tri Cities Airport 212

D.35 Total (wet+dry) SO_4^{2-} deposition estimated for September 1990 resulting from a 28.8 g/s (1000 tpy) hypothetical SO_2 emission source located at Chattanooga/Lovell Field 213

FIGURE **PAGE**

D.36 Total (wet+dry) SO_4^{2-} deposition estimated for September 1990 resulting from a 28.8 g/s (1000 tpy) hypothetical SO_2 emission source located in Crossville 214

D.37 Total (wet+dry) SO_4^{2-} deposition estimated for October 1990 resulting from a 28.8 g/s (1000 tpy) hypothetical SO_2 emission source located at Knoxville/McGhee Tyson Airport 215

D.38 Total (wet+dry) SO_4^{2-} deposition estimated for October 1990 resulting from a 28.8 g/s (1000 tpy) hypothetical SO_2 emission source located at Bristol/Tri Cities Airport 216

D.39 Total (wet+dry) SO_4^{2-} deposition estimated for October 1990 resulting from a 28.8 g/s (1000 tpy) hypothetical SO_2 emission source located at Chattanooga/Lovell Field 217

D.40 Total (wet+dry) SO_4^{2-} deposition estimated for October 1990 resulting from a 28.8 g/s (1000 tpy) hypothetical SO_2 emission source located in Crossville 218

D.41 Total (wet+dry) SO_4^{2-} deposition estimated for November 1990 resulting from a 28.8 g/s (1000 tpy) hypothetical SO_2 emission source located at Knoxville/McGhee Tyson Airport 219

D.42 Total (wet+dry) SO_4^{2-} deposition estimated for November 1990 resulting from a 28.8 g/s (1000 tpy) hypothetical SO_2 emission source located at Bristol/Tri Cities Airport 220

D.43 Total (wet+dry) SO_4^{2-} deposition estimated for November 1990 resulting from a 28.8 g/s (1000 tpy) hypothetical SO_2 emission source located at Chattanooga/Lovell Field 221

D.44 Total (wet+dry) SO_4^{2-} deposition estimated for November 1990 resulting from a 28.8 g/s (1000 tpy) hypothetical SO_2 emission source located in Crossville 222

FIGURE **PAGE**

D.45 Total (wet+dry) SO_4^{2-} deposition estimated for December 1990 resulting from a 28.8 g/s (1000 tpy) hypothetical SO_2 emission source located at Knoxville/McGhee Tyson Airport 223

D.46 Total (wet+dry) SO_4^{2-} deposition estimated for December 1990 resulting from a 28.8 g/s (1000 tpy) hypothetical SO_2 emission source located at Bristol/Tri Cities Airport 224

D.47 Total (wet+dry) SO_4^{2-} deposition estimated for December 1990 resulting from a 28.8 g/s (1000 tpy) hypothetical SO_2 emission source located at Chattanooga/Lovell Field 225

D.48 Total (wet+dry) SO_4^{2-} deposition estimated for December 1990 resulting from a 28.8 g/s (1000 tpy) hypothetical SO_2 emission source located in Crossville 226

E.1 Total (wet+dry) NO_x deposition estimated for January 1990 resulting from a 28.8 g/s (1000 tpy) hypothetical NO_x emission source located at Knoxville/McGhee Tyson Airport 228

E.2 Total (wet+dry) NO_x deposition estimated for January 1990 resulting from a 28.8 g/s (1000 tpy) hypothetical NO_x emission source located at Bristol/Tri Cities Airport 229

E.3 Total (wet+dry) NO_x deposition estimated for January 1990 resulting from a 28.8 g/s (1000 tpy) hypothetical NO_x emission source located at Chattanooga/Lovell Field 230

E.4 Total (wet+dry) NO_x deposition estimated for January 1990 resulting from a 28.8 g/s (1000 tpy) hypothetical NO_x emission source located in Crossville 231

E.5 Total (wet+dry) NO_x deposition estimated for February 1990 resulting from a 28.8 g/s (1000 tpy) hypothetical NO_x emission source located at Knoxville/McGhee Tyson Airport 232

FIGURE **PAGE**

E.6 Total (wet+dry) NO_x deposition estimated for February 1990 resulting from a 28.8 g/s (1000 tpy) hypothetical NO_x emission source located at Bristol/Tri Cities Airport 233

E.7 Total (wet+dry) NO_x deposition estimated for February 1990 resulting from a 28.8 g/s (1000 tpy) hypothetical NO_x emission source located at Chattanooga/Lovell Field 234

E.8 Total (wet+dry) NO_x deposition estimated for February 1990 resulting from a 28.8 g/s (1000 tpy) hypothetical NO_x emission source located in Crossville 235

E.9 Total (wet+dry) NO_x deposition estimated for March 1990 resulting from a 28.8 g/s (1000 tpy) hypothetical NO_x emission source located at Knoxville/McGhee Tyson Airport 236

E.10 Total (wet+dry) NO_x deposition estimated for March 1990 resulting from a 28.8 g/s (1000 tpy) hypothetical NO_x emission source located at Bristol/Tri Cities Airport 237

E.11 Total (wet+dry) NO_x deposition estimated for March 1990 resulting from a 28.8 g/s (1000 tpy) hypothetical NO_x emission source located at Chattanooga/Lovell Field 238

E.12 Total (wet+dry) NO_x deposition estimated for March 1990 resulting from a 28.8 g/s (1000 tpy) hypothetical NO_x emission source located in Crossville 239

E.13 Total (wet+dry) NO_x deposition estimated for April 1990 resulting from a 28.8 g/s (1000 tpy) hypothetical NO_x emission source located at Knoxville/McGhee Tyson Airport 240

E.14 Total (wet+dry) NO_x deposition estimated for April 1990 resulting from a 28.8 g/s (1000 tpy) hypothetical NO_x emission source located at Bristol/Tri Cities Airport 241

FIGURE PAGE

E.15 Total (wet+dry) NO_x deposition estimated for April 1990 resulting from a 28.8 g/s (1000 tpy) hypothetical NO_x emission source located at Chattanooga/Lovell Field 242

E.16 Total (wet+dry) NO_x deposition estimated for April 1990 resulting from a 28.8 g/s (1000 tpy) hypothetical NO_x emission source located in Crossville 243

E.17 Total (wet+dry) NO_x deposition estimated for May 1990 resulting from a 28.8 g/s (1000 tpy) hypothetical NO_x emission source located at Knoxville/McGhee Tyson Airport 244

E.18 Total (wet+dry) NO_x deposition estimated for May 1990 resulting from a 28.8 g/s (1000 tpy) hypothetical NO_x emission source located at Bristol/Tri Cities Airport 245

E.19 Total (wet+dry) NO_x deposition estimated for May 1990 resulting from a 28.8 g/s (1000 tpy) hypothetical NO_x emission source located at Chattanooga/Lovell Field 246

E.20 Total (wet+dry) NO_x deposition estimated for May 1990 resulting from a 28.8 g/s (1000 tpy) hypothetical NO_x emission source located in Crossville 247

E.21 Total (wet+dry) NO_x deposition estimated for June 1990 resulting from a 28.8 g/s (1000 tpy) hypothetical NO_x emission source located at Knoxville/McGhee Tyson Airport 248

E.22 Total (wet+dry) NO_x deposition estimated for June 1990 resulting from a 28.8 g/s (1000 tpy) hypothetical NO_x emission source located at Bristol/Tri Cities Airport 249

E.23 Total (wet+dry) NO_x deposition estimated for June 1990 resulting from a 28.8 g/s (1000 tpy) hypothetical NO_x emission source located at Chattanooga/Lovell Field 250

FIGURE PAGE

E.24 Total (wet+dry) NO_x deposition estimated for June 1990 resulting from a 28.8 g/s (1000 tpy) hypothetical NO_x emission source located in Crossville 251

E.25 Total (wet+dry) NO_x deposition estimated for July 1990 resulting from a 28.8 g/s (1000 tpy) hypothetical NO_x emission source located at Knoxville/McGhee Tyson Airport 252

E.26 Total (wet+dry) NO_x deposition estimated for July 1990 resulting from a 28.8 g/s (1000 tpy) hypothetical NO_x emission source located at Bristol/Tri Cities Airport 253

E.27 Total (wet+dry) NO_x deposition estimated for July 1990 resulting from a 28.8 g/s (1000 tpy) hypothetical NO_x emission source located at Chattanooga/Lovell Field 254

E.28 Total (wet+dry) NO_x deposition estimated for July 1990 resulting from a 28.8 g/s (1000 tpy) hypothetical NO_x emission source located in Crossville 255

E.29 Total (wet+dry) NO_x deposition estimated for August 1990 resulting from a 28.8 g/s (1000 tpy) hypothetical NO_x emission source located at Knoxville/McGhee Tyson Airport 256

E.30 Total (wet+dry) NO_x deposition estimated for August 1990 resulting from a 28.8 g/s (1000 tpy) hypothetical NO_x emission source located at Bristol/Tri Cities Airport 257

E.31 Total (wet+dry) NO_x deposition estimated for August 1990 resulting from a 28.8 g/s (1000 tpy) hypothetical NO_x emission source located at Chattanooga/Lovell Field 258

E.32 Total (wet+dry) NO_x deposition estimated for August 1990 resulting from a 28.8 g/s (1000 tpy) hypothetical NO_x emission source located in Crossville 259

FIGURE **PAGE**

E.33 Total (wet+dry) NO_x deposition estimated for September 1990 resulting from a 28.8 g/s (1000 tpy) hypothetical NO_x emission source located at Knoxville/McGhee Tyson Airport 260

E.34 Total (wet+dry) NO_x deposition estimated for September 1990 resulting from a 28.8 g/s (1000 tpy) hypothetical NO_x emission source located at Bristol/Tri Cities Airport 261

E.35 Total (wet+dry) NO_x deposition estimated for September 1990 resulting from a 28.8 g/s (1000 tpy) hypothetical NO_x emission source located at Chattanooga/Lovell Field 262

E.36 Total (wet+dry) NO_x deposition estimated for September 1990 resulting from a 28.8 g/s (1000 tpy) hypothetical NO_x emission source located in Crossville 263

E.37 Total (wet+dry) NO_x deposition estimated for October 1990 resulting from a 28.8 g/s (1000 tpy) hypothetical NO_x emission source located at Knoxville/McGhee Tyson Airport 264

E.38 Total (wet+dry) NO_x deposition estimated for October 1990 resulting from a 28.8 g/s (1000 tpy) hypothetical NO_x emission source located at Bristol/Tri Cities Airport 265

E.39 Total (wet+dry) NO_x deposition estimated for October 1990 resulting from a 28.8 g/s (1000 tpy) hypothetical NO_x emission source located at Chattanooga/Lovell Field 266

E.40 Total (wet+dry) NO_x deposition estimated for October 1990 resulting from a 28.8 g/s (1000 tpy) hypothetical NO_x emission source located in Crossville 267

E.41 Total (wet+dry) NO_x deposition estimated for November 1990 resulting from a 28.8 g/s (1000 tpy) hypothetical NO_x emission source located at Knoxville/McGhee Tyson Airport 268

FIGURE **PAGE**

E.42 Total (wet+dry) NO_x deposition estimated for November 1990 resulting from a 28.8 g/s (1000 tpy) hypothetical NO_x emission source located at Bristol/Tri Cities Airport 269

E.43 Total (wet+dry) NO_x deposition estimated for November 1990 resulting from a 28.8 g/s (1000 tpy) hypothetical NO_x emission source located at Chattanooga/Lovell Field 270

E.44 Total (wet+dry) NO_x deposition estimated for November 1990 resulting from a 28.8 g/s (1000 tpy) hypothetical NO_x emission source located in Crossville 271

E.45 Total (wet+dry) NO_x deposition estimated for December 1990 resulting from a 28.8 g/s (1000 tpy) hypothetical NO_x emission source located at Knoxville/McGhee Tyson Airport 272

E.46 Total (wet+dry) NO_x deposition estimated for December 1990 resulting from a 28.8 g/s (1000 tpy) hypothetical NO_x emission source located at Bristol/Tri Cities Airport 273

E.47 Total (wet+dry) NO_x deposition estimated for December 1990 resulting from a 28.8 g/s (1000 tpy) hypothetical NO_x emission source located at Chattanooga/Lovell Field 274

E.48 Total (wet+dry) NO_x deposition estimated for December 1990 resulting from a 28.8 g/s (1000 tpy) hypothetical NO_x emission source located in Crossville 275

F.1 Total (wet+dry) HNO_3 deposition estimated for January 1990 resulting from a 28.8 g/s (1000 tpy) hypothetical NO_x emission source located at Knoxville/McGhee Tyson Airport 277

F.2 Total (wet+dry) HNO_3 deposition estimated for January 1990 resulting from a 28.8 g/s (1000 tpy) hypothetical NO_x emission source located at Bristol/Tri Cities Airport 278

FIGURE **PAGE**

F.3 Total (wet+dry) HNO_3 deposition estimated for January 1990 resulting from a 28.8 g/s (1000 tpy) hypothetical NO_x emission source located at Chattanooga/Lovell Field 279

F.4 Total (wet+dry) HNO_3 deposition estimated for January 1990 resulting from a 28.8 g/s (1000 tpy) hypothetical NO_x emission source located in Crossville 280

F.5 Total (wet+dry) HNO_3 deposition estimated for February 1990 resulting from a 28.8 g/s (1000 tpy) hypothetical NO_x emission source located at Knoxville/McGhee Tyson Airport 281

F.6 Total (wet+dry) HNO_3 deposition estimated for February 1990 resulting from a 28.8 g/s (1000 tpy) hypothetical NO_x emission source located at Bristol/Tri Cities Airport 282

F.7 Total (wet+dry)HNO_3 deposition estimated for February 1990 resulting from a 28.8 g/s (1000 tpy) hypothetical NO_x emission source located at Chattanooga/Lovell Field 283

F.8 Total (wet+dry)HNO_3 deposition estimated for February 1990 resulting from a 28.8 g/s (1000 tpy) hypothetical NO_x emission source located in Crossville 284

F.9 Total (wet+dry) HNO_3 deposition estimated for March 1990 resulting from a 28.8 g/s (1000 tpy) hypothetical NO_x emission source located at Knoxville/McGhee Tyson Airport 285

F.10 Total (wet+dry) HNO_3 deposition estimated for March 1990 resulting from a 28.8 g/s (1000 tpy) hypothetical NO_x emission source located at Bristol/Tri Cities Airport 286

F.11 Total (wet+dry) HNO_3 deposition estimated for March 1990 resulting from a 28.8 g/s (1000 tpy) hypothetical NO_x emission source located at Chattanooga/Lovell Field 287

FIGURE PAGE

F.12 Total (wet+dry) HNO_3 deposition estimated for March 1990 resulting from a 28.8 g/s (1000 tpy) hypothetical NO_x emission source located in Crossville 288

F.13 Total (wet+dry) HNO_3 deposition estimated for April 1990 resulting from a 28.8 g/s (1000 tpy) hypothetical NO_x emission source located at Knoxville/McGhee Tyson Airport 289

F.14 Total (wet+dry) HNO_3 deposition estimated for April 1990 resulting from a 28.8 g/s (1000 tpy) hypothetical NO_x emission source located at Bristol/Tri Cities Airport 290

F.15 Total (wet+dry) HNO_3 deposition estimated for April 1990 resulting from a 28.8 g/s (1000 tpy) hypothetical NO_x emission source located at Chattanooga/Lovell Field 291

F.16 Total (wet+dry) HNO_3 deposition estimated for April 1990 resulting from a 28.8 g/s (1000 tpy) hypothetical NO_x emission source located in Crossville 292

F.17 Total (wet+dry) HNO_3 deposition estimated for May 1990 resulting from a 28.8 g/s (1000 tpy) hypothetical NO_x emission source located at Knoxville/McGhee Tyson Airport 293

F.18 Total (wet+dry) HNO_3 deposition estimated for May 1990 resulting from a 28.8 g/s (1000 tpy) hypothetical NO_x emission source located at Bristol/Tri Cities Airport 294

F.19 Total (wet+dry) HNO_3 deposition estimated for May 1990 resulting from a 28.8 g/s (1000 tpy) hypothetical NO_x emission source located at Chattanooga/Lovell Field 295

F.20 Total (wet+dry) HNO_3 deposition estimated for May 1990 resulting from a 28.8 g/s (1000 tpy) hypothetical NO_x emission source located in Crossville 296

FIGURE **PAGE**

F.21 Total (wet+dry) HNO_3 deposition estimated for June 1990 resulting from a 28.8 g/s (1000 tpy) hypothetical NO_x emission source located at Knoxville/McGhee Tyson Airport 297

F.22 Total (wet+dry) HNO_3 deposition estimated for June 1990 resulting from a 28.8 g/s (1000 tpy) hypothetical NO_x emission source located at Bristol/Tri Cities Airport 298

F.23 Total (wet+dry) HNO_3 deposition estimated for June 1990 resulting from a 28.8 g/s (1000 tpy) hypothetical NO_x emission source located at Chattanooga/Lovell Field 299

F.24 Total (wet+dry) HNO_3 deposition estimated for June 1990 resulting from a 28.8 g/s (1000 tpy) hypothetical NO_x emission source located in Crossville 300

F.25 Total (wet+dry) HNO_3 deposition estimated for July 1990 resulting from a 28.8 g/s (1000 tpy) hypothetical HNO_3 emission source located at Knoxville/McGhee Tyson Airport 301

F.26 Total (wet+dry) NO_x deposition estimated for July 1990 resulting from a 28.8 g/s (1000 tpy) hypothetical HNO_3 emission source located at Bristol/Tri Cities Airport 302

F.27 Total (wet+dry) HNO_3 deposition estimated for July 1990 resulting from a 28.8 g/s (1000 tpy) hypothetical NO_x emission source located at Chattanooga/Lovell Field 303

F.28 Total (wet+dry) HNO_3 deposition estimated for July 1990 resulting from a 28.8 g/s (1000 tpy) hypothetical HNO_3 emission source located in Crossville 304

F.29 Total (wet+dry) NO_x deposition estimated for August 1990 resulting from a 28.8 g/s (1000 tpy) hypothetical HNO_3 emission source located at Knoxville/McGhee Tyson Airport 305

FIGURE PAGE

F.30 Total (wet+dry) NO_x deposition estimated for August 1990 resulting from a 28.8 g/s (1000 tpy) hypothetical NO_x emission source located at Bristol/Tri Cities Airport 306

F.31 Total (wet+dry) HNO_3 deposition estimated for August 1990 resulting from a 28.8 g/s (1000 tpy) hypothetical NO_x emission source located at Chattanooga/Lovell Field 307

F.32 Total (wet+dry) HNO_3 deposition estimated for August 1990 resulting from a 28.8 g/s (1000 tpy) hypothetical NO_x emission source located in Crossville 308

F.33 Total (wet+dry) HNO_3 deposition estimated for September 1990 resulting from a 28.8 g/s (1000 tpy) hypothetical NO_x emission source located at Knoxville/McGhee Tyson Airport 309

F.34 Total (wet+dry) HNO_3 deposition estimated for September 1990 resulting from a 28.8 g/s (1000 tpy) hypothetical NO_x emission source located at Bristol/Tri Cities Airport 310

F.35 Total (wet+dry) HNO_3 deposition estimated for September 1990 resulting from a 28.8 g/s (1000 tpy) hypothetical NO_x emission source located at Chattanooga/Lovell Field 311

F.36 Total (wet+dry) HNO_3 deposition estimated for September 1990 resulting from a 28.8 g/s (1000 tpy) hypothetical NO_x emission source located in Crossville 312

F.37 Total (wet+dry) HNO_3 deposition estimated for October 1990 resulting from a 28.8 g/s (1000 tpy) hypothetical NO_x emission source located at Knoxville/McGhee Tyson Airport 313

F.38 Total (wet+dry) HNO_3 deposition estimated for October 1990 resulting from a 28.8 g/s (1000 tpy) hypothetical NO_x emission source located at Bristol/Tri Cities Airport 314

FIGURE **PAGE**

F.39 Total (wet+dry) HNO_3 deposition estimated for October 1990 resulting from a 28.8 g/s (1000 tpy) hypothetical NO_x emission source located at Chattanooga/Lovell Field 315

F.40 Total (wet+dry) HNO_3 deposition estimated for October 1990 resulting from a 28.8 g/s (1000 tpy) hypothetical NO_x emission source located in Crossville 316

F.41 Total (wet+dry) HNO_3 deposition estimated for November 1990 resulting from a 28.8 g/s (1000 tpy) hypothetical NO_x emission source located at Knoxville/McGhee Tyson Airport 317

F.42 Total (wet+dry) HNO_3 deposition estimated for November 1990 resulting from a 28.8 g/s (1000 tpy) hypothetical NO_x emission source located at Bristol/Tri Cities Airport 318

F.43 Total (wet+dry) HNO_3 deposition estimated for November 1990 resulting from a 28.8 g/s (1000 tpy) hypothetical NO_x emission source located at Chattanooga/Lovell Field 319

F.44 Total (wet+dry) HNO_3 deposition estimated for November 1990 resulting from a 28.8 g/s (1000 tpy) hypothetical NO_x emission source located in Crossville 320

F.45 Total (wet+dry) HNO_3 deposition estimated for December 1990 resulting from a 28.8 g/s (1000 tpy) hypothetical NO_x emission source located at Knoxville/McGhee Tyson Airport 321

F.46 Total (wet+dry) HNO_3 deposition estimated for December 1990 resulting from a 28.8 g/s (1000 tpy) hypothetical NO_x emission source located at Bristol/Tri Cities Airport 322

F.47 Total (wet+dry) HNO_3 deposition estimated for December 1990 resulting from a 28.8 g/s (1000 tpy) hypothetical NO_x emission source located at Chattanooga/Lovell Field 323

FIGURE PAGE

F.48 Total (wet+dry) HNO_3 deposition estimated for December 1990 resulting from a 28.8 g/s (1000 tpy) hypothetical NO_x emission source located in Crossville 324

G.1 Total (wet+dry) NO_3^- deposition estimated for January 1990 resulting from a 28.8 g/s (1000 tpy) hypothetical NO_x emission source located at Knoxville/McGhee Tyson Airport 326

G.2 Total (wet+dry) NO_3^- deposition estimated for January 1990 resulting from a 28.8 g/s (1000 tpy) hypothetical NO_x emission source located at Bristol/Tri Cities Airport 327

G.3 Total (wet+dry) NO_3^- deposition estimated for January 1990 resulting from a 28.8 g/s (1000 tpy) hypothetical NO_x emission source located at Chattanooga/Lovell Field 328

G.4 Total (wet+dry) NO_3^- deposition estimated for January 1990 resulting from a 28.8 g/s (1000 tpy) hypothetical NO_x emission source located in Crossville 329

G.5 Total (wet+dry) NO_3^- deposition estimated for February 1990 resulting from a 28.8 g/s (1000 tpy) hypothetical NO_x emission source located at Knoxville/McGhee Tyson Airport 330

G.6 Total (wet+dry) NO_3^- deposition estimated for February 1990 resulting from a 28.8 g/s (1000 tpy) hypothetical NO_3^- emission source located at Bristol/Tri Cities Airport 331

G.7 Total (wet+dry) NO_x deposition estimated for February 1990 resulting from a 28.8 g/s (1000 tpy) hypothetical NO_3^- emission source located at Chattanooga/Lovell Field 332

G.8 Total (wet+dry) NO_3^- deposition estimated for February 1990 resulting from a 28.8 g/s (1000 tpy) hypothetical NO_x emission source located in Crossville 333

FIGURE PAGE

G.9 Total (wet+dry) NO_3^- deposition estimated for March 1990 resulting from a 28.8 g/s (1000 tpy) hypothetical NO_3^- emission source located at Knoxville/McGhee Tyson Airport 334

G.10 Total (wet+dry) NO_x deposition estimated for March 1990 resulting from a 28.8 g/s (1000 tpy) hypothetical NO_3^- emission source located at Bristol/Tri Cities Airport 335

G.11 Total (wet+dry) NO_x deposition estimated for March 1990 resulting from a 28.8 g/s (1000 tpy) hypothetical NO_3^- emission source located at Chattanooga/Lovell Field 336

G.12 Total (wet+dry) NO_3^- deposition estimated for March 1990 resulting from a 28.8 g/s (1000 tpy) hypothetical NO_x emission source located in Crossville 337

G.13 Total (wet+dry) NO_3^- deposition estimated for April 1990 resulting from a 28.8 g/s (1000 tpy) hypothetical NO_x emission source located at Knoxville/McGhee Tyson Airport 338

G.14 Total (wet+dry) NO_3^- deposition estimated for April 1990 resulting from a 28.8 g/s (1000 tpy) hypothetical NO_x emission source located at Bristol/Tri Cities Airport 339

G.15 Total (wet+dry) NO_3^- deposition estimated for April 1990 resulting from a 28.8 g/s (1000 tpy) hypothetical NO_x emission source located at Chattanooga/Lovell Field 340

G.16 Total (wet+dry) NO_3^- deposition estimated for April 1990 resulting from a 28.8 g/s (1000 tpy) hypothetical NO_3^- emission source located in Crossville 341

G.17 Total (wet+dry) NO_x deposition estimated for May 1990 resulting from a 28.8 g/s (1000 tpy) hypothetical NO_3^- emission source located at Knoxville/McGhee Tyson Airport 342

FIGURE **PAGE**

G.18 Total (wet+dry) NO_x deposition estimated for May 1990 resulting from a 28.8 g/s (1000 tpy) hypothetical NO_3^- emission source located at Bristol/Tri Cities Airport 343

G.19 Total (wet+dry) NO_3^- deposition estimated for May 1990 resulting from a 28.8 g/s (1000 tpy) hypothetical NO_x emission source located at Chattanooga/Lovell Field 344

G.20 Total (wet+dry) NO_3^- deposition estimated for May 1990 resulting from a 28.8 g/s (1000 tpy) hypothetical NO_x emission source located in Crossville 345

G.21 Total (wet+dry) NO_3^- deposition estimated for June 1990 resulting from a 28.8 g/s (1000 tpy) hypothetical NO_x emission source located at Knoxville/McGhee Tyson Airport 346

G.22 Total (wet+dry) NO_3^- deposition estimated for June 1990 resulting from a 28.8 g/s (1000 tpy) hypothetical NO_x emission source located at Bristol/Tri Cities Airport 347

G.23 Total (wet+dry) NO_3^- deposition estimated for June 1990 resulting from a 28.8 g/s (1000 tpy) hypothetical NO_x emission source located at Chattanooga/Lovell Field 348

G.24 Total (wet+dry) NO_3^- deposition estimated for June 1990 resulting from a 28.8 g/s (1000 tpy) hypothetical NO_x emission source located in Crossville 349

G.25 Total (wet+dry) NO_3^- deposition estimated for July 1990 resulting from a 28.8 g/s (1000 tpy) hypothetical NO_x emission source located at Knoxville/McGhee Tyson Airport 350

G.26 Total (wet+dry) NO_3^- deposition estimated for July 1990 resulting from a 28.8 g/s (1000 tpy) hypothetical NO_x emission source located at Bristol/Tri Cities Airport 351

FIGURE PAGE

G.27 Total (wet+dry) NO_3^- deposition estimated for July 1990 resulting from a 28.8 g/s (1000 tpy) hypothetical NO_3^- emission source located at Chattanooga/Lovell Field 352

G.28 Total (wet+dry) NO_x deposition estimated for July 1990 resulting from a 28.8 g/s (1000 tpy) hypothetical NO_3^- emission source located in Crossville 353

G.29 Total (wet+dry) NO_x deposition estimated for August 1990 resulting from a 28.8 g/s (1000 tpy) hypothetical NO_3^- emission source located at Knoxville/McGhee Tyson Airport 354

G.30 Total (wet+dry) NO_3^- deposition estimated for August 1990 resulting from a 28.8 g/s (1000 tpy) hypothetical NO_x emission source located at Bristol/Tri Cities Airport 355

G.31 Total (wet+dry) NO_3^- deposition estimated for August 1990 resulting from a 28.8 g/s (1000 tpy) hypothetical NO_3^- emission source located at Chattanooga/Lovell Field 356

G.32 Total (wet+dry) NO_3^- deposition estimated for August 1990 resulting from a 28.8 g/s (1000 tpy) hypothetical NO_x emission source located in Crossville 357

G.33 Total (wet+dry) NO_3^- deposition estimated for September 1990 resulting from a 28.8 g/s (1000 tpy) hypothetical NO_x emission source located at Knoxville/McGhee Tyson Airport 358

G.34 Total (wet+dry) NO_3^- deposition estimated for September 1990 resulting from a 28.8 g/s (1000 tpy) hypothetical NO_x emission source located at Bristol/Tri Cities Airport 359

G.35 Total (wet+dry) NO_3^- deposition estimated for September 1990 resulting from a 28.8 g/s (1000 tpy) hypothetical NO_x emission source located at Chattanooga/Lovell Field 360

FIGURE PAGE

G.36 Total (wet+dry) NO_3^- deposition estimated for September 1990 resulting from a 28.8 g/s (1000 tpy) hypothetical NO_x emission source located in Crossville 361

G.37 Total (wet+dry) NO_3^- deposition estimated for October 1990 resulting from a 28.8 g/s (1000 tpy) hypothetical NO_x emission source located at Knoxville/McGhee Tyson Airport 362

G.38 Total (wet+dry) NO_3^- deposition estimated for October 1990 resulting from a 28.8 g/s (1000 tpy) hypothetical NO_x emission source located at Bristol/Tri Cities Airport 363

G.39 Total (wet+dry) NO_3^- deposition estimated for October 1990 resulting from a 28.8 g/s (1000 tpy) hypothetical NO_x emission source located at Chattanooga/Lovell Field 364

G.40 Total (wet+dry) NO_3^- deposition estimated for October 1990 resulting from a 28.8 g/s (1000 tpy) hypothetical NO_x emission source located in Crossville 365

G.41 Total (wet+dry) NO_3^- deposition estimated for November 1990 resulting from a 28.8 g/s (1000 tpy) hypothetical NO_x emission source located at Knoxville/McGhee Tyson Airport 366

G.42 Total (wet+dry) NO_3^- deposition estimated for November 1990 resulting from a 28.8 g/s (1000 tpy) hypothetical NO_x emission source located at Bristol/Tri Cities Airport 367

G.43 Total (wet+dry) NO_3^- deposition estimated for November 1990 resulting from a 28.8 g/s (1000 tpy) hypothetical NO_x emission source located at Chattanooga/Lovell Field 368

G.44 Total (wet+dry) NO_3^- deposition estimated for November 1990 resulting from a 28.8 g/s (1000 tpy) hypothetical NO_x emission source located in Crossville 369

FIGURE PAGE

G.45 Total (wet+dry) NO_3^- deposition estimated for December 1990 resulting from a 28.8 g/s (1000 tpy) hypothetical NO_x emission source located at Knoxville/McGhee Tyson Airport 370

G.46 Total (wet+dry) NO_3^- deposition estimated for December 1990 resulting from a 28.8 g/s (1000 tpy) hypothetical NO_x emission source located at Bristol/Tri Cities Airport 371

G.47 Total (wet+dry) NO_3^- deposition estimated for December 1990 resulting from a 28.8 g/s (1000 tpy) hypothetical NO_x emission source located at Chattanooga/Lovell Field 372

G.48 Total (wet+dry) NO_3^- deposition estimated for December 1990 resulting from a 28.8 g/s (1000 tpy) hypothetical NO_x emission source located in Crossville 373

H.1 Maximum 3-h average SO_2 concentrations estimated for 1990 resulting from a 28.8 g/s (1000 tpy) hypothetical SO_2 emission source located at Knoxville/McGhee Tyson Airport 375

H.2 Maximum 3-h average SO_2 concentrations estimated for 1990 resulting from a 28.8 g/s (1000 tpy) hypothetical SO_2 emission source located at Chattanooga/Lovell Field 376

H.3 Maximum 3-h average SO_2 concentrations estimated for 1990 resulting from a 28.8 g/s (1000 tpy) hypothetical SO_2 emission source located at Bristol/Tri Cities Airport 377

H.4 Maximum 3-h average SO_2 concentrations estimated for 1990 resulting from a 28.8 g/s (1000 tpy) hypothetical SO_2 emission source located in Crossville 378

H.5 Maximum 24-h average SO_2 concentrations estimated for 1990 resulting from a 28.8 g/s (1000 tpy) hypothetical SO_2 emission source located at Knoxville/McGhee Tyson Airport 379

H.6 Maximum 24-h average SO_2 concentrations estimated for 1990 resulting from a 28.8 g/s (1000 tpy) hypothetical SO_2 emission source located at Chattanooga/Lovell Field 380

FIGURE PAGE

H.7 Maximum 24-h average SO_2 concentrations estimated for 1990 resulting from a 28.8 g/s (1000 tpy) hypothetical SO_2 emission source located at Bristol/Tri Cities Airport 381

H.8 Maximum 24-h average SO_2 concentrations estimated for 1990 resulting from a 28.8 g/s (1000 tpy) hypothetical SO_2 emission source located in Crossville 382

H.9 Annual average SO_2 concentrations estimated for 1990 resulting from a 28.8 g/s (1000 tpy) hypothetical SO_2 emission source located at Knoxville/McGhee Tyson Airport 383

H.10 Annual average SO_2 concentrations estimated for 1990 resulting from a 28.8 g/s (1000 tpy) hypothetical SO_2 emission source located at Chattanooga/Lovell Field 384

H.11 Annual average SO_2 concentrations estimated for 1990 resulting from a 28.8 g/s (1000 tpy) hypothetical SO_2 emission source located at Bristol/Tri Cities Airport 385

H.12 Annual average SO_2 concentrations estimated for 1990 resulting from a 28.8 g/s (1000 tpy) hypothetical SO_2 emission source located in Crossville 386

H.13 Annual average NO_x concentrations estimated for 1990 resulting from a 28.8 g/s (1000 tpy) hypothetical NO_x emission source located at Knoxville/McGhee Tyson Airport 387

H.14 Annual average NO_x concentrations estimated for 1990 resulting from a 28.8 g/s (1000 tpy) hypothetical NO_x emission source located at Chattanooga/Lovell Field 388

H.15 Annual average NO_x concentrations estimated for 1990 resulting from a 28.8 g/s (1000 tpy) hypothetical NO_x emission source located at Bristol/Tri Cities Airport 389

H.16 Annual average NO_x concentrations estimated for 1990 resulting from a 28.8 g/s (1000 tpy) hypothetical NO_x emission source located in Crossville 390

LIST OF ACRONYMS, INITIALISMS, AND ABBREVIATIONS

AHN	Athens Municipal Airport
AQRV	air quality related value
ARM3	Acid Rain Mountain Mesoscale Model
ATDD	Atmospheric Turbulence and Diffusion Division
BNA	Nashville Metropolitan Airport
CALMET	meteorological preprocessor to the CALPUFF model
CALPUFF	California Puff Model
CAPTEX	Cross Appalachian Tracer Experiment
CFR	Code of Federal Regulations
CHA	Chattanooga/Lovell Field
CRO	Crossville
CTDMPLUS	Complex Terrain Dispersion Model
CWA	Cohutta Wilderness Area
EPA	Environmental Protection Agency
ET	Eastern Time
°F	degrees Fahrenheit
Fig.	figure
FLM	Federal Land Manager
fpm	feet per minute
ft	feet
g/s	grams per second
g/g-mol	grams per gram-mole
GMT	Greenwich Mean Time
GSMNP	The Great Smoky Mountains National Park
GSO	Greensboro High Point/Winston Salem Airport
h	hour
H_2O_2	hydrogen peroxide
H_2SO_4	sulfuric acid
ha	hectare
HNO_3	nitric acid
HTS	Huntington Tri-State Airport
ISC	Industrial Source Complex air dispersion model
IWAQM	Interagency Workgroup on Air Quality Modeling
JKWA	Joyce Kilmer Wilderness Area
kg/ha	kilograms per hectare
km	kilometer
$\mu g/m^3$	micrograms per cubic meter
m	meter
MESOPAC	meteorological preprocessor to the MESOPUFF model
MESOPUFF	Mesoscale Puff Model
MM4-FDDA	Penn State/NCAR Mesoscale Model (Version 4) with four dimensional data assimilation
NADP	National Acid Deposition Program

NAPAP	National Acid Precipitation Assessment Program
NCDC	National Climatic Data Center
NDDN	National Dry Deposition Network
NH_3	ammonia
NO_3^-	nitrate
NO_x	oxides of nitrogen
NPS	National Park Service
NWS	National Weather Service
O_3	ozone
OH	hydroxyl radical
ORO	Oak Ridge Operations
PSD	Prevention of Significant Deterioration
Sect.	section
SO_2	sulfur dioxide
SO_4^{2-}	sulfate
tpy	tons per year
TRI	Bristol/Tri Cities Airport
TYS	Knoxville/McGhee Tyson Airport
USFS	United States Forest Service
USFWS	United States Fish and Wildlife Service
UTM	Universal Transverse Mercator
VOC	volatile organic compound

1. INTRODUCTION

In the February 5, 1992, issue of the *Federal Register*, the National Park Service (NPS) announced that existing air pollution levels were causing adverse impacts on terrestrial and aquatic resources, as well as visibility, at the Great Smoky Mountains National Park. In this notice, the NPS stated its position that new emission sources, or major modifications to existing sources, would contribute to these adverse impacts. The intent of the NPS was to recommend that permits for new emission sources [located within 200 km (130 miles) of the park] be denied unless proposed pollutant increases were mitigated. Such mitigations would have to ensure that no net increase in adverse impact on park resources was incurred (Shaver *et al.*, 1994).

The purpose of this thesis is to report on the development and demonstration of a modeling protocol, which addresses impacts from modification or construction of major point sources emitting oxides of nitrogen (NO_x) and sulfur dioxide (SO_2) in East Tennessee. Impacts to the Great Smoky Mountains National Park and other specially protected areas located in East Tennessee (i.e., Joyce Kilmer Wilderness Area and Cohutta Wilderness Area) are the focus of this study. The scope of this report is concerned with estimating acidic deposition resulting from SO_2 and NO_x emissions in these specially protected areas. Impacts to park ecosystems resulting from ozone exposure and visibility degradation resulting from anthropogenic emissions in East Tennessee are not discussed in this thesis.

Chapter 2 presents background information on the formation of acidic particles and gases in the atmosphere, and subsequent deposition of acidic species resulting from SO_2 and NO_x emissions. Information is also provided on the regulatory environment influencing the selection of the air dispersion model, MESOPUFF II, used to estimate the transport and dispersion of emissions at the regional scale [50-500 km (30-300 miles)].

Chapter 3 describes the modeling method developed for this thesis. Development of gridded meteorological data fields, necessary for the modeling analysis are discussed, as well as selection of hypothetical SO_2 and NO_x emission sources used to demonstrate the modeling protocol.

Chapter 4 presents the results of the modeling study. Monthly and annual deposition estimates for the four baseline and two sensitivity scenarios are discussed. Maps showing deposition potential are presented. These maps may be used as a screening tool to make acidic deposition estimates in the Great Smoky Mountains National Park, and Joyce Kilmer and Cohutta Wilderness Area resulting from emission sources located anywhere in East Tennessee.

Chapter 5 discusses the recommendations and conclusions reached from the development and demonstration of the modeling protocol. A series of appendices is included containing a user's guide for those performing MESOPUFF II modeling studies in the East Tennessee area (Appendix A), contour plots showing deposition and concentration values estimated during the modeling protocol (Appendices B-H), and code listings of programs used in the modeling protocol (Appendices I-L).

2. BACKGROUND

2.1 INTRODUCTION

Federal land managers (FLMs) of national parks and wilderness areas are concerned that air pollution and air pollution related phenomena, such as acidic deposition, are adversely affecting air quality and air quality related values (AQRVs)[1] in lands under their administration. The Clean Air Act (Public Law 95-95, 1977 as amended) designated all national parks greater than 2,430 ha (6,000 acres) and many wilderness areas as Prevention of Significant Deterioration (PSD) Class I areas in order to greatly restrict the degradation of ambient air quality in these protected public lands. In recent years, FLMs have asserted that the PSD permitting process for new emission sources (e.g., electricity-generating power plants and industrial boilers) is failing to protect Class I areas (Paine and Heinhold, 1995; EPA 1993). In particular, the FLMs expressed a need for regional transport modeling techniques that permitting authorities could use to assess the impacts on AQRVs from emission sources located at relatively long distances [50-500 km (30-300 miles)] from Class I areas.

During the late 1980s, two agencies that administer Class I areas, the NPS and the U. S. Forest Service (USFS), as well as, the U. S. Environmental Protection Agency (EPA),were working independently to develop regional transport models for assessing impacts of emission sources on Class I areas. There was a concern, primarily among state regulators, that the potential existed for the three agencies to develop divergent modeling protocols that would make permitting a single source unnecessarily difficult (EPA, 1993). Because of this concern, the Interagency Workgroup on Air Quality Modeling (IWAQM) was formed in 1991 to coordinate the development of technically

[1]AQRVs are qualities of general public importance (e.g., good visibility and healthy ecosystems) that may be detrimentally impacted by air pollution.

sound, regional air quality models for regulatory assessment of Class I areas (EPA, 1993). The IWAQM is comprised of members representing the three agencies that administer Class I areas: (1) the NPS, (2) the USFS and (3) the U. S. Fish and Wildlife Service (USFWS). In addition, EPA has a representative member on IWAQM. The EPA serves as the link between the FLMs and state regulators, and is responsible for approving air quality modeling methods.

In 1992, the IWAQM initiated a multi-year workplan to develop a modeling approach for the permitting of new and modified sources impacting Class I areas (EPA, 1993). Because the scope of this report is concerned with the adverse affect of acidic deposition on Class I area ecosystems found in East Tennessee, this section first provides background information on the formation of acidic particles and vapors in the atmosphere, and subsequent deposition on ecosystems, and the impacts of acidic deposition on Class I areas in East Tennessee. Second, this section discusses the influences of the IWAQM workplan on the selection of MESOPUFF as the regional transport model used to estimate acidic deposition in the East Tennessee.

2.2 FORMATION AND DEPOSITION OF ACIDIC PARTICLES AND VAPORS

Acidic deposition is a general term referring to the removal of acidic particles and gases from the atmosphere. The term "acid rain" is commonly used, but technically only applies to acidic compounds removed from the atmosphere during rain events. Acidic deposition is associated with all forms of precipitation (e.g., rain and snow) and fog, collectively known as "wet deposition," and also is associated with the settling of aerosols, particles, or gases suspended in the atmosphere to the ground. This settling process of dry acidic compounds is known as dry deposition. Figure 2.1 is a schematic of the acidic deposition process as related specifically to sulfur compounds. In Fig. 2.1, the sulfur budget is shown for the United States and Canada, where 30% of total emissions are

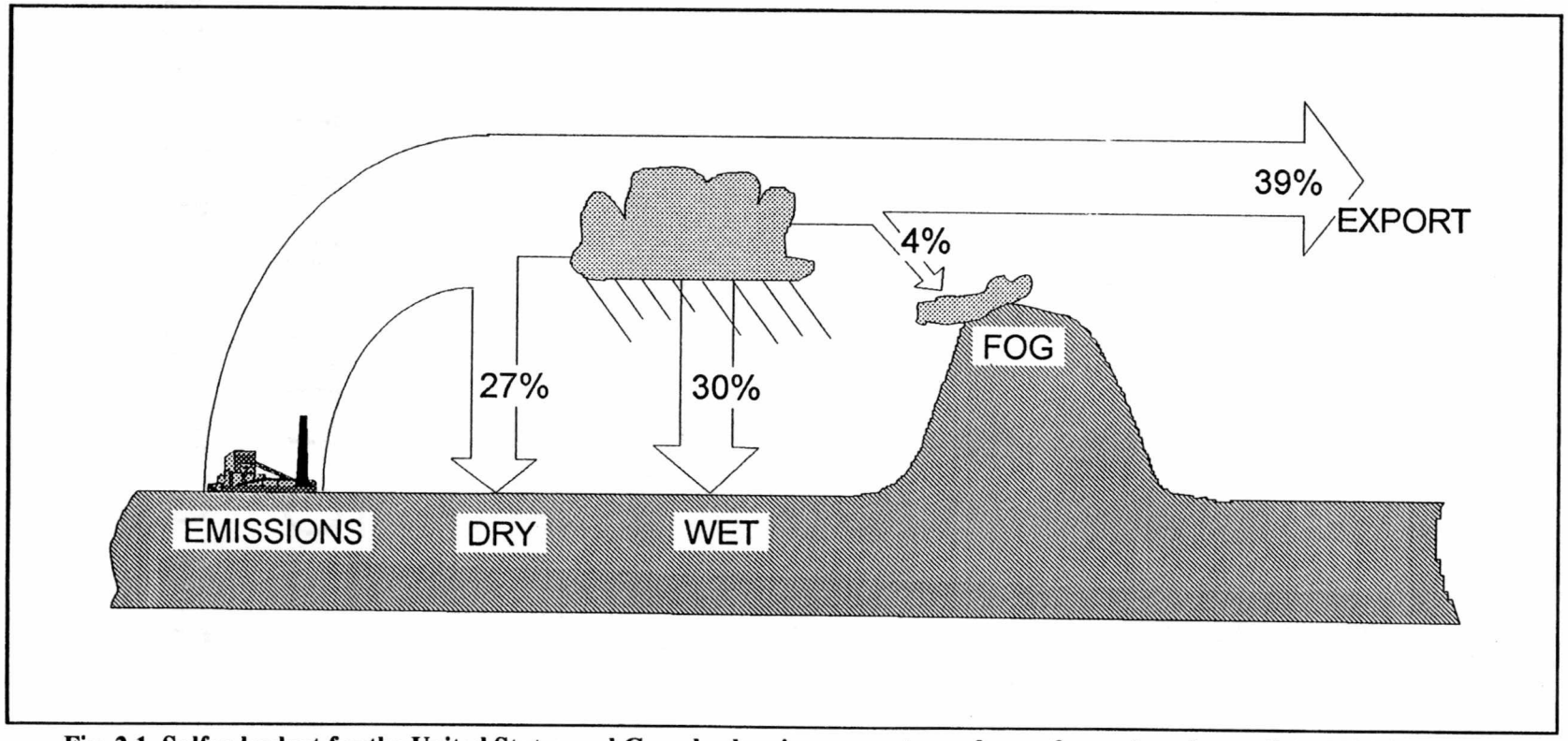

Fig. 2.1. Sulfur budget for the United States and Canada showing percentage of mass for each pathway (from NAPAP, 1991).

deposited by precipitation, 27% by dry deposition, and about 4% by vegetation scavenging of cloud (fog) droplets. The remaining 39% of emissions move beyond the North American Continent, primarily to the Atlantic Ocean (NAPAP, 1991). This schematic illustrates that both wet and dry deposition must be considered in assessing the impacts of acidic deposition.

2.2.1 Emissions of Acidic Precursor Species

Emissions of SO_2, NO_x, and volatile organic compounds (VOCs) contribute to the formation of acidic gases and particles in the atmosphere. Table 2.1 shows major emission source categories of SO_2, NO_x and reactive precursor species (i.e., VOCs) in the United States. Approximately 70% of anthropogenic SO_2 emissions occur from electricity-generating power plants that burn fossil-fuels, primarily coal (EPA, 1995e). Just under 33% of anthropogenic NO_x emissions also occur from electricity-generating power plants; however mobile sources, primarily automobiles, contribute a larger percentage (44%) of total anthropogenic NO_x emissions (EPA, 1995e). Automobiles are also a primary source (contributing about 27% of the total anthropogenic emissions) of reactive precursor species (i.e., VOCs) (EPA, 1995e).

2.2.2 Transformation and Transport of Acidic Precursor Species and Compounds

Acidic compounds form in the atmosphere when SO_2 and NO_x emissions are oxidized, primarily by hydroxyl radicals, hydrogen peroxide, and ozone. These oxidants are secondary pollutants formed in the atmosphere via photochemical reactions of NO_x and VOCs. Figures 2.2 and 2.3 show schematically the atmospheric oxidation pathways of SO_2 and NO_x.

SO_2 emissions, which come primarily from tall (e.g., *not* vent) stacks, can be transported considerable distances downwind. During this travel time, SO_2 is oxidized to sulfate (SO_4^{2-}), and is

Table 2.1. Major emissions source categories in the United States and their contribution to total emissions of each pollutant in 1992

Pollutant	Emission source	Percent contribution
SO_2[a]	Electric utility fuel combustion	70
	Industrial fuel combustion	14
	Metals processing	4
	Mobile sources (e.g., automobiles)	4
	Other fuel combustion	3
	All other sources	5
NO_x[a]	Mobile sources (e.g., automobiles)	44
	Electric utility fuel combustion	33
	Industrial fuel combustion	15
	Other fuel combustion	3
	All other sources	5
VOCs[a]	Mobile sources (e.g., automobiles)	36
	Solvent utilization	27
	Waste disposal and recycling	10
	All other sources	27

[a]Abbreviations: SO_2 = sulfur dioxide, NO_x = oxides of nitrogen, VOCs = volatile organic compounds.

Source: U. S. Environmental Protection Agency, *Acid Deposition Standard Feasibility Study Report to Congress*, EPA 430-R-95-001a, Office of Air and Radiation, Acid Rain Division (6204J), Washington, D C., 1995.

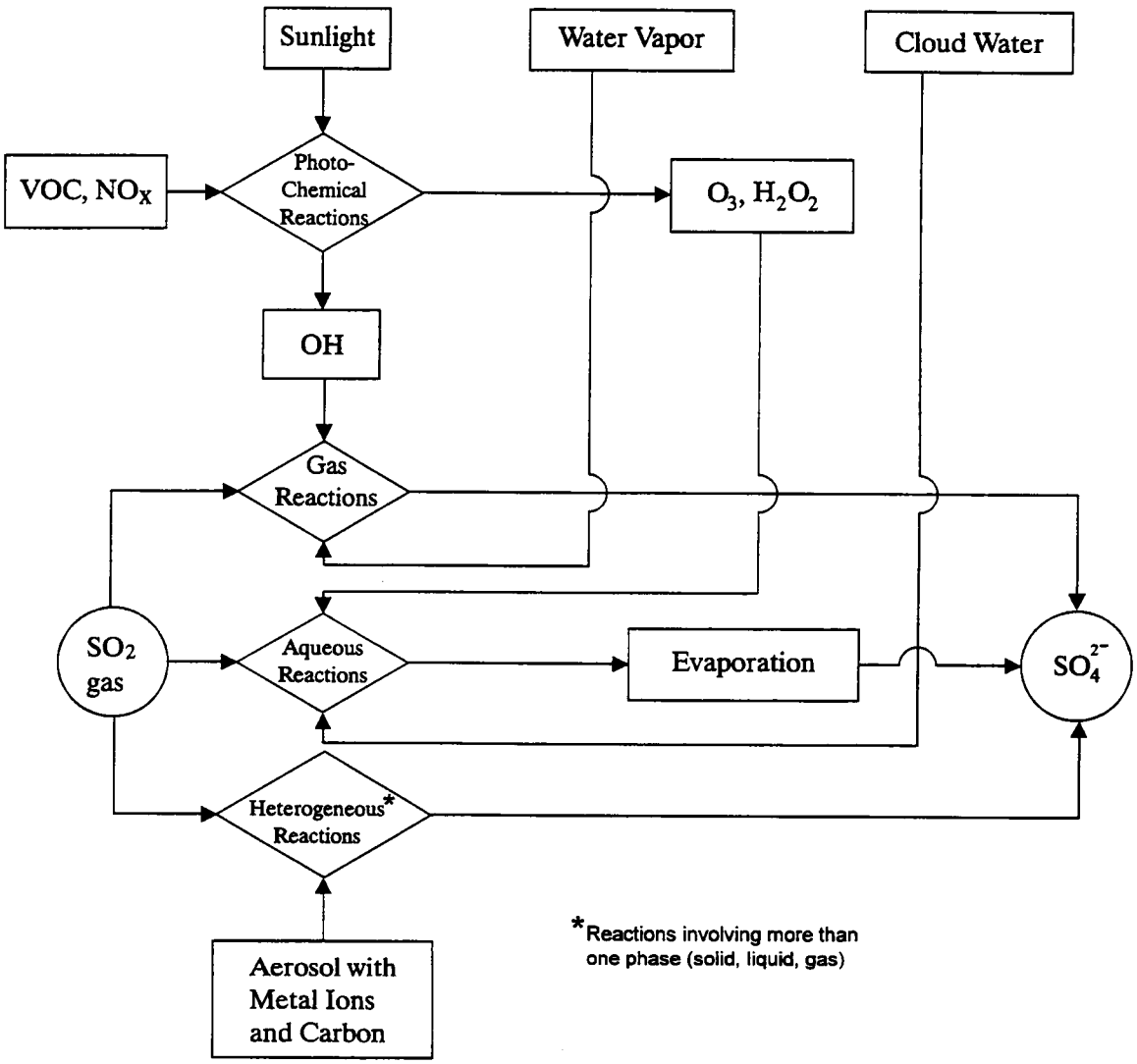

Fig. 2.2. SO_2 oxidation pathways (from Scire *et al.*, 1984).

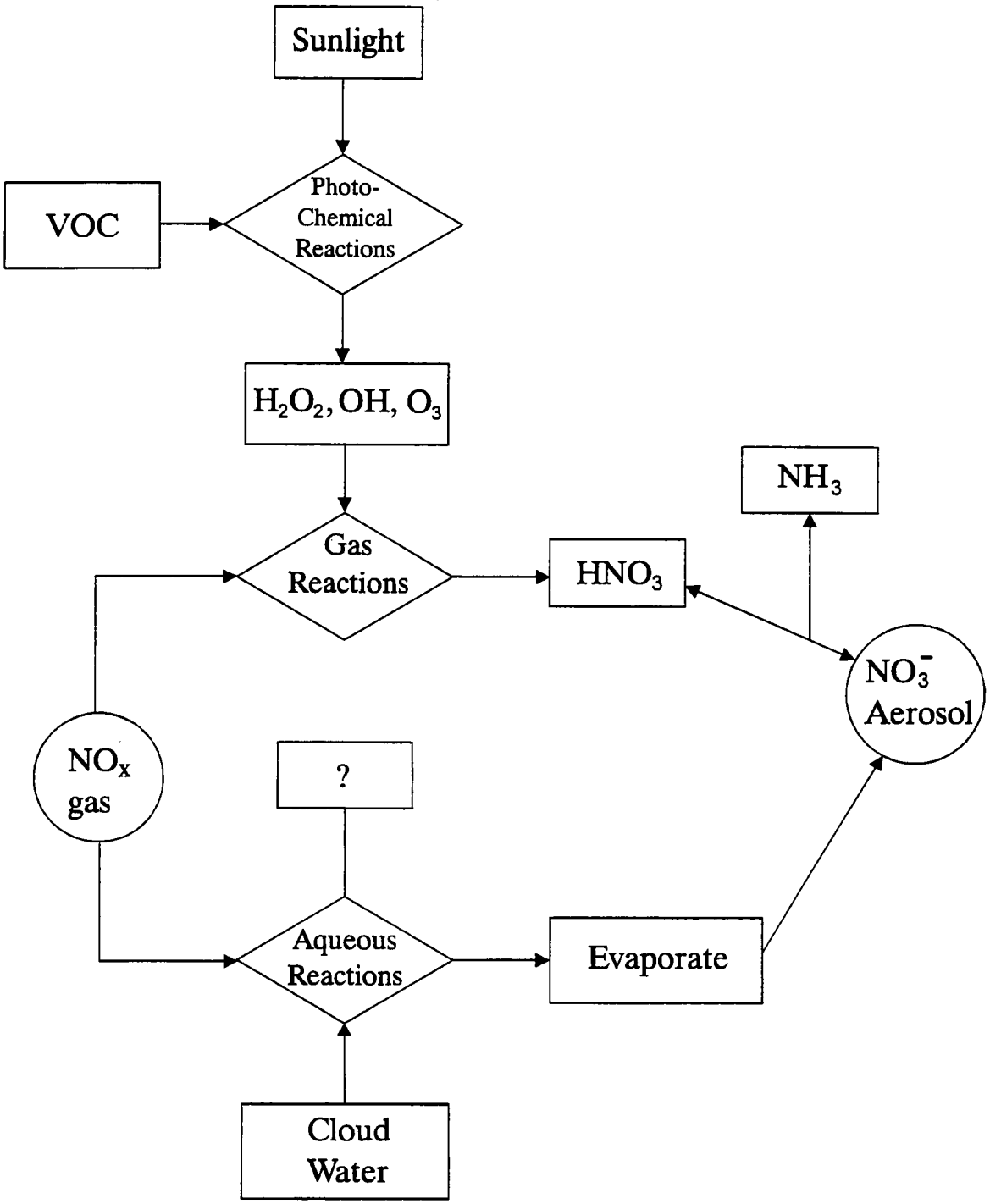

Fig. 2.3. NO_x oxidation pathways (from Scire *et al.*, 1984).

subsequently deposited on the ground as dry particles or removed from the atmosphere as sulfuric acid (H_2SO_4) during precipitation events. During the summer, wind speeds are generally lower than in winter and precipitation intensity is greater (primarily due to thunderstorm activity). Therefore, wet SO_4^{2-} is removed more quickly in summer than in winter (NAPAP, 1991). Dry deposition processes remove SO_2 from the atmosphere efficiently, particularly in summer due to increased scavenging by vegetation. Sulfate particles are not removed by dry deposition processes as efficiently as SO_2. Therefore dry deposition is primarily in the form of SO_2 near the source and SO_4^{2-} particles far from the source for all seasons (NAPAP, 1991).

About half of NO_x emissions occur primarily from mobile sources at ground level, with the other half occurring from tall stacks. Nitric acid (HNO_3) and nitrate (NO_3^-) particles form more quickly from NO_x emissions than do SO_4^{2-} particles from SO_2 emissions. HNO_3 deposits efficiently in wet and dry form, and therefore, a higher percentage is deposited relatively near the source. The distance from the source at which NO_3^- deposits is similar to SO_4^{2-} for both wet and dry removal processes (i.e., NO_3^- does not deposit efficiently) (NAPAP, 1991).

2.2.3 Monitoring of Acidic Deposition

Wet deposition is monitored nationally at almost 200 sites in the United States as part of the National Atmospheric Deposition Program (NADP). Figures 2.4 and 2.5 show the patterns of wet SO_4^{2-} and NO_3^- deposition in the United States during 1991 (NAPAP, 1992). On these figures, deposition values are indicated by the wet flux in units of kilograms of pollutant per hectare (kg/ha). Three NADP sites are located in or near the East Tennessee Class I areas: (1) Oak Ridge, Tennessee, (2) Sugarlands, Tennessee (note that Sugarlands is located in the Great Smoky Mountains National Park), and (3) Coweeta, North Carolina.

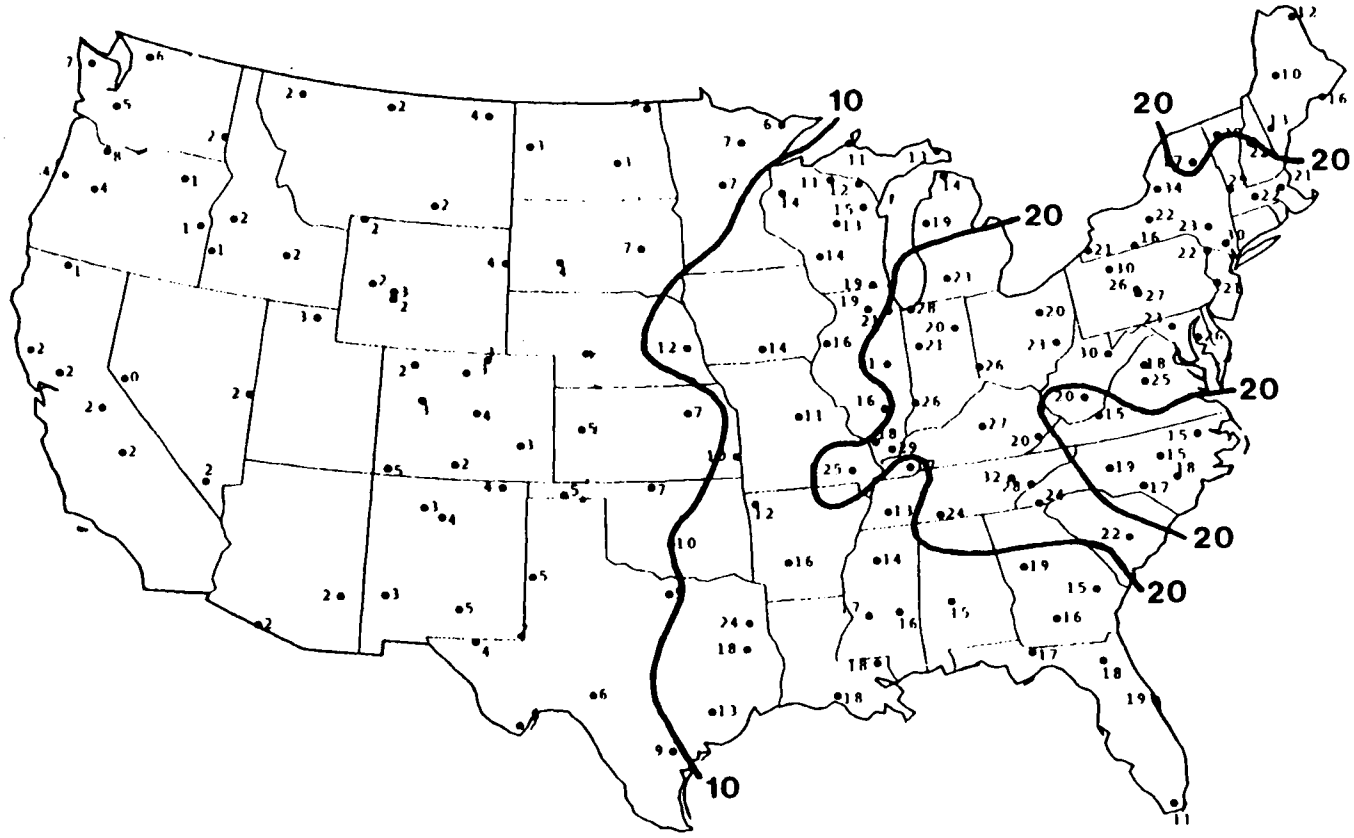

Fig. 2.4. 1991 wet SO_4^{2-} deposition (kilograms per hectare) (from NAPAP, 1992).

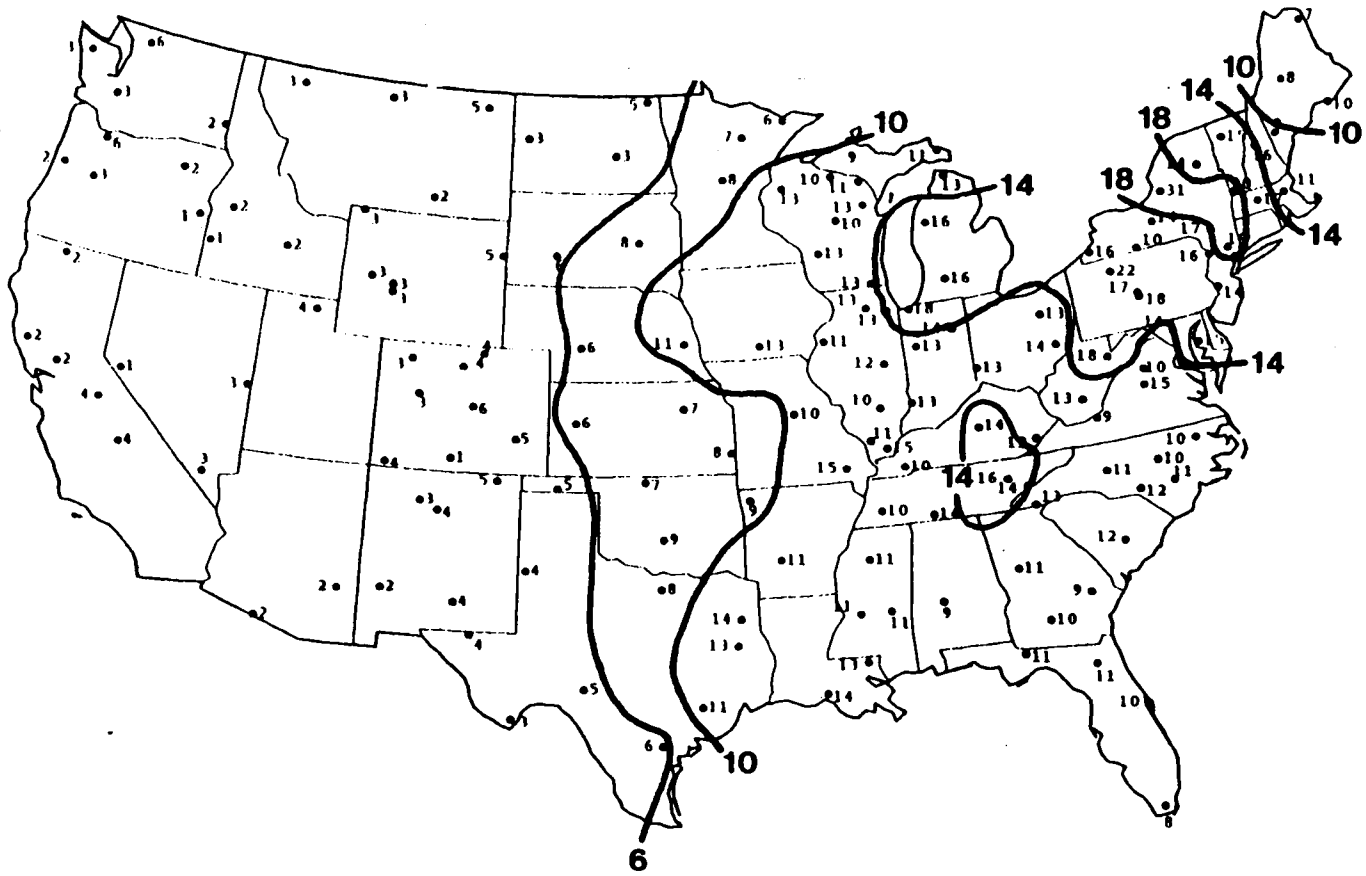

Fig. 2.5. 1991 wet NO_3^- deposition (kilograms per hectare) (from NAPAP, 1992).

For total wet SO_4^{2-} deposition measured during 1991 (Fig. 2.4), the highest value measured in the country was at Oak Ridge (32 kg/ha). The value at Sugarlands (28 kg/ha) was the fifth highest in the country, and the value measured at Coweeta, North Carolina (24 kg/ha) was in the top 10% of all monitoring stations. Typically, wet SO_4^{2-} deposition values in East Tennessee are above average, but not the highest in the country. Between 1985 and 1987 the highest annual wet SO_4^{2-} deposition values were measured in the area east of the Ohio River Valley, stretching across Pennsylvania and New York, where the average annual maximum was 43 kg/ha (NAPAP, 1990). Over this same period, 1985-1987, the average annual wet SO_4^{2-} deposition in the East Tennessee area ranged from about 17 kg/ha to 28 kg/ha.

During 1991, the maximum annual wet NO_3^- deposition occurred at a station located in the Adirondack Mountains of New York (31 kg/ha). Annual wet NO_3^- deposition in the East Tennessee area was one-third to one-half of the national maximum, ranging from a low of 13 kg/ha at Coweeta and 14 kg/ha at Sugarlands to a high of 16 kg/ha at Oak Ridge. These values are similar to 1985-1987 measurements where annual wet NO_3^- deposition averaged about 13 kg/ha in East Tennessee.

Dry deposition is measured at 50 sites in the United States. These 50 sites comprise the National Dry Deposition Network (NDDN) established by the EPA in 1987. Because direct measurement of dry deposition is considerably more difficult than direct measurement of acidic precipitation (Clarke and Edgerton, 1992; NAPAP, 1992), dry deposition is estimated at these monitoring locations using an inferential model developed by Hicks *et al.* (1985). The inferential model estimates dry deposition as the product of the measured atmospheric pollutant concentration and the deposition velocity determined from meteorological measurements. Three NDDN stations are located near the East Tennessee Class I areas: (1) Speedwell, Tennessee, (2) Cranberry, North Carolina, and (3) Coweeta, North Carolina. Figures 2.6 and 2.7 show the annual SO_2 and HNO_3 dry deposition fluxes estimated by the NDDN during 1991.

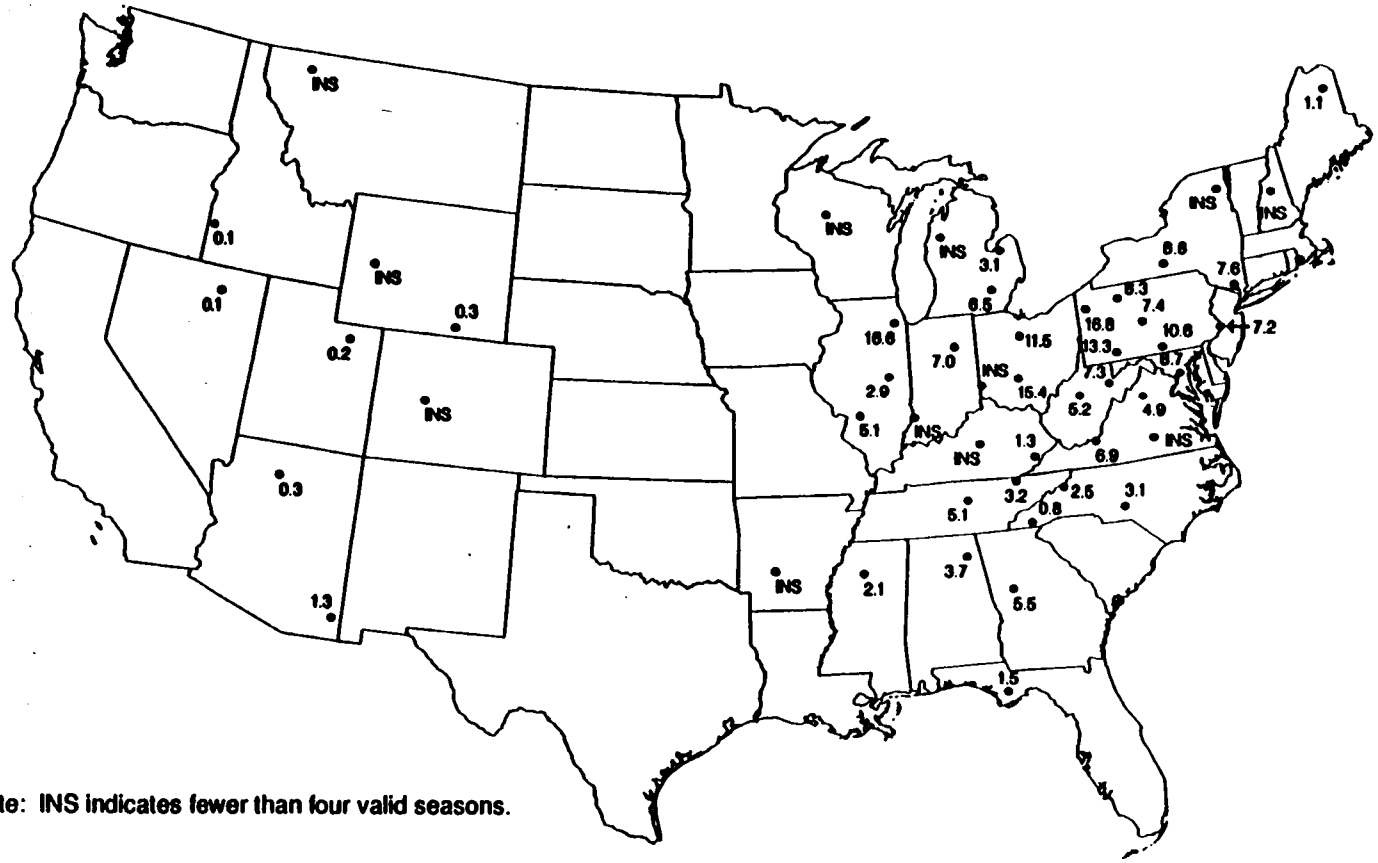

Note: INS indicates fewer than four valid seasons.

Fig. 2.6. 1991 mean annual SO_2 dry deposition fluxes (kilograms per hectare) (from Clark and Edgerton, 1992).

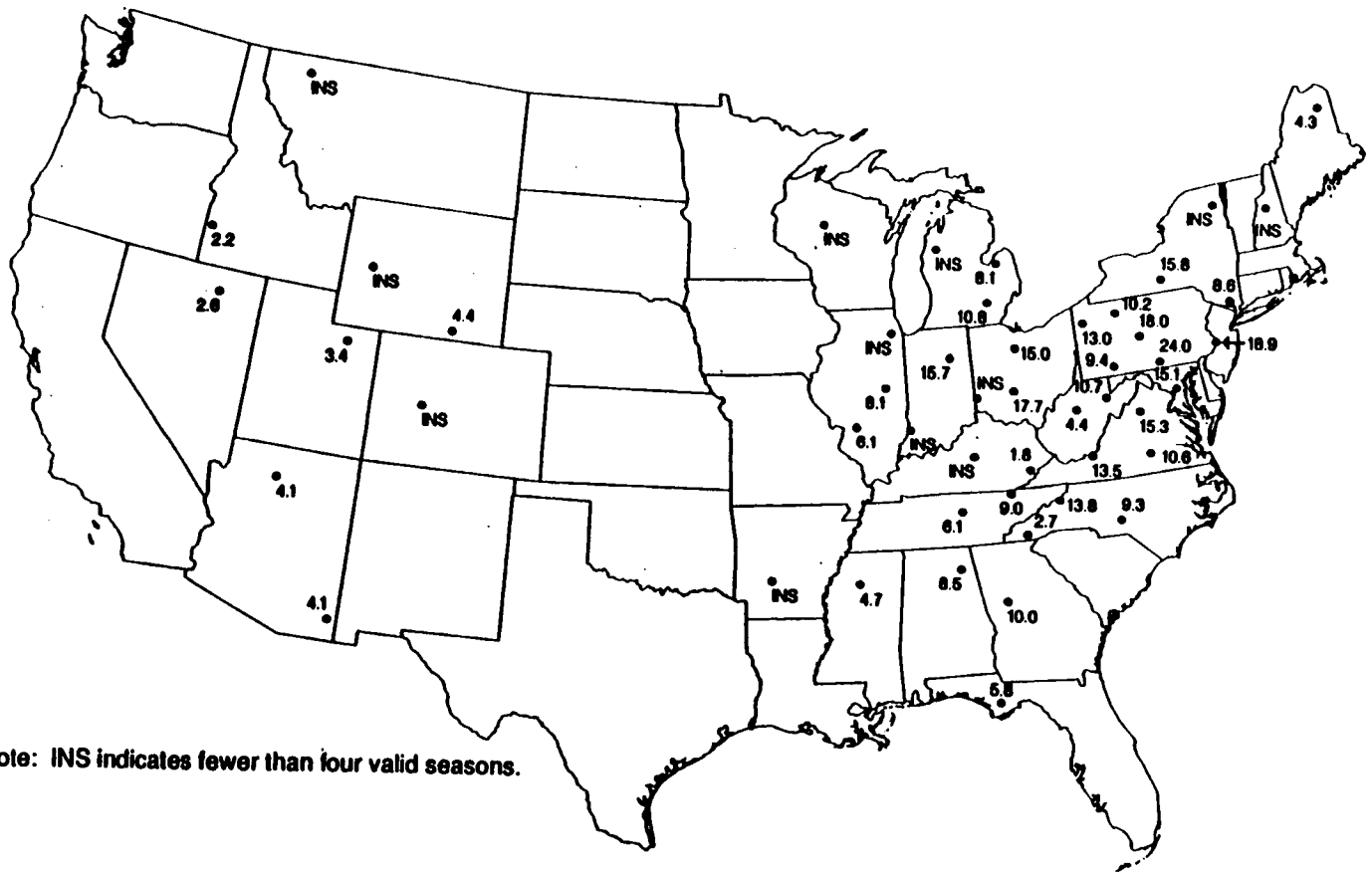

Fig. 2.7. 1991 mean annual HNO_3 dry deposition fluxes (kilograms per hectare) (from Clark and Edgerton, 1992).

Total dry SO_2 fluxes estimated for 1991 at stations located in or near East Tennessee were relatively low compared to most of the eastern United States (Fig. 2.6). The maximum value in or near East Tennessee was estimated for Speedwell, TN (3.2 kg/ha), with a slightly lower value at Cranberry, NC (2.5 kg/ha) and a much lower value at Coweeta (0.8 kg/ha). During 1991, the maximum dry SO_2 flux in the country was located in western Pennsylvania (16.8 kg/ha).

Total dry HNO_3 fluxes estimated for 1991 for stations located near the East Tennessee Class I areas ranged from a low of 2.7 kg/ha at Coweeta to 13.8 kg/ha in Cranberry, North Carolina.

2.3 IMPACTS OF ACIDIC DEPOSITION ON CLASS I ECOSYSTEMS IN EAST TENNESSEE

Impacts of acidic deposition are a concern for watersheds and high elevation spruce-fir forests in Class I areas located in East Tennessee (NAPAP, 1991; EPA 1995e). Currently, only 1-3% of the streams in East Tennessee are chronically acidic (EPA, 1995e). However, streams in the Great Smoky Mountains National Park have the highest NO_3^- concentrations of any in the United States draining undisturbed watersheds (Stoddard, 1994). Additionally, watersheds in the Great Smoky Mountains National Park are potentially sensitive to future acidification due to steep mountain slopes and shallow soils (EPA, 1995e). These characteristics are expected to lead to reduced NO_3^- and SO_4^{2-} retention capacity of the watershed, and therefore, a greater potential for migration of acidic species to aquatic systems (EPA, 1995e; NAPAP, 1991).

Episodic acidification caused by short-term storm events has been modeled and monitored in the Great Smoky Mountains National Park. Model estimates indicate that 2-7% of the streams in the Southern Appalachians have episodes of acute acidity during strong rain events (NAPAP, 1991). Cook *et al.* (1994) measured increased SO_4^{2-} and dissolved organic compounds during acidic episodes in streams in the Great Smoky Mountains National Park. No negative effects from acidic

episodes have been observed in the park. However, studies in the Northeastern U. S. show that acidic episodes impact fish and invertebrate populations similar to those found in the Southern Appalachians (Wigington *et al.*, 1990).

Impact of acidic deposition on high-elevation spruce-fir populations in East Tennessee are currently being studied. The Great Smoky Mountains National Park contains the largest area of "old-growth" red spruce and fraser fir ecosystem in the world (Shaver *et al.*, 1994). Tree studies conducted since the 1950s show increased copper, aluminum, iron, cadmium, and nitrogen, and decreased manganese in xylem tissue of several coniferous trees in the Great Smoky Mountains National Park (Baes and McLaughlin, 1986). A field plot study by Stam *et al.* (1990) supports these data and concludes that changes in metal concentrations can be largely attributed to acidic deposition. There is experimental evidence that acid deposition and associated pollutants can alter the resistance of red spruce to winter injury (Barnard and Lucier, 1990) and through this mechanism, acidic deposition may have contributed to red spruce decline at high elevations in the northern Appalachians (EPA. 1995e; NAPAP, 1991).

EPA has been investigating the establishment of acidic deposition standards to provide a predetermined level of protection to aquatic and terrestrial resources. A recent EPA report to Congress stated that "establishing specific needs and appropriate limits for deposition standards requires advancing the scientific understanding of factors key to (1) defining times to watershed nitrogen saturation (i.e., how long before deposition occurs and adverse effects become difficult to reverse) and (2) the interaction of sulfur and nitrogen in acidifying watersheds and surface waters" (EPA, 1995e). Because these processes are not well understood, EPA did not recommend specific acidic deposition standards.

The absence of an acidic deposition standard makes assessment of impacts from emission sources more difficult. FLMs believe that Class I areas, particularly in the Eastern United States,

have experienced ecosystem degradation from acidic deposition and want to cease future decline of aquatic and terrestrial resources (Shaver *et al.*, 1994).

2.4 PHASE I OF THE IWAQM WORKPLAN

Regional atmospheric transport models are one of the key tools used to gauge the impacts of acidic deposition on Class I areas. These models estimate the surface deposition flux from emission sources located at distances greater than 50 km (30 miles) from the area of interest. In 1992, the IWAQM identified an immediate need for a regional transport model that would assess the impact of emission sources on Class I areas. This model would be used primarily for ongoing permit activity. In Phase I of their workplan, the IWAQM decided that a preexisting (immediately available) model would be used on an interim basis to satisfy this immediate need until a model could be developed and tested in Phase II.

The IWAQM consulted EPA's *Guideline for Air Quality Models (Revised)* (40 CFR 51, App. W) as part of its Phase I model selection (EPA, 1993). The guideline does not specifically recommend a model for use in regional transport assessments; however it does provide three general criteria for selecting an appropriate model in those cases when one is not otherwise specifically recommended:

1. the model can be demonstrated to be applicable to the problem on a theoretical basis,
2. the data bases which are necessary to perform the analysis are available and adequate, and
3. performance evaluations of the model in similar circumstances have shown that the model is not biased toward underestimates.

The IWAQM adopted these three criteria in selecting a interim regional transport model.

Two models were considered in Phase I that would meet the immediate need for regional transport assessment: the Acid Rain Mountain Mesoscale Model (ARM3) (Morris *et al.*, 1988) and MESOPUFF. ARM3 was originally developed by EPA Region 8 and adopted by the NPS for regional transport modeling studies prior to the IWAQM's formation. The development of MESOPUFF was originally sponsored by EPA in the early 1980s. MESOPUFF is currently listed as a potential alternate model for regulatory applications (40 CFR 51, App. W).

ARM3 and MESOPUFF were each compared to other regional transport models. Both models demonstrated better performance than other models involved in the studies when compared to measured tracer data (i.e., ARM3 and MESOPUFF were relatively accurate in simulating data) (Carhart *et al.*, 1980; Moore *et al.*, 1990). Based on these comparisons, the other models were eliminated by the IWAQM from further consideration.

The IWAQM performed a study directly comparing the performance of ARM3 and MESOPUFF. The results of this comparison are summarized in the following excerpt taken from the IWAQM's Phase I report (EPA, 1993).

> Until a more refined technique can be evaluated [Phase II], neither of the models under consideration by the IWAQM to use in the interim are totally satisfactory. With respect to the meteorological preproccessors, the MESOPUFF II processor should incorporate a weighted interpolation algorithm in the calculation of mixing depths to avoid the extreme gradients in the current formulation. The ARM3 processor, on the other hand, should employ different algorithms for calculating mixing depths and should change the order of analysis in the diagnostic wind field calculations to start out with a field interpolated from the observations as the first-guess field, upon which the kinematic and blocking effects of terrain should be applied.
>
> The MESOPUFF II model does not explicitly include any treatment for the effects of terrain on long range transport and dispersion. This is a relatively major deficiency with respect to the needs of the IWAQM. While the ARM3 model incorporates algorithms to treat such effects, the model has been found to have a number of coding errors which render its use suspect.

The IWAQM considered ARM3's coding errors correctable. However, due to these errors, previous evaluation analyses involving ARM3 were invalidated. Because the time required to validate the code would not satisfy the need for an immediate, interim regional transport model, ARM3 was eliminated as a candidate Phase I model. Therefore, MESOPUFF was selected as the interim Phase I model for immediate regulatory use.

The IWAQM also recommended that MESOPUFF be used with a steady-state Gaussian plume model [e.g., the Industrial Source Complex (ISC) air dispersion model (40 CFR 51, App. W)] in assessing impacts to Class I areas. The use of the Gaussian plume model to provide initial estimates of concentrations in Class I areas is called a "Level I analysis" by the IWAQM. If Level I estimates indicate that adverse conditions may occur in the Class I areas, then a "Level II analysis" using MESOPUFF would be required. The IWAQM concluded its Phase I report by stating "that the interim system [a combination Level I analysis using ISC and Level II analysis using MESOPUFF] is the best of currently available alternatives for simulating the impacts of long range transport on . . . AQRVs." Since the Phase I recommendations were published in 1993, several Level II analyses have been conducted using MESOPUFF to assess impacts on Class I areas in Virginia, Florida, South Carolina, and Colorado (EPA, 1995a).

2.5 PHASE II OF THE IWAQM WORKPLAN

The purpose of Phase II of the IWAQM's multi-year work plan was to identify and develop refined techniques for assessment of the impact of the regional transport of air pollutants on Class I areas. One of the major efforts of Phase II was to enhance and evaluate the CALMET and CALPUFF models (EPA, 1995b). CALMET is a meteorological model that is able to use hourly gridded wind fields created by the Penn State/NCAR Mesoscale Model with four dimensional (length, width, height, and time) data assimilation (MM4-FDDA) as a supplement to observational

data. Additionally, the CALMET model has been modified to include the effects of terrain on winds and mixing layer heights (EPA 1995c). CALPUFF is a multi-layer puff dispersion model that uses meteorological data prepared by CALMET. Although CALPUFF employs the same basic dispersion methodology as MESOPUFF, it is more advanced in that it incorporates the following features not found in MESOPUFF (EPA 1995b): (1) subgrid scale complex terrain algorithms similar to those found in the EPA recommended Complex Terrain Dispersion Model (CTDMPLUS) (Perry *et al.*, 1989); (2) wind shear effects allowing individual puffs to be split by wind shear occurring between different vertical layers; (3) building downwash algorithms currently used by the EPA recommended ISC model, and (4) overwater and coastal interaction effects designed to model the effects of bodies of water on plume transport, dispersion and deposition.

As part of Phase II, a study was conducted which compared the performance of MESOPUFF II to the enhanced CALMET/CALPUFF model system (EPA, 1995d). The performance of the models was evaluated using tracer data collected during the Cross-Appalachian Tracer Experiment (CAPTEX). The study results show that using the CALPUFF model with MM4-FDDA data performed better in simulating the CAPTEX data than using MESOPUFF as originally specified in the Phase I interim modeling approach (i.e., running MESOPUFF with wind fields created by its meteorological preprocessor, MESOPAC) (EPA, 1995d).

A major conclusion drawn from the study was that the selection of the wind field model had a much larger influence on model performance than selection of the dispersion models themselves. In the IWAQM-sponsored study, MESOPUFF simulations were run using the MM4-FDDA wind fields, as well as with wind fields created by MESOPAC. The CALPUFF model with MM4-FDDA data matched the tracer data better than MESOPUFF with MM4-FDDA data, but the difference in results was much less significant compared to those MESOPUFF runs using wind fields created by MESOPAC (EPA, 1995d). It should be noted that the model options chosen in CALPUFF for the

CAPTEX tracer simulations were selected to closely simulate MESOPUFF features (e.g., only two layer wind fields were used). This was done so that the effects of different wind field models and data inputs could be isolated and identified (EPA, 1995d).

Phase II has not been completed even though the CALPUFF model has been enhanced to the IWAQM's specifications and model comparisons indicate that CALPUFF outperforms MESOPUFF. CALMET and CALPUFF are currently undergoing a formal public review so that EPA can determine whether the models are suitable for routine regulatory use. EPA has not specified when this formal public review will conclude. Additionally, as of August 1995, the IWAQM has depleted its funding. The workgroup estimates that the earliest date by which its Phase II recommendation will be complete is August 1996 (EPA, 1995a).

2.6 REGIONAL TRANSPORT MODEL SELECTED FOR THIS STUDY

MESOPUFF is the current regional transport model recommended by the IWAQM to use for evaluating impacts of air pollutants from emission sources located more than 50 km (30 miles) from Class I areas. This recommendation is valid until MESOPUFF is replaced by the model chosen at the completion of Phase II of the IWAQM's workplan (most likely CALPUFF). Because IWAQM's Phase II recommendation will not be issued until fall 1996, at earliest, MESOPUFF (with meteorological data fields generated by MESOPAC) was chosen to develop and demonstrate a regional transport modeling protocol for East Tennessee. If another model (e.g., CALPUFF) is used in a subsequent study, a detailed comparison of those results with the results of this study would be expected to provide much useful information.

3. MODELING METHOD

3.1 INTRODUCTION

Per IWAQM recommendations, MESOPUFF was chosen to estimate acidic deposition resulting from emission sources located in East Tennessee. The following discussion highlights some features of MESOPUFF that are described in more detail in Scire *et al.* (1984) and EPA (1995f).

MESOPUFF employs the Gaussian puff method where a continuous plume is divided into a series of discrete puffs at the emission point. Each puff has a Gaussian distribution of pollutants in three dimensions (length, width and height). Puffs are superimposed upon a wind field which varies over space and time, and each puff will follow its own trajectory through the wind field (i.e., Lagrangian motion). Because it allows for a changing wind field to transport pollutants for long distances, the Gaussian puff method is particularly suited for modeling atmospheric dispersion of pollutants in the regional scale [50-500 km (30-300 miles)] (Hanna *et al.*, 1982).

MESOPUFF simulates the chemical oxidation of SO_2 and NO_x that produces acidic species in the atmosphere (i.e., SO_2 is converted to SO_4^{2-} and NO_x is converted to HNO_3 and NO_3^-). The model uses empirical chemical transformation rate equations that simulate a wide range of environmental conditions over space and time.

Wet and dry deposition algorithms are incorporated into MESOPUFF. The model simulates dry deposition using a resistance model that calculates the dry deposition flux as the product of the estimated pollutant concentration in the atmosphere times the deposition velocity (Hicks *et al.*, 1984). Wet removal is simulated using actual precipitation scavenging ratios associated with different acidic species (Maul, 1980).

MESOPUFF has the following limitations relevant to the East Tennessee area: (1) the model assumes flat terrain over the modeling domain, and therefore, does not account for terrain effects on dispersion and deposition; and (2) the model does not account for puff splitting that may occur with vertical wind shear.

The remainder of this section discusses the development of gridded meteorological data fields used by MESOPUFF to simulate atmospheric conditions in East Tennessee, and the development of scenarios used for analyzing the impacts to Class I areas located in the modeling domain from hypothetical SO_2 and NO_x emission sources located in East Tennessee.

3.2 INPUTS TO MESOPAC

MESOPUFF uses meteorological data fields created by the preprocessor MESOPAC-II Version 2.4 (MESOPAC) (Scire *et al.* 1984, EPA 1995f). MESOPAC constructs hourly gridded meteorological fields from hourly surface and twice-daily rawinsonde data measured at multiple sites.

3.2.1 Extent of the Meteorological Grid

Three cartesian coordinate grid systems are used in MESOPUFF: (1) a meteorological grid, (2) a computational grid, and (3) a sampling grid. The meteorological grid is established using MESOPAC and is the basic reference frame for all spatial inputs (e.g., locations of meteorological stations and sources) to both MESOPAC and MESOPUFF. Meteorological parameters, such as wind speed and direction, are determined by MESOPAC at each grid point. The southwest corner of the modeling domain (Fig.3.1) lies at Universal Transverse Mercator (UTM) coordinates 3825 km Northing, 655 km Easting (approximately 55 km due south of Chattanooga). The modeling domain is enclosed by a rectangle extending 330 km (200 miles) east and 220 km (140 miles) north from

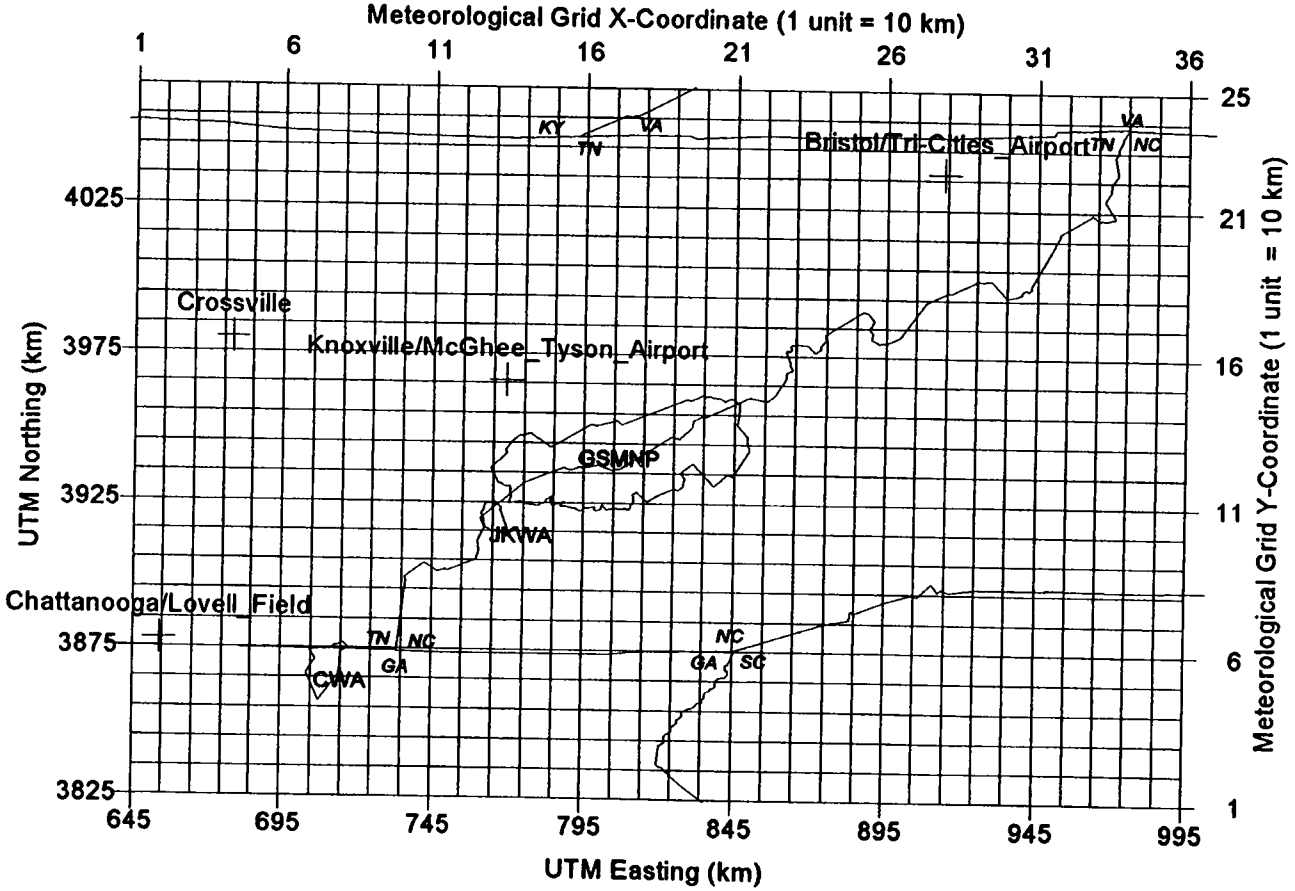

Fig. 3.1. The MESOPUFF II meteorological grid defining the East Tennessee modeling domain.

the southwest corner, and was selected to encompass the East Tennessee River Valley (including the cities of Chattanooga, Knoxville, and Bristol) and the affected Class I areas (i.e., Great Smoky Mountains National Park, Joyce Kilmer Wilderness Area, and Cohutta Wilderness Area). Both the computational and sampling grids must lie within the areal extent of the meteorological grid (EPA, 1995f). The meteorological grid extends beyond the modeling domain by 10 km in the east, north, and west directions. The author decided not to extend the meteorological grid 10 km beyond the southern boundary of the modeling domain because this boundary is well south of the southernmost Class I area (Cohutta Wilderness Area) and the Tennessee-Georgia border [about 35 km (22 miles) and 55 km (34 miles), respectively]. Any further extension would have included a large area that is not relevant to the study. Therefore, the southwest corner of the meteorological grid is at UTM coordinates 3825 km Northing, 645 km Easting. The meteorological grid extends 350 km (220 miles) east and 230 km (140 miles) north from the southwest corner.

3.2.2 Selection of Meteorological Stations

Figure 3.2 shows the meteorological data stations used to construct the meteorological grid. Table 3.1 gives the latitudes, longitudes, and UTM coordinates for these stations.

Four rawinsonde stations [located at Nashville Metropolitan Airport, Tennessee (BNA); Huntington Tri-State Airport, West Virginia (HTS); Greensboro High Point/Winston Salem Airport, North Carolina (GSO); and Athens Municipal Airport, Georgia (GSO)] were used in developing the meteorological grid. These are the closest rawinsonde stations to the modeling domain and are almost equidistant from the center of the area. There are no rawinsonde stations located in the East Tennessee Valley that make regular, twice-daily upper-air soundings.

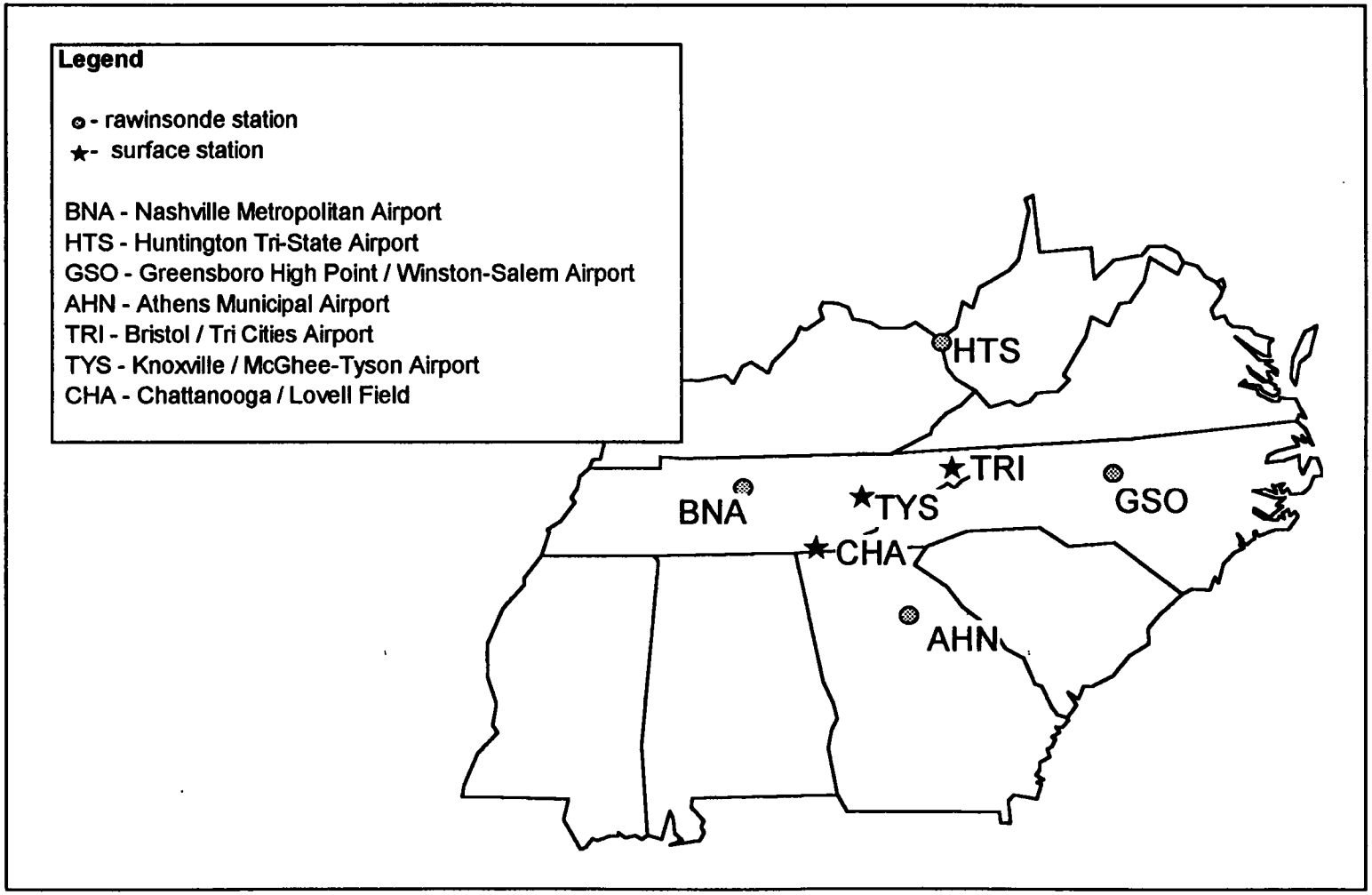

Fig. 3.2. Location of rawinsonde and surface data stations used to construct the East Tennessee meteorological grid.

Table 3.1. Locations of surface and rawinsonde stations and surface roughnesses and anemometer heights for surface stations

Station	Latitude (deg)	Longitude (deg)	UTM Coordinates (km)		Anemometer height (m)	Surface roughness (m)
			Northing	Easting[a]		
CHA[b]	35°02'	85°12'	3879	654	10	0.1
TRI[b]	36°29'	82°24'	4038	914	6.1	0.1
TYS[b]	35°48'	84°00'	3967	769	4.3	0.1
AHN[b]	33°57'	83°19'	3759	825	na[b]	na
BNA[b]	36°07'	86°41'	3999	529	na	na
GSO[b]	36°05'	79°57'	3994	1035	na	na
HTS[b]	38°22'	82°33'	4247	905	na	na

[a]All UTM Easting coordinates are referenced to Zone 16.
[b]Abbreviations: CHA = Chattanooga/Lovell Field, Tennessee; TRI = Bristol/Tri Cities Airport, Tennessee; TYS = Knoxville/McGhee Tyson Airport, AHN = Athens Municipal, Airport, Georgia; Nashville Metropolitan Airport, Tennessee; Greensboro High Point Airport, North Carolina; Huntington/Tri-State, Airport, West Virginia.; na = not applicable.

Three surface meteorological stations all located in Tennessee [Chattanooga/Lovell Field (CHA), Knoxville/McGhee Tyson Airport (TYS), and Bristol/Tri-Cities Airport (TRI)] were used in developing the meteorological grid. These National Weather Service (NWS) sites were selected because they provide quality-assured data that collectively are representative of wind flow in the East Tennessee Valley. Additionally, data from these sites are readily available from the National Climatic Data Center (NCDC) in the format needed for MESOPAC. Anemometer heights and representative surface roughness lengths (equal to about one-tenth of the height of average protuberances at the station location) for the three surface stations are shown in Table 3.1.

3.2.3 Meteorological Grid Construction

IWAQM made several recommendations for running MESOPAC and MESOPUFF to determine impacts to Class I areas, including the resolution of the meteorological grid (EPA, 1993). IWAQM recommended that grid resolution should be at least one-third the median distance between meteorological observation stations (i.e., a grid point spacing greater than one-third the median distance is too coarse, but a finer spacing is acceptable). The distance between Knoxville/McGhee Tyson Airport and Chattanooga/Lovell Field is 145 km (90 miles), and the distance between Knoxville/McGhee Tyson Airport and Bristol/Tri-Cities Airport is 165 km (100 miles). One-third of the average distance between the stations is 51 km (32 miles). The average distance was used instead of the median distance because only two distances were involved in the calculation. The rawinsonde stations were not included in the grid resolution calculation because these stations lie outside of the modeling domain. Therefore, based on IWAQM's recommendation, the meteorological grid spacing should be approximately 50 km (30 miles).

The resolution of the meteorological grid must be equal to the resolution of the computational grid. Transport, dispersion, and deposition calculations are made at points in the computational grid. A finer computational resolution allows for more precision in these calculations. Therefore, the author chose a meteorological and computational grid resolution equal to 10 km (6 miles) because this close spacing increases precision in model estimates. A grid resolution of 20, 40 or 50 km (12, 25, or 30 miles) would have lowered the size of the meteorological files created by MESOPAC and speeded up MESOPUFF runs; however, degradation of model precision in transport and dispersion calculations at these lower resolutions was undesirable for the purpose of this study.

3.2.4 Land Use/Land Cover Data

Roughness lengths associated with specific land use/land cover categories are used by MESOPAC to calculate meteorological parameters at each grid point (e.g., mixing height and friction velocity). Additionally, MESOPUFF uses land use data to calculate dry deposition flux. Land use data for the East Tennessee River watershed were obtained from maps constructed by the Tennessee Valley Authority using 30 m (100 ft) resolution Landsat satellite imagery (Yankee, 1995). Table 3.2 shows the land use category read from the Landsat map and the corresponding land uses category number, and roughness height used by MESOPAC.

Portions of the East Tennessee modeling domain extend beyond the limits of the East Tennessee River Valley (i.e, the Cumberland Plateau west and north of Crossville, and western North Carolina). Land use/land cover data were not available on the TVA maps for those areas

Table 3.2. Land use/land cover data categories used in Tennessee Valley Authority (TVA) maps made using Landsat satellite imagery to corresponding categories and roughness lengths used by MESOPAC/MESOPUFF

Land use/land cover category			
TVA Landsat data	MESOPAC/MESOPUFF	Category number	Roughness length (m)
Pasture	Cropland and pasture	1	0.20
Agriculture	Irrigated crops	1	0.05
Deciduous forest	Ungrazed forest and woodland	5	1.00
Coniferous forest	Ungrazed forest and woodland	5	1.00
Forested wetland	Swamp	9	0.20
Scrub or shrub	Desert scrub land	8	0.30
Open water	Lake or ocean	12	1×10^{-4}
Urban	Metropolitan city	11	1.00

outside of the East Tennessee River Valley. The author conducted a sensitivity study to determine the effects of filling missing data with different land use/land cover types. MESOPUFF runs were made with meteorological fields created using missing data filled with a high roughness land use category (ungrazed forest and woodland with a 1 m roughness length) and compared to runs made with meteorological fields created using missing data filled with a low roughness land use category (crop land and pasture with a 0.2 m roughness length). There was virtually no difference in the results. Therefore, missing land use data were filled assuming a land use category corresponding to a high roughness length (ungrazed forest and woodland) because this is a predominant land use/land cover category in the domain.

3.3 IMPLEMENTING MESOPAC

MESOPAC calculates wind fields at two levels, referred to as the lower and upper layer, in which the lower layer represents flow in the planetary boundary layer and the upper layer represents flow above the planetary boundary layer (Scire et. al 1984). The turbulent nature of the planetary boundary layer readily leads to the uniform mixing of pollutant emissions, and because of this, is often referred to as the mixing layer. For the remainder of this report, the term mixing layer is used for the lower planetary boundary layer.

The lower layer wind field is created by MESOPAC using hourly surface and twice-daily rawinsonde data measured at sites in or near the modeling domain. The model calculates an average wind speed and direction for the mixing layer at each point in the meteorological grid using the following five-step procedure adapted from Draxler (1979), as reported in the MESOPUFF user's manual (EPA 1995f).

1. A representative rawinsonde sounding [00 or 12 Greenwich Mean Time (GMT)] is selected based upon the stability class at the nearest surface station to the grid point and the time of day. Neutral/unstable and stable classes are assumed to be represented by the 00 GMT and 12 GMT soundings, respectively.

2. Using the sounding selected in Step (1), vertically averaged u (easterly) and v (northerly) wind components are computed throughout the layer from the surface to the mixing height calculated at that grid point.

3. The ratio, R, of the layer-averaged wind speed to the surface wind speed *at the rawinsonde station*, and the angular difference in wind direction, $\Delta\theta$, between the layer averaged and surface wind *at the rawinsonde station* are calculated.

4. The hourly surface wind data are used to calculate spatially interpolated surface wind components (u_s, v_s) at each grid point. The u (easterly wind component) and v (northerly wind component) data from k surface stations within a user-specified "scan-radius" of the grid point are used to compute (u_s, v_s) according to:

$$(u_s,v_s)_{ij} = \frac{\sum \frac{\alpha_s}{r_s^2} \cdot (u_k,v_k)}{\sum \frac{\alpha_s}{r_s^2}} \qquad (3.1)$$

where, u_s, v_s are the easterly and northerly components of the surface wind at grid point *(i,j)*, u_k, v_k are the easterly and northerly components of the surface wind at surface station k, r_s is

the distance from the surface station to grid point *(i,j)*, and α_s is the alignment weighting factor described by:.

$$\alpha_s = 1 - 0.5|\sin\phi_s| \tag{3.2}$$

where, ϕ_s is the angle between the observed wind direction and the line from the surface station to the grid point. Alignment weighting gives observations directly upwind and downwind from the grid point the greatest weight. This is consistent with empirical observations where isotach lines (lines of constant wind speed) tend to be elongated in the direction of flow (Draxler, 1979). For equal values of r_s, alignment weighting causes winds at a station directly upwind or downwind of a grid point to be weighted twice as heavily as winds for a station at right angles to the wind with respect to the grid point.

5. The mixed-layer averaged wind at the grid point is calculated by multiplying the surface wind speed at the grid point computed in Step (4) by the wind speed ratio, *R*, at the *nearest* rawinsonde site. Similarly, the surface wind direction is adjusted by the wind direction factor, $\Delta\theta$.

The above method was modified to create wind fields that are more representative of flow in the East Tennessee Valley. Specifically, the author adjusted the way in which mixed-layer average wind direction and speed are calculated as described in the following section.

3.3.1 Wind Direction in the East Tennessee Modeling Domain

Surface winds are strongly affected by frictional forces that occur as air flows over terrain. Friction tends to deflect the wind across isobars toward areas of low pressure. With increasing

height above the surface, frictional forces decrease and winds reach a state of equilibrium between the Coriolis force (induced by the earth's rotation) and the pressure gradient force (induced by variations in air pressure over the earth's surface). The state of equilibrium between these two forces is called geostrophic balance and winds generated by this balance are called geostrophic winds. Geostrophic winds flow parallel to isobars. Upper atmospheric winds are typically geostrophic and as height increases from the surface to the level of geostrophic winds, direction will shift in a clockwise motion (i.e., opposite to the Northern Hemisphere's rotation).

Generally, frictional forces on the wind flow are greater with more rugged terrain and geostrophic balance is reached at a greater height above the surface. The East Tennessee Valley, although broad [averaging about 70 km (45 miles)], is "corrugated" by parallel ridges that rise 50-150 m (160-480 ft) above the valley floor at intervals of 2-3 km (1-2 miles) (Whiteman and Doran, 1993). The overall effect of this parallel ridge system is to increase the surface roughness appreciably from that due to vegetative elements (e.g., trees). Roughness can be estimated as one-tenth the average height of protuberances in an area; therefore, the roughness of the valley is about 10 m (30 ft). This high roughness leads to increased friction, and subsequently, a higher altitude is attained before geostrophic winds occur. The rawinsonde stations are not located in the valley and lie in regions where the roughness height is, at maximum, about 1 m (3 ft). Wind direction at these sites would shift clockwise more rapidly because geostrophic winds would occur at much lower altitudes than would be expected in the East Tennessee Valley. Therefore, $\Delta\theta$ calculated using these sites would be too great for the East Tennessee Valley region.

The question then arises as to how wind direction shifts as it increases with height in the Tennessee Valley. A report detailing a comprehensive meteorological data collection effort in Eastern Tennessee during the late 1940s and early 1950s, concluded that winds from the surface to at least 500 m (1640 ft) above ground level flow predominately up and down the southwest-

northeast axis of the East Tennessee Valley (ORO, 1953). During the summer and fall seasons, mountain-valley temperature gradients cause the wind to flow up-valley during the day and down-valley at night. Up-valley winds are predominant in the spring because this is the direction of the general circulation pattern in the region. During winter, winds flow up- and down-valley during clear and cold weather associated with high pressure systems, but winds are more variable when cyclonic systems that frequently traverse the valley dominate the flow system (ORO, 1953).

Unpublished data collected by the National Oceanic and Atmospheric Administration's (NOAA's) Atmospheric Turbulence and Diffusion Division (ATDD) located in Oak Ridge, Tennessee confirm the conclusions of the earlier study. Surface and upper-air data collected by ATDD at sites in the Cumberland Mountains, Oak Ridge Tennessee, and the Great Smoky Mountains show that wind flow up to the top of the mixed layer is generally along the valley axis (Pendergrass, 1995).

A study conducted by Whiteman and Doran (1993) showed that winds typically move up or down the axis of the East Tennessee Valley. The depth of the within-valley winds is defined by the height of the Cumberland Mountains which rise about 700 m to the north and west of the valley, and the Great Smoky Mountains, which rise as high as 1700 m above the valley floor. Whiteman and Doran state that winds flow along the valley axis primarily because of "pressure-driven channeling," in which the winds in the valley are driven by the component of the geostrophic pressure gradient along the valley's length. Pressure-driven channeling is similar to forced channeling winds (those winds directed by the valley sidewalls), because for both mechanisms, winds blow predominately along the valley axis. However, in forced channeling, sudden changes in wind direction occur when geostrophic winds shift across a line normal to the valley axis. In pressure-driven channeling, shifts in the pressure gradient in the valley axis cause the wind to change 90 degrees out of phase compared to forced channeling shifts. In pressure-driven channeling, winds can blow directly

opposite of above-valley winds (e.g., winds *in the valley* may blow from the southwest when winds *aloft* are from the northeast). Whiteman and Doran call these valley winds "countercurrents" and cite similar studies by Wippermann and Gross (1981), Wippermann (1984), and Gross and Wippermann (1987) that discuss countercurrent development in the terrain such as the East Tennessee Valley due to pressure-driven channeling.

Based on the findings of ORO (1953) and Whiteman and Doran (1993), and data collected by the ATDD, the author fixed the value of $\Delta\theta$ in Equation 3.1 to 1. By setting $\Delta\theta$ equal to 1, the direction of the lower-layer wind field is based solely on the surface stations which are representative of along-valley axis flow found in the East Tennessee Valley and are not influenced in any way by rawinsonde data. For the purposes of this study, Step 4 (as detailed above) is the only step used in determining wind direction at each point in the meteorological grid.

3.3.2 Smoothing of Wind Speeds

The mixed-layer average wind speed is calculated by multiplying the surface wind speed at a particular grid point by the wind speed ratio, R, determined for the *nearest* rawinsonde site. Values of R can vary largely between rawinsonde stations and this may lead to sharp discontinuities in calculated wind field speed. These discontinuities occur at adjacent grid points where the nearest rawinsonde station shifts from one site to another. Fig. 3.3 shows a MESOPAC generated wind field with sharp discontinuities in wind speed between adjacent grid points, where the lengths of the arrows on the figure indicate the magnitude of the relative wind speed. The longer arrows at the top (north) and right (east) indicate grid points that are under the influence of data collected at Huntington Tri-State Airport and Greensboro High Point/Winston-Salem Airport, respectively,

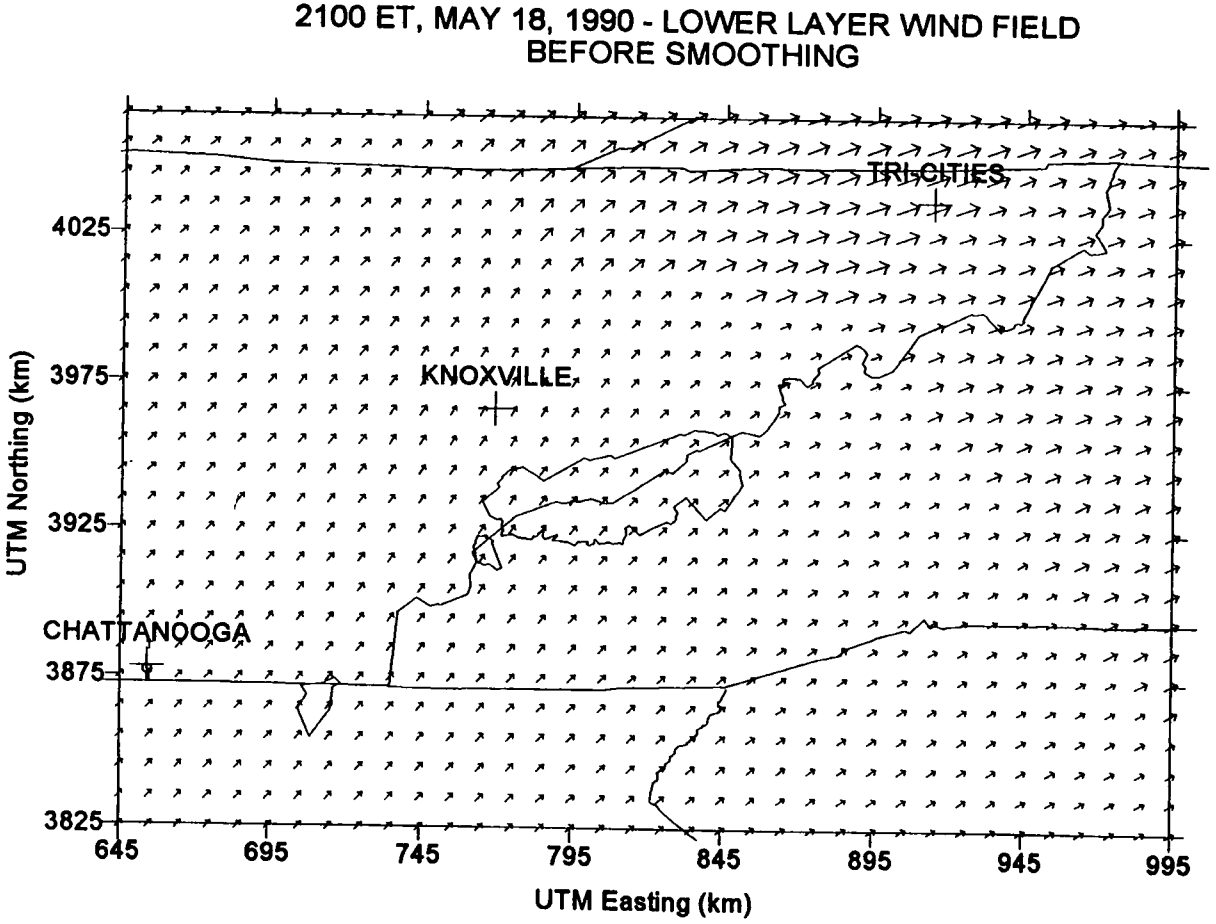

Fig. 3.3. Lower-layer wind field generated using MESOPAC II for 2100 ET, May 18, 1990 before smoothing routine was implemented.

where wind speeds in the upper atmosphere are relatively large. The shorter arrows in the left, middle, and bottom of the figure indicate grid points that are under the influence of data collected at Nashville Metropolitan Airport and Athens Municipal Airport, respectively, where wind speeds are relatively low. Definite boundaries are seen where an arrow at one grid point is small and at an adjacent point is large. Such boundaries are not representative of wind speeds in East Tennessee, but occur because of the way that MESOPAC applies a singular *R* value to a specific grid point.

For this study, wind speeds were smoothed by applying a weighted-sum *R* value that varies with each grid point. Weighting factors for each grid point were based on the inverse-squared distance of the grid point *(i,j)* to each rawinsonde station using the following equation:

$$\beta_k = \frac{\frac{1}{r_k^2}}{\sum \frac{1}{r_k^2}} \tag{3.3}$$

where, β_k is the weighting factor for rawinsonde station k (the value of k varies from one to four because there were four rawinsonde stations used in the study) and r_k is the distance from the grid point (i,j) to rawinsonde station k. The weighted-sum *R* value for each grid point (i,j) is calculated as:

$$R_{ws(i,j)} = \sum \beta_k R_K \tag{3.4}$$

where, $R_{ws(i,j)}$ is the weighted-sum *R* value for each grid point (i,j), R_k is the R value calculated at rawinsonde station k using Step 3 as described above. By using $R_{ws(i,j)}$, wind speeds are smoothed in the lower-layer. This wind field shown in Fig. 3.4 represents the flow at the same hour and

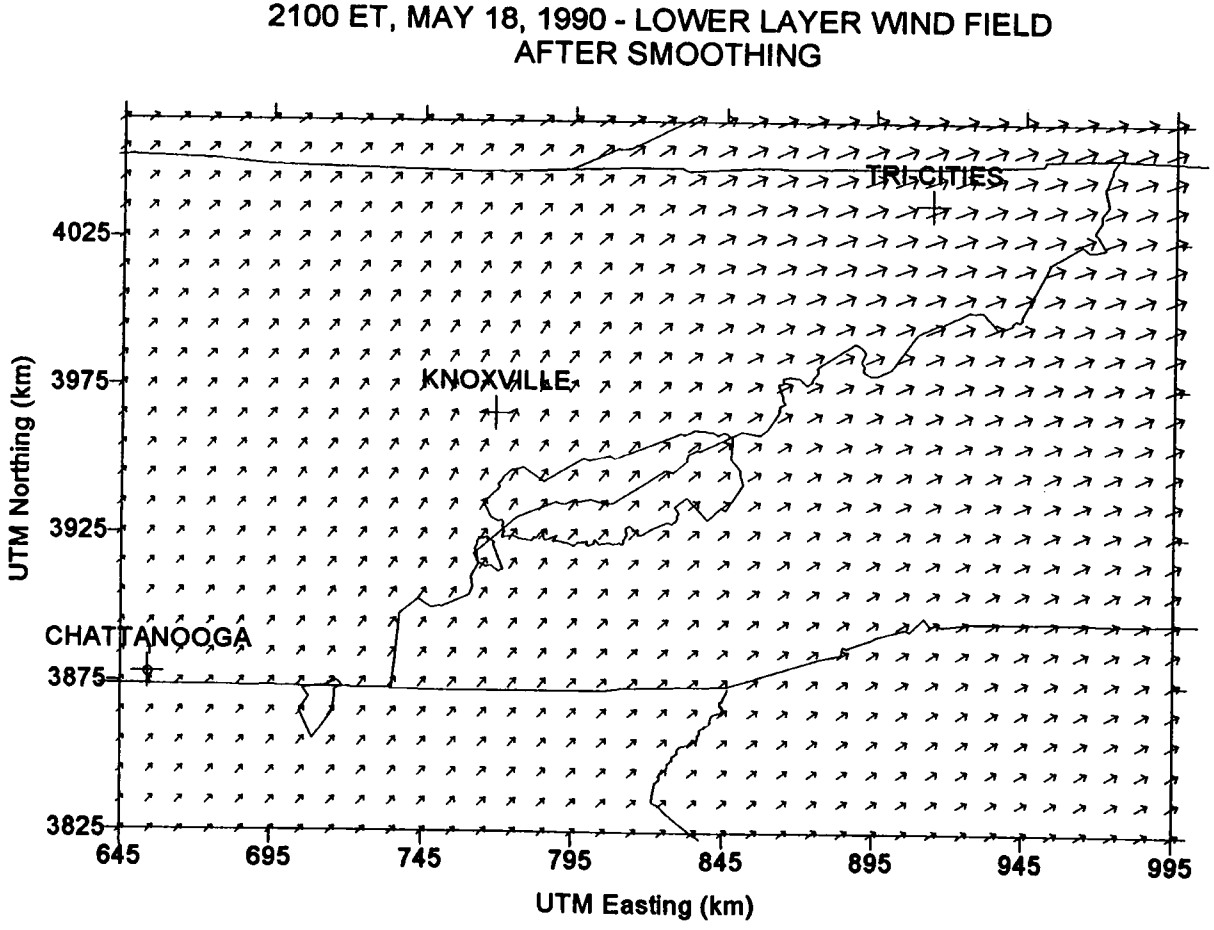

Fig. 3.4. Lower-layer wind field generated using MESOPAC II for 2100 ET, May 18, 1990 after smoothing routine was implemented.

time as Fig. 3.3, but with smoothed wind speeds. Note that in Fig. 3.4, there are no discontinuities in wind speed between adjacent grid points.

For this study, the upper-layer wind field extends from the top of the mixing layer, to the 700 mb height as recommended by EPA (1993). MESOPAC constructs the upper-layer wind field using Equation 3.1, with the summation over rawinsonde stations instead of surface stations. No modifications were made to upper-layer wind field calculations for this study. Beside calculating winds, MESOPAC calculates mixing heights, surface friction velocities, surface Pasquill-Gifford stability categories, and surface temperatures at each grid point. As with upper-layer winds, no modifications were made in the way that MESOPAC calculates these parameters.

3.4 DEVELOPMENT OF HYPOTHETICAL EMISSION SOURCES

Baseline scenarios were developed to determine the impact on Class I areas in the East Tennessee modeling domain from a hypothetical point source emitting 28.8 g/s (1000 tpy) of SO_2 and NO_x located at four different sites in the domain. The four locations selected were: (1) Knoxville/McGhee Tyson Airport, (2) Chattanooga/Lovell Field, (3) Bristol/Tri-Cities Airport, and (4) Crossville. The first three are located at the sites of the surface meteorological stations, which are also the largest urban areas in the modeling domain. These sites represent likely locations of future point sources constructed in the modeling domain. The last location, Crossville, is an urban area at the western edge of the modeling domain.

Emission and stack parameters are shown in Table 3.3 for a baseline scenario source. The hypothetical sources have emissions similar to a large industrial point source (28.8 g/s of SO_2 and NO_x) at a continuous level throughout the entire year of 1990 (the year represented by the meteorological data, which was selected to be consistent with a parallel study concerning ozone modeling). The height of the stack was set at 65 m (210 ft), because this is the maximum height

Table 3.3. Emission and stack exit parameters of a hypothetical baseline scenario sources to be used in the SO_2 and NO_x Modeling Study Performed as part of the Development and Demonstration of Modeling Protocols for East Tennessee

Parameter	Value
SO_2 emission rate	28.8 g/s (1000 tpy)
NO_x emission rate	28.8 g/s (1000 tpy)
Stack height	65 m (210 ft)
Stack exit temperature	273 K (32°F)
Stack exit velocity	0.1 m/s (20 fpm)
Stack exit diameter	0.1 m (0.3 ft)

allowed by the EPA for modeling studies from sources that are not affected by building downwash (EPA 1987). Stack exit parameters were set to virtually eliminate buoyant plume rise so as to keep puff centers equal to the stack height. Major new sources would likely have stack heights and exit parameters that would result in a final puff center height greater than 65 m. Therefore, by limiting the puff center height to 65 m, deposition fluxes and pollutant concentrations at the Class I areas are maximized providing an upper bound estimate of impacts. The steps used to run MESOPUFF and associated postprocessors for the baseline scenarios are detailed in Appendix A.

Two sensitivity scenarios were developed as comparisons to the baseline scenarios. Hypothetical emission sources at the four locations with stack heights of 200 m (660 ft) were used to show the sensitivity of stack heights on results. The time period of comparison was for August 1990 because that month had the highest deposition and atmospheric concentration values. Sensitivity of results relative to emission rates was also determined by comparing emission rates of 2.88 g/s (100 tpy) and 288 g/s (10,000 tpy) at the four locations to baseline scenarios. The time

period of the emission rate sensitivity runs was also August 1990. All modeling results, including those of sensitivity studies, are discussed in Chapter 4.

4. MODELING RESULTS

4.1 INTRODUCTION

This section discusses the results of the modeling analysis performed for the four baseline and two sensitivity scenarios. The discussion on the baseline scenario is divided into four parts: the first part (Sect. 4.2.1) discusses the pollutant mass balance; the second part (Sect. 4.2.2) focuses on the monthly variations in deposition over the entire modeling domain; the third part (Sect. 4.2.3) details maximum annual deposition estimated to occur in the target Class I areas (i.e., Great Smoky Mountains National Park, and Joyce Kilmer and Cohutta Wilderness Areas); and the fourth part (Sect. 4.2.4) discusses maximum concentration values estimated in the target Class I areas. The sensitivity scenarios are discussed in Section 4.3, specifically, the effects of varying emission rate and puff height on maximum deposition values estimated for the Class I areas. Section 4.4 discusses the development of deposition potential maps to be used as tools in estimating impacts on the target Class I areas from a source located anywhere in the modeling domain.

4.2 BASELINE SCENARIO RESULTS

The baseline scenarios were run to show the variations in pollutant transport, dispersion and deposition from a hypothetical source positioned at each of four locations in the East Tennessee modeling domain. The four sites chosen were: (1) Knoxville/Tyson McGhee Airport, (2) Bristol/Tri Cities Airport, (3) Chattanooga/Lovell Field, and (4) Crossville. MESOPUFF runs were made for each hypothetical source location separately (i.e., estimated concentrations and deposition values result from only one point source).

4.2.1 Mass Balance

The mass of sulfur and nitrogen deposited over the modeling domain resulting from the four hypothetical source locations is shown in Table 4.1. For each chemical species [i.e., SO_2 and SO_4^{2-} resulting from SO_2 emissions, and NO_x, HNO_3, and NO_3^- resulting from NO_x ($NO + NO_2$) emissions], wet and dry annual deposition values were calculated using monthly MESOPUFF output. From these calculations, annual sulfur deposition (in both wet and dry form), D_S (in units of kg/ha), was determined using the following equation:

$$D_S = \frac{MW_S}{MW_{SO_2}} D_{SO_2} + \frac{MW_S}{MW_{SO_4^{2-}}} D_{SO_4^{2-}} \tag{4.1}$$

where: MW_S is the molecular weight of sulfur (32.07 g/g-mol), MW_{SO_2} is the molecular weight of SO_2 (64.07 g/g-mol), D_{SO_2} is the average annual SO_2 deposition (kg/ha) over the modeling domain, $MW_{SO_4^{2-}}$ is the molecular weight of SO_4^{2-} (96.06 g/g-mol), and $D_{SO_4^{2-}}$ is the average annual SO_4^{2-} deposition (kg/ha) over the modeling domain. Similarly, both wet and dry annual nitrogen deposition values, D_N (kg/ha), were calculated using the following equation:

$$D_N = \frac{MW_N}{MW_{NO_2}} D_{NO_2} + \frac{MW_N}{MW_{HNO_3}} D_{HNO_3} + \frac{MW_N}{MW_{NO_3^-}} D_{NO_3^-} \tag{4.2}$$

where: MW_N is the molecular weight of nitrogen (14.01 g/g-mol), MW_{NO_2} is the molecular weight of NO_2 (46.01 g/g-mol), D_{NO_2} is the average annual NO_2 deposition (kg/ha) over the domain (approximated as being equal to the maximum annual NO_x deposition), MW_{HNO_3} is the molecular weight of HNO_3 (63.01 g/g-mol), D_{HNO_3} is the average annual HNO_3 deposition (kg/ha) over the domain, $MW_{NO_3^-}$ is the molecular weight of NO_3^- (62.01 g/g-mol), and $D_{NO_3^-}$ is the average annual NO_3^- deposition (kg/ha). Approximating NO_x deposition

Table 4.1. Sulfur and nitrogen mass balance (percent of emitted pollutant that is deposited) from a hypothetical source located in the East Tennessee modeling domain

Site of hypothetical source	Average annual deposition (kg/ha) over the modeling domain estimated using the MESOPUFF II model		Total mass of sulfur deposited (kg) in the modeling domain[a]	Percent of emissions deposited in the modeling domain[b]
	Wet	Dry		
		sulfur		
Knoxville/McGhee Tyson Airport	1.3×10^{-3}	2.2×10^{-2}	1.7×10^{5}	38%
Bristol/ Tri Cities Airport	6.0×10^{-4}	1.2×10^{-2}	9.0×10^{4}	20%
Chattanooga/Lovell Field	7.8×10^{-4}	8.2×10^{-3}	6.6×10^{4}	14%
Crossville	8.2×10^{-4}	2.0×10^{-2}	1.5×10^{5}	33%
		nitrogen		
Knoxville/McGhee Tyson Airport	3.6×10^{-4}	6.2×10^{-3}	4.8×10^{4}	17%
Bristol/ Tri Cities Airport	1.5×10^{-4}	3.3×10^{-3}	2.5×10^{4}	9%
Chattanooga/Lovell Field	1.8×10^{-4}	2.6×10^{-3}	2.0×10^{4}	7%
Crossville	2.1×10^{-4}	5.7×10^{-3}	4.3×10^{4}	16%

[a]The total mass of pollutant deposited is equal to the sum of the wet and dry deposition times the area of the MESOPUFF II sampling domain (7.3×10^{6} ha).

[b]The mass of sulfur emitted is equal to the annual SO_2 emission rate [9.1×10^{5} kg (1000 tons)] times the ratio of the molecular weight of sulfur to the molecular weight of SO_2 (0.501). The mass of nitrogen emitted is equal to the annual NO_x emission rate [9.1×10^{5} kg (1000 tons)] times the ratio of the molecular weight of nitrogen to the molecular weight of NO_x (approximated to be completely NO_2) (0.305).

to be entirely in the form of NO_2 results in a slight under-prediction of nitrogen mass deposited, because a very small fraction of deposited NO_x will be NO.

The percent of pollutant emissions that was deposited in the modeling domain varied among the different source locations. Siting the hypothetical source at Knoxville/Tyson McGhee Airport resulted in the largest percentages of sulfur (38%) and nitrogen (17%) deposited because this location is in the middle of the domain. The percent of sulfur and nitrogen deposited for the Bristol/Tri Cities Airport or Chattanooga/Lovell Field sites where about half the amount of the Knoxville source because these source locations are on the northeast and southwest edge of the modeling domain, respectively. Bristol had a slightly larger percent of sulfur and nitrogen deposited than Chattanooga because annual deposition maxima occurred to the southwest of all source sites (i.e., in the direction of prevailing nighttime winds). With Chattanooga lying at the southwest corner of the domain, a larger pollutant mass was exported out of the domain. The percent mass deposited from the Crossville source site was only slightly lower than the Knoxville site even though Crossville lies much closer to the edge of the domain [about 40 km (25 miles) to the nearest domain boundary] than Knoxville [about 100 km (60 miles) to the nearest domain boundary] . This is because most of the pollutant mass is deposited within about 40 km (25 miles) of the source.

For all source locations, the mass of sulfur deposited is more than twice the amount of nitrogen deposited (e.g., 38% of sulfur deposited compared to 17% of nitrogen deposited for the Knoxville site). This is caused by the large amount of SO_2 that deposits within the modeling domain compared to NO_x and HNO_3. Deposition values of NO_3^- and SO_4^{2-} are approximately equal. Contour maps showing annual deposition over the modeling domain are found in Appendix B. Deposition of each species is discussed in more detail in the next section.

4.2.2 Monthly Variations

Contour maps of monthly total (wet + dry) deposition for each species are shown in Appendices C (SO_2), D (SO_4^{2-}), E (NO_x), F (HNO_3), and G (NO_3^-). These plots show the variations in deposition patterns caused by a hypothetical source emitting 28.8 g/s (1000 tpy) of SO_2 and NO_x positioned at the four site locations. For all source locations and most months, the deposition pattern is roughly elliptical in shape with the major axis aligned parallel to the axis of the East Tennessee Valley. This pattern results from the along-valley wind flow which occurs in East Tennessee and was simulated using MESOPAC (see Sect. 3.3.1). During the fall months, the deposition pattern is more circular reflecting the light and variable winds that occur most frequently during this season.

For all source locations and most months, maximum deposition of all species occurred about 15-30 km (9-19 miles) southwest of the source. These maxima were associated with nighttime winds, that generally flow down the East Tennessee Valley (i.e., southwest) at relatively low speeds under neutral or stable conditions (i.e., little atmospheric turbulence). Secondary, and occasionally tertiary, relative maxima associated with daytime winds are also evident, particularly for SO_4^{2-} and NO_3^- deposition. These relative maxima generally occur farther from the source and to the northeast during the summer and winter, and to the east-northeast during the spring and fall, reflecting wind patterns of those seasons. For each source location, contours are more loosely spaced in the northeast quadrant compared to tighter spacing in the southwest quadrant. Again, this demonstrates the up-valley flow with stronger daytime winds, less atmospheric stability and greater horizontal standard deviation of wind direction (σ_θ) distributing pollutants over a wider area and yielding lower deposition per unit area. At night, down-valley flow is light, atmospheric

stability is high, σ_θ is less and deposition per unit area is higher, thereby creating tighter spacing between contours.

Figures 4.1 through 4.4 show the maximum estimated deposition values over all grid points in the modeling domain estimated for each month in 1990 from each source location. Each figure contains five plots, one for each of the five pollutant species considered (note that the vertical scale is logarithmic). For all sources and species, the greatest deposition occurred during the summer months with most maxima occurring in August. Deposition is greatest in the summer because winds are generally lighter, which limits dispersion, increases deposition and inhibits resuspension. Production of SO_4^{2-} and NO_3^- is also greater during the summer because increased solar radiation enhances photochemical reactions forming more species that oxidize SO_2 and NO_x. Rainfall is most intense in the summer leading to increased wet deposition. Over the year, the range of maximum monthly deposition varies only by about one order of magnitude for each species.

The relative deposition values associated with each pollutant species are also similar for each source location. Of all the pollutant species, maximum SO_2 deposition is greatest ranging from 0.05 to 0.6 kg/ha. The range of deposition values of HNO_3 and NO_x are approximately one order of magnitude less than SO_2 (0.006 to 0.09 kg/ha), with the range of deposition values of NO_3^- and SO_4^{2-} approximately two orders of magnitude less than SO_2 (0.0002 to 0.02 kg/ha).

The reason for greater maximum SO_2 deposition is illustrated in Figs. 4.5 and 4.6. These figures show comparisons of annual average concentrations at every grid point in the modeling domain from the Knoxville source location. Figure 4.5 shows the sum of the annual average *concentration* of the two nitrogen species gases ($NO_x + HNO_3$), $C_{HNO3+NOx}$, versus the annual average concentration of SO_2, C_{SO2}, for every grid point. The linear, least squares regression

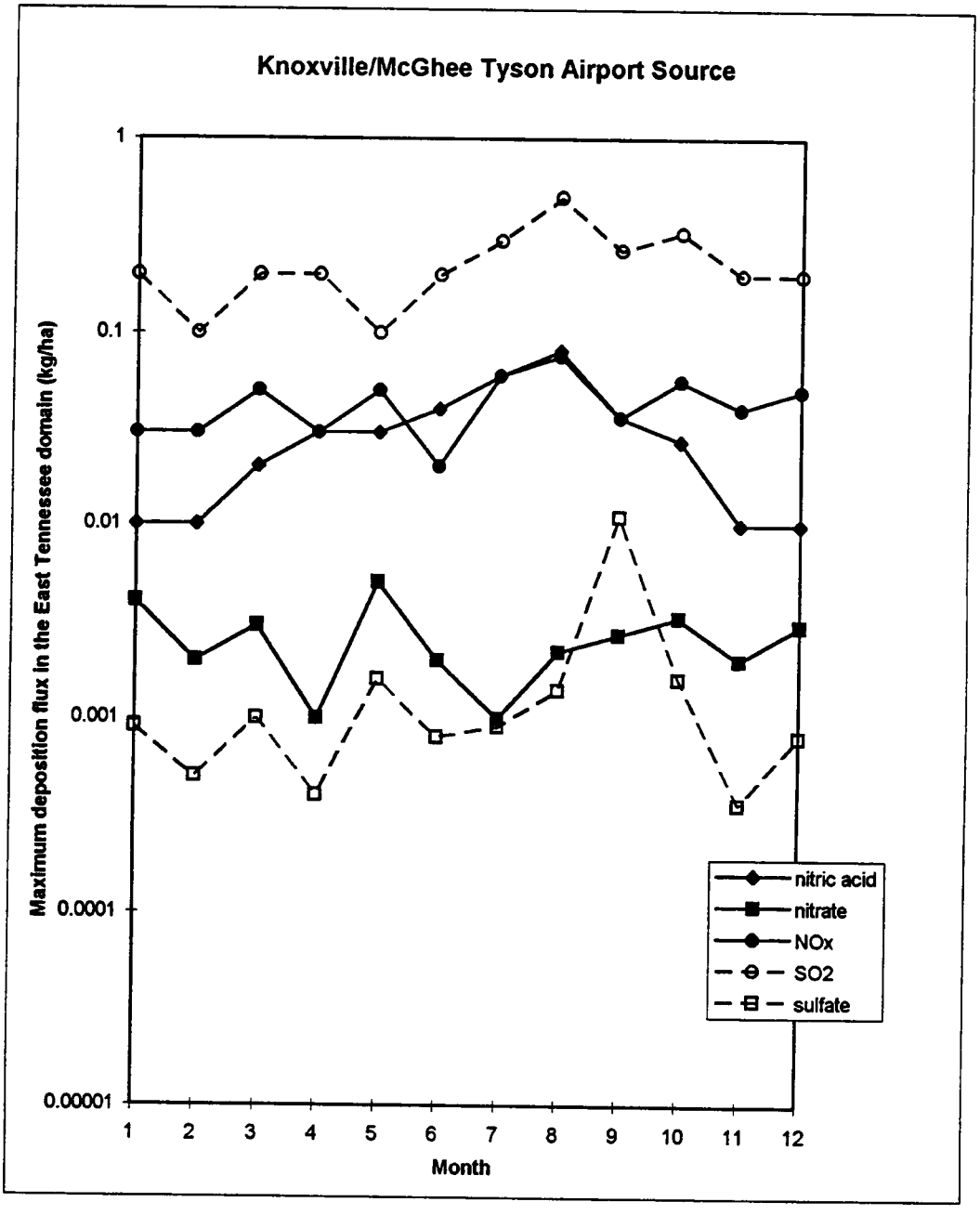

Fig. 4.1. Maximum monthly deposition (kg/ha) for five species estimated for 1990 from a hypothetical, 65 m (210 ft) tall point source located at Knoxville/McGhee Tyson Airport emitting 28.8 g/s (1000 tpy) each of SO_2 and NO_x.

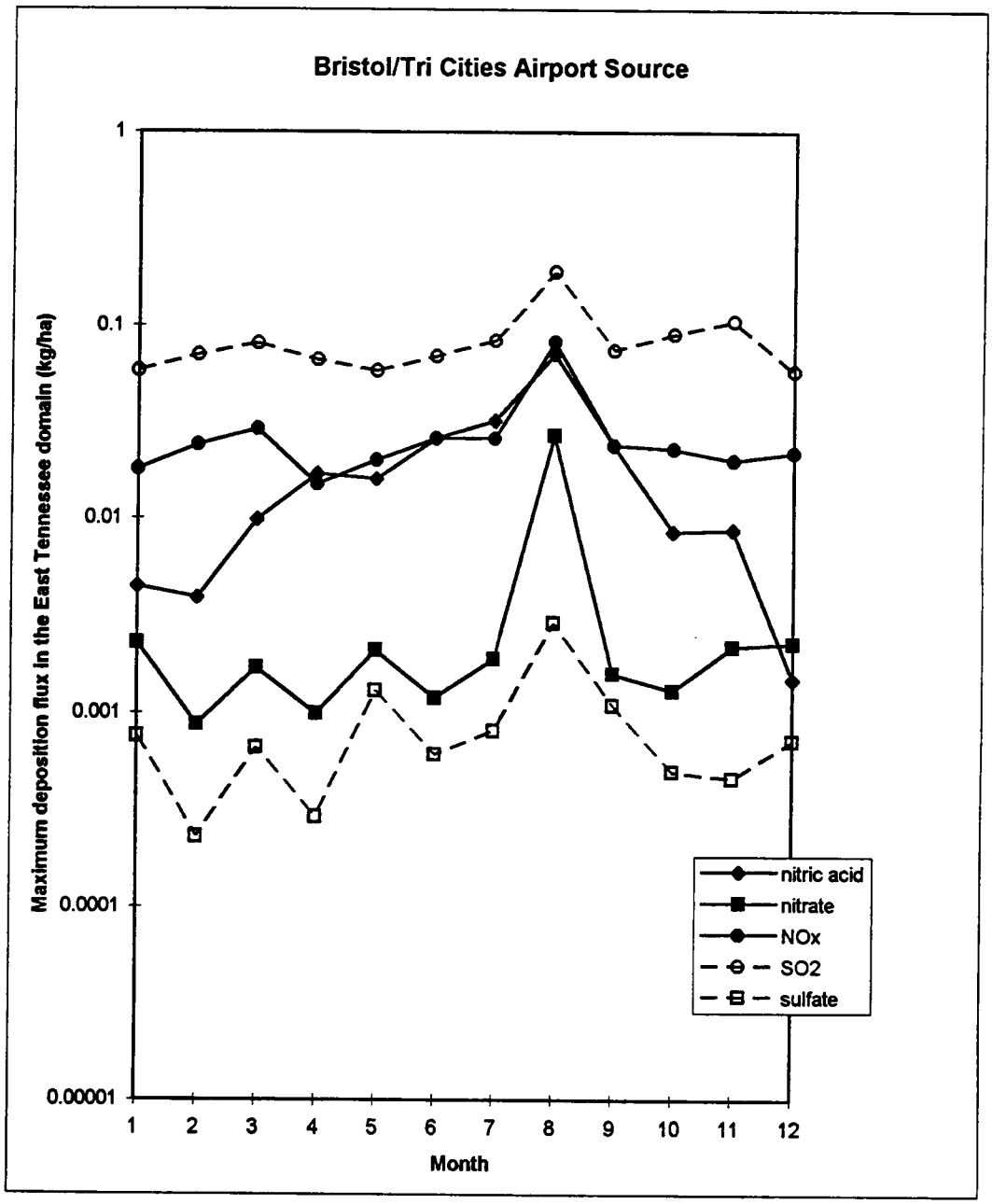

Fig. 4.2. Maximum monthly deposition (kg/ha) for five species estimated for 1990 from a hypothetical, 65 m (210 ft) tall point source located at Bristol/Tri Cities Airport emitting 28.8 g/s (1000 tpy) each of SO_2 and NO_x.

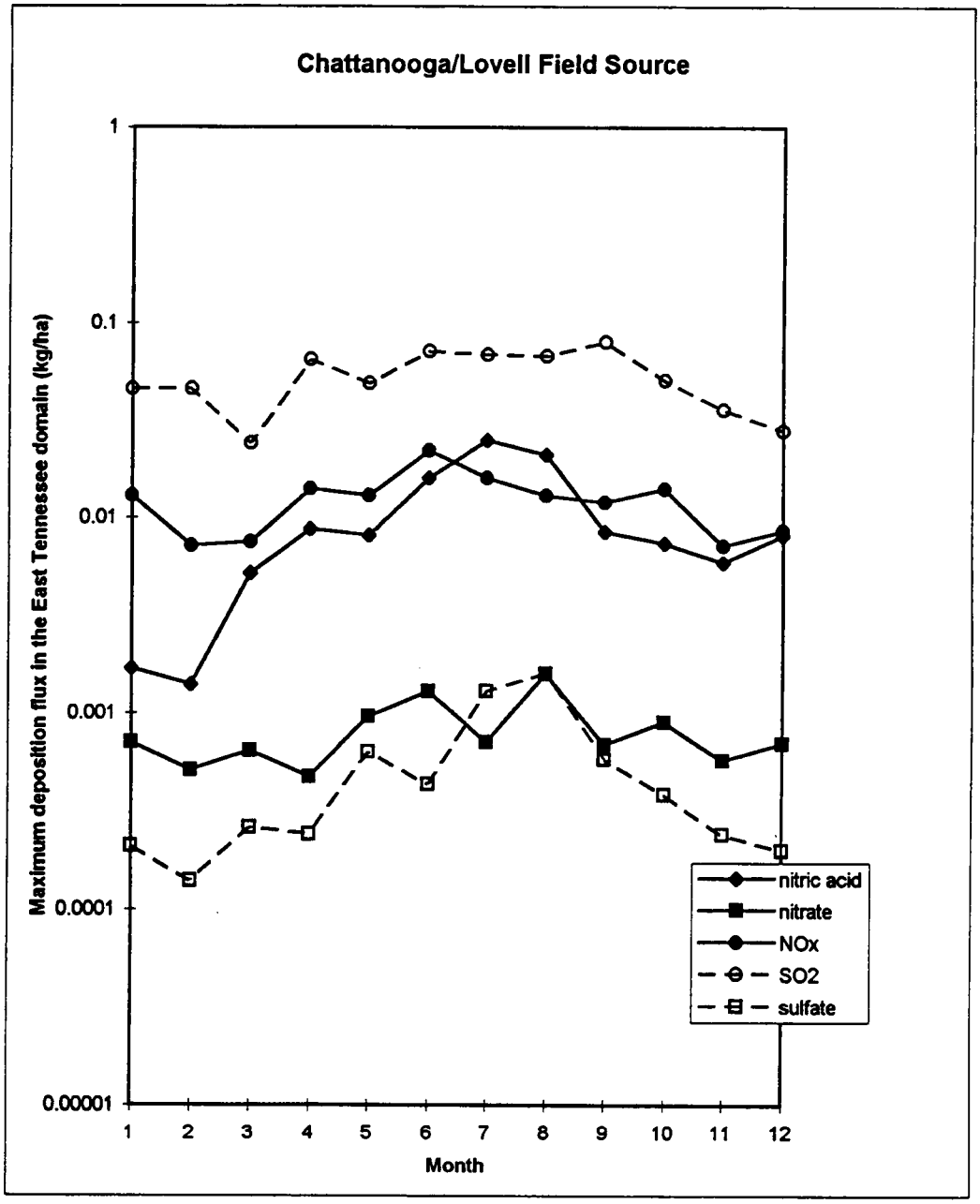

Fig. 4.3. Maximum monthly deposition (kg/ha) for five species estimated for 1990 from a hypothetical, 65 m (210 ft) tall point source located at Chattanooga/Lovell Field emitting 28.8 g/s (1000 tpy) each of SO_2 and NO_x.

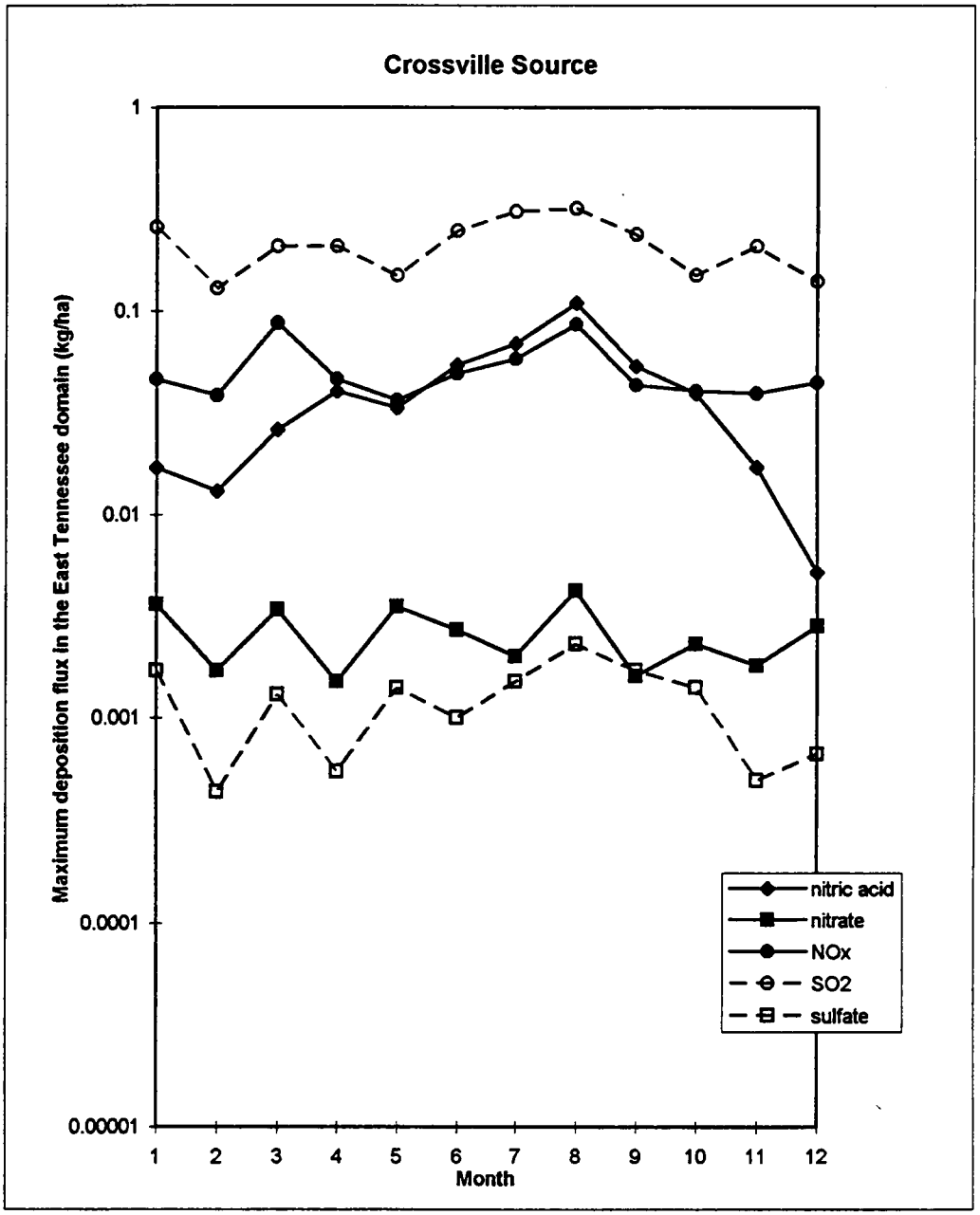

Fig. 4.4. Maximum monthly deposition (kg/ha) for five species estimated for 1990 from a hypothetical, 65 m (210 ft) tall point source located in Crossville emitting 28.8 g/s (1000 tpy) each of SO_2 and NO_x.

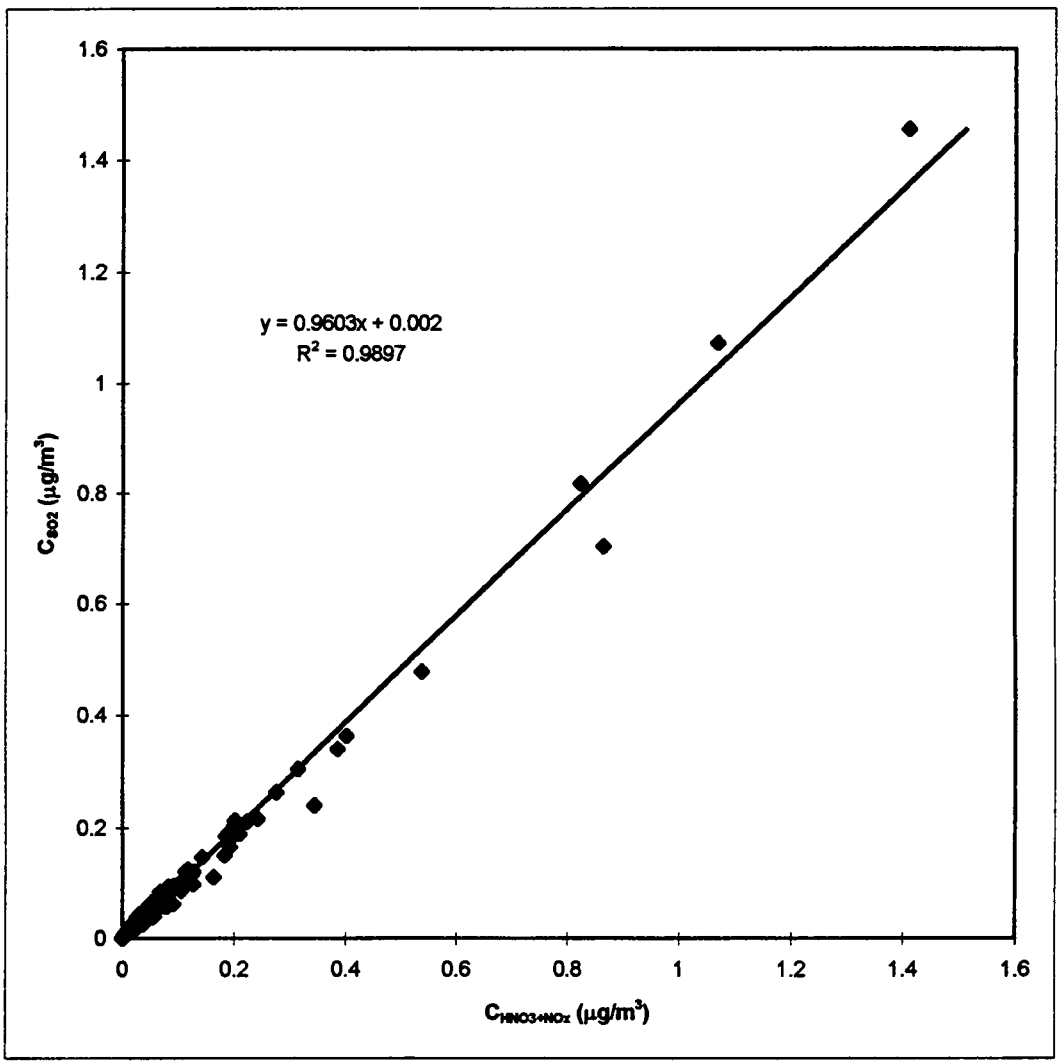

Fig. 4.5. Comparison of annual average (1990) concentrations from a hypothetical source located at Knoxville/Tyson McGhee Airport emitting 28.8 g/s (1000 tpy) each of SO_2 and NO_x. The plot shows the annual concentrations of the sum of nitrogen gas species (HNO_3 + NO_x) versus annual concentrations of SO_2 at every grid point in the East Tennessee modeling domain.

indicates that relationship between the two annual average concentrations is nearly one to one when all grid points in the modeling domain are considered. MESOPUFF quickly partitions NO_x emissions to HNO_3 and NO_x. Therefore, atmospheric concentrations of SO_2 are greater than NO_x. The model also allows SO_2 to deposit more readily than NO_x and HNO_3. These effects are shown in Fig. 4.6 where C_{SO2} is plotted versus the ratio of $C_{HNO3+NOx}$ to C_{SO2}. In Fig. 4.6, the higher concentrations (indicated by points on the right-hand side of the figure) are generally receptors located closer to the source. The points on the left of the graph show concentrations at receptors farthest from the source, where the concentration bias is clearly toward the nitrogen species. Because more of the SO_2 has deposited close to the source, SO_2 concentrations far from the source are less.

4.2.3 Maximum Annual Deposition Estimated for the Target Class I Areas

Figures 4.7 through 4.10 show the maximum annual deposition of sulfur (wet and dry) and nitrogen (wet and dry) in the target Class I areas resulting from the baseline hypothetical source at each of the four selected locations. Both wet and dry maximum annual sulfur deposition values were calculated using Equations 4.1 and 4.2. For all of the source locations, maximum deposition values occurred at receptors located on the boundary of the Class I area nearest the source.

The highest annual sulfur and nitrogen deposition values (both dry and wet) for the Great Smoky Mountains National Park were associated with siting the hypothetical source at Knoxville/McGhee Tyson Airport. The distance from the Knoxville source to the nearest boundary of the Great Smoky Mountains National Park is approximately 25 km (15 miles). This

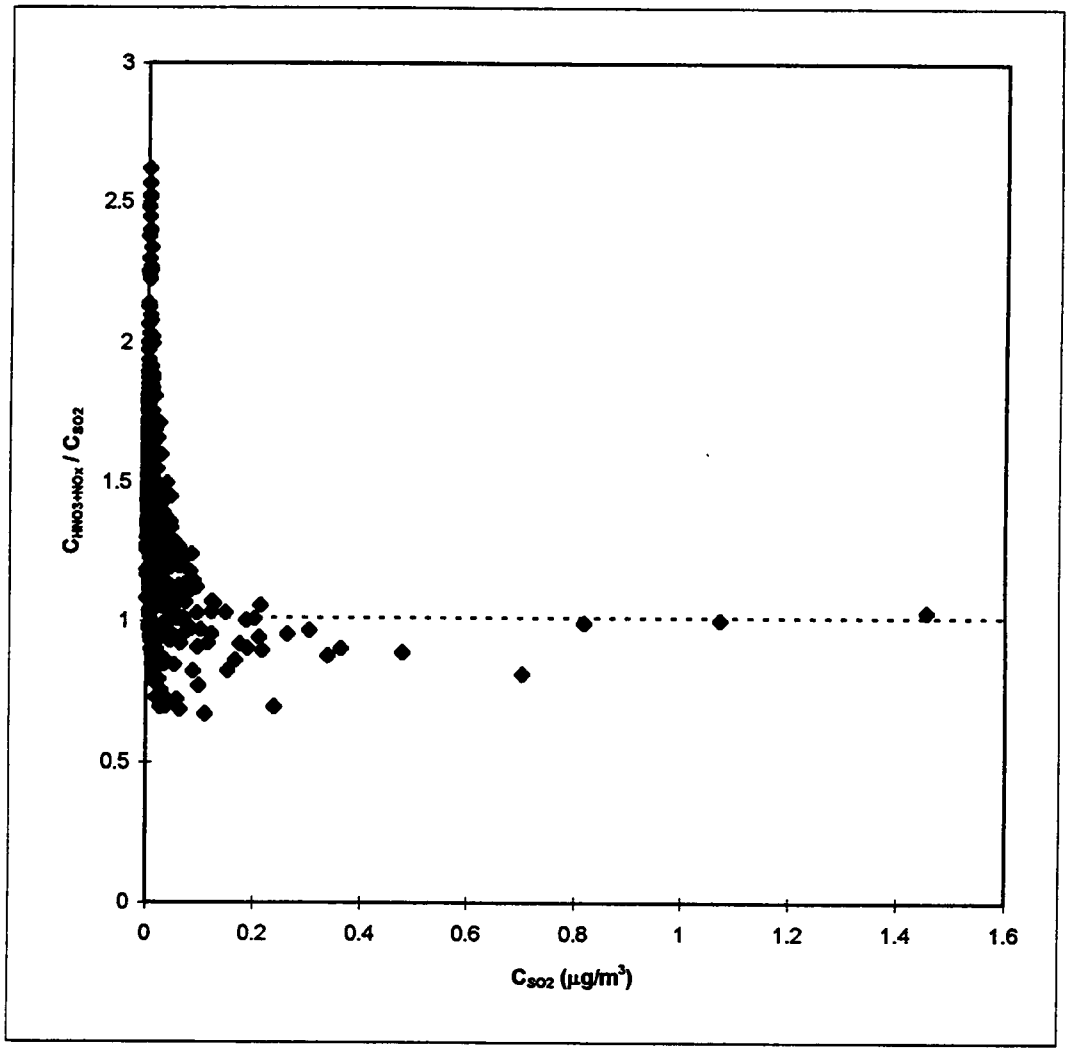

Fig. 4.6. Annual average (1990) SO_2 concentrations versus the ratio of the sum of nitrogen gas species (HNO_3 + NO_z) annual concentrations to SO_2 annual concentrations. Annual concentrations at every grid point in the East Tennessee modeling domain result from a hypothetical source located at Knoxville/Tyson McGhee Airport emitting 28.8 g/s (1000 tpy) each of SO_2 and NO_x.

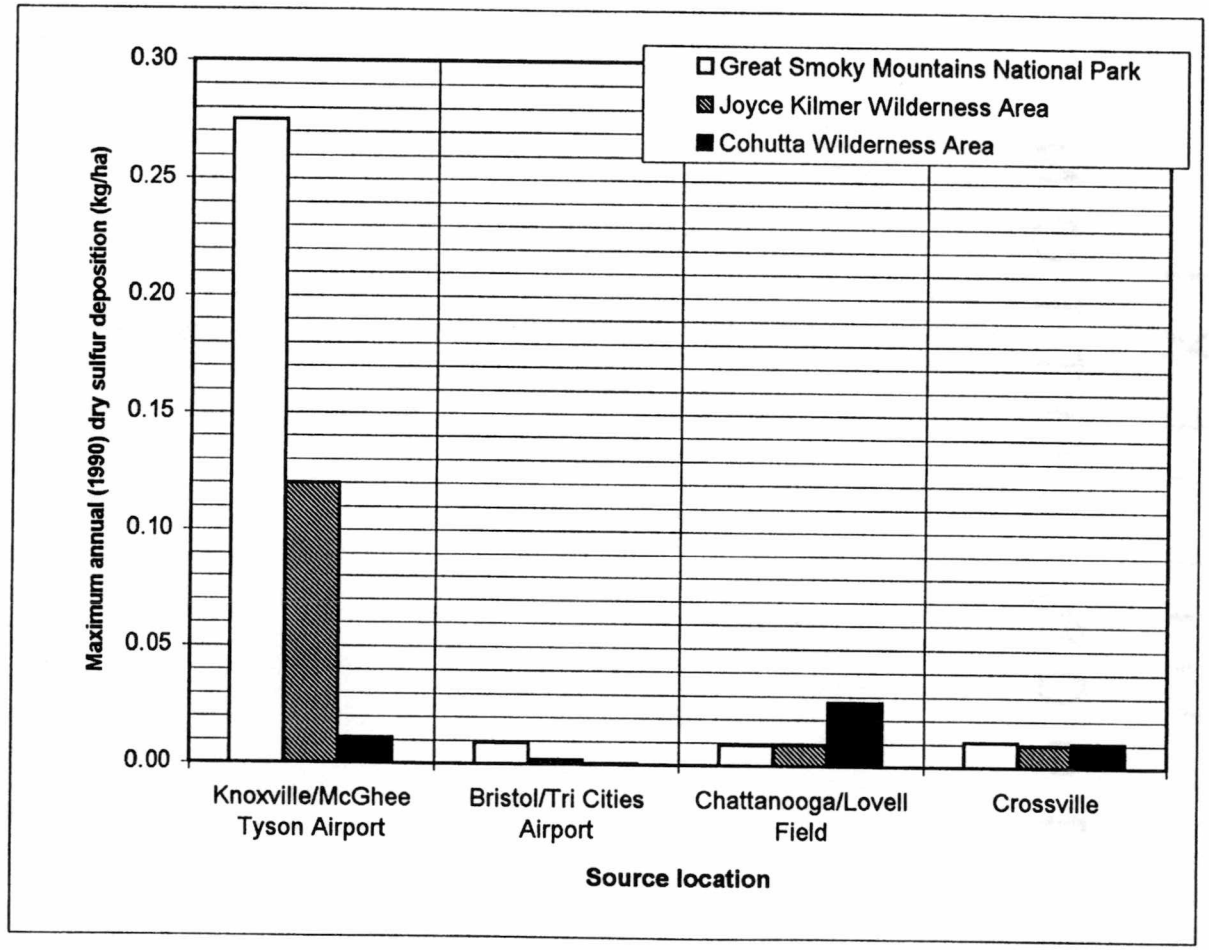

Fig. 4.7. Maximum annual dry sulfur deposition estimated for 1990 on Class I areas in the East Tennessee modeling domain from a 65 m (210 ft), 28.8 g/s (1000 tpy) SO_2 emission source.

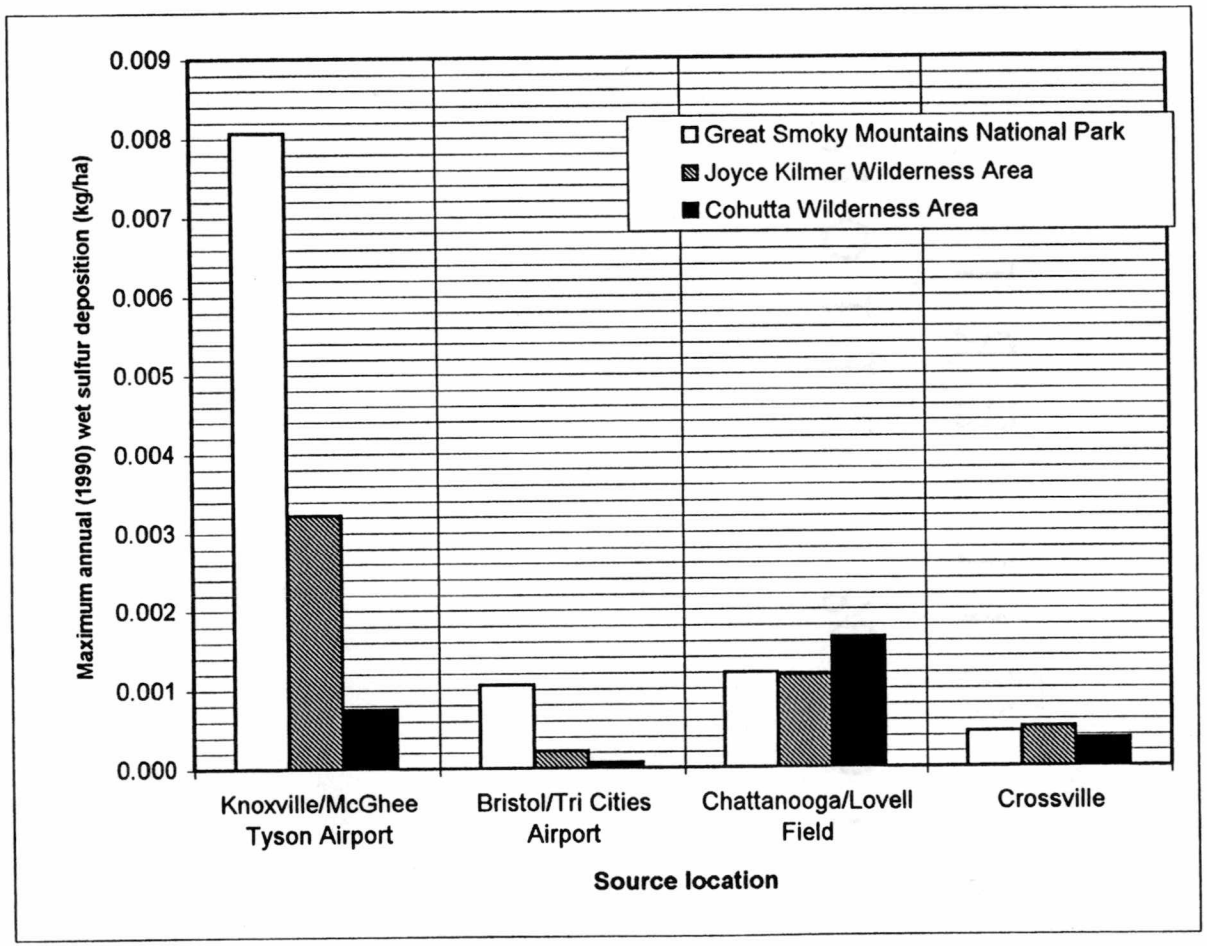

Fig. 4.8. Maximum annual wet sulfur deposition estimated for 1990 on Class I areas in the East Tennessee modeling domain from a 65 m (210 ft), 28.8 g/s (1000 tpy) SO_2 emission source.

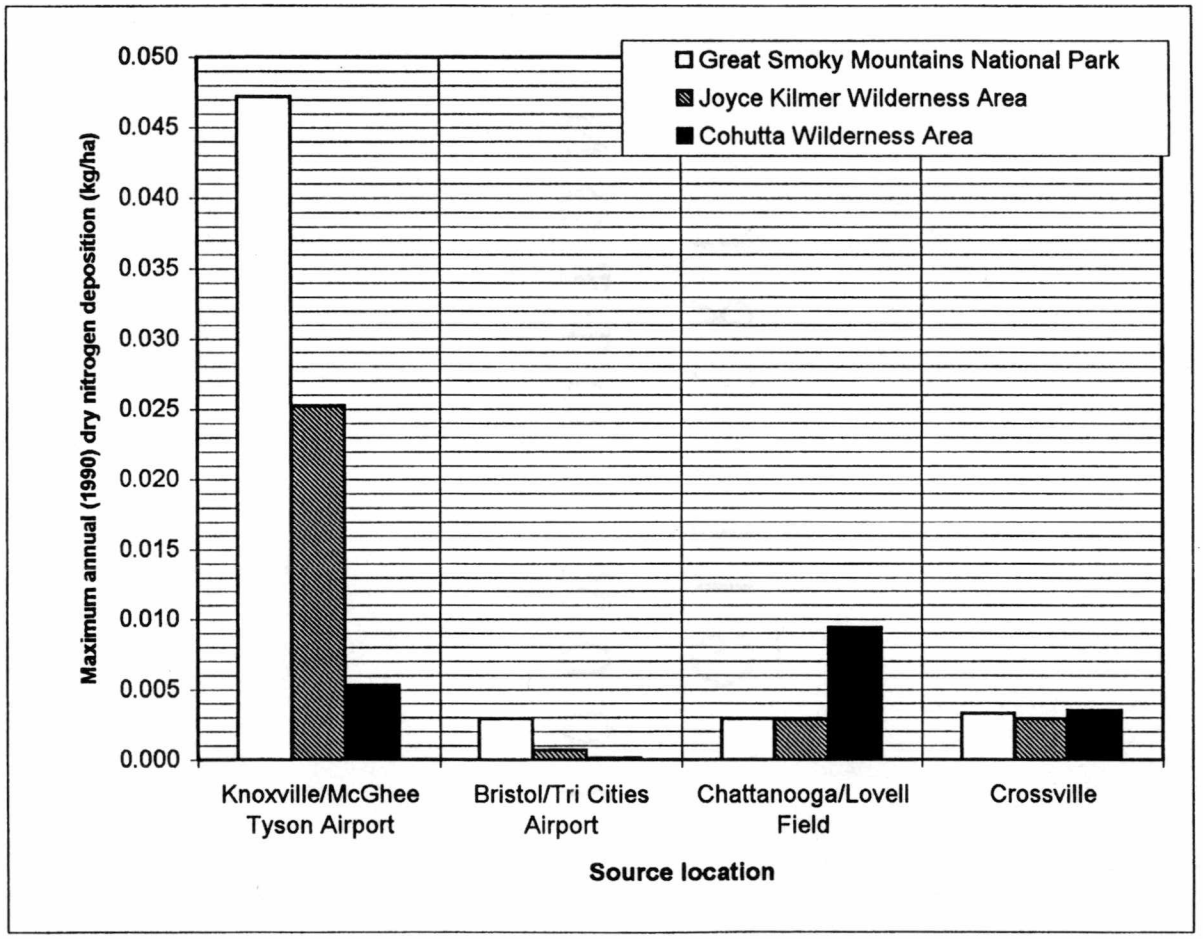

Fig. 4.9. Maximum annual dry nitrogen deposition estimated for 1990 on Class I areas in the East Tennessee modeling domain from a 65 m (210 ft), 28.8 g/s (1000 tpy) NO_x emission source.

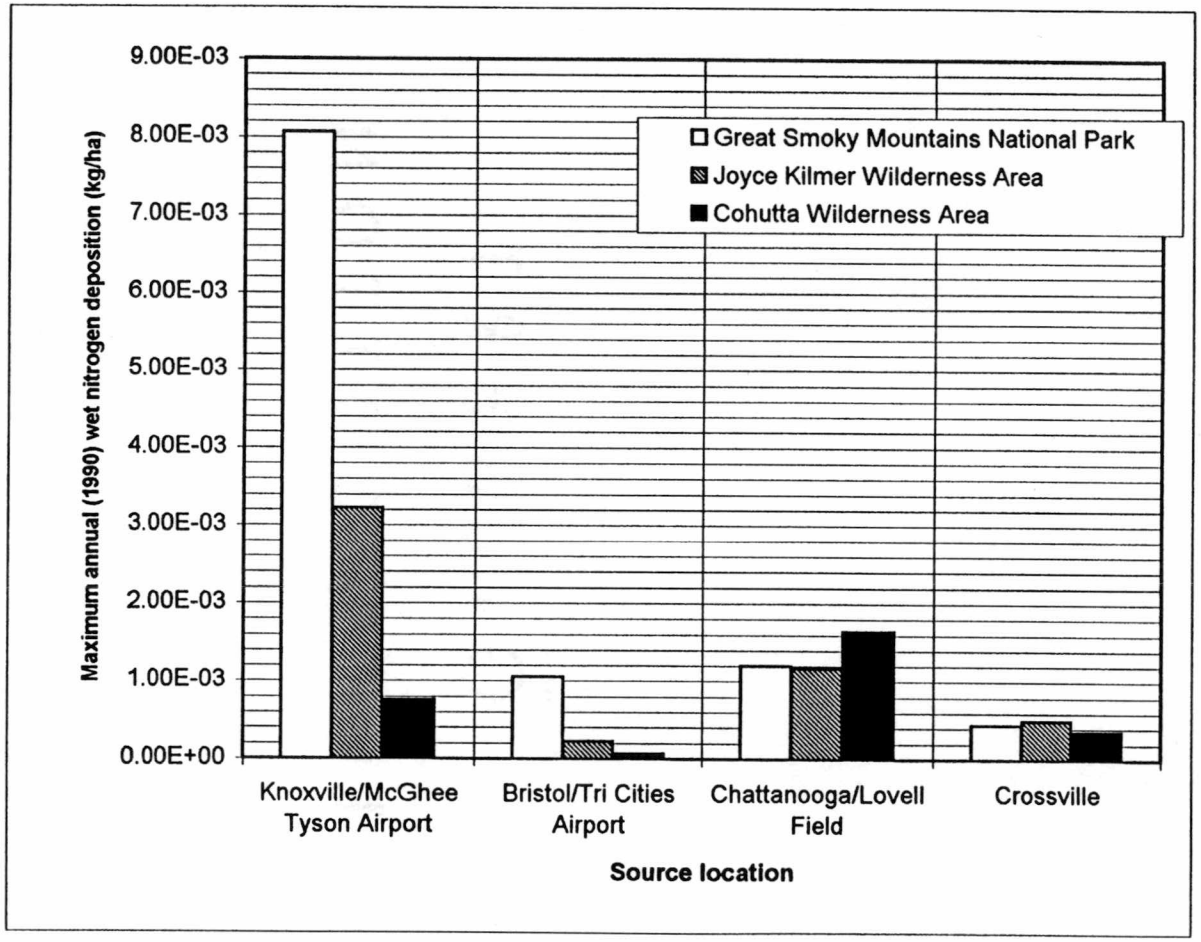

Fig. 4.10. Maximum annual wet nitrogen deposition estimated for 1990 on Class I areas in the East Tennessee modeling domain from a 65 m (210 ft), 28.8 g/s (1000 tpy) NO_x emission source.

distance is much closer than Crossville [100 km (62 miles)], Tri Cities [105 km (65 miles)], and Chattanooga [125 km (77 miles)].

MESOPUFF estimates show that the hypothetical baseline source located in Crossville, Tri Cities, or Chattanooga would produce about the same maximum annual dry sulfur and nitrogen deposition values in the Great Smoky Mountains National Park. These three sites are almost equidistant from the park, but mixed layer winds blowing up and down the East Tennessee Valley should result in higher deposition in the park from a Chattanooga or Tri Cities source. However, for a substantial part of the year, upper-level winds blow from west to east, and thus, there is a high chance that emissions from the Crossville source would be transported directly to the park if they reach the upper-layer. This effect might show up even more clearly if the relatively high elevation of Crossville was taken into account (i.e., if elevation effects were in the model). Generally, upper-level winds have higher speeds than lower-level winds, contributing to higher dispersion, but upper-level winds blow persistently to the east, counteracting the increased dispersion. This effect does not occur with wet deposition because the model does not allow pollutants to be efficiently removed from the upper layer by precipitation scavenging. Wet sulfur and nitrogen deposition on the Great Smoky Mountains National Park from the Crossville site is less than half that from the Bristol and Chattanooga source locations.

In Joyce Kilmer Wilderness Area, estimated maximum deposition values are highest when the hypothetical source is in Knoxville. The distance from Knoxville/Tyson McGhee airport to Joyce Kilmer Wilderness Area is almost twice that to the Great Smoky Mountains National Park [40 km vs. 25 km (25 vs. 15 miles)] with deposition values one-half to one-third of those in the park. Dry deposition values resulting from a source located either in Chattanooga or Crossville are approximately equal. Wet deposition is about twice as much from Chattanooga as

from Crossville because the model does not allow efficient precipitation scavenging from the upper-layer, as discussed above. Very low deposition values (both wet and dry) occur in Joyce Kilmer Wilderness Area from a source sited at Tri Cities due to the relatively large distance between source and receptor.

Because of its close proximity, a hypothetical source located in Chattanooga results in the highest deposition values in Cohutta Wilderness Area. Maximum deposition resulting from siting the source in Knoxville and Crossville is about one-half to one-third that from the Chattanooga source. As with Joyce Kilmer Wilderness Area, locating the source in Tri Cities results in comparatively small deposition on Cohutta Wilderness Area.

4.2.4 Maximum Concentrations Estimated for the Target Class I Areas

Contour maps showing maximum SO_2 and NO_x concentrations over the modeling domain are shown in Appendix H. For the target Class I areas, maximum concentrations are summarized in Tables 4.2 through 4.4. These concentrations were compared to the maximum cumulative allowable SO_2 and NO_x PSD increments for Class I areas (40 CFR 51.166). Locating the hypothetical baseline source at Knoxville/McGhee Tyson Airport would result in exceedances of the allowable 3-h and 24-h average SO_2 increments at Great Smoky Mountains National Park, and an exceedance of the 3-h SO_2 increment in Joyce Kilmer Wilderness Area. Locating the hypothetical source at Chattanooga/Lovell Field would result in an exceedance of the 3-h and 24-h average Class I increments at Cohutta Wilderness Area. Locating the hypothetical sources at Bristol/Tri Cities Airport and Crossville resulted in no exceedances of the allowable increments at any of the Class I areas.

Table 4.2. Maximum concentrations estimated in the Great Smoky Mountains National Park from a hypothetical 28.8 g/s (1000 tpy) SO_2 and NO_x emission source

Pollutant	Averaging Time	Source Location	Maximum Concentration ($\mu g/m^3$)[a]	Percent of Class I PSD Increment[b]
SO_2	3-h	TYS	71	*280*
		TRI	4.0	16
		CHA	5.3	21
		CRO	7.7	31
	24-h	TYS	8.9	*180*
		TRI	0.50	10
		CHA	0.67	13
		CRO	0.88	18
	annual	TYS	0.19	10
		TRI	0.0070	0.35
		CHA	0.0099	0.50
		CRO	0.015	7.5
NO_x[c]	annual	TYS	0.012	1.2
		TRI	0.0018	0.18
		CHA	0.0016	0.16
		CRO	0.0026	0.26

Abbreviations: PSD = Prevention of Significant Deterioration; SO_2 = sulfur dioxide; NO_x = oxides of nitrogen; TYS = Knoxville/McGhee Tyson Airport, TRI = Bristol/Tri Cities Airport, CHA = Chattanooga/Lovell Field; CRO = Crossville.

[a]Concentrations were estimated using the MESOPUFF II air dispersion model.

[b]Class I PSD increments for SO_2 are 25 $\mu g/m^3$ (maximum 3-h average), 5 $\mu g/m^3$ (maximum 24-h average), and 2 $\mu g/m^3$ (annual average) The Class I PSD increments for NO_2 is 1 $\mu g/m^3$ (maximum annual average).

[c]Approximated to be completely NO_2 for comparison to the Class I PSD Increment. Note that NO_x concentrations do not include concentrations of nitric acid.

Table 4.3. Maximum concentrations estimated in Joyce Kilmer Wilderness Area from a hypothetical 28.8 g/s (1000 tpy) SO_2 and NO_x emission source

Pollutant	Averaging Time	Source Location	Maximum Concentration ($\mu g/m^3$)[a]	Percent of Class I PSD Increment[b]
SO_2	3-h	TYS	37	*150*
		TRI	1.5	6.0
		CHA	4.8	19
		CRO	5.5	22
	24-h	TYS	4.6	92
		TRI	0.19	3.8
		CHA	0.60	12
		CRO	0.69	14
	annual	TYS	0.087	4.4
		TRI	0.0020	0.10
		CHA	0.0097	0.49
		CRO	0.012	0.66
NO_x[c]	annual	TYS	0.0082	0.92
		TRI	0.00080	0.080
		CHA	0.0016	0.16
		CRO	0.0023	0.23

Abbreviations: PSD = Prevention of Significant Deterioration; SO_2 = sulfur dioxide; NO_x = oxides of nitrogen; TYS = Knoxville/McGhee Tyson Airport, TRI = Bristol/Tri Cities Airport, CHA = Chattanooga/Lovell Field; CRO = Crossville.

[a]Concentrations were estimated using the MESOPUFF II air dispersion model.

[b]Class I PSD increments for SO_2 are 25 $\mu g/m^3$ (maximum 3-h average), 5 $\mu g/m^3$ (maximum 24-h average), and 2 $\mu g/m^3$ (annual average) The Class I PSD increments for NO_2 is 1 $\mu g/m^3$ (maximum annual average).

[c]Approximated to be completely NO_2 for comparison to the Class I PSD Increment. Note that NO_x concentrations do not include concentrations of nitric acid.

Table 4.4. Maximum concentrations estimated in Cohutta Wilderness Area from a hypothetical 28.8 g/s (1000 tpy) SO_2 and NO_x emission source

Pollutant	Averaging Time	Source Location	Maximum Concentration ($\mu g/m^3$)[a]	Percent of Class I PSD Increment[b]
SO_2	3-h	TYS	4.4	18
		TRI	0.47	1.9
		CHA	40	*160*
		CRO	7.2	29
	24-h	TYS	0.55	11
		TRI	0.059	1.2
		CHA	5.0	*100*
		CRO	0.90	18
	annual	TYS	0.011	0.55
		TRI	0.00057	0.029
		CHA	0.047	2.4
		CRO	0.012	0.60
NO_x[c]	annual	TYS	0.0027	0.27
		TRI	0.00029	0.029
		CHA	0.0031	0.31
		CRO	0.0018	0.18

Abbreviations: PSD = Prevention of Significant Deterioration; SO_2 = sulfur dioxide; NO_x = oxides of nitrogen; TYS = Knoxville/McGhee Tyson Airport, TRI = Bristol/Tri Cities Airport, CHA = Chattanooga/Lovell Field; CRO = Crossville.

[a]Concentrations were estimated using the MESOPUFF II air dispersion model.

[b]Class I PSD increments for SO_2 are 25 $\mu g/m^3$ (maximum 3-h average), 5 $\mu g/m^3$ (maximum 24-h average), and 2 $\mu g/m^3$ (annual average) The Class I PSD increments for NO_2 is 1 $\mu g/m^3$ (maximum annual average).

[c]Approximated to be completely NO_2 for comparison to the Class I PSD Increment. Note that NO_x concentrations do not include concentrations of nitric acid.

Maximum annual average NO_x concentrations in the target Class I areas range from 6 to 51% of the annual SO_2 concentrations depending on the distance to the Class I area. As stated earlier, MESOPUFF simulates rapid conversion of NO_x ($NO + NO_2$) to a mix of HNO_3 and NO_x (still assumed to be $NO + NO_2$). Also, the model allows the HNO_3 and NO_x mix to convert to NO_3^- more quickly than SO_2 is converted to SO_4^{2-}. Therefore, for sources located close to the target Class I area, the annual NO_x concentrations are much lower than annual SO_2 concentrations. For sources located farther from the target Class I area, annual NO_x concentrations are about half of the annual SO_2 concentrations because more SO_2 has oxidized to SO_4^{2-}. If HNO_3 concentrations were included, the NO_x concentration would increase by a median factor of about 2.5 (i.e., 2.5 is the median ratio of HNO_3 to NO_x over all grid points in the modeling domain).

4.3 SENSITIVITY SCENARIOS

Two sensitivity scenarios where run from the same four hypothetical source locations to determine the effect of (1) different emission rates and (2) different stack heights on model estimates. Sensitivity runs were conducted for the month of August because this month generally had the highest deposition values from all source locations and all species.

Runs were made with emission rates of 2.88 g/s (100 tpy) and 288 g/s (10,000 tpy) and compared to the baseline scenario [28.8 g/s (1000 tpy)]. All deposition values and concentrations estimated using MESOPUFF were linearly proportional to the emission rate. For example, with the baseline source located at Knoxville/McGhee Tyson Airport, the maximum monthly (August 1990) dry sulfur deposition in Great Smoky Mountains National Park was estimated to be about 0.03 kg/ha. With an emission rate of 2.88 g/s, the maximum dry sulfur deposition in the park was

estimated to be 0.003 kg/ha, and with an emission rate of 288 g/s, the maximum dry sulfur deposition in the park was estimated to be 0.3 kg/ha. Therefore, deposition estimates made for the baseline scenario may be used to determine the impact of different emission rates by adjusting values linearly, at least within the broad range of emission values considered in this thesis.

The sensitivity of estimated deposition to stack height was determined by comparing results from a 200 m (125 ft) stack to the baseline source (65 m). Stack exit parameters (i.e., temperature, diameter, and effluent velocity) where the same as the baseline scenarios (see Sect. 3.4).

The relationships between modeled deposition at the target Class I areas from the 65-m stack, D_{65}, and from the 200-m stack, D_{200}, are shown in Figs 4.11 [total (wet + dry) sulfur] and 4.12 [total (wet + dry) nitrogen]. These figures show the maximum monthly D_{65} values plotted against the maximum monthly D_{200} values. Twelve points are plotted on each figure, representing the maximum monthly deposition values predicted to occur at the three target Class I areas from each of the four hypothetical source locations.

Using a least-squares linear regression two equations were generated which show the relationship between deposition values for a 65-m stack and a 200-m stack. The first equation for total maximum sulfur deposition is:

$$D_{200} = 1.05 D_{65}^{0.968} \tag{4.3}$$

where, the R^2 value of the linear regression is 0.945. For total maximum nitrogen deposition, the equation is:

$$D_{200} = 0.868 D_{65}^{0.964} \tag{4.4}$$

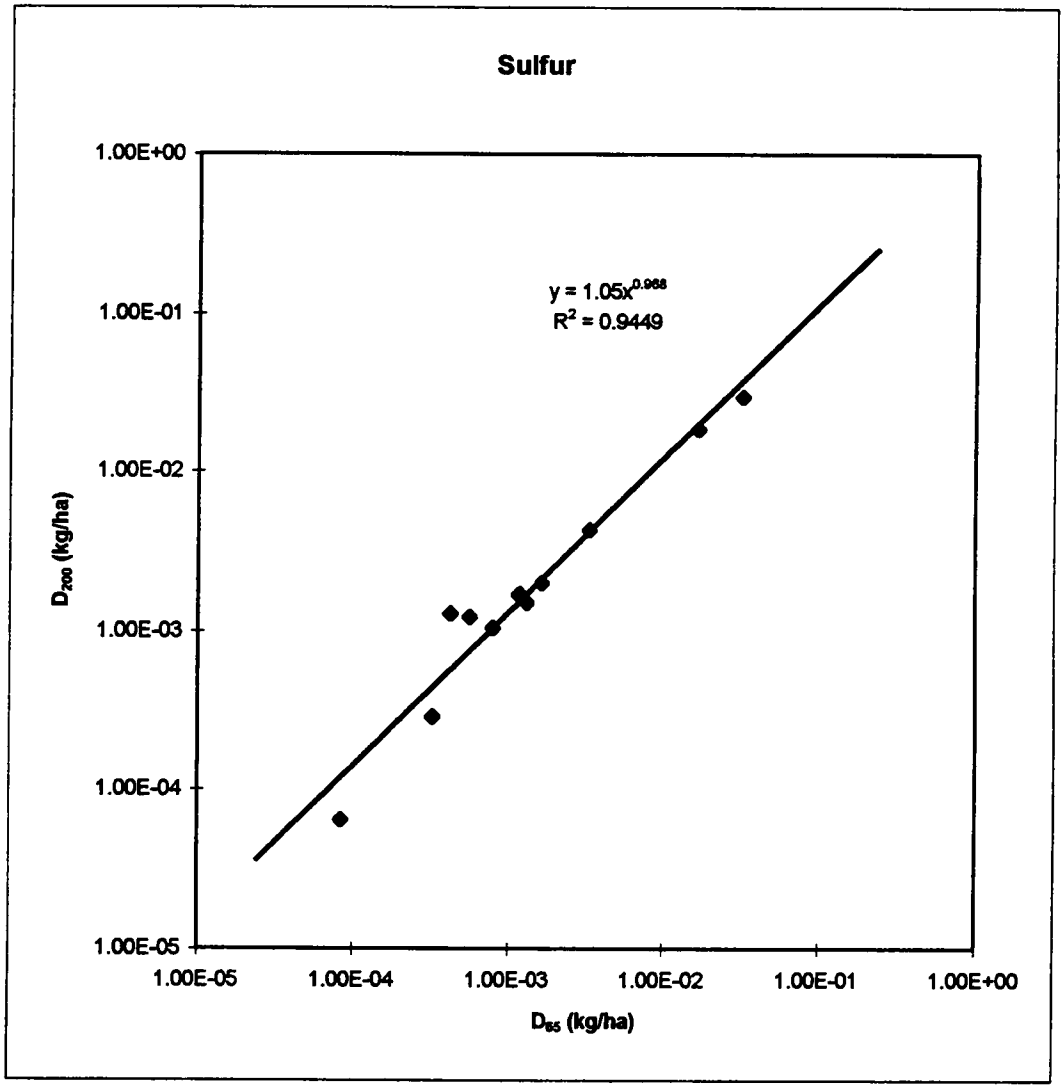

Fig. 4.11. Comparison of maximum annual (1990) total sulfur (wet + dry) deposition estimated for Class I areas in East Tennessee from a hypothetical 28.8 g/s SO_2 source with a stack height of 65 m (210 ft) versus the same source with a stack height of 200 m (660 ft). The hypothetical source was located at each of four different locations in the East Tennessee modeling domain.

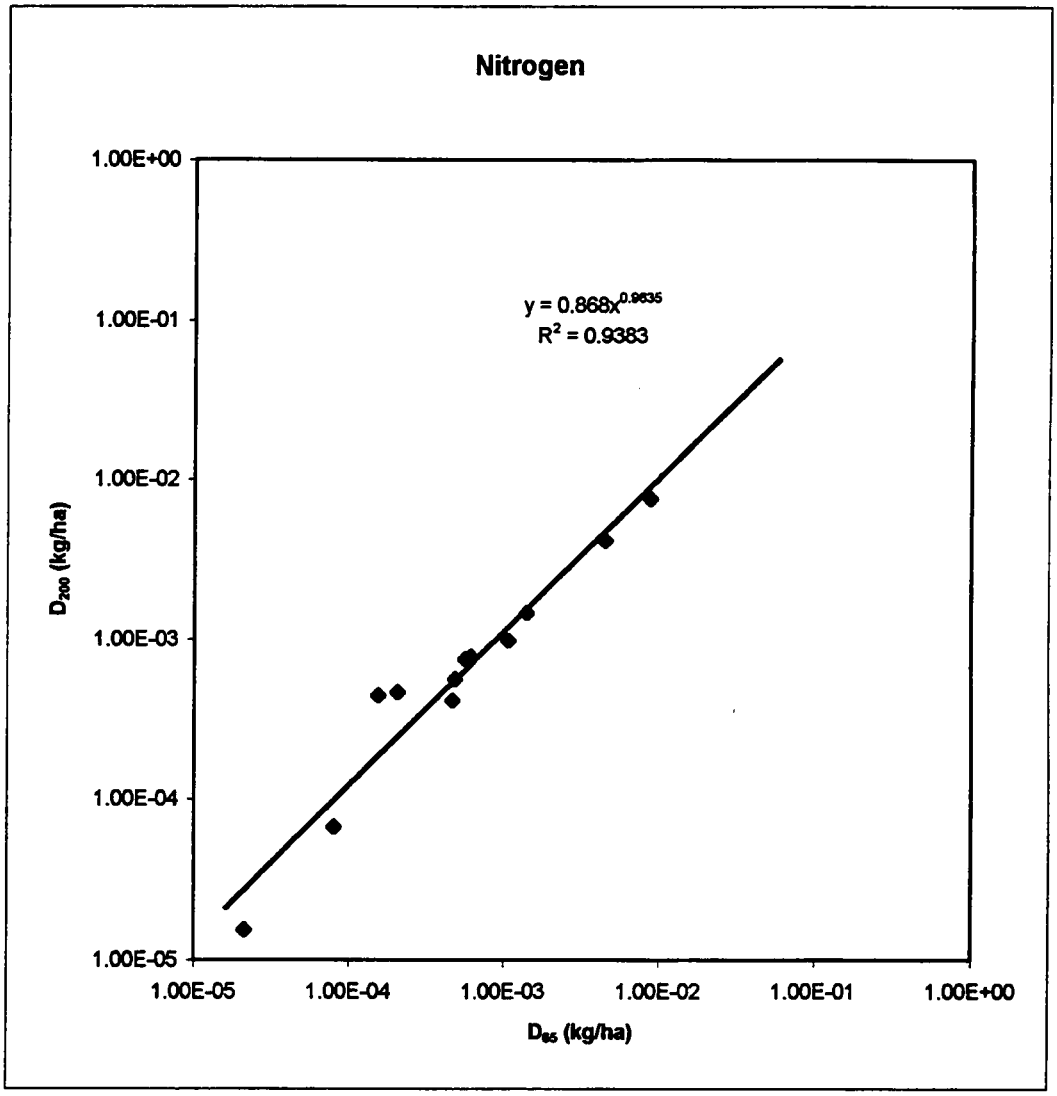

Fig. 4.12. Comparison of maximum annual (1990) total nitrogen (wet + dry) deposition estimated for Class I areas in East Tennessee from a hypothetical 28.8 g/s NO_x source with a stack height of 65 m (210 ft) versus the same source with a stack height of 200 m (660 ft). The hypothetical source was located at each of four different locations in the East Tennessee modeling domain.

where, the R^2 value of the linear regression is 0.938. Both of these equations show that there is relatively little difference in the maximum monthly deposition estimated for the target Class I areas with respect to stack height. For total sulfur (Equation 4.3), the deposition values for a 200-m stack are within 5% of those for a 65-m stack, and for total nitrogen (Equation 4.4), the deposition values for a 200-m stack are within 14% of those for a 65-m stack. This relatively low sensitivity results from the puffs being well mixed in the vertical at distances of about 40 to 50 km (25 to 30 miles) from the source. Because puffs are well mixed, pollutant concentrations are virtually the same throughout the mixed layer despite the initial emission height. For sources located closer than 50 km to the target Class I areas (i.e. a source located at Knoxville/Tyson McGhee Airport), puffs are not completely mixed in the vertical and resulting deposition values decrease with increasing stack height.

4.4 DEPOSITION POTENTIAL

The author developed maps of *deposition potential* for the East Tennessee modeling domain (Figs. 4.13 through 4.18). These maps show the maximum deposition per unit area at a specific location that would result from a 65-m high source emitting 28.8 g/s (1000 tpy) each of NO_x and SO_2 as a function of source location within the modeling domain. For each target Class I area, maps were constructed by calculating the maximum annual deposition at the nearest Class I area boundary estimated from each of the four hypothetical source locations, entering the result for each source location on the map, and contouring the result. The author labeled the resulting contours as *deposition potential*. These maps are fundamentally different from maps showing deposition patterns from a single source because they show the potential maximum deposition that would occur at the nearest boundary of a particular Class I area from every location in the

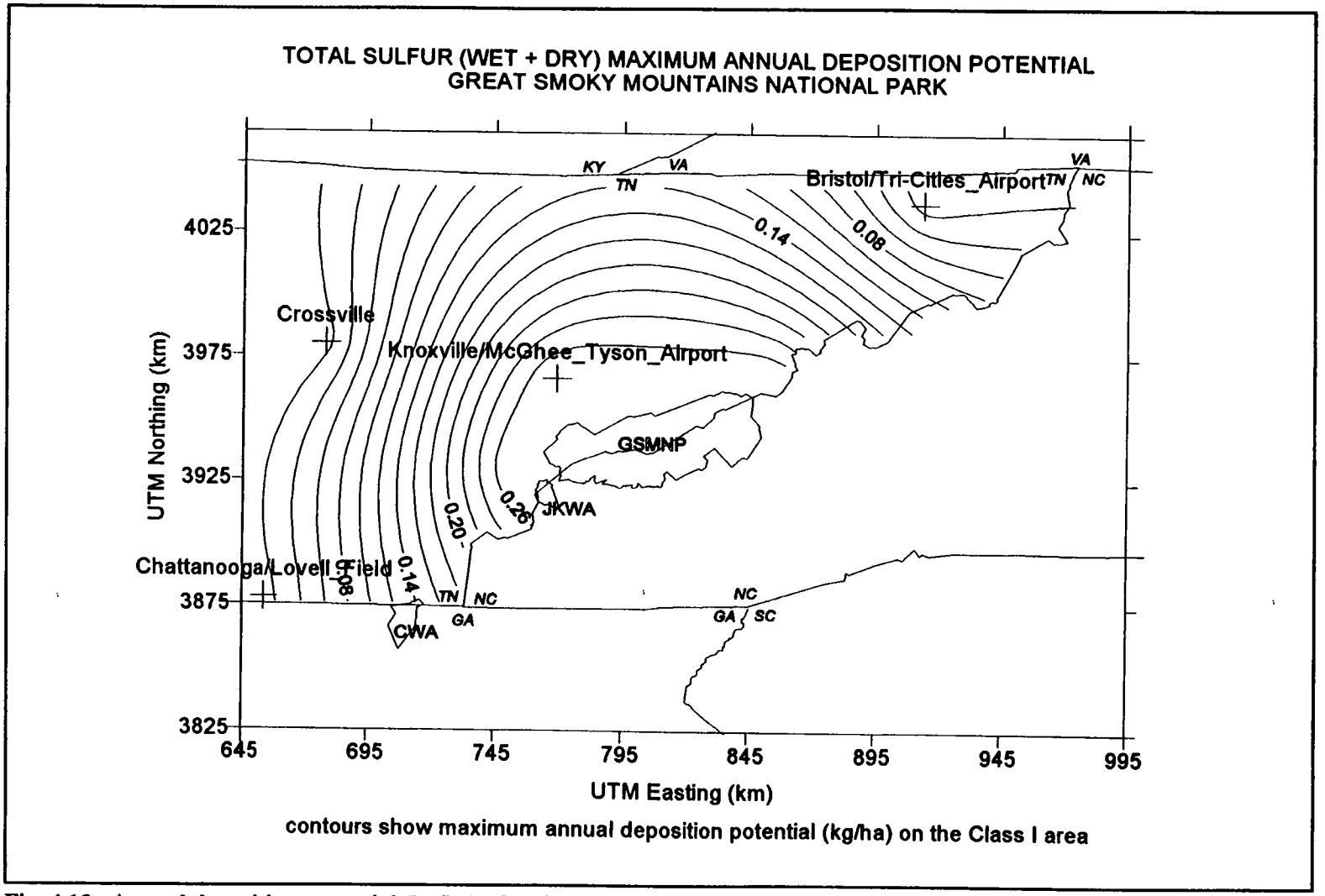

Fig. 4.13. Annual deposition potential (kg/ha) of sulfur at the nearest boundary of the Great Smoky Mountains National Park corresponding to a continuous emission of 28.8 g/s (1000 tpy) of SO_2 from a 65 m (210 ft) tall point source.

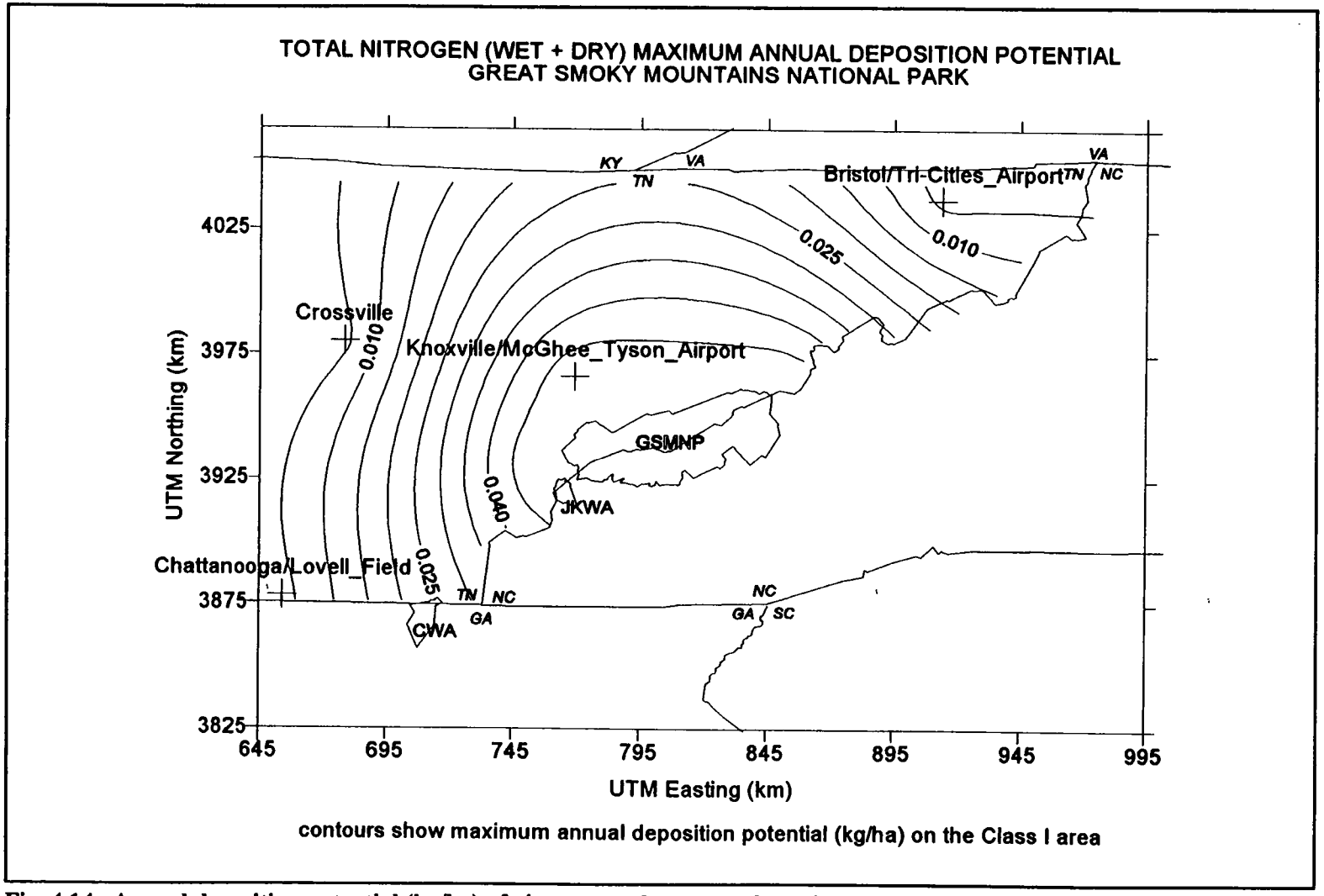

Fig. 4.14. Annual deposition potential (kg/ha) of nitrogen at the nearest boundary of the Great Smoky Mountains National Park corresponding to a continuous emission of 28.8 g/s (1000 tpy) of NO_x from a 65 m (210 ft) tall point source.

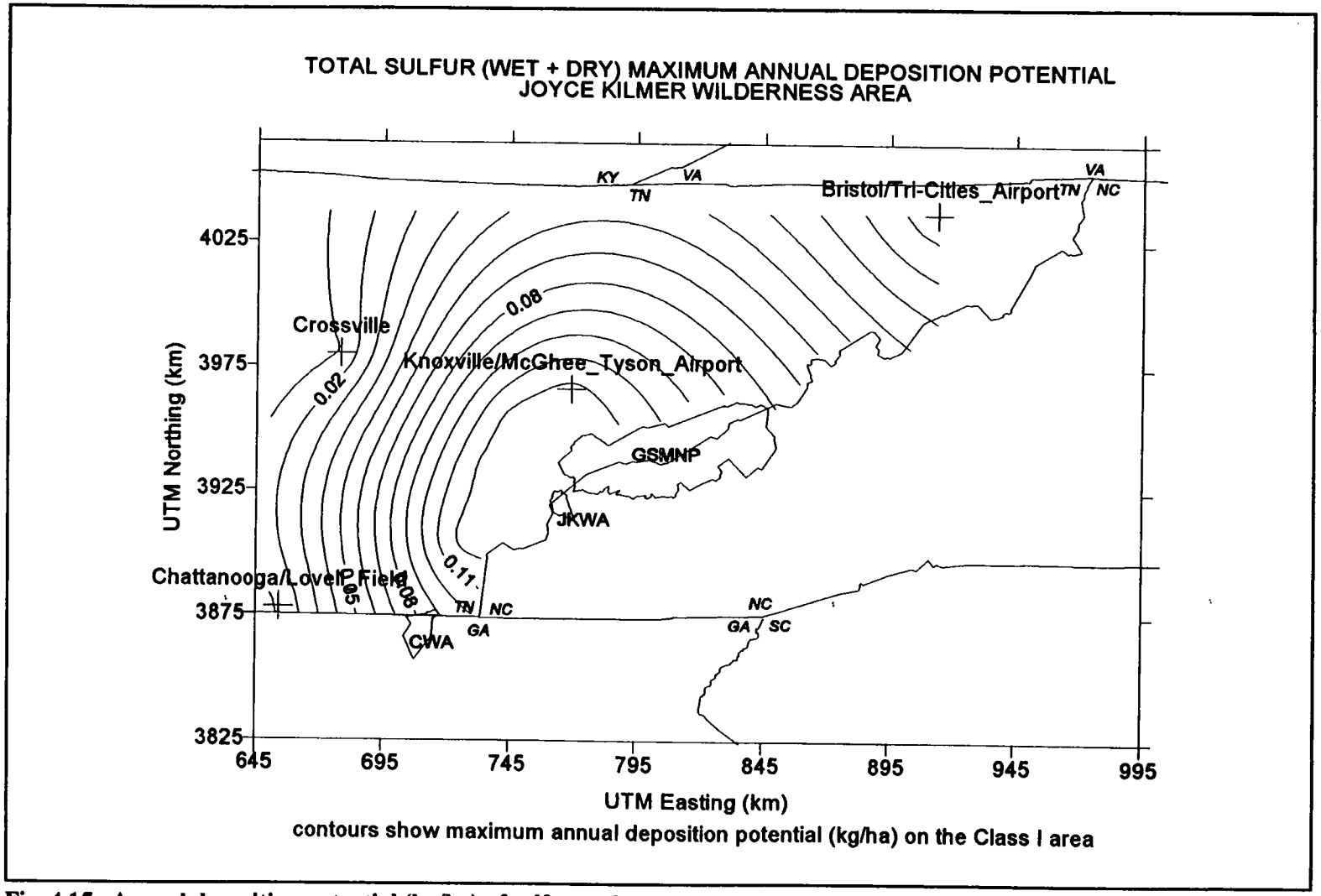

Fig. 4.15. Annual deposition potential (kg/ha) of sulfur at the nearest boundary of Joyce Kilmer Wilderness Area corresponding to a continuous emission of 28.8 g/s (1000 tpy) of SO_2 from a 65 m (210 ft) tall point source.

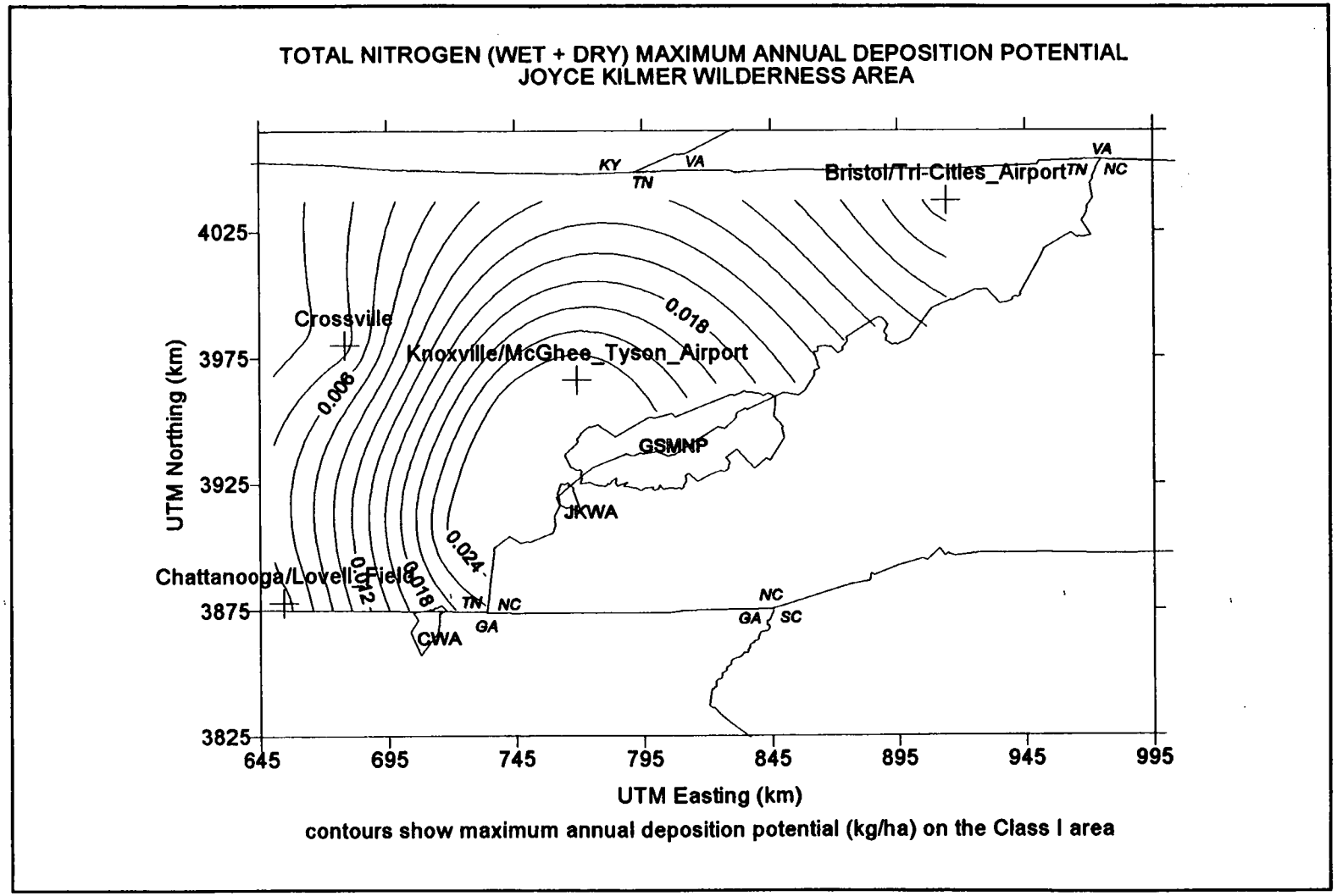

Fig. 4.16. Annual deposition potential (kg/ha) of nitrogen at the nearest boundary of Joyce Kilmer Wilderness Area corresponding to a continuous emission of 28.8 g/s (1000 tpy) of NO_x from a 65 m (210 ft) tall point source.

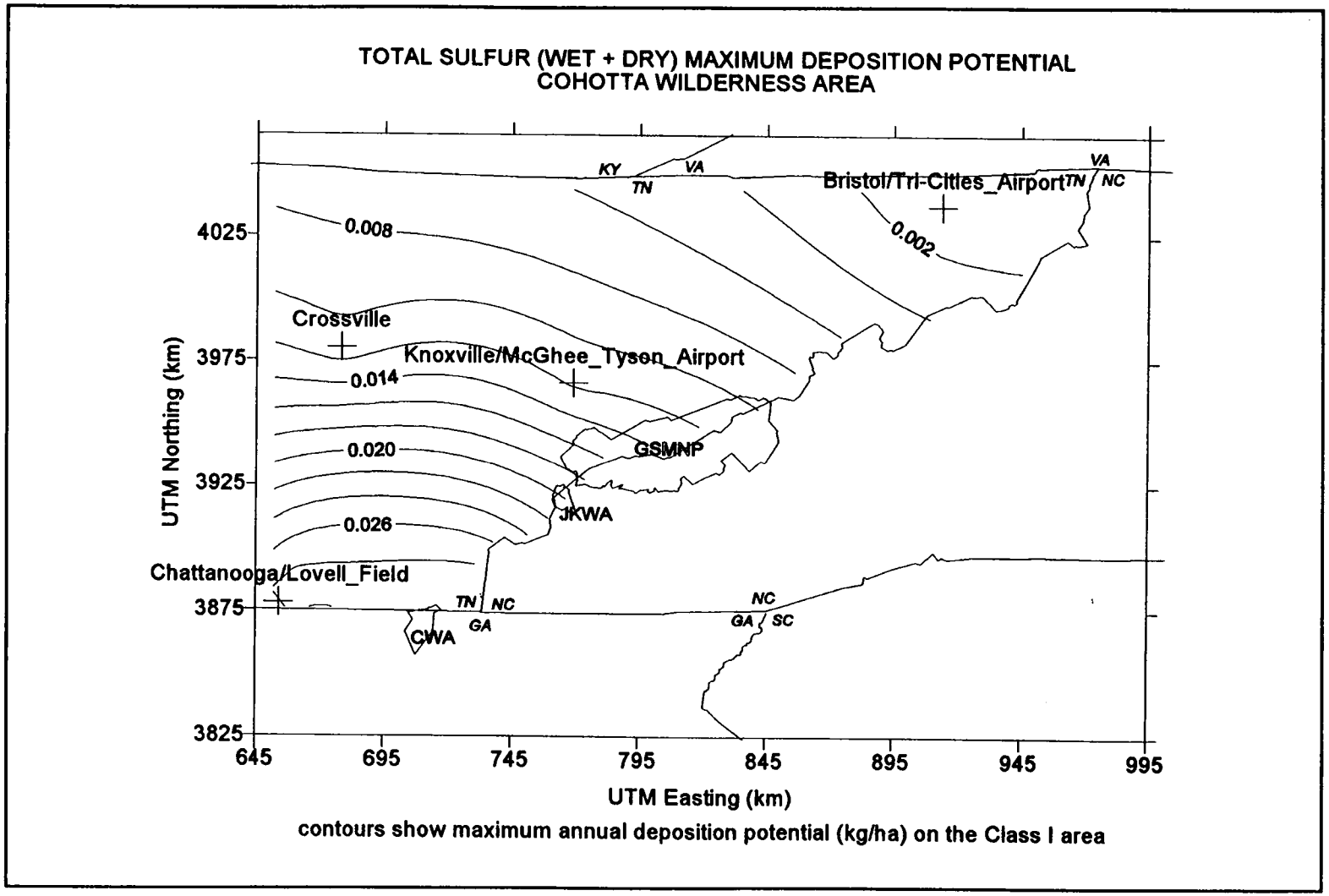

Fig. 4.17. Annual deposition potential (kg/ha) of sulfur at the nearest boundary of Cohutta Wilderness Area corresponding to a continuous emission of 28.8 g/s (1000 tpy) of SO_2 from a 65 m (210 ft) tall point source.

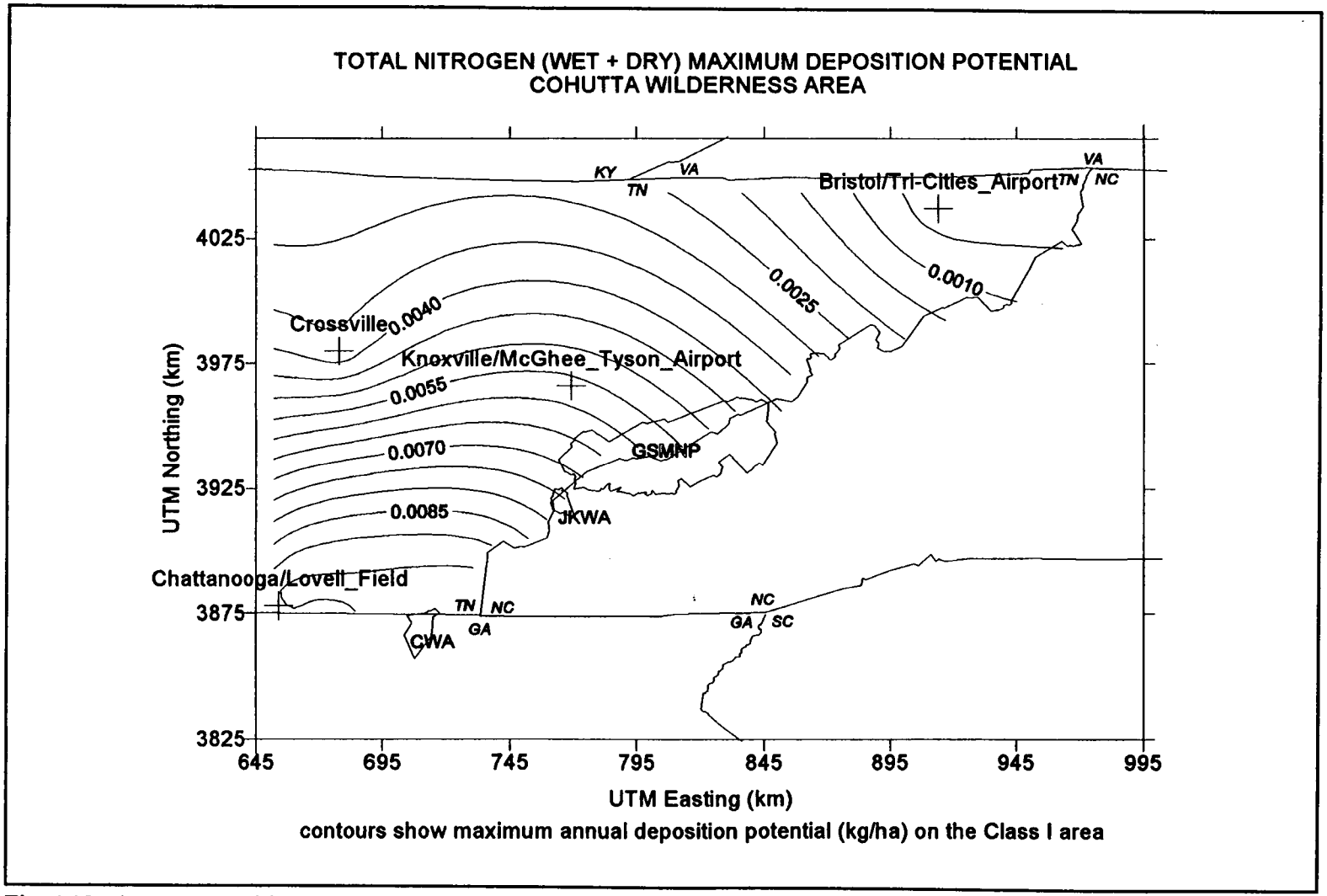

Fig. 4.18. Annual deposition potential (kg/ha) of nitrogen at the nearest boundary of Cohutta Wilderness Area corresponding to a continuous emission of 28.8 g/s (1000 tpy) of NO_x from a 65 m (210 ft) tall point source.

modeling domain. For example, in Fig. 4.13, the 0.26 contour shows those locations at which the hypothetical baseline source would lead to annual average sulfur deposition of 0.26 kg/ha at the nearest park boundary. Six maps were created showing total (wet + dry) maximum annual deposition for the two pollutants (sulfur and nitrogen) for each of the three target Class I areas. On these figures, contours were not drawn close to the Class I area because of the uncertainty in deposition estimates from sources close to the park. Deposition potential close to the target Class I area would be greater than the maximum contour value.

The maps may be used to estimate the emission offsets that would be required to ensure a net zero increase in deposition on a target Class I area. For example, if a 28.8 g/s SO_2 emission source with a 65-m stack was proposed to be built in Athens, Tennessee (UTM coordinates 3926 km Northing, 718 km Easting), the total sulfur (wet + dry) maximum annual deposition potential would be about 0.14 kg/ha on the Great Smoky Mountains National Park (see Fig. 4.13). If emission offsets (i.e., emission reductions resulting in no net maximum deposition) were sought from a 65 m emission source located in Kingsport, Tennessee (UTM coordinates 4045 km Northing, 904 km Easting), which has a total sulfur maximum annual deposition potential of about 0.04 kg/ha, the required emission reduction from this Kingsport source would be about 100 g/s (3500 tpy) of SO_2. In other words, a source located in Athens, Tennessee has about 3.5 times (0.14/0.04) the potential to deposit sulfur on the Great Smoky Mountains National Park as a source located in Kingsport, Tennessee.

Although, these maps have been constructed for a 65-m stack, they may be used for sources with different stack heights because of the low sensitivity on deposition estimates from stack height variations (as described by Equations 4.3 and 4.4). As discussed in the previous section, the error introduced by using these deposition potential maps for stack heights greater

than 65 m would be less than 15%. Therefore, prior to running MESOPUFF, these maps could be used by modelers and planners to make estimates of the maximum potential deposition that would occur on target Class I areas for sources located in the East Tennessee modeling domain. These deposition potential maps should not be used for sources closer than 40 km (25 miles) to the target Class I areas (e.g., the distance represented by the 0.26 kg/ha contour on Fig. 4.13). A steady-state Gaussian plume model [e.g., the Industrial Source Complex (ISC) air dispersion model (40 CFR 51, App. W)] should be used at close distances, with acidic deposition calculated per IWAQM guidelines (EPA, 1993).

5. RECOMMENDATIONS AND CONCLUSIONS

A modeling protocol to estimate atmospheric concentration and deposition of acidic pollutants has been developed and demonstrated for the East Tennessee domain. MESOPUFF II was the air dispersion model used to estimate concentrations and deposition values in the modeling domain from emission sources located at four hypothetical locations in East Tennessee. The focus of the protocol was to estimate acidic deposition on the Class I areas located in East Tennessee: (1) the Great Smoky Mountains National Park, (2) Joyce Kilmer Wilderness Area, and (3) Cohutta Wilderness Area. The following is a list of recommendations and conclusions reached by the author in development and demonstration of the MESOPUFF II modeling protocol.

1. Winds in the mixing layer generally flow up and down the East Tennessee Valley. A modification was made in the MESOPAC meteorological preprocessor to represent this flow. The MESOPAC preprocessor was also modified so that discontinuities in the lower-layer wind field were smoothed.

2. For a single source, deposition and concentration estimates are linearly proportional to the emission rate (i.e., increasing the emission rate by a factor of 10 results in similar increases in estimated deposition and concentration). Additionally, estimated maximum deposition and concentration values in the target Class I areas are relatively insensitive to changes in stack height for sources located more than 50 km (30 miles) from the area. Because of these two results, it was possible to generate maps of *deposition potential* that can be used as screening tools to estimate maximum deposition on target Class I

areas from a proposed new source located anywhere in the East Tennessee modeling domain. These maps may be used by planners early in the permitting process (i.e., before using MESOPUFF) to determine an optimally efficient and effective modeling strategy. However, these deposition potential maps should only be used for sources located farther than about 40 km (25 miles) from the target Class I area. For sources closer than 40 km, a steady-state Gaussian plume model should be used in accordance with IWAQM recommendations.

REFERENCES

REFERENCES

Baes, III, C. F. and S. B. McLaughlin, 1984. "Trace Elements in Tree Rings: Evidence of Recent and Historical Air Pollution," *Science* **224**, 494-497.

Barnard, J. and A. A. Lucier, 1990. *Changes in Forest Health and Productivity in the United States and Canada*, State of Science and Technology Report 15, National Acid Precipitation Assessment Program, Washington, D. C.

Carhart, R. A., A. J. Policastro, M. Wastag, and L. Coke, 1989. "Evaluation of Eight Short-Term Long Range Transport Models Using Field Data," *Atmos. Envir.*, **23**(1):85-105.

Clarke, J. F. and E. S. Edgerton, 1992. *Dry Deposition Flux Calculations for the National Dry Deposition Network*, U. S. Environmental Protection Agency, Atmospheric Research and Exposure Assessment Laboratory, Office of Research and Development, Research Triangle Park, North Carolina.

Cook, R. B., J. W. Elwood, R. R. Turner, M. A. Bogle, P. J. Mulholland, and A. V. Palumbo, 1994. "Acid-base Chemistry of High-elevation Streams in the Great Smoky Mountains National Park," *Water, Air and Soil Pollution* **72**:331-356.

Draxler, R. R., 1979. "Modeling the Results of Two Recent Mesoscale Dispersion Experiments," *Atmos. Environ.* **13**:1523-1533.

EPA (U. S. Environmental Protection Agency), 1985. *Guideline for Determination of Good Engineering Practice Stack Height (Technical Support Document for the Stack Height Regulations) (Revised)*, Office of Air Quality Planning and Standards, Research Triangle Park, North Carolina.

EPA (U. S. Environmental Protection Agency), 1993. *Interagency Workgroup on Air Quality Modeling (IWAQM) Phase I Report: Interim Recommendation for Modeling Long Range Transport and Impacts on Regional Visibility*, EPA-454/R-93-015, Technical Support Division (MD-14), Research Triangle Park, Raleigh, North Carolina.

EPA (U. S. Environmental Protection Agency), 1995a. *Official Record from the Sixth Conference on Air Quality Modeling*, AQM-95-01, B-1, Technical Support Division (MD-14), Research Triangle Park, Raleigh, North Carolina.

EPA (U. S. Environmental Protection Agency), 1995b. *A User's Guide for the CALPUFF Dispersion Model*, EPA-454/B-95-006, Office of Air Quality Planning and Standards, Research Triangle Park, North Carolina.

EPA (U. S. Environmental Protection Agency), 1995c. *A User's Guide for the CALMET Meteorological Model*, EPA-454/B-95-002, Emissions, Monitoring and Analysis Division (MD-14), Research Triangle Park, Raleigh, North Carolina.

EPA (U. S. Environmental Protection Agency), 1995d. *Testing of Meteorological and Dispersion Models for Use in Regional Air Quality Modeling*, EPA-454/R-95-005, Emissions, Monitoring and Analysis Division (MD-14), Research Triangle Park, Raleigh, North Carolina.

EPA (U. S. Environmental Protection Agency), 1995e. *Acid Deposition Standard Feasibility Study Report to Congress*, EPA 430-R-95-001a, Office of Air and Radiation, Acid Rain Division, Washington, D. C.

EPA (U. S. Environmental Protection Agency), 1995f. *A Revised User's Guide to MESOPUFF II (V5.1)*, EPA-454/B-94-025, Office of Air Quality Planning and Standards, Research Triangle Park, North Carolina.

Gross, G. and F. Wippermann, 1987. "Channeling and Countercurrents in the Upper Rhine Valley: Numerical Simulations," *J. Climate Appl. Meteor.*, **26**:1293-1304.

Hicks, B. B., D. D. Baldocchi, R. P. Hosker, B. A. Hutcherson, D. R. Matt, R. T. McMillen, and L. C. Satterfield, 1985. *On the Use of Monitored Air Concentrations to Infer Dry Deposition*, National Oceanic and Atmospheric Administration Technical Memorandum ERLARL-141, Oak Ridge, Tennessee.

Moore, G. E., R. E. Morris, S. G. Douglas, and R. E. Kessler, 1990. *Rocky Mountain Acid Deposition Model Assessment: ARM3 Model Performance Evaluation*. EPA-600/3-90-024, U. S. Environmental Protection Agency, Atmospheric Research and Exposure Laboratory, Research Triangle Park, North Carolina.

Morris, R. E., R. C. Kessler, S. G. Douglas, K. R. Styles, and G. E. Moore, 1988. *Rocky Mountain Acid Deposition Model Assessment: Acid Rain Mountain Mesoscale Model (ARM3)*, EPA-600/3-88-042, U. S. Environmental Protection Agency, Atmospheric Research and Exposure Laboratory, Research Triangle Park, North Carolina.

NAPAP (National Acid Precipitation Assessment Program), 1990. *National Acid Precipitation Assessment Program: 1990 Report to Congress*, Office of the Director, Washington, D. C.

NAPAP (National Acid Precipitation Assessment Program), 1991. *National Acid Precipitation Assessment Program: 1990 Integrated Assessment Report*, Office of the Director, Washington, D. C.

NAPAP (National Acid Precipitation Assessment Program), 1992. *National Acid Precipitation Assessment Program: 1992 Report to Congress*, Office of the Director, Washington, D. C.

Paine, R. J. and D. W. Heinhold, 1995. "Long Range Transport Modeling: Assessment of MESOPUFF II Performance," *Proceedings from the 1995 Annual Meeting of the Air and Waste Management Association*, San Antonio, Texas.

Pendergrass W., 1995. William Pendegrass, NOAA Atmospheric and Turbulence Division, Oak Ridge, Tennessee, personal communication with Douglas A. Lombardi, University of Tennessee, Knoxville, Tennessee, July 24, 1995.

Perry, S. G., D.J. Burns, L. H. Adams, R. J. Paine, M.G. Dennis, M.T. Mills, D. G. Strimaitis, R. J. Yamartino, E. M. Insley, 1989. *User's Guide to the Complex Terrain Dispersion Model Plus Algorithms for Unstable Situations (CTDMPLUS) Volume 1: Model Description and User Instructions*, EPA/600/8-89/041, U.S. Environmental Protection Agency, Research Triangle Park, North Carolina

Scire, J. S., F. W. Lurmann, A. Bass, S. R. Hanna, 1984. *Development of the MESOPUFF II Dispersion Model*, EPA-600/3-84-057, prepared for the Environmental Sciences Research Laboratory, U. S. Environmental Protection Agency, Research Triangle Park, North Carolina.

Shaver, C. L., K. A. Tonnessen, and T. G. Maniero, 1994. "Clearing the Air at Great Smoky Mountains National Park," *Ecological Applications* 4(4):690-701.

Stam, A. C., S. B. McLaughlin, and J. F. McCormick, 1990, *Effects of Acidic Precipitation on the Soil Chemistry and Bioavailability of Aluminum, Manganese, and Copper*, ORNL/TM-11569, Oak Ridge, National Laboratory, Oak Ridge, Tennessee.

Stoddard, J., 1994. "Long-term Changes in Watershed Retention of Nitrogen: Its Causes and Aquatic Consequences," pp. 223-284 in L. A. Baker, ed., *Environmental Chemistry of Lakes and Reservoirs*, Advances in Chemistry Series Number 237, American Chemical Society, Washington, D. C.

Whiteman, C. D. and J. C. Doran, 1993. "The Relationship Between Overlying Synoptic Scale Flows and Winds Within a Valley," *J. Appl. Meteor.* 12(11):1669-1682.

Wigington, P. J., T. D. Davies, M. Tranter, and K. Eshlelman, 1990. *Episodic Acidification of Surface Waters due to Acidic Deposition*, State of Science and Technology Report 12, National Acid Precipitation Assessment Program , Washington, D. C.

Wippermann, F. and G. Gross 1981. "On the Contribution of Orographically Influenced Wind Roses for Given Distributions of the Large-scale Wind," *Contrib. Atmos. Phys.*, **54**:492-501.

Wippermann, F., 1984. "Air Flow Over and in Broad Valleys: Channeling and Countercurrents," *Contrib. Atmos. Phys.*, **57**:92-105.

Yankee, D. H., 1995. Dennis Yankee, Technology Transfer, Tennessee Valley Authority, Norris, Tennessee, Landsat 30 meter resolution satellite imagery land use/land cover map, provided to Douglas A. Lombardi, University of Tennessee, Knoxville, Tennessee, October 10, 1995.

A PROTOCOL FOR MODELING ATMOSPHERIC TRANSPORT AND DEPOSITION OF ACIDIC SPECIES IN EAST TENNESSEE USING MESOPUFF II

A Thesis
Presented for the Master of Science
Degree
The University of Tennessee, Knoxville

Douglas Adler Lombardi
May 1996

VOLUME 2

APPENDICES

APPENDIX A

GUIDE FOR USING MESOPUFF II IN THE EAST TENNESSEE MODELING DOMAIN

A.1 INTRODUCTION

This appendix was written to serve as a guide for those using the MESOPUFF II Regional Transport Model, Version 5.1 (referred to in this document as MESOPUFF) in the East Tennessee modeling domain (Fig. A.1). It is a supplement to *A Revised User's Guide to MESOPUFF II (V5.1)*[1]. This guide addresses model input parameters appropriate for estimating impacts of the modification or construction of major point sources emitting oxides of nitrogen (NO_x) and oxides of sulfur (SO_x) on Class I Prevention of Significant Deterioration (PSD) areas in East Tennessee. These areas include the Great Smoky Mountains National Park (GSMNP) in Tennessee and North Carolina, the Joyce Kilmer Wilderness Area (JKWA) in Tennessee and North Carolina, and the Cohutta Wilderness Area (CWA) in Tennessee and Georgia.

This material is divided into five sections. Section A.1 provides background information on model preparation (including construction of meteorological data files) performed by the author; Sect. A.2 discusses computer system requirements the user should consider before running MESOPUFF; Sect. A.3 describes the steps the user must follow to construct the run control file; Sect. A.4 describes a MESOPUFF run; and Sect. A.5 discusses running the postprocessors to obtain concentration and deposition data.

A.2 BACKGROUND

The author downloaded the MESOPUFF code listing via modem from EPA's Support Center for Regulatory Air Dispersion Models (SCRAM) Bulletin Board Service (BBS)

---

[1]U. S. Environmental Protection Agency, *A Revised User's Guide to MESOPUFF II (V5.1)*, EPA-454/B-94-025, Technical Support Division (MD-14), Research Triangle Park, North Carolina, August 1994.

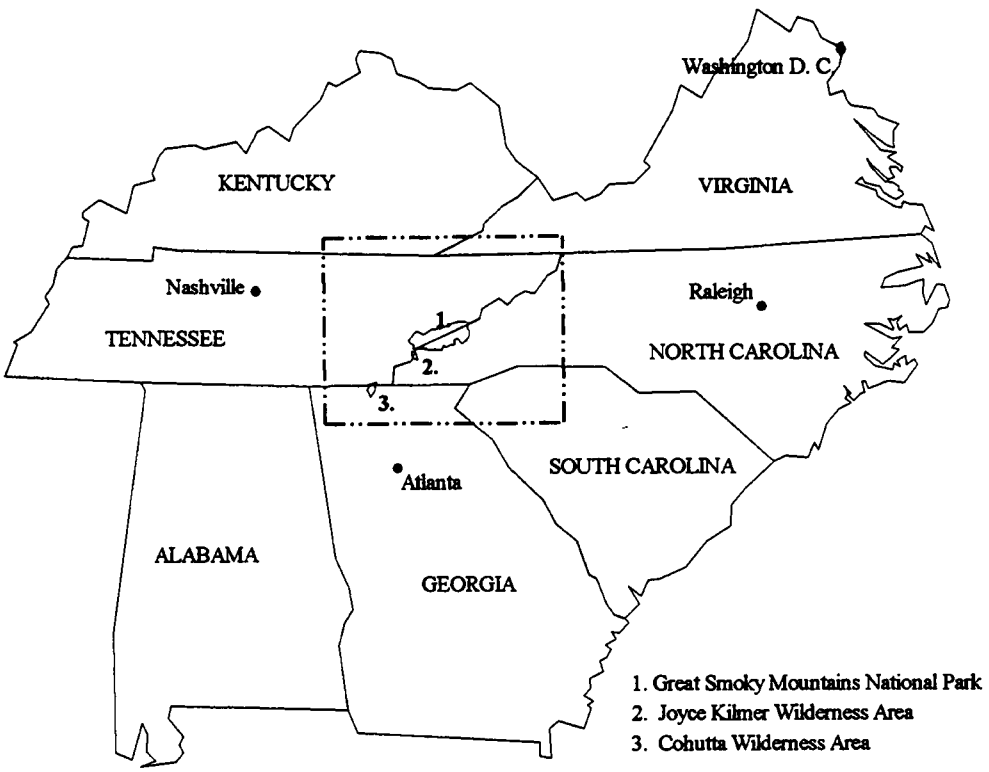

Figure A.1. Location of the East Tennessee Modeling domain (dashed lines).

maintained by the Office of Air Quality Planning and Standards. In addition to the code listing, the MESOPUFF executable file may be obtained from the SCRAM BBS; however, the author chose to recompile the MESOPUFF code using an updated compiler. The executable file available over the SCRAM BBS was produced using Lahey Fortran Compiler Version 5.0 and is quite large [approximately 3.4 megabytes (MB)]. It is necessary to run this large file from a DOS window in the Windows 3.x operating environment. The code was recompiled using Lahey Fortran Compiler Version 5.2, which reduced the size of the executable file to approximately 1.8 MB. The recompiled executable also runs more quickly and will run under a variety of operating environments.

In addition to recompiling the executable file, the author has prepared files of 1990 meteorological data for the East Tennessee modeling domain in a format ready for use by MESOPUFF. The files were created using MESOPAC II Version 2.4 (MESOPAC).

MESOPAC calculates meteorological parameters, such as wind speed and direction, at points located on a Cartesian coordinate grid. This meteorological grid is established using MESOPAC and is the basic reference frame for all spatial inputs (e.g., location of meteorological data stations and emission sources) to both MESOPAC and MESOPUFF. The rectangular meteorological grid includes the East Tennessee modeling domain, with the southwest corner at Universal Transverse Mercator (UTM) coordinate 3825 km Northing, 645 km Easting in zone 16. The meteorological grid extends 350 km east and 240 km north from the southwest corner, and grid points are spaced 10 km apart in both directions (Fig. A.2).

Figure A.3 shows the meteorological data stations used to construct the meteorological grid. Four rawinsonde stations [located in Nashville, Tennessee (BNA); Huntington, West

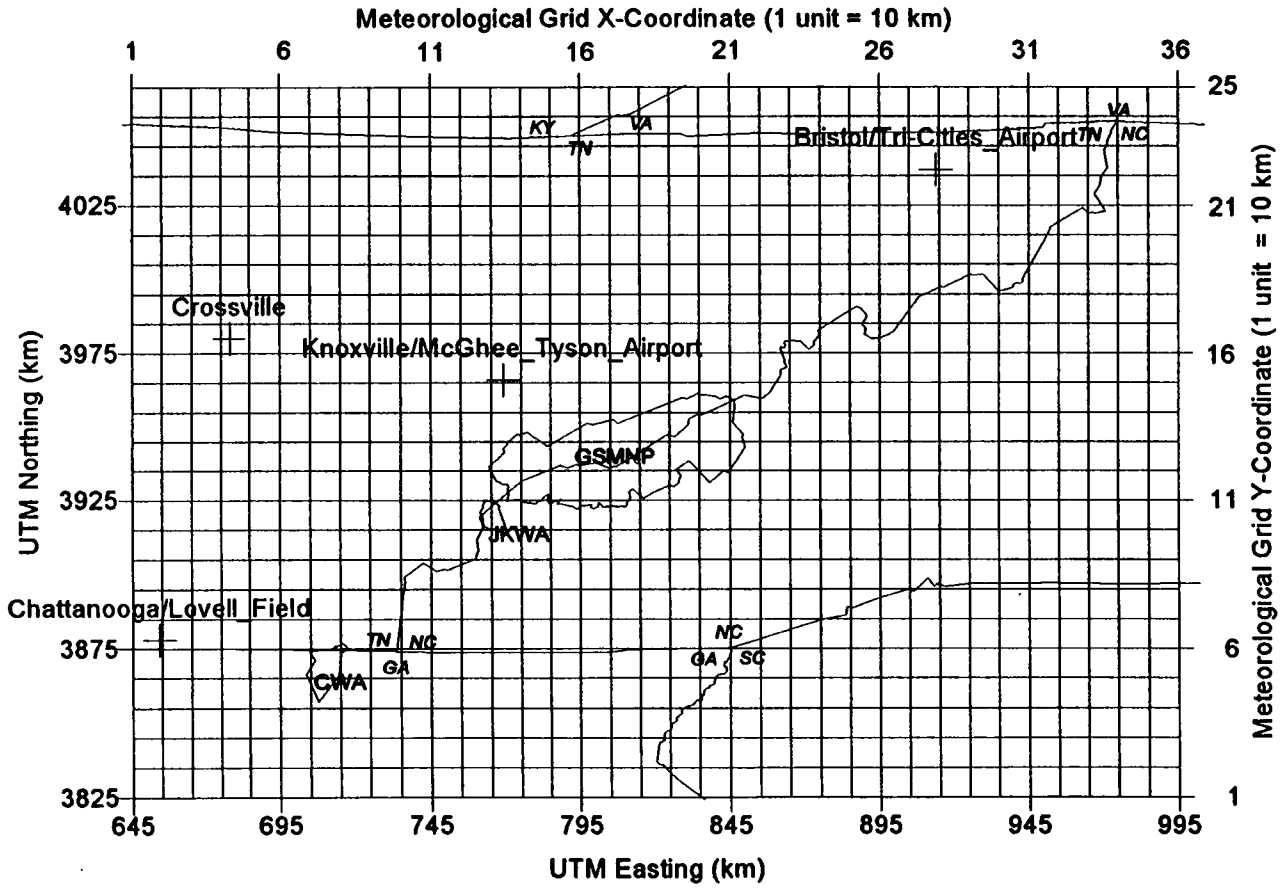

Fig. A.2. The MESOPUFF II meteorological grid defining the East Tennessee modeling domain.

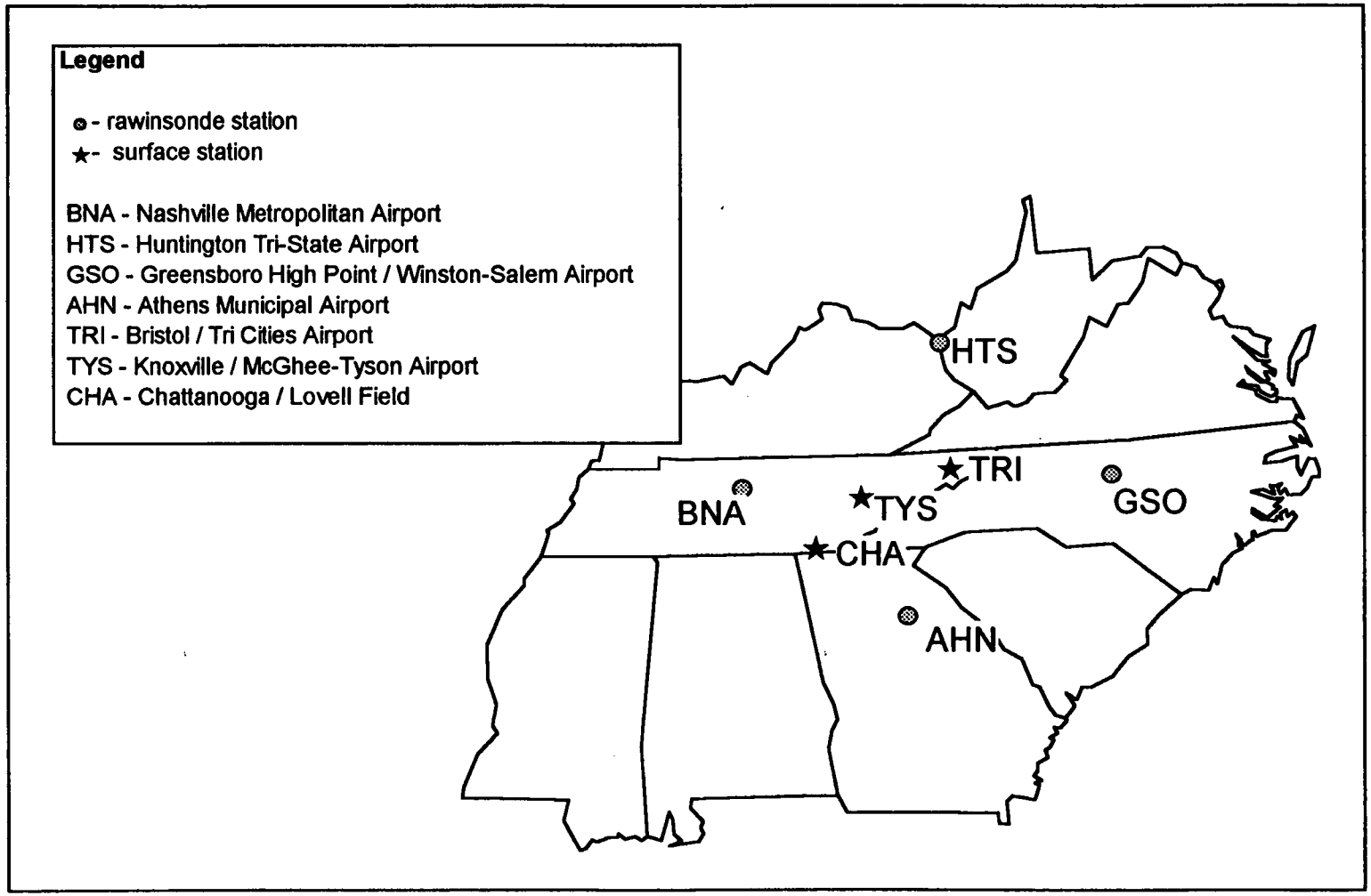

Fig. A.3. Location of rawinsonde and surface data stations used to construct the East Tennessee meteorological grid.

Virginia (HTS); Greensboro, North Carolina (GSO); and Athens, Georgia (GSO)] provided upper-air data and three surface meteorological stations [located in Tennessee at Chattanooga (CHA), Knoxville (TYS), and Bristol (TRI)] were used in developing the meteorological grid.

Table A.1 lists the meteorological data files created using MESOPAC for each month in 1990. The author named the files using the following code: xxx-MET.DAT, where xxx is the three letter month code (e.g., JAN = January and DEC = December). These files contain hourly meteorological parameters for every point in the meteorological grid. The meteorological input files occupy 26.0-28.7 MB of disk space depending on the number of days in the month.

The additional files listed in Table A.1 were also developed by the author to accompany this guide. MESOPUFF.EXE is the recompiled executable file, PUFF.INP is a sample MESOPUFF run control file, READDEP.IN and READCON.IN are run control files for the postprocessors READDEP.EXE and READCON.EXE, respectively. MAXPARK.EXE is a postprocessor which produces text files listing concentration and deposition values at receptors in the Class I areas. The application of these files is discussed in Sect. A.5.

A.3 COMPUTER SYSTEM REQUIREMENTS

Computer system requirements for running MESOPUFF are listed in Table A.2. The recompiled executable file uses extended memory management; therefore, a personal computer with at least an Intel 80386 microprocessor or equivalent is required. Just under 336 MB of storage space is consumed by one year of meteorological data input files. Additionally, MESOPUFF generates about 32-35 MB of output per simulated month to be read by postprocessors. The postprocessors create 0.5-MB concentration and deposition files for each simulated month. The total size of files required or generated in a MESOPUFF run simulating a

Table A.1. Files developed to use with MESOPUFF II for studies in the East Tennessee modeling domain

File Name	Description
MESOPUFF.EXE	MESOPUFF II Executable file recompiled using Lahey Fortran Compiler 5.20.
JAN-MET.DAT, FEB-MET.DAT, MAR-MET.DAT, APR-MET.DAT MAY-MET.DAT, JUN-MET.DAT JUL-MET.DAT, AUG-MET.DAT SEP-MET.DAT, OCT-MET.DAT NOV-MET.DAT, DEC-MET.DAT	Monthly meteorological data files for 1990. These files are to be used specifically in the East Tennessee modeling domain.
PUFF.INP	A sample MESOPUFF II run control file.
READDEP.EXE	A postprocessor used to read MESOPUFF deposition output.
READDEP.IN	A sample run control file for the READDEP postprocessor.
READCON.EXE	A postprocessor used to read MESOPUFF concentration output.
READCON.IN	A sample run control file for the READCON postprocessor.
MAXPARK.EXE	A postprocessor used to show concentration and deposition values at receptors located in the Class I areas.

Table A.2. Computer system requirements to run MESOPUFF II for the East Tennessee modeling domain

Component	Requirement
Microprocessor	Intel 80386, 80486, Pentium or compatible.
Operating system	MS-DOS Version 5.0 or higher, Windows 3.x, Windows 95, Windows NT 3.5 or higher, or OS/2 Version 2.1 or higher.
Storage space for executable, input, and output files	765 megabytes for a one-year simulation.

one-year period is about 765 MB. The large storage requirements for model input, output, and post-processed files necessitates a large hard disk (i.e., at least 850 MB of storage). For situations where multiple scenarios are run, a very large hard disk [e.g., 5-10 gigabytes (GB)] is required.

An alternative to using a large hard disk is to archive input and output files to a backup device. A one-month meteorological data file could be dearchived manually for use in MESOPUFF, and rearchived manually after use. MESOPUFF output files would be archived manually after being read by postprocessors.

A.4 SETTING UP THE MESOPUFF RUN CONTROL

The file that controls the MESOPUFF run is a text (ASCII) formatted file and can be edited using a standard text editor, such as EDIT.EXE included with MS-DOS. This run control file is formatted in the fashion of input card decks that were commonly used before the proliferation of personal computers in the mid-1980s. Each line in the run control file represents a card with the parameter values at specified locations on the line. These specified locations are

called columns, where column 1 represents the first space in the line and column 80, typically the last column allowed, is the eightieth space in the line.

Figure A.4 shows a sample MESOPUFF run control file (PUFF.INP). This input file is for a point located in Knoxville emitting 28.8 grams per second (g/s) [1000 tons per year (tpy)] of SO_2 and NO_X. The stack height is 65 m (210 ft) and stack exit parameters are set so as to virtually eliminate plume rise (i.e., the plume height is equal to the stack height). The run uses January 1990 meteorological data. A line-by-line description is provided in the following paragraphs.

		1	1	2	2	3	3	4	4	5	5	6	6	7
Column	1 5	0	5	0	5	0	5	0	5	0	5	0	5	0
Line 1	MESOPUFF II DEMO CASE - JAN 90 - POINT SOURCE AT KNOXVILLE													
Line 2	90	1	0	744	1	0	0	5	0					
Line 3	1	4	2	T	2.	T	900.							
Line 4	2	35	2	24	2	35	2	24	1					
Line 5	T	T	T	T	T									
Line 6	T	F	0	F	0	0	T	F	T	F	T	F	1	0
Line 7	000000													
Line 8	13.4 15.2	65.	0.1	0.1	273.		28.8		0.0		28.8			

Fig. A.4. Example run control file, PUFF.INP, to MESOPUFF II for the studies in the East Tennessee modeling domain.

Run control variables important for use in the East Tennessee modeling domain and their descriptions are listed in Tables A.3 through A.10. A complete description of the run control variables used in MESOPUFF is given in Table 6-9 of the *MESOPUFF II User's Guide*. Additionally, in 1993, the Interagency Working Group on Air Quality Modeling (IWAQM) published a report which specified recommended input values for the MESOPUFF run control

file[2]. These recommendations, where appropriate, have been adopted for the East Tennessee modeling domain.

The title of the MESOPUFF run is specified in input group 1, which is the first line in the run control file (Table A.3). Up to 80 alphanumeric characters are allowed for the title.

Table A.3. MESOPUFF II inputs specific for the East Tennessee modeling domain - title

Input Group 1 (Line 1) - Format 20A4

Columns	Type[a]	Variable	Description	Value
1-80	CA	TITLE	This is the title of the MESOPUFF II run. The maximum length of the title can be 80 characters.	As appropriate

Input group 2, the second line in the run control file (Table A.4), specifies the general run information, such as the time period spanned by the modeling run. For modeling in the East Tennessee domain, the model has been set up so that runs will be made in monthly increments. Therefore, twelve runs, and subsequently twelve run control files, will be required to simulate the impact of a point source over a one-year period.

Input group 3, the third line in the run control file (Table A.5), specifies the computational variables. The values for variables in input group 3 were all adopted from IWAQM recommendations.

[2]U. S. Environmental Protection Agency, *Interagency Workgroup On Air Quality Modeling (IWAQM) Phase I Report: Interim Recommendation for Modeling Long Range Transport and Impacts on Regional Visibility*, Technical Support Division (MD-14), Research Triangle Park, North Carolina, April 1993.

Table A.4 MESOPUFF II inputs specific for the East Tennessee modeling domain - general run information

Input Group 2 (Line 2) - Format 9I5

Columns	Type[a]	Variable	Description	Value
1-5	I	NSYR	Two-digit year of run.	This value should be set equal to 90 because this is the year in which the meteorological data files were created.
6-10	I	NSDAY	Starting Julian day.	The following are starting Julian days for each month for a non-leap year: Jan = 001, Feb = 032, Mar = 060, Apr = 91, May = 121, Jun = 152, Jul = 182, Aug = 213, Sep = 244, Oct = 274, Nov = 305, Dec=335.
11-15	I	NSHR	Starting hour.	This value can range from 00-23. For one month runs, NSHR = 00.
16-20	I	NADVTS	Number of hours in run.	For months with 31 days, NADVTS = 744 and for months with 30 days, NADVTS = 720. NADVTS = 672 for February.
21-25	I	NPTS	Number of point sources.	This number should not exceed 1000.
26-30	I	NAREAS	Number of area sources.	This number should not exceed 200.
31-35	I	NREC	Number of non-gridded receptors.	For this study, no non-gridded receptors were used. Non-gridded receptors may be used, but the post-processors designed specifically for the East Tennessee modeling domain will not work.
36-40	I	NSPEC	Number of chemical species to model.	NSPEC can equal 1, 2, 3, or 5. NSPEC = 1 for SO_2, NSPEC = 2 for SO_2, and SO_4^{2-}, NSPEC = 3 for SO_2, SO_4^{2-}, NO_x, and NSPEC = 5 for SO_2, SO_4^{2-}, NO_x, HNO_3, and NO_3^-.
41-45	I	ICONT	Continuation run?	0 = no and 1 = yes.

[a] I = Integer.

Table A.5. MESOPUFF II inputs specific for the East Tennessee modeling domain - computational variables

Input Group 3 (Line 3) - Format 3I5, L5, F5.1, L5, F5.0

Columns	Type[a]	Variable	Description	Value
1-5	I	IAVG	Concentration averaging time.	IAVG should be set to 1.
6-10	I	NPUF	Puff release rate (puffs/hour).	NPUF was set to 4 as recommended by the Interagency Workgroup on Air Quality Modeling (EPA 1993). To conserve storage space, NPUF may be set to 2 or 1.
11-15	I	NSAMAD	Minimum sampling rate (samples/hour).	NSAMAD should be set to 2.
16-20	L	LVSAMP	Control variable for sampling rate option.	LVSAMP should be set to T so that the puff sampling rate increases with wind speed.
21-25	R	WSAMP	Reference wind speed (m/s) used in variable sampling rate option (i.e., when LVSAMP = T).	WSAMP should be set equal to 2.
26-30	L	LSGRID	Control variable for concentration computations at sampling grid points.	LSGRID should be set to T so that concentrations are calculated at sampling grid points.
31-35	R	AGEMIN	Minimum age of puffs to be sampled (in seconds). This option eliminates near-field concentration spikes at receptors located very close to sources.	AGEMIN should be set to 900.

[a]I = Integer, L = Logical, R = Real.

Input group 4, the fourth line in the run control file (Table A.6), specifies the grid information to be used in the MESOPUFF run. Three nested grid systems are used by MESOPUFF: (1) the meteorological grid, (2) the computational grid, and (3) the sampling grid. The extent and resolution of the meteorological grid are defined as inputs to MESOPAC and are not required for the MESOPUFF run control file. However, the meteorological grid serves as the spatial reference for the two other grids, which are defined in the MESOPUFF run control files. The southwest corner of the meteorological grid is designated as $(x,y) = (1.0, 1.0)$, where 1 meteorological grid unit equals 10 km in the East Tennessee modeling domain (Fig. A.2). Puffs are advected in the computational grid. To avoid possible boundary effects, the computational grid lies one grid point away from the edges of the meteorological grid. The sampling grid defines the set of gridded receptors. For the East Tennessee modeling domain, the computational and sampling grid are the same.

Input group 5, the fifth line in the run control file (Table A.7), specifies the technical options employed by the model. These values were adopted from IWAQM recommendations.

Input group 6, the sixth line in the run control file (Table A.8), specifies the output options. Printer output should be disabled to avoid creating very large data files. Additionally, MESOPUFF has a restart option that allows large simulations to be broken into a series of manageable, smaller runs. This feature has been employed for the East Tennessee modeling domain, where a run for the entire year has been broken into twelve smaller monthly runs. The restart feature, which is set in input group 6, should be specified for all months except December.

Table A.6. MESOPUFF II inputs specific for the East Tennessee modeling domain - grid information

Input Group 4 (Line 4) - Grid Information (Format 9I5)

Columns	Type[a]	Variable	Description	Value
1-5	I	IASTAR	Element number of the meteorological grid defining the beginning of the computational grid in the x-direction.	IASTAR should be set to 2.
6-10	I	IASTOP	Element number of the meteorological grid defining the end the computational grid in the x-direction.	IASTOP should be set to 35.
11-15	I	JASTAR	Element number of the meteorological grid defining the beginning of the computational grid in the y-direction.	JASTAR should be set to 2.
16-20	I	JASTOP	Element number of the meteorological grid defining the end of the computational grid in the y-direction.	JASTOP should be set to 24.
21-25	I	ISASTR	Element number of the meteorological grid defining the beginning of the sampling grid in the x-direction.	ISASTR should be set to 2.
26-30	I	ISASTP	Element number of the meteorological grid defining the end of the sampling grid in the x-direction.	ISASTP should be set to 35.
31-35	I	JSASTR	Element number of the meteorological grid defining the beginning of the sampling grid in the y-direction.	JSASTR should be set to 2.
36-40	I	JSASTP	Element number of the meteorological grid defining the end of the sampling grid in the y-direction.	JSASTP should be set to 24.
41-45	I	MESHDN	Sampling spacing factor.	MESHDN should be set to 1.

Table A.7 MESOPUFF II inputs specific for the East Tennessee modeling domain - technical options

Input Group 5 (Line 5) - Format 5L5

Columns	Type[a]	Variable	Description	Value
1-5	L	LGAUSS	Vertical concentration distribution option.	LGAUSS should be set to T so that a Gaussian vertical concentration distribution with reflection terms is assumed for each puff.
6-10	L	LCHEM	Chemical transformation option.	LCHEM should be set to T so that chemical transformation processes are modeled as necessary for deposition calculations.
11-15	L	LDRY	Dry deposition option.	LDRY should be set to T.
16-20	L	LWET	Wet removal option.	LWET should be set to T.
21-25	L	L3VL	Three vertical layer deposition option.	L3VL should be set to T so that the 3-layer deposition model is used for puffs that have been mixed uniformly in the vertical.

[a]L = Logical.

Table A.8. MESOPUFF II inputs specific for the East Tennessee modeling domain - output options

Input Group 6 (Line 6) - Format 2L5, I5, L5, 2I5, 6L5, 2I5

Columns	Type[a]	Variable	Description	Value
1-5	L	LSAVE	Disk output control variable.	LSAVE should be set to T.
6-10	L	LPRINT	Printer output control variable.	LPRINT should be set to F.
11-15	I	IPRINF	Printing interval (in hours) of concentrations if LPRINT = T.	IPRINF should be set to 0.
16-20	L	LDB	Control variable for printing of computed puff data.	LDB should be set to F.
21-25	I	NN1	Time step of printing intermediate puff data begins.	NN1 should be set to 0.
26-30	I	NN2	Time step of printing intermediate puff data ends.	NN2 should be set to 0.
31-35	L	LWETG	Wet flux control variable for gridded receptors.	LWETG should be set to T.
36-40	L	LWETNG	Wet flux control variable for non-gridded receptors.	LWETNG should be set to F unless non-gridded receptors are used.
41-45	L	LDRYG	Dry flux control variable for gridded receptors.	LDRYG should be set to T.
46-50	L	LDRYNG	Dry flux control variable for non-gridded receptors.	LDRYNG should be set to F unless non-gridded receptors are used.
51-55	L	LSAVEF	Disk output control variable for fluxes.	LSAVEF should be set to T.
56-60	L	LPRFLX	Printer output control variables for fluxes.	LPRFLX should be set to F.
61-65	I	IRES	Save results for restart option.	IRES should be set to 1 for all monthly runs except December.
66-70	I	IINT	Frequency (in hours) of restart.	IINT should be set to 0 so that only the last hour of the run is saved for restart.

[a]I = Integer, L = Logical.

Input Group 7, the seventh line in the run control file (Table A.9), specifies the default override options. The IWAQM recommends that none of the defaults should be overridden and all of these run control variables should be set to 0. Because defaults are not to be overridden, input groups 8 through 13 do not need to be entered into the run control file.

The last line in the run control file is input group 14 (Table A.10), which specifies the point source data. This line is repeated for each point source in the modeling run. Note that coordinates for point sources must be in meteorological grid units (e.g., 13.4 = 13.4 grid units = 134 km east of 645 km Easting).

Table A.9. MESOPUFF II inputs specific for the East Tennessee modeling domain - default override options

Input Group 7 (Line 7) - Format 2L5, I5, L5, 2I5, 6L5, 2I5

Columns	Type[a]	Variable	Description	Value
1	IAE	IOPTS(1)	Control variable for input of dispersion parameters.	IOPTS(1) should be set to 0 (i.e., default option is used).
2	IAE	IOPTS(2)	Control variable for input of vertical diffusivity constants.	IOPTS(2) should be set to 0 (i.e., default option is used).
3	IAE	IOPTS(3)	Control variable for input of SO_2 canopy resistances.	IOPTS(3) should be set to 0 (i.e., default option is used).
4	IAE	IOPTS(4)	Control variable for input of dry deposition parameters.	IOPTS(4) should be set to 0 (i.e., default option is used).
5	IAE	IOPTS(5)	Control variable for input of wet removal parameters.	IOPTS(5) should be set to 0 (i.e., default option is used).

Table A.10. MESOPUFF II inputs specific for the East Tennessee modeling domain - point source data

Input Group 14 (Line 8) - Point Source Data (Format 2F2.5, F5.1, 2F5.2, F5.1, 5F10.2)				
Columns	Type[a]	Variable	Description	Value
1-5	RAE	XSTAK	X-coordinate of point source in meteorological grid units.	Coordinates should be converted from UTM to meteorological grid coordinates. The southwest corner of the meteorological grid is at UTM coordinates 645 km Easting, 3824 km Northing which equals coordinates 1, 1 in meteorological grid units.
6-10	RAE	YSTAK	Y-coordinate of point source in meteorological grid units.	
11-15	RAE	HTSTAK	Stack height in meters.	As appropriate.
16-20	RAE	D	Stack diameter in meters.	As appropriate.
21-25	RAE	W	Exit velocity in meters per second.	As appropriate.
26-30	RAE	TSTAK	Stack gas exit temperature in Kelvins.	As appropriate.
31-80	RAE	EMIS	Emission rate, in grams per second for pollutants 1-5.	The SO_2 and NO_x emission rates should be entered in columns 31-40 and 51-60, respectively. For the others the emission rate is 0.

[a]RAE = Real Array Element.

A.5 PERFORMING A MESOPUFF RUN

Three input files are required to perform a MESOPUFF run:

1. PUFF.INP, the run control file described in Sect. A.4, above;
2. PACOUT.DAT, the meteorological data file created by MESOPAC; and
3. PREVIOUS.DAT, the restart file, which allows a run to be continued from a previous run (note that PREVIOUS.DAT will not be required for the January run).

These files must be located in the same directory as the executable file, MESOPUFF.EXE. If MESOPUFF runs are made in monthly segments, the meteorological data file for the month being modeled should be copied into the MESOPUFF directory and renamed PACOUT.INP. It is recommended that all run control files be prepared at the same time for improved accuracy and efficiency. If this is done, the run control for the month being modeled must be copied into the MESOPUFF directory and renamed PUFF.INP.

MESOPUFF creates the following output files:

1. PUFF.LST, a text file that contains general information on the MESOPUFF run;
2. PUFFOUT.DAT, an unformatted file containing gridded concentrations for each hour;
3. FLUXWET.DAT, an unformatted file containing gridded wet fluxes for each hour;
4. FLUXDRY.DAT, an unformatted file containing gridded dry fluxes for each hour; and
5. RESTART.DAT, an unformatted file containing restart information allowing the run to be continued.

These files (except RESTART.DAT) must be copied into another directory and renamed (e.g., JAN-CON.DAT, for the January concentration data) at the end of each monthly run segment for postprocessing. Additionally, RESTART.DAT should be renamed PREVIOUS.DAT before starting the next month's run.

With one point source, the time required for a one-month MESOPUFF run ranges from 46 to 210 minutes using a 486/66MHz processor. The summer and fall months require the greatest run times, and the winter and spring months require the shortest run times. The total time required for a one-year simulation is almost 24 hours, including running the model, and copying files into and renaming files in the MESOPUFF directory. An MS-DOS batch file can be used to automate these tasks.

A.6 RUNNING THE POSTPROCESSORS

The concentration files and wet and dry flux files created as output by MESOPUFF are unformatted; therefore, postprocessors are required to convert the data in these files to text format. A postprocessor, MESOFILE II, is available with the MESOPUFF model on the SCRAM BBS. MESOFILE II requires a complex command input file to produce wet and dry deposition and concentration output in the format desired by the user. Because of the complexity of MESOFILE II, the author developed two much simpler postprocessors specifically designed for use in the East Tennessee modeling domain. Two postprocessors, called READEP and READCON, produce deposition (wet, dry and total) and concentration data files in text format. These postprocessors will only work when modeling all five chemical species. A third postprocessor, MAXPARK, produces text files showing deposition and concentration values at receptors located in the Class I areas.

A.6.1 READDEP

READDEP reads the wet and dry flux output files produced by MESOPUFF and calculates the deposition over the time period of the run (e.g., one month) for the pollutants

modeled (e.g., SO_2, SO_4^{2-}, NO_x, HNO_3, and NO_3^-). Deposition is calculated at each grid point in the East Tennessee modeling domain in units of kilograms of pollutant per hectare (kg/ha).

READDEP requires a run control file, READDEP.IN, which specifies the names of the wet and dry flux files output from MESOPUFF that are to be read by the postprocessor, as well as the user-specified names of the text-formatted deposition files created by the postprocessor. Figure A.5 shows an example of the run control file used to process a December run. Table A.11 lists the required inputs and format of READDEP.IN.

```
                1   1   2   2   3   3   4   4   5   5   6   6   7
Column 1    5   0   5   0   5   0   5   0   5   0   5   0   5   0
Line 1  DEC-DRY.DAT  DEC-WET.DAT     DECD.OUT     DECW.OUT     DECT.OUT
Line 2  DECSO2T.DAT  DECSO4T.DAT  DECNOXT.DAT  DECHNO3T.DAT  DECNO3T.DAT
```

Fig. A.5. Example run control file to READDEP, called READDEP.IN.

The user specifies the names of the wet and dry flux files produced by MESOPUFF on line 1 of READDEP.IN. MESOPUFF calls the wet and dry flux files, FLUXWET.DAT and FLUXDRY.DAT, respectively. However, a user who makes multiple MESOPUFF runs simulating a one-year period may copy and rename the FLUXWET.DAT and FLUXDRY.DAT files after each monthly run segment into another directory (e.g., for a January run, the user would rename FLUXWET.DAT and FLUXDRY.DAT to JAN-WET.DAT and JAN-DRY.DAT, respectively). The file names produced by READDEP that summarize deposition of all

Table A.11. Inputs specified in the READDEP run control file, READDEP.IN

Line 1 - Input and Output Files (Format 1X, A12, 1X, A12, 1X, A12, 1X, A12, 1X)

Columns	Type	Variable	Description
2-13	Character	FNAME5	The unformatted dry flux MESOPUFF II output file to be read by READDEP.
15-26	Character	FNAME6	The unformatted wet flux MESOPUFF II output file to be read by READDEP.
28-39	Character	FNAME7	The text-formatted dry deposition summary output file produced by READDEP.
41-52	Character	FNAME8	The text-formatted wet deposition summary output file produced by READDEP.
54-65	Character	FNAME9	The text-formatted total (wet + dry) deposition summary output file produced by READDEP.

Line 2 - Pollutant-Specific Output Files (Format 1X, A12, 1X, A12, 1X, A12, 1X, A12, 1X)

Columns	Type	Variable	Description
2-13	Character	FNAME10	The text-formatted total (wet + dry) SO_2 deposition output file produced by READDEP.
15-26	Character	FNAME11	The text-formatted total (wet + dry) SO_4^{2-} deposition output file produced by READDEP.
28-39	Character	FNAME12	The text-formatted total (wet + dry) NO_x deposition output file produced by READDEP.
41-52	Character	FNAME13	The text-formatted total (wet + dry) HNO_3 deposition output file produced by READDEP.
54-65	Character	FNAME14	The text-formatted total (wet + dry) NO_3^- deposition output file produced by READDEP.

pollutants at each grid point are also specified on line 1 of the run control file. Three deposition files are created by the post processor: one that lists dry deposition, one that lists wet deposition, and one that lists total (wet + dry) deposition. Deposition data are arranged in three columns, with columns 1 and 2 specifying the location of the grid point in UTM coordinates Easting km and Northing km, respectively, and column 3 containing the deposition value at that grid point in kg/ha.

Individual total deposition files for each pollutant are also created by READDEP and are specified in line 2 of the run control file. These files repeat the information found in the total deposition file defined in line 1, but a separate filename is assigned for each pollutant, and no header information is included in the file. This eases data import into a contour plotting program, such as SURFER. Data are organized in three columns as described above.

A.6.2 READCON

READCON reads the concentration output file that is produced by MESOPUFF and calculates maximum and average concentrations over the time period of the run (e.g., one month) for the pollutants modeled (e.g., SO_2, SO_4^{2-}, NO_x, HNO_3, and NO_3^-). Maximum 3-h and 24-h average concentrations are calculated at each grid point in the East Tennessee modeling domain for SO_2, and maximum 1-h average concentrations are calculated at each grid point for SO_4^{2-}, NO_x, HNO_3, and NO_3^-. Concentrations are calculated in units of micrograms of pollutant per cubic meter of air ($\mu g/m^3$).

READCON requires a run control file, READCON.IN, which specifies the name of the concentration file output from MESOPUFF to be read by the postprocessor, as well as the names of the text-formatted concentration files created by the postprocessor. Figure A.6 shows an

```
                1   1   2   2   3   3   4   4   5   5   6   6   7
Column 1   5    0   5   0   5   0   5   0   5   0   5   0   5   0
Line 1   DEC-CON.DAT      DECC.OUT
Line 2  DECSO203.DAT DECSO224.DAT  DECSO2P.DAT
Line 3   DECSO41.DAT  DECSO4P.DAT
Line 4   DECNOX1.DAT  DECNOXP.DAT
Line 5  DECHNO31.DAT DECHNO3P.DAT
Line 6   DECNO31.DAT  DECNO3P.DAT
```

Fig. A.6. Example run control file to READCON, called READCON.IN.

example of the run control file for a December run. Table A.12 lists the required inputs and format of READCON.IN.

The run control file for READCON is very similar to that used by READDEP. The user specifies the names of the concentration file produced by MESOPUFF on line 1 of READCON.IN. MESOPUFF calls the concentration file PUFFOUT.DAT. However, a user who makes multiple MESOPUFF runs simulating a one-year period may copy and rename PUFFOUT.DAT into another directory after each monthly run segment (e.g., for a January run, the user would rename PUFFOUT.DAT to JAN-CON.DAT).

The name of the text-formatted file produced by READCON that summarizes concentration values of all pollutants over various averaging times is also specified on line 1 of the run control file. In addition, individual concentration files for each pollutant are created by READCON and are specified in lines 2-6 of the run control file. These files repeat the information found in the summary concentration file defined in line 1, but a separate filename is assigned for each pollutant, and no header information is included in these files. This eases data import into a contour plotting program, such as SURFER. In all of these files, concentration data are arranged in three columns, with columns 1 and 2 specifying the location of the grid point in

Table A.12. Inputs specified in the READCON run control file, READCON.IN

Line 1 - Input and Output Files (Format 1X, A12, 1X, A12)

Columns	Type	Variable	Description
2-13	Character	FNAME5	The unformatted concentration MESOPUFF II output file to be read by READCON.
15-26	Character	FNAME6	The text-formatted concentration summary output file produced by READCON.

Line 2 - SO_2 Output Files (Format 1X, A12, 1X, A12, 1X, A12)

28-39	Character	FNAME7	The text-formatted maximum 3-h average SO_2 concentration.
41-52	Character	FNAME8	The text-formatted maximum 24-h average SO_2 concentration.
54-65	Character	FNAME9	The text-formatted average period SO_2 concentration file.

Line 3 - SO_4^{2-} Output Files (Format 1X, A12, 1X, A12)

Columns	Type	Variable	Description
2-13	Character	FNAME10	The text-formatted maximum 1-h average SO_4^{2-} concentration.
15-26	Character	FNAME11	The text-formatted average period SO_4^{2-} concentration file.

Line 4 - NO_x Output Files (Format 1X, A12, 1X, A12)

Columns	Type	Variable	Description
2-13	Character	FNAME12	The text-formatted maximum 1-h average NO_x concentration.
15-26	Character	FNAME13	The text-formatted average period NO_x concentration file.

Line 5 - HNO_3 Output Files (Format 1X, A12, 1X, A12)

Columns	Type	Variable	Description
2-13	Character	FNAME14	The text-formatted maximum 1-h average HNO_3 concentration.
15-26	Character	FNAME15	The text-formatted average period HNO_3 concentration file.

Line 6 - NO_3^- Output Files (Format 1X, A12, 1X, A12)

Columns	Type	Variable	Description
2-13	Character	FNAME16	The text-formatted maximum 1-h average NO_3^- concentration.

UTM coordinates, Easting km and Northing km, respectively, and column 3 containing the concentration value at that grid point (in $\mu g/m^3$).

A.6.3 MAXPARK

MAXPARK reads the text files produced by READDEP and READCON and produces text files that show the deposition and concentration values in the Great Smoky Mountains National Park, and Joyce Kilmer and Cohutta Wilderness Areas. As with READDEP and READCON, data are arranged in three columns, with columns 1 and 2 specifying the location of the Class I area receptor in UTM coordinates, in Easting (km) and Northing (km), respectively, and column 3 containing the deposition or concentration value. The maximum value is also printed in the output file for each of the three Class I areas.

The program is run at the MS-DOS prompt in the following fashion:

```
c:\dirname> MAXPARK  filename.in  filename.out
```

where, dirname is the name of the directory that contains MAXPARK.EXE; the input file, filename.in; and the output file, filename.out. MAXPARK does not identify the difference between concentration and deposition values. Therefore, the user should carefully name output files so that concentration and deposition data are not confused.

APPENDIX B
ANNUAL DEPOSITION CONTOUR MAPS

The following figures are contour maps of annual deposition in the East Tennessee modeling domain. One contour map for each of the four hypothetical source locations has been generated for each of the pollutant forms as follows: (1) total dry sulfur deposition (Figs. B.1 through B.4) , (2) total wet sulfur deposition (Figs. B.5 through B.8), (3) total dry nitrogen deposition (Figs. B.9 through B.12) and (4) total wet nitrogen deposition (Figs. B.13 through B.16).

The following abbreviations are used on the contour maps:

GSMNP	=	The Great Smoky Mountains National Park
JKWA	=	Joyce Kilmer Wilderness Area
CWA	=	Cohutta Wilderness Area
TN	=	Tennessee
NC	=	North Carolina
GA	=	Georgia
VA	=	Virginia
KY	=	Kentucky
UTM	=	Universal Transverse Mercator

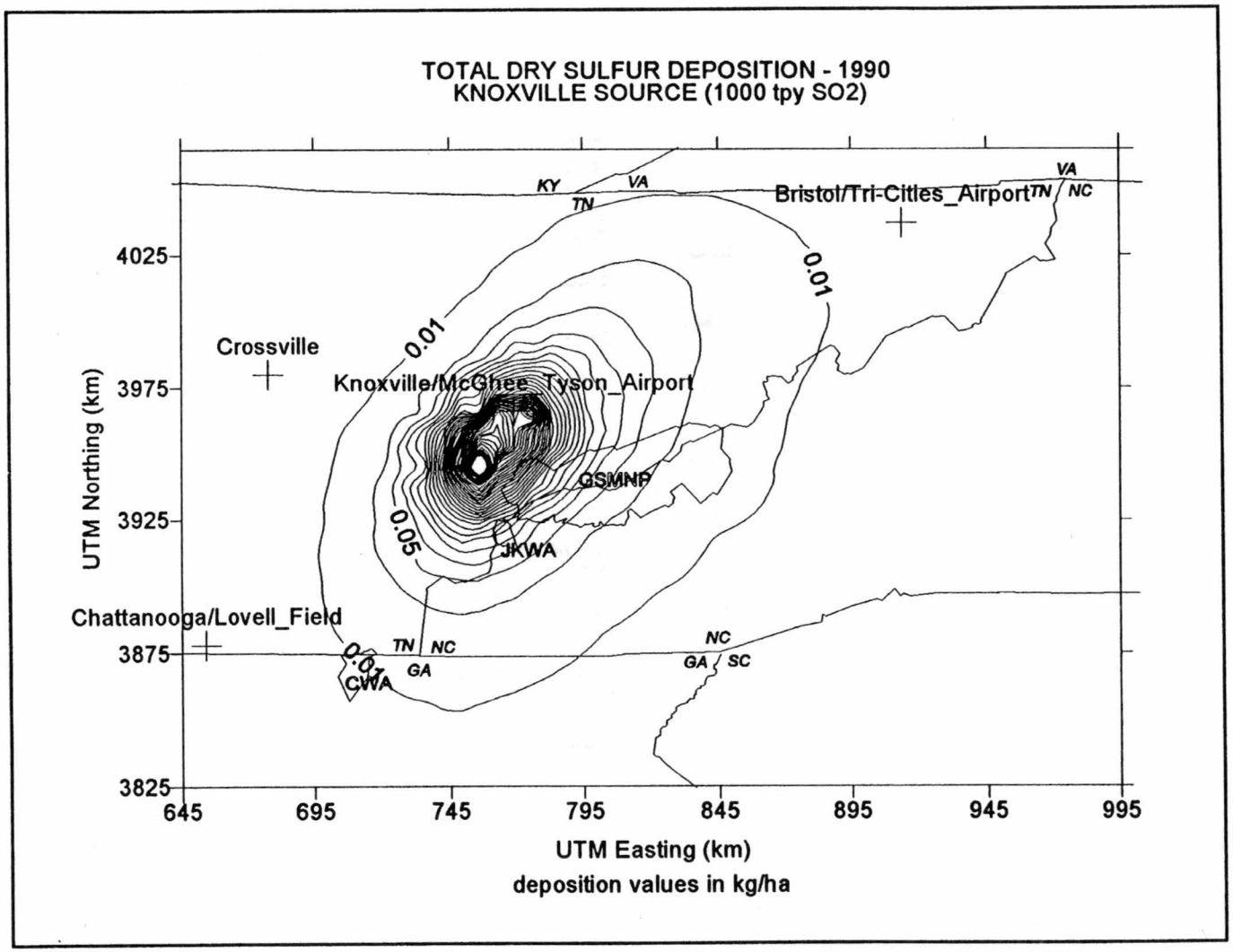

Fig. B.1. Total annual dry sulfur deposition estimated for 1990 resulting from a hypothetical 28.8 g/s (1000 tpy) SO_2 emission source located at Knoxville/McGhee Tyson Airport.

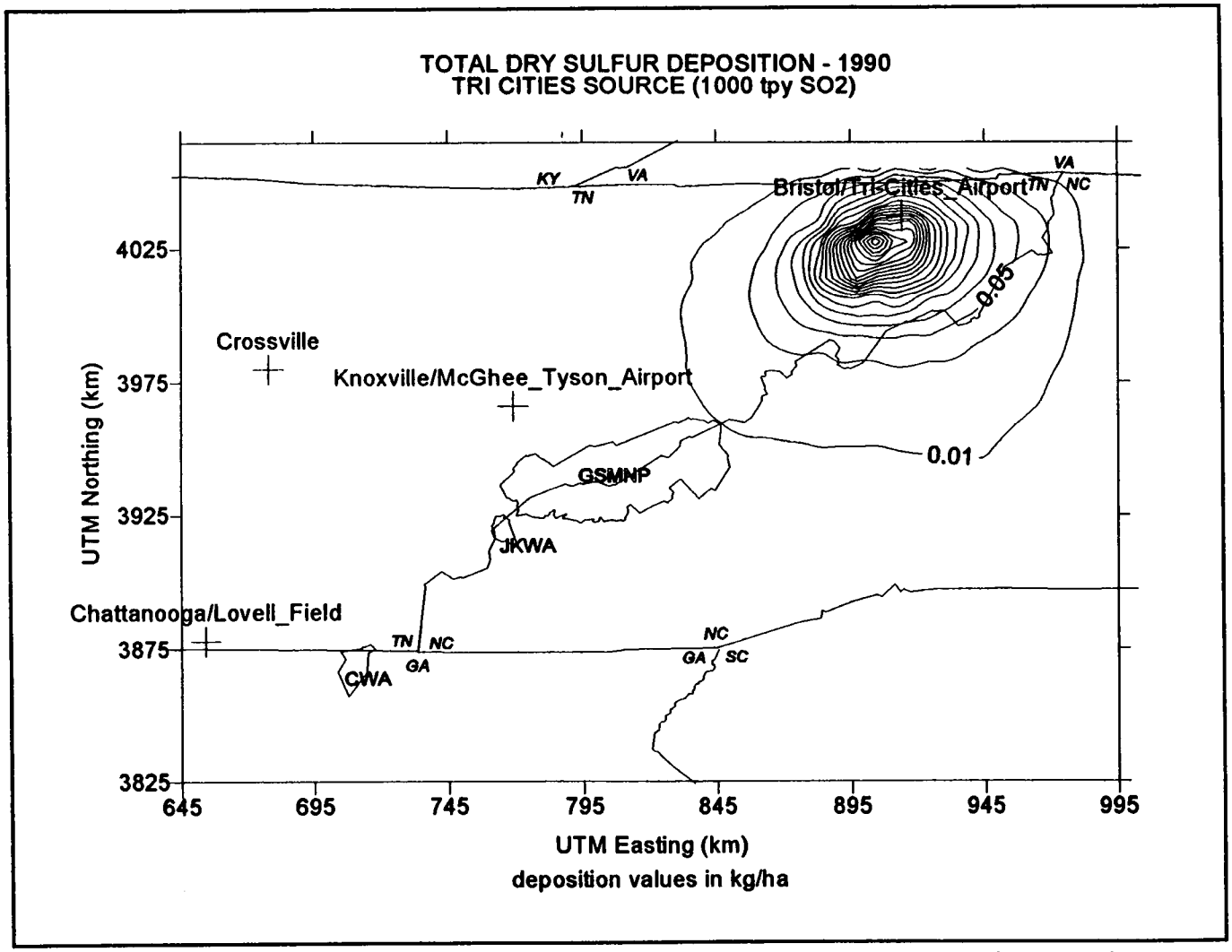

Fig. B.2. Total annual dry sulfur deposition estimated for 1990 resulting from a hypothetical 28.8 g/s (1000 tpy) SO_2 emission source located at Bristol/Tri Cities Airport.

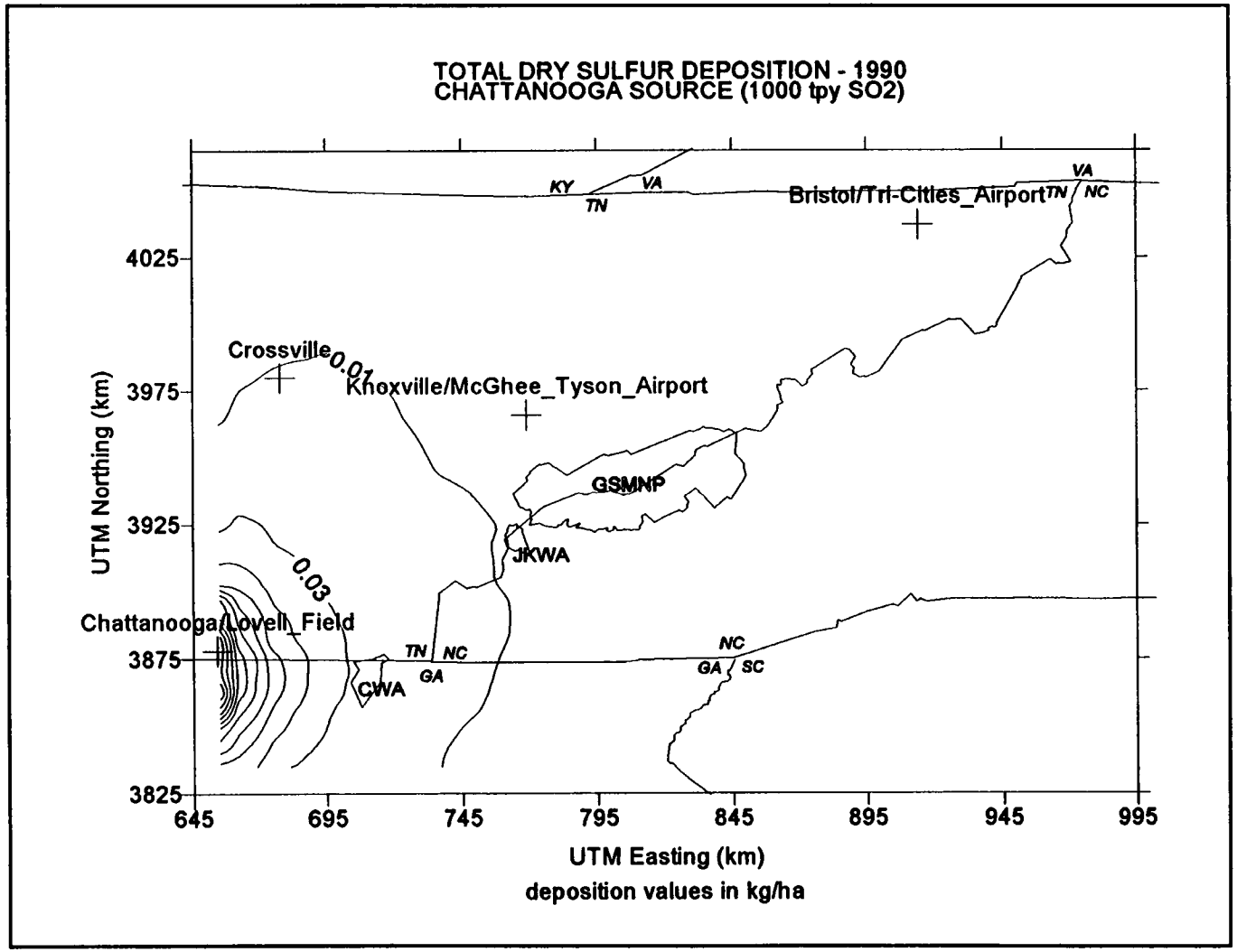

Fig. B.3. Total annual dry sulfur deposition estimated for 1990 resulting from a hypothetical 28.8 g/s (1000 tpy) SO_2 emission source located at Chattanooga/Lovell Field.

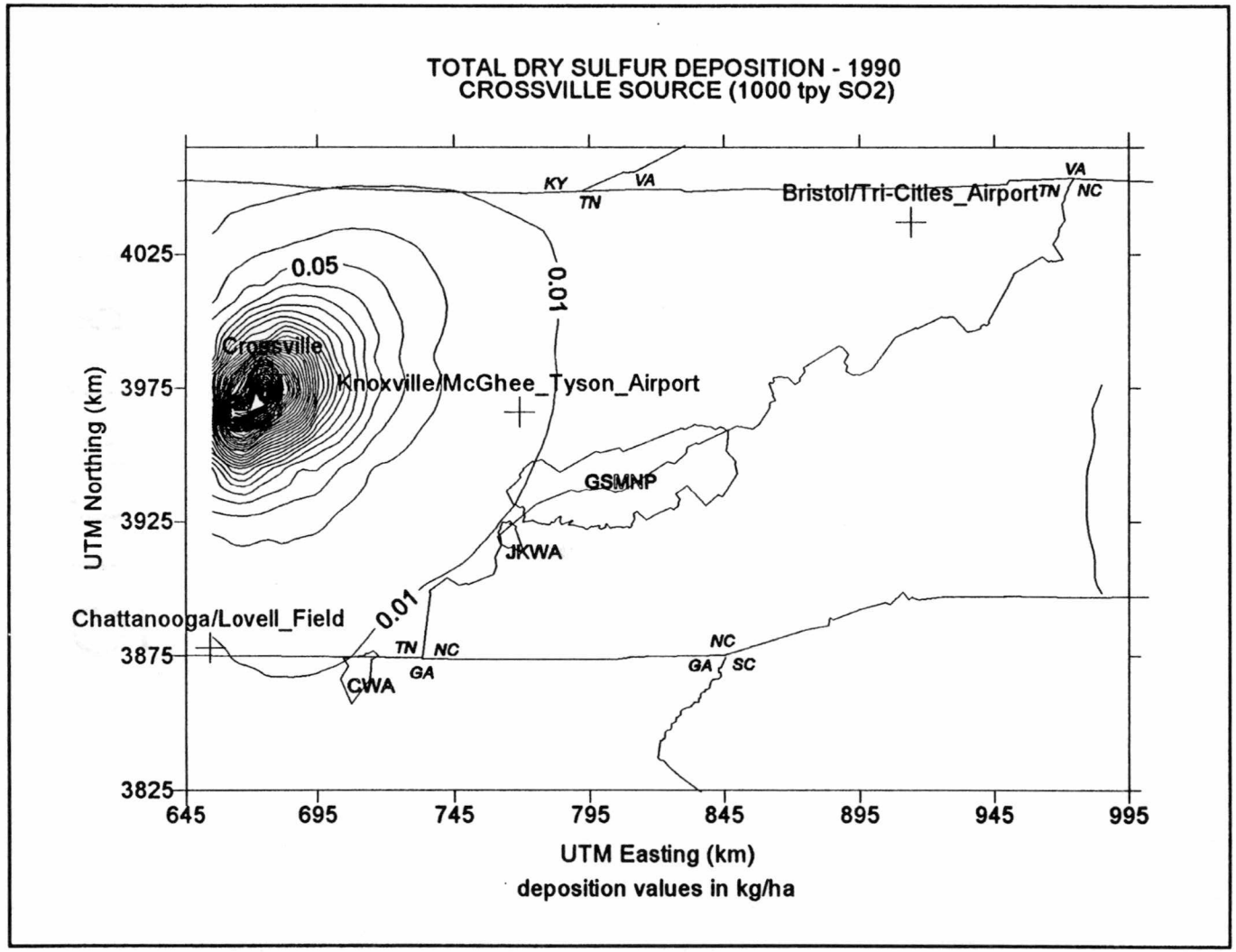

Fig. B.4. Total annual dry sulfur deposition estimated for 1990 resulting from a hypothetical 28.8 g/s (1000 tpy) SO_2 emission source located in Crossville.

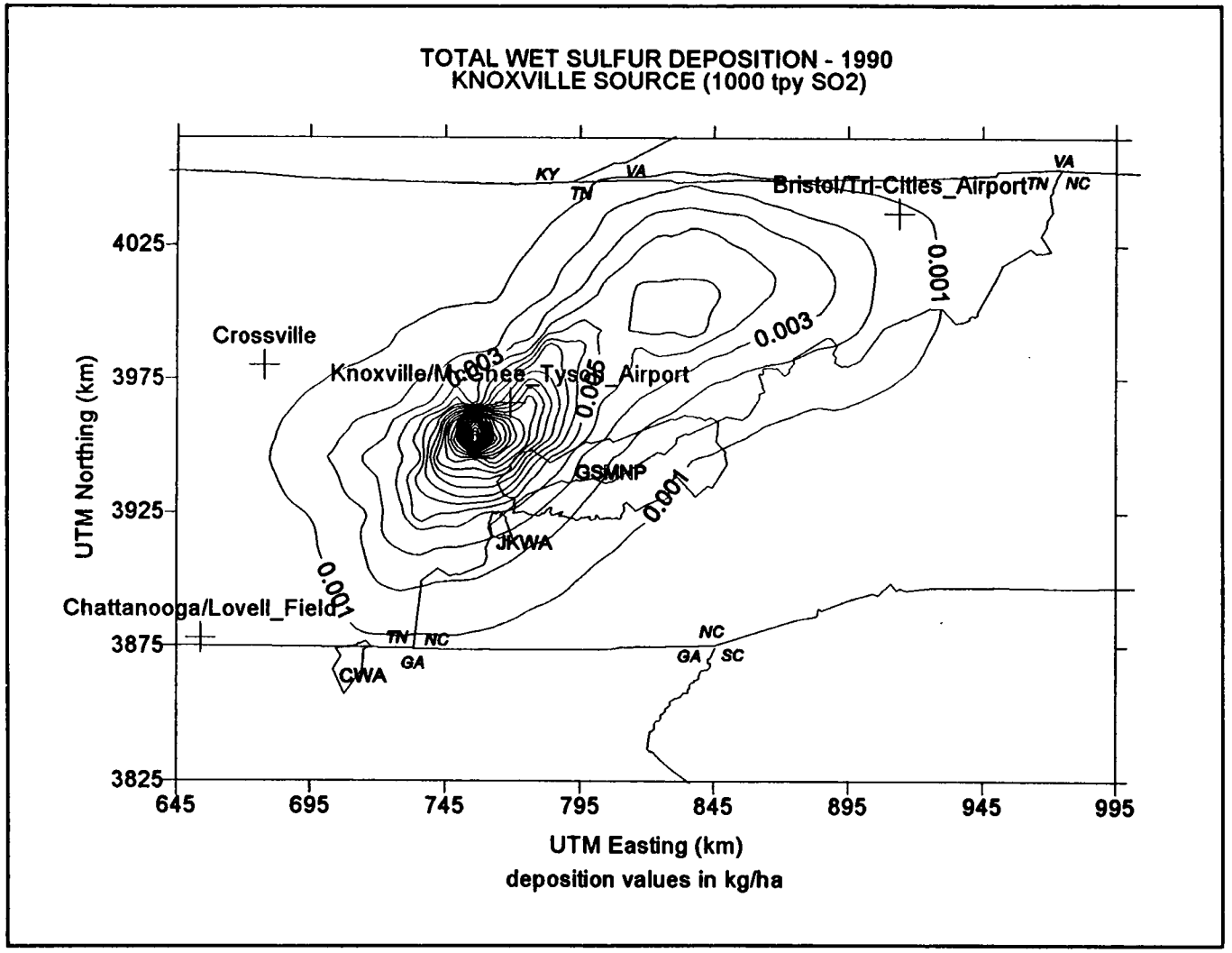

Fig. B.5. Total annual wet sulfur deposition estimated for 1990 resulting from a hypothetical 28.8 g/s (1000 tpy) SO_2 emission source located at Knoxville/McGhee Tyson Airport.

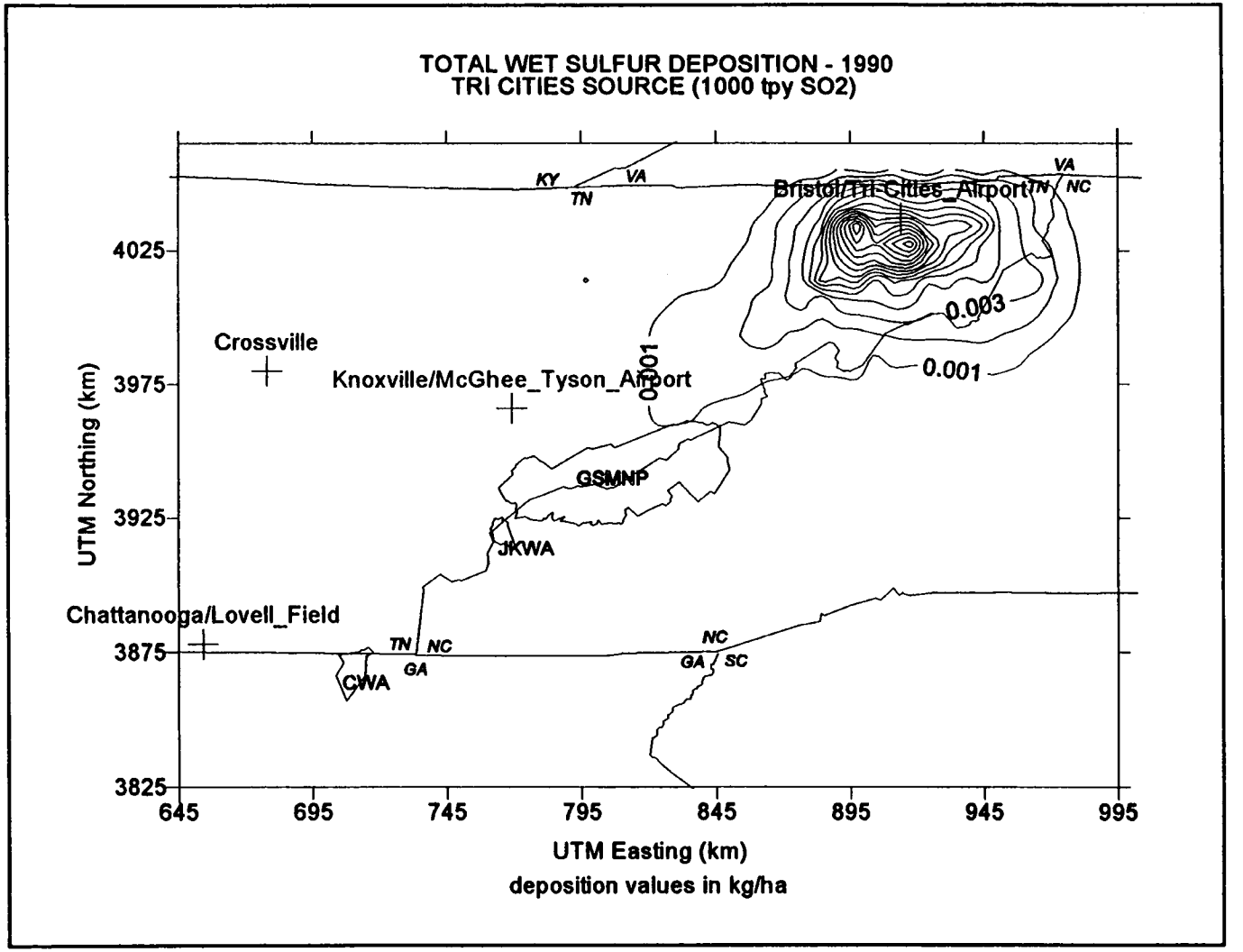

Fig. B.6. Total annual wet sulfur deposition estimated for 1990 resulting from a hypothetical 28.8 g/s (1000 tpy) SO_2 emission source located at Bristol/Tri Cities Airport.

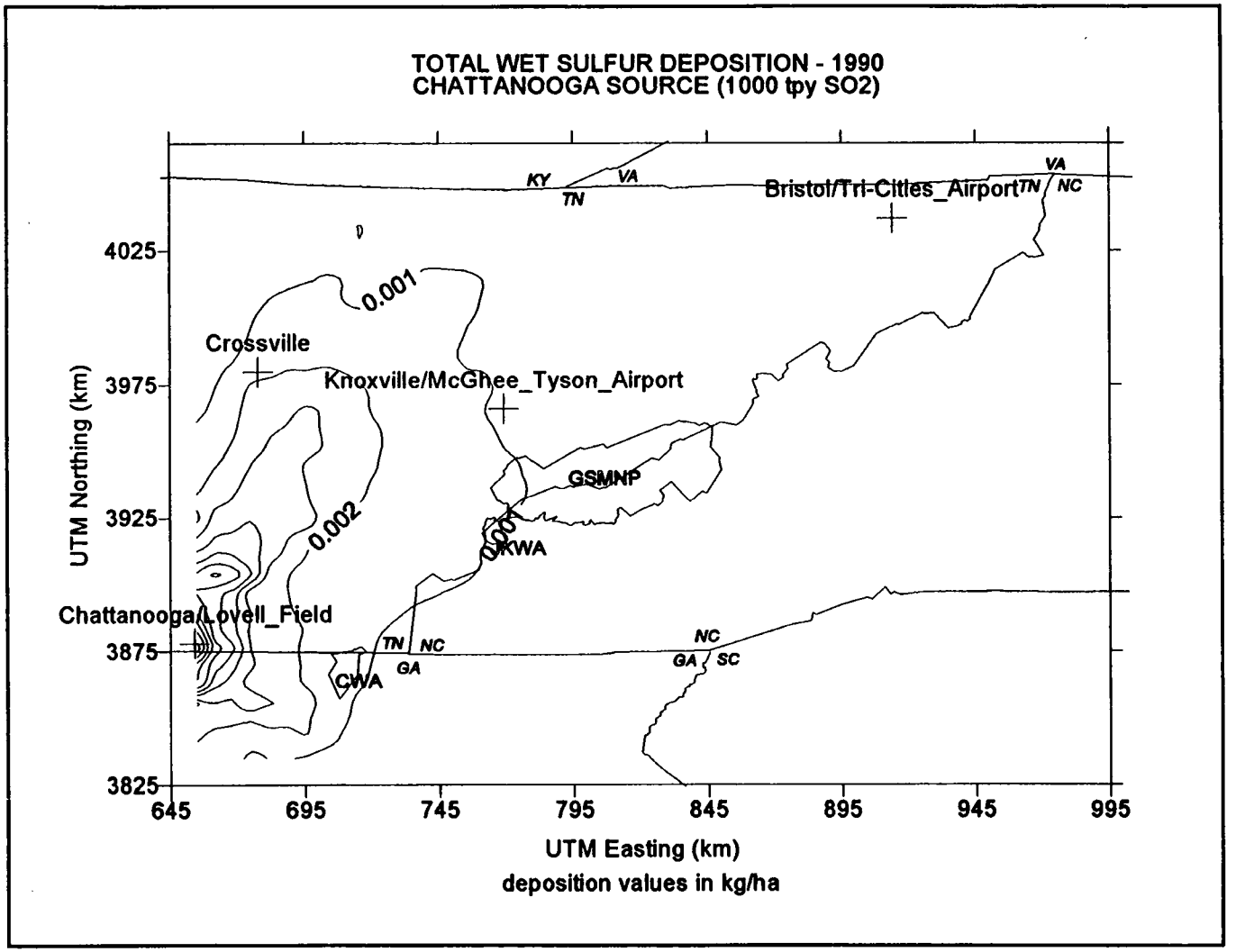

Fig. B.7. Total annual wet sulfur deposition estimated for 1990 resulting from a hypothetical 28.8 g/s (1000 tpy) SO_2 emission source located at Chattanooga/Lovell Field.

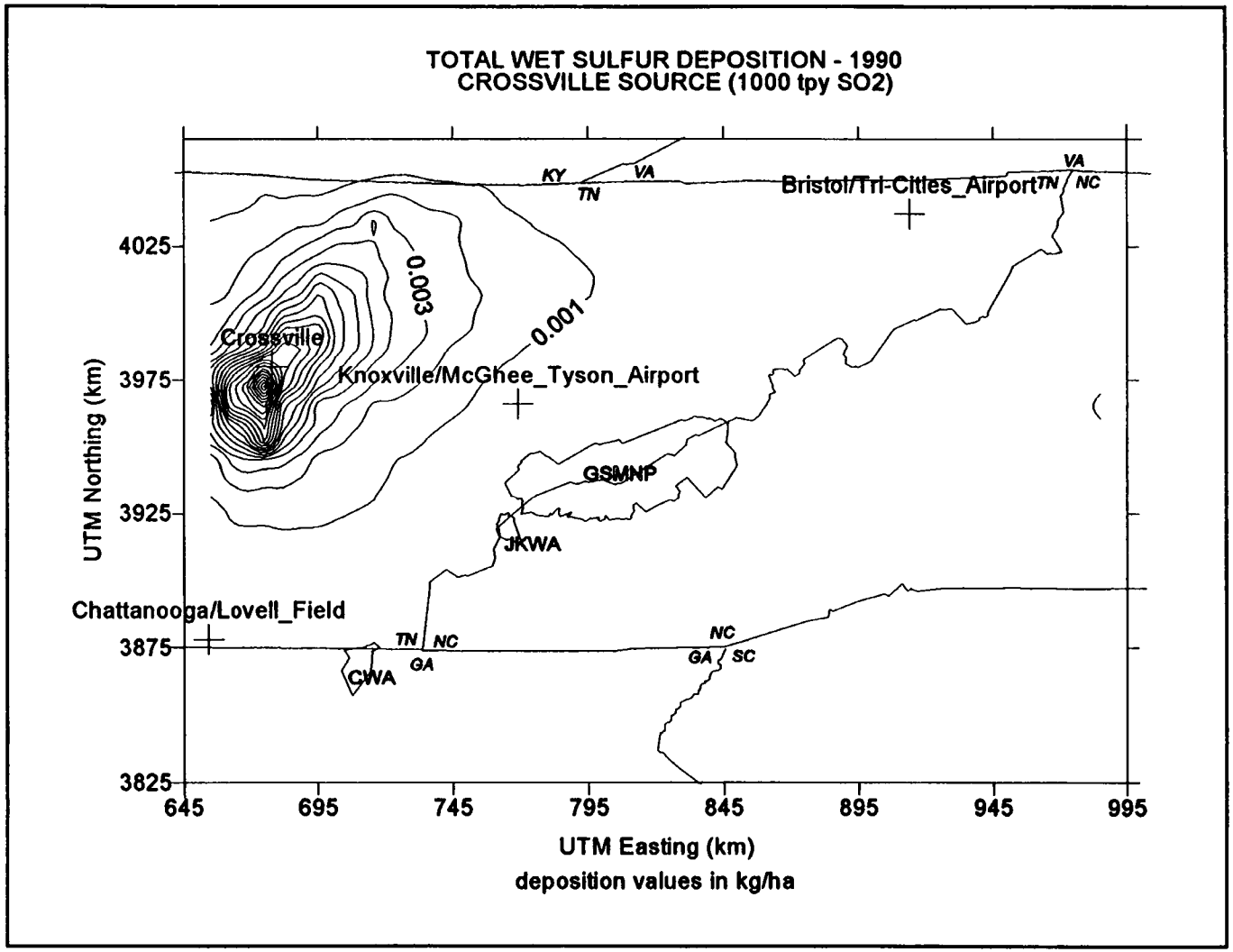

Fig. B.8. Total annual wet sulfur deposition estimated for 1990 resulting from a hypothetical 28.8 g/s (1000 tpy) SO_2 emission source located in Crossville.

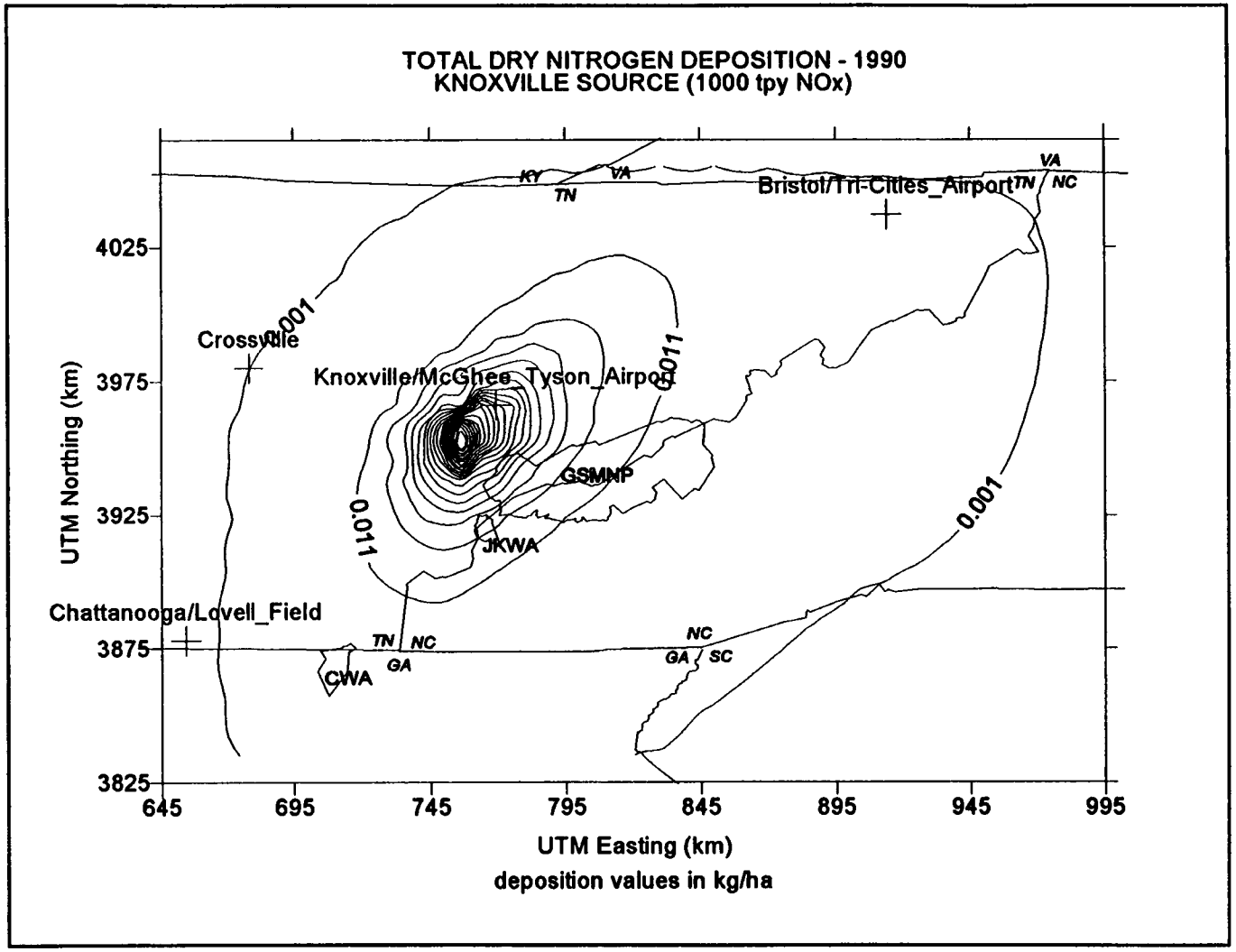

Fig. B.9. Total annual dry nitrogen deposition estimated for 1990 resulting from a hypothetical 28.8 g/s (1000 tpy) NO_x emission source located at Knoxville/McGhee Tyson Airport.

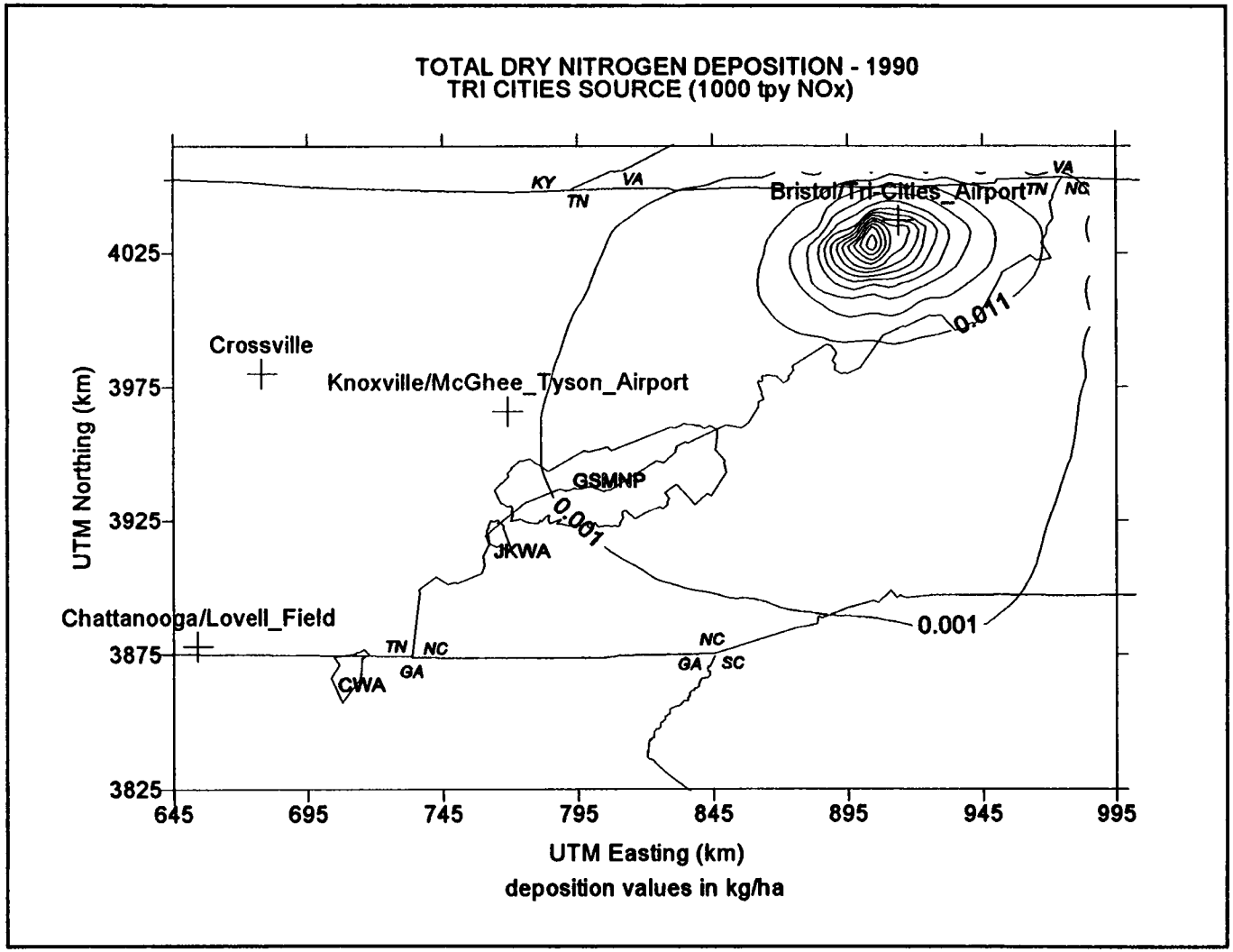

Fig. B.10. Total annual dry nitrogen deposition estimated for 1990 resulting from a hypothetical 28.8 g/s (1000 tpy) NO_x emission source located at Bristol/Tri Cities Airport.

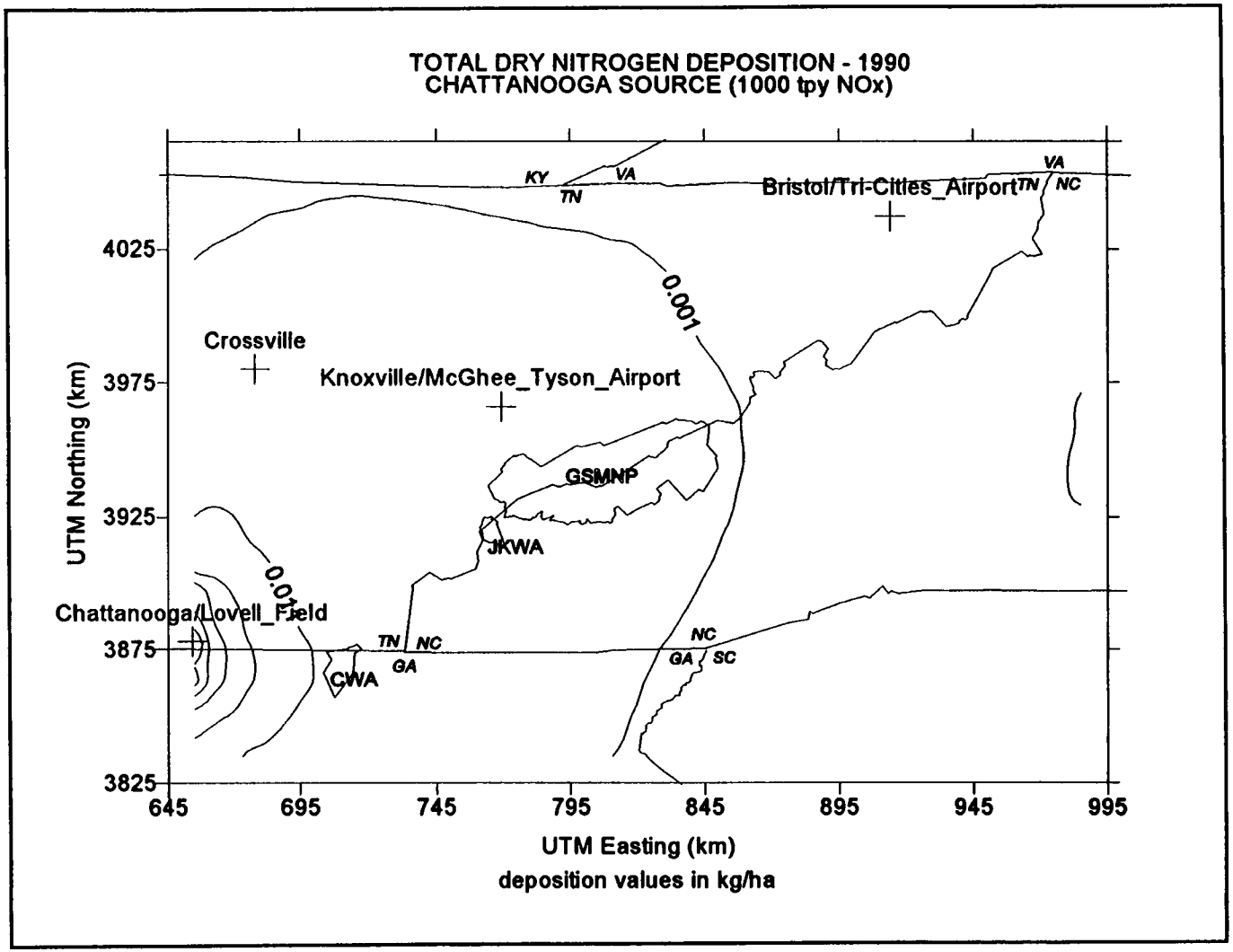

Fig. B.11. Total annual dry nitrogen deposition estimated for 1990 resulting from a hypothetical 28.8 g/s (1000 tpy) NO_x emission source located at Chattanooga/Lovell Field.

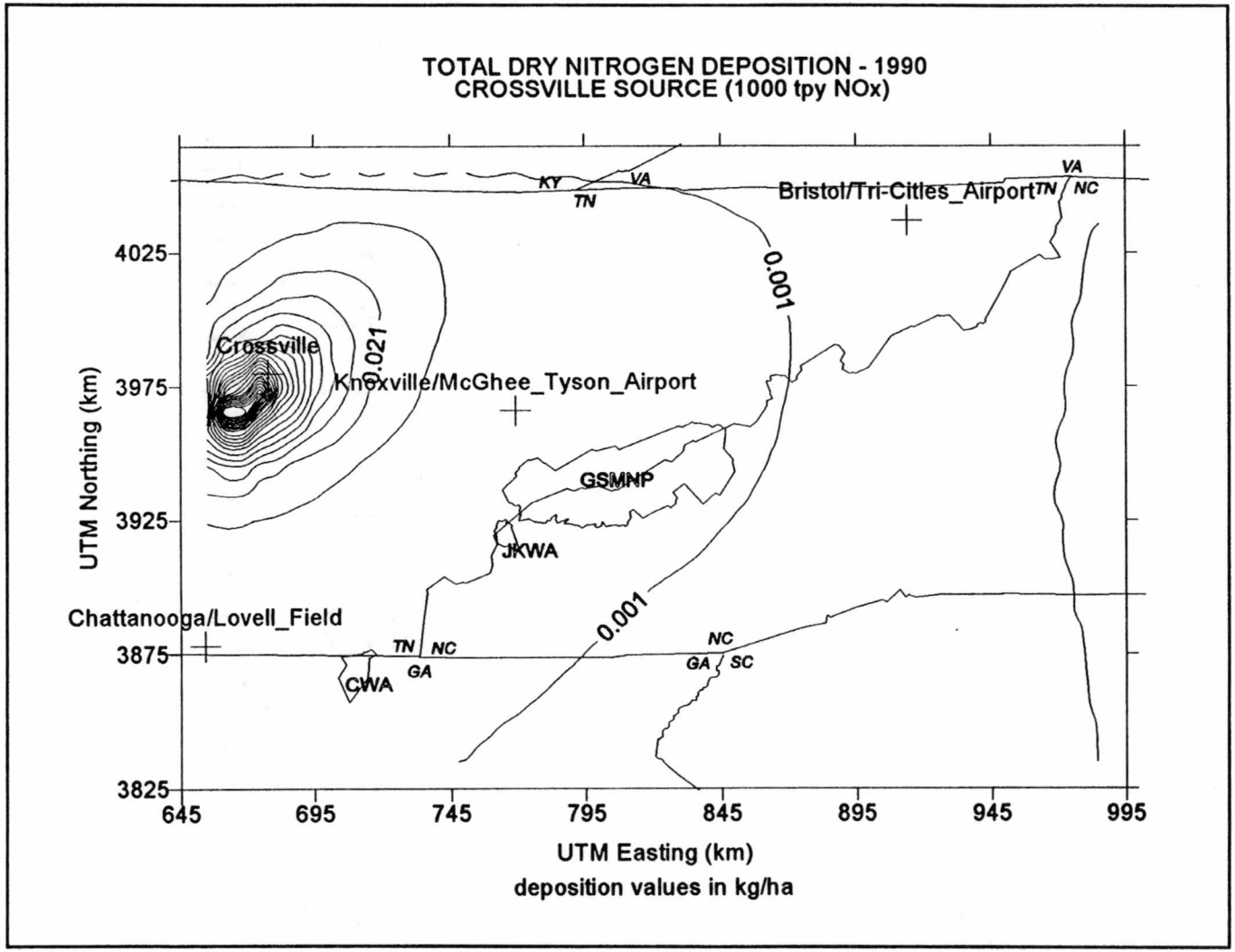

Fig. B.12. Total annual dry nitrogen deposition estimated for 1990 resulting from a hypothetical 28.8 g/s (1000 tpy) NO_x emission source located in Crossville.

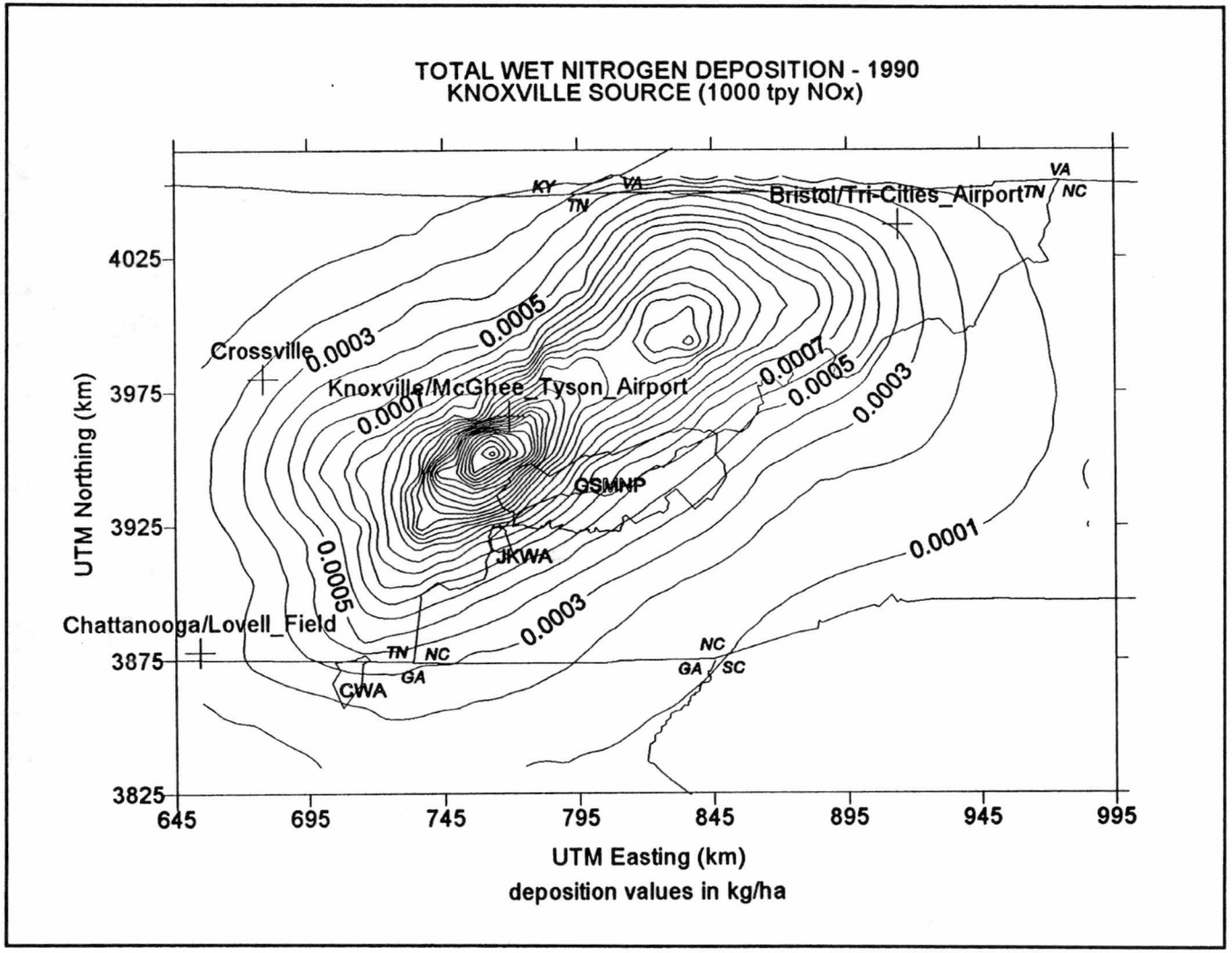

Fig. B.13. Total annual wet nitrogen deposition estimated for 1990 resulting from a hypothetical 28.8 g/s (1000 tpy) NO_x emission source located at Knoxville/McGhee Tyson Airport.

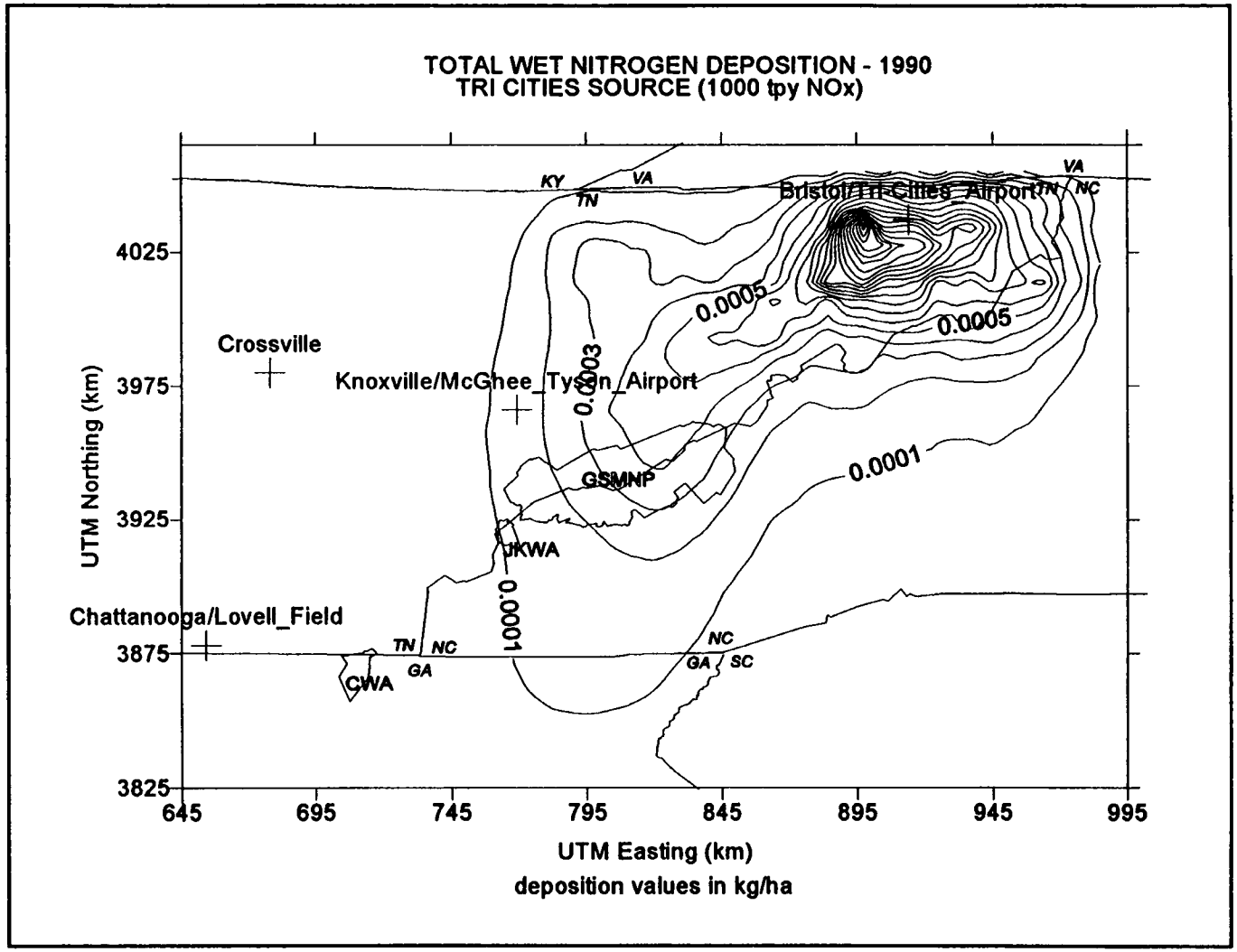

Fig. B.14. Total annual wet nitrogen deposition estimated for 1990 resulting from a hypothetical 28.8 g/s (1000 tpy) NO_x emission source located at Bristol/Tri Cities Airport.

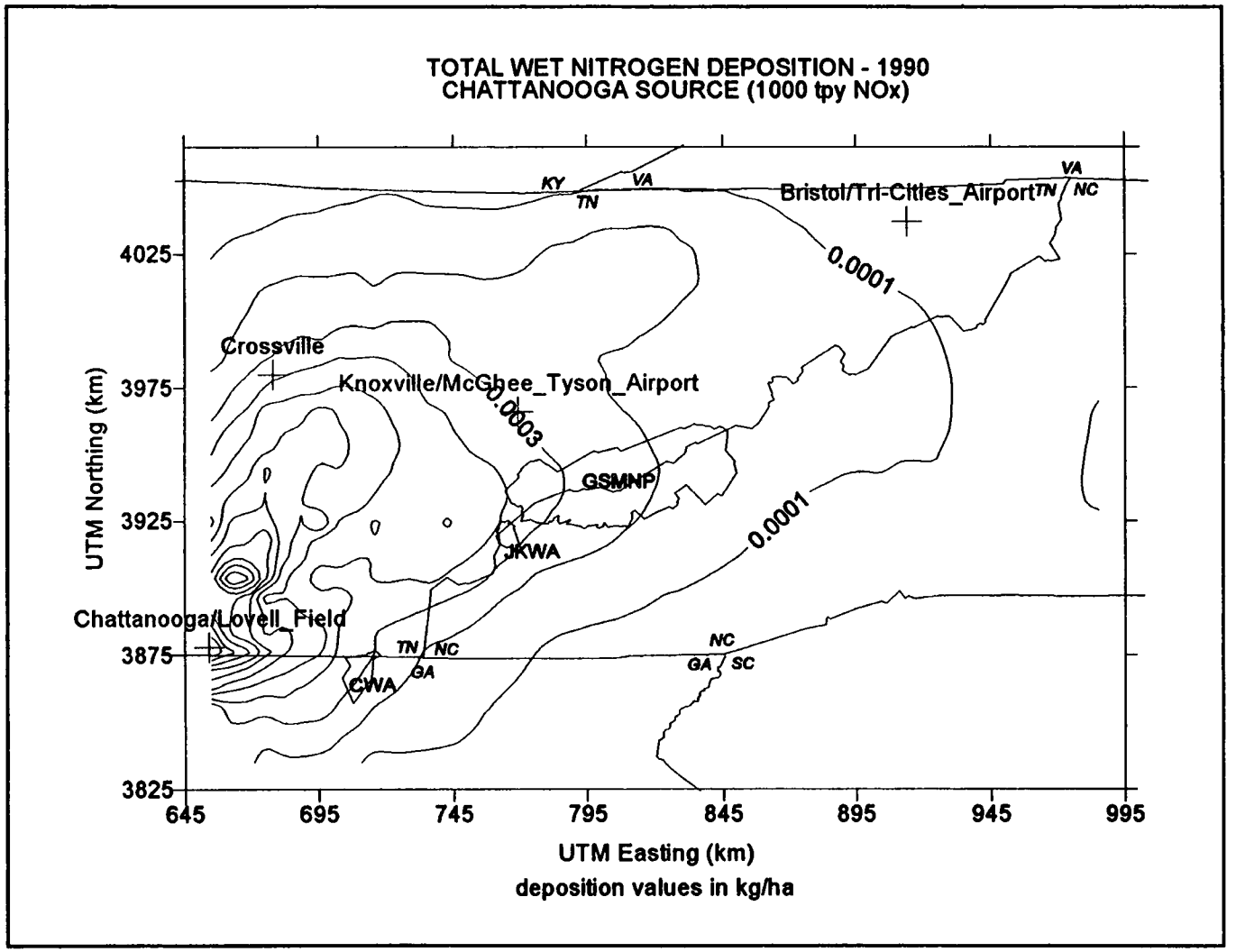

Fig. B.15. Total annual wet nitrogen deposition estimated for 1990 resulting from a hypothetical 28.8 g/s (1000 tpy) NO_x emission source located at Chattanooga/Lovell Field.

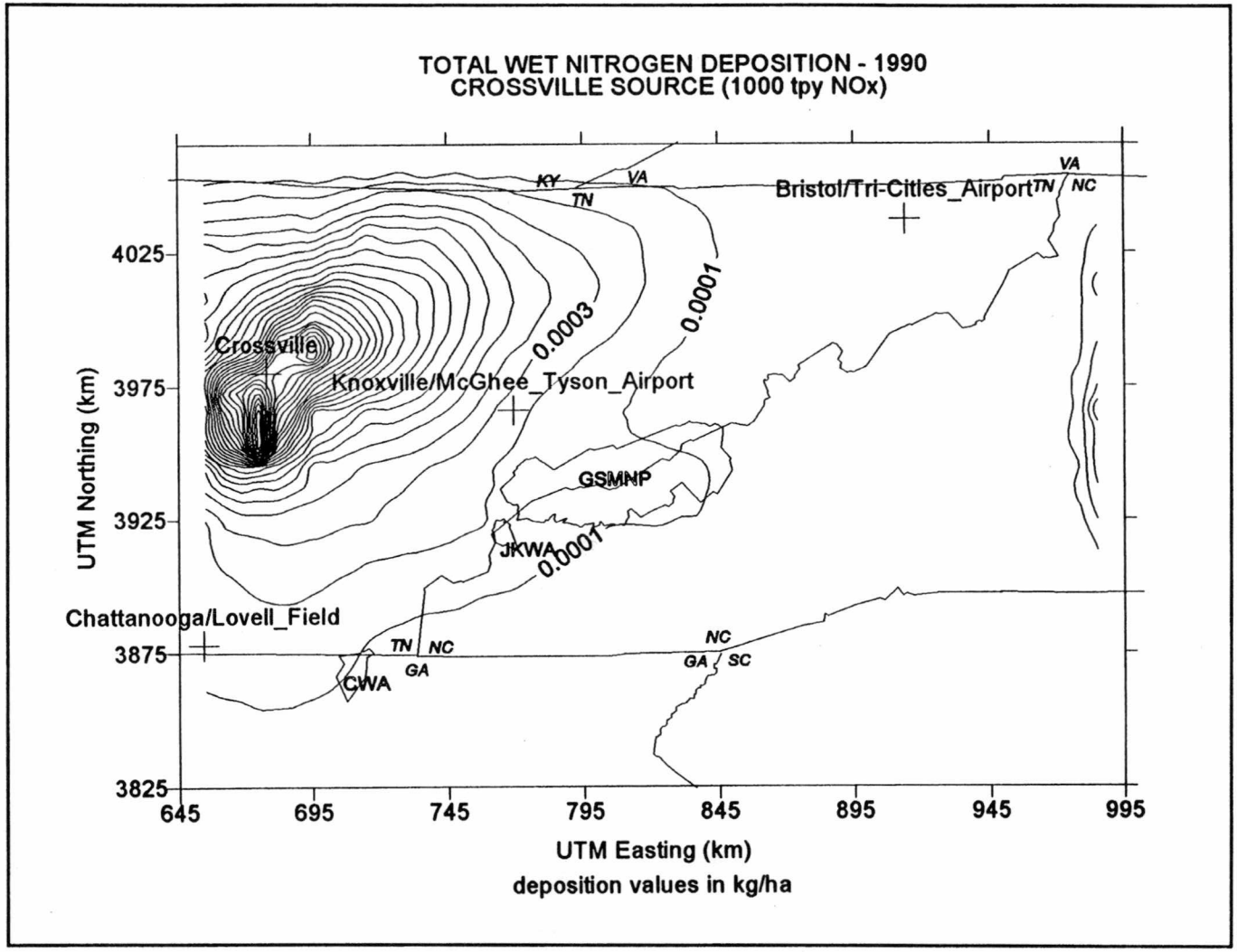

Fig. B.16. Total annual wet nitrogen deposition estimated for 1990 resulting from a hypothetical 28.8 g/s (1000 tpy) NO_x emission source located in Crossville.

APPENDIX C
MONTHLY SO_2 DEPOSITION CONTOUR MAPS

The following figures are contour maps of monthly total (wet + dry) SO_2 deposition in the East Tennessee modeling domain. One contour map per month has been generated for each of the four hypothetical source locations.

The following abbreviations are used on the contour maps:

GSMNP	=	The Great Smoky Mountains National Park
JKWA	=	Joyce Kilmer Wilderness Area
CWA	=	Cohutta Wilderness Area
TN	=	Tennessee
NC	=	North Carolina
GA	=	Georgia
VA	=	Virginia
KY	=	Kentucky
UTM	=	Universal Transverse Mercator

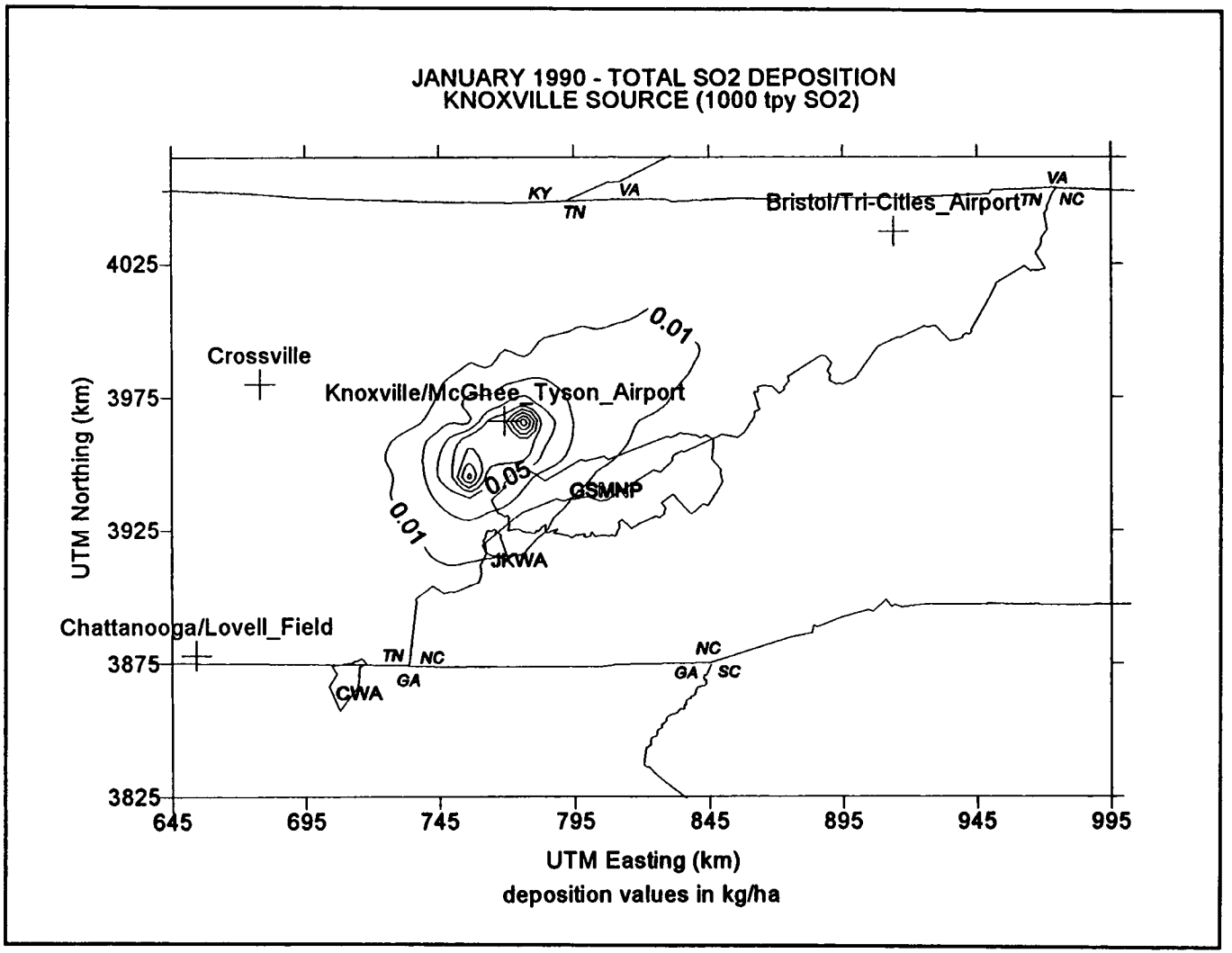

Fig. C.1. Total (wet+dry) SO_2 deposition estimated for January 1990 resulting from a 28.8 g/s (1000 tpy) hypothetical SO_2 emission source located at Knoxville /McGhee Tyson Airport.

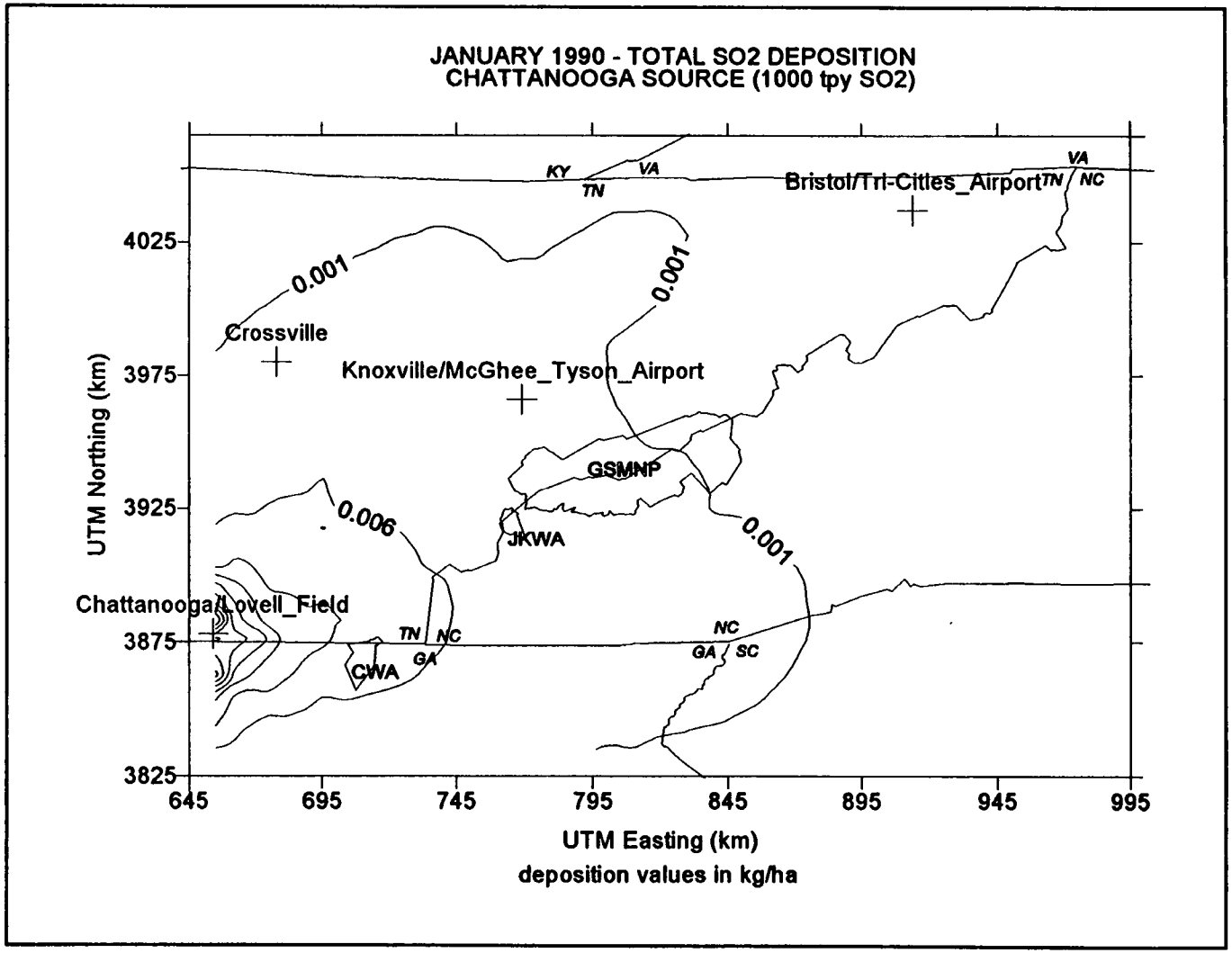

Fig. C.2. Total (wet+dry) SO_2 deposition estimated for January 1990 resulting from a 28.8 g/s (1000 tpy) hypothetical SO_2 emission source located at Chattanooga/Lovell Field.

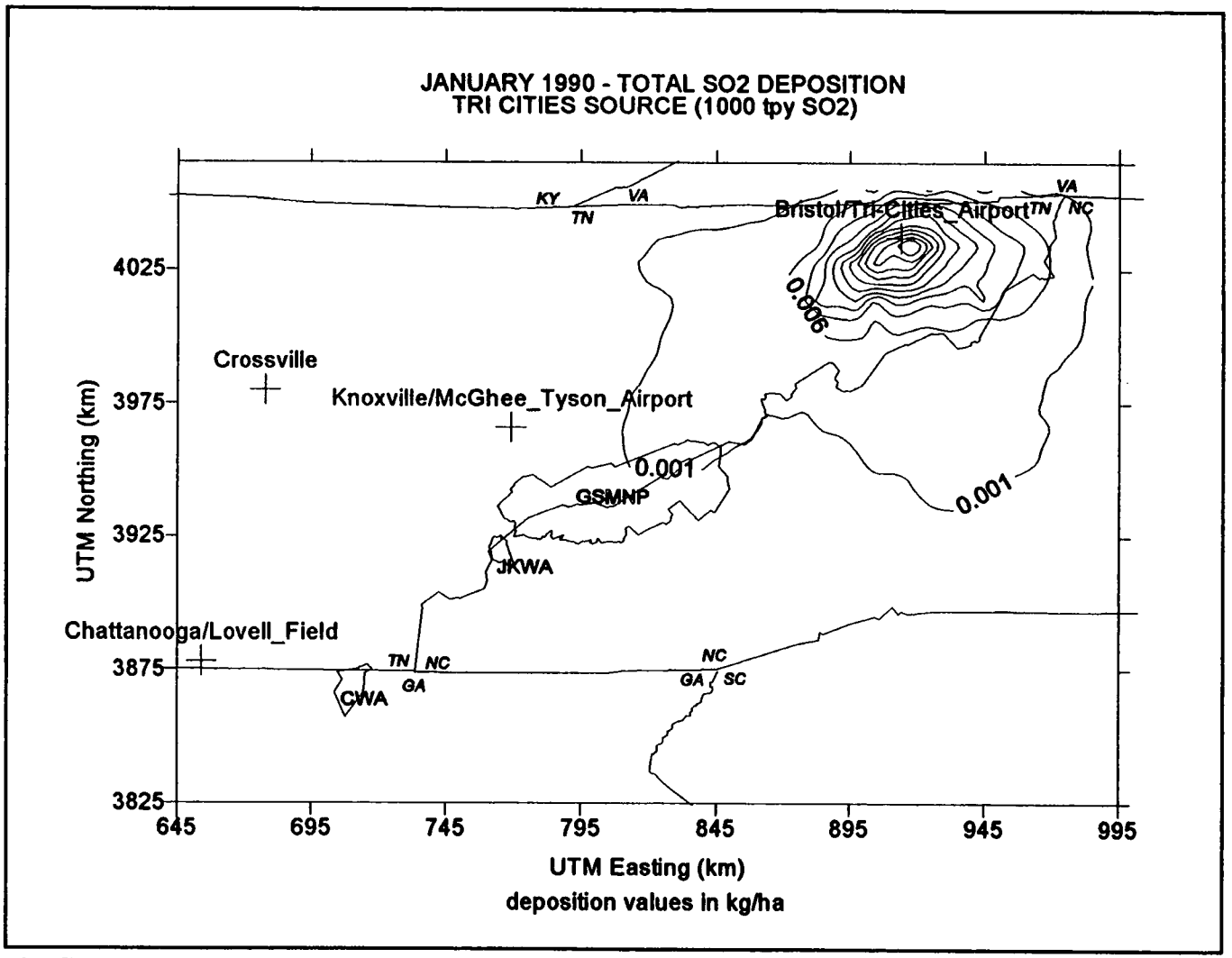

Fig. C.3. Total (wet+dry) SO_2 deposition estimated for January 1990 resulting from a 28.8 g/s (1000 tpy) hypothetical SO_2 emission source located at Bristol/Tri Cities Airport.

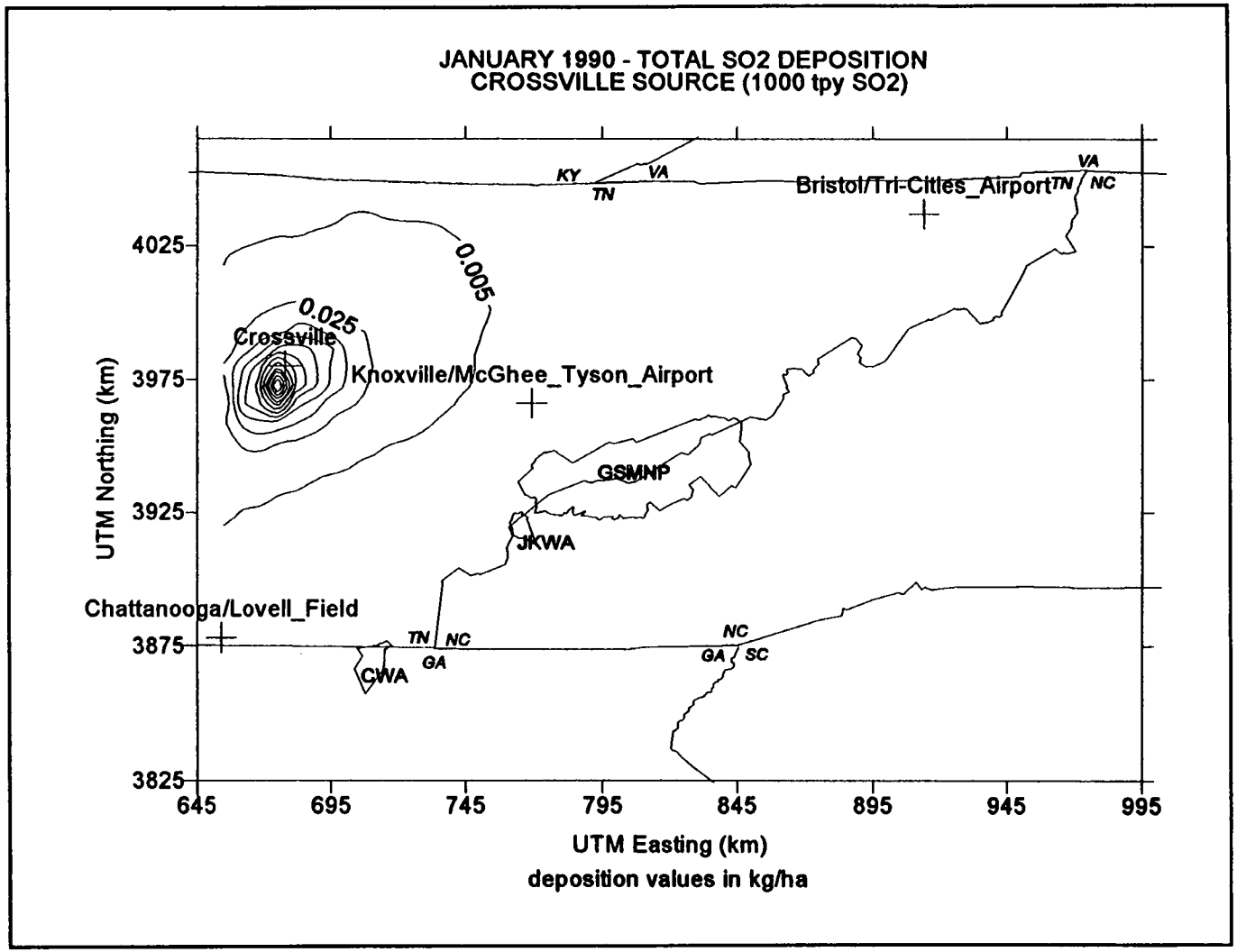

Fig. C.4. Total (wet+dry) SO_2 deposition estimated for January 1990 resulting from a 28.8 g/s (1000 tpy) hypothetical SO_2 emission source located in Crossville.

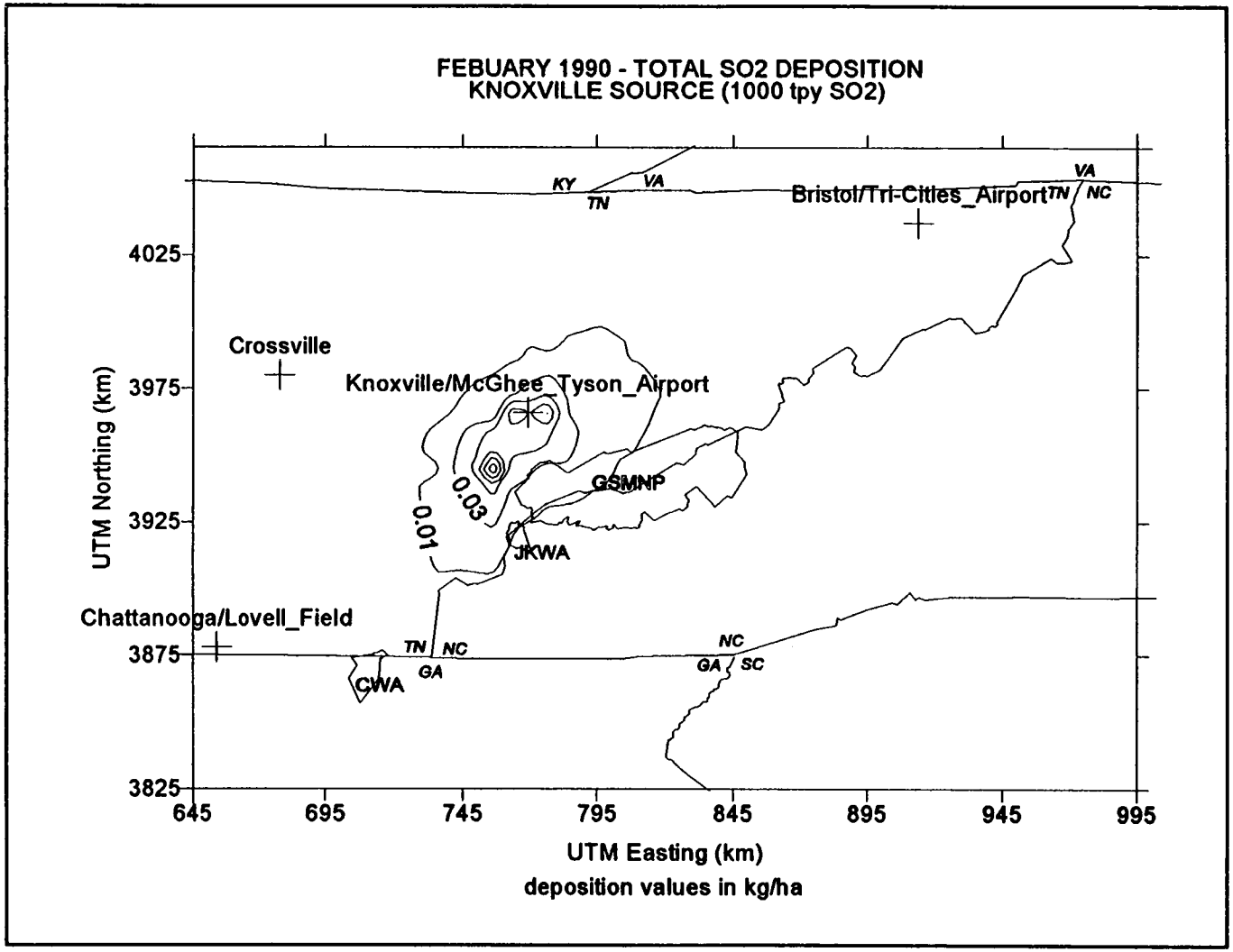

Fig. C.5. Total (wet+dry) SO_2 deposition estimated for February 1990 resulting from a 28.8 g/s (1000 tpy) hypothetical SO_2 emission source located at Knoxville /McGhee Tyson Airport.

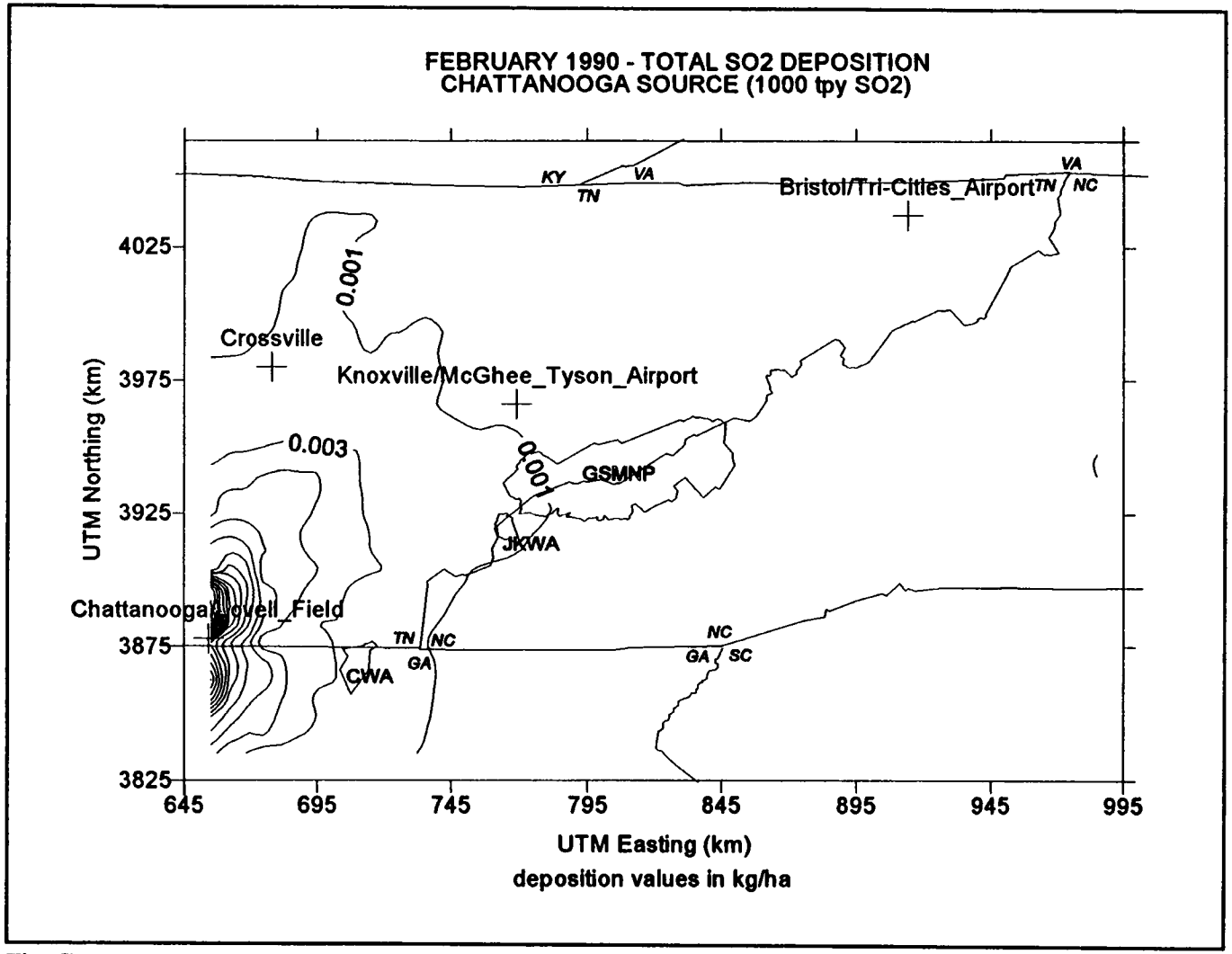

Fig. C.6. Total (wet+dry) SO_2 deposition estimated for February 1990 resulting from a 28.8 g/s (1000 tpy) hypothetical SO_2 emission source located at Chattanooga/Lovell Field.

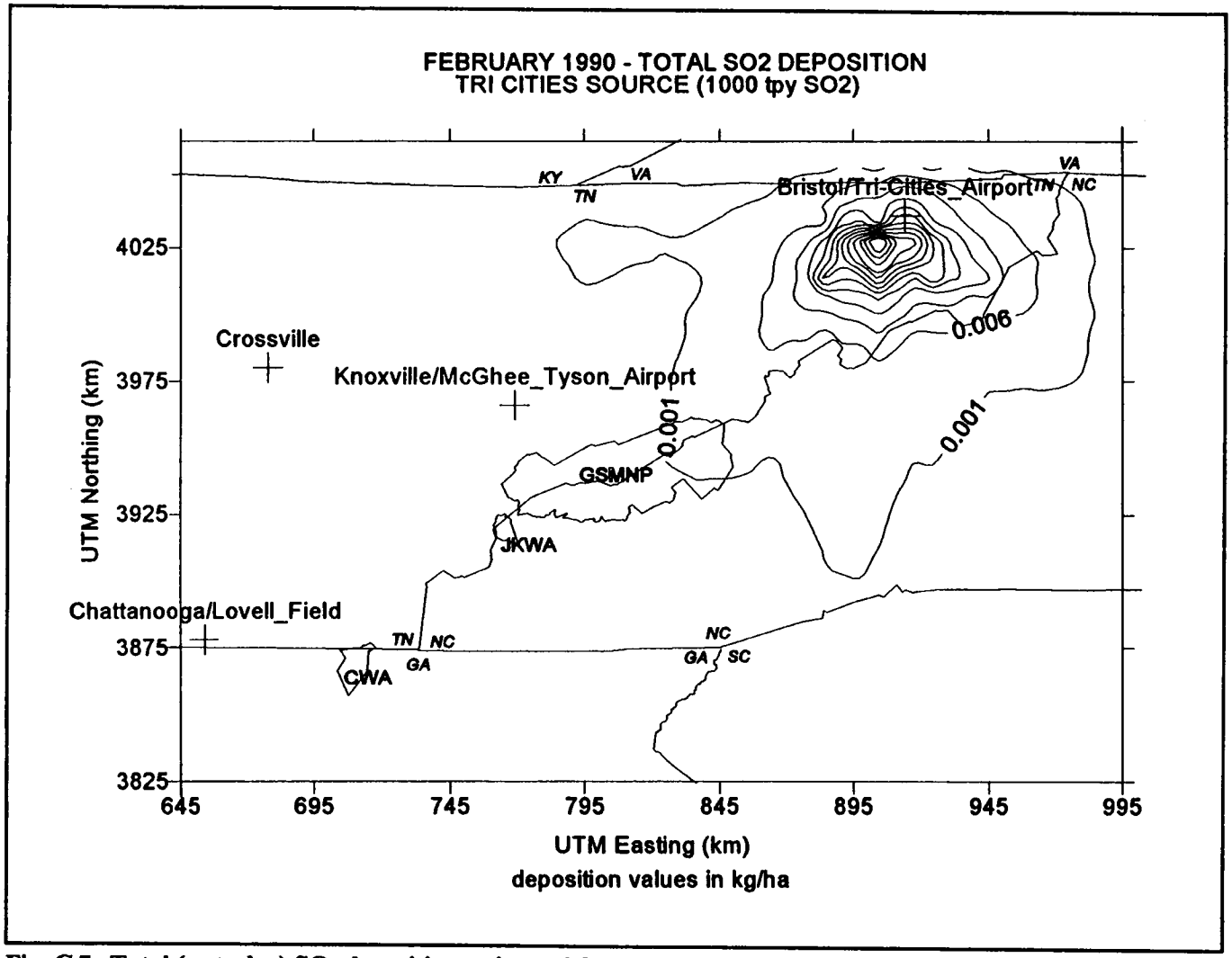

Fig. C.7. Total (wet+dry) SO_2 deposition estimated for February 1990 resulting from a 28.8 g/s (1000 tpy) hypothetical SO_2 emission source located at Bristol/Tri Cities Airport.

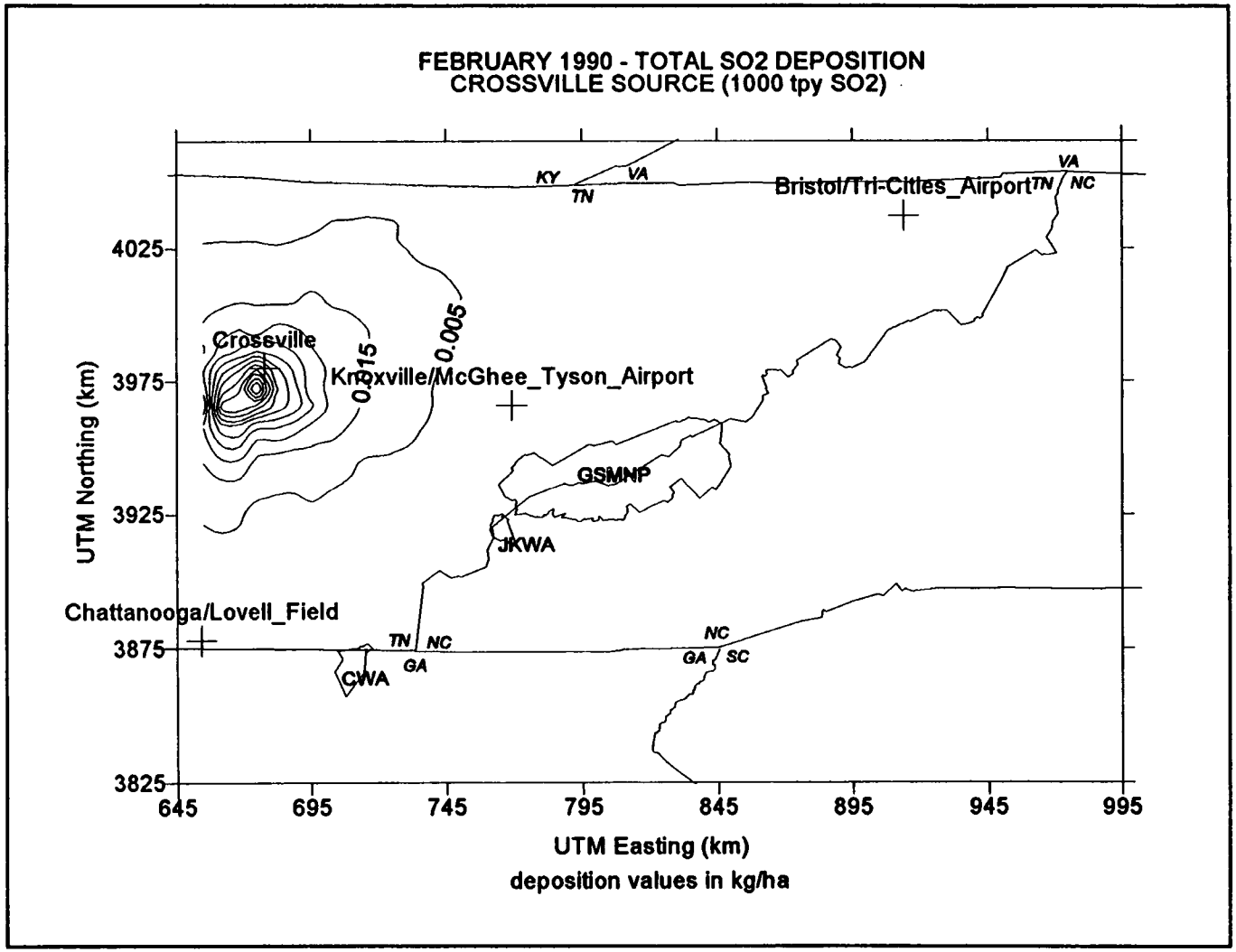

Fig. C.8. Total (wet+dry) SO_2 deposition estimated for February 1990 resulting from a 28.8 g/s (1000 tpy) hypothetical SO_2 emission source located in Crossville.

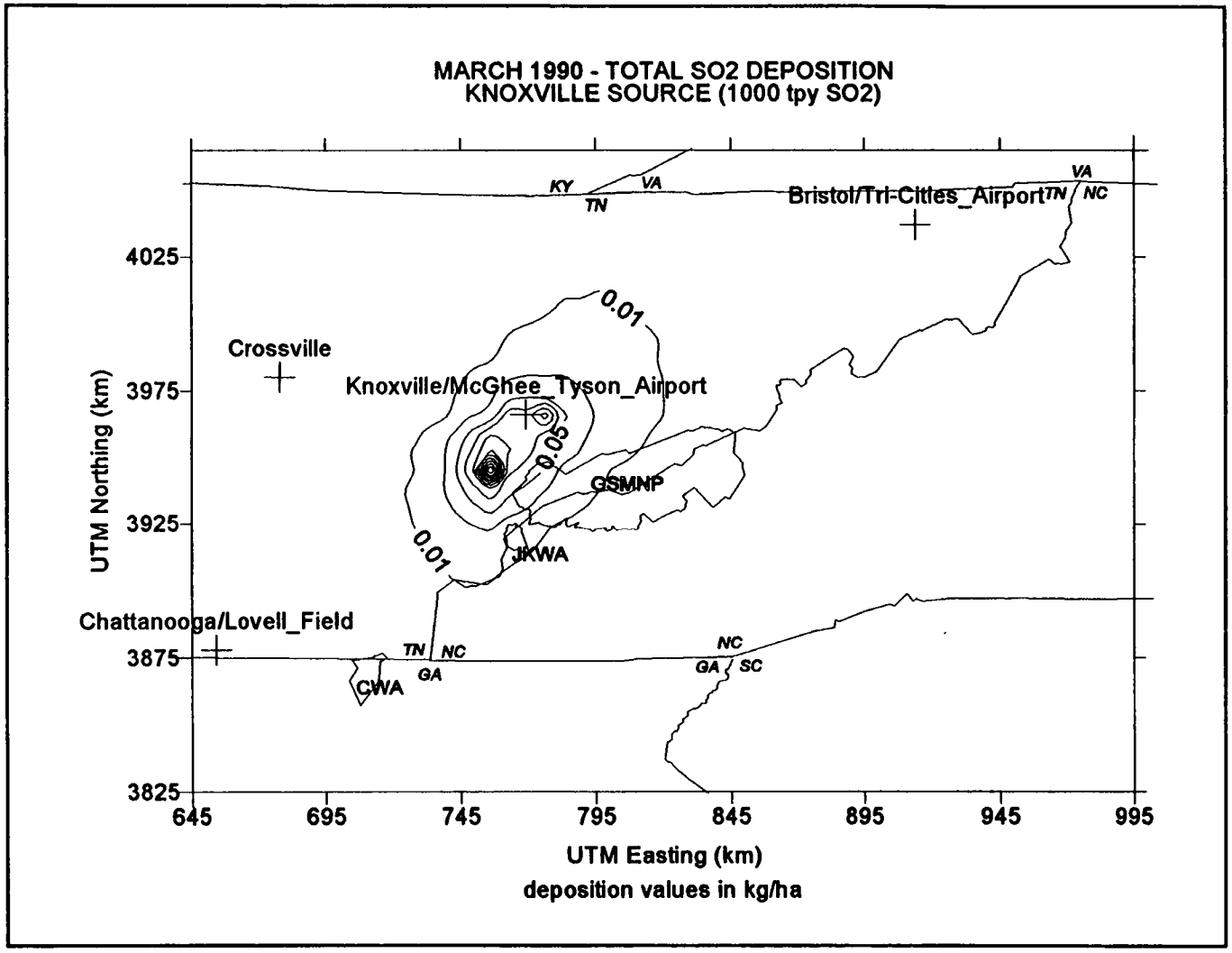

Fig. C.9. Total (wet+dry) SO_2 deposition estimated for March 1990 resulting from a 28.8 g/s (1000 tpy) hypothetical SO_2 emission source located at Knoxville /McGhee Tyson Airport.

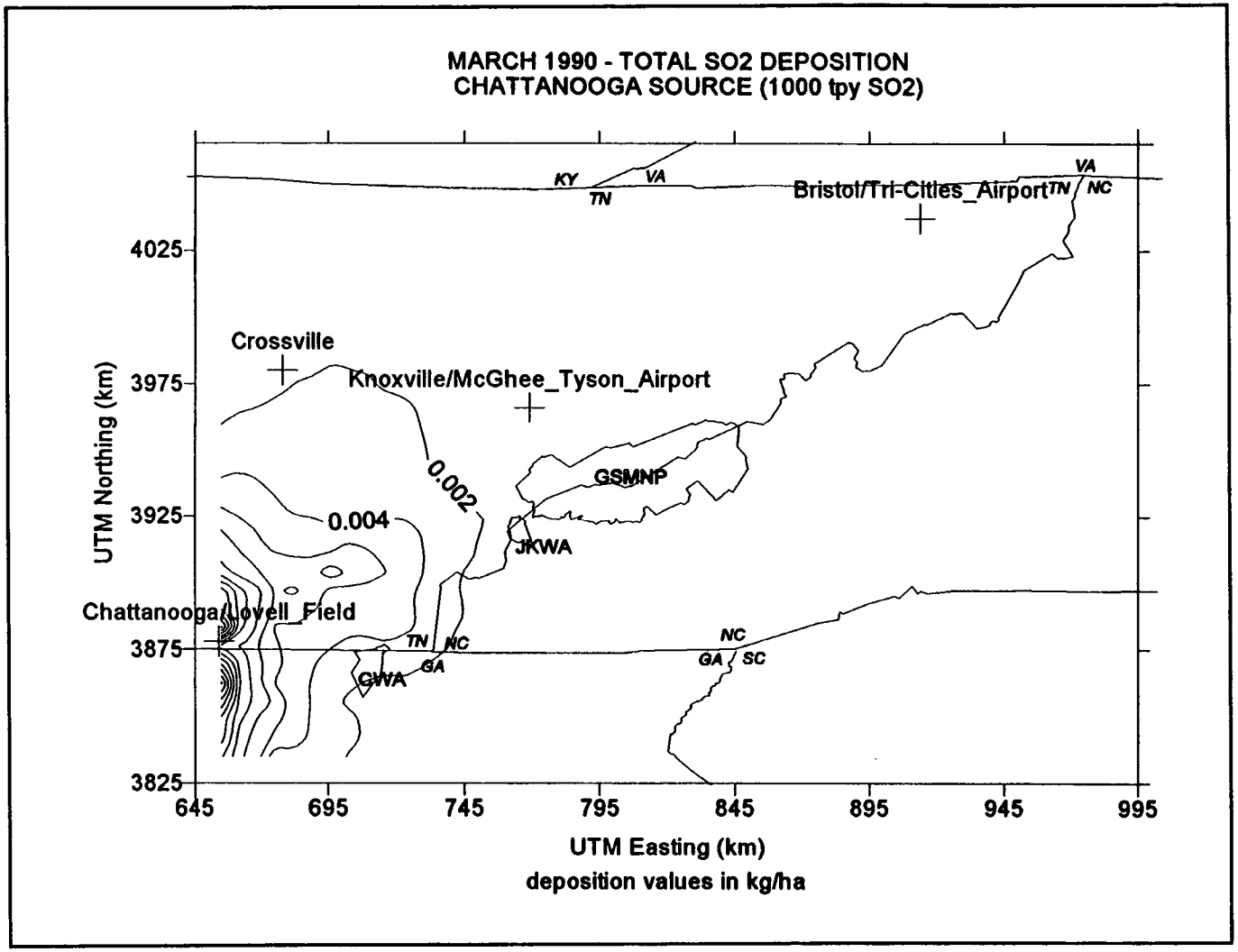

Fig. C.10. Total (wet+dry) SO_2 deposition estimated for March 1990 resulting from a 28.8 g/s (1000 tpy) hypothetical SO_2 emission source located at Chattanooga/Lovell Field.

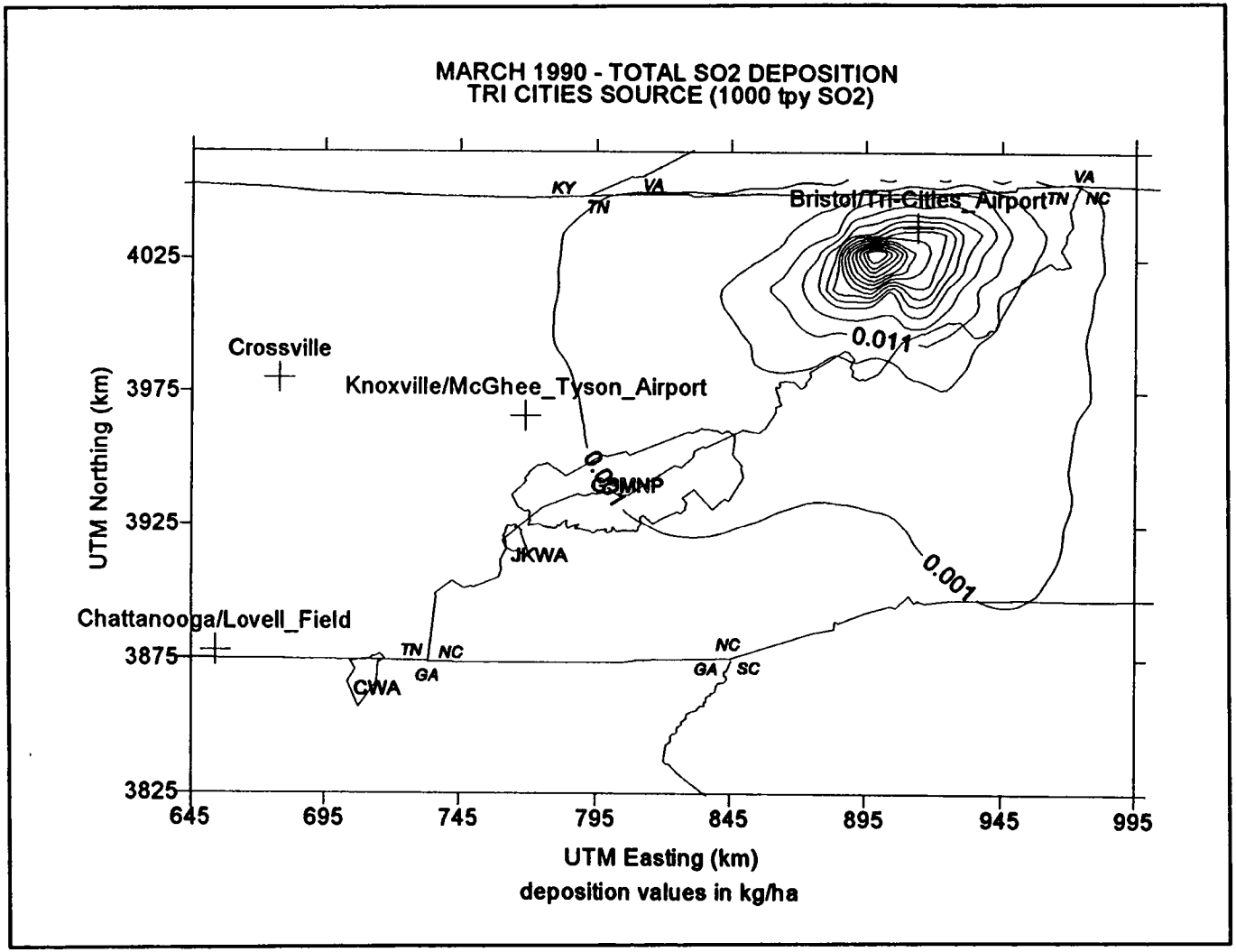

Fig. C.11. Total (wet+dry) SO_2 deposition estimated for March 1990 resulting from a 28.8 g/s (1000 tpy) hypothetical SO_2 emission source located at Bristol/Tri Cities Airport.

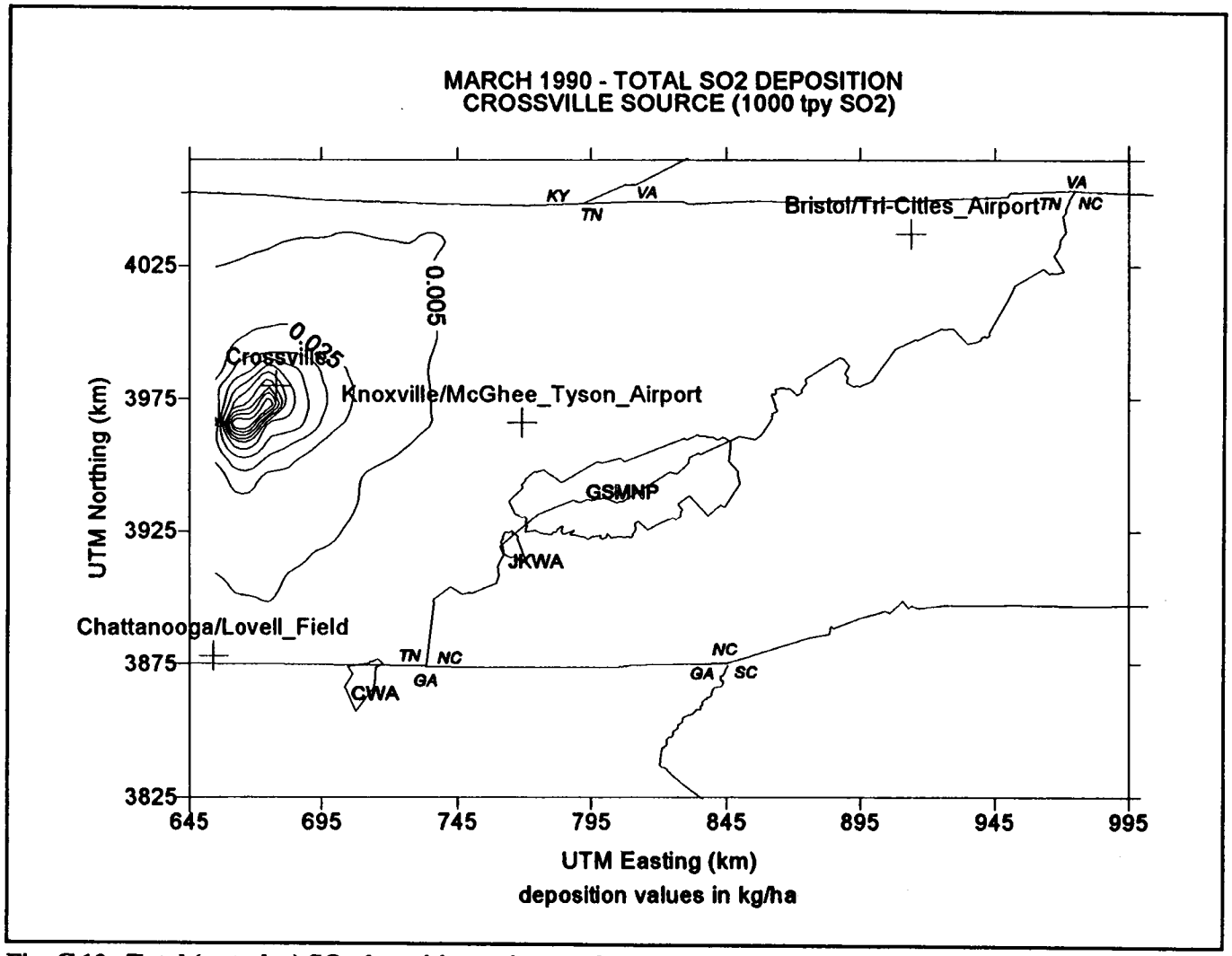

Fig. C.12. Total (wet+dry) SO_2 deposition estimated for March 1990 resulting from a 28.8 g/s (1000 tpy) hypothetical SO_2 emission source located in Crossville.

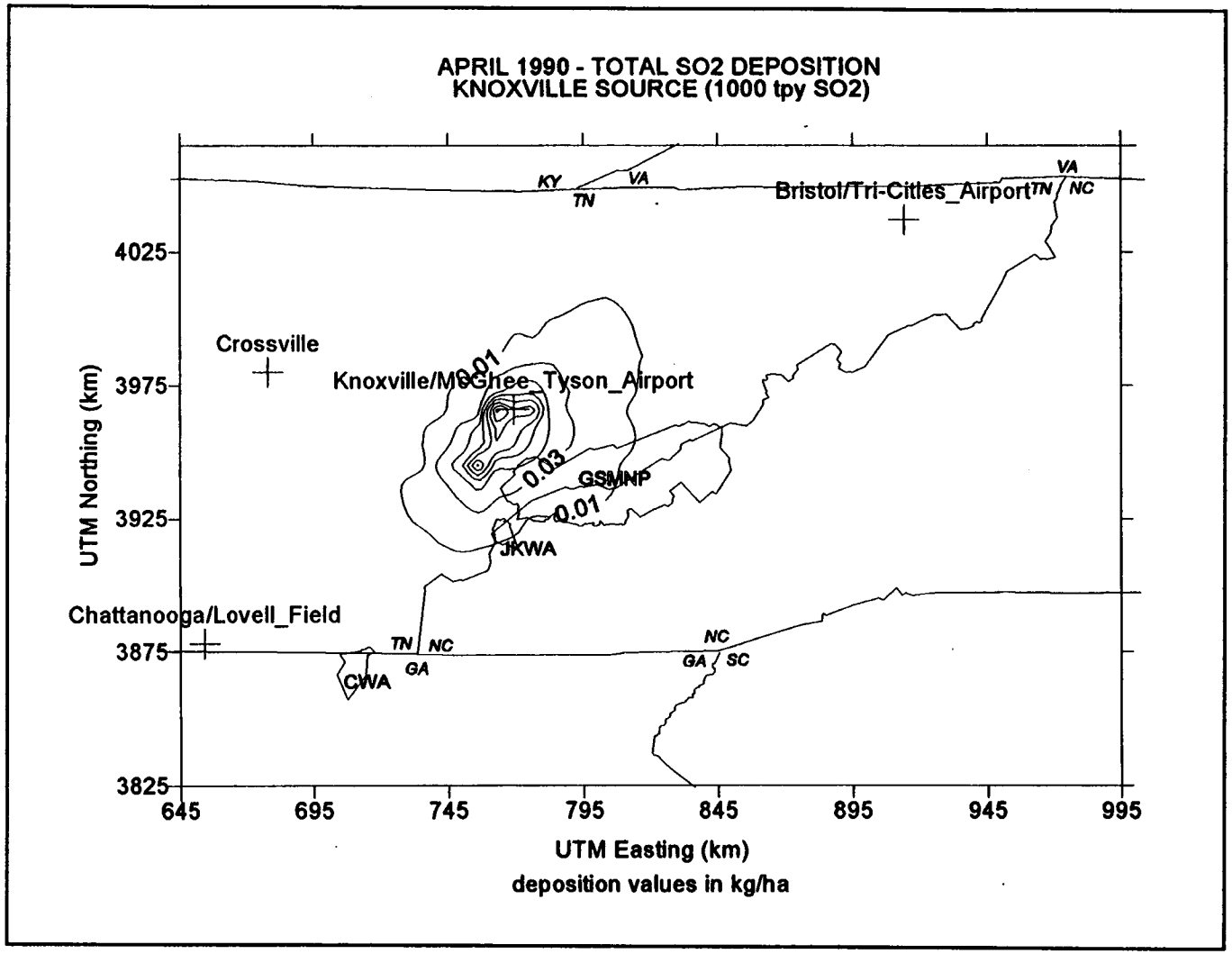

Fig. C.13. Total (wet+dry) SO_2 deposition estimated for April 1990 resulting from a 28.8 g/s (1000 tpy) hypothetical SO_2 emission source located at Knoxville /McGhee Tyson Airport.

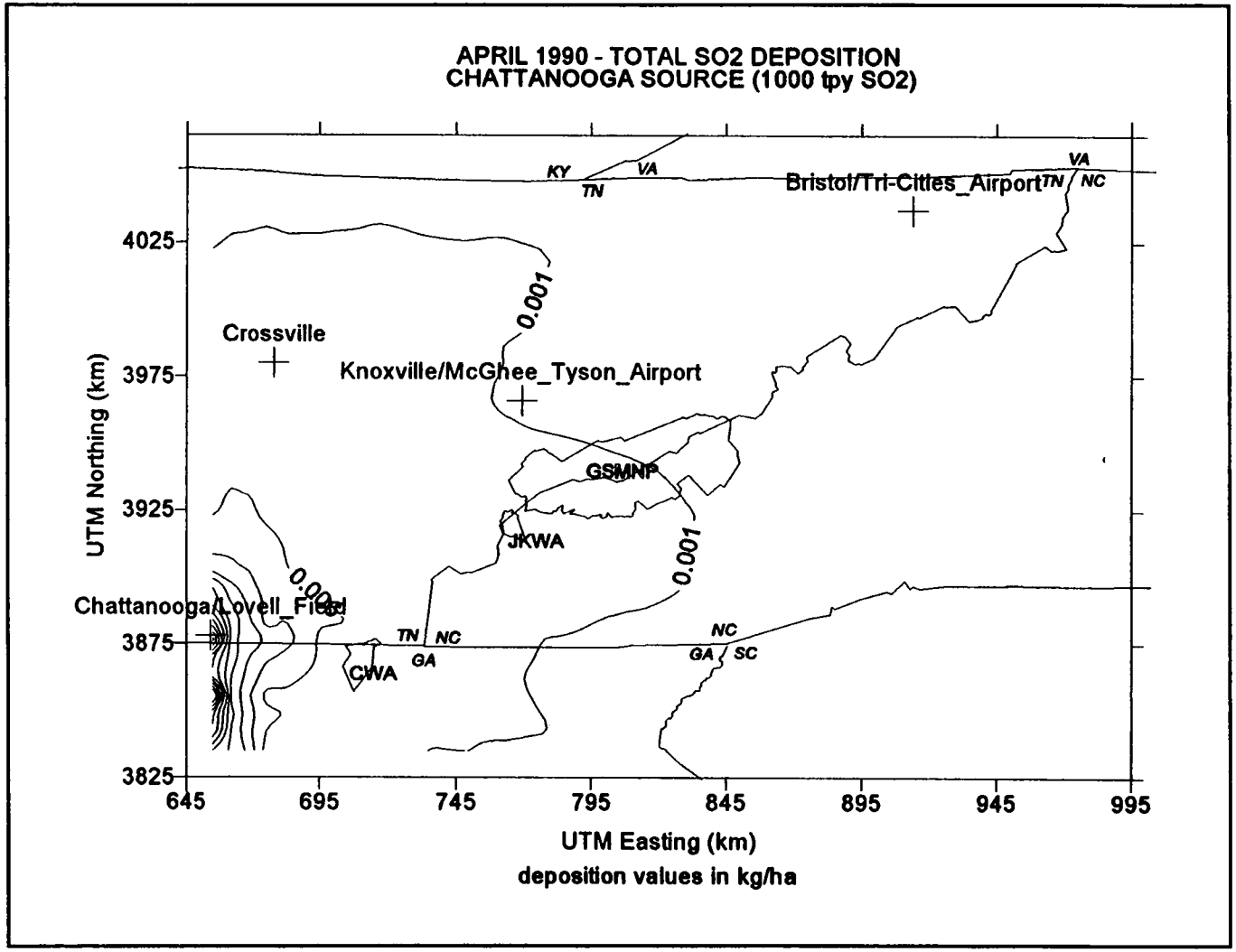

Fig. C.14. Total (wet+dry) SO_2 deposition estimated for April 1990 resulting from a 28.8 g/s (1000 tpy) hypothetical SO_2 emission source located at Chattanooga/Lovell Field.

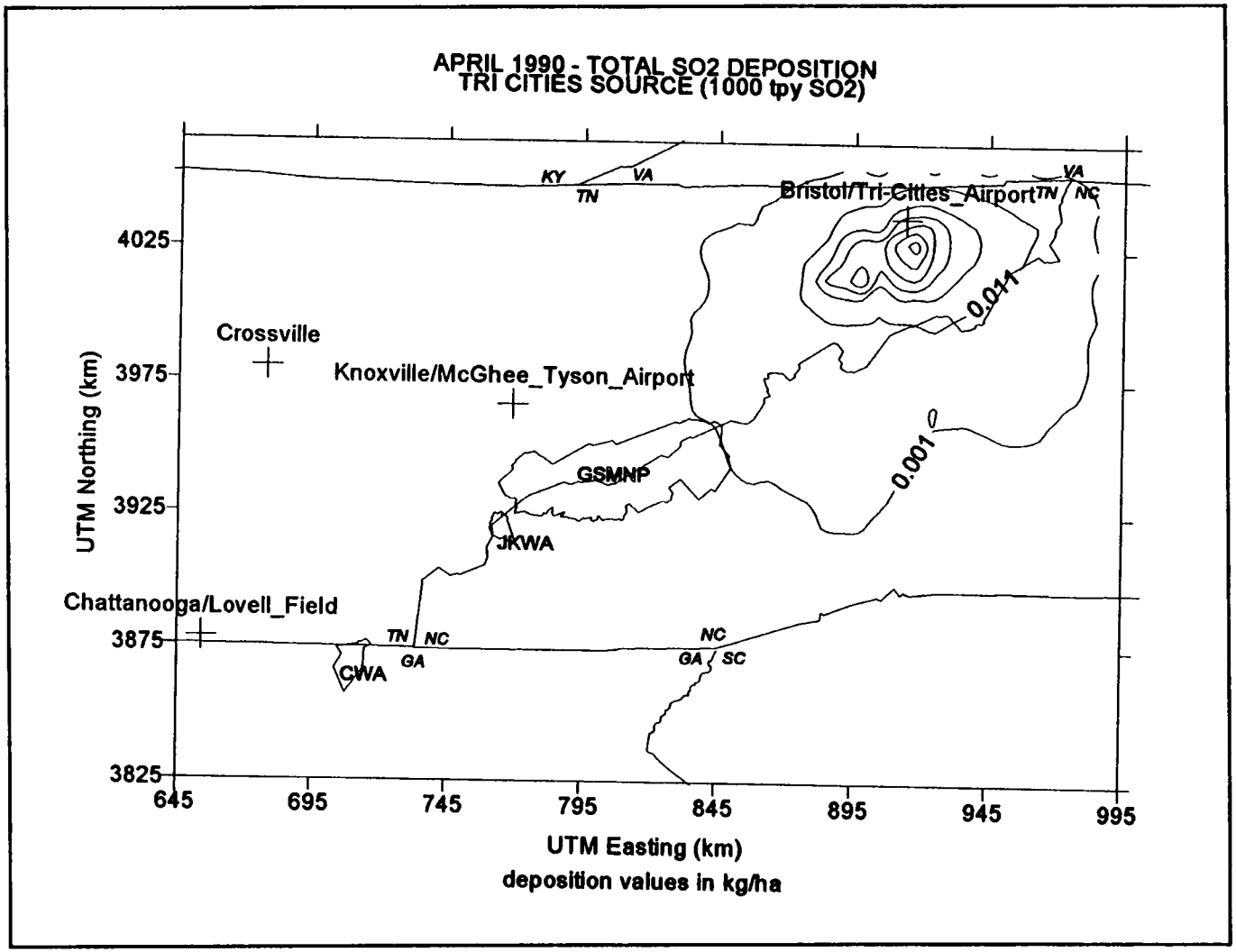

Fig. C.15. Total (wet+dry) SO_2 deposition estimated for April 1990 resulting from a 28.8 g/s (1000 tpy) hypothetical SO_2 emission source located at Bristol/Tri Cities Airport.

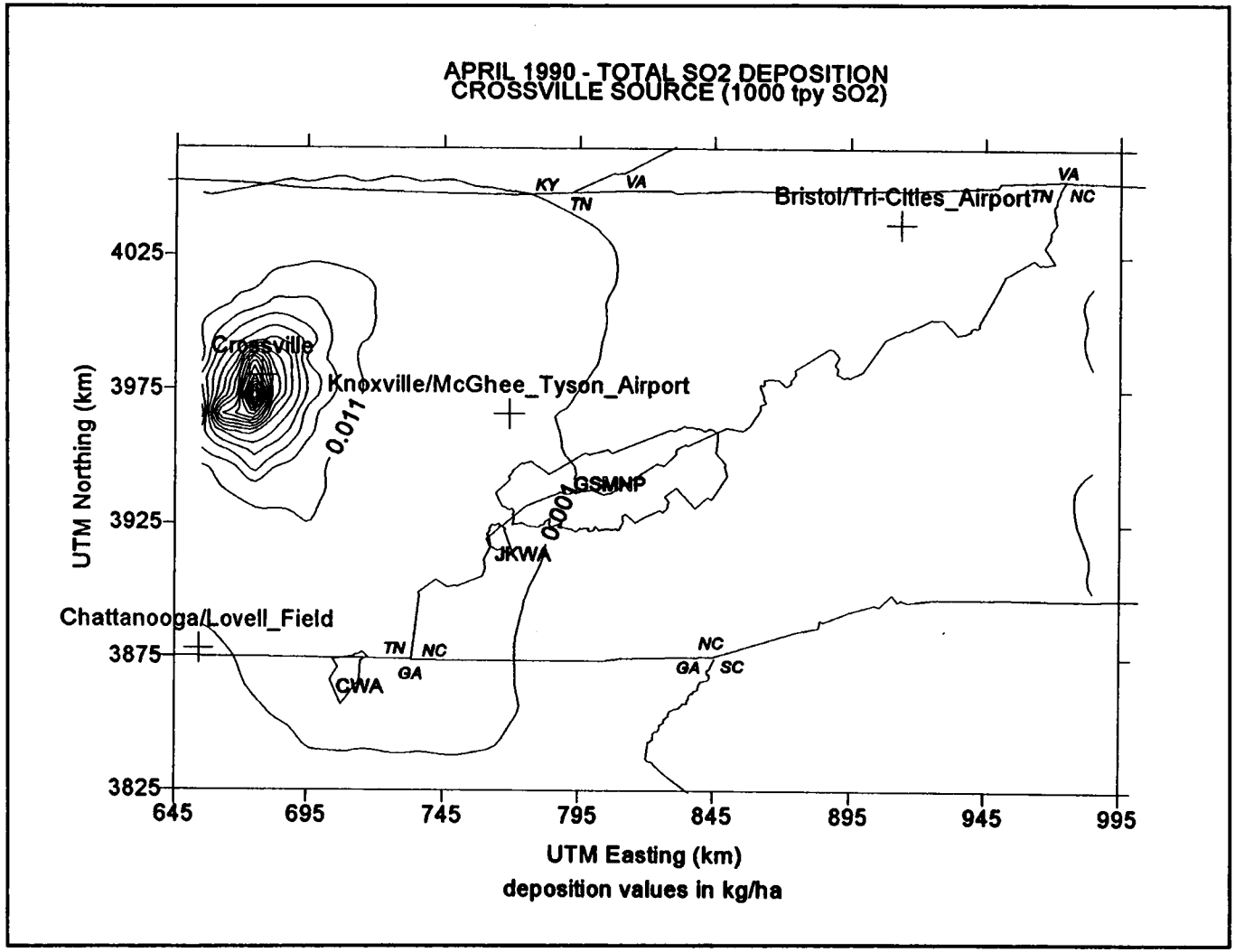

Fig. C.16. Total (wet+dry) SO_2 deposition estimated for April 1990 resulting from a 28.8 g/s (1000 tpy) hypothetical SO_2 emission source located in Crossville.

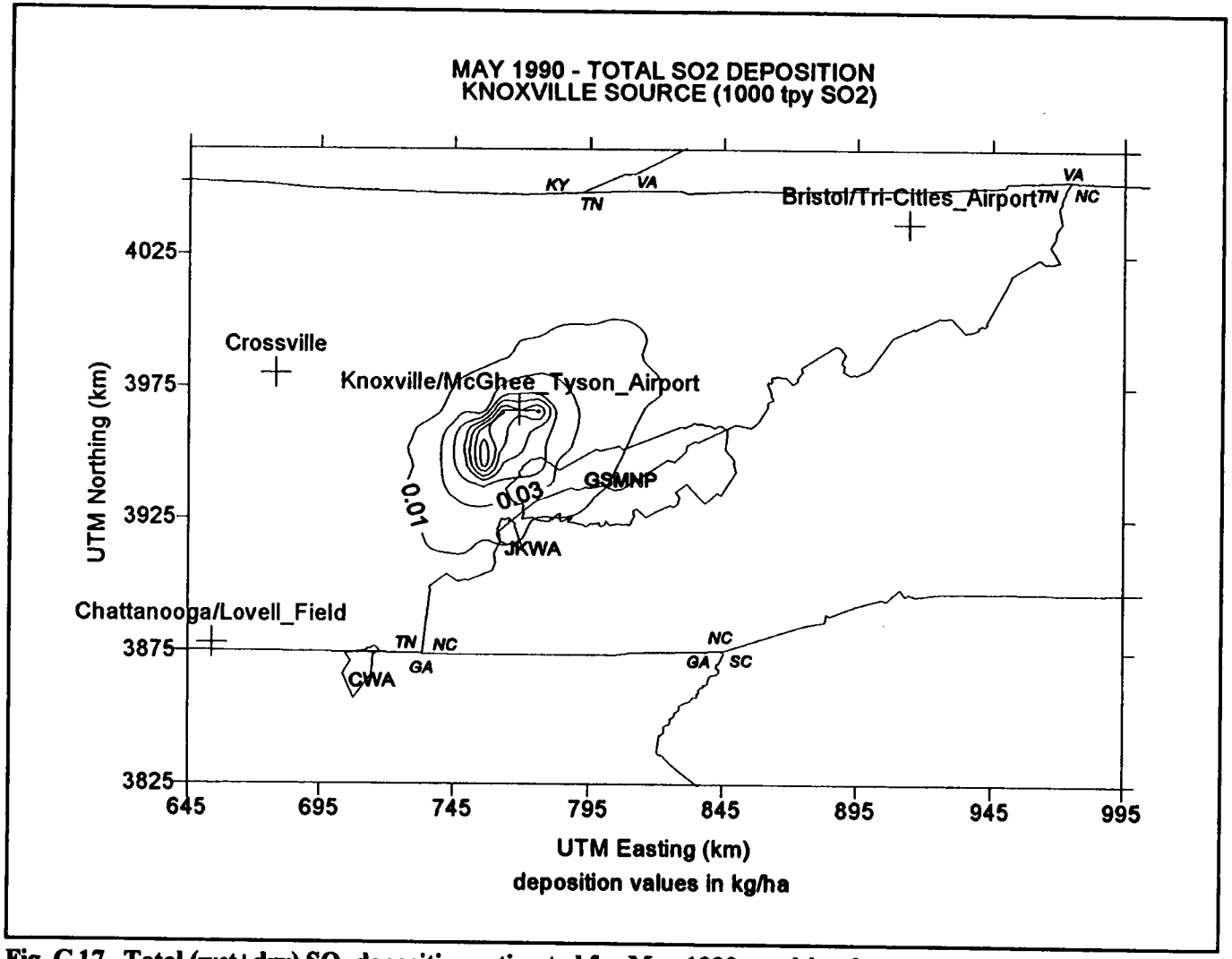

Fig. C.17. Total (wet+dry) SO_2 deposition estimated for May 1990 resulting from a 28.8 g/s (1000 tpy) hypothetical SO_2 emission source located at Knoxville /McGhee Tyson Airport.

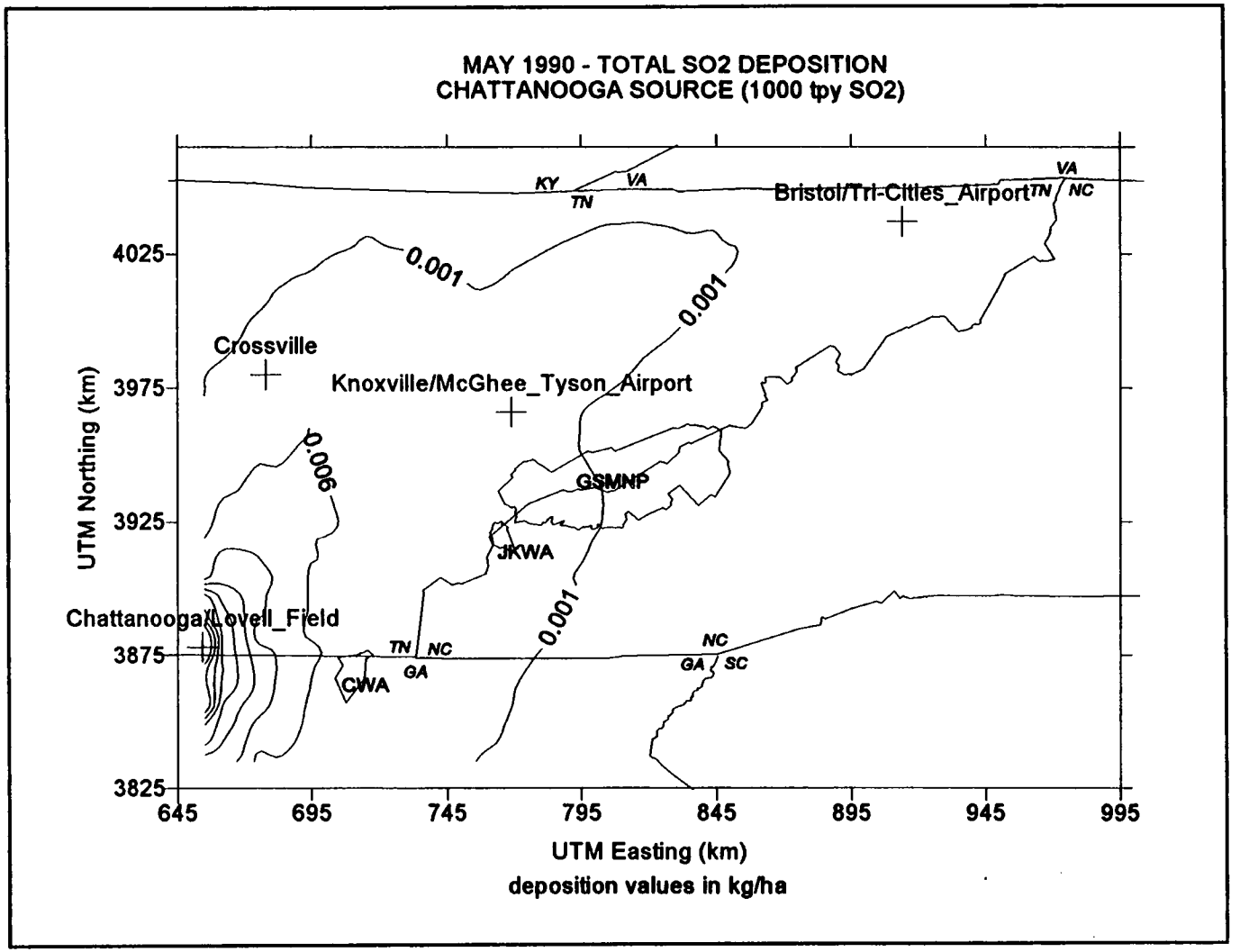

Fig. C.18. Total (wet+dry) SO_2 deposition estimated for May 1990 resulting from a 28.8 g/s (1000 tpy) hypothetical SO_2 emission source located at Chattanooga/Lovell Field.

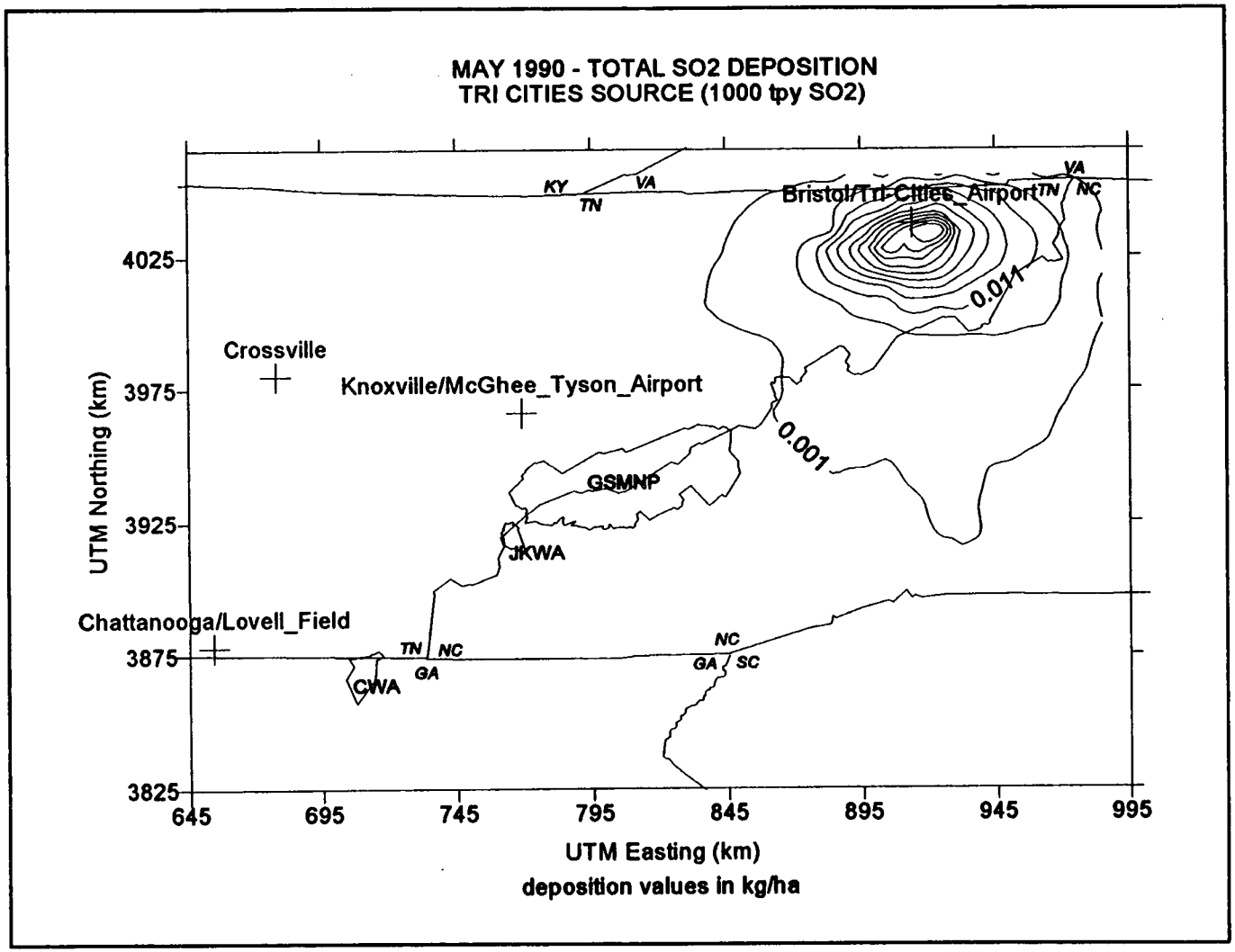

Fig. C.19. Total (wet+dry) SO_2 deposition estimated for May 1990 resulting from a 28.8 g/s (1000 tpy) hypothetical SO_2 emission source located at Bristol/Tri Cities Airport.

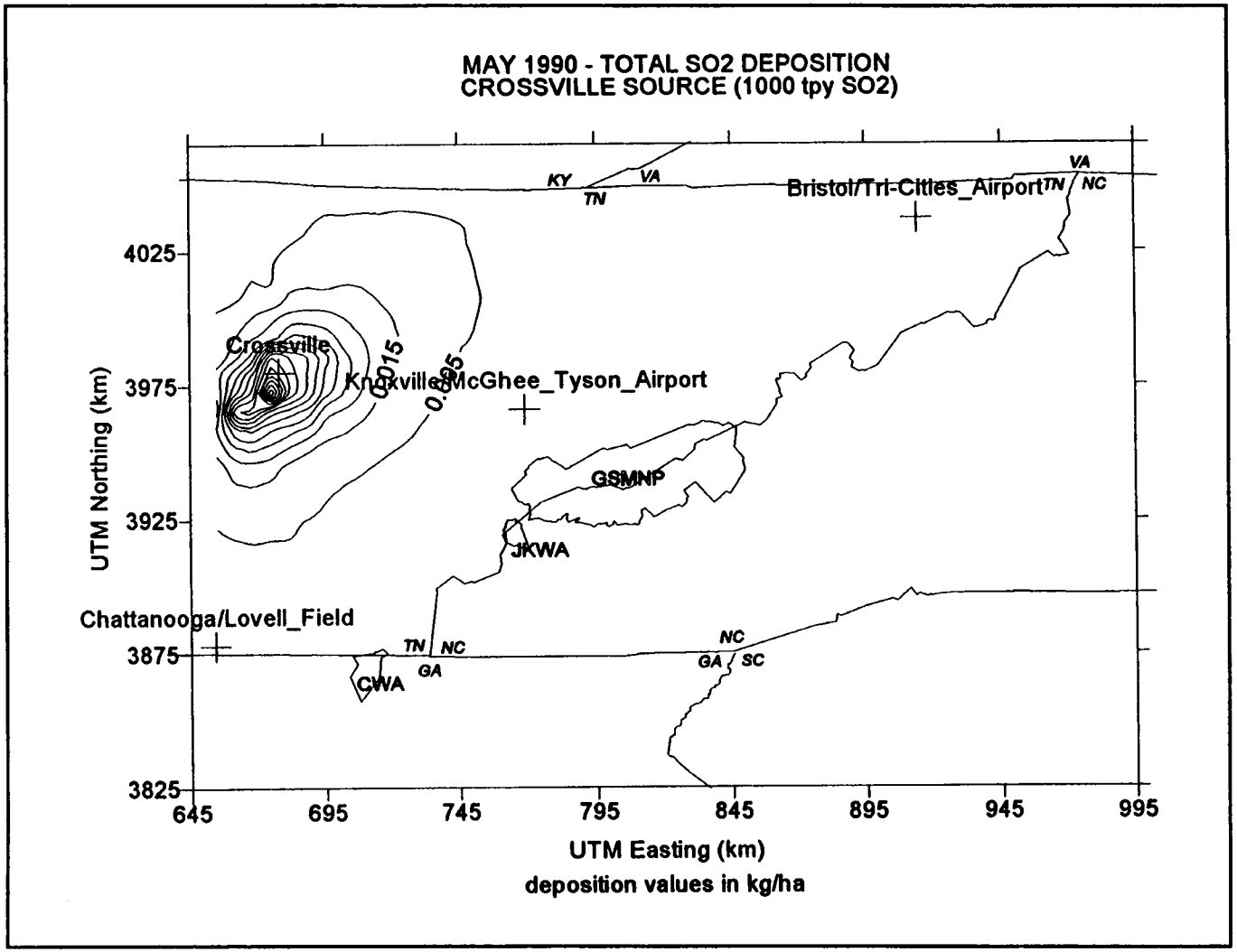

Fig. C.20. Total (wet+dry) SO_2 deposition estimated for May 1990 resulting from a 28.8 g/s (1000 tpy) hypothetical SO_2 emission source located in Crossville.

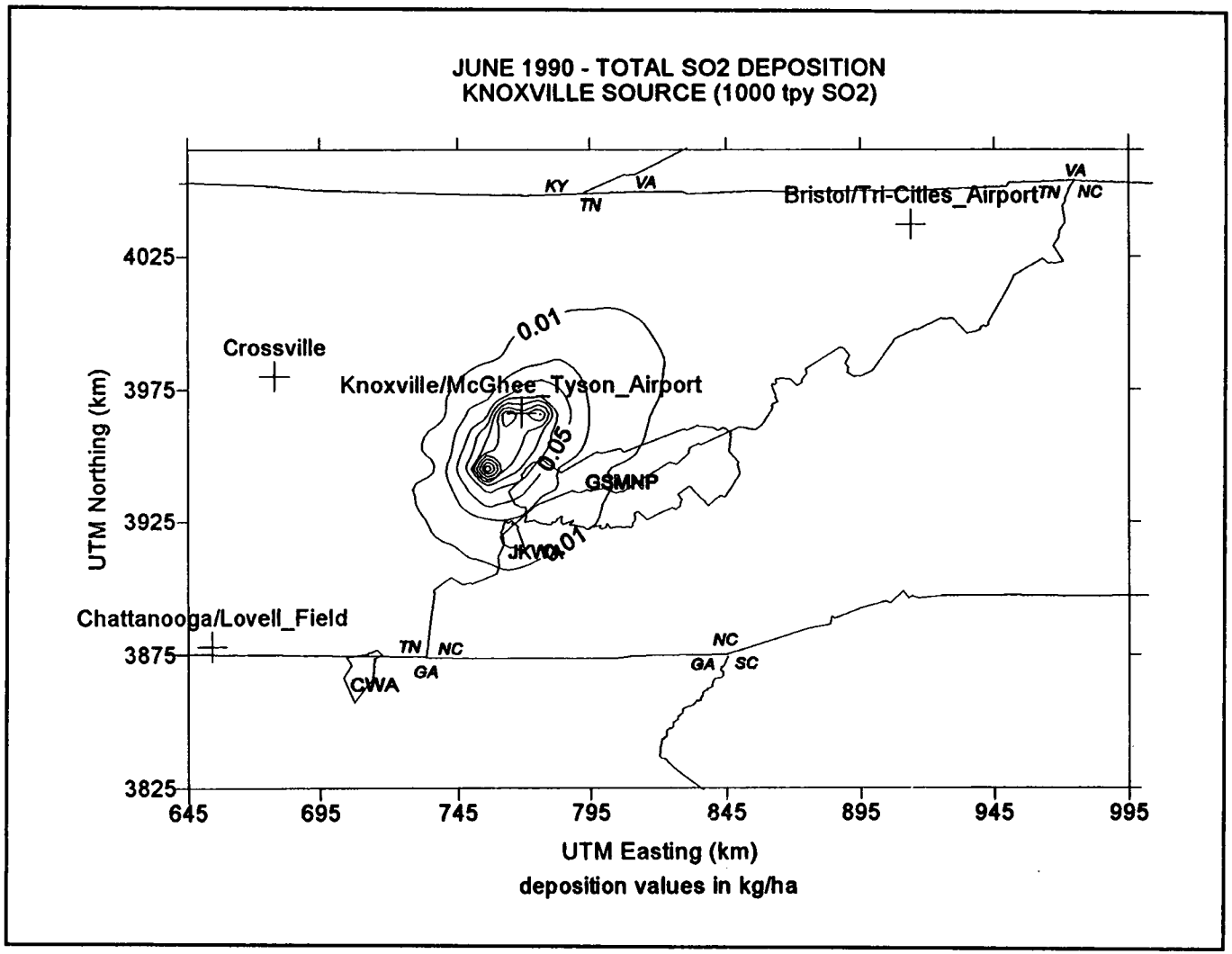

Fig. C.21. Total (wet+dry) SO_2 deposition estimated for June 1990 resulting from a 28.8 g/s (1000 tpy) hypothetical SO_2 emission source located at Knoxville /McGhee Tyson Airport.

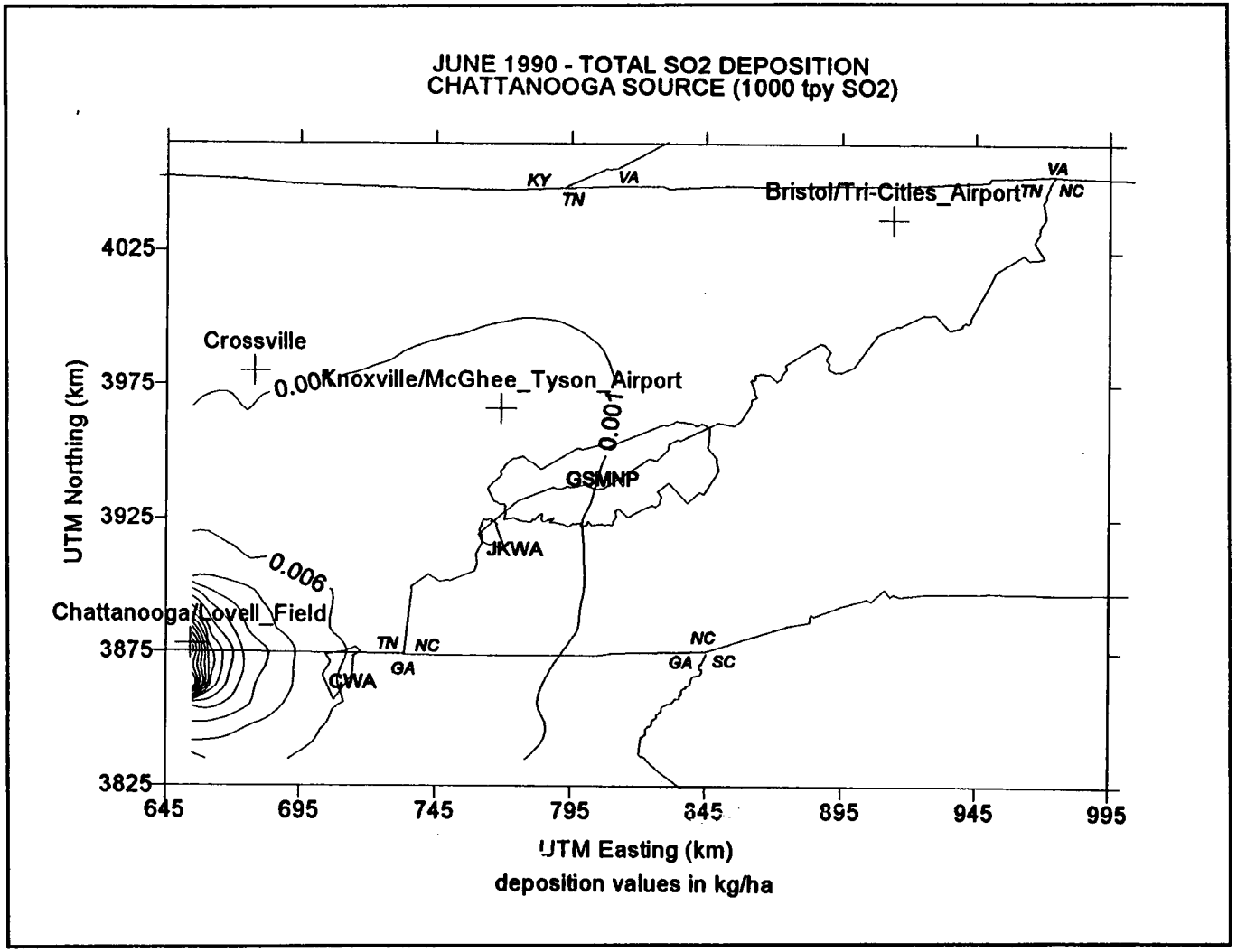

Fig. C.22. Total (wet+dry) SO_2 deposition estimated for June 1990 resulting from a 28.8 g/s (1000 tpy) hypothetical SO_2 emission source located at Chattanooga/Lovell Field.

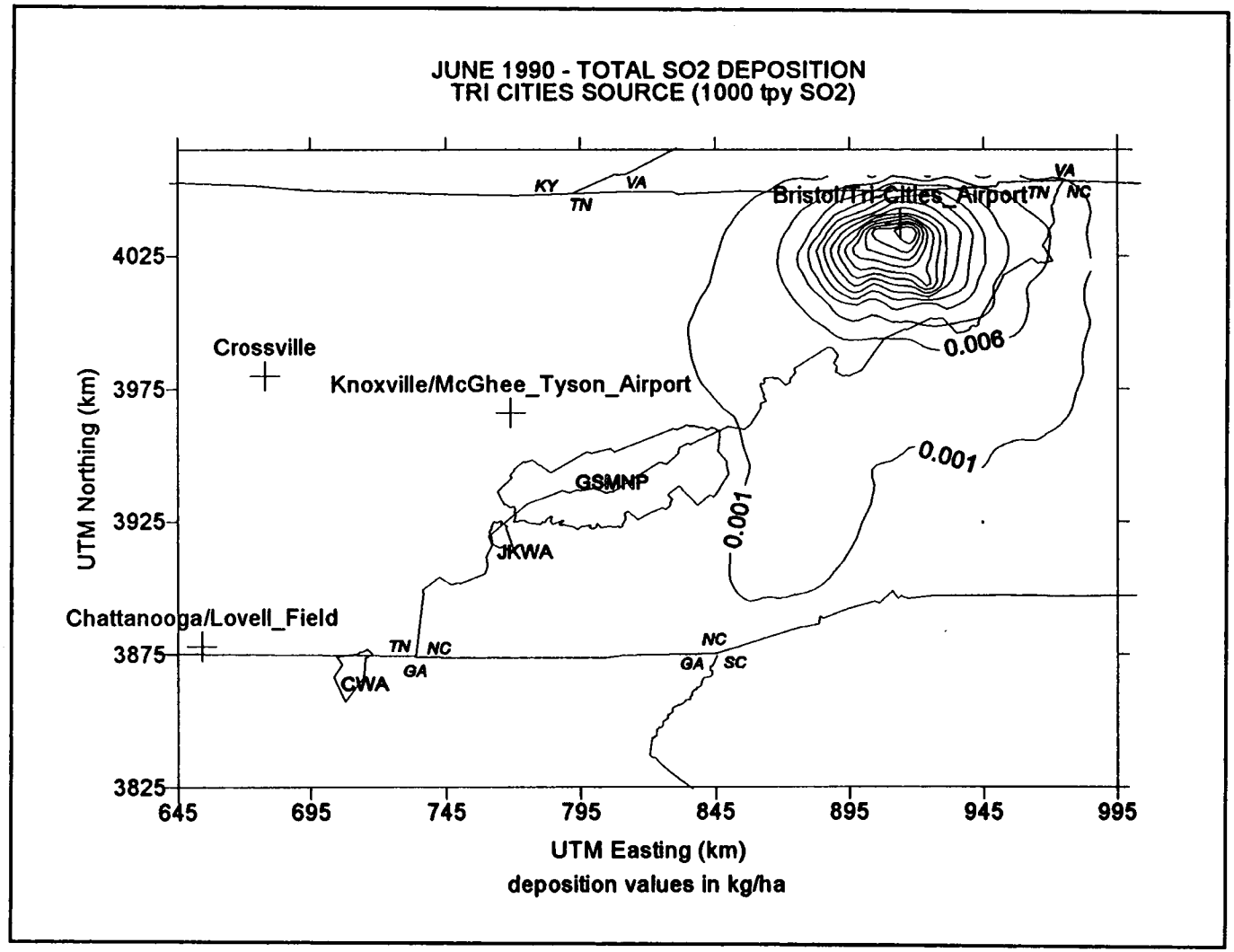

Fig. C.23. Total (wet+dry) SO_2 deposition estimated for June 1990 resulting from a 28.8 g/s (1000 tpy) hypothetical SO_2 emission source located at Bristol/Tri Cities Airport.

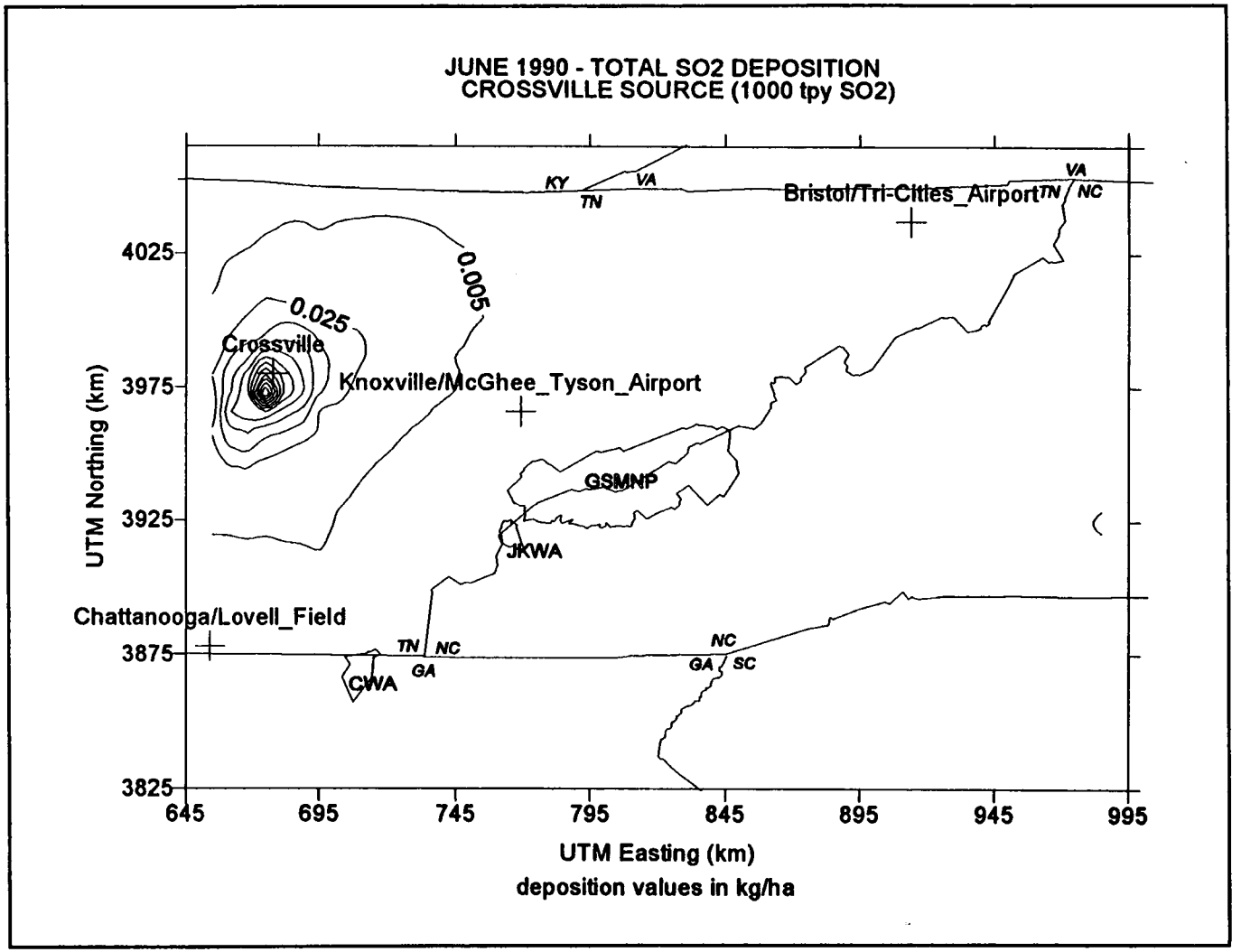

Fig. C.24. Total (wet+dry) SO_2 deposition estimated for June 1990 resulting from a 28.8 g/s (1000 tpy) hypothetical SO_2 emission source located in Crossville.

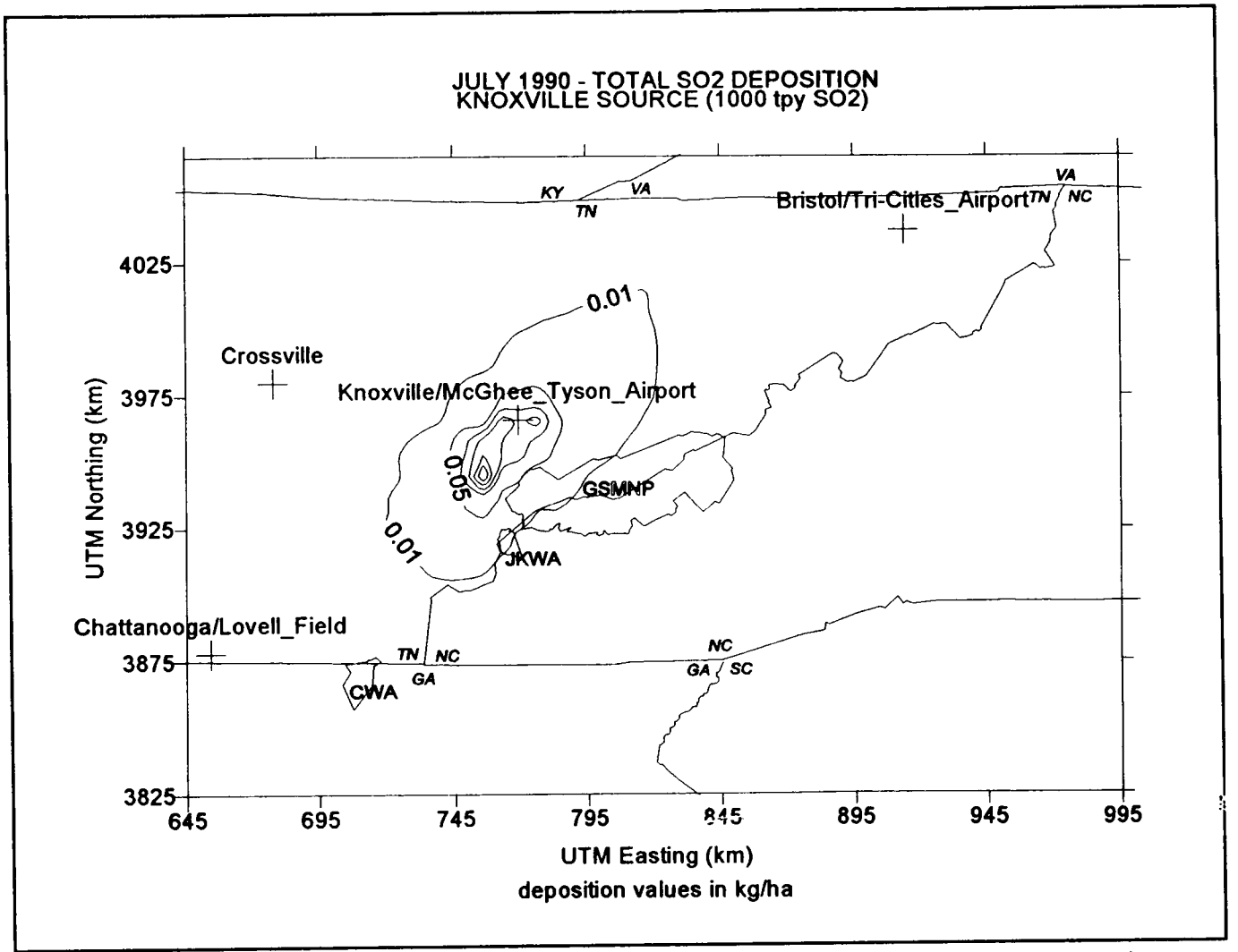

Fig. C.25. Total (wet+dry) SO_2 deposition estimated for July 1990 resulting from a 28.8 g/s (1000 tpy) hypothetical SO_2 emission source located at Knoxville /McGhee Tyson Airport.

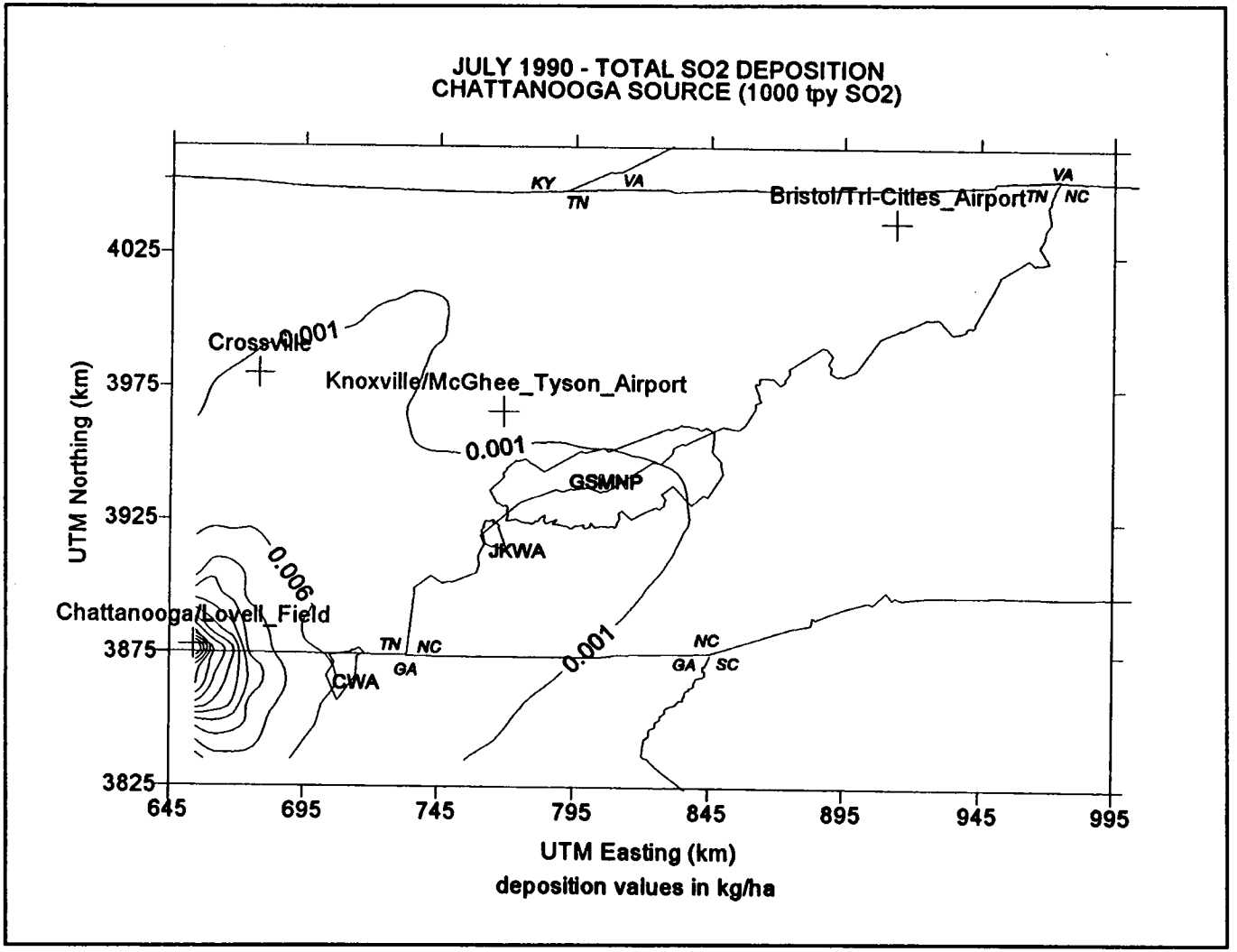

Fig. C.26. Total (wet+dry) SO_2 deposition estimated for July 1990 resulting from a 28.8 g/s (1000 tpy) hypothetical SO_2 emission source located at Chattanooga/Lovell Field.

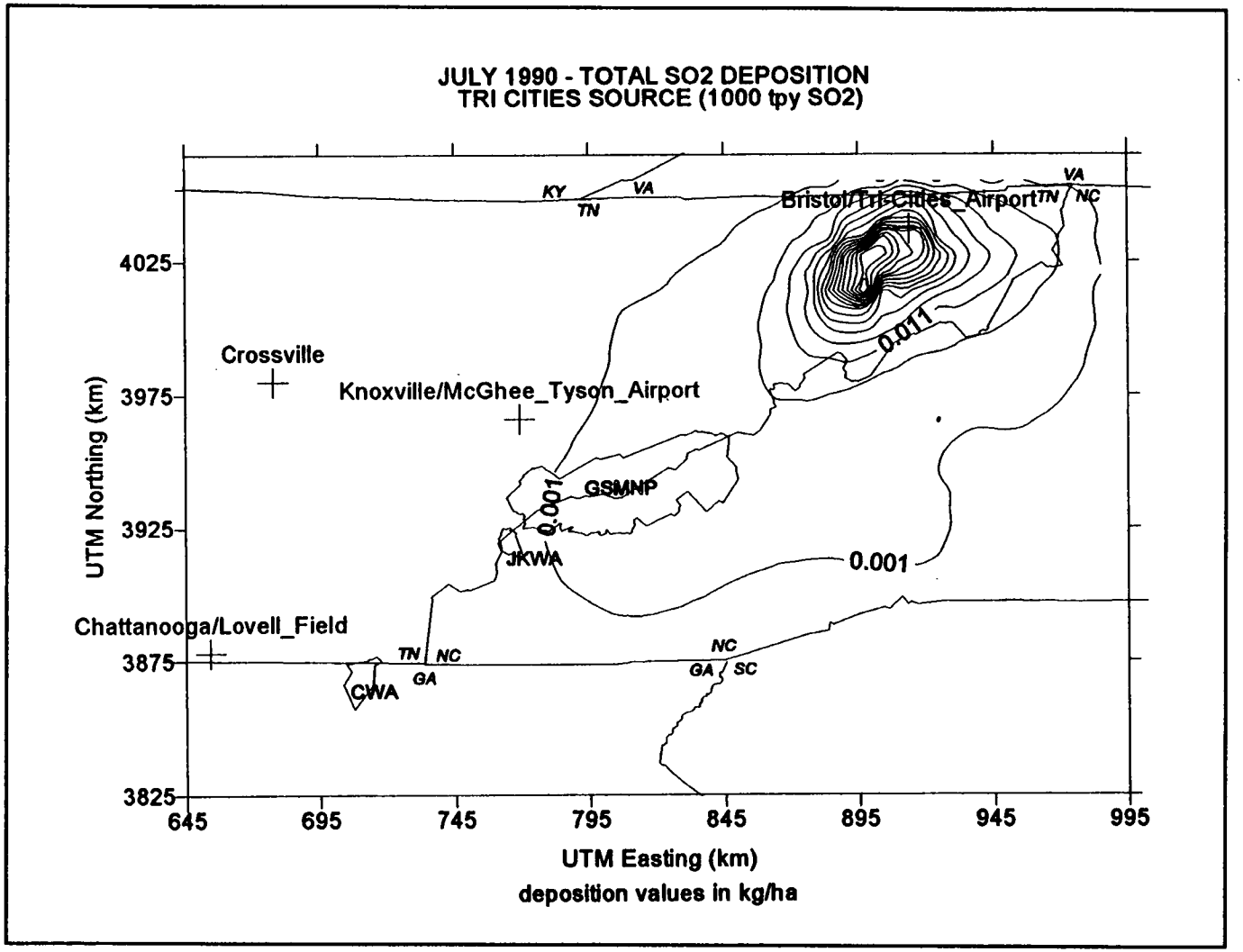

Fig. C.27. Total (wet+dry) SO_2 deposition estimated for July 1990 resulting from a 28.8 g/s (1000 tpy) hypothetical SO_2 emission source located at Bristol/Tri Cities Airport.

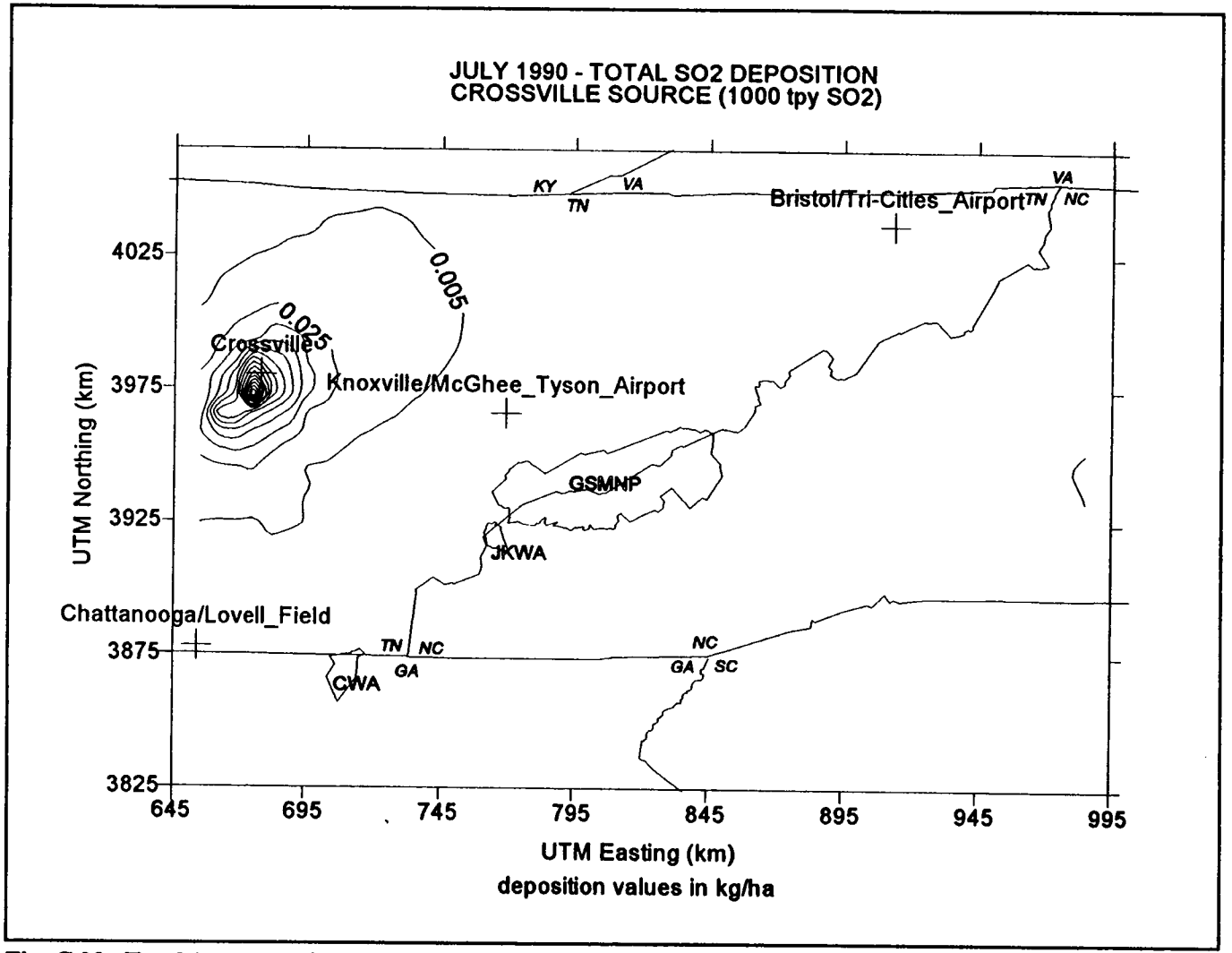

Fig. C.28. Total (wet+dry) SO_2 deposition estimated for July 1990 resulting from a 28.8 g/s (1000 tpy) hypothetical SO_2 emission source located in Crossville.

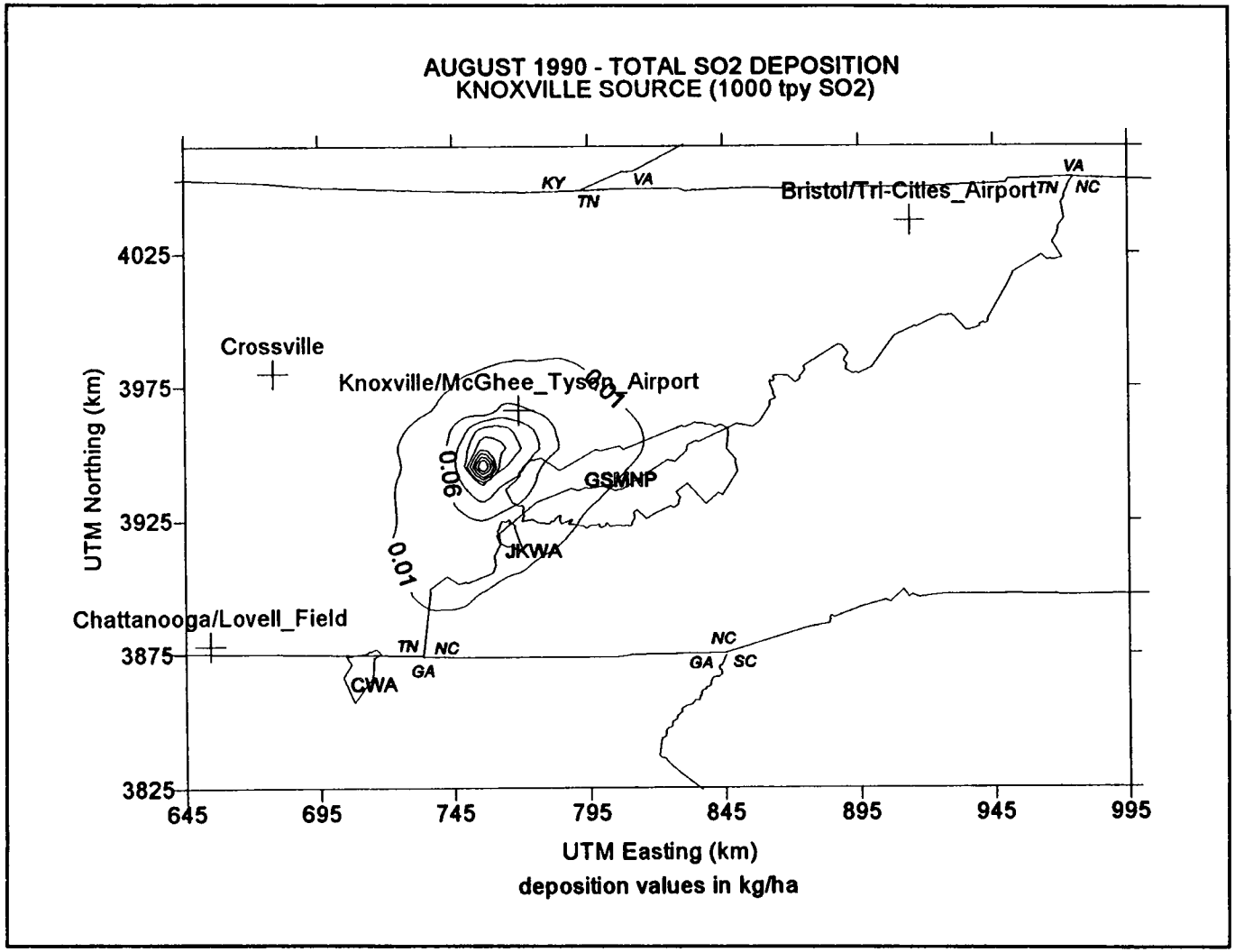

Fig. C.29. Total (wet+dry) SO_2 deposition estimated for August 1990 resulting from a 28.8 g/s (1000 tpy) hypothetical SO_2 emission source located at Knoxville /McGhee Tyson Airport.

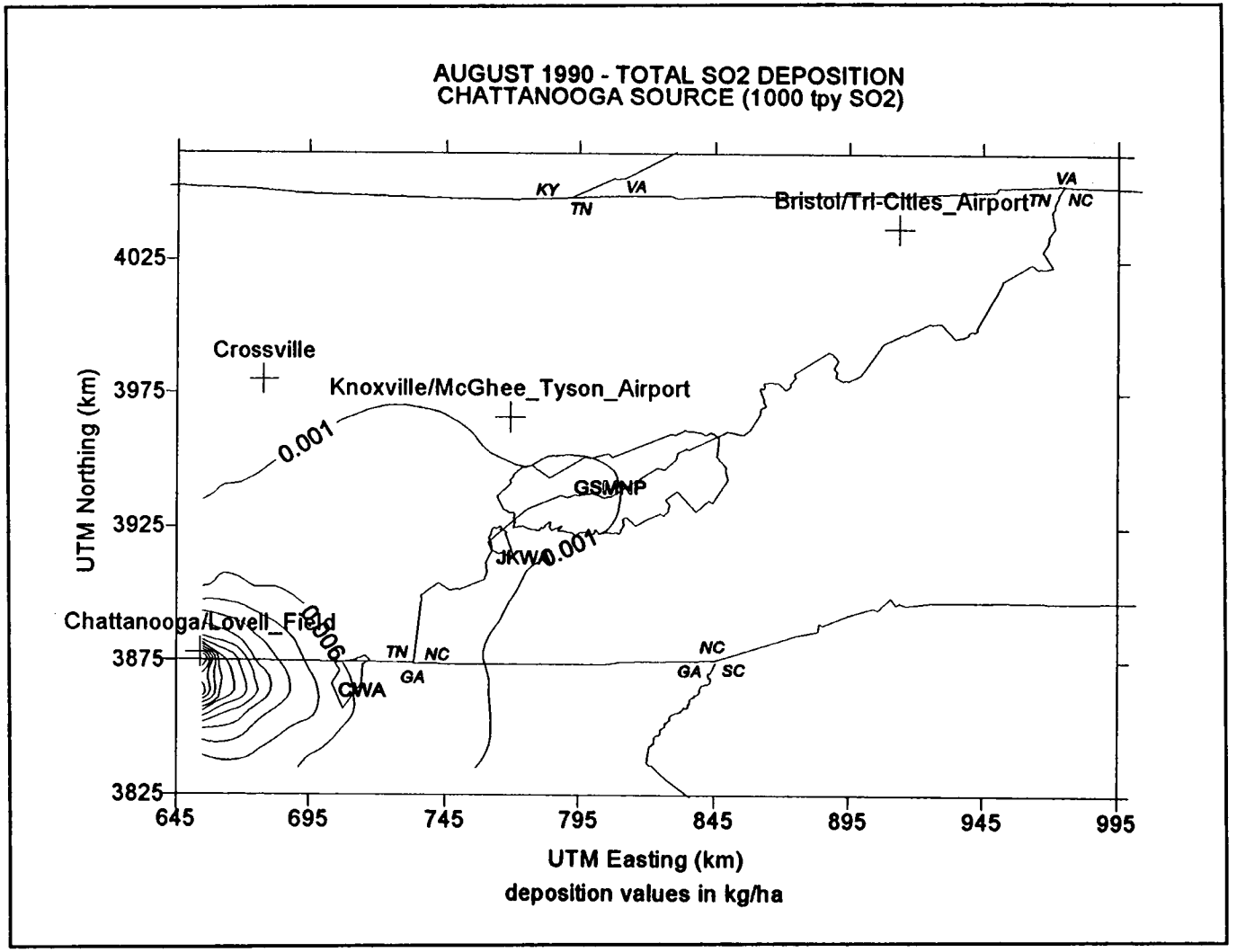

Fig. C.30. Total (wet+dry) SO_2 deposition estimated for August 1990 resulting from a 28.8 g/s (1000 tpy) hypothetical SO_2 emission source located at Chattanooga/Lovell Field.

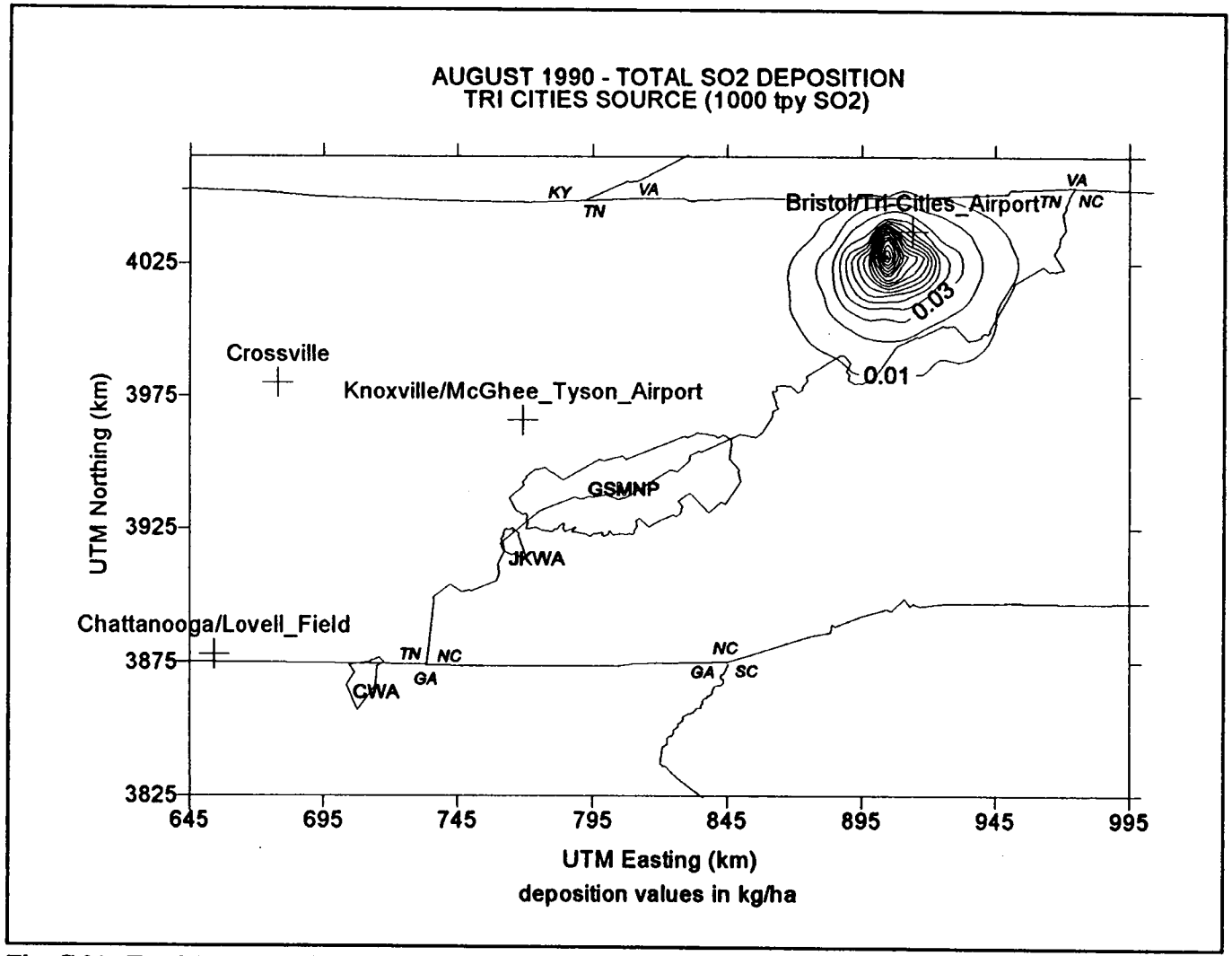

Fig. C.31. Total (wet+dry) SO_2 deposition estimated for August 1990 resulting from a 28.8 g/s (1000 tpy) hypothetical SO_2 emission source located at Bristol/Tri Cities Airport.

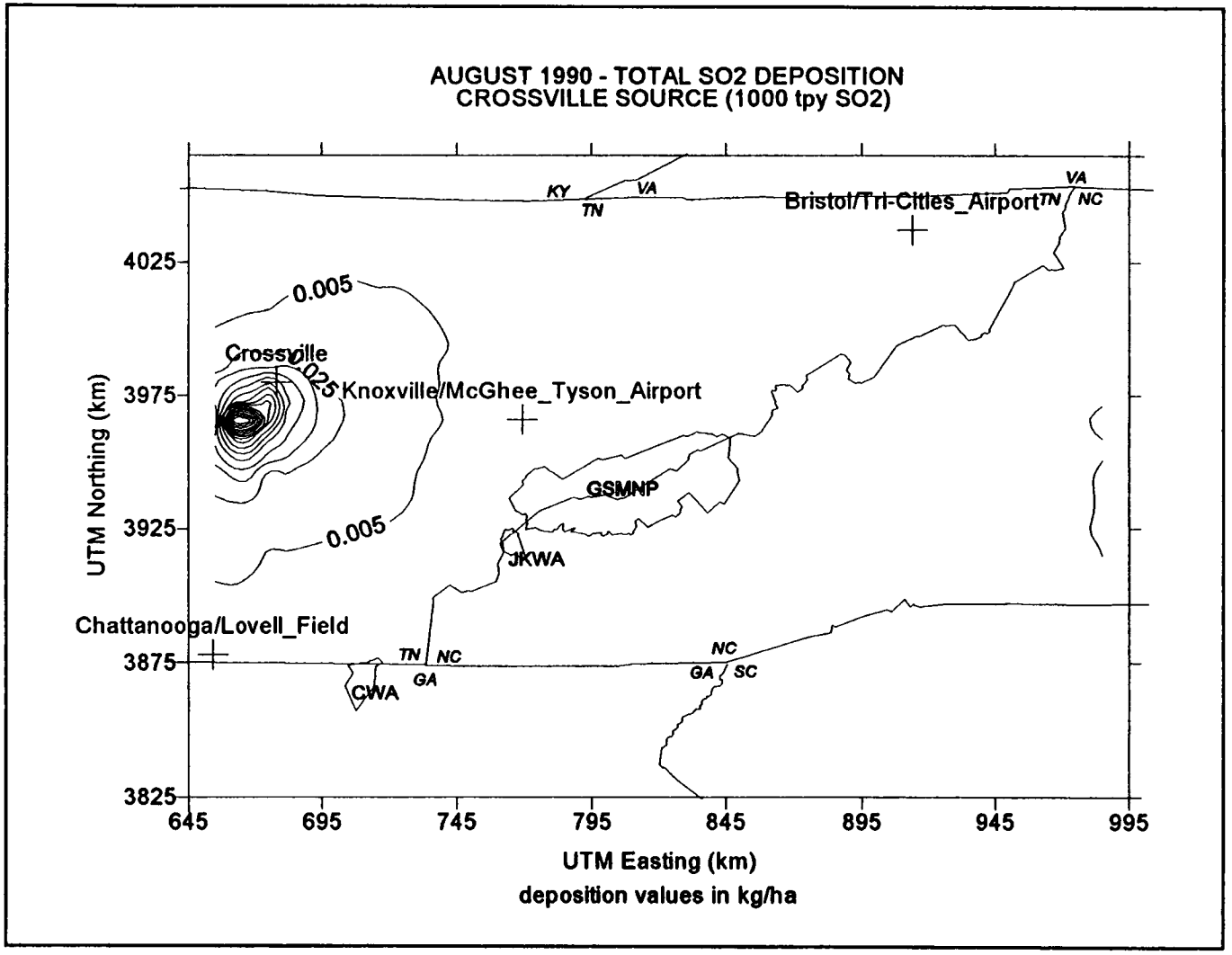

Fig. C.32. Total (wet+dry) SO_2 deposition estimated for August 1990 resulting from a 28.8 g/s (1000 tpy) hypothetical SO_2 emission source located in Crossville.

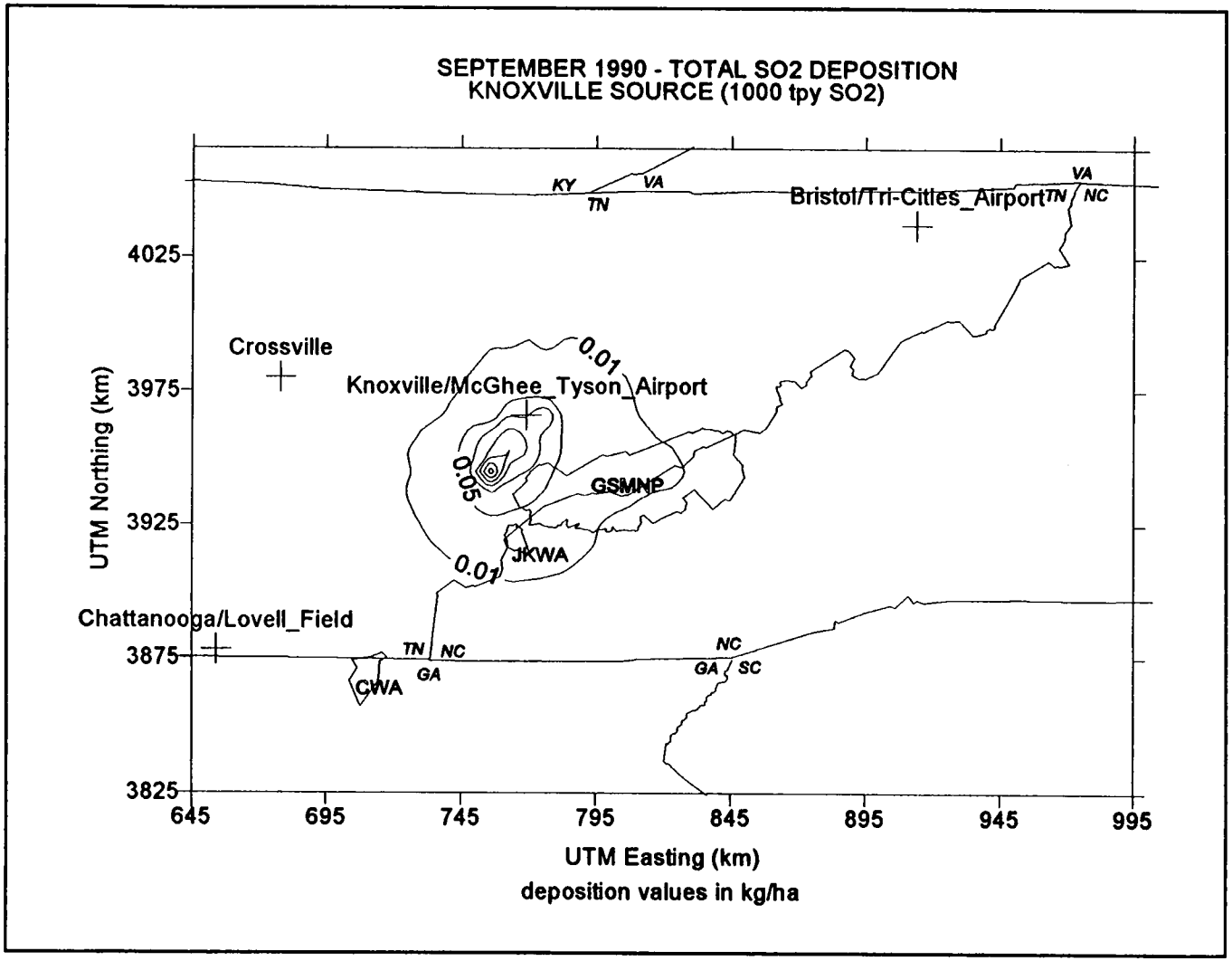

Fig. C.33. Total (wet+dry) SO_2 deposition estimated for September 1990 resulting from a 28.8 g/s (1000 tpy) hypothetical SO_2 emission source located at Knoxville /McGhee Tyson Airport.

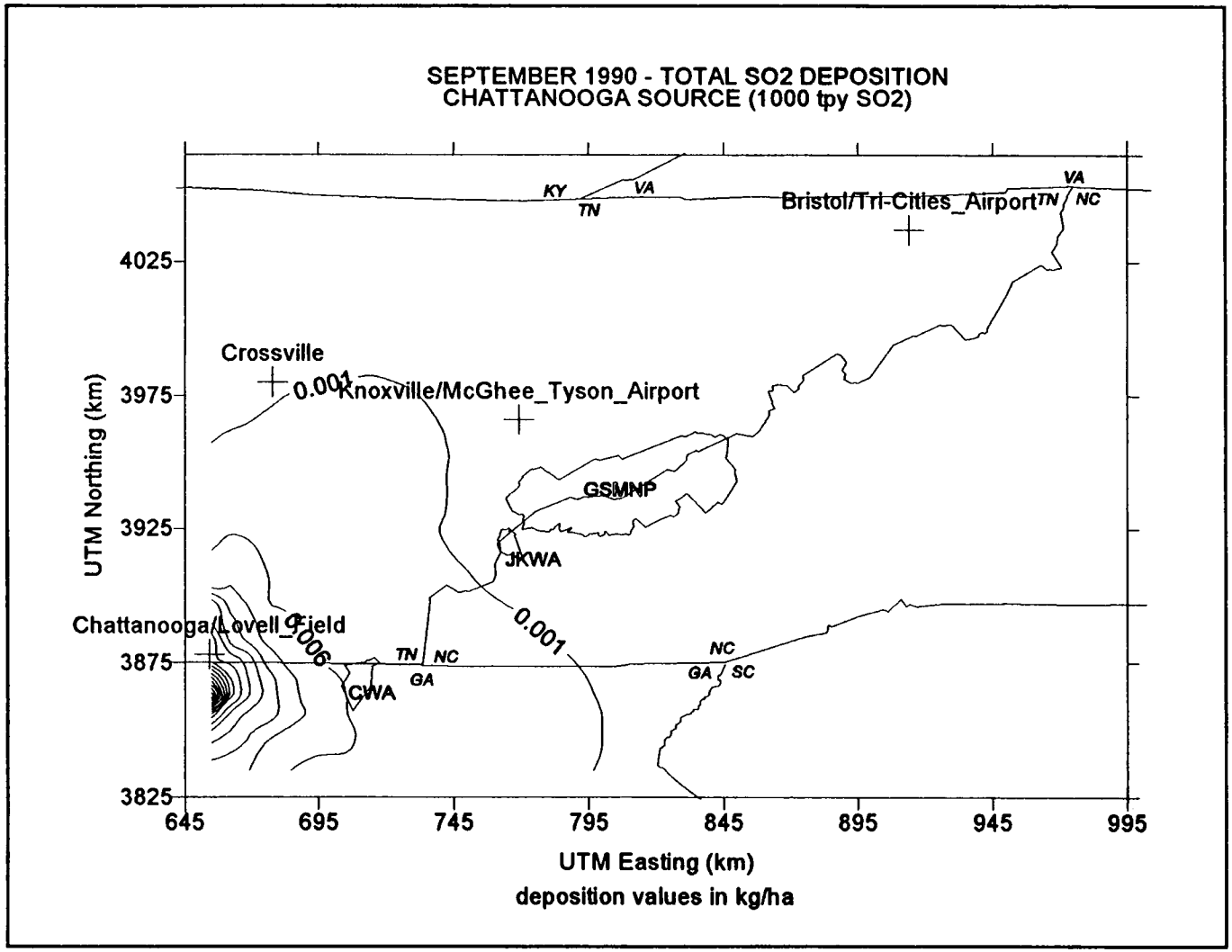

Fig. C.34. Total (wet+dry) SO_2 deposition estimated for September 1990 resulting from a 28.8 g/s (1000 tpy) hypothetical SO_2 emission source located at Chattanooga/Lovell Field.

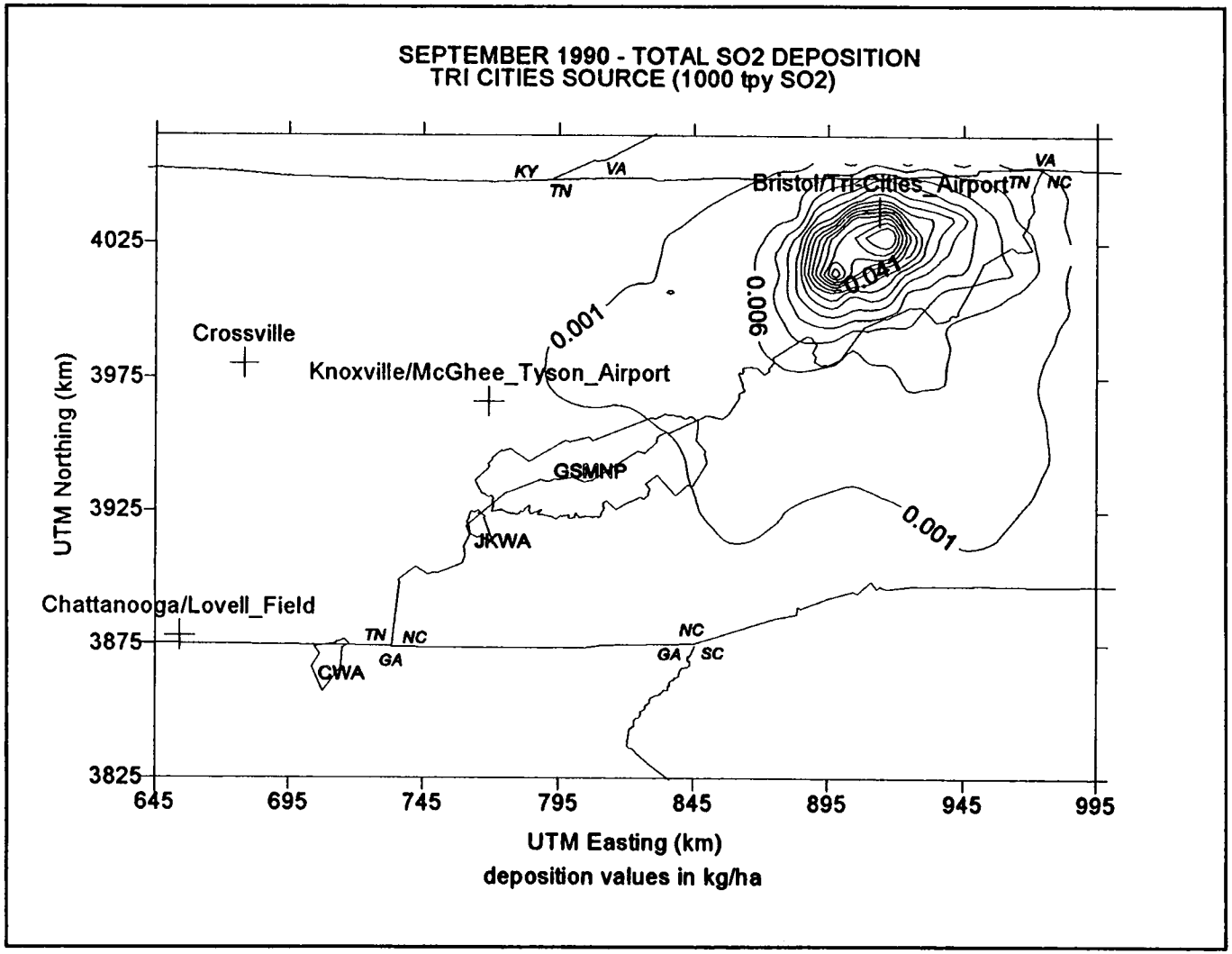

Fig. C.35. Total (wet+dry) SO_2 deposition estimated for September 1990 resulting from a 28.8 g/s (1000 tpy) hypothetical SO_2 emission source located at Bristol/Tri Cities Airport.

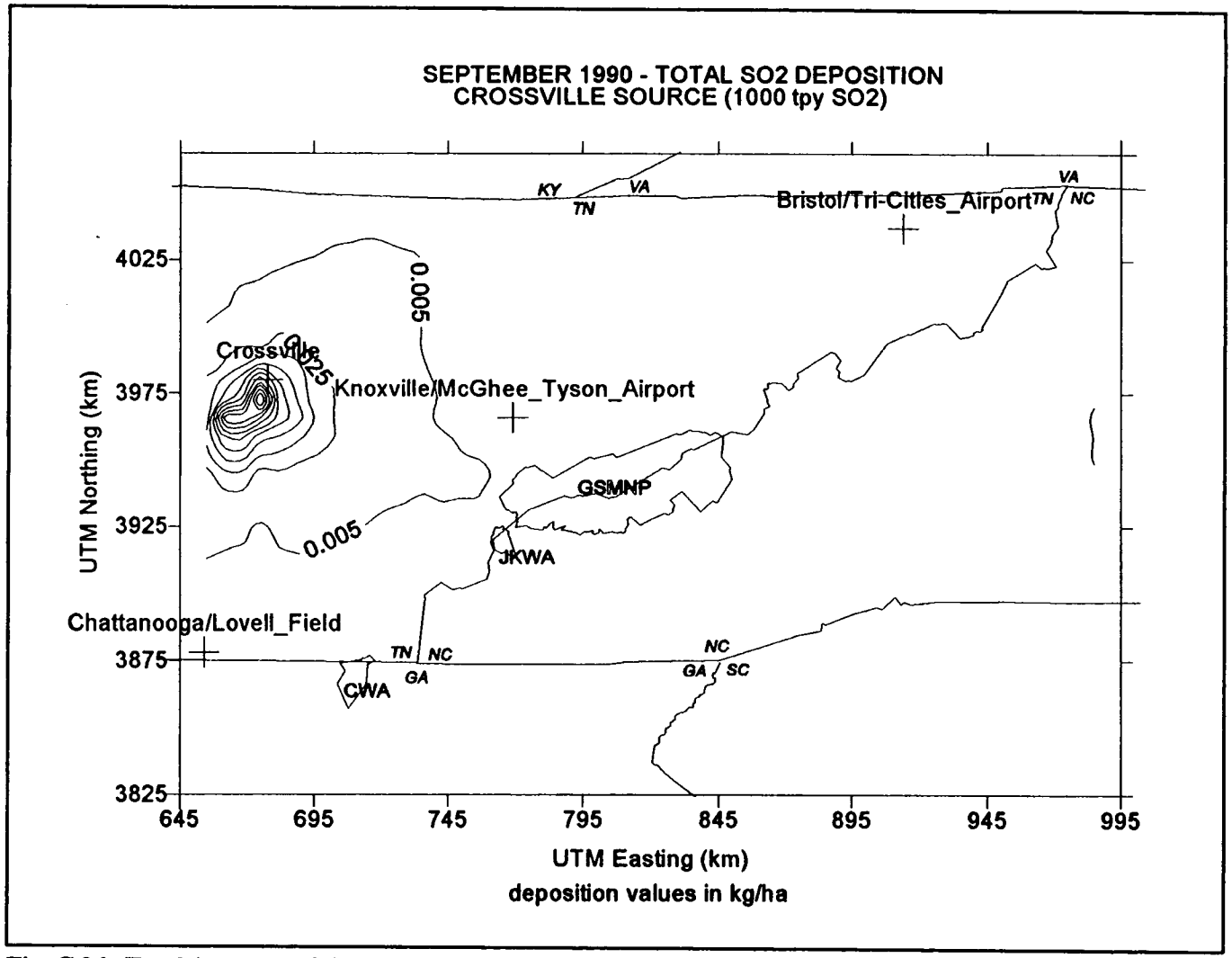

Fig. C.36. Total (wet+dry) SO_2 deposition estimated for September 1990 resulting from a 28.8 g/s (1000 tpy) hypothetical SO_2 emission source located in Crossville.

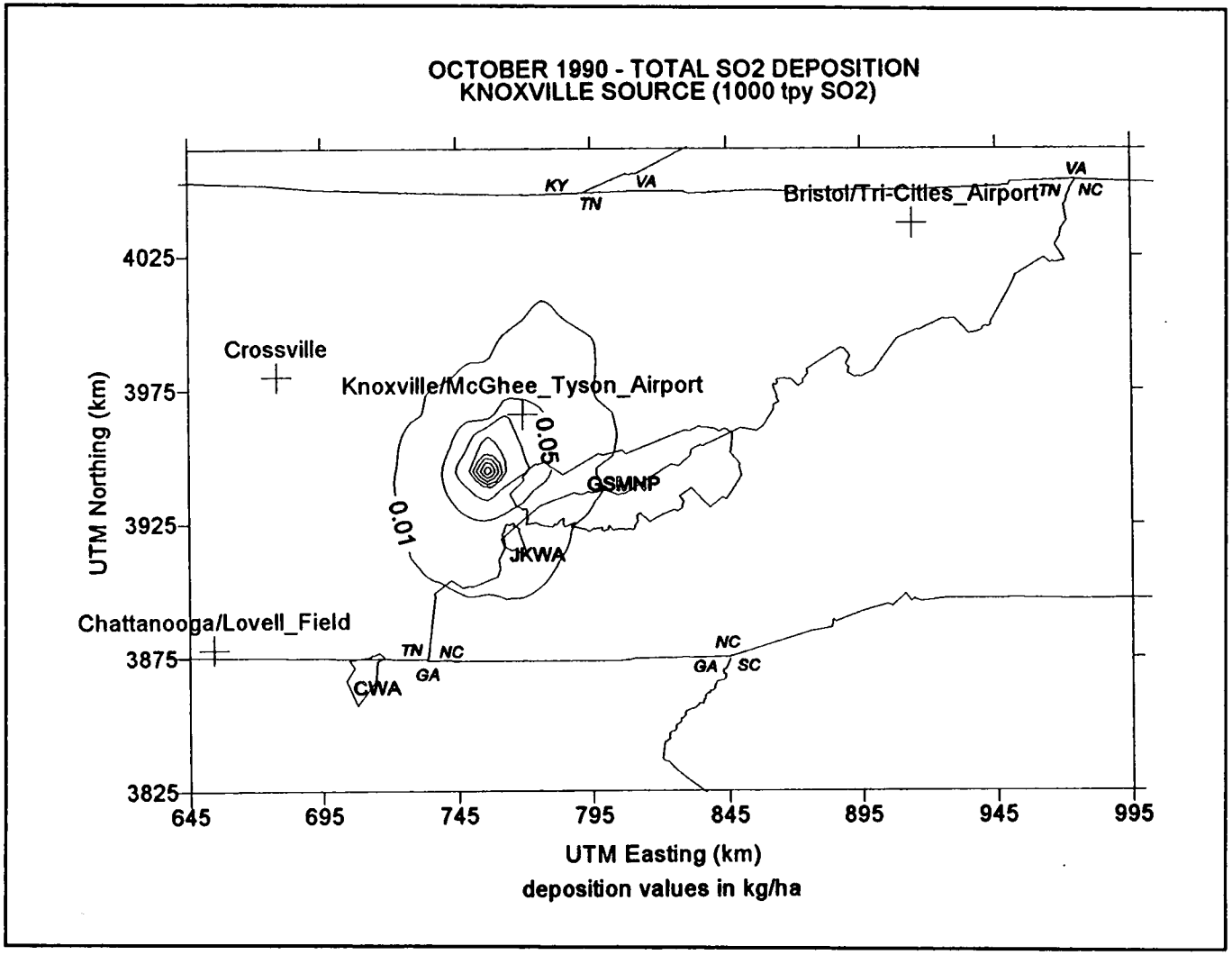

Fig. C.37. Total (wet+dry) SO_2 deposition estimated for October 1990 resulting from a 28.8 g/s (1000 tpy) hypothetical SO_2 emission source located at Knoxville /McGhee Tyson Airport.

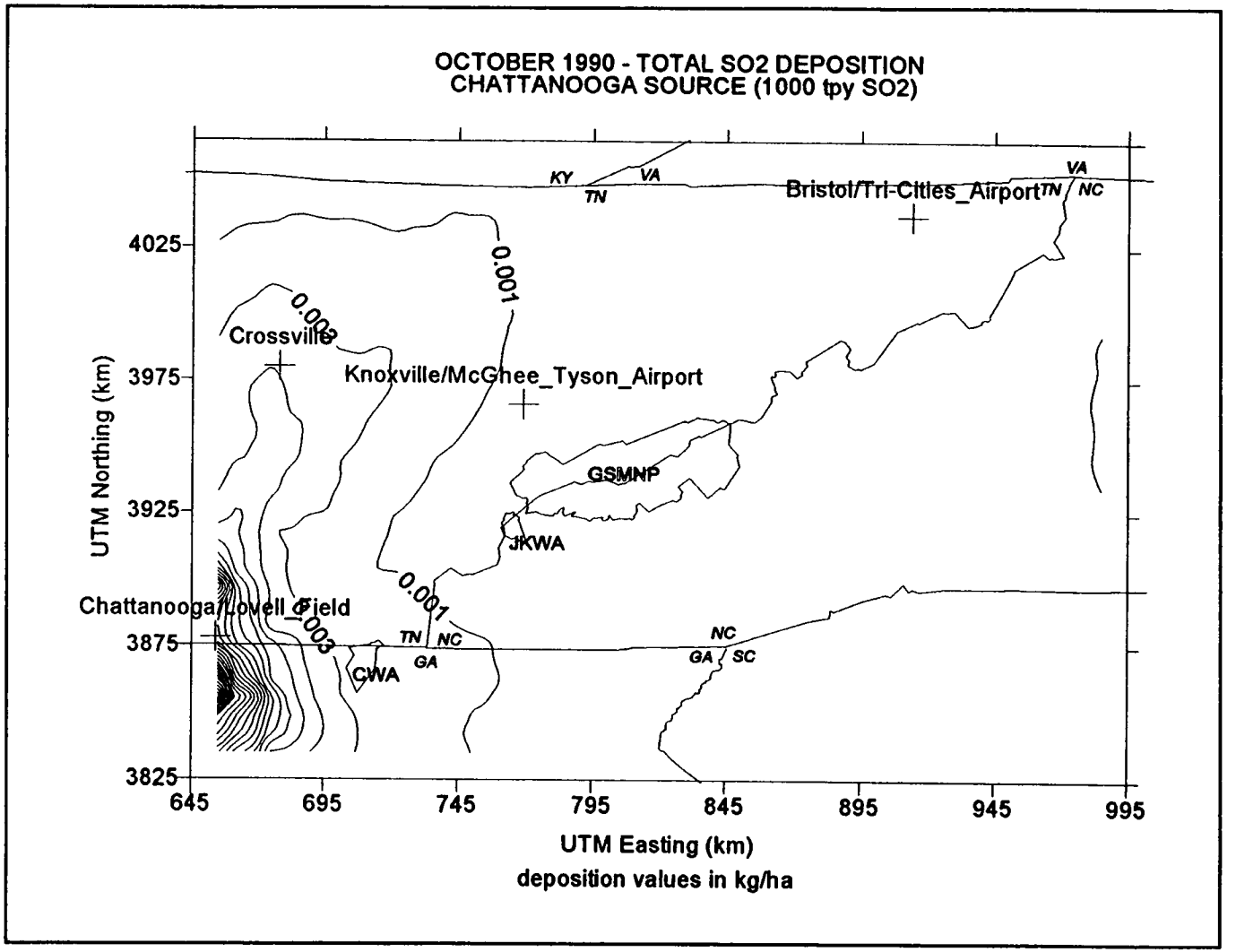

Fig. C.38. Total (wet+dry) SO_2 deposition estimated for October 1990 resulting from a 28.8 g/s (1000 tpy) hypothetical SO_2 emission source located at Chattanooga/Lovell Field.

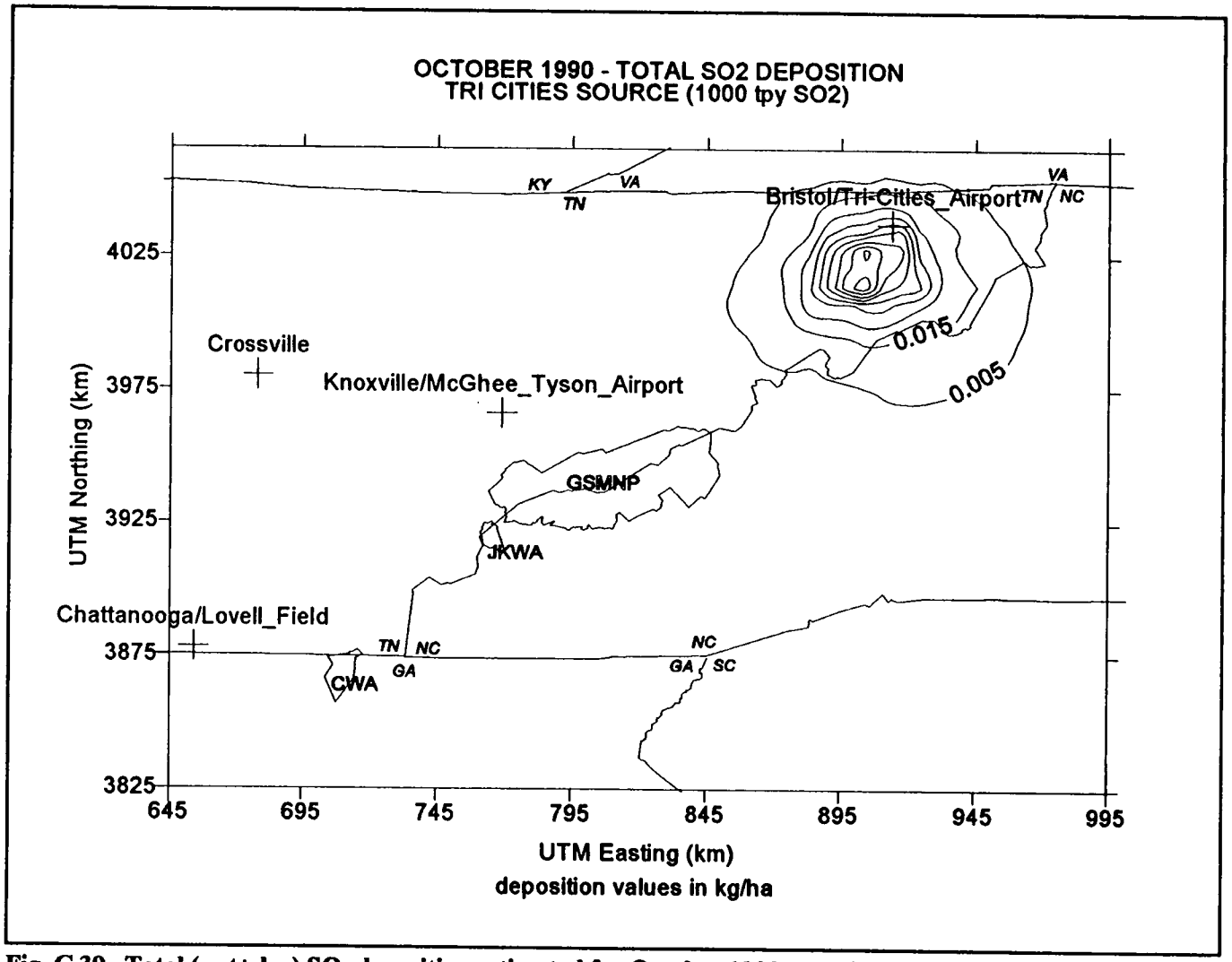

Fig. C.39. Total (wet+dry) SO_2 deposition estimated for October 1990 resulting from a 28.8 g/s (1000 tpy) hypothetical SO_2 emission source located at Bristol/Tri Cities Airport.

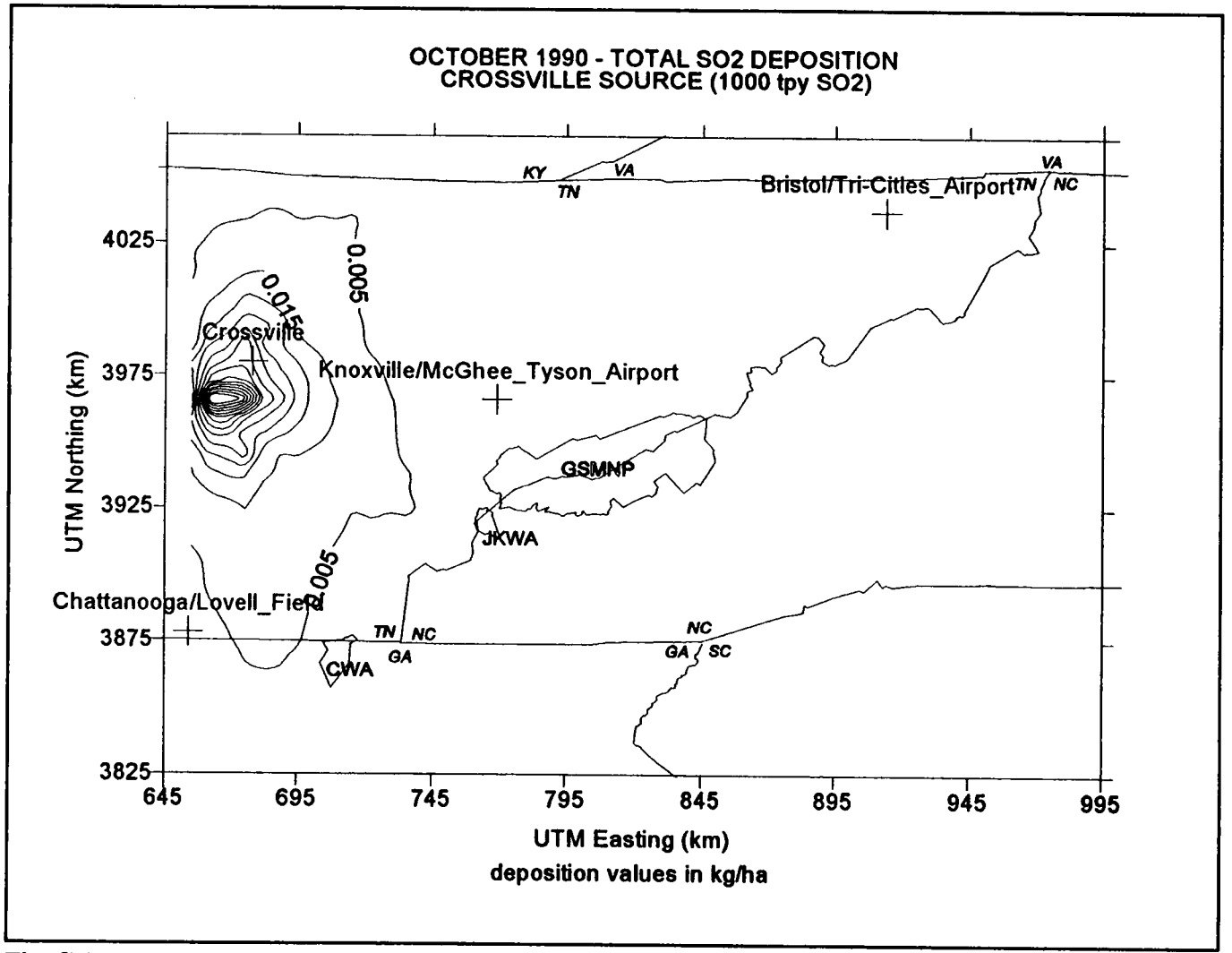

Fig. C.40. Total (wet+dry) SO_2 deposition estimated for October 1990 resulting from a 28.8 g/s (1000 tpy) hypothetical SO_2 emission source located in Crossville.

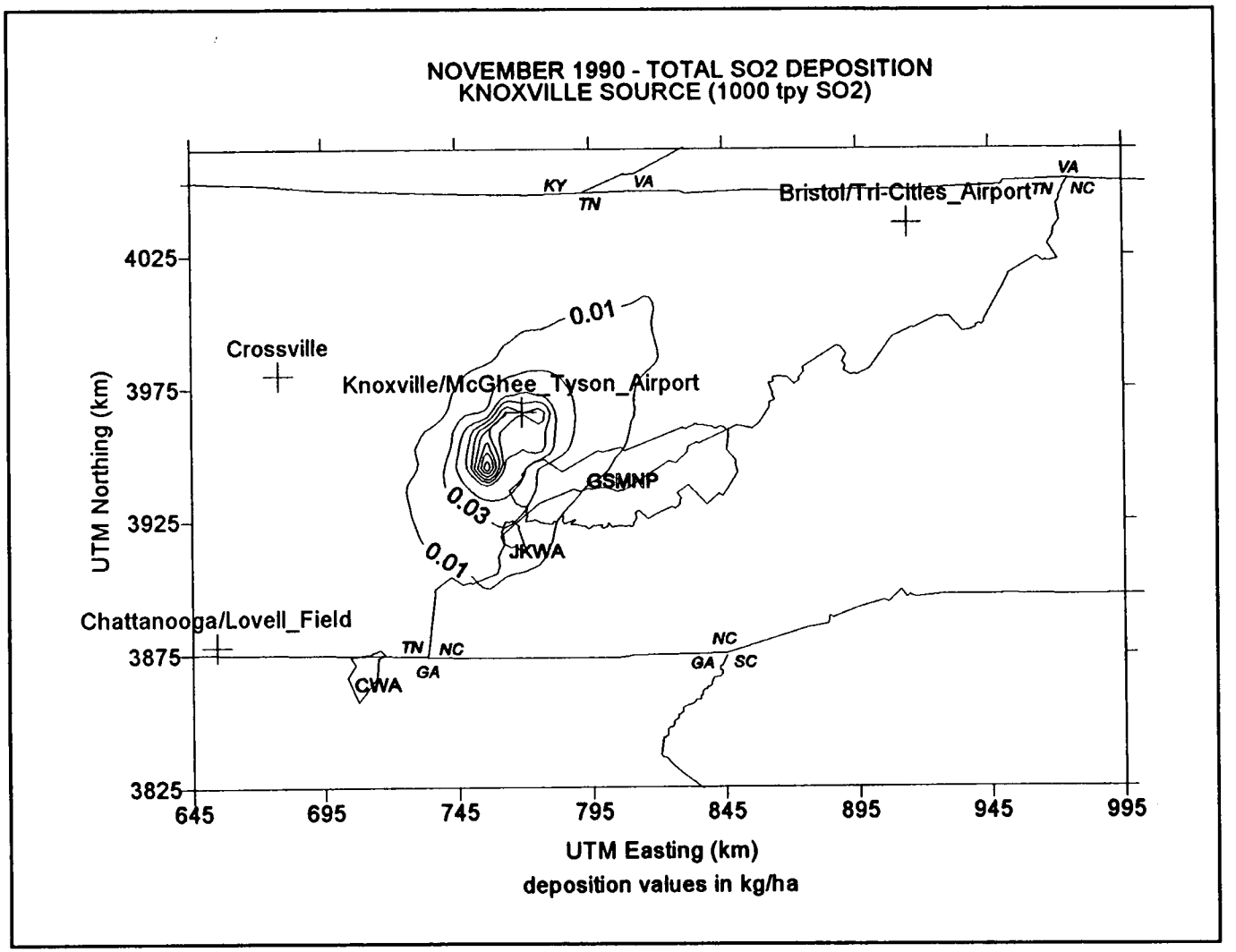

Fig. C.41. Total (wet+dry) SO_2 deposition estimated for November 1990 resulting from a 28.8 g/s (1000 tpy) hypothetical SO_2 emission source located at Knoxville /McGhee Tyson Airport.

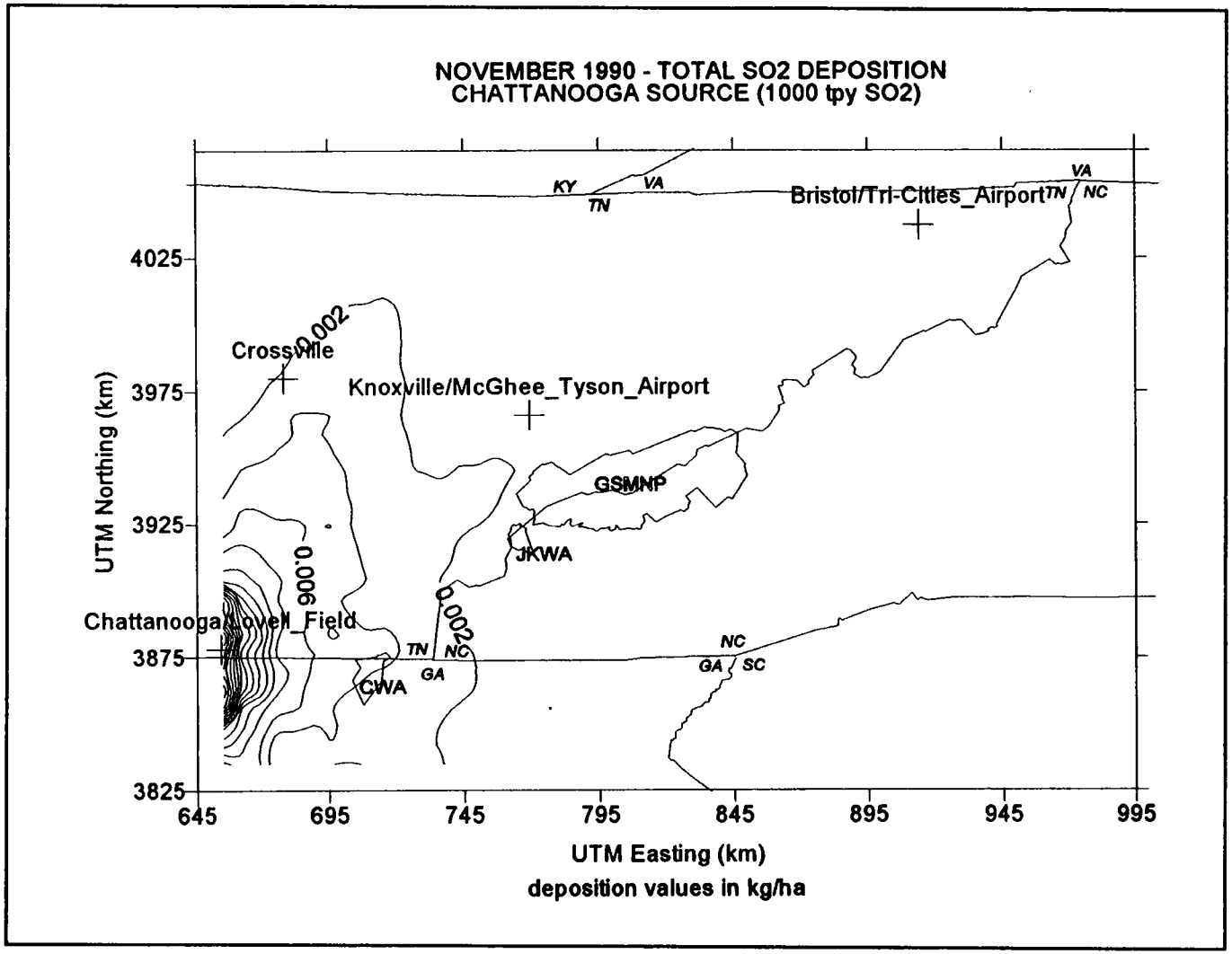

Fig. C.42. Total (wet+dry) SO_2 deposition estimated for November 1990 resulting from a 28.8 g/s (1000 tpy) hypothetical SO_2 emission source located at Chattanooga/Lovell Field.

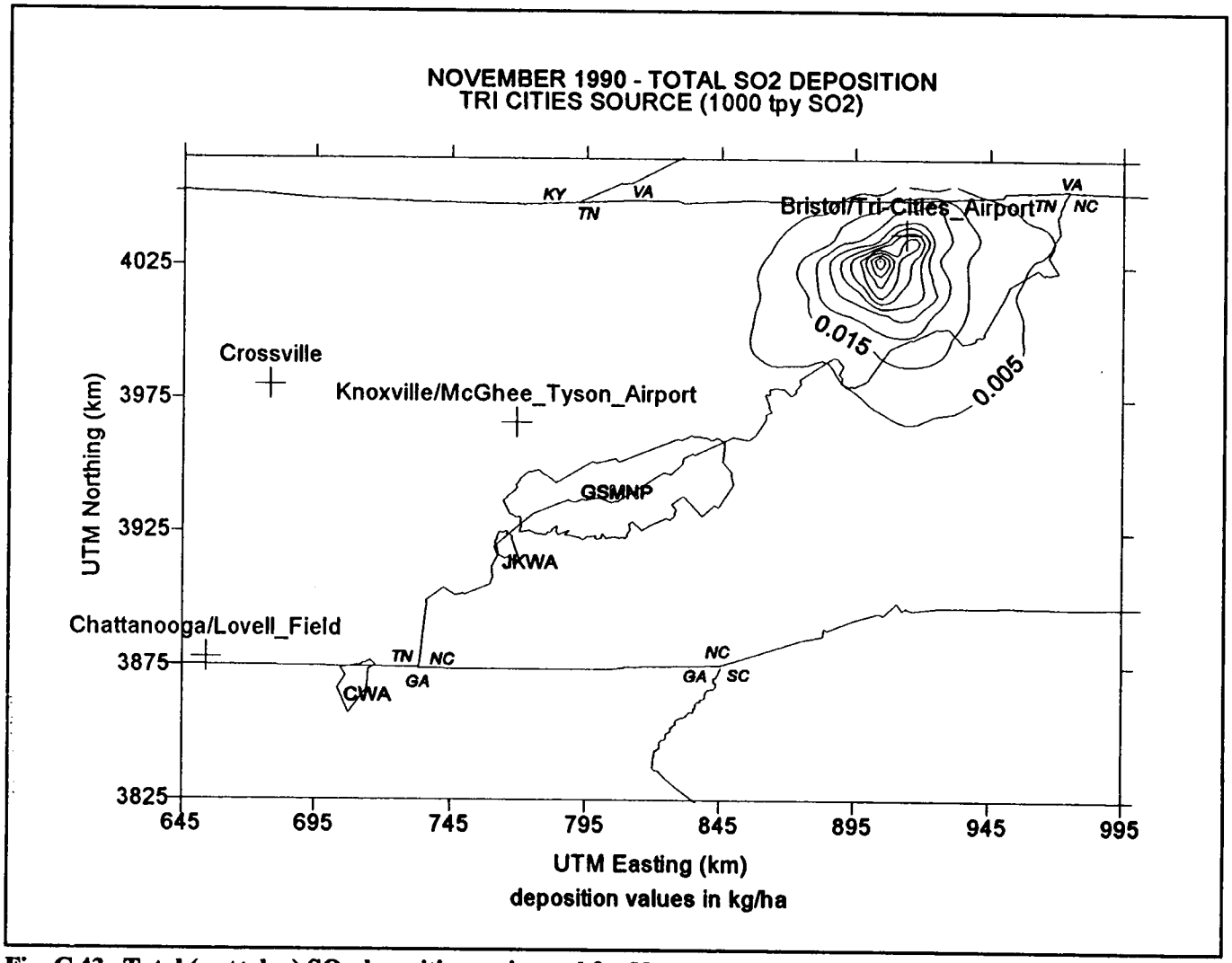

Fig. C.43. Total (wet+dry) SO_2 deposition estimated for November 1990 resulting from a 28.8 g/s (1000 tpy) hypothetical SO_2 emission source located at Bristol/Tri Cities Airport.

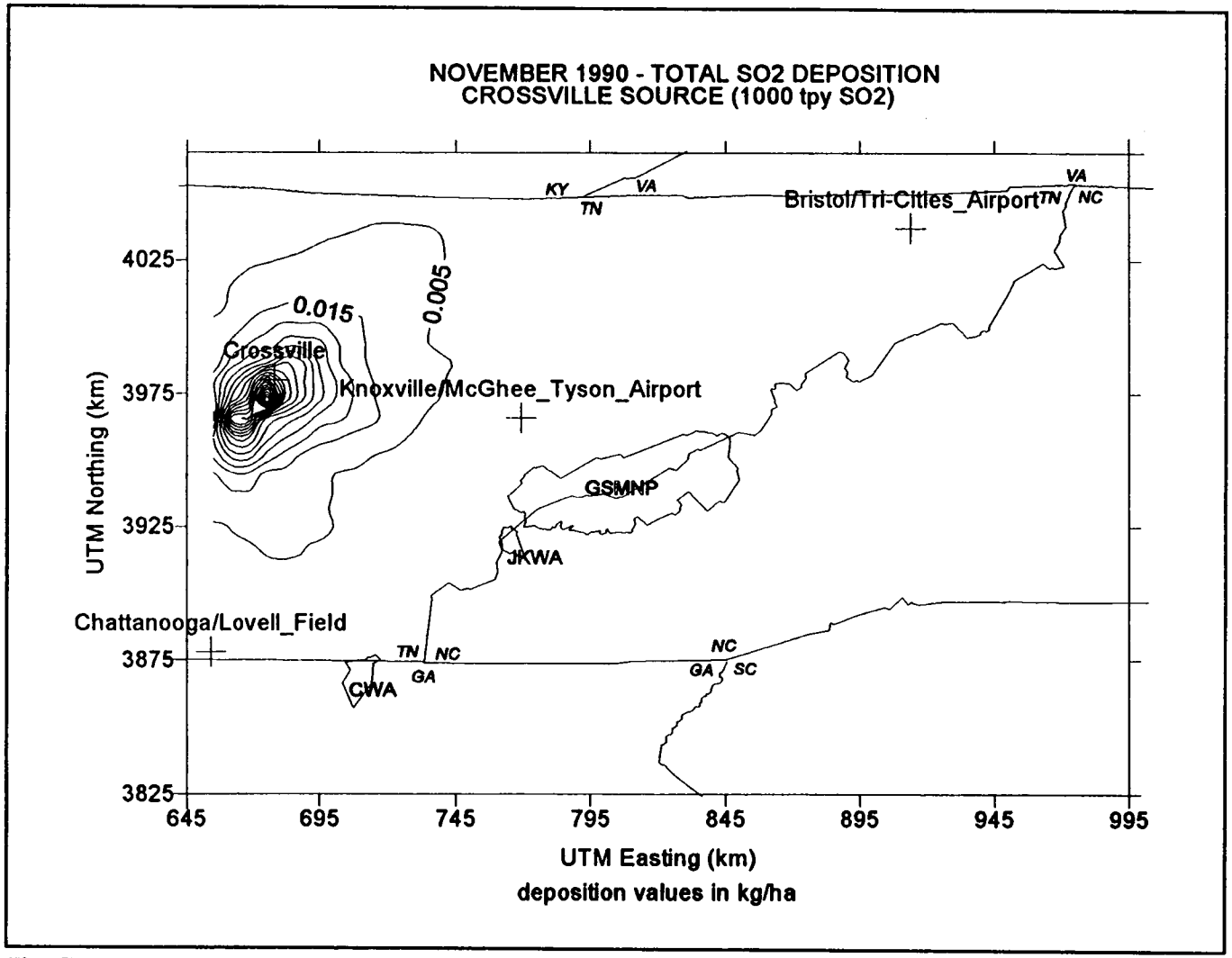

Fig. C.44. Total (wet+dry) SO_2 deposition estimated for November 1990 resulting from a 28.8 g/s (1000 tpy) hypothetical SO_2 emission source located in Crossville.

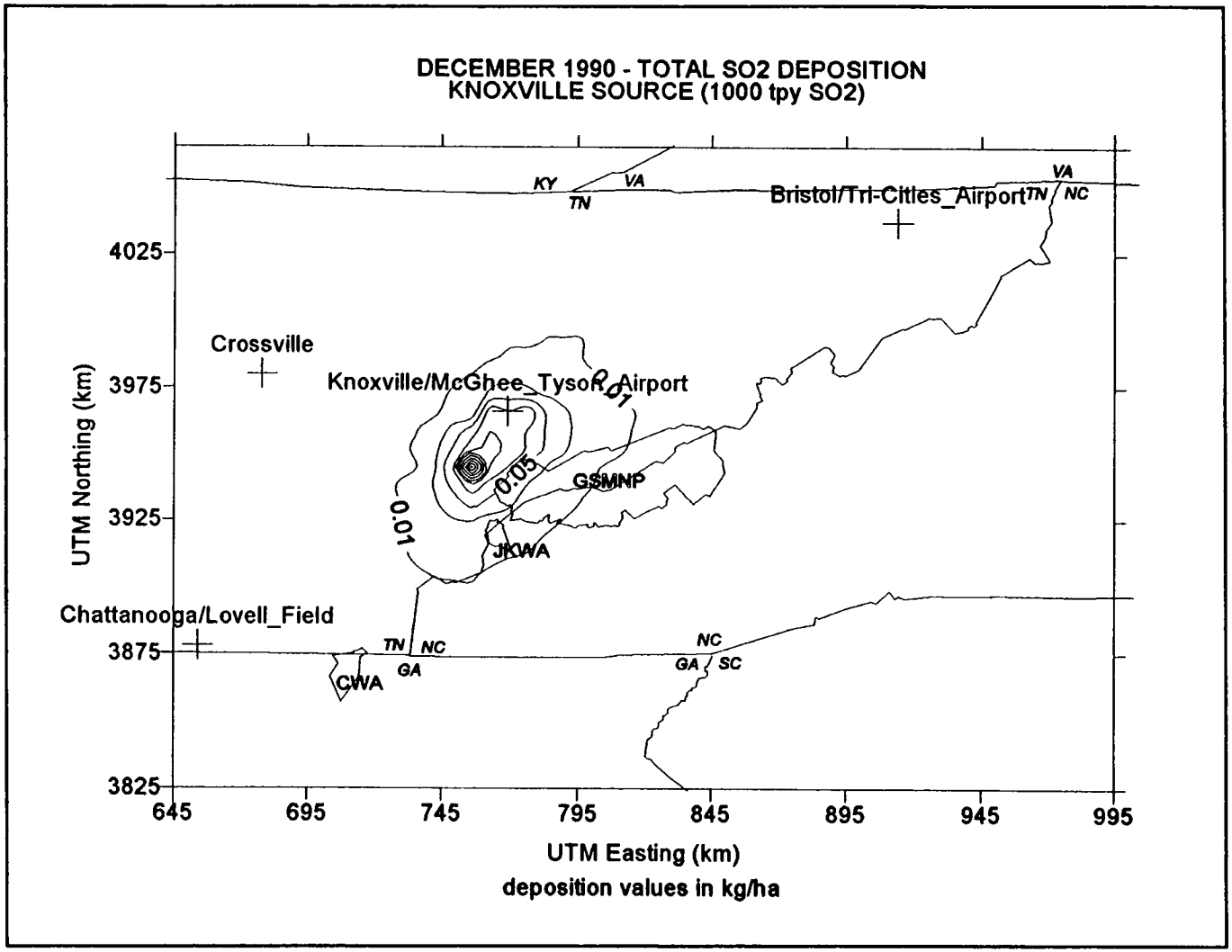

Fig. C.45. Total (wet+dry) SO_2 deposition estimated for December 1990 resulting from a 28.8 g/s (1000 tpy) hypothetical SO_2 emission source located at Knoxville /McGhee Tyson Airport.

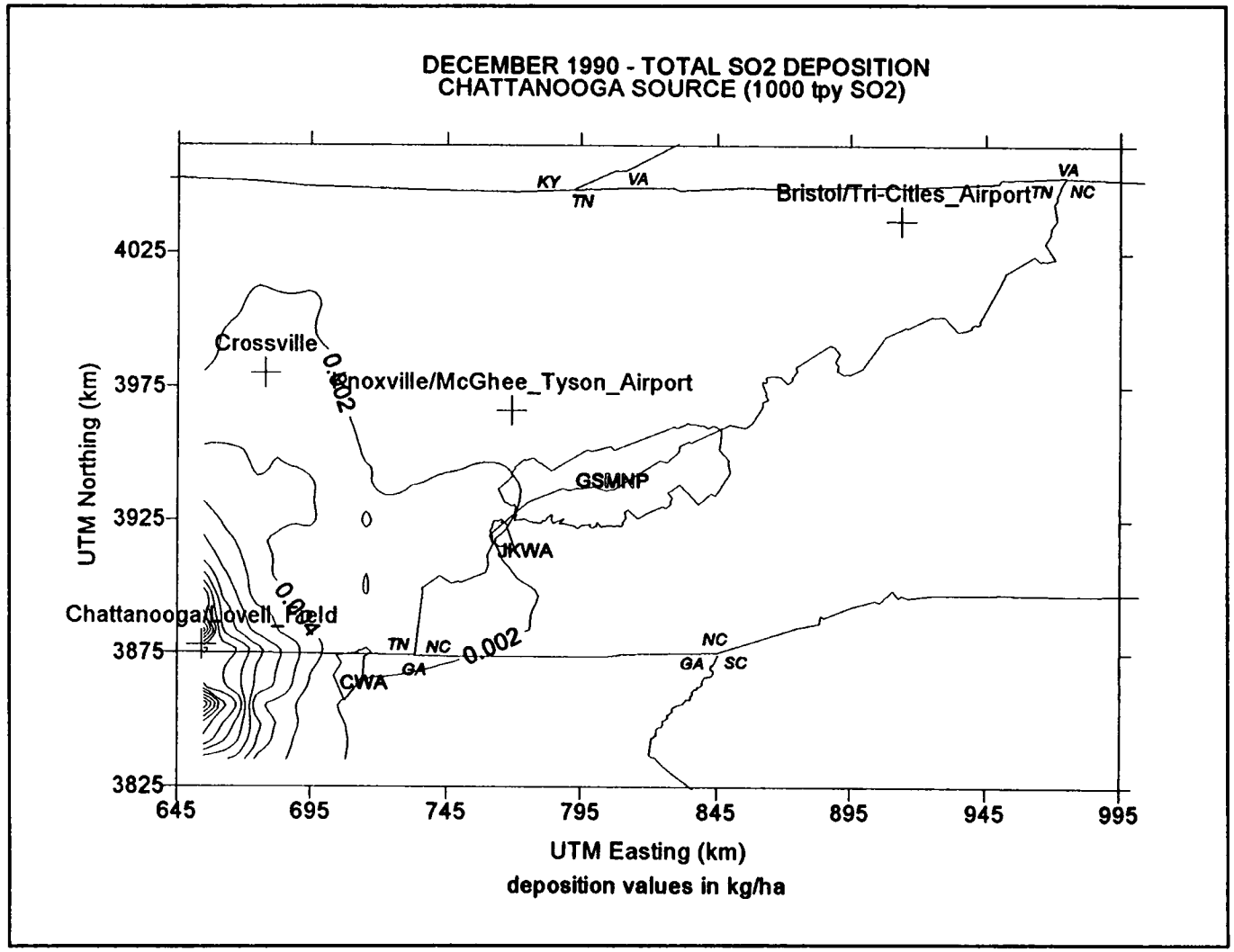

Fig. C.46. Total (wet+dry) SO_2 deposition estimated for December 1990 resulting from a 28.8 g/s (1000 tpy) hypothetical SO_2 emission source located at Chattanooga/Lovell Field.

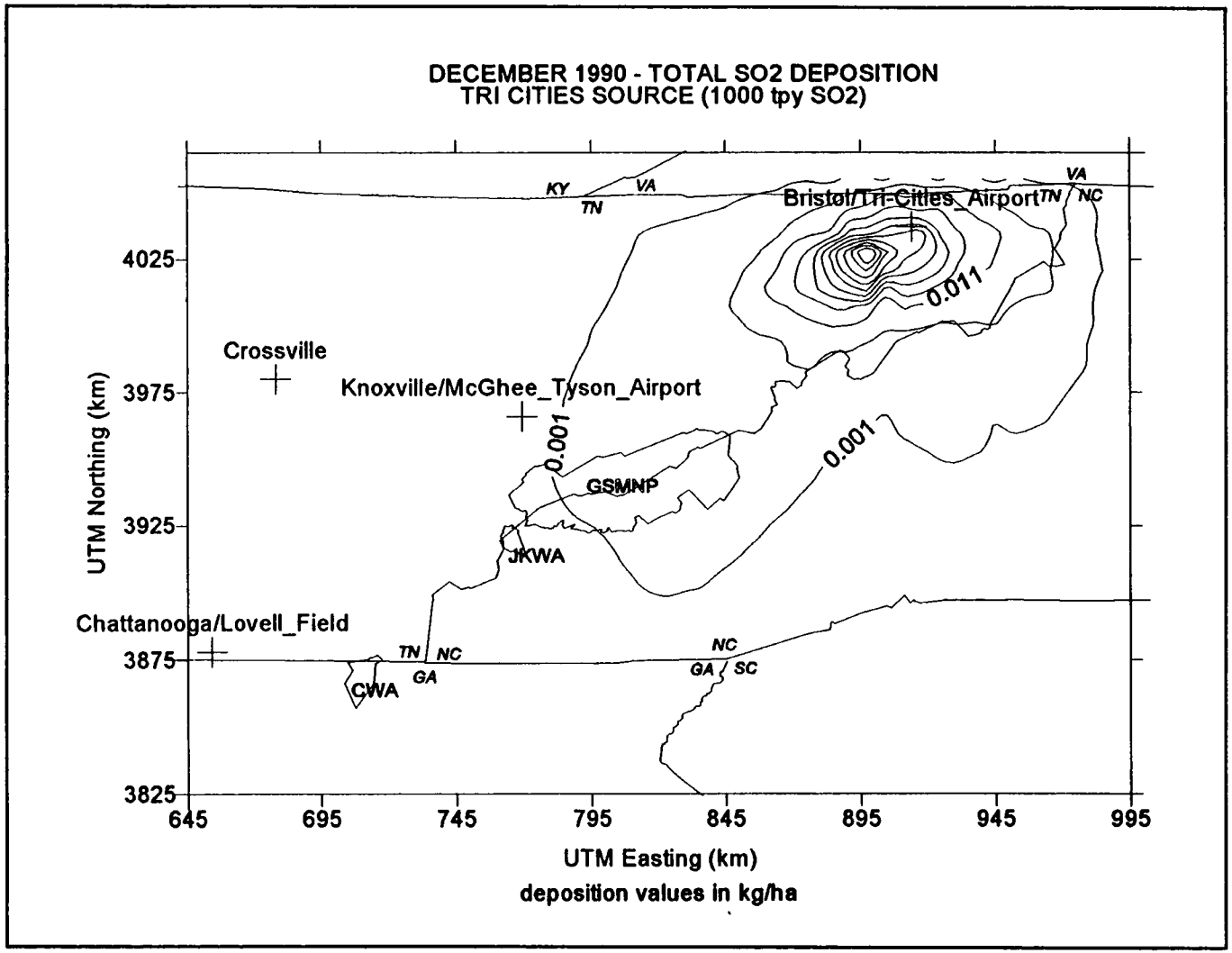

Fig. C.47. Total (wet+dry) SO_2 deposition estimated for December 1990 resulting from a 28.8 g/s (1000 tpy) hypothetical SO_2 emission source located at Bristol/Tri Cities Airport.

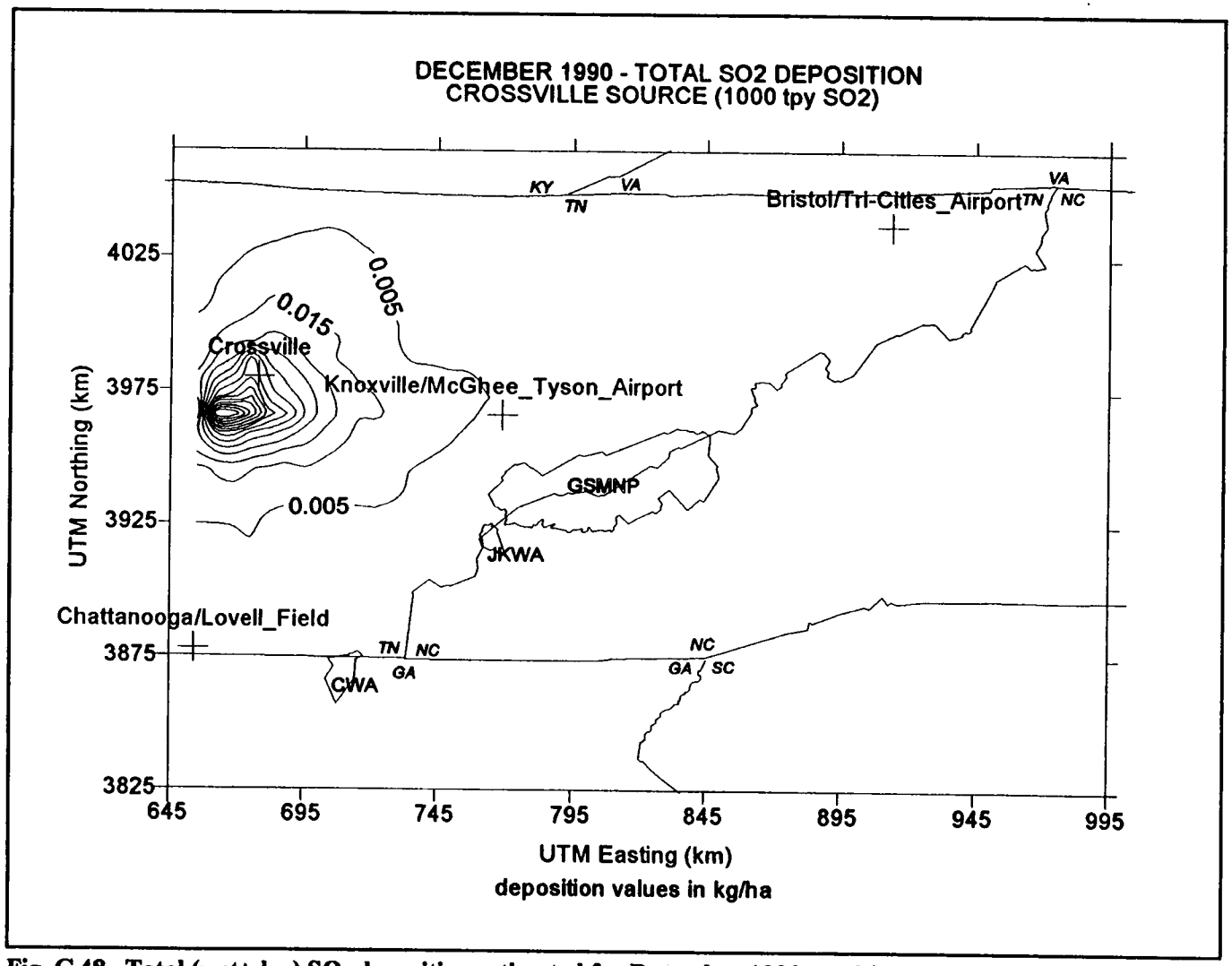

Fig. C.48. Total (wet+dry) SO_2 deposition estimated for December 1990 resulting from a 28.8 g/s (1000 tpy) hypothetical SO_2 emission source located in Crossville.

APPENDIX D
MONTHLY SO_4^{2-} DEPOSITION CONTOUR MAPS

The following figures are contour maps of monthly total (wet + dry) SO_4^{2-} deposition in the East Tennessee modeling domain. One contour map per month has been generated for each of the four hypothetical source locations.

The following abbreviations are used on the contour maps:

GSMNP	=	The Great Smoky Mountains National Park
JKWA	=	Joyce Kilmer Wilderness Area
CWA	=	Cohutta Wilderness Area
TN	=	Tennessee
NC	=	North Carolina
GA	=	Georgia
VA	=	Virginia
KY	=	Kentucky
UTM	=	Universal Transverse Mercator

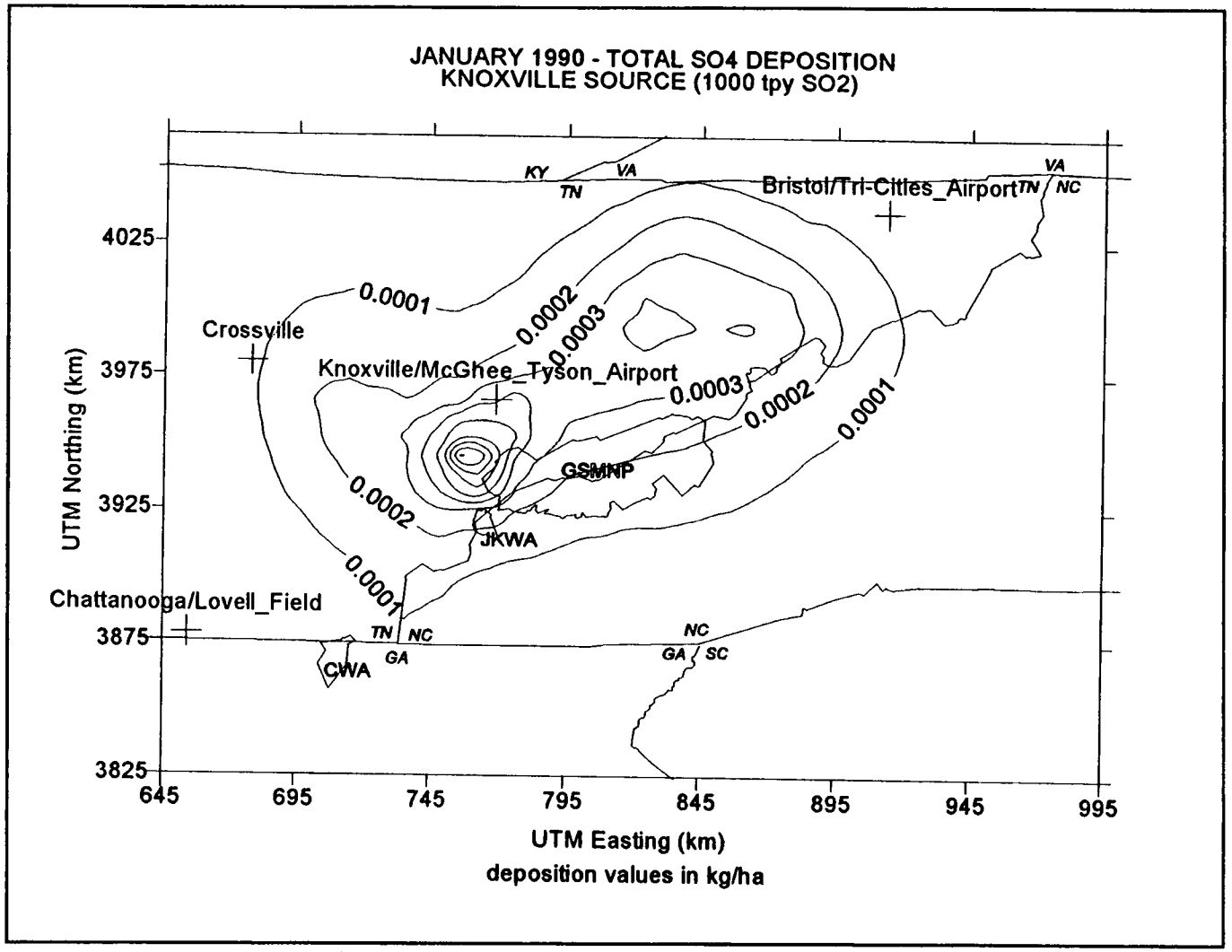

Fig. D.1. Total (wet+dry) SO_4^{2-} deposition estimated for January 1990 resulting from a 28.8 g/s (1000 tpy) hypothetical SO_2 emission source located at Knoxville /McGhee Tyson Airport.

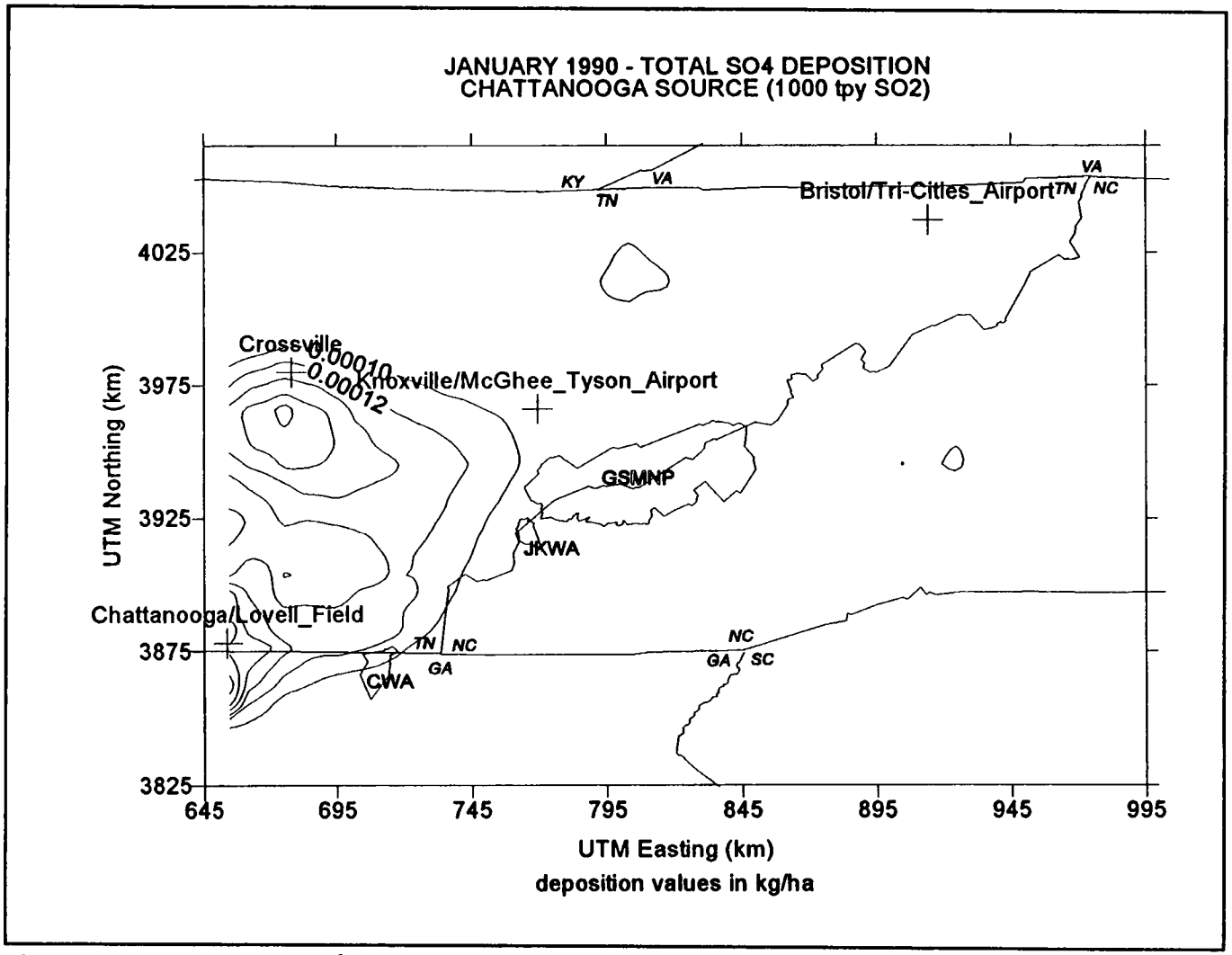

Fig. D.2. Total (wet+dry) SO_4^{2-} deposition estimated for January 1990 resulting from a 28.8 g/s (1000 tpy) hypothetical SO_2 emission source located at Chattanooga/Lovell Field.

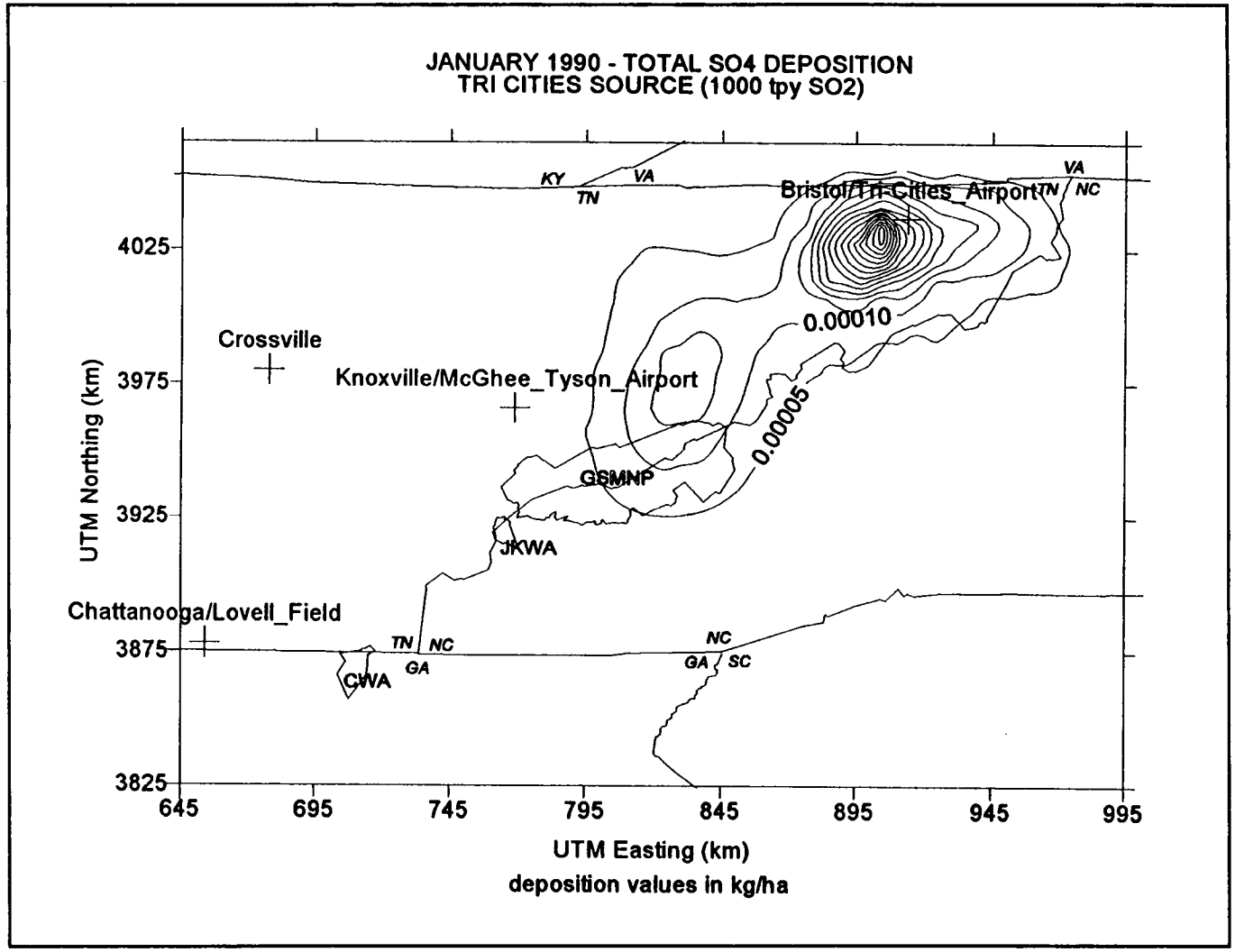

Fig. D.3. Total (wet+dry) SO_4^{2-} deposition estimated for January 1990 resulting from a 28.8 g/s (1000 tpy) hypothetical SO_2 emission source located at Bristol/Tri Cities Airport.

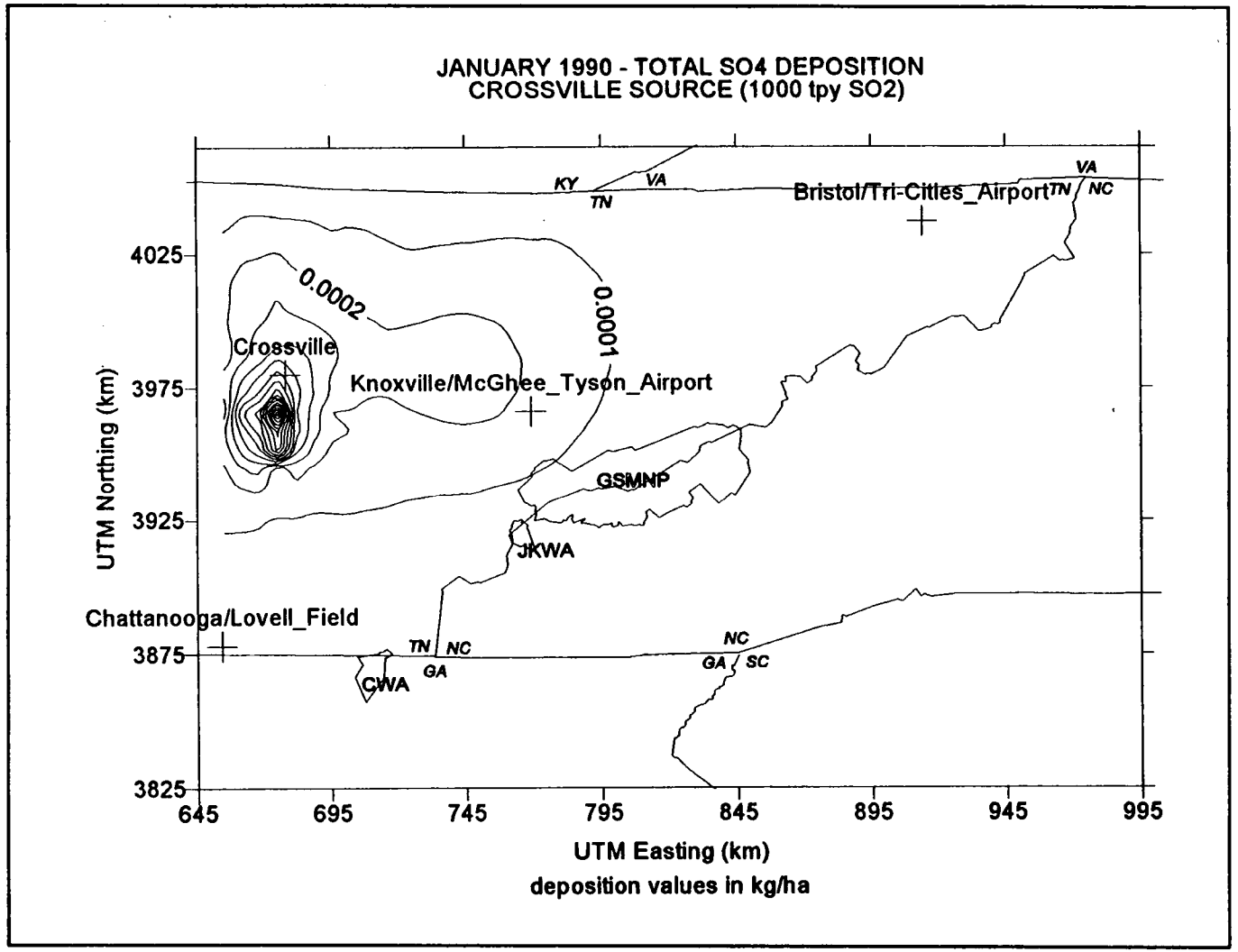

Fig. D.4. Total (wet+dry) SO_4^{2-} deposition estimated for January 1990 resulting from a 28.8 g/s (1000 tpy) hypothetical SO_2 emission source located in Crossville.

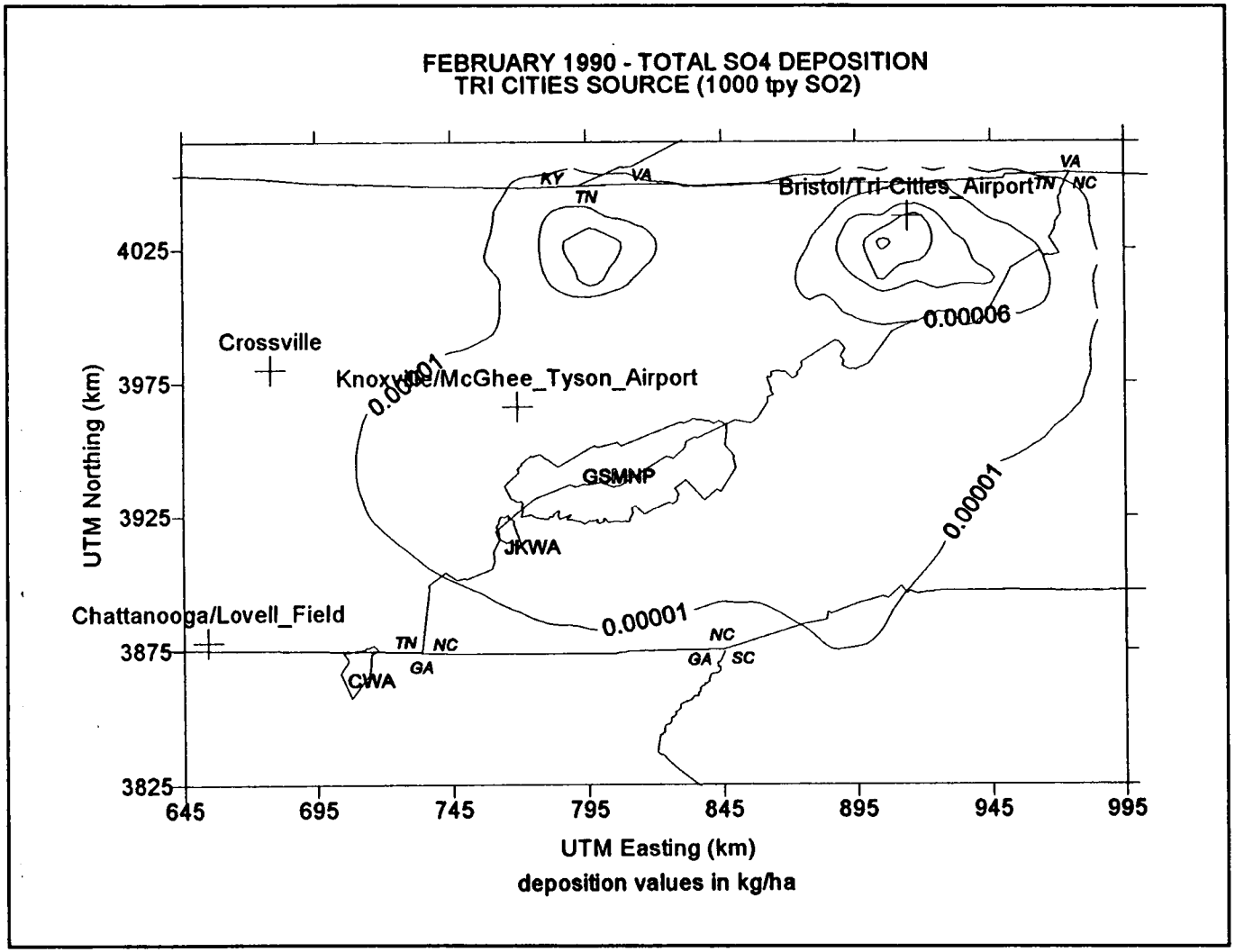

Fig. D.7. Total (wet+dry) SO_4^{2-} deposition estimated for February 1990 resulting from a 28.8 g/s (1000 tpy) hypothetical SO_2 emission source located at Bristol/Tri Cities Airport.

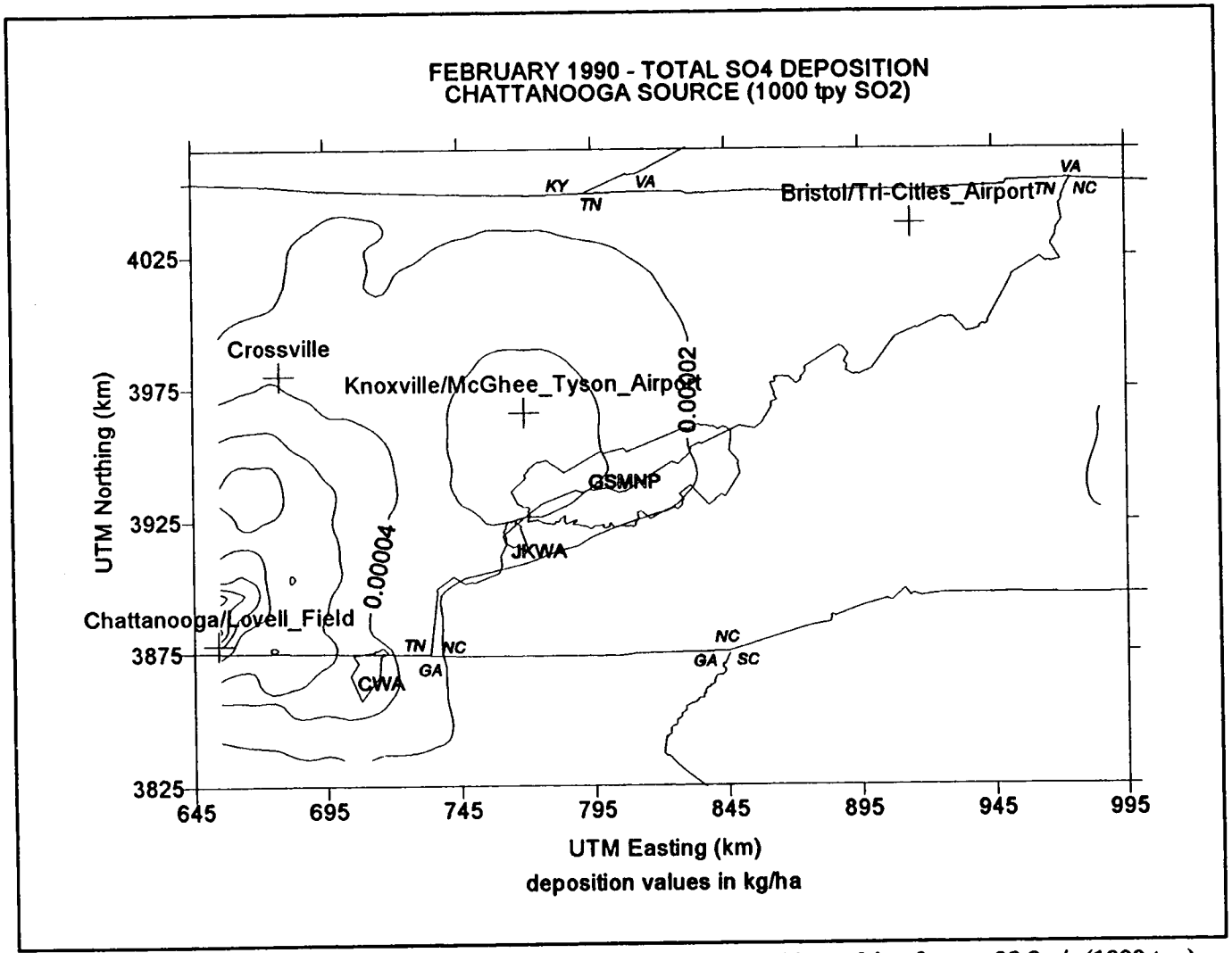

Fig. D.6. Total (wet+dry) SO_4^{2-} deposition estimated for February 1990 resulting from a 28.8 g/s (1000 tpy) hypothetical SO_2 emission source located at Chattanooga/Lovell Field.

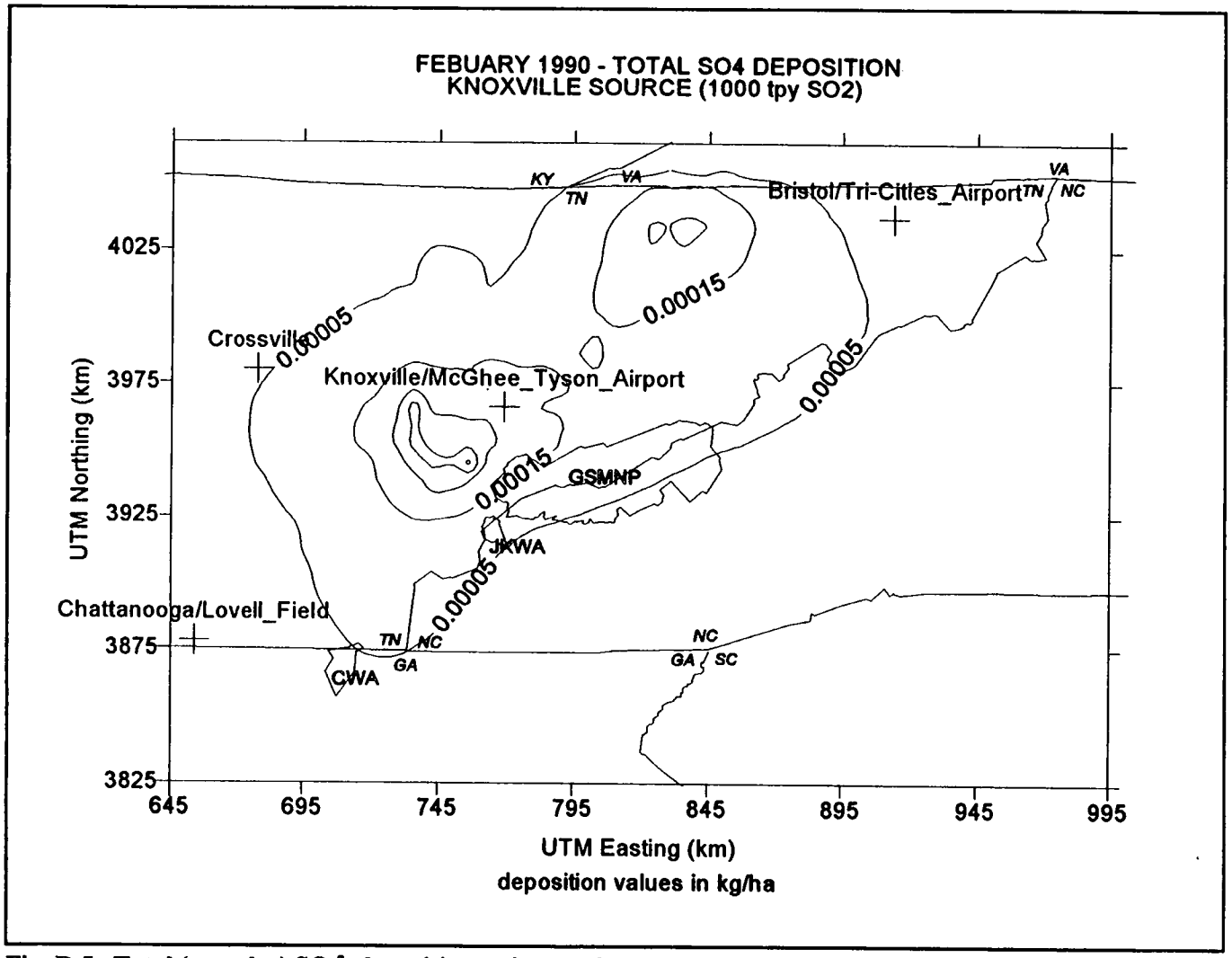

Fig. D.5. Total (wet+dry) SO_4^{2-} deposition estimated for February 1990 resulting from a 28.8 g/s (1000 tpy) hypothetical SO_2 emission source located at Knoxville /McGhee Tyson Airport.

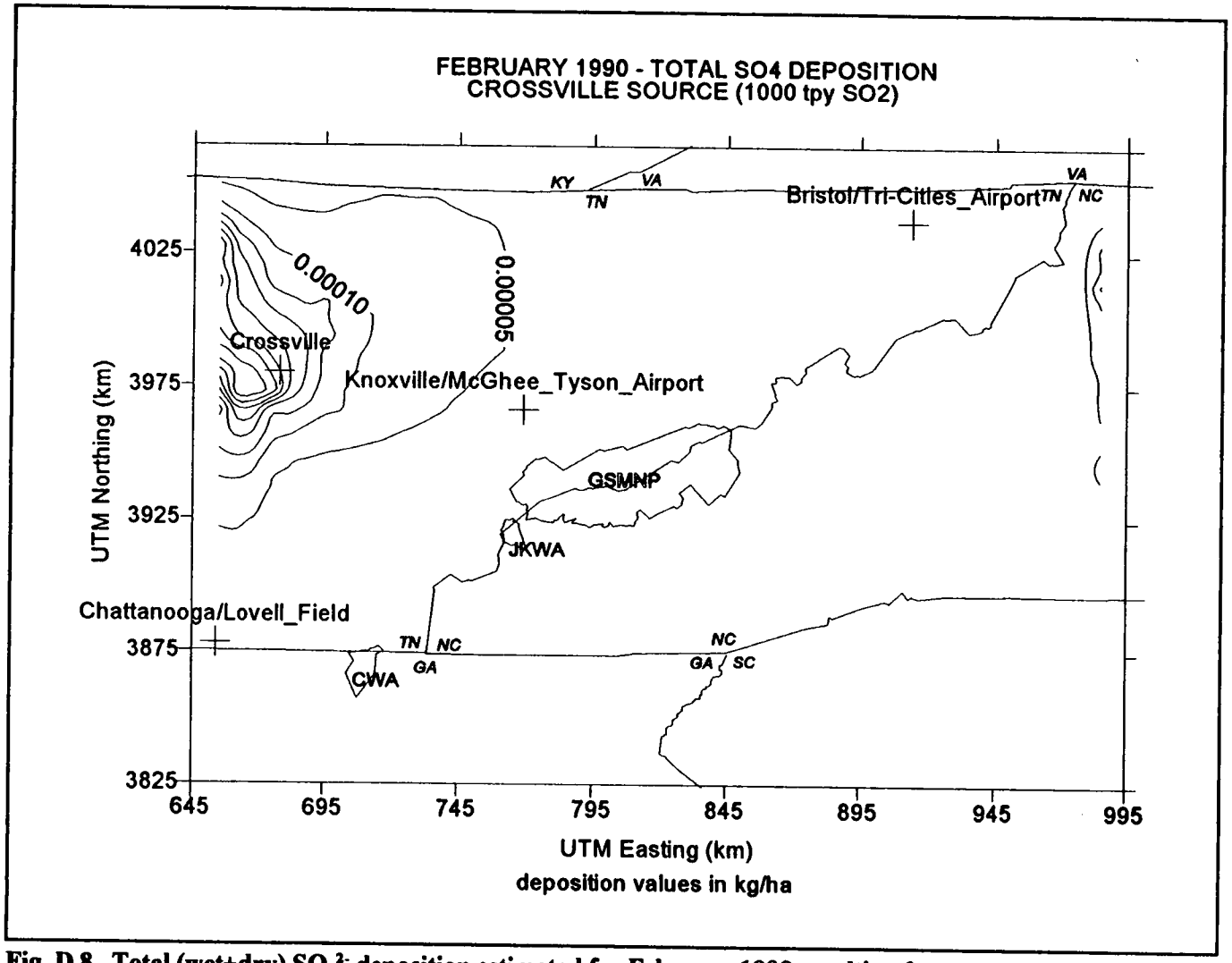

Fig. D.8. Total (wet+dry) SO_4^{2-} deposition estimated for February 1990 resulting from a 28.8 g/s (1000 tpy) hypothetical SO_2 emission source located in Crossville.

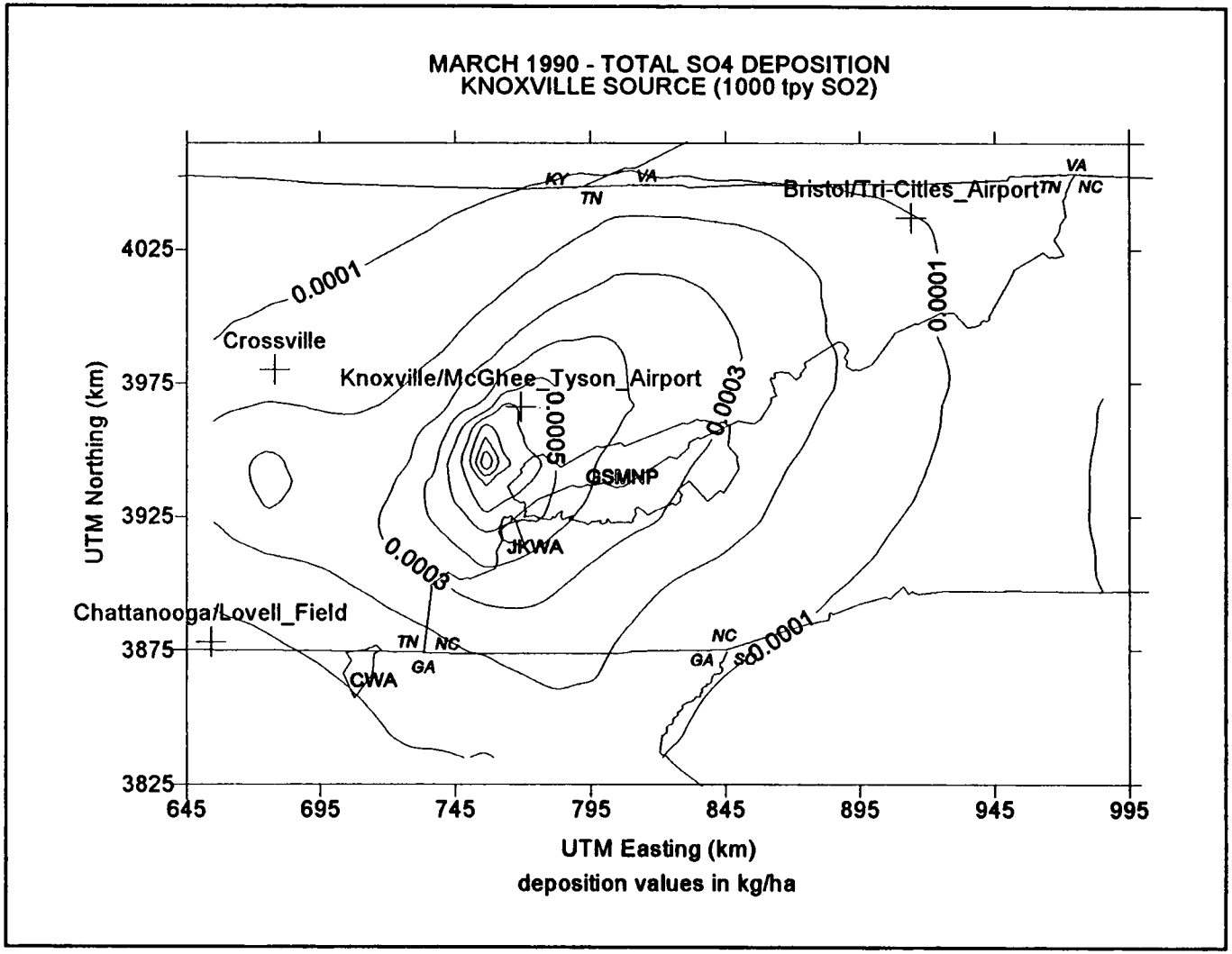

Fig. D.9. Total (wet+dry) SO_4^{2-} deposition estimated for March 1990 resulting from a 28.8 g/s (1000 tpy) hypothetical SO_2 emission source located at Knoxville /McGhee Tyson Airport.

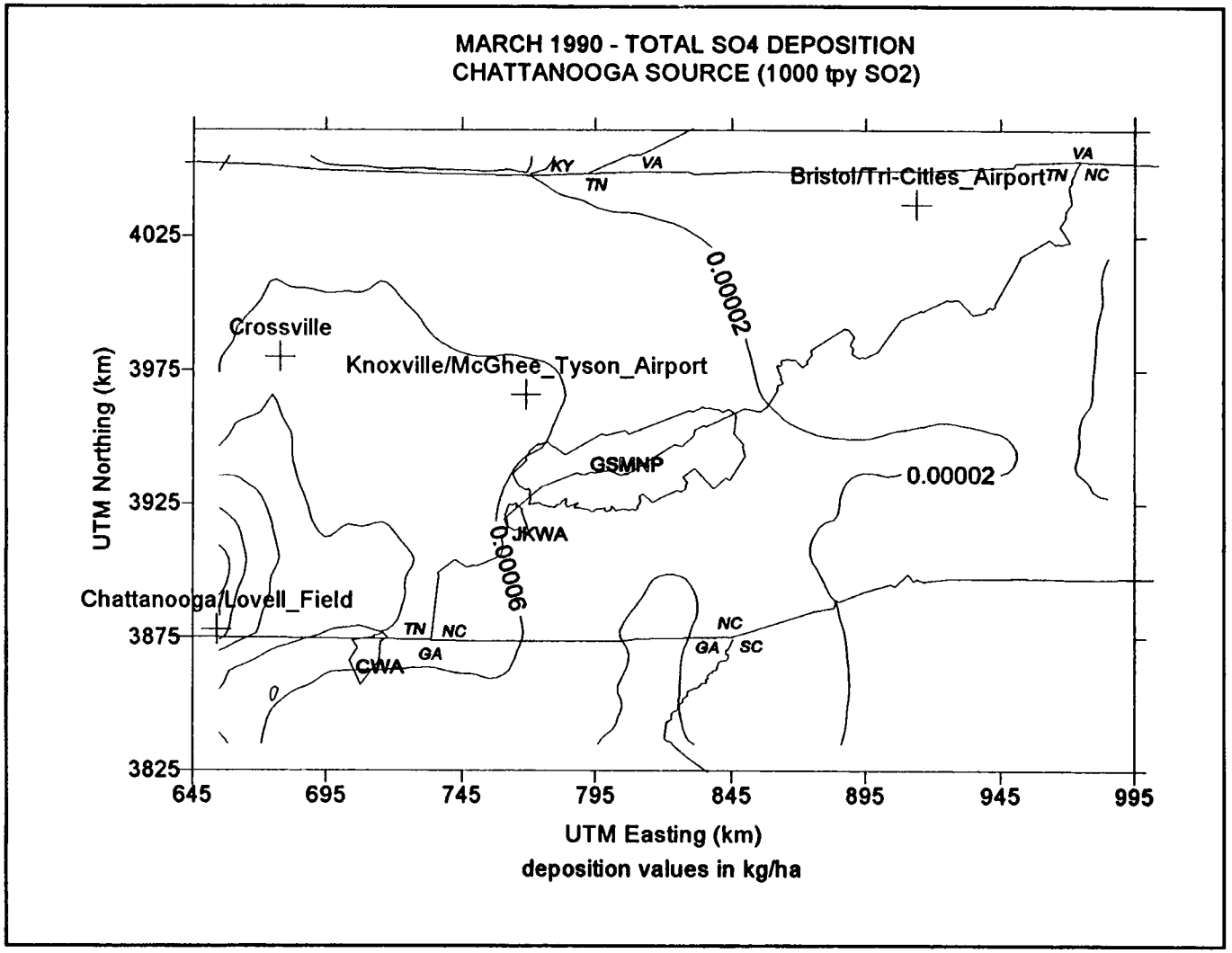

Fig. D.10. Total (wet+dry) SO_4^{2-} deposition estimated for March 1990 resulting from a 28.8 g/s (1000 tpy) hypothetical SO_2 emission source located at Chattanooga/Lovell Field.

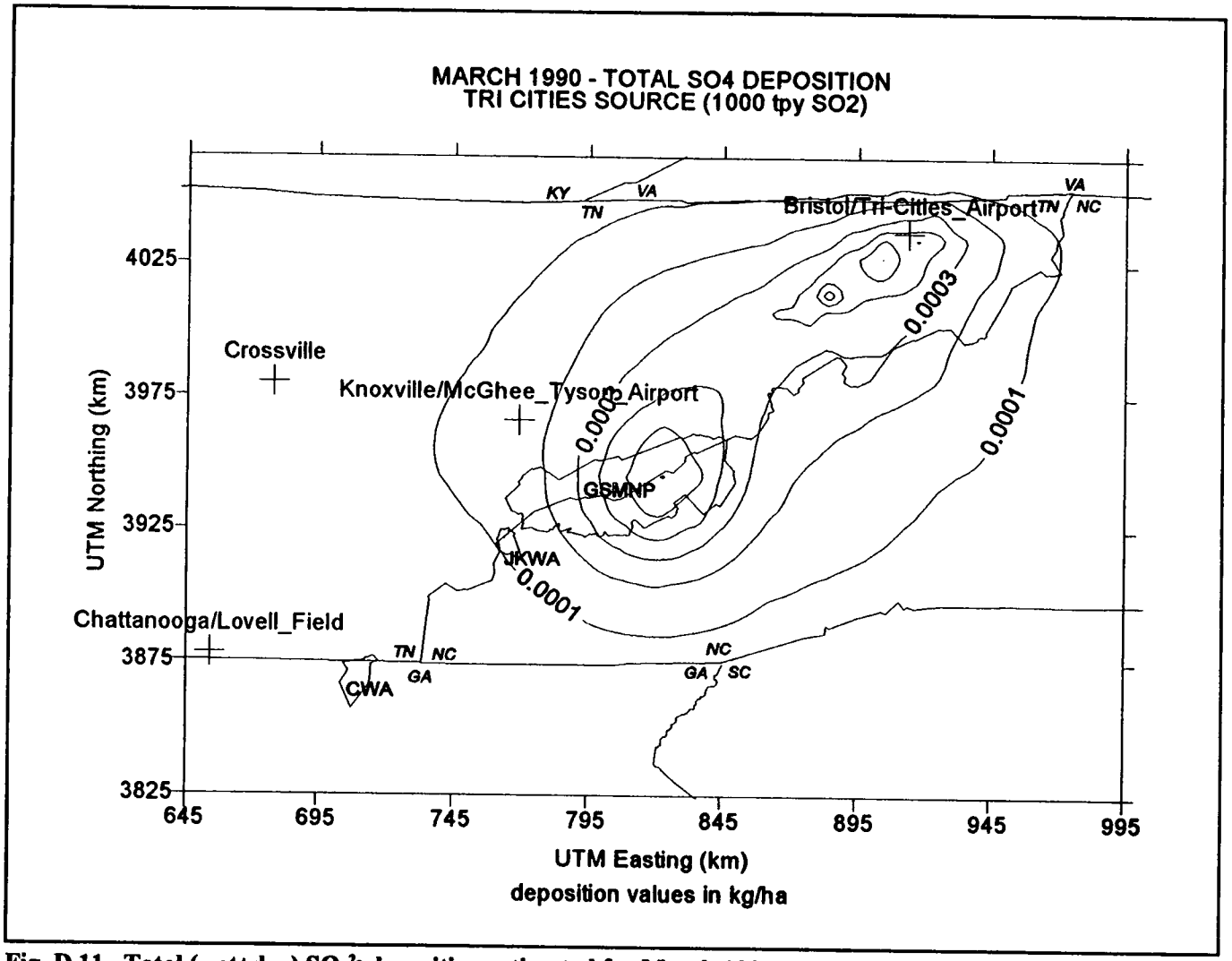

Fig. D.11. Total (wet+dry) SO_4^{2-} deposition estimated for March 1990 resulting from a 28.8 g/s (1000 tpy) hypothetical SO_2 emission source located at Bristol/Tri Cities Airport.

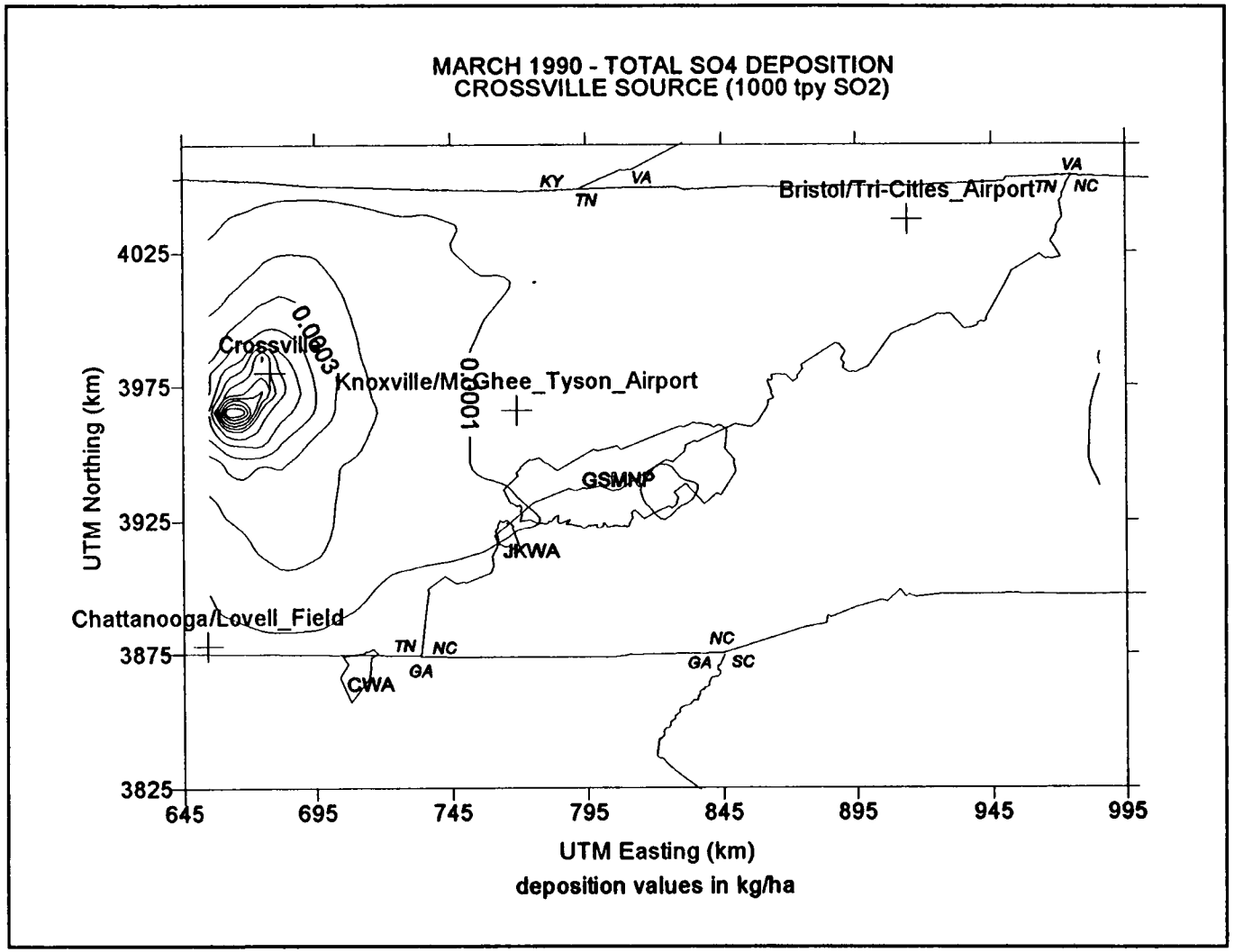

Fig. D.12. Total (wet+dry) SO_4^{2-} deposition estimated for March 1990 resulting from a 28.8 g/s (1000 tpy) hypothetical SO_2 emission source located in Crossville.

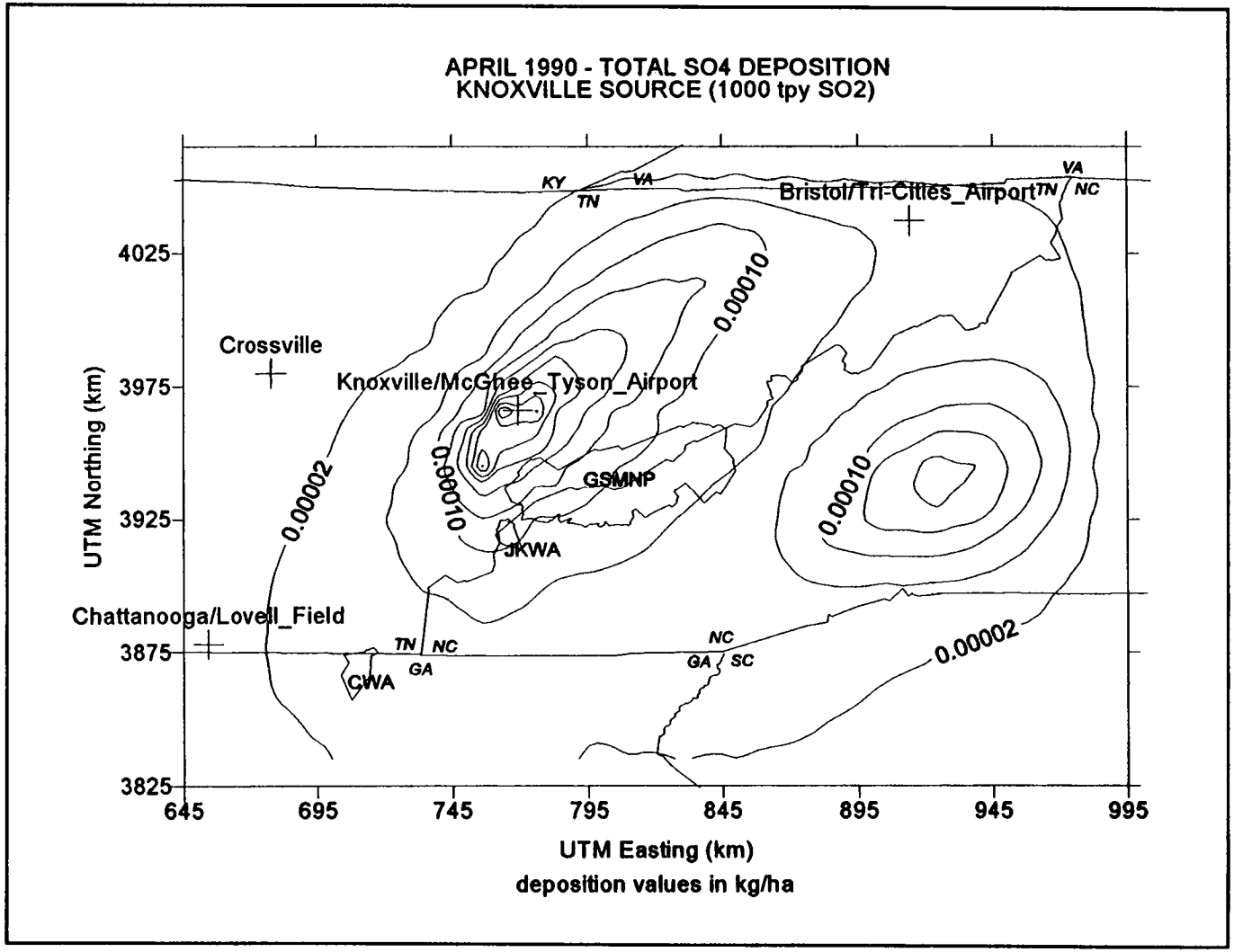

Fig. D.13. Total (wet+dry) SO_4^{2-} deposition estimated for April 1990 resulting from a 28.8 g/s (1000 tpy) hypothetical SO_2 emission source located at Knoxville /McGhee Tyson Airport.

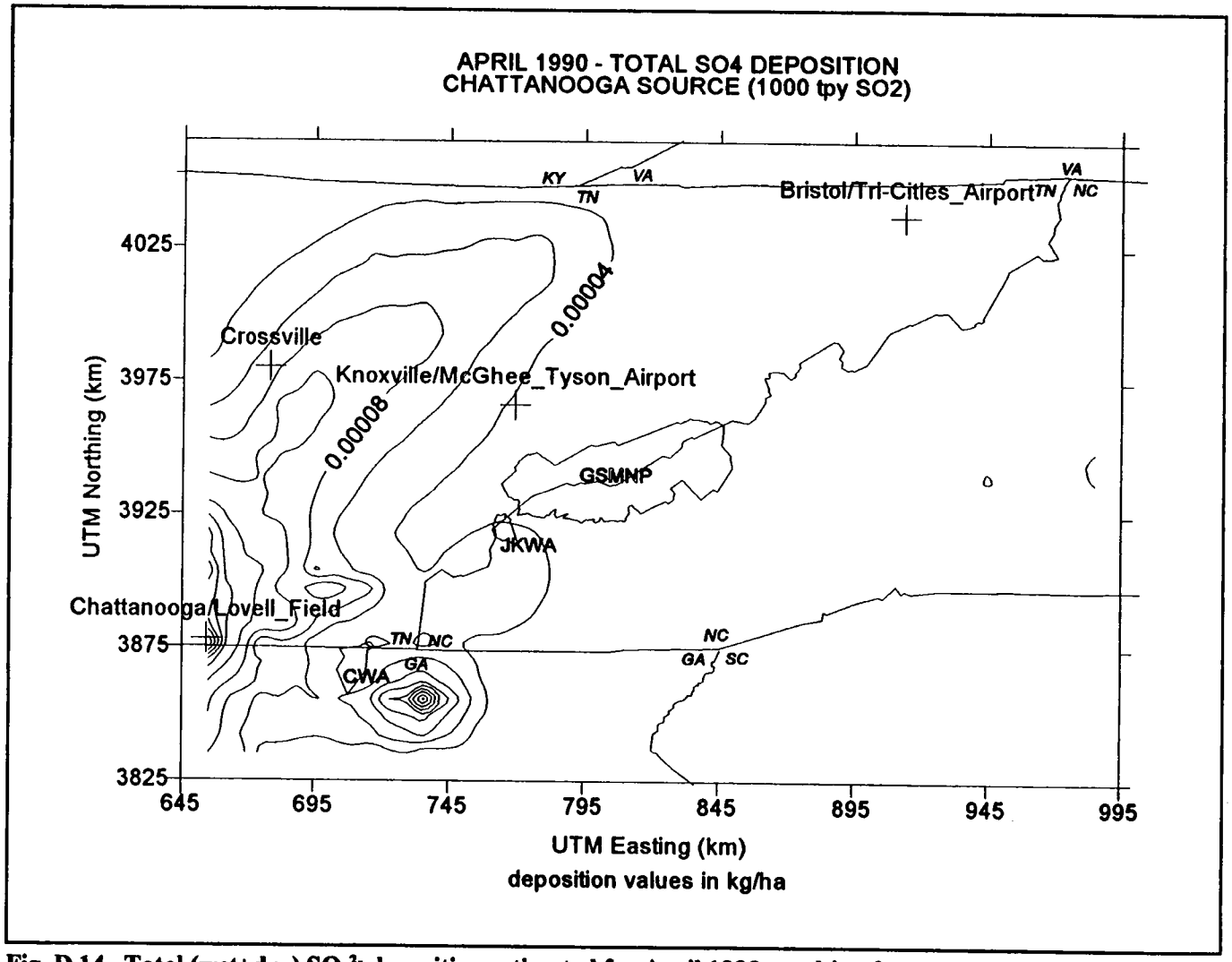

Fig. D.14. Total (wet+dry) SO_4^{2-} deposition estimated for April 1990 resulting from a 28.8 g/s (1000 tpy) hypothetical SO_2 emission source located at Chattanooga/Lovell Field.

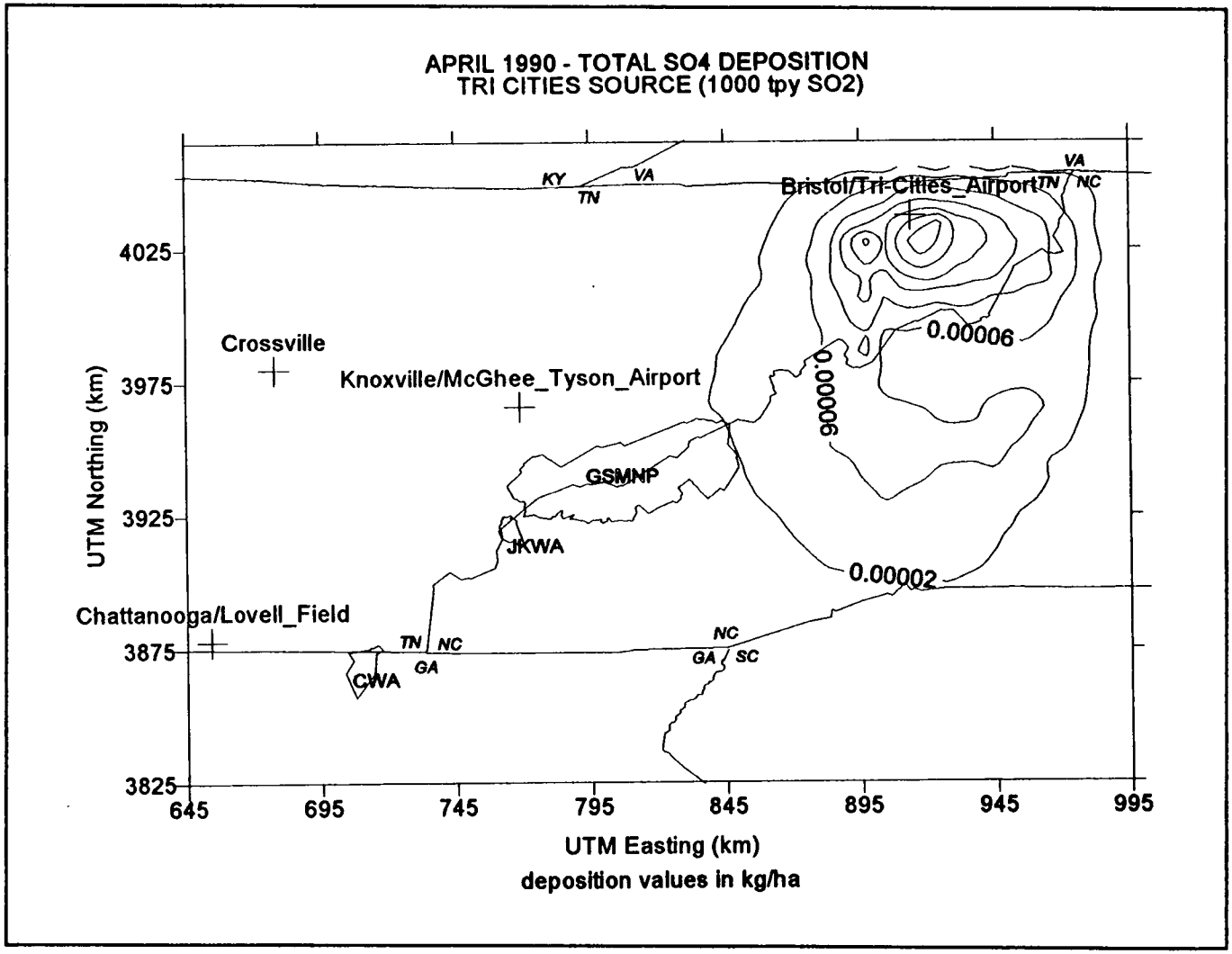

Fig. D.15. Total (wet+dry) SO_4^{2-} deposition estimated for April 1990 resulting from a 28.8 g/s (1000 tpy) hypothetical SO_2 emission source located at Bristol/Tri Cities Airport.

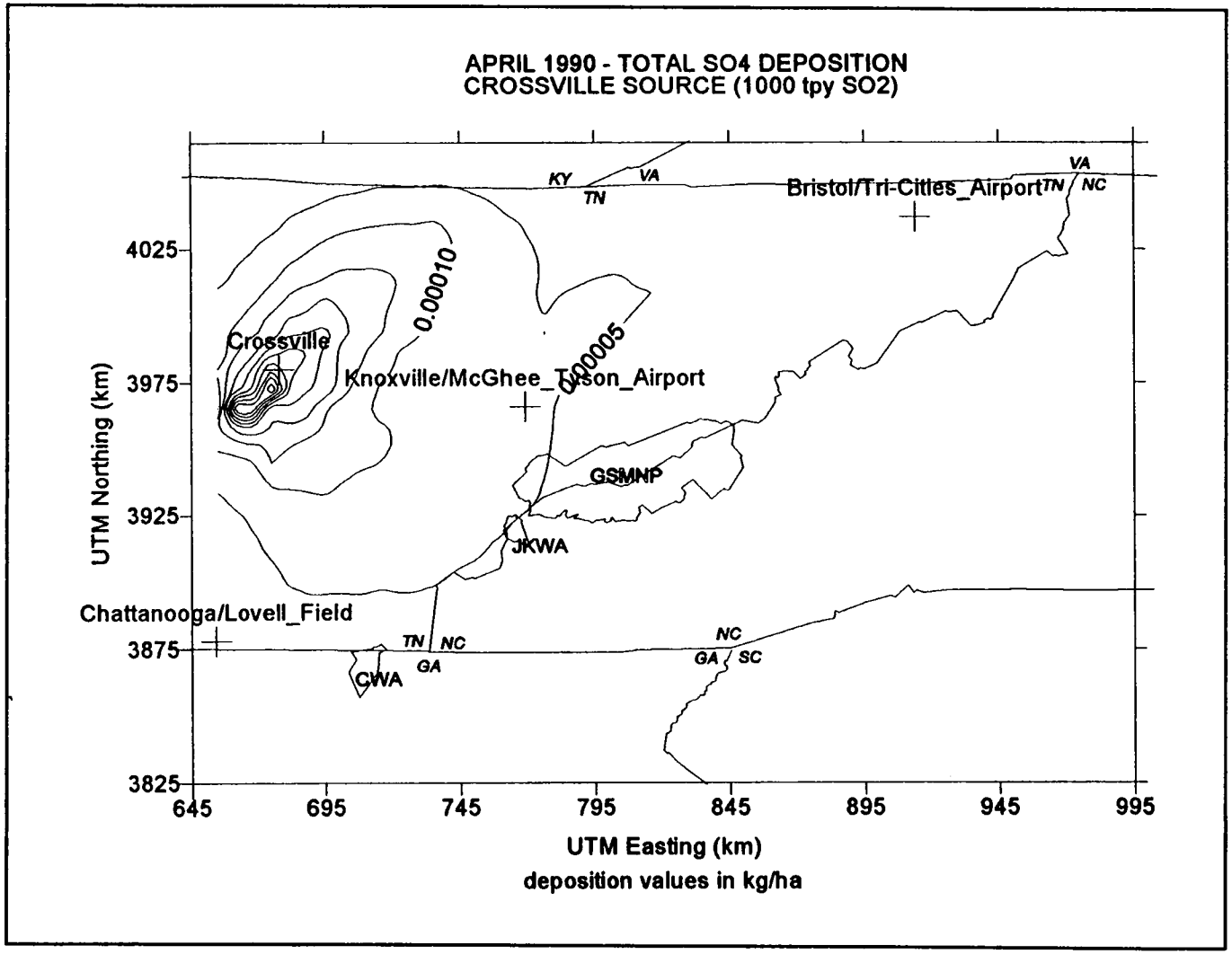

Fig. D.16. Total (wet+dry) SO_4^{2-} deposition estimated for April 1990 resulting from a 28.8 g/s (1000 tpy) hypothetical SO_2 emission source located in Crossville.

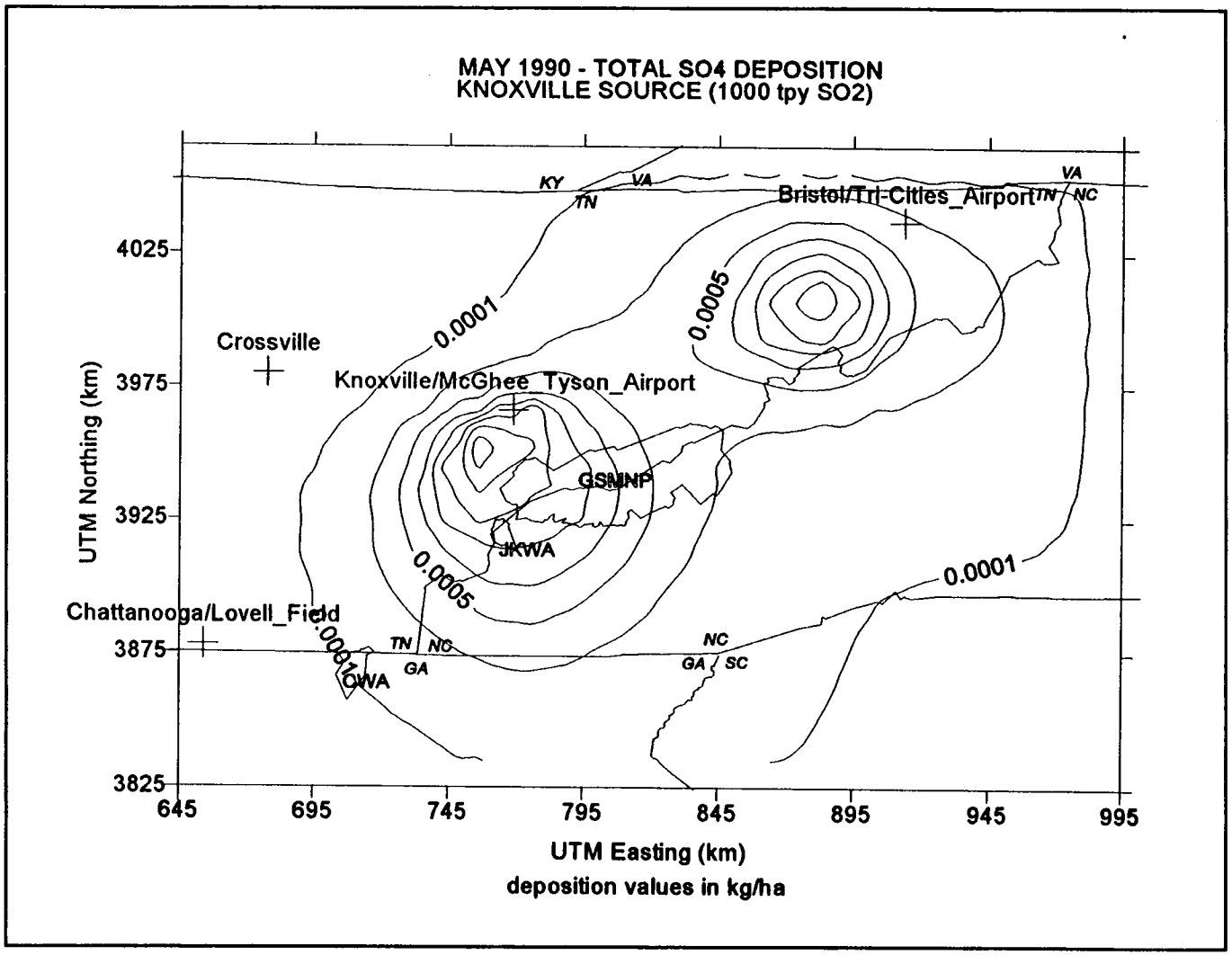

Fig. D.17. Total (wet+dry) SO_4^{2-} deposition estimated for May 1990 resulting from a 28.8 g/s (1000 tpy) hypothetical SO_2 emission source located at Knoxville /McGhee Tyson Airport.

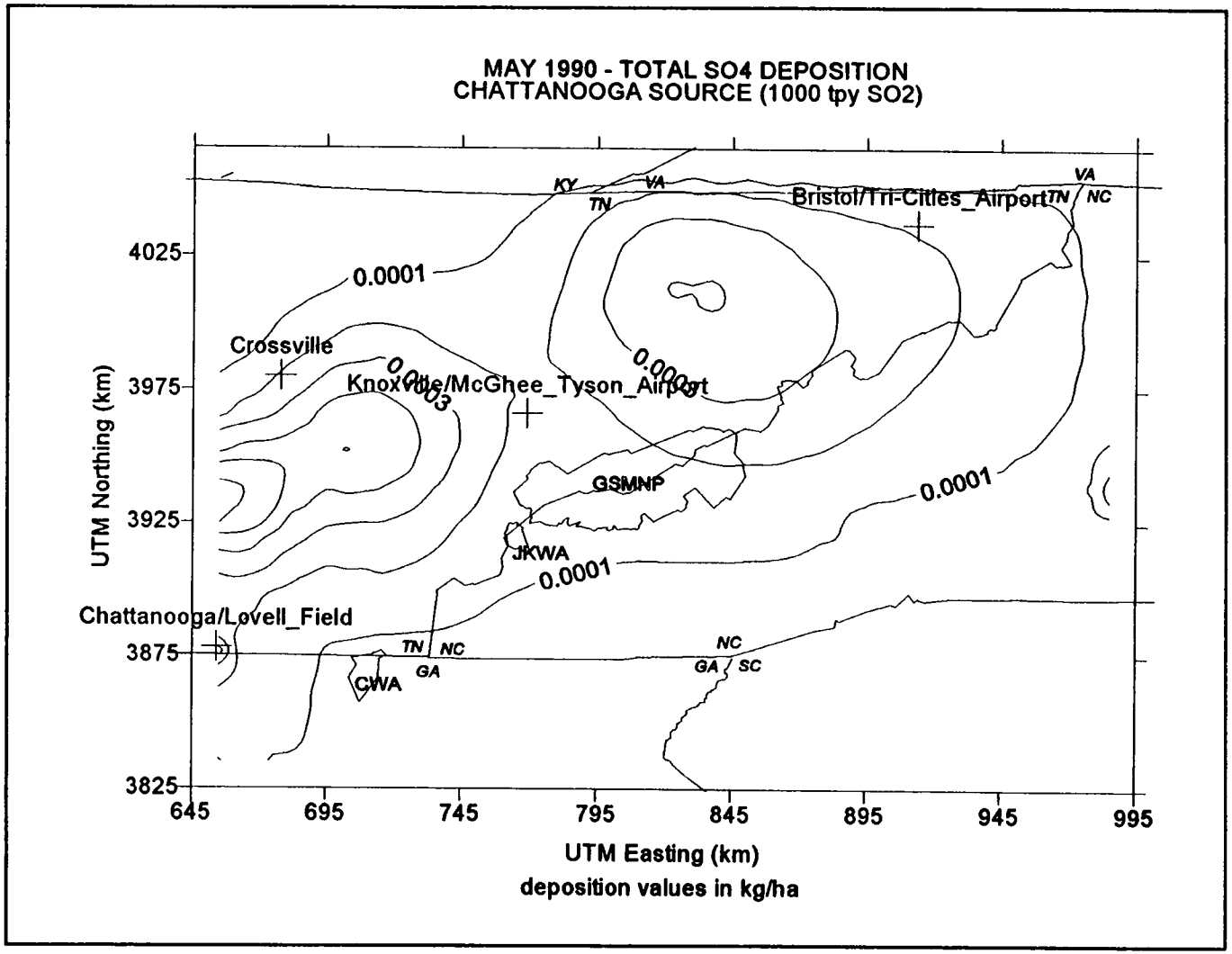

Fig. D.18. Total (wet+dry) SO_4^{2-} deposition estimated for May 1990 resulting from a 28.8 g/s (1000 tpy) hypothetical SO_2 emission source located at Chattanooga/Lovell Field.

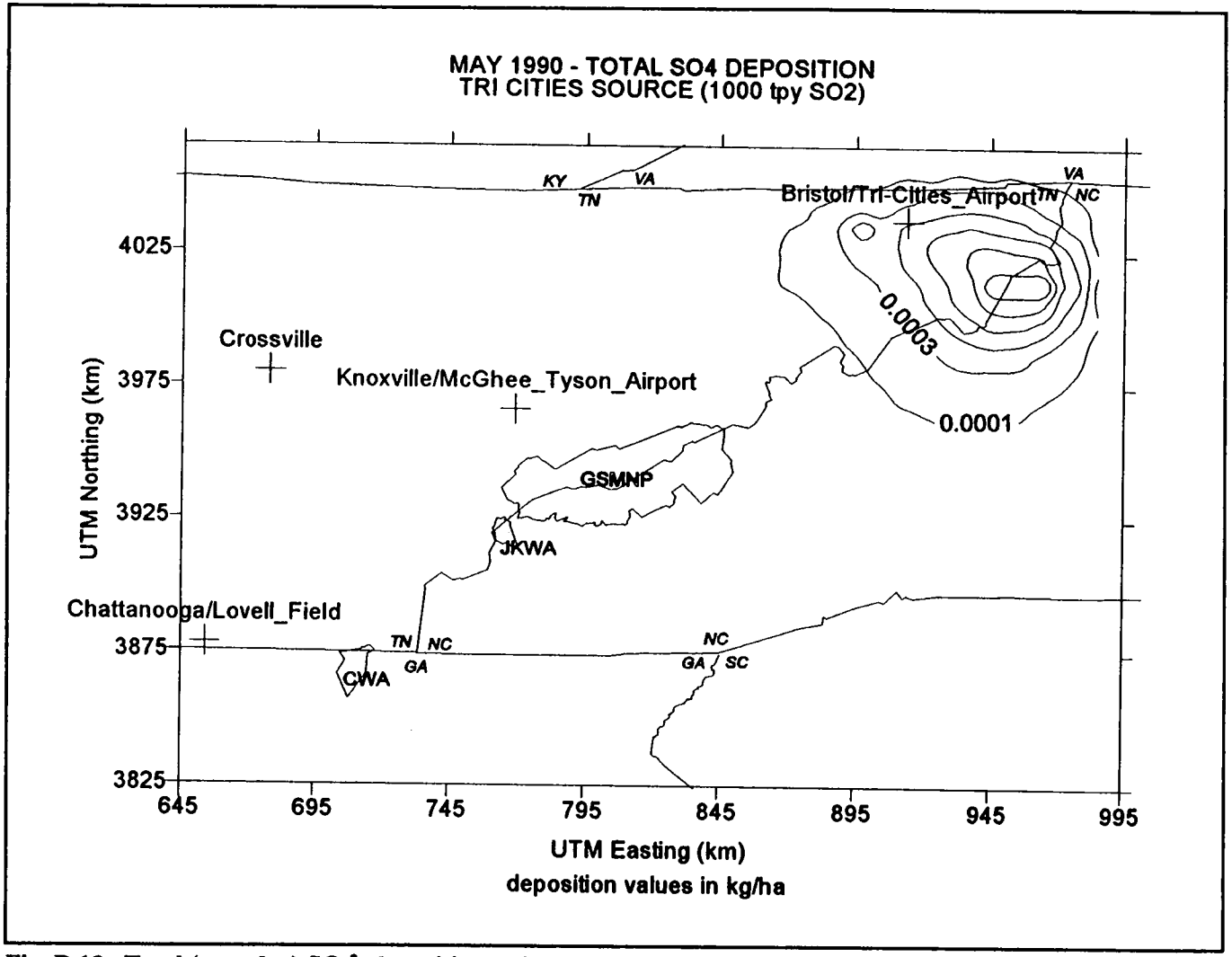

Fig. D.19. Total (wet+dry) SO_4^{2-} deposition estimated for May 1990 resulting from a 28.8 g/s (1000 tpy) hypothetical SO_2 emission source located at Bristol/Tri Cities Airport.

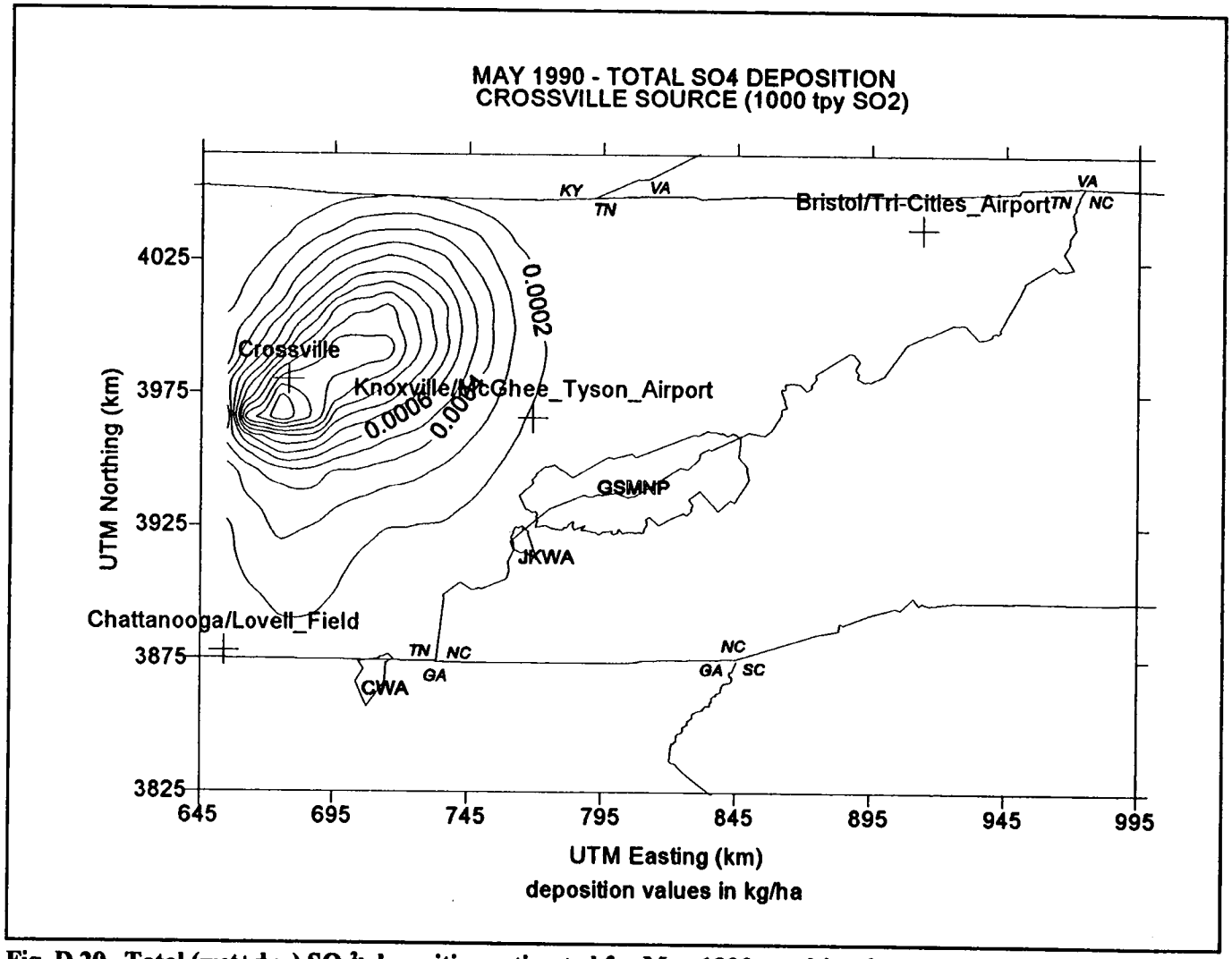

Fig. D.20. Total (wet+dry) SO_4^{2-} deposition estimated for May 1990 resulting from a 28.8 g/s (1000 tpy) hypothetical SO_2 emission source located in Crossville.

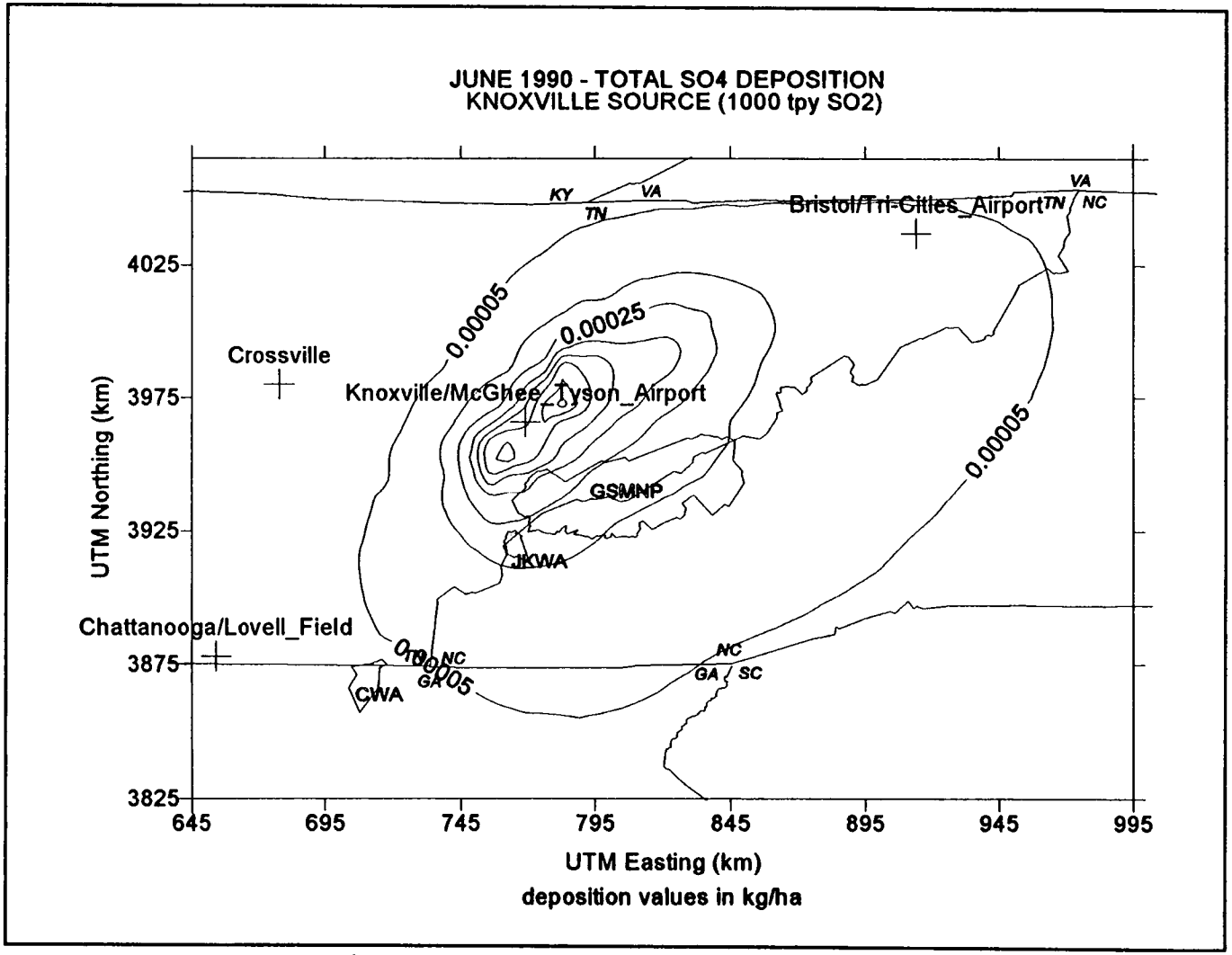

Fig. D.21. Total (wet+dry) SO_4^{2-} deposition estimated for June 1990 resulting from a 28.8 g/s (1000 tpy) hypothetical SO_2 emission source located at Knoxville /McGhee Tyson Airport.

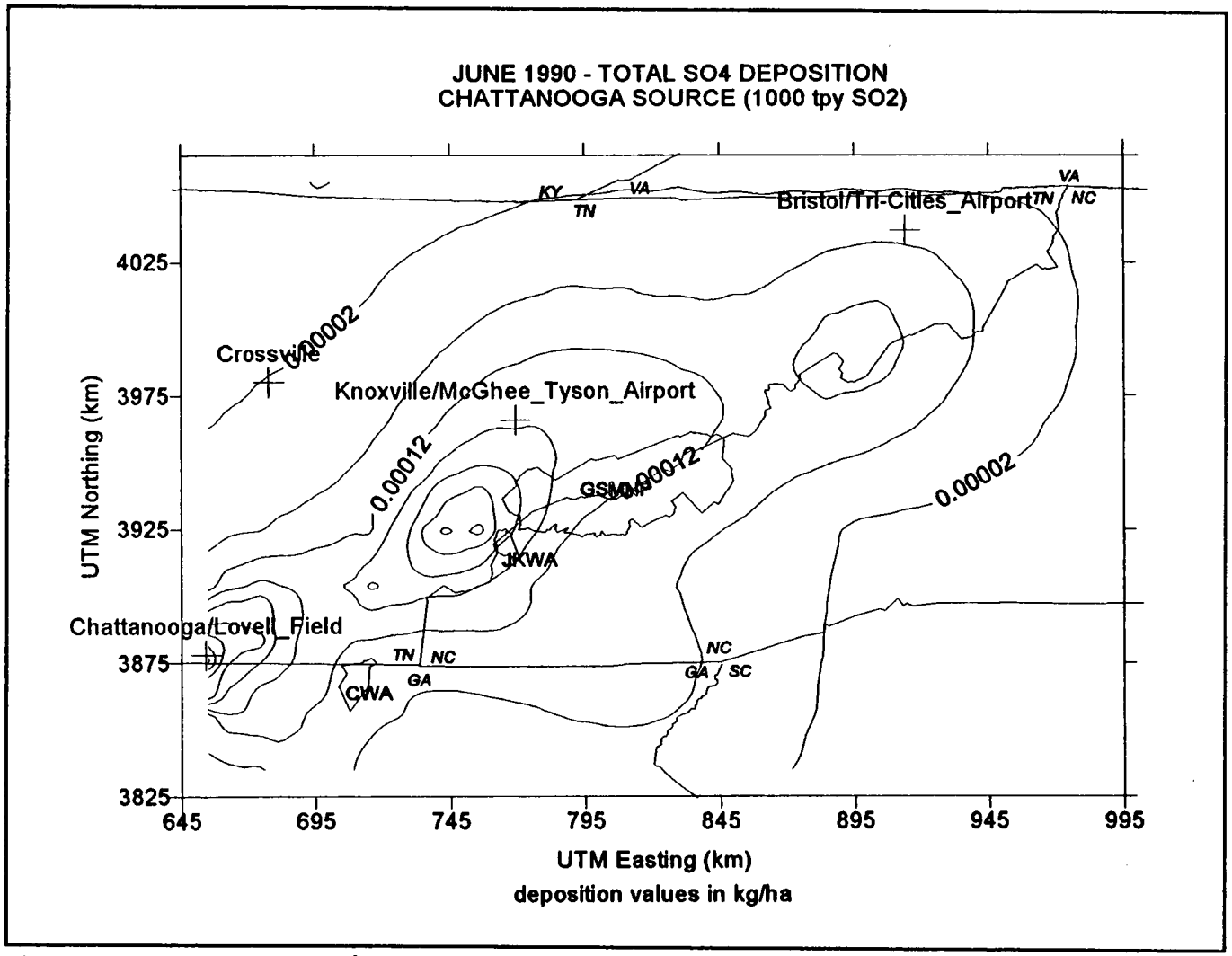

Fig. D.22. Total (wet+dry) SO_4^{2-} deposition estimated for June 1990 resulting from a 28.8 g/s (1000 tpy) hypothetical SO_2 emission source located at Chattanooga/Lovell Field.

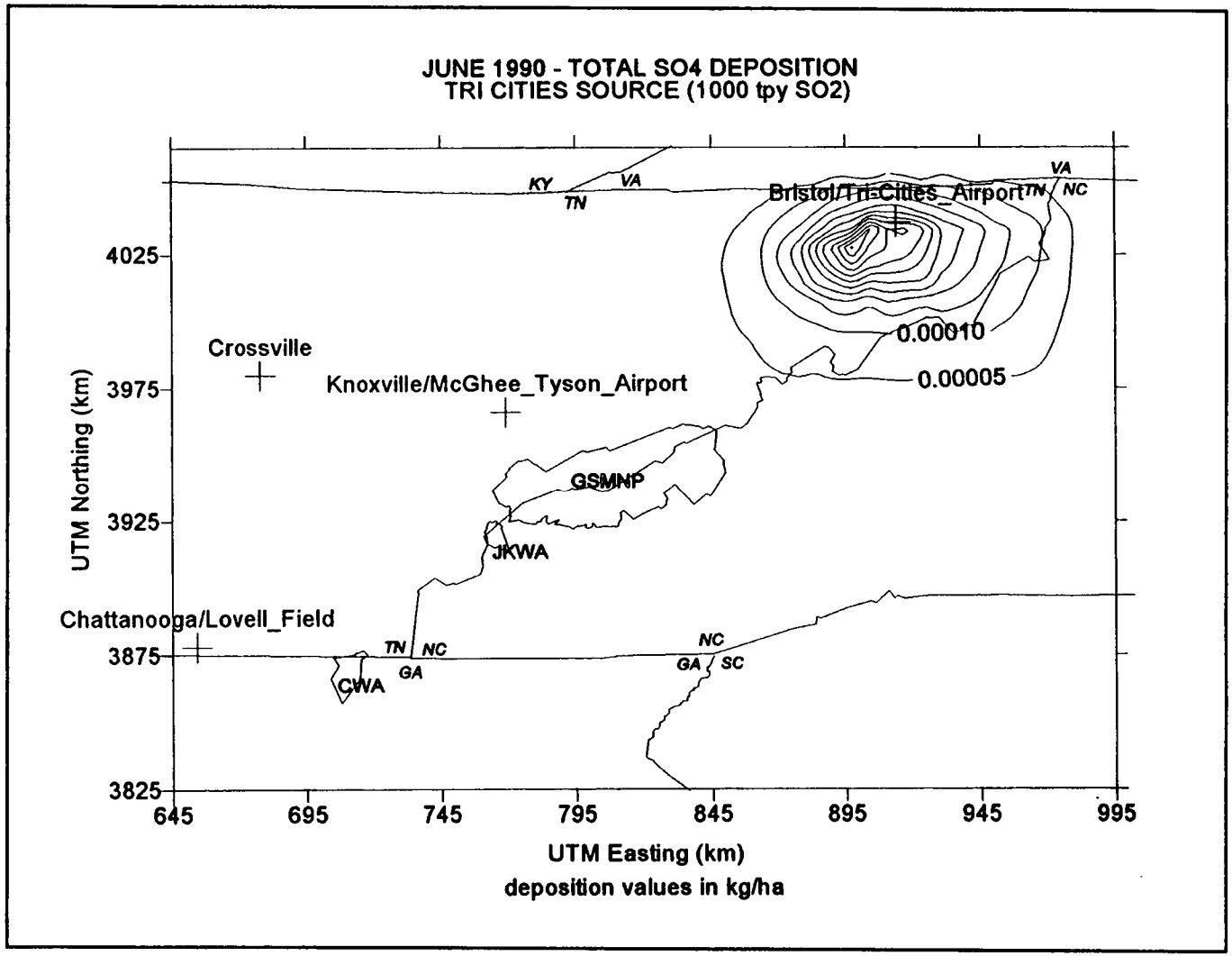

Fig. D.23. Total (wet+dry) SO_4^{2-} deposition estimated for June 1990 resulting from a 28.8 g/s (1000 tpy) hypothetical SO_2 emission source located at Bristol/Tri Cities Airport.

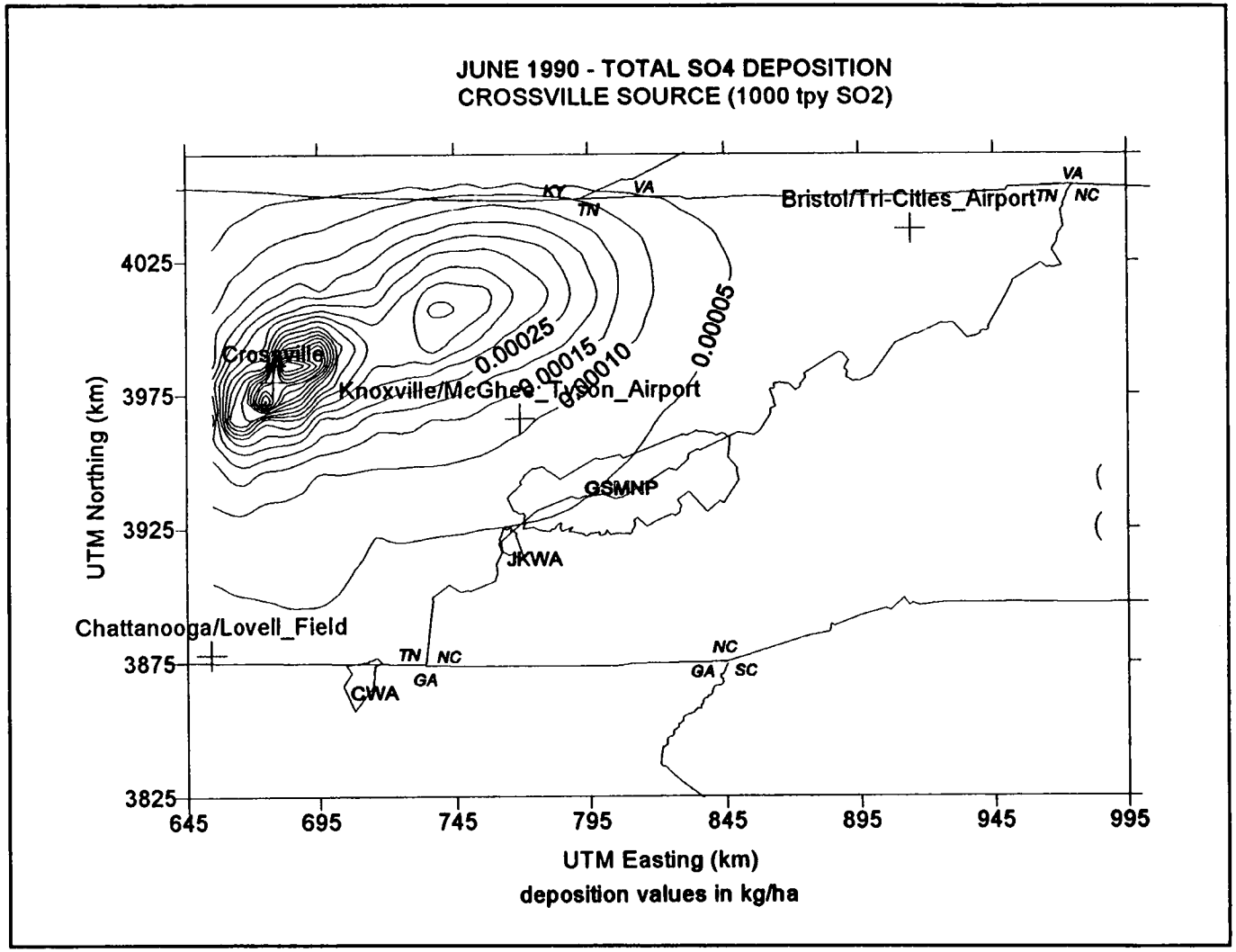

Fig. D.24. Total (wet+dry) SO_4^{2-} deposition estimated for June 1990 resulting from a 28.8 g/s (1000 tpy) hypothetical SO_2 emission source located in Crossville.

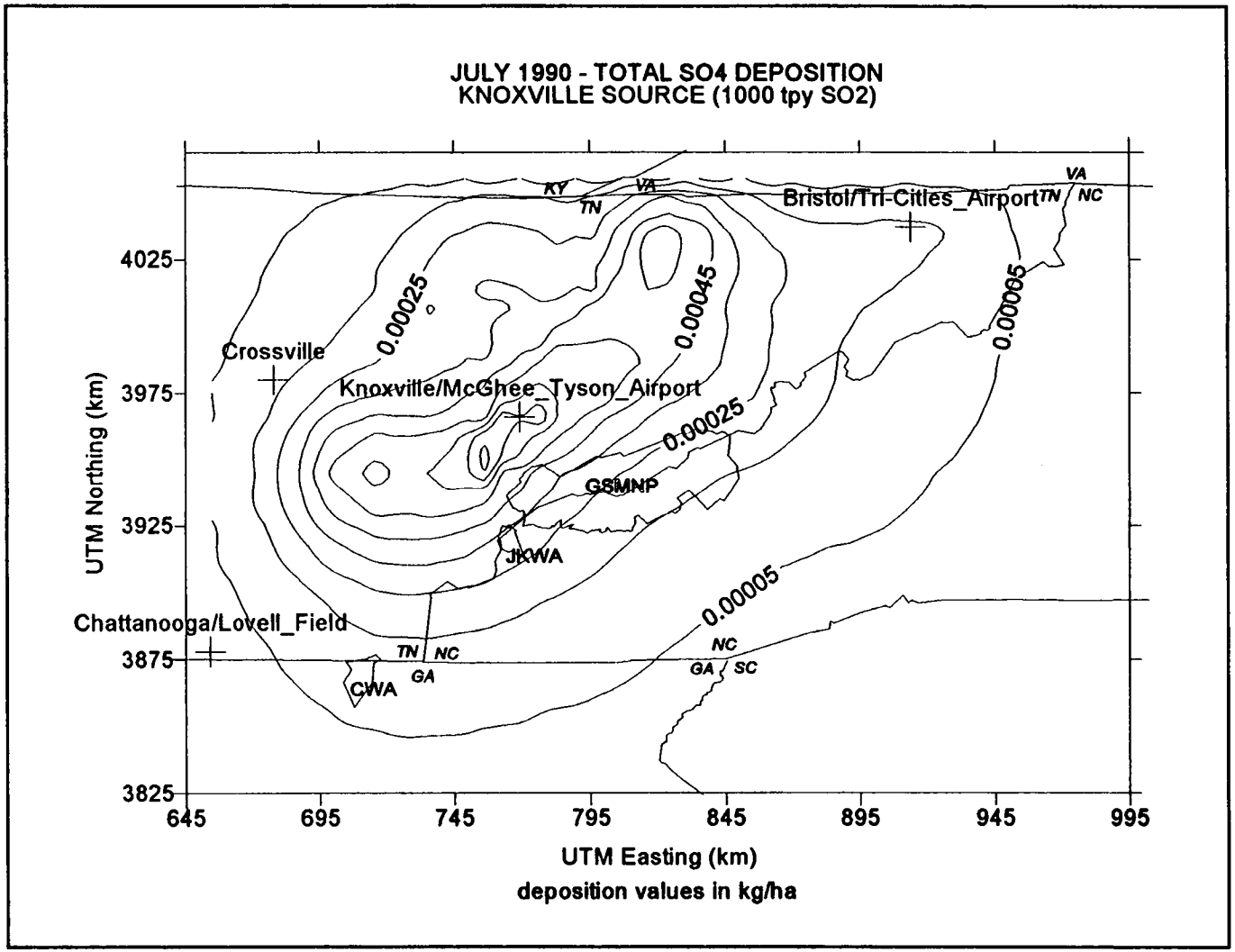

Fig. D.25. Total (wet+dry) SO_4^{2-} deposition estimated for July 1990 resulting from a 28.8 g/s (1000 tpy) hypothetical SO_2 emission source located at Knoxville /McGhee Tyson Airport.

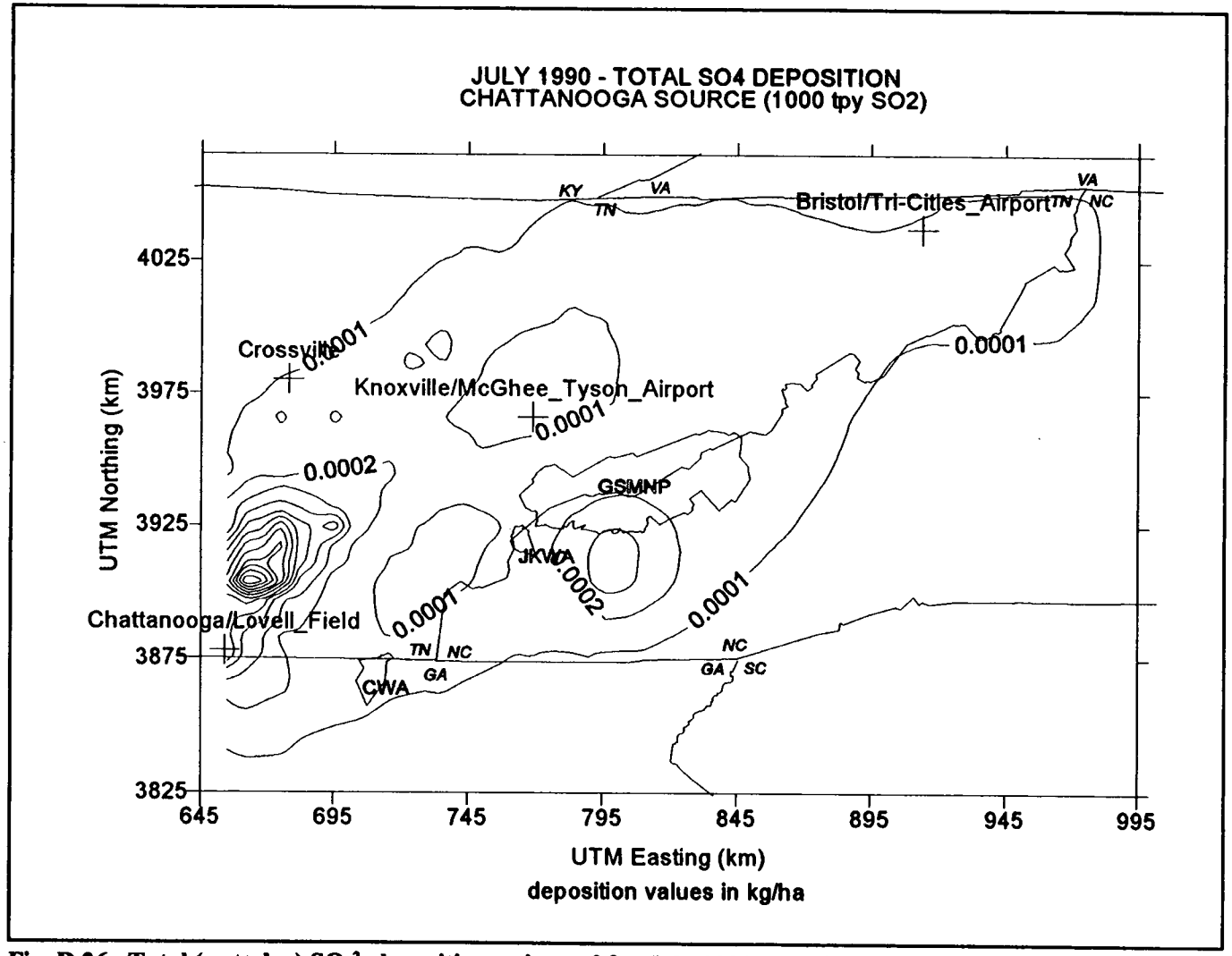

Fig. D.26. Total (wet+dry) SO_4^{2-} deposition estimated for July 1990 resulting from a 28.8 g/s (1000 tpy) hypothetical SO_2 emission source located at Chattanooga/Lovell Field.

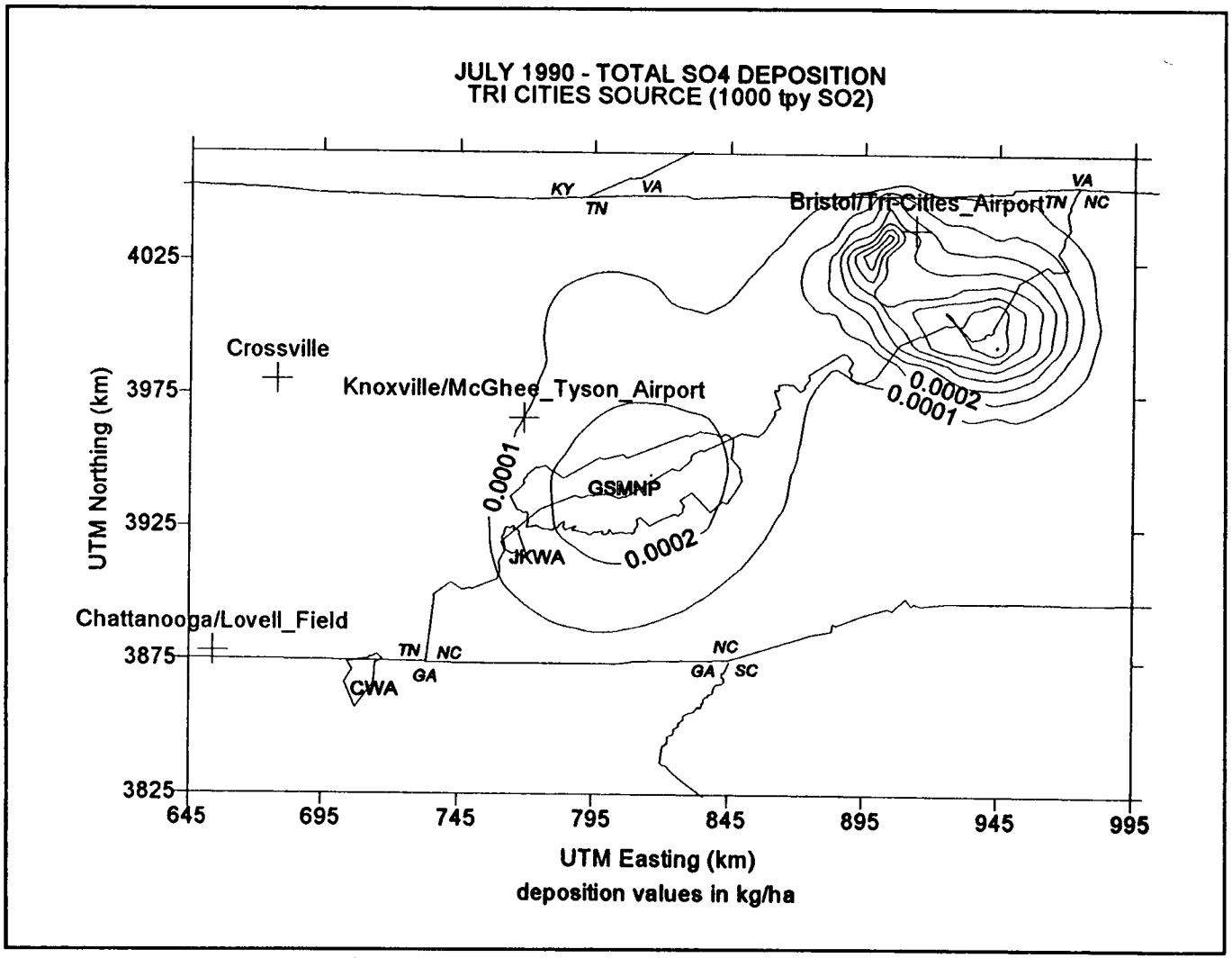

Fig. D.27. Total (wet+dry) SO_4^{2-} deposition estimated for July 1990 resulting from a 28.8 g/s (1000 tpy) hypothetical SO_2 emission source located at Bristol/Tri Cities Airport.

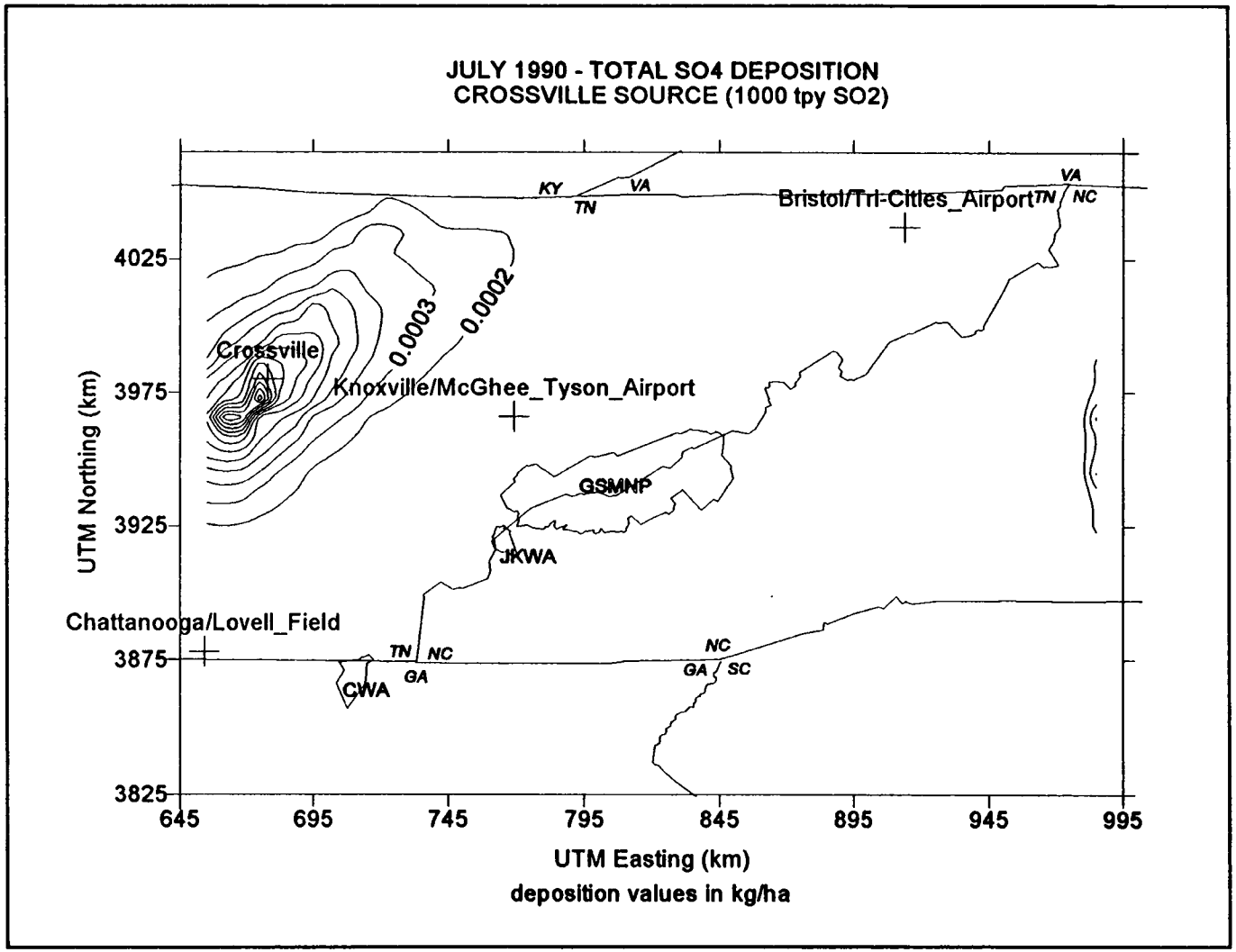

Fig. D.28. Total (wet+dry) SO_4^{2-} deposition estimated for July 1990 resulting from a 28.8 g/s (1000 tpy) hypothetical SO_2 emission source located in Crossville.

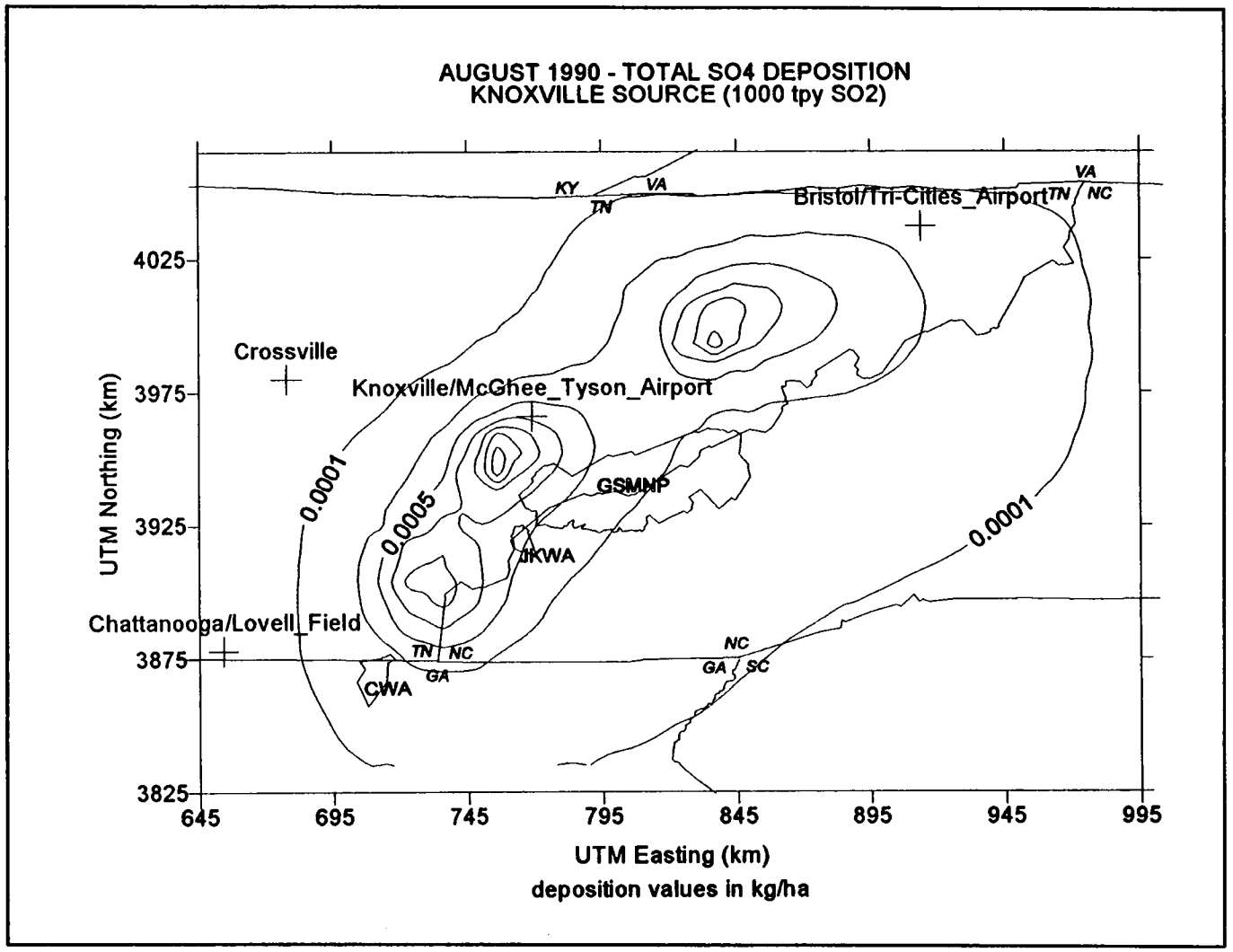

Fig. D.29. Total (wet+dry) SO_4^{2-} deposition estimated for August 1990 resulting from a 28.8 g/s (1000 tpy) hypothetical SO_2 emission source located at Knoxville /McGhee Tyson Airport.

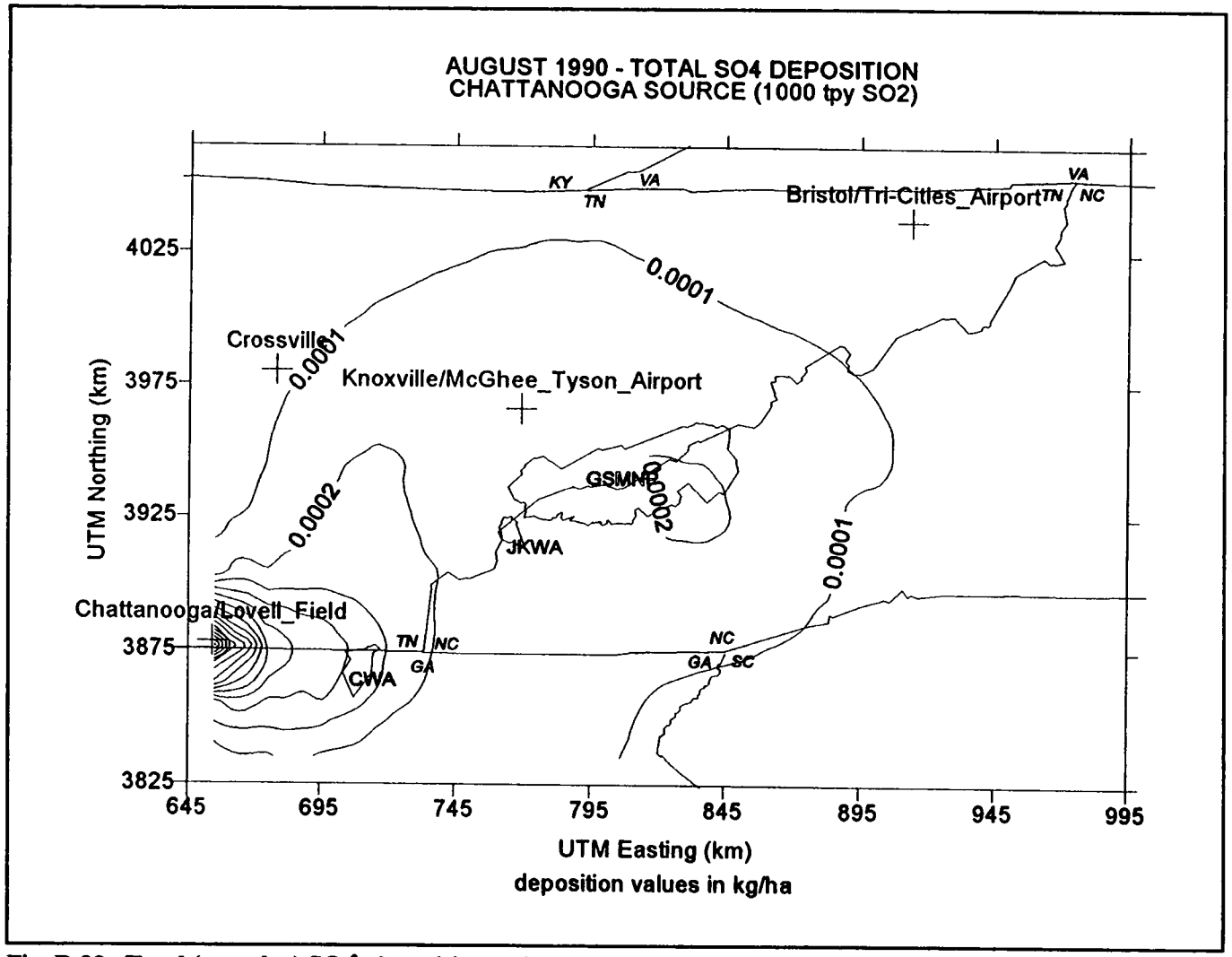

Fig. D.30. Total (wet+dry) SO_4^{2-} deposition estimated for August 1990 resulting from a 28.8 g/s (1000 tpy) hypothetical SO_2 emission source located at Chattanooga/Lovell Field.

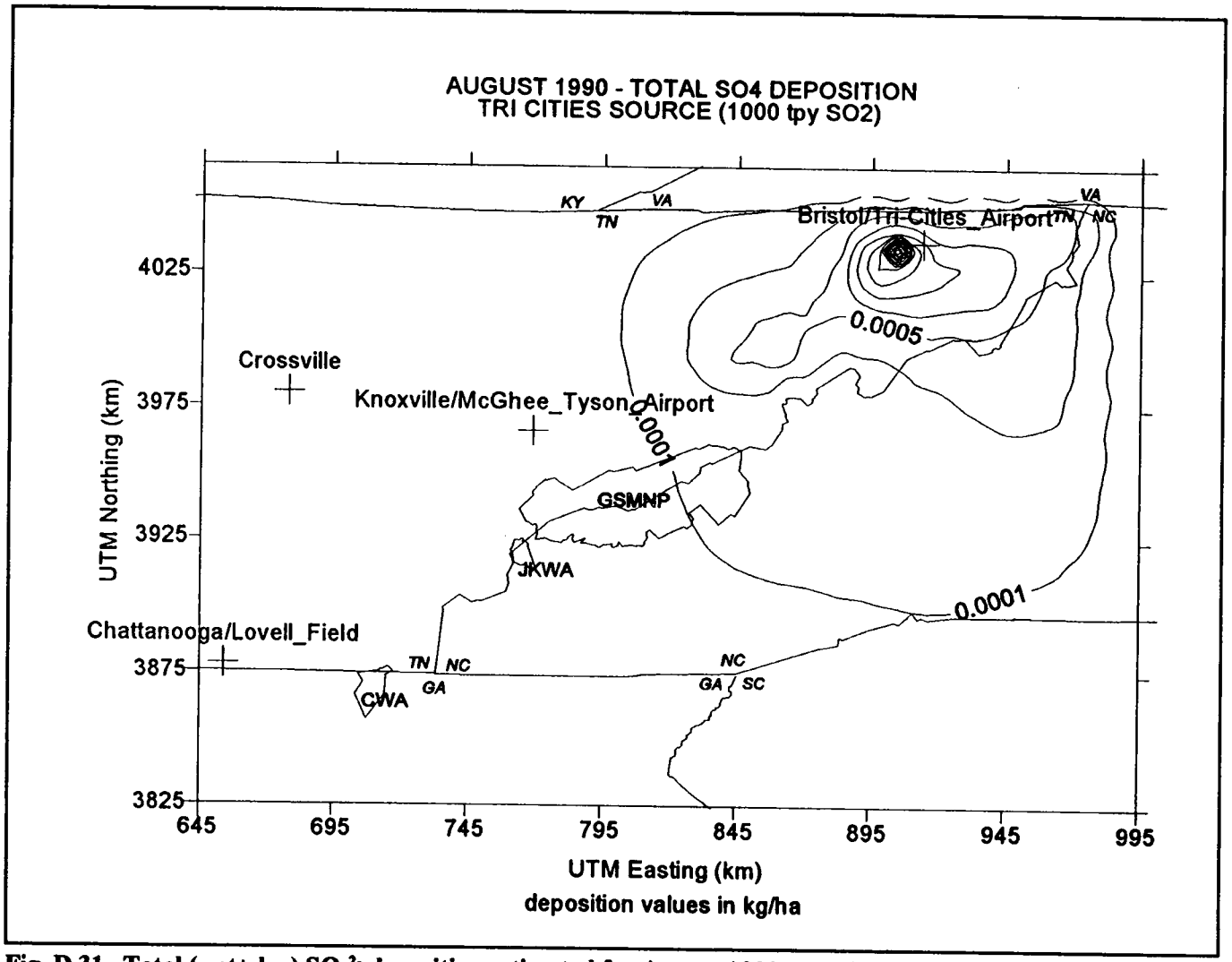

Fig. D.31. Total (wet+dry) SO_4^{2-} deposition estimated for August 1990 resulting from a 28.8 g/s (1000 tpy) hypothetical SO_2 emission source located at Bristol/Tri Cities Airport.

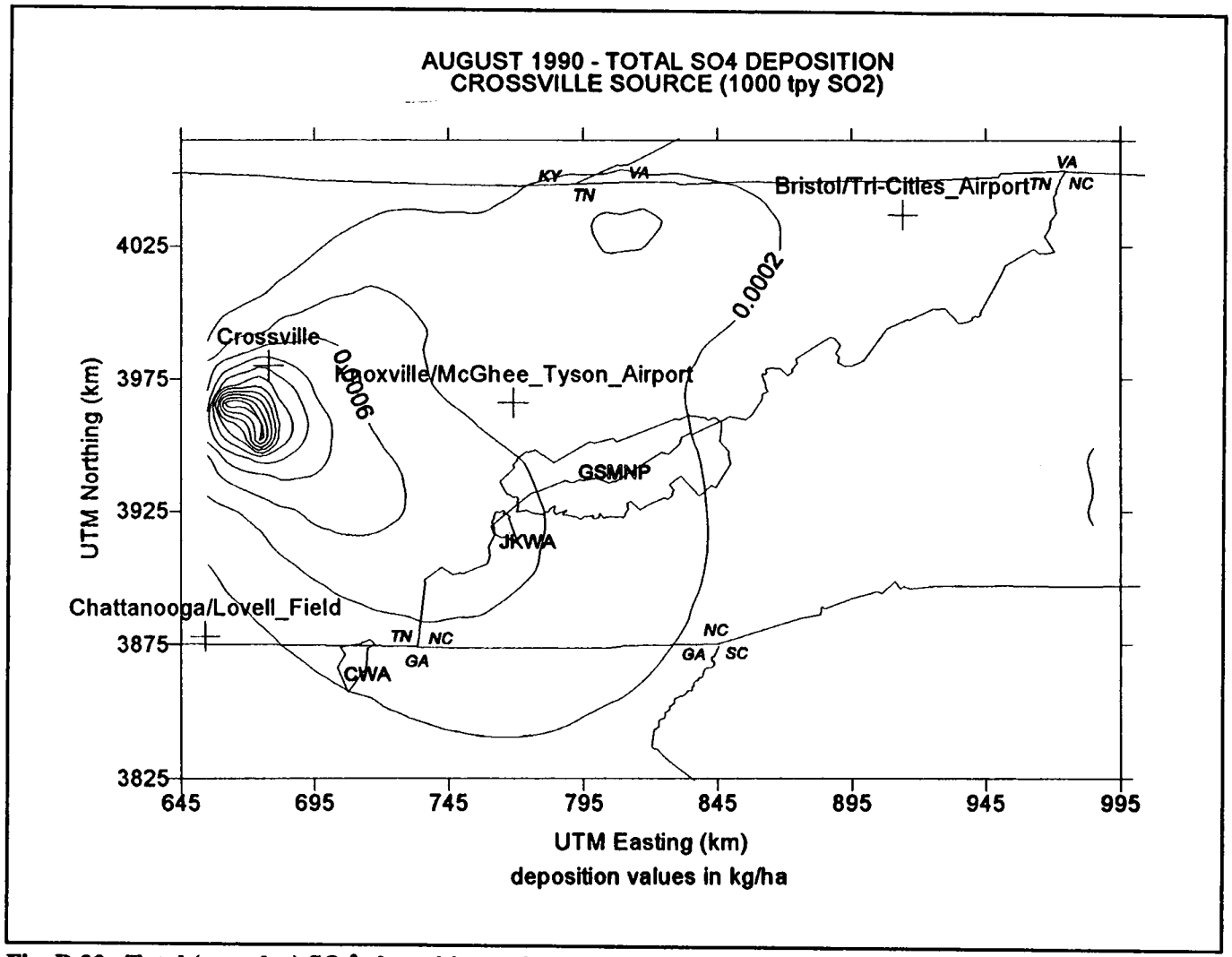

Fig. D.32. Total (wet+dry) SO_4^{2-} deposition estimated for August 1990 resulting from a 28.8 g/s (1000 tpy) hypothetical SO_2 emission source located in Crossville.

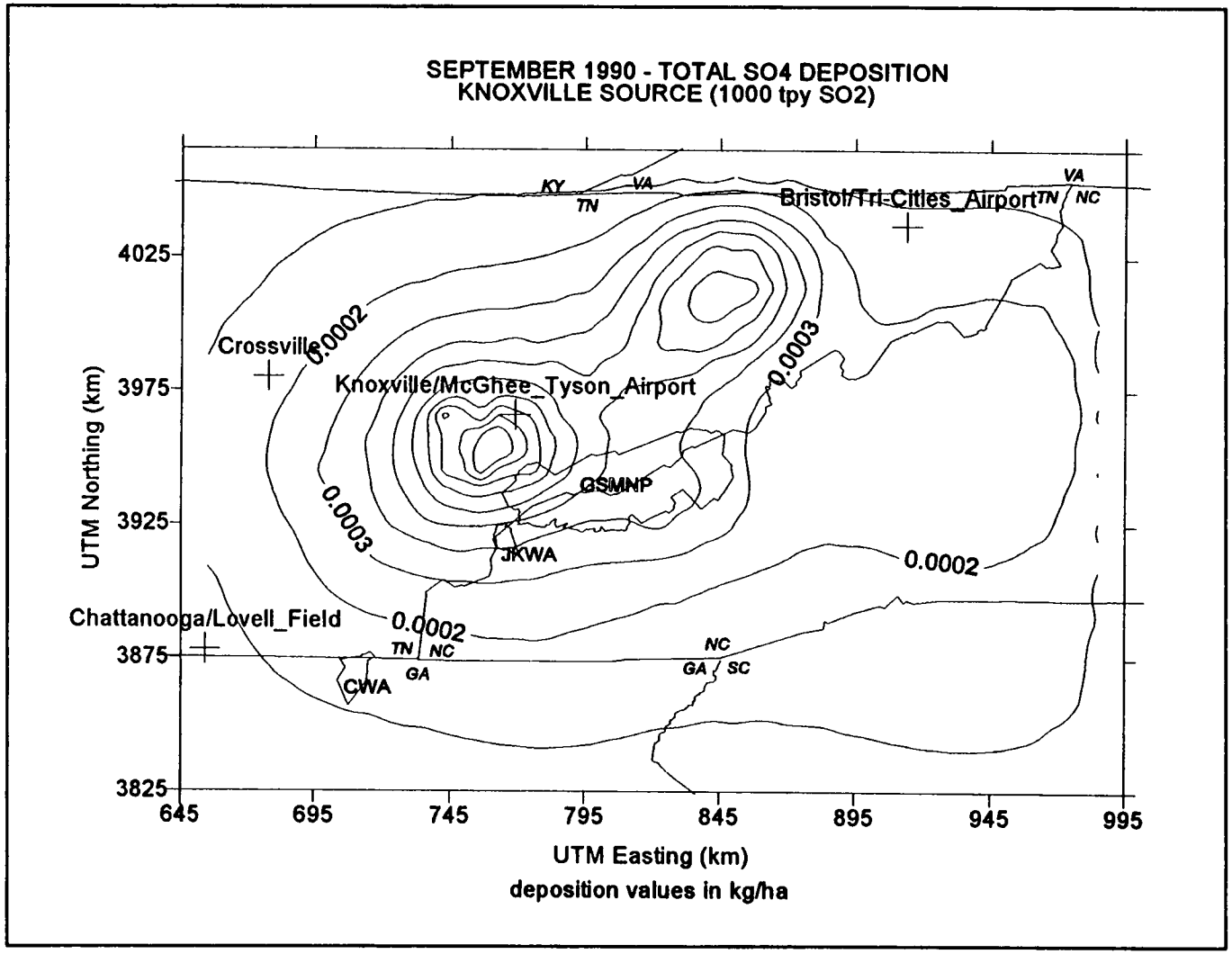

Fig. D.33. Total (wet+dry) SO_4^{2-} deposition estimated for September 1990 resulting from a 28.8 g/s (1000 tpy) hypothetical SO_2 emission source located at Knoxville /McGhee Tyson Airport.

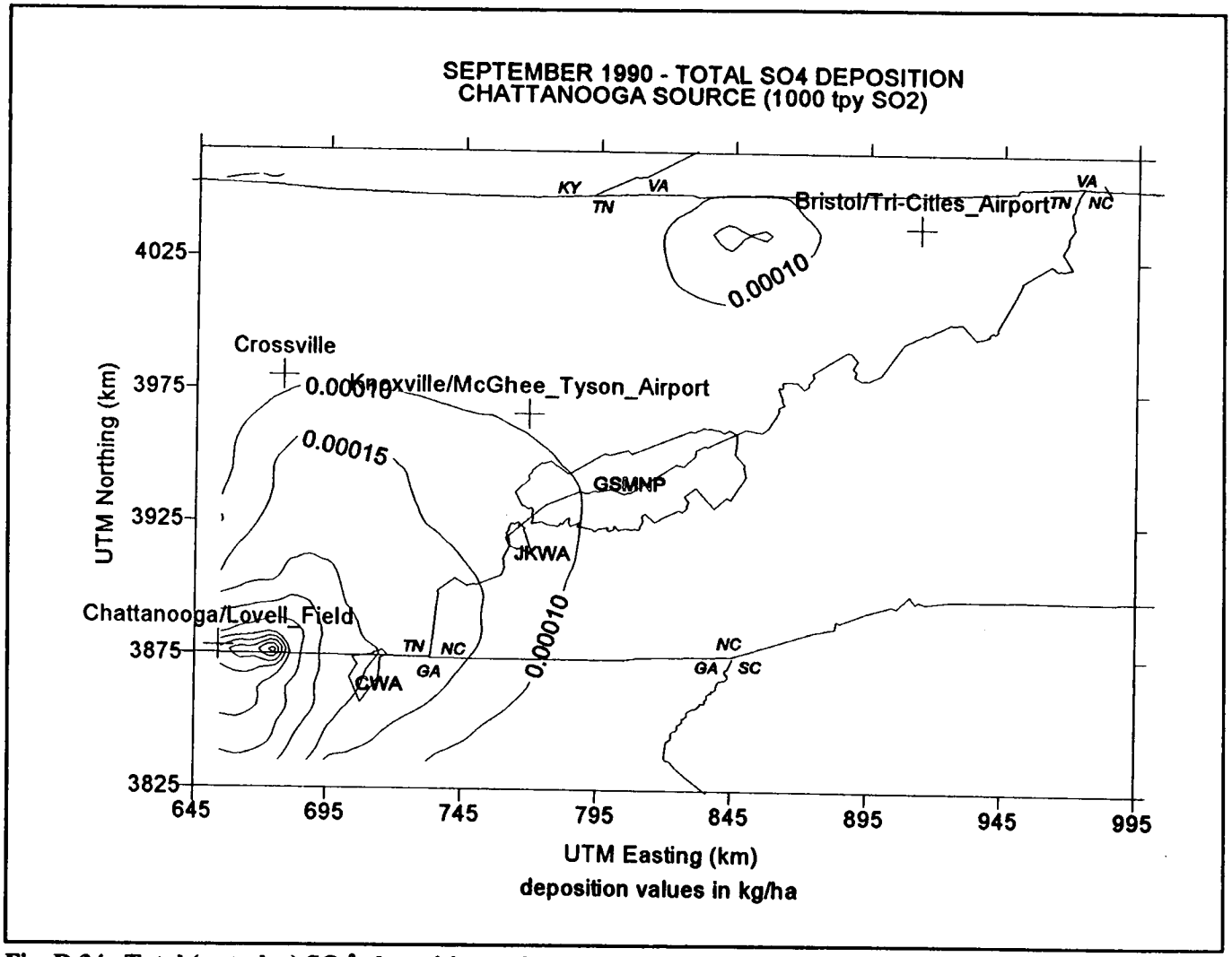

Fig. D.34. Total (wet+dry) SO_4^{2-} deposition estimated for September 1990 resulting from a 28.8 g/s (1000 tpy) hypothetical SO_2 emission source located at Chattanooga/Lovell Field.

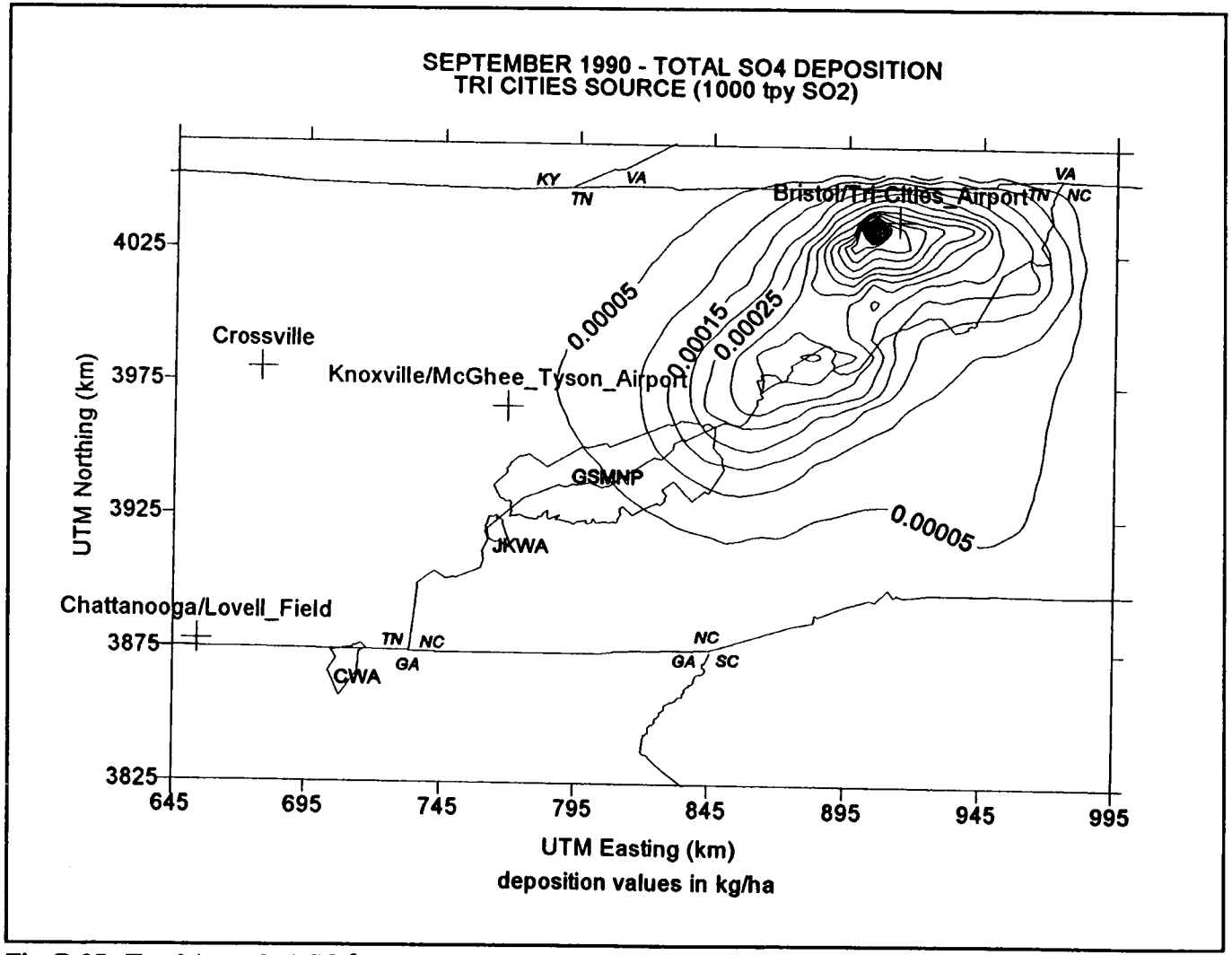

Fig. D.35. Total (wet+dry) SO_4^{2-} deposition estimated for September 1990 resulting from a 28.8 g/s (1000 tpy) hypothetical SO_2 emission source located at Bristol/Tri Cities Airport.

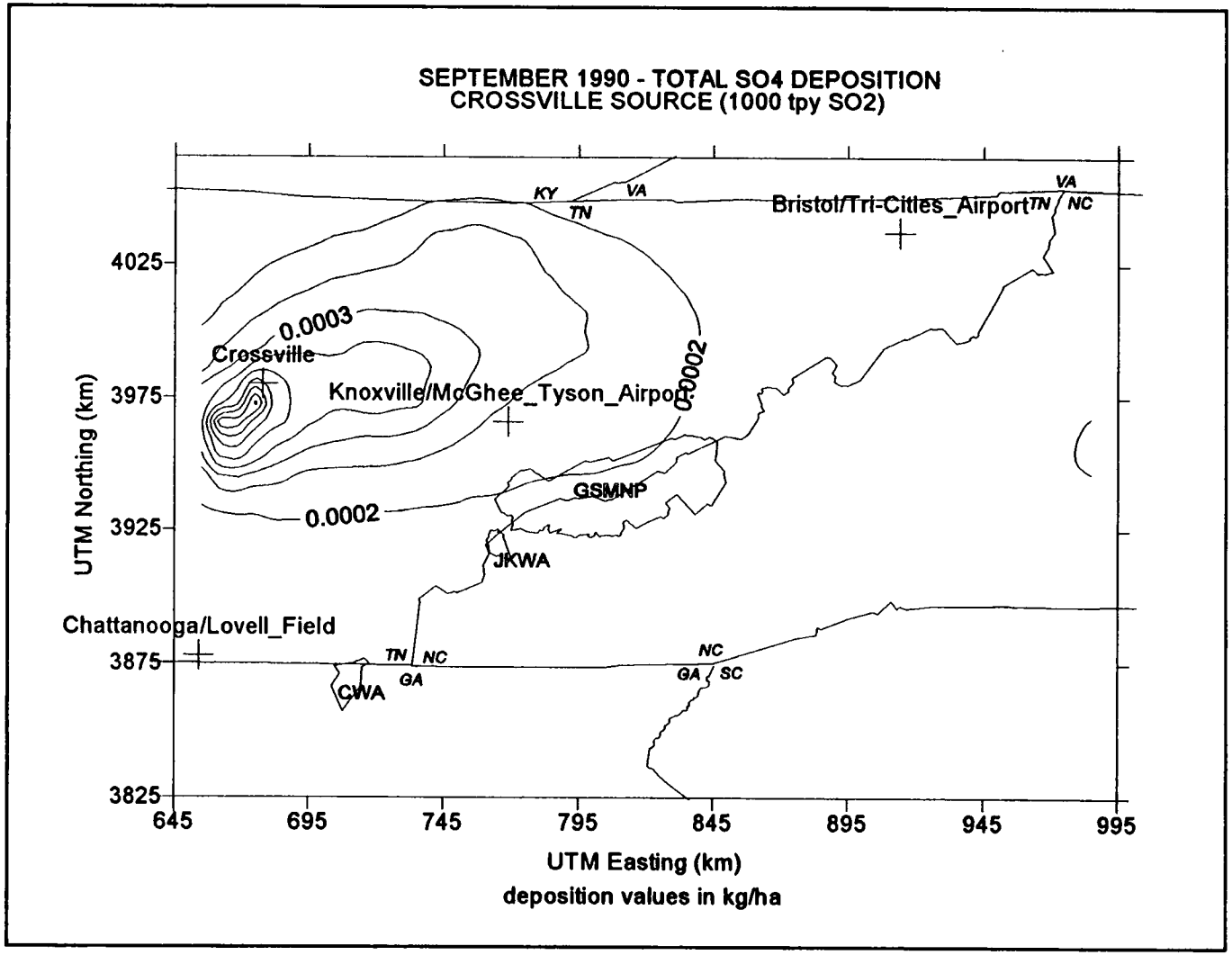

Fig. D.36. Total (wet+dry) SO_4^{2-} deposition estimated for September 1990 resulting from a 28.8 g/s (1000 tpy) hypothetical SO_2 emission source located in Crossville.

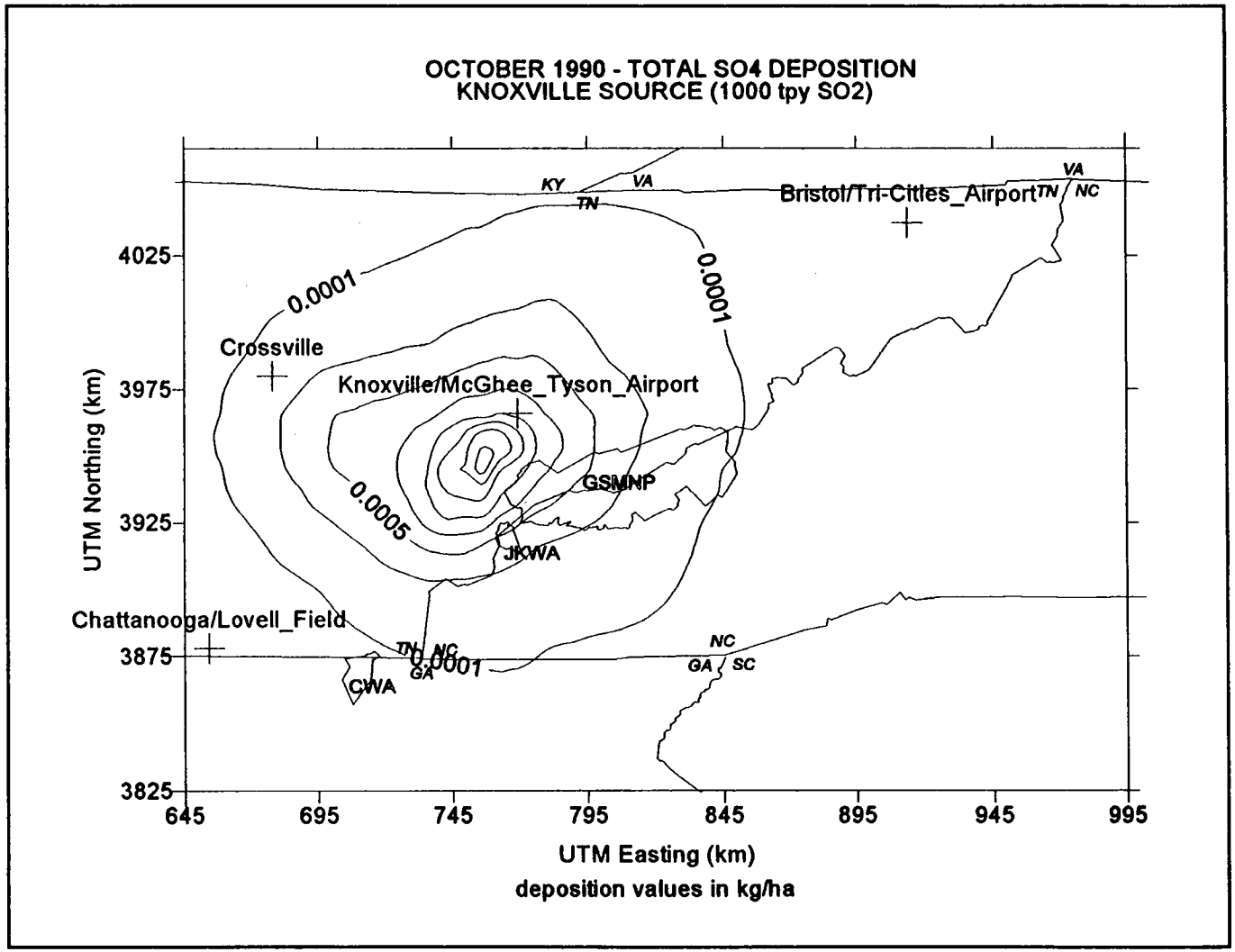

Fig. D.37. Total (wet+dry) SO_4^{2-} deposition estimated for October 1990 resulting from a 28.8 g/s (1000 tpy) hypothetical SO_2 emission source located at Knoxville /McGhee Tyson Airport.

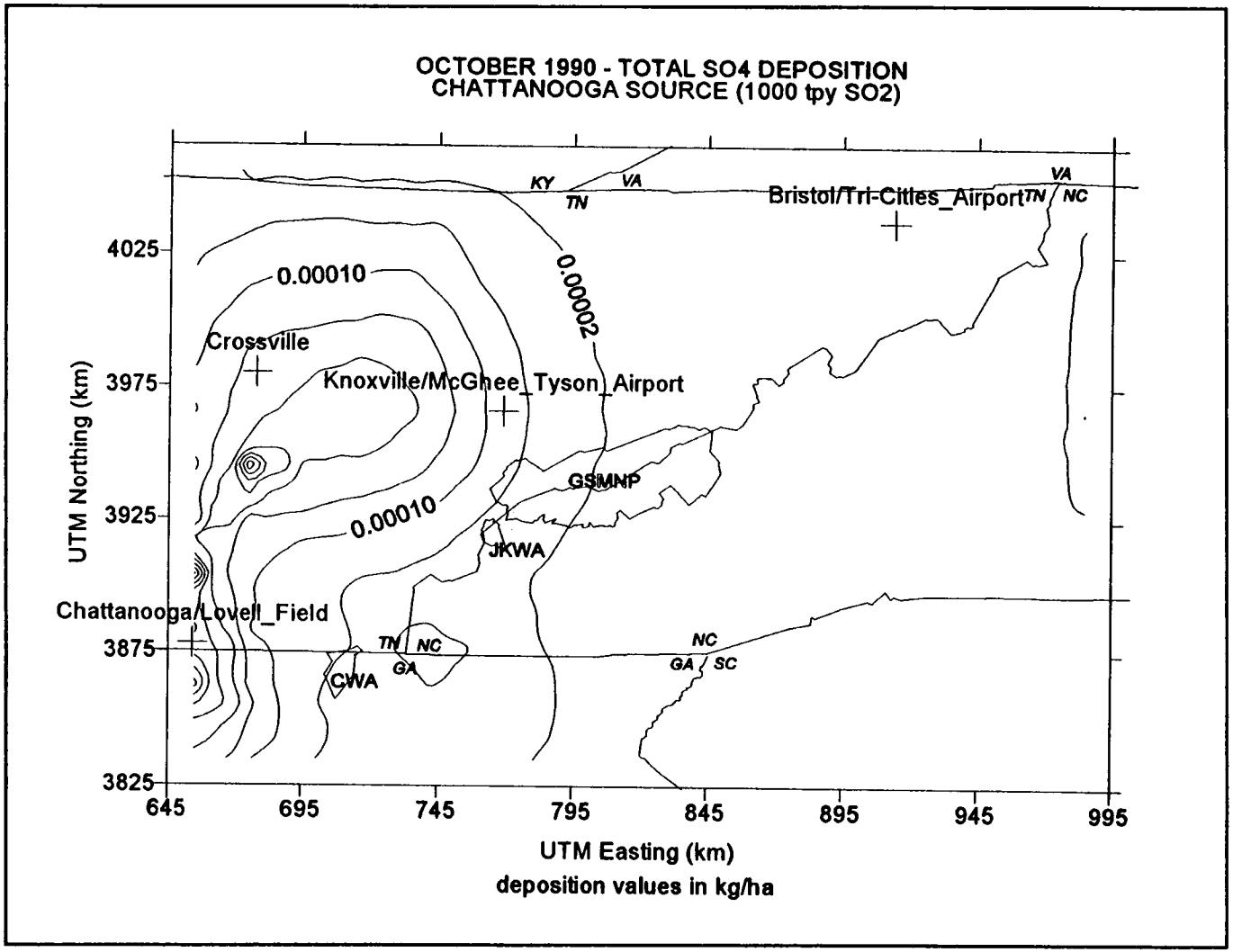

Fig. D.38. Total (wet+dry) SO_4^{2-} deposition estimated for October 1990 resulting from a 28.8 g/s (1000 tpy) hypothetical SO_2 emission source located at Chattanooga/Lovell Field.

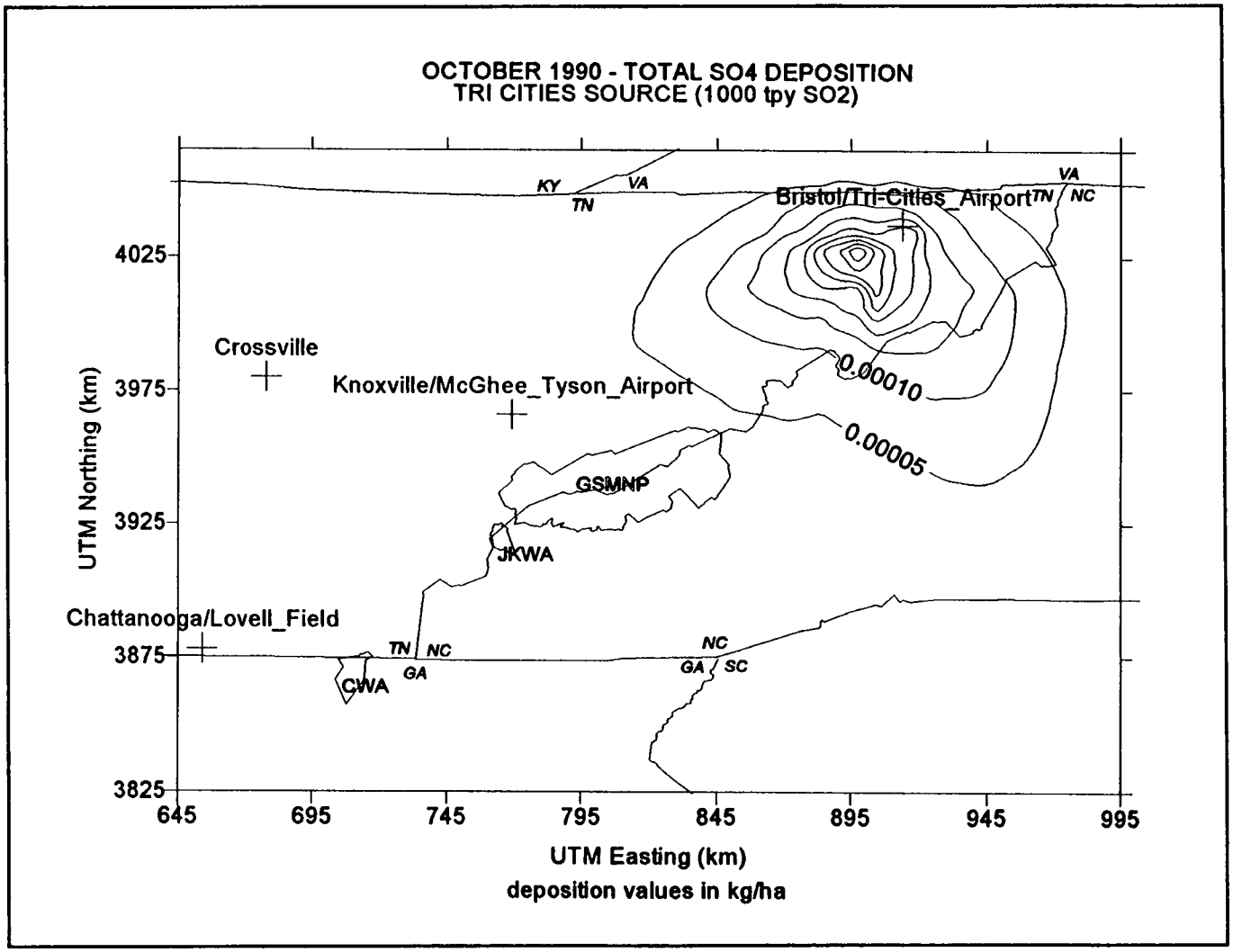

Fig. D.39. Total (wet+dry) SO_4^{2-} deposition estimated for October 1990 resulting from a 28.8 g/s (1000 tpy) hypothetical SO_2 emission source located at Bristol/Tri Cities Airport.

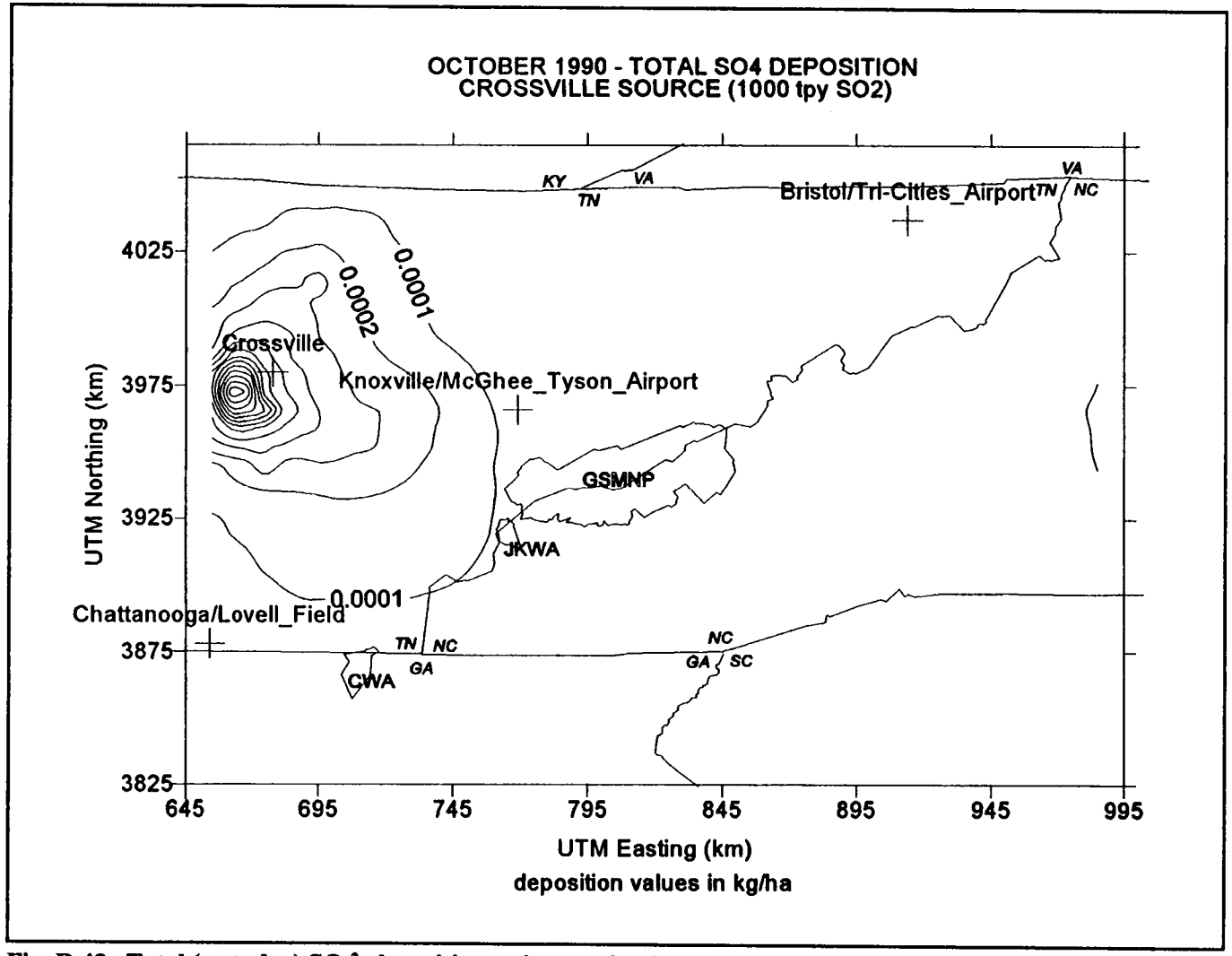

Fig. D.40. Total (wet+dry) SO_4^{2-} deposition estimated for October 1990 resulting from a 28.8 g/s (1000 tpy) hypothetical SO_2 emission source located in Crossville.

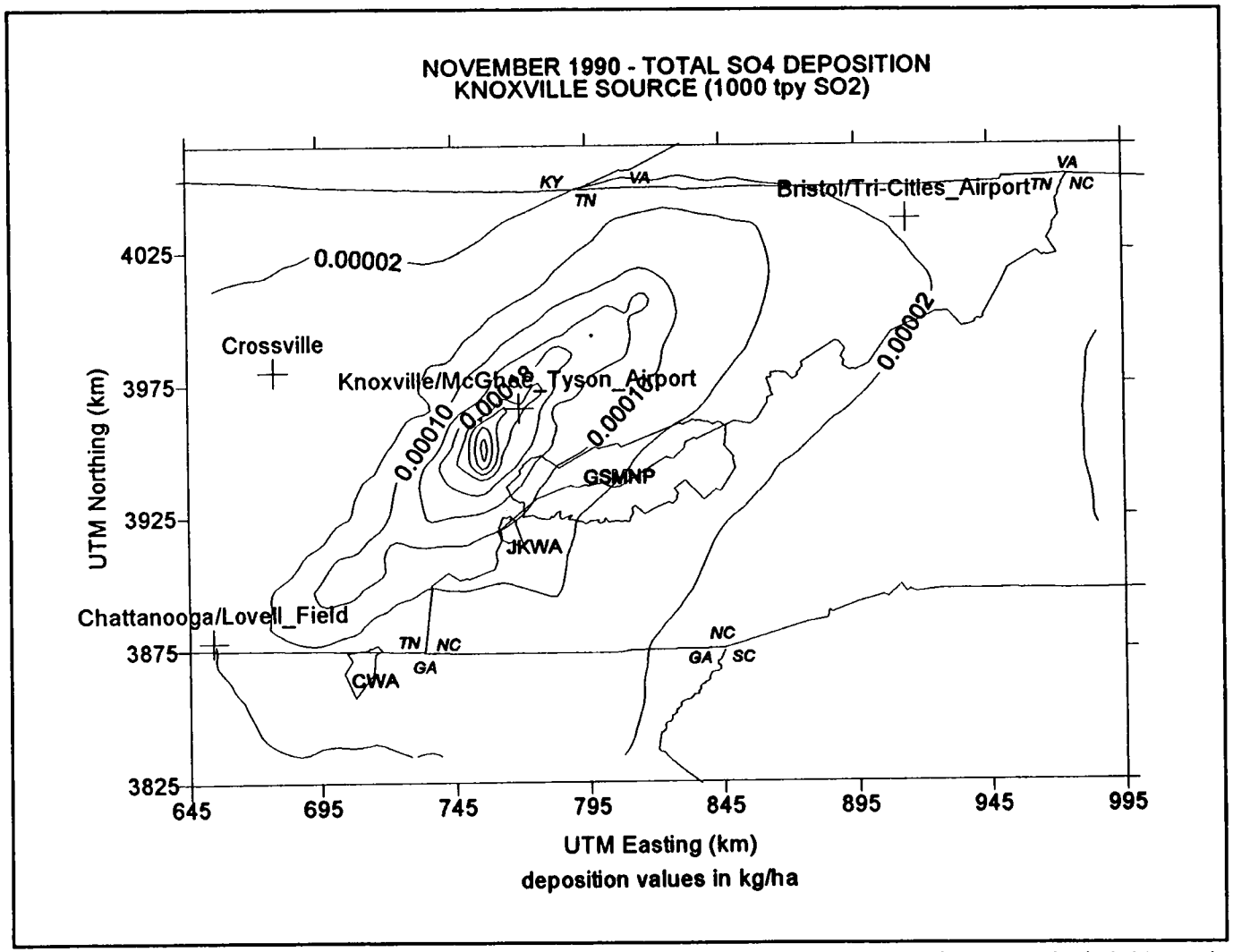

Fig. D.41. Total (wet+dry) SO_4^{2-} deposition estimated for November 1990 resulting from a 28.8 g/s (1000 tpy) hypothetical SO_2 emission source located at Knoxville /McGhee Tyson Airport.

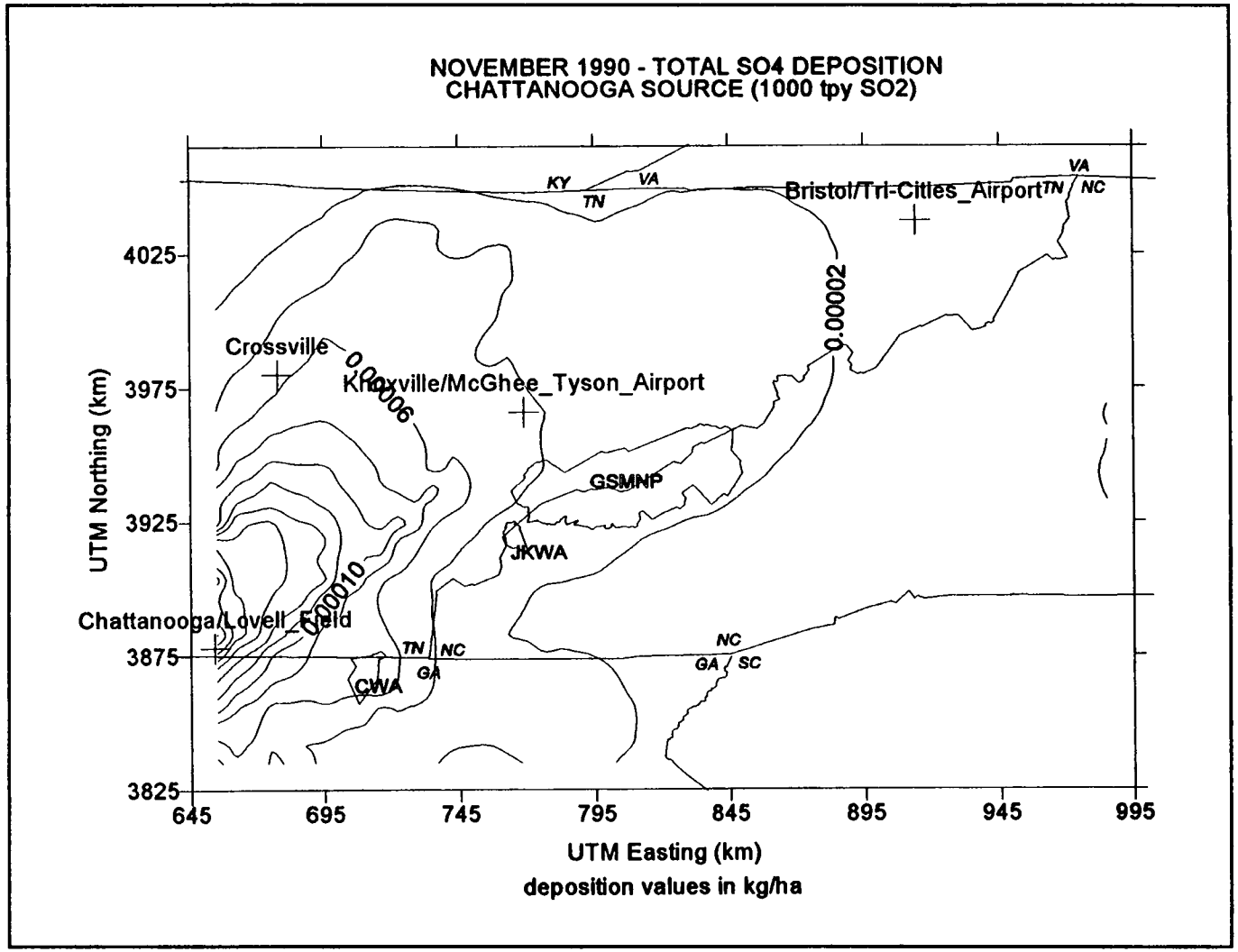

Fig. D.42. Total (wet+dry) SO_4^{2-} deposition estimated for November 1990 resulting from a 28.8 g/s (1000 tpy) hypothetical SO_2 emission source located at Chattanooga/Lovell Field.

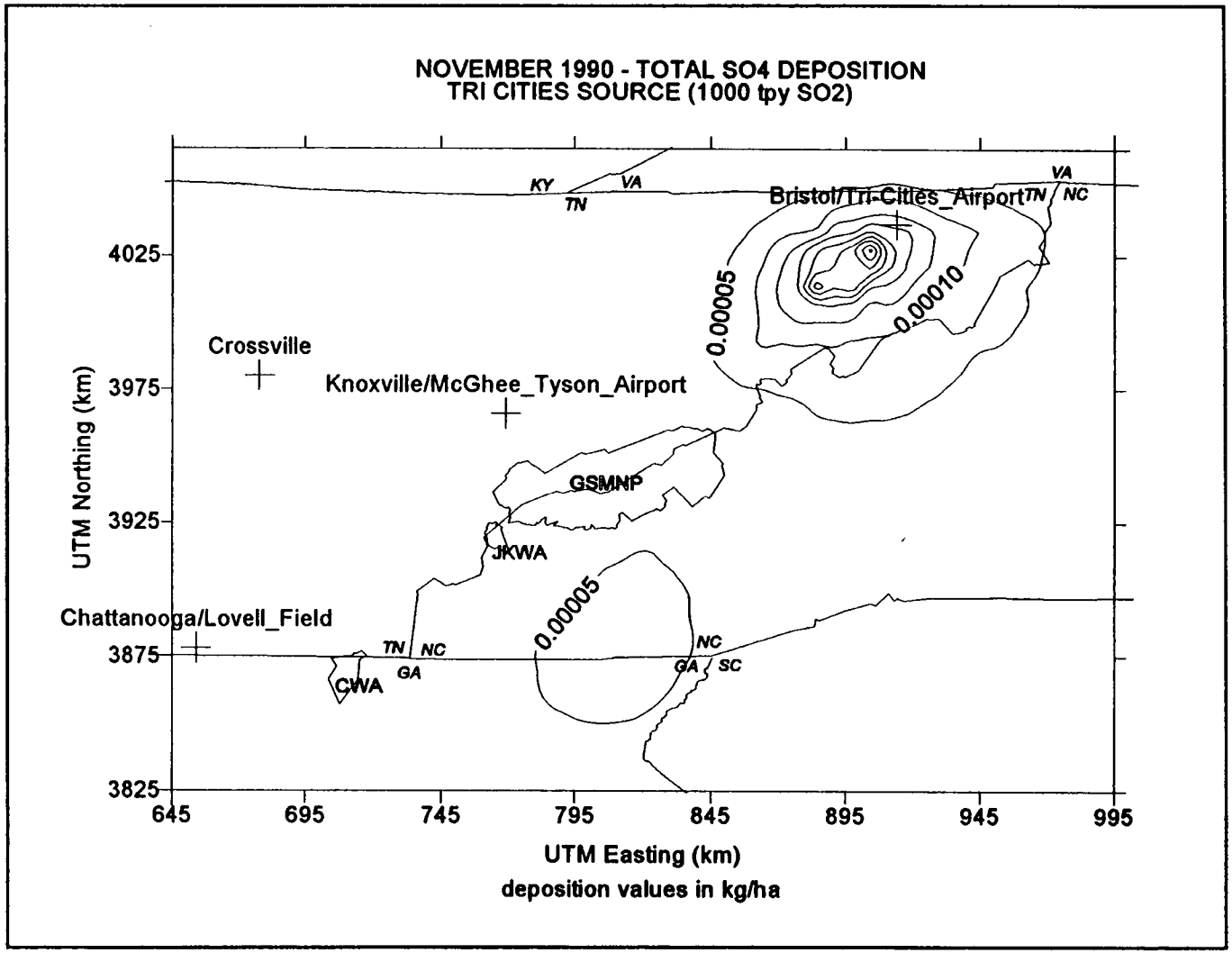

Fig. D.43. Total (wet+dry) SO_4^{2-} deposition estimated for November 1990 resulting from a 28.8 g/s (1000 tpy) hypothetical SO_2 emission source located at Bristol/Tri Cities Airport.

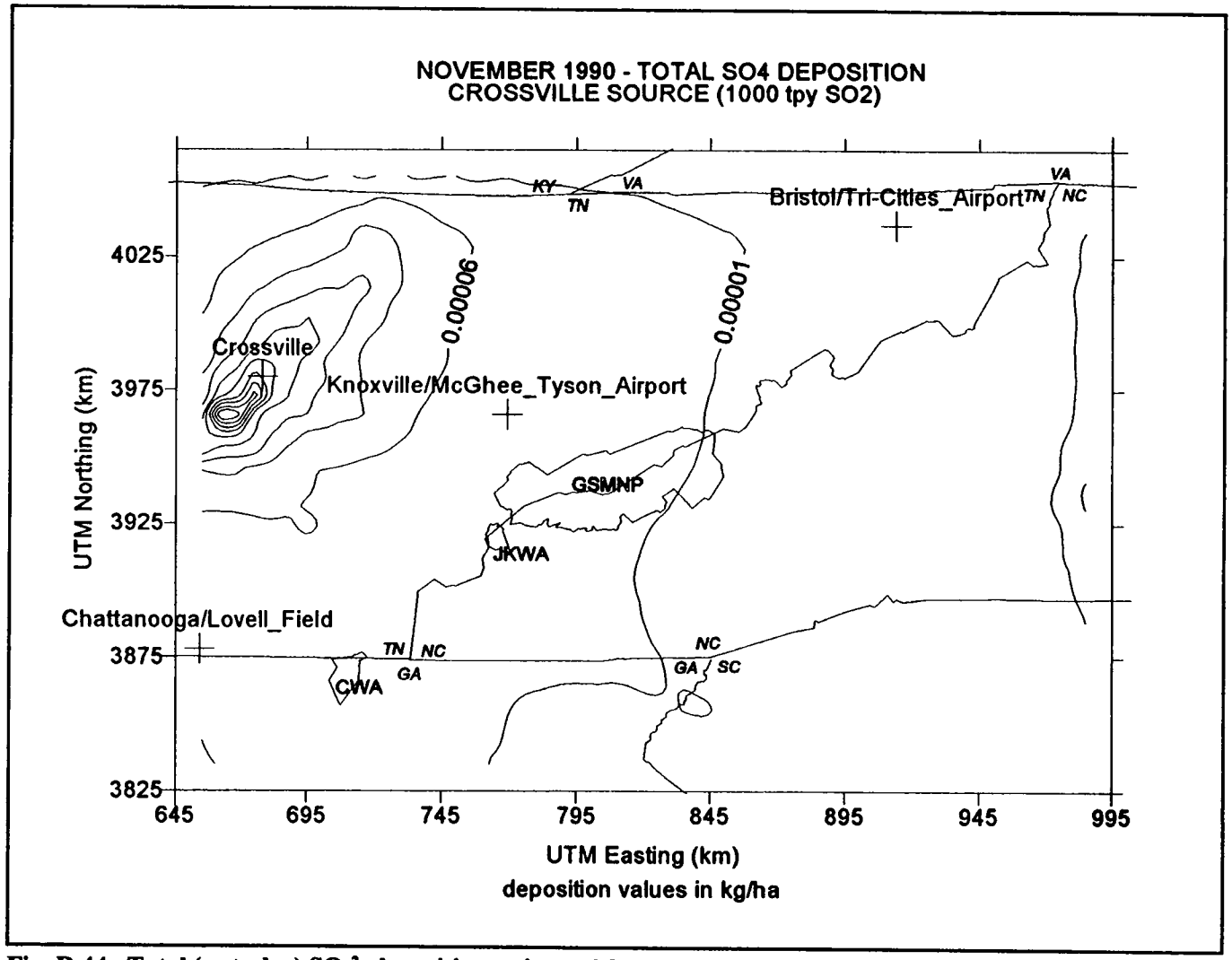

Fig. D.44. Total (wet+dry) SO_4^{2-} deposition estimated for November 1990 resulting from a 28.8 g/s (1000 tpy) hypothetical SO_2 emission source located in Crossville.

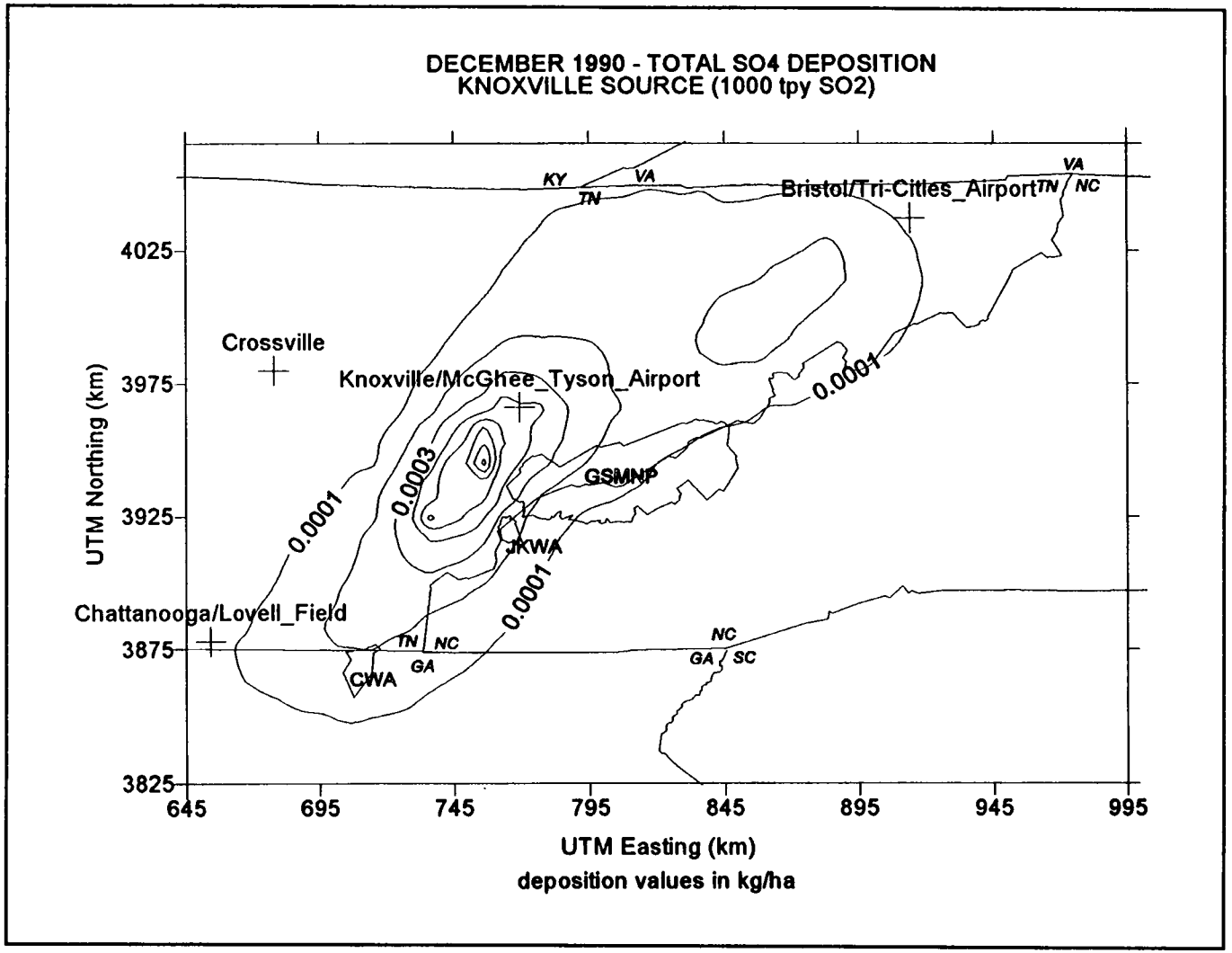

Fig. D.45. Total (wet+dry) SO_4^{2-} deposition estimated for December 1990 resulting from a 28.8 g/s (1000 tpy) hypothetical SO_2 emission source located at Knoxville /McGhee Tyson Airport.

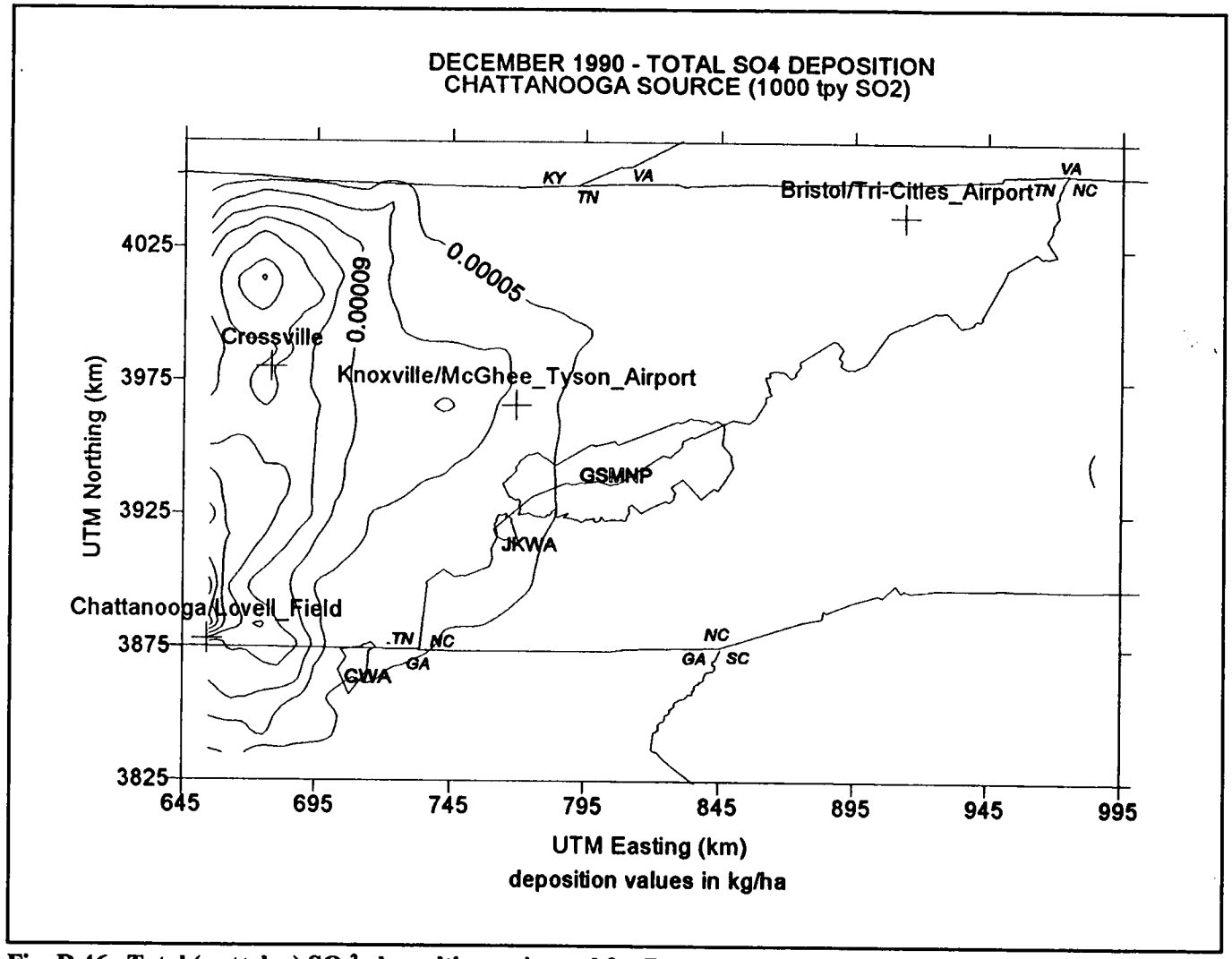

Fig. D.46. Total (wet+dry) SO_4^{2-} deposition estimated for December 1990 resulting from a 28.8 g/s (1000 tpy) hypothetical SO_2 emission source located at Chattanooga/Lovell Field.

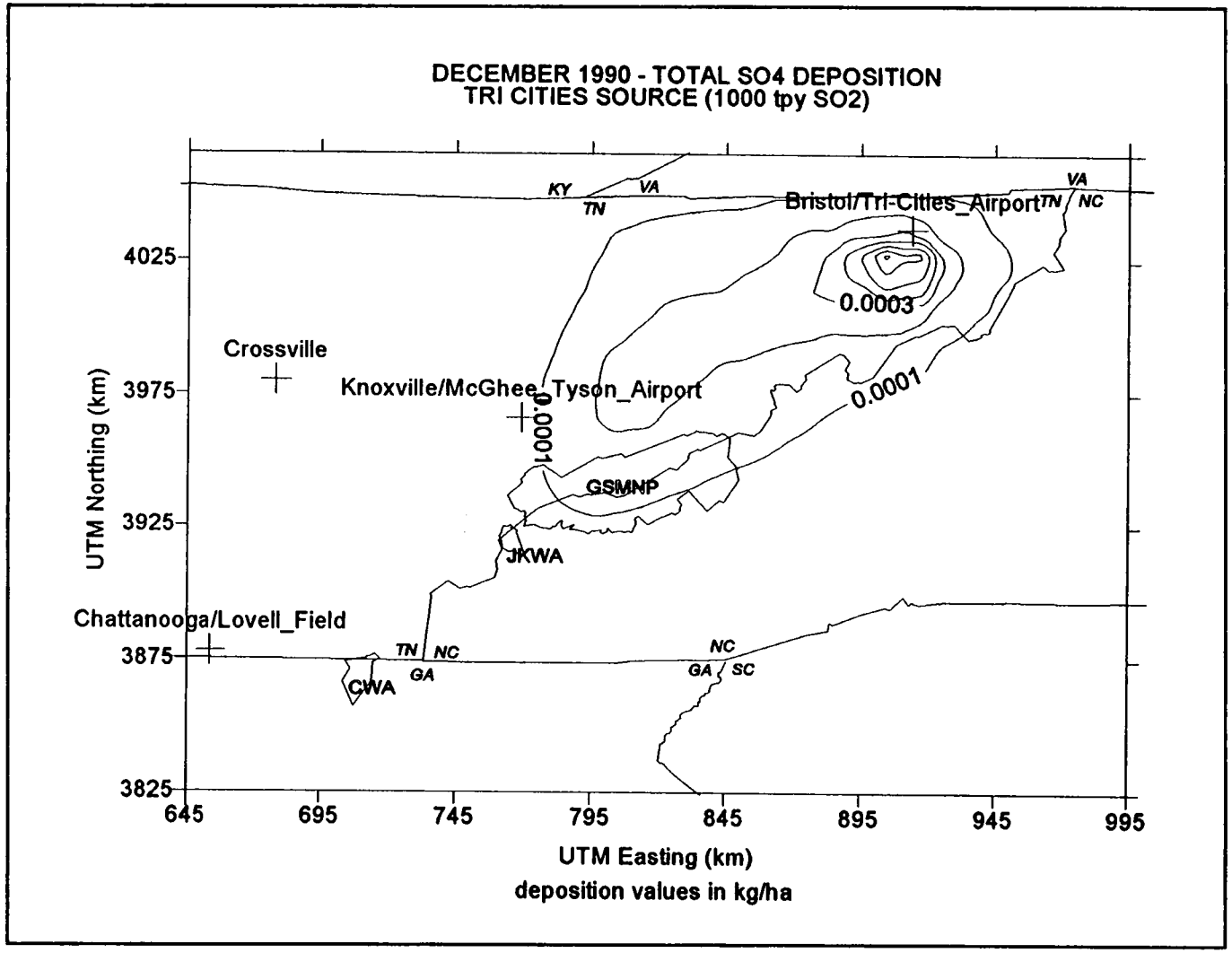

Fig. D.47. Total (wet+dry) SO_4^{2-} deposition estimated for December 1990 resulting from a 28.8 g/s (1000 tpy) hypothetical SO_2 emission source located at Bristol/Tri Cities Airport.

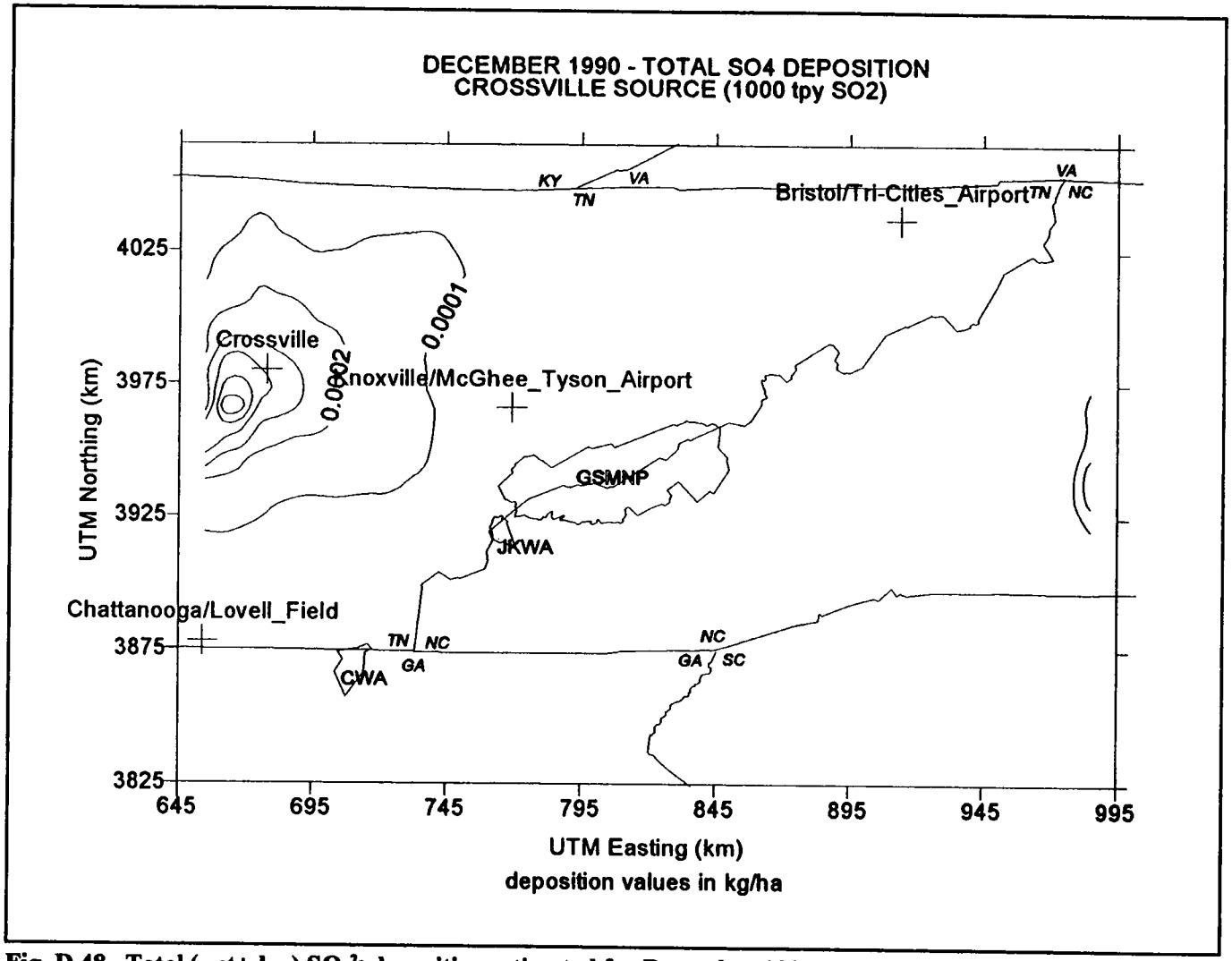

Fig. D.48. Total (wet+dry) SO_4^{2-} deposition estimated for December 1990 resulting from a 28.8 g/s (1000 tpy) hypothetical SO_2 emission source located in Crossville.

APPENDIX E
MONTHLY NOx DEPOSITION CONTOUR MAPS

The following figures are contour maps of monthly total (wet + dry) NO_x deposition in the East Tennessee modeling domain. One contour map per month has been generated for each of the four hypothetical source locations.

The following abbreviations are used on the contour maps:

GSMNP	=	The Great Smoky Mountains National Park
JKWA	=	Joyce Kilmer Wilderness Area
CWA	=	Cohutta Wilderness Area
TN	=	Tennessee
NC	=	North Carolina
GA	=	Georgia
VA	=	Virginia
KY	=	Kentucky
UTM	=	Universal Transverse Mercator

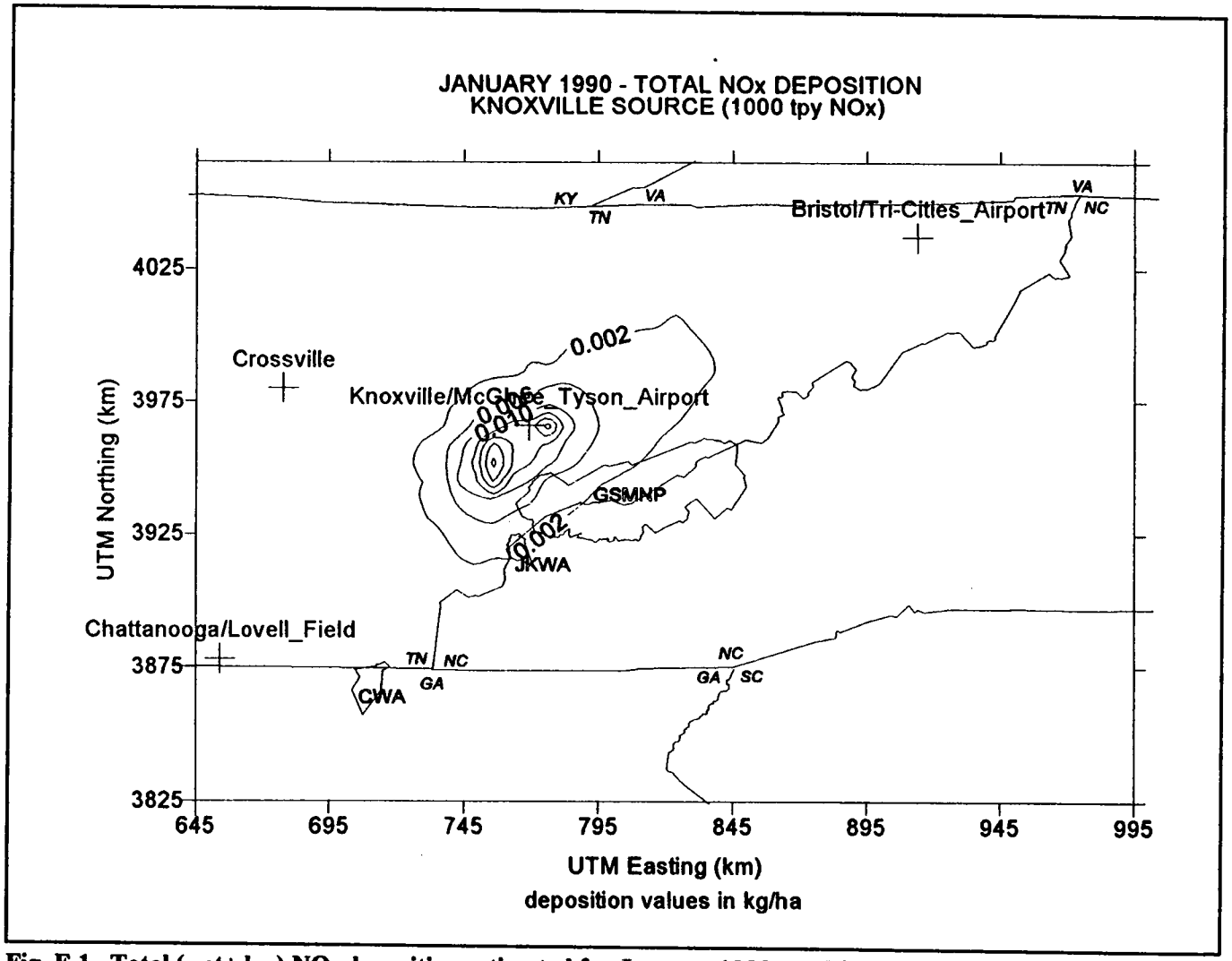

Fig. E.1. Total (wet+dry) NO_x deposition estimated for January 1990 resulting from a 28.8 g/s (1000 tpy) hypothetical NO_x emission source located at Knoxville /McGhee Tyson Airport.

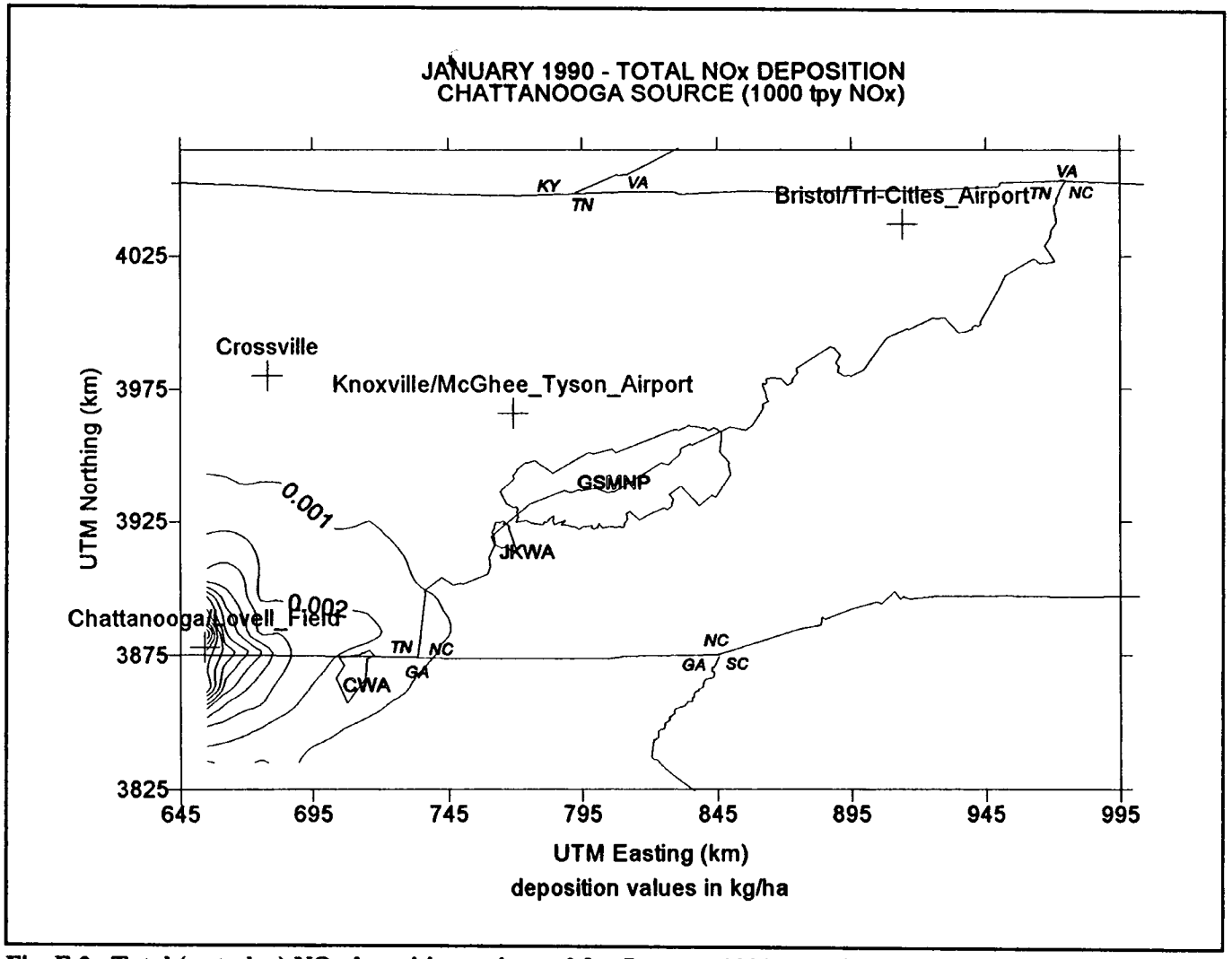

Fig. E.2. Total (wet+dry) NO_x deposition estimated for January 1990 resulting from a 28.8 g/s (1000 tpy) hypothetical NO_x emission source located at Chattanooga/Lovell Field.

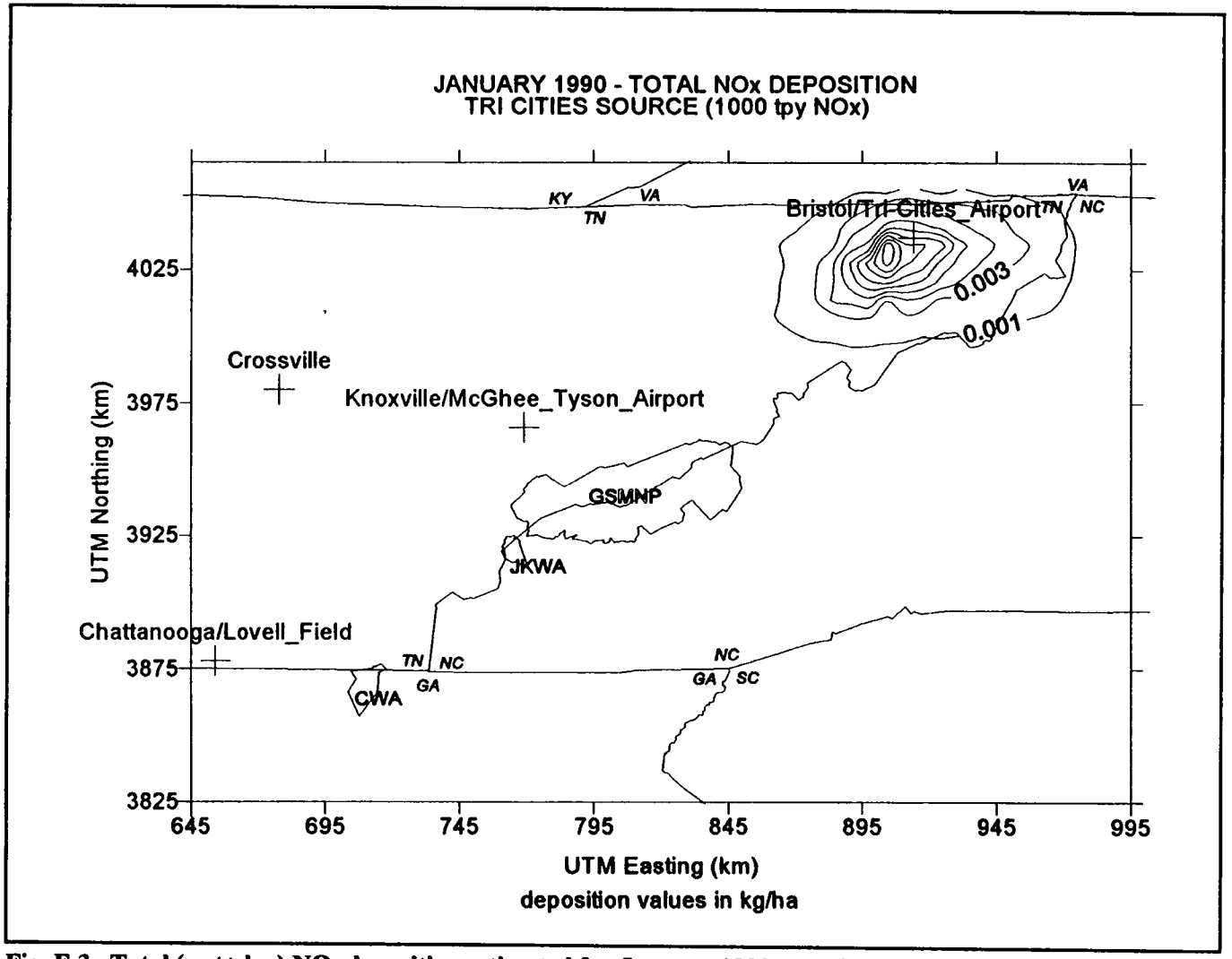

Fig. E.3. Total (wet+dry) NO_x deposition estimated for January 1990 resulting from a 28.8 g/s (1000 tpy) hypothetical NO_x emission source located at Bristol/Tri Cities Airport.

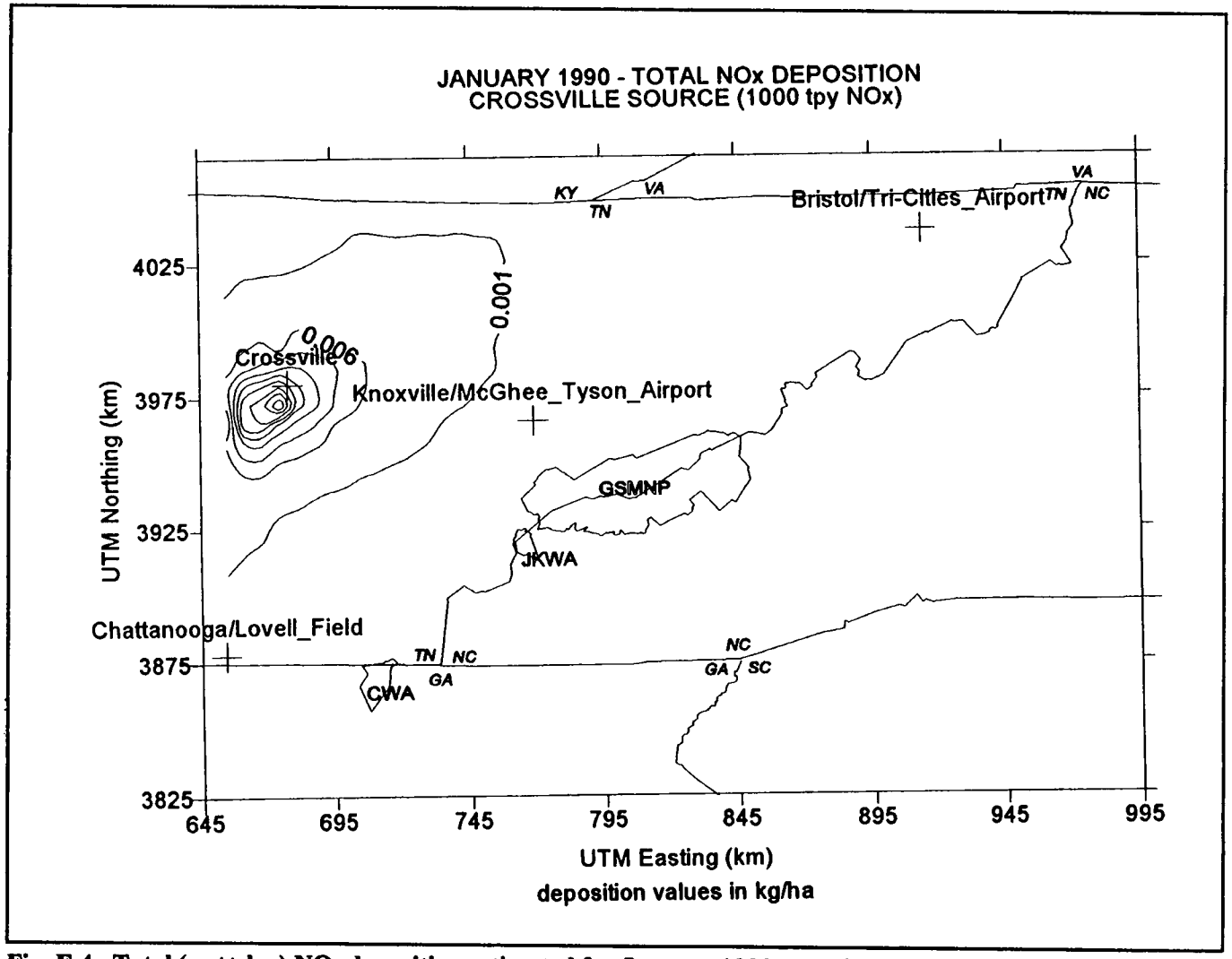

Fig. E.4. Total (wet+dry) NO_x deposition estimated for January 1990 resulting from a 28.8 g/s (1000 tpy) hypothetical NO_x emission source located in Crossville.

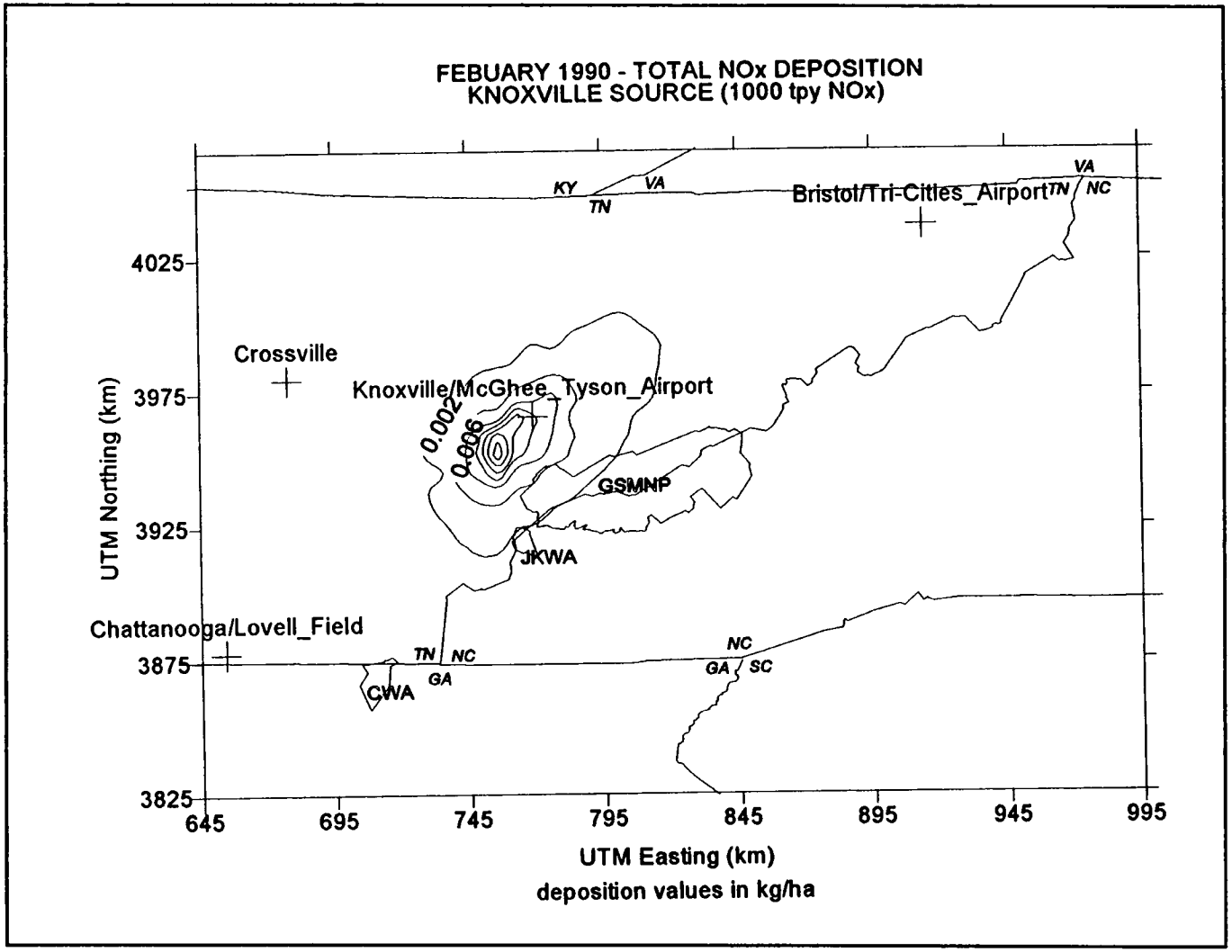

Fig. E.5. Total (wet+dry) NO_x deposition estimated for February 1990 resulting from a 28.8 g/s (1000 tpy) hypothetical NO_x emission source located at Knoxville /McGhee Tyson Airport.

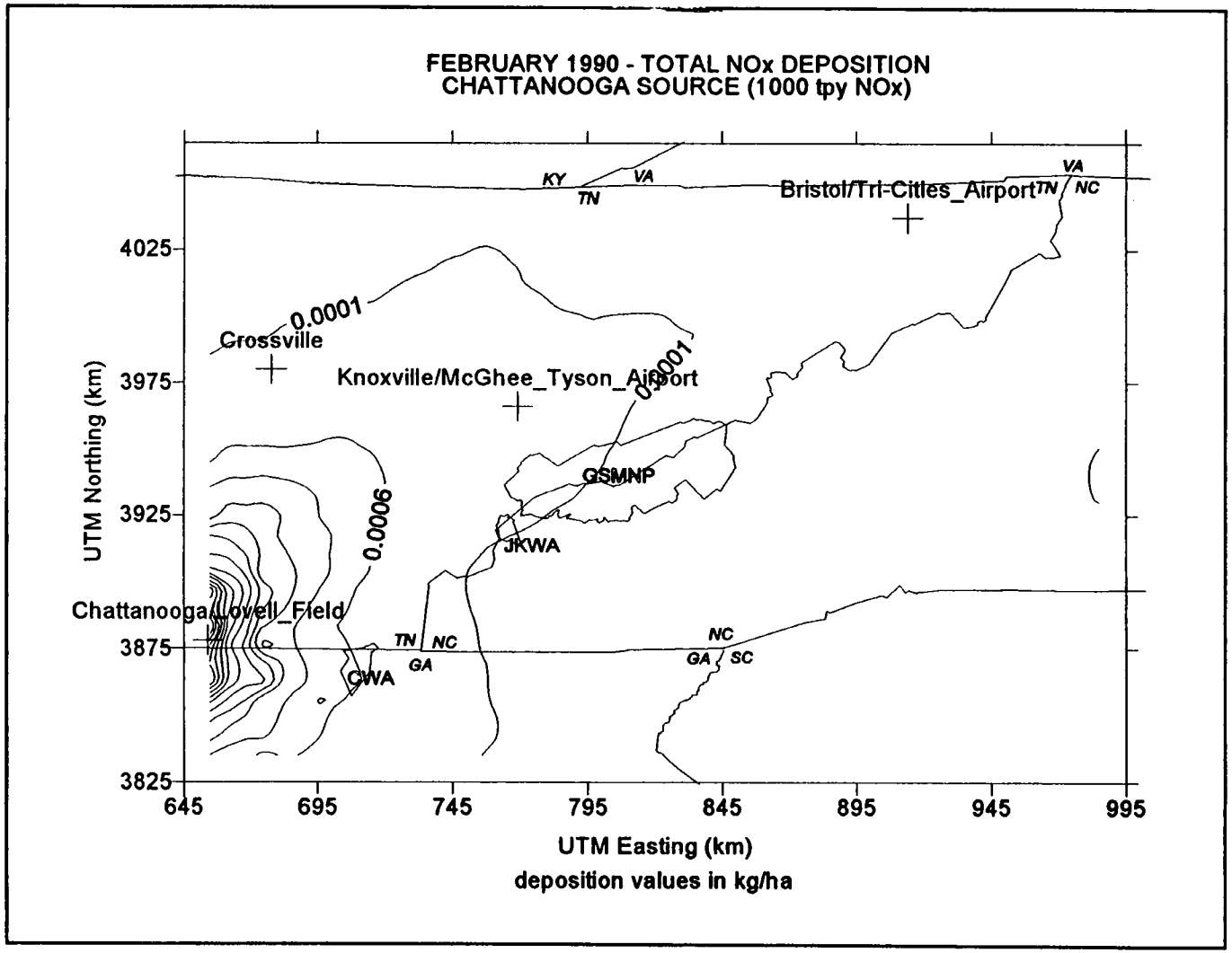

Fig. E.6. Total (wet+dry) NO_x deposition estimated for February 1990 resulting from a 28.8 g/s (1000 tpy) hypothetical NO_x emission source located at Chattanooga/Lovell Field.

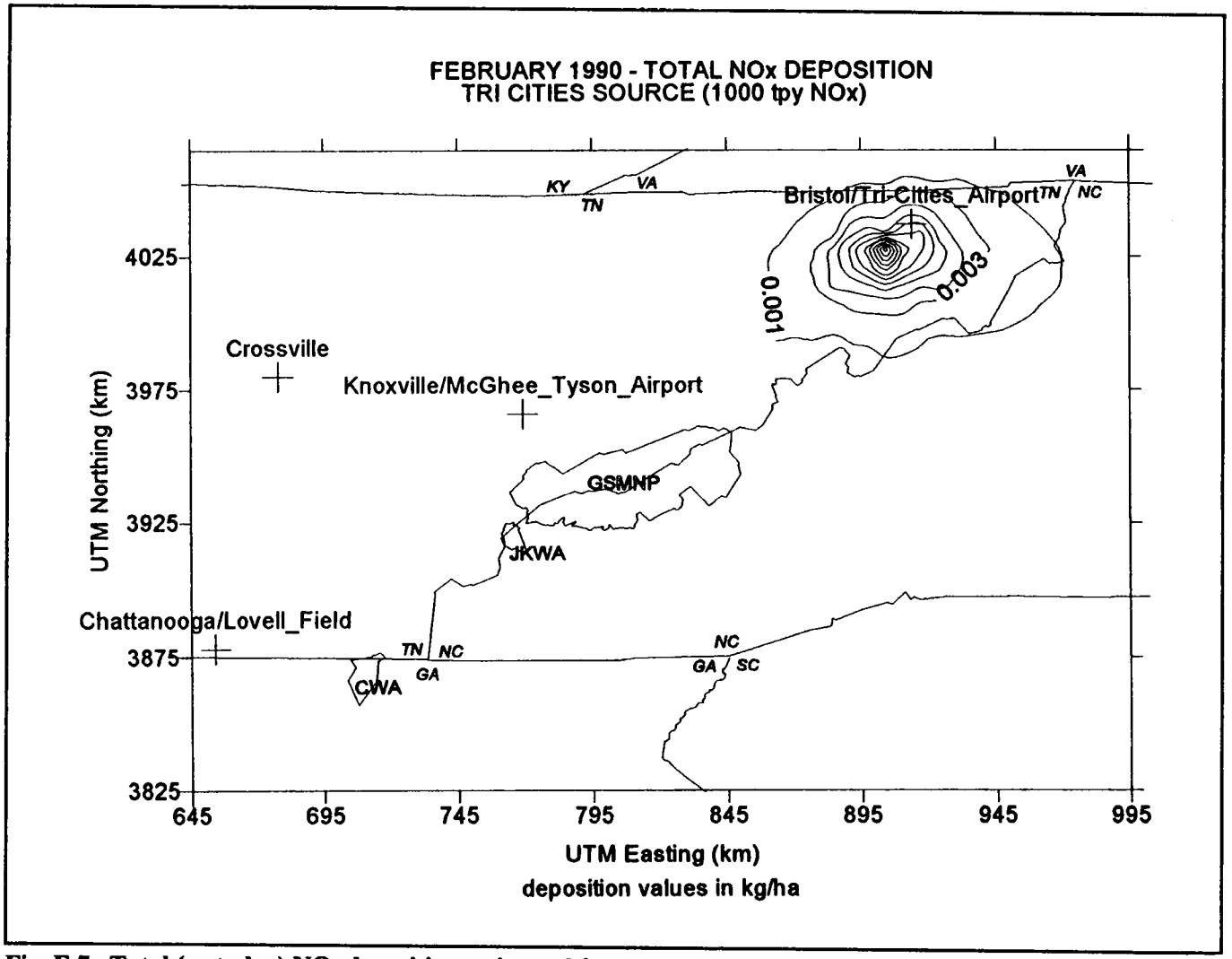

Fig. E.7. Total (wet+dry) NO_x deposition estimated for February 1990 resulting from a 28.8 g/s (1000 tpy) hypothetical NO_x emission source located at Bristol/Tri Cities Airport.

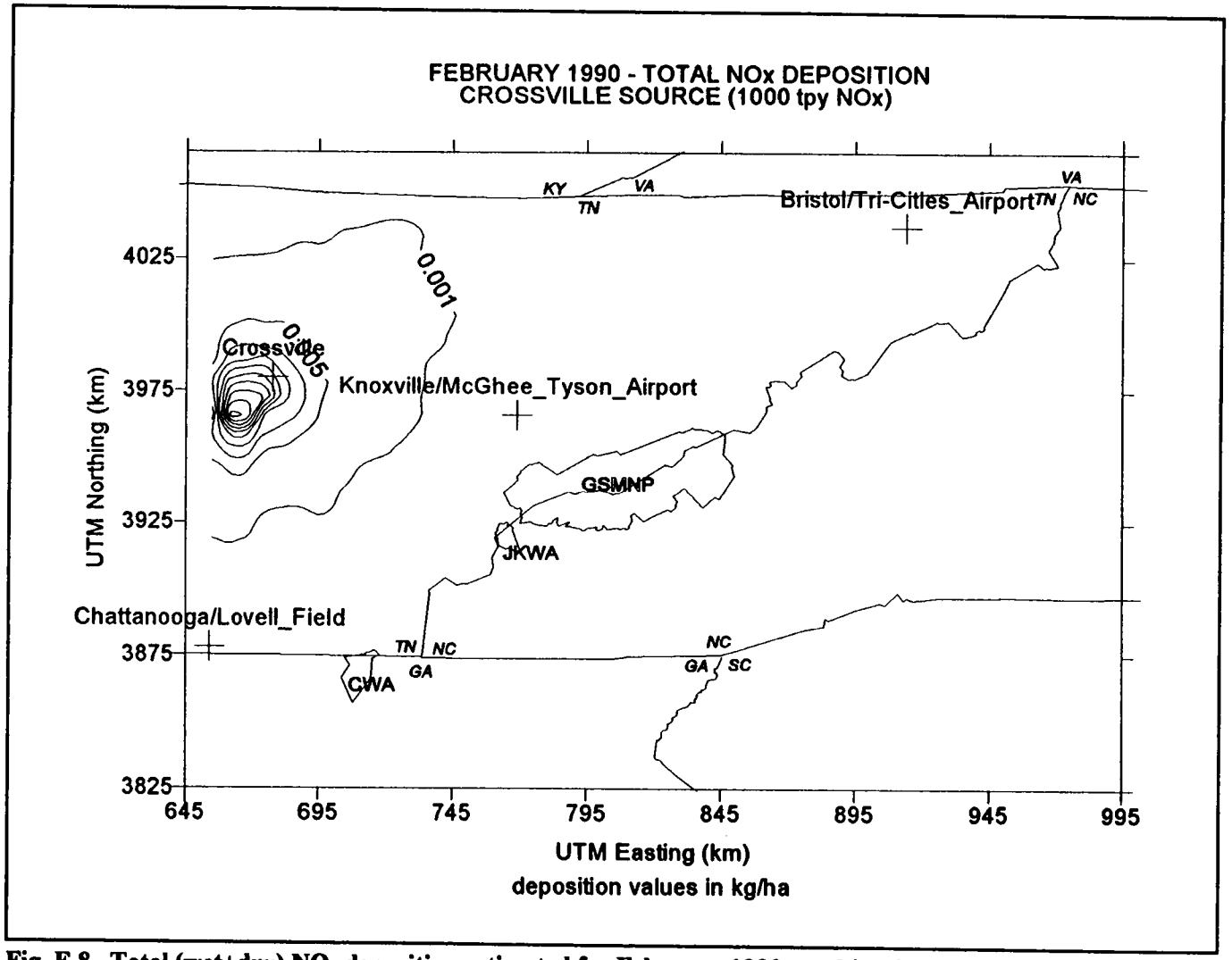

Fig. E.8. Total (wet+dry) NO_x deposition estimated for February 1990 resulting from a 28.8 g/s (1000 tpy) hypothetical NO_x emission source located in Crossville.

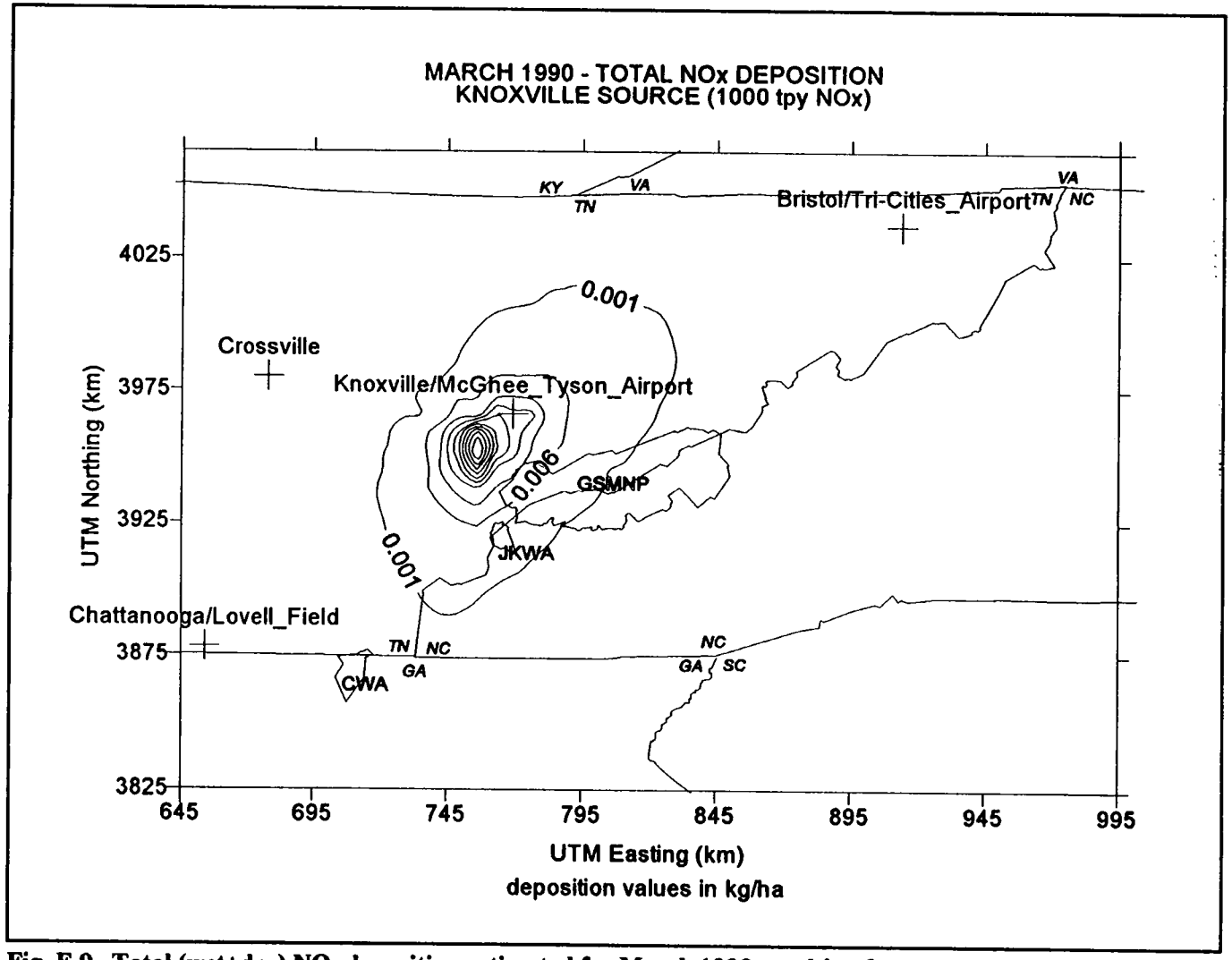

Fig. E.9. Total (wet+dry) NO_x deposition estimated for March 1990 resulting from a 28.8 g/s (1000 tpy) hypothetical NO_x emission source located at Knoxville /McGhee Tyson Airport.

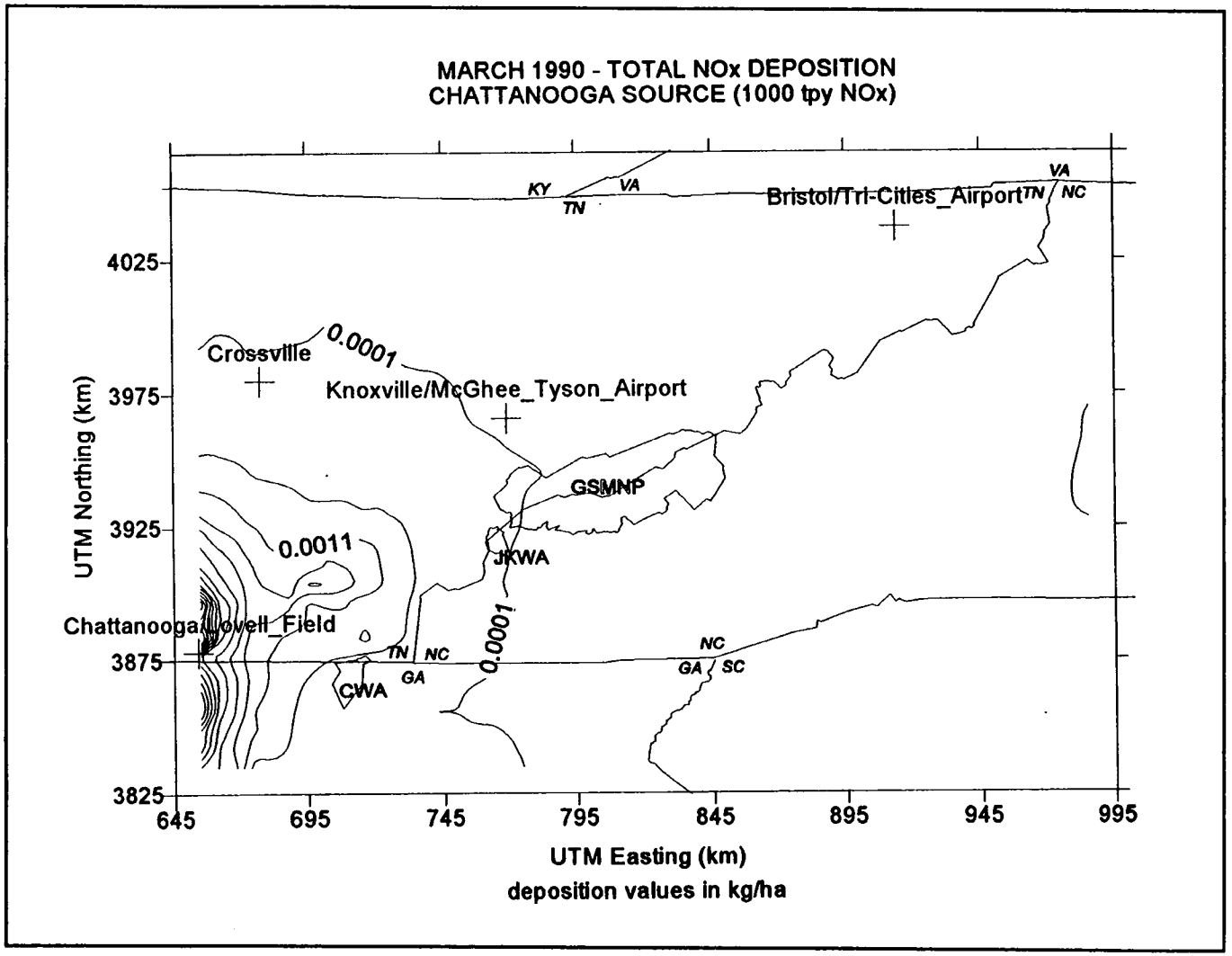

Fig. E.10. Total (wet+dry) NO_x deposition estimated for March 1990 resulting from a 28.8 g/s (1000 tpy) hypothetical NO_x emission source located at Chattanooga/Lovell Field.

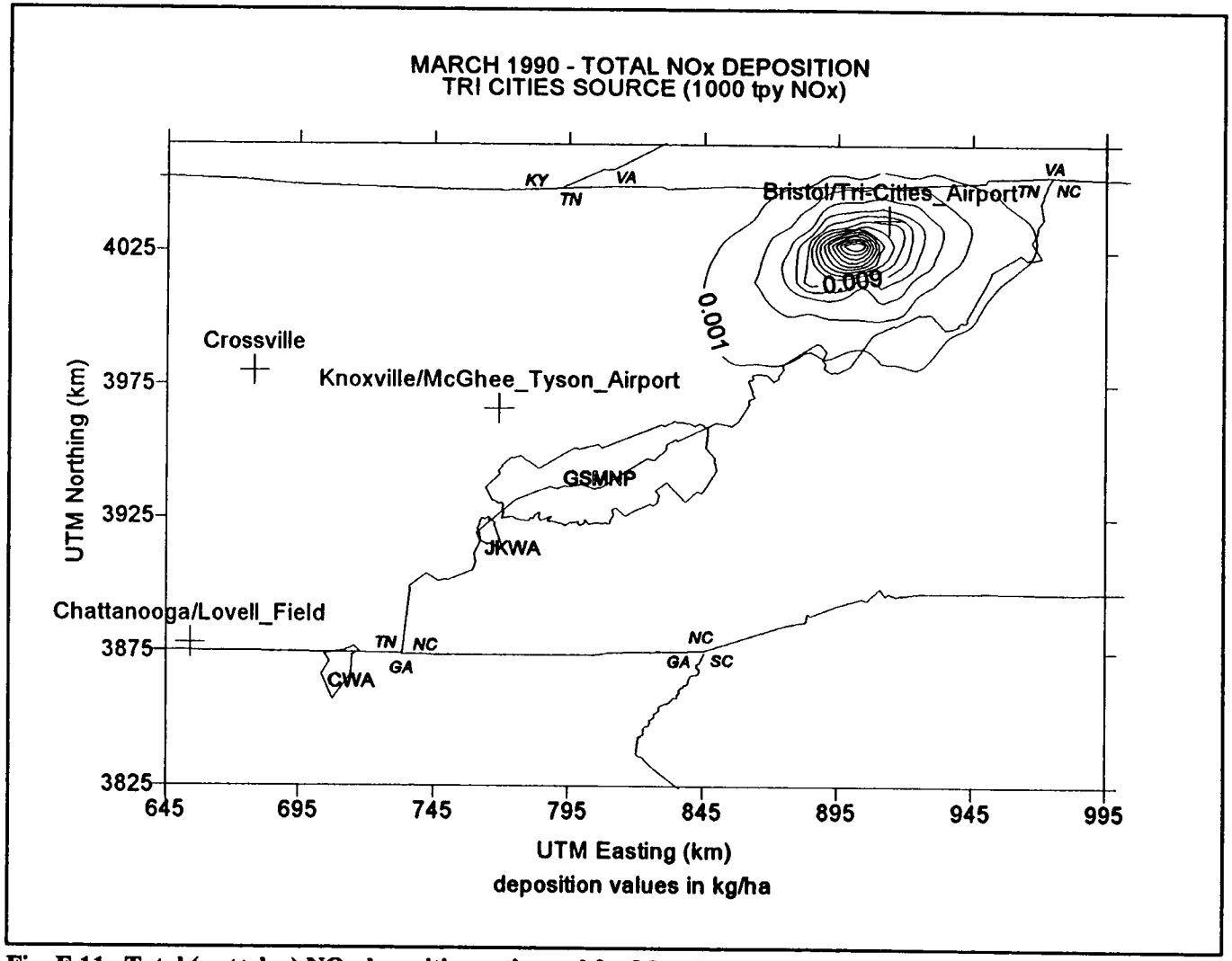

Fig. E.11. Total (wet+dry) NO_x deposition estimated for March 1990 resulting from a 28.8 g/s (1000 tpy) hypothetical NO_x emission source located at Bristol/Tri Cities Airport.

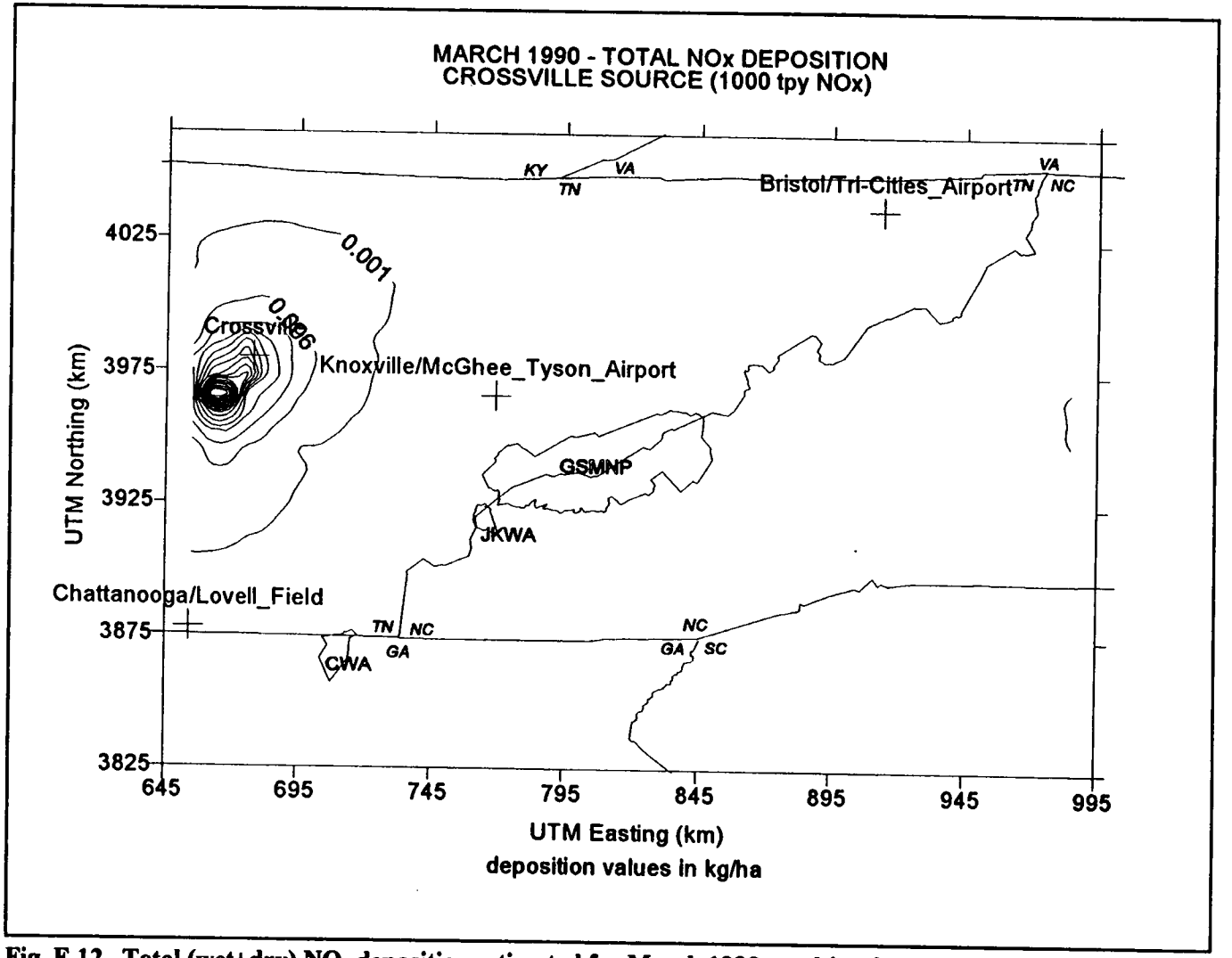

Fig. E.12. Total (wet+dry) NO_x deposition estimated for March 1990 resulting from a 28.8 g/s (1000 tpy) hypothetical NO_x emission source located in Crossville.

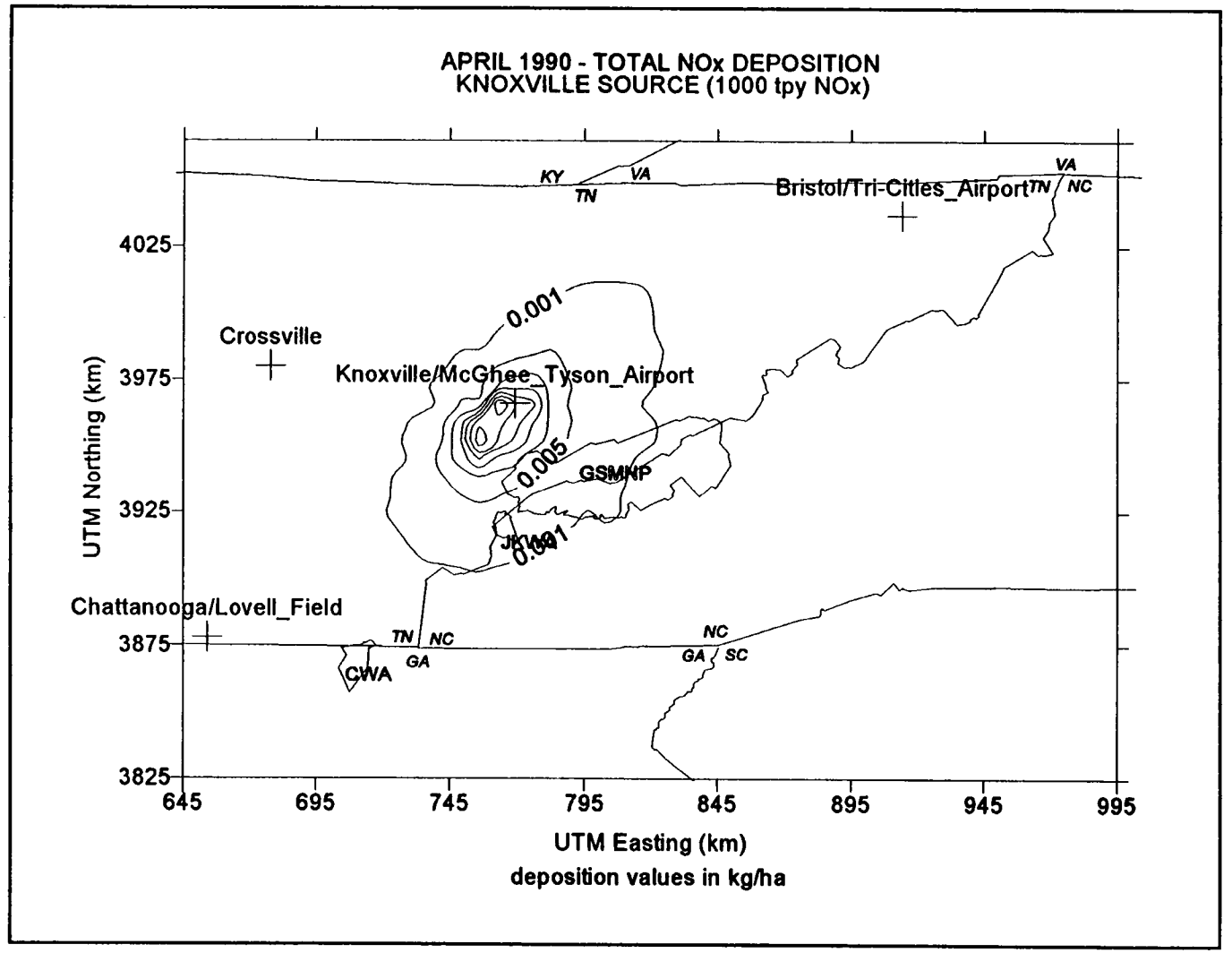

Fig. E.13. Total (wet+dry) NO_x deposition estimated for April 1990 resulting from a 28.8 g/s (1000 tpy) hypothetical NO_x emission source located at Knoxville /McGhee Tyson Airport.

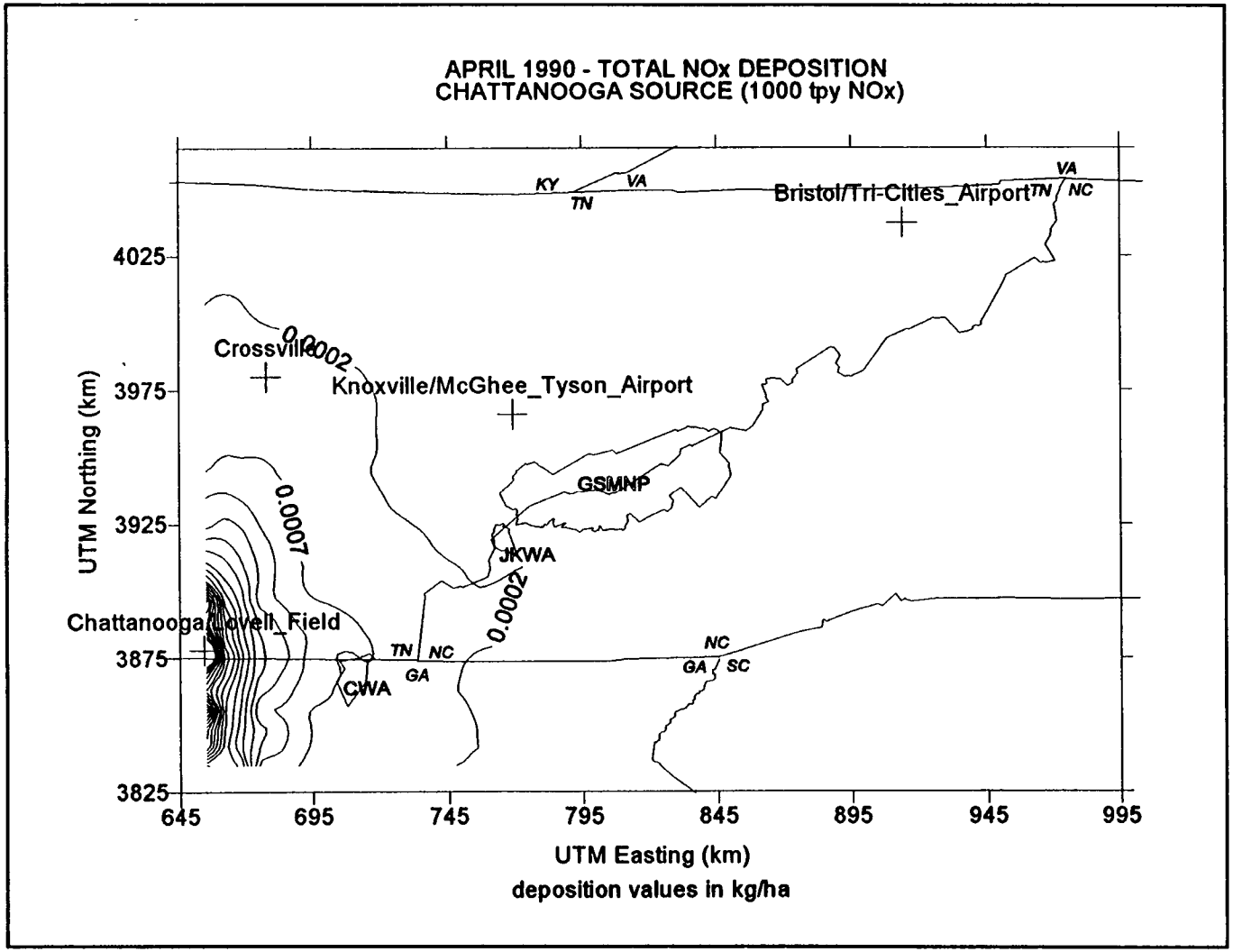

Fig. E.14. Total (wet+dry) NO_x deposition estimated for April 1990 resulting from a 28.8 g/s (1000 tpy) hypothetical NO_x emission source located at Chattanooga/Lovell Field.

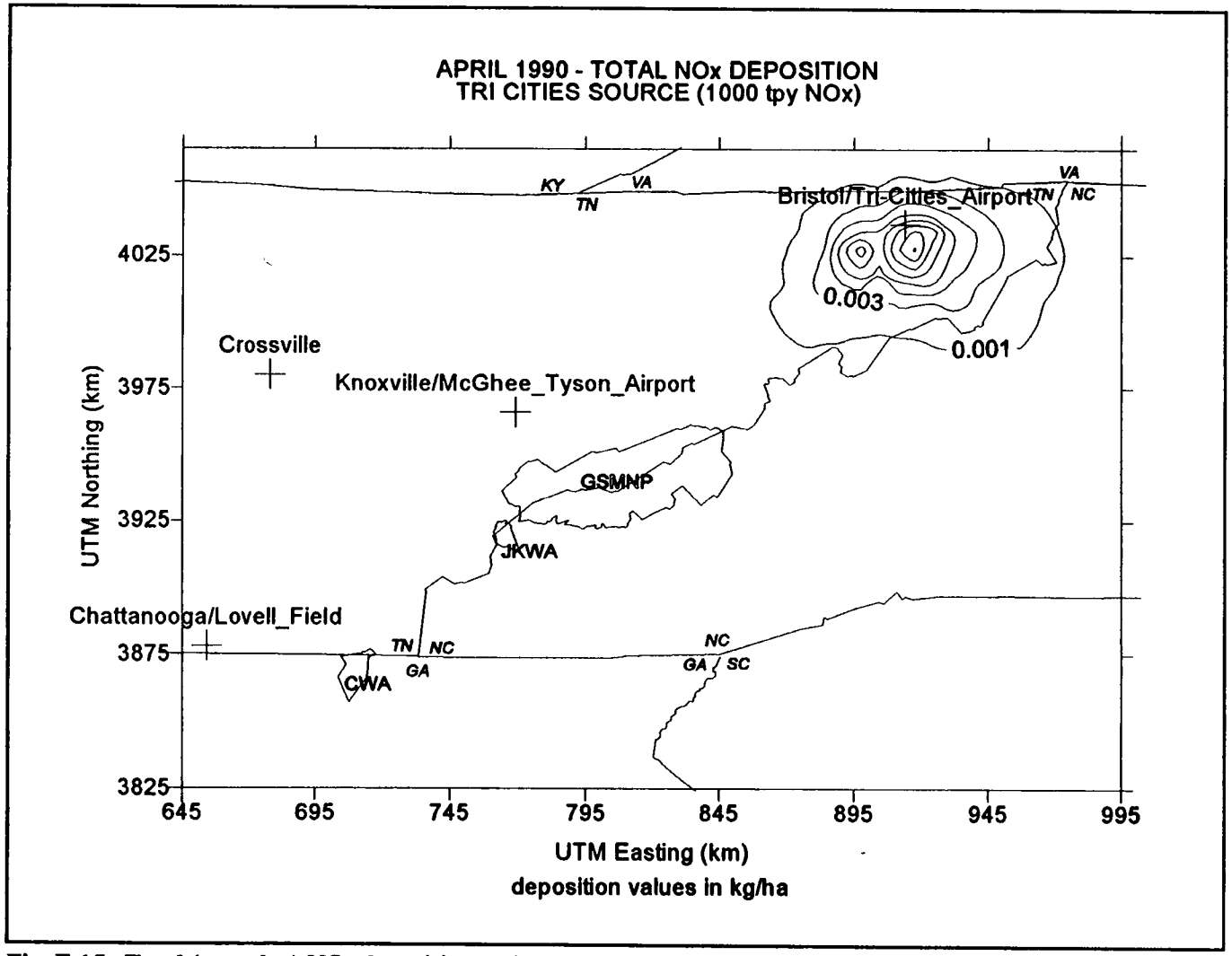

Fig. E.15. Total (wet+dry) NO_x deposition estimated for April 1990 resulting from a 28.8 g/s (1000 tpy) hypothetical NO_x emission source located at Bristol/Tri Cities Airport.

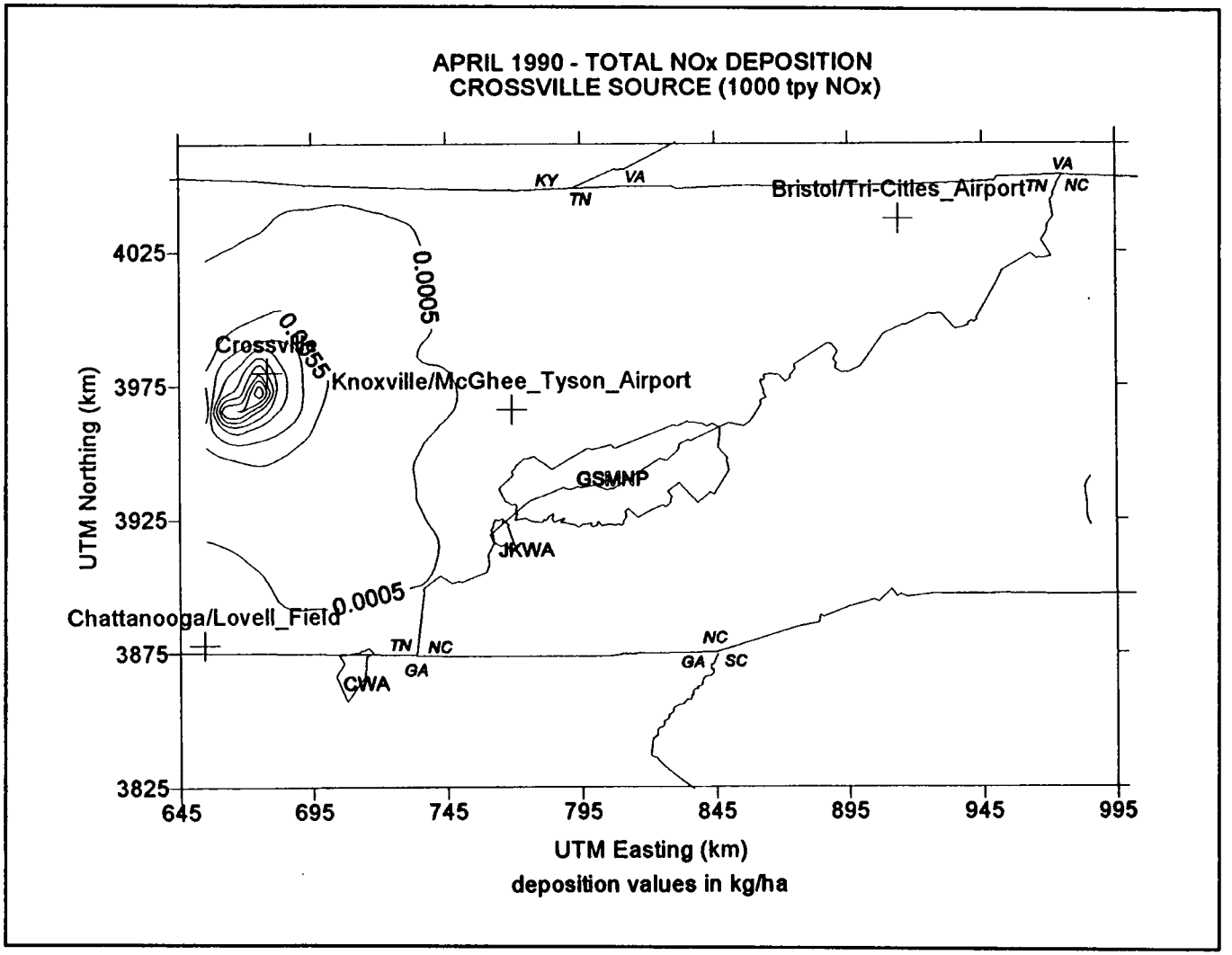

Fig. E.16. Total (wet+dry) NO_x deposition estimated for April 1990 resulting from a 28.8 g/s (1000 tpy) hypothetical NO_x emission source located in Crossville.

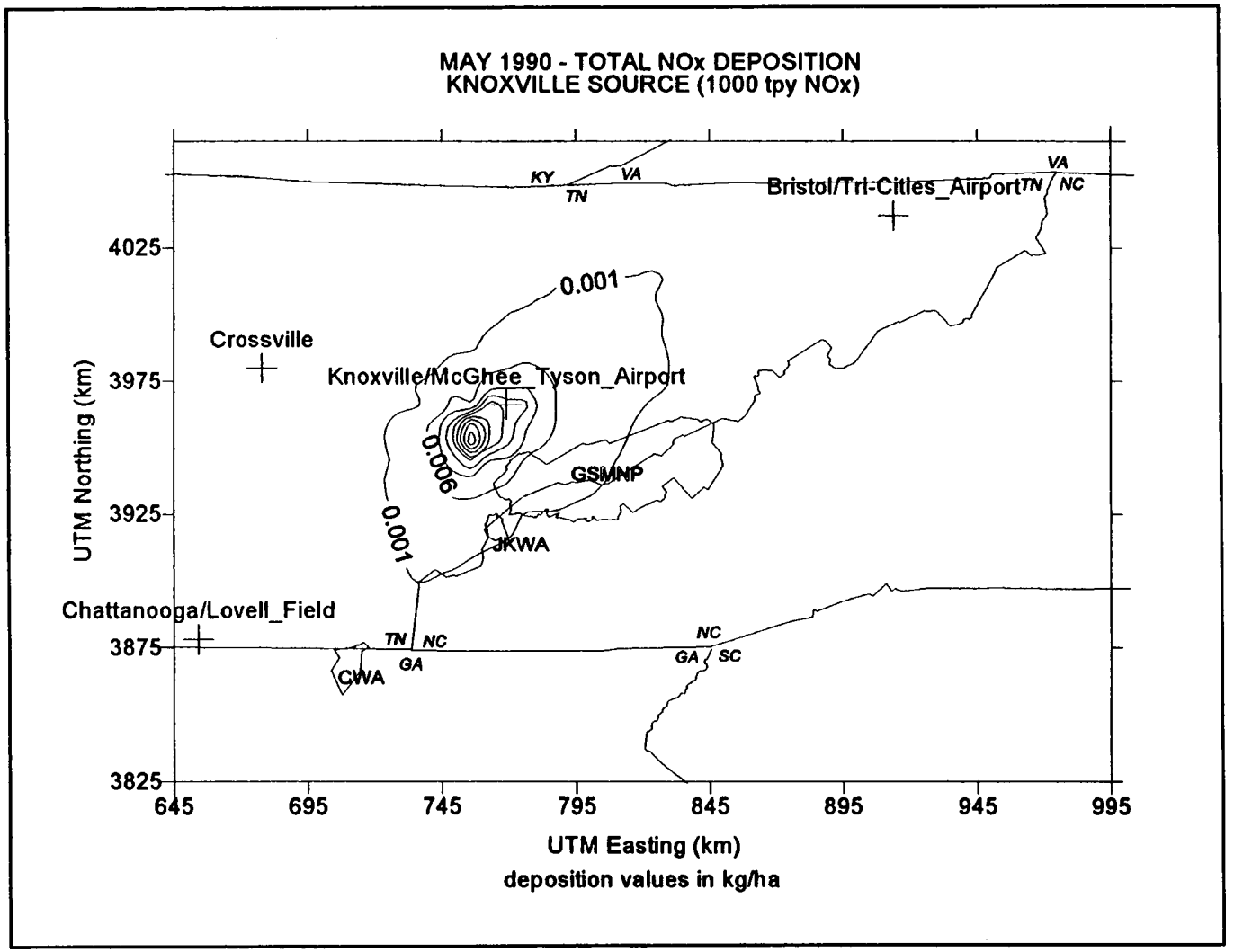

Fig. E.17. Total (wet+dry) NO_x deposition estimated for May 1990 resulting from a 28.8 g/s (1000 tpy) hypothetical NO_x emission source located at Knoxville /McGhee Tyson Airport.

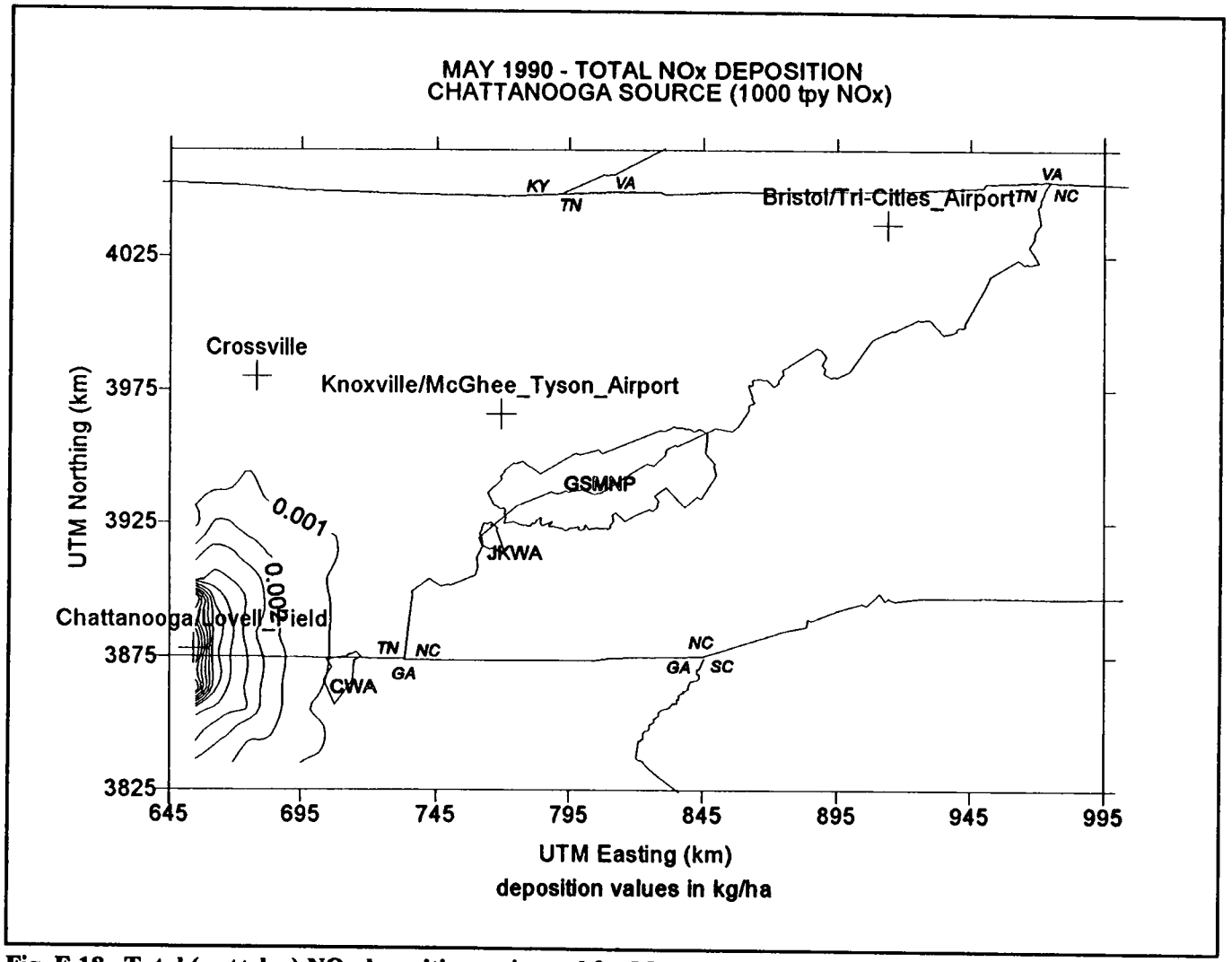

Fig. E.18. Total (wet+dry) NO_x deposition estimated for May 1990 resulting from a 28.8 g/s (1000 tpy) hypothetical NO_x emission source located at Chattanooga/Lovell Field.

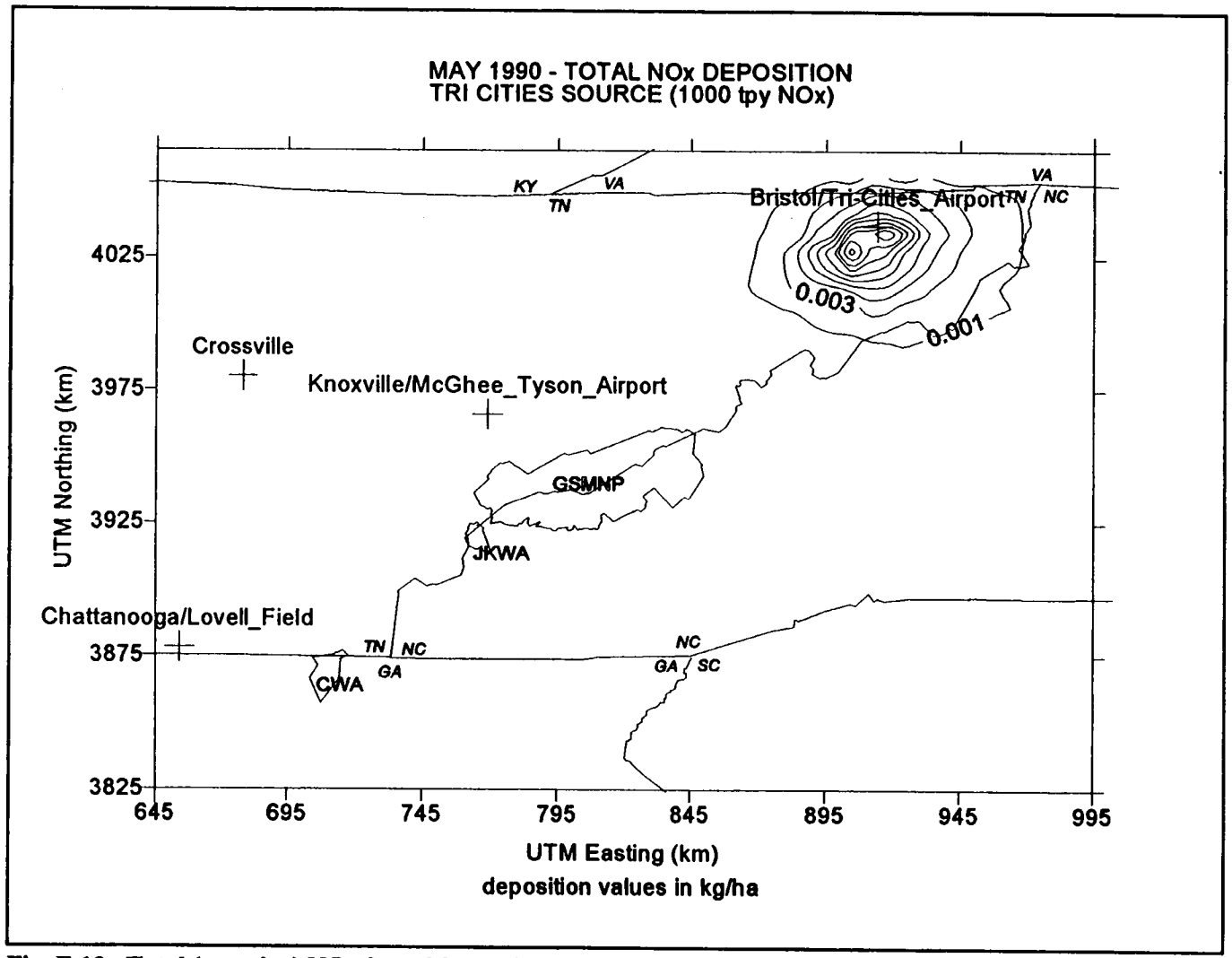

Fig. E.19. Total (wet+dry) NO_x deposition estimated for May 1990 resulting from a 28.8 g/s (1000 tpy) hypothetical NO_x emission source located at Bristol/Tri Cities Airport.

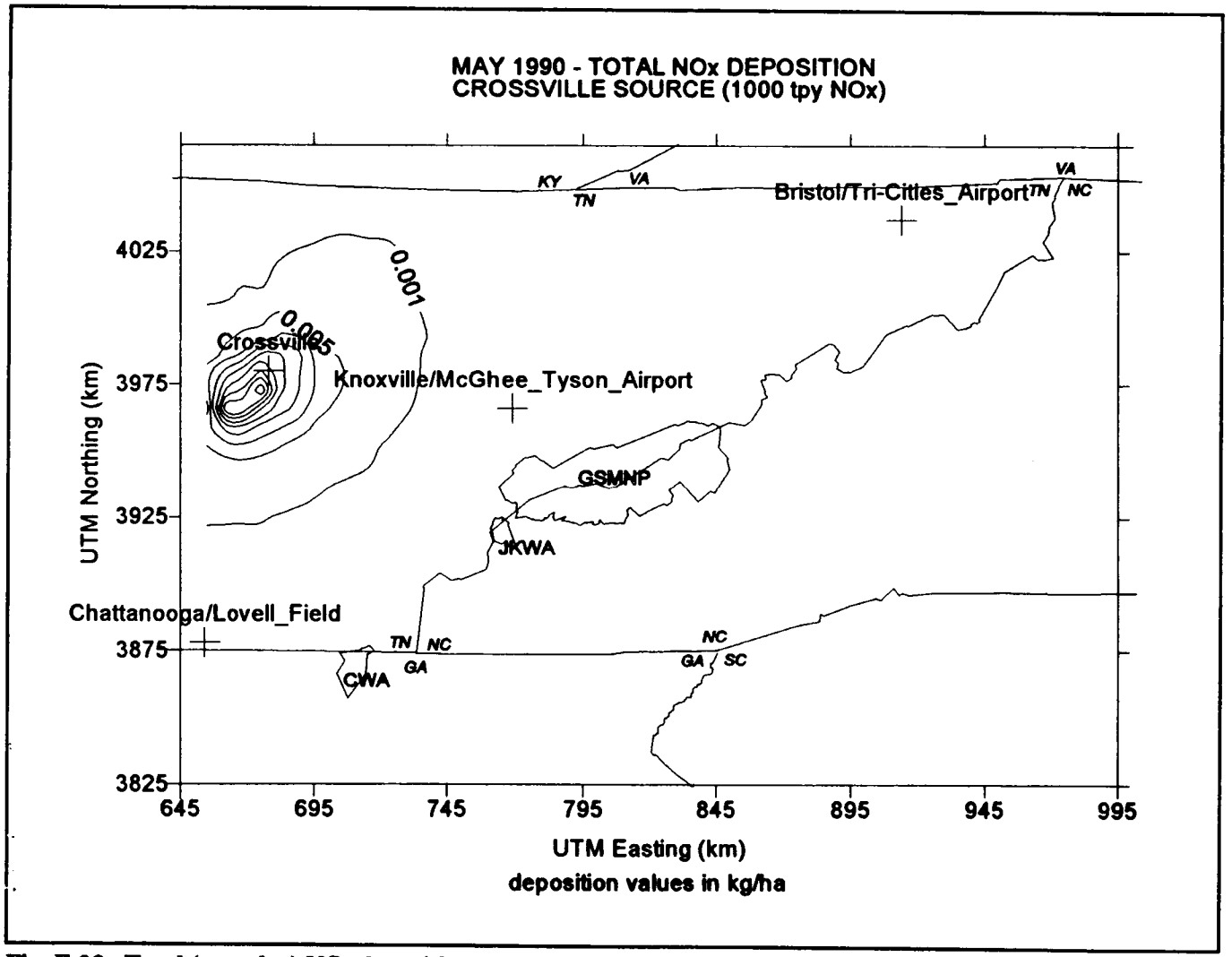

Fig. E.20. Total (wet+dry) NO_x deposition estimated for May 1990 resulting from a 28.8 g/s (1000 tpy) hypothetical NO_x emission source located in Crossville.

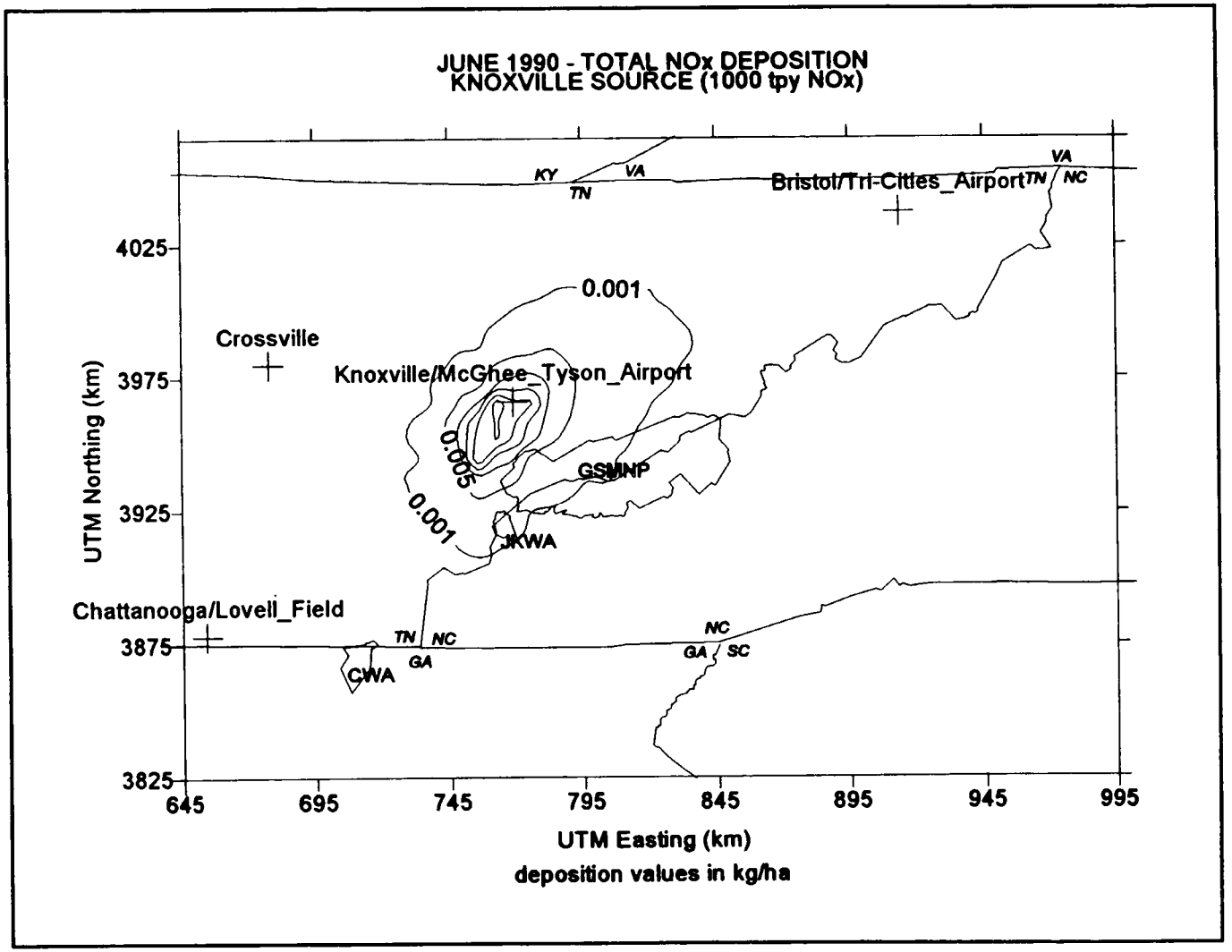

Fig. E.21. Total (wet+dry) NO_x deposition estimated for June 1990 resulting from a 28.8 g/s (1000 tpy) hypothetical NO_x emission source located at Knoxville /McGhee Tyson Airport.

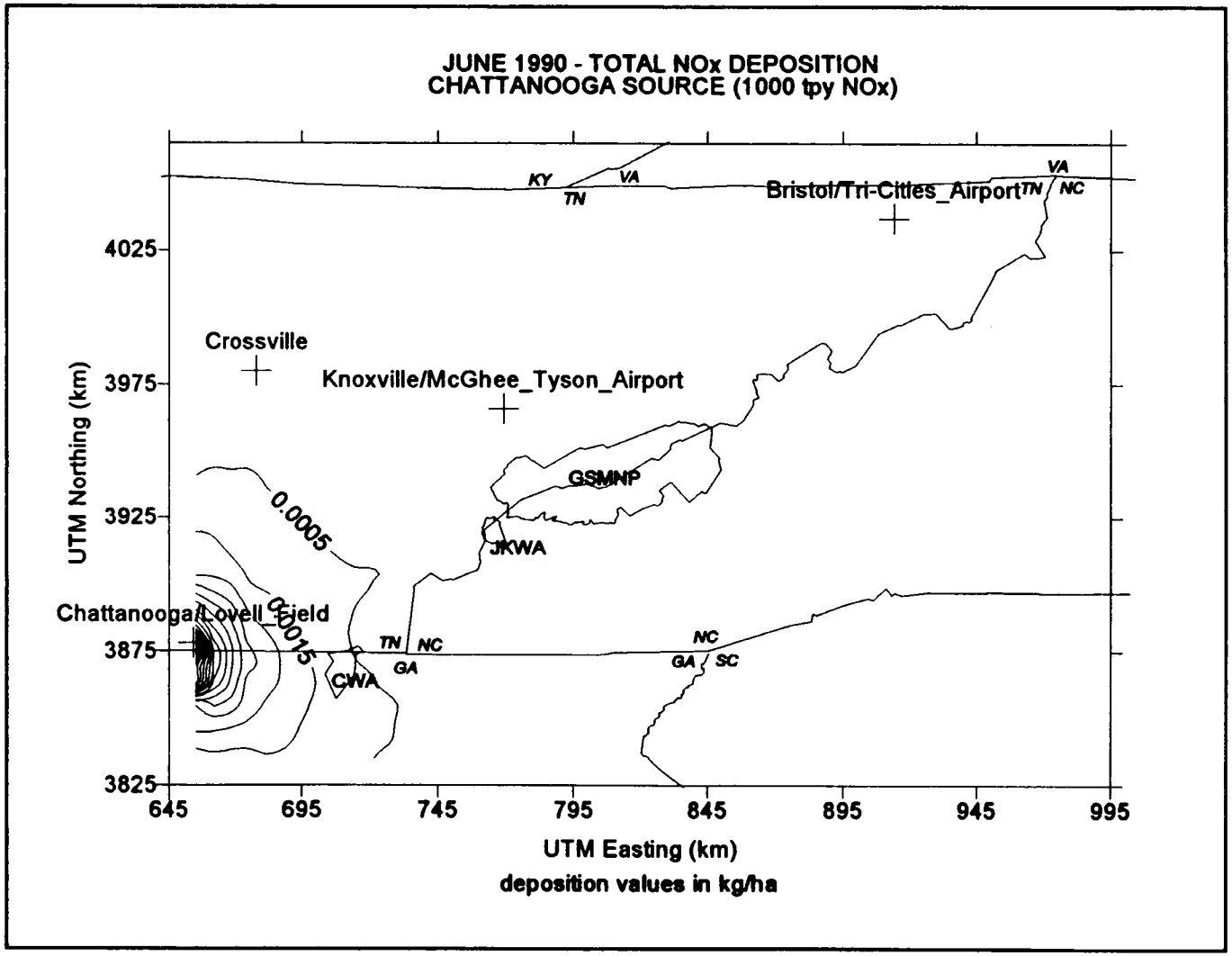

Fig. E.22. Total (wet+dry) NO_x deposition estimated for June 1990 resulting from a 28.8 g/s (1000 tpy) hypothetical NO_x emission source located at Chattanooga/Lovell Field.

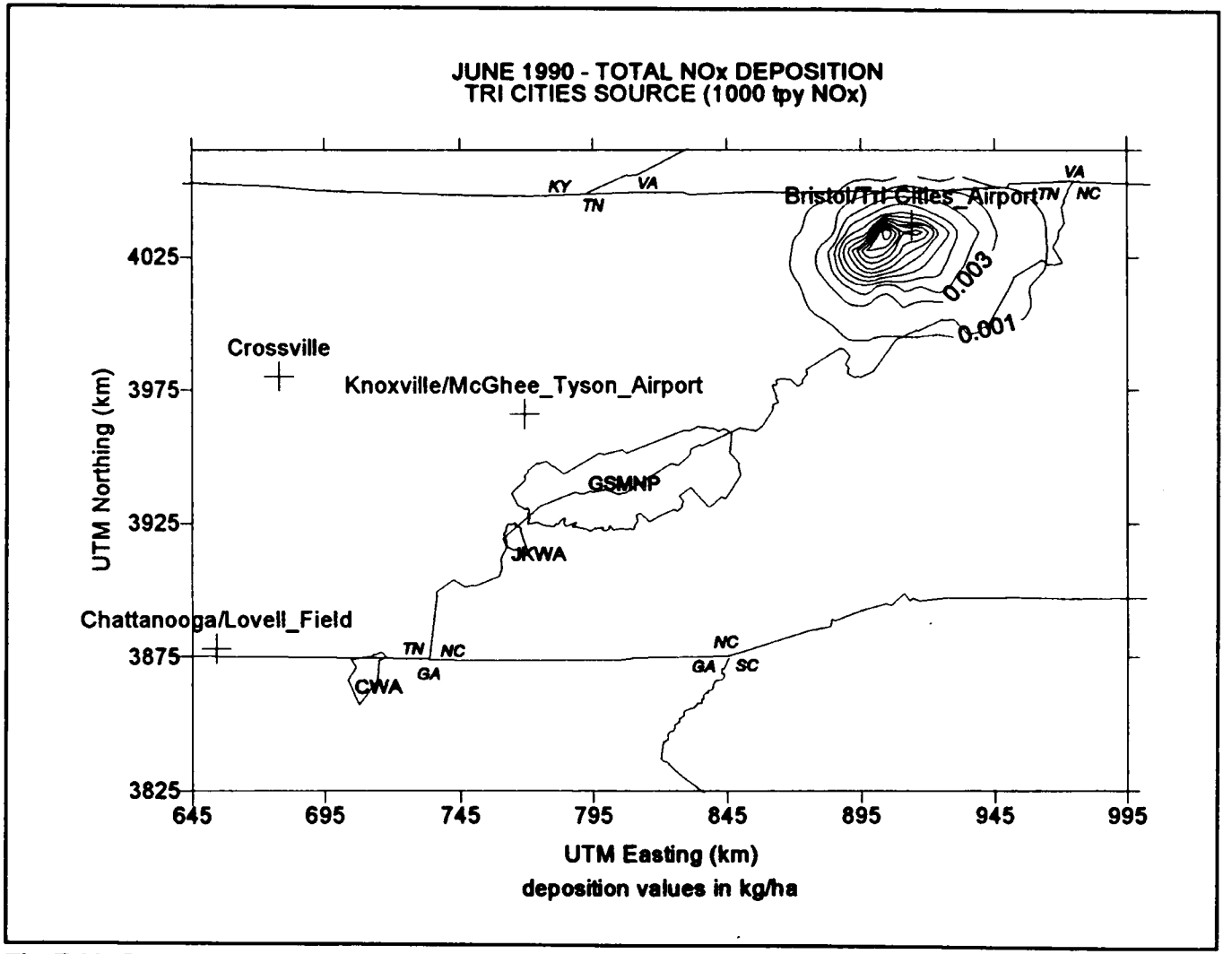

Fig. E.23. Total (wet+dry) NO_x deposition estimated for June 1990 resulting from a 28.8 g/s (1000 tpy) hypothetical NO_x emission source located at Bristol/Tri Cities Airport.

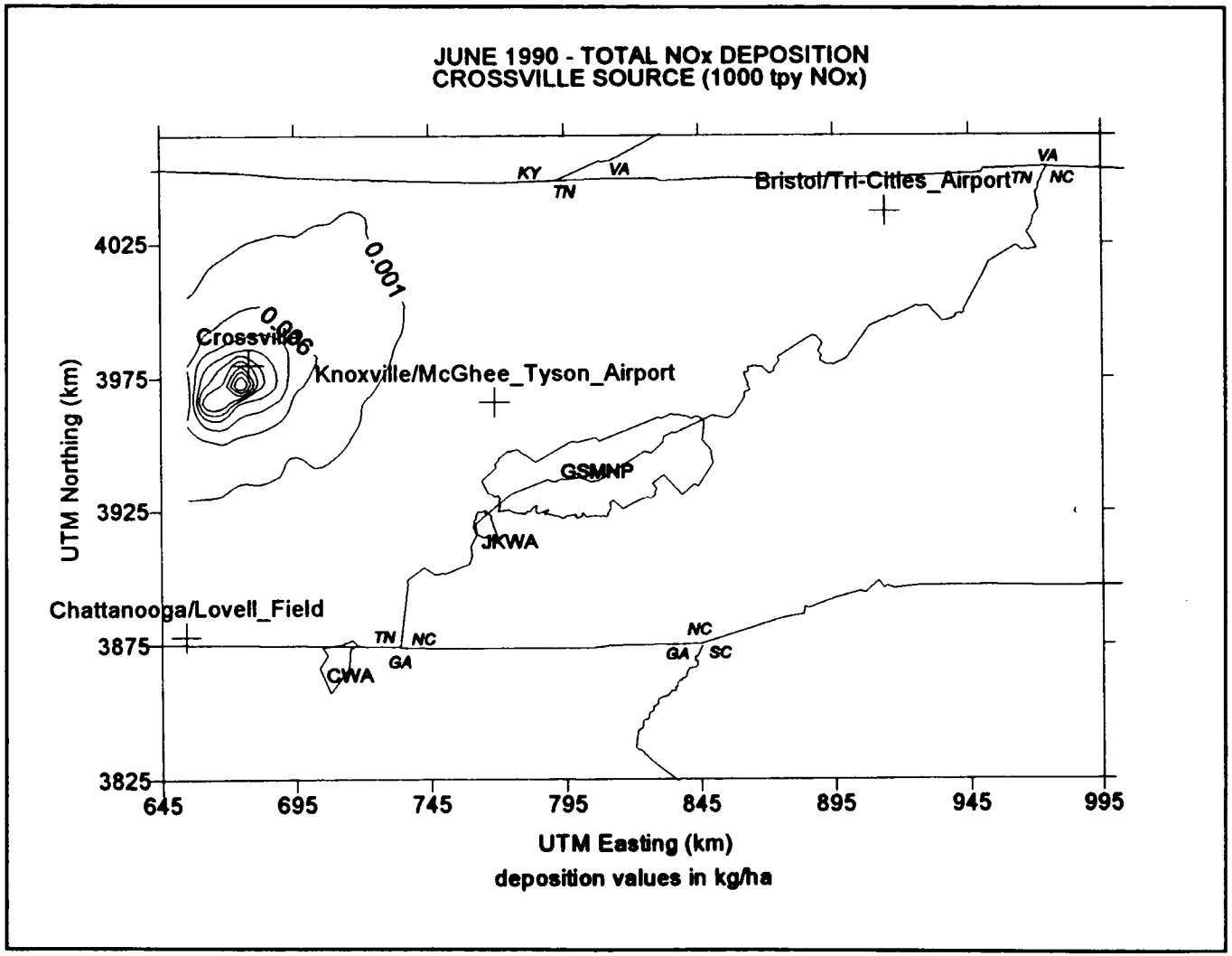

Fig. E.24. Total (wet+dry) NO_x deposition estimated for June 1990 resulting from a 28.8 g/s (1000 tpy) hypothetical NO_x emission source located in Crossville.

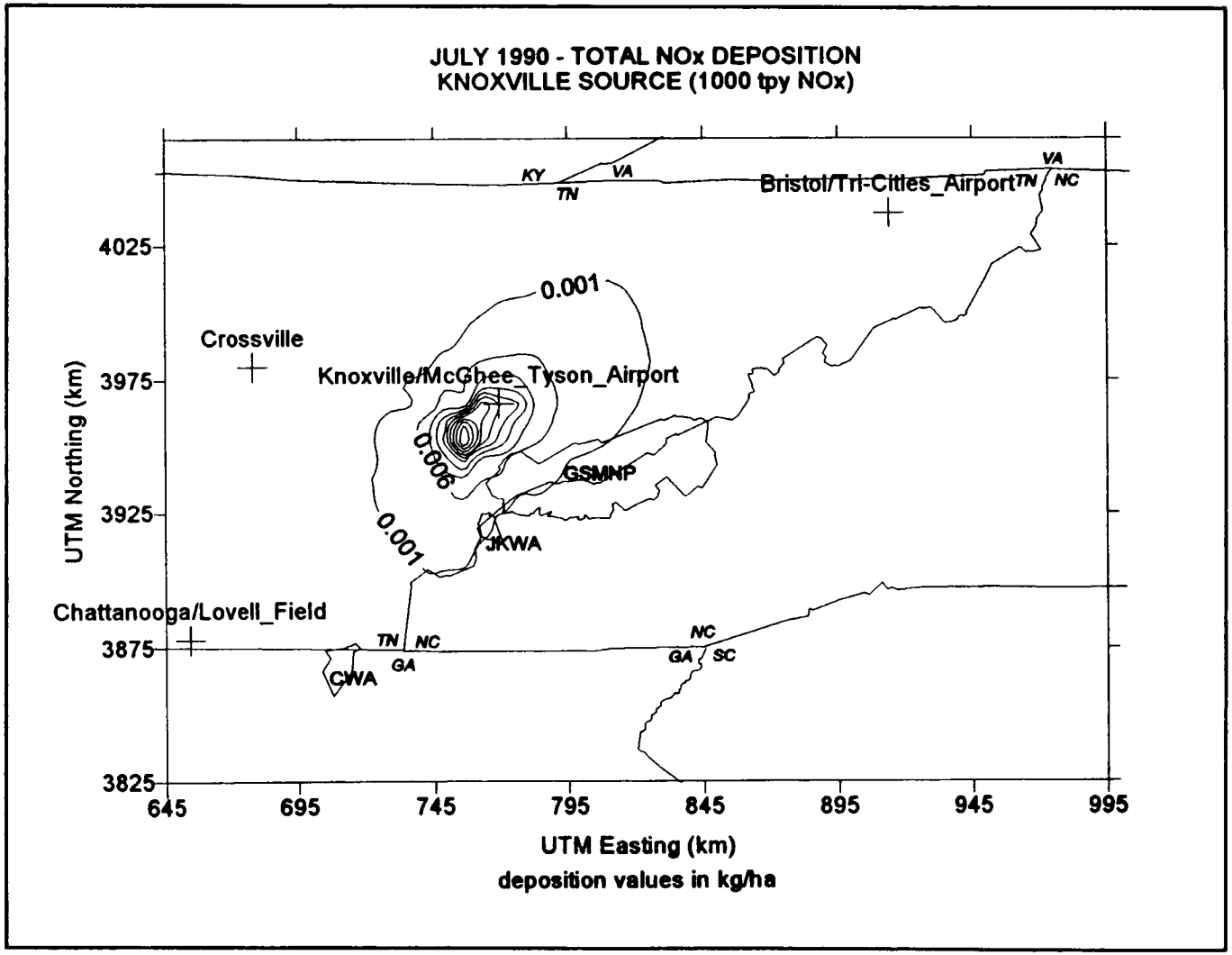

Fig. E.25. Total (wet+dry) NO_x deposition estimated for July 1990 resulting from a 28.8 g/s (1000 tpy) hypothetical NO_x emission source located at Knoxville /McGhee Tyson Airport.

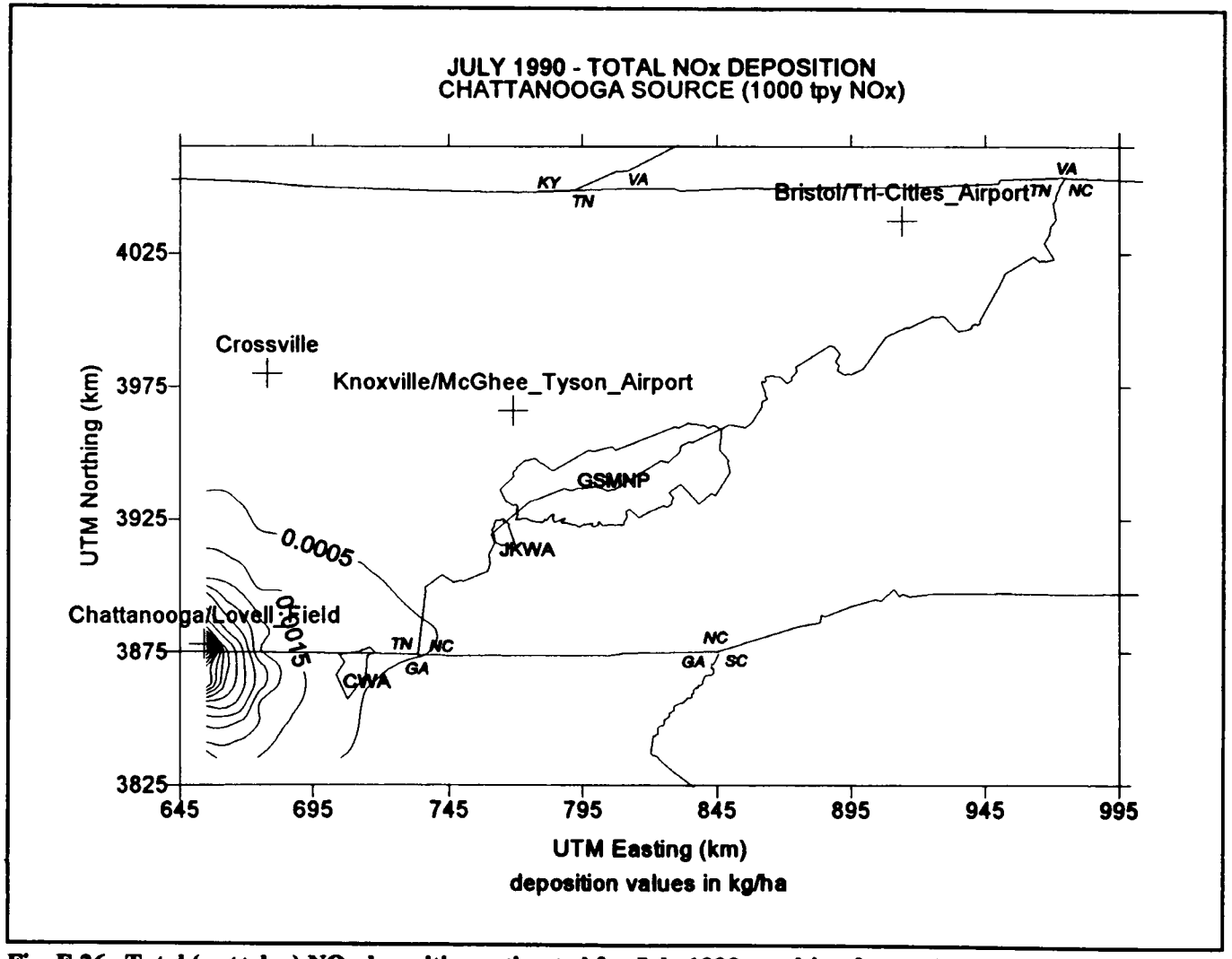

Fig. E.26. Total (wet+dry) NO_x deposition estimated for July 1990 resulting from a 28.8 g/s (1000 tpy) hypothetical NO_x emission source located at Chattanooga/Lovell Field.

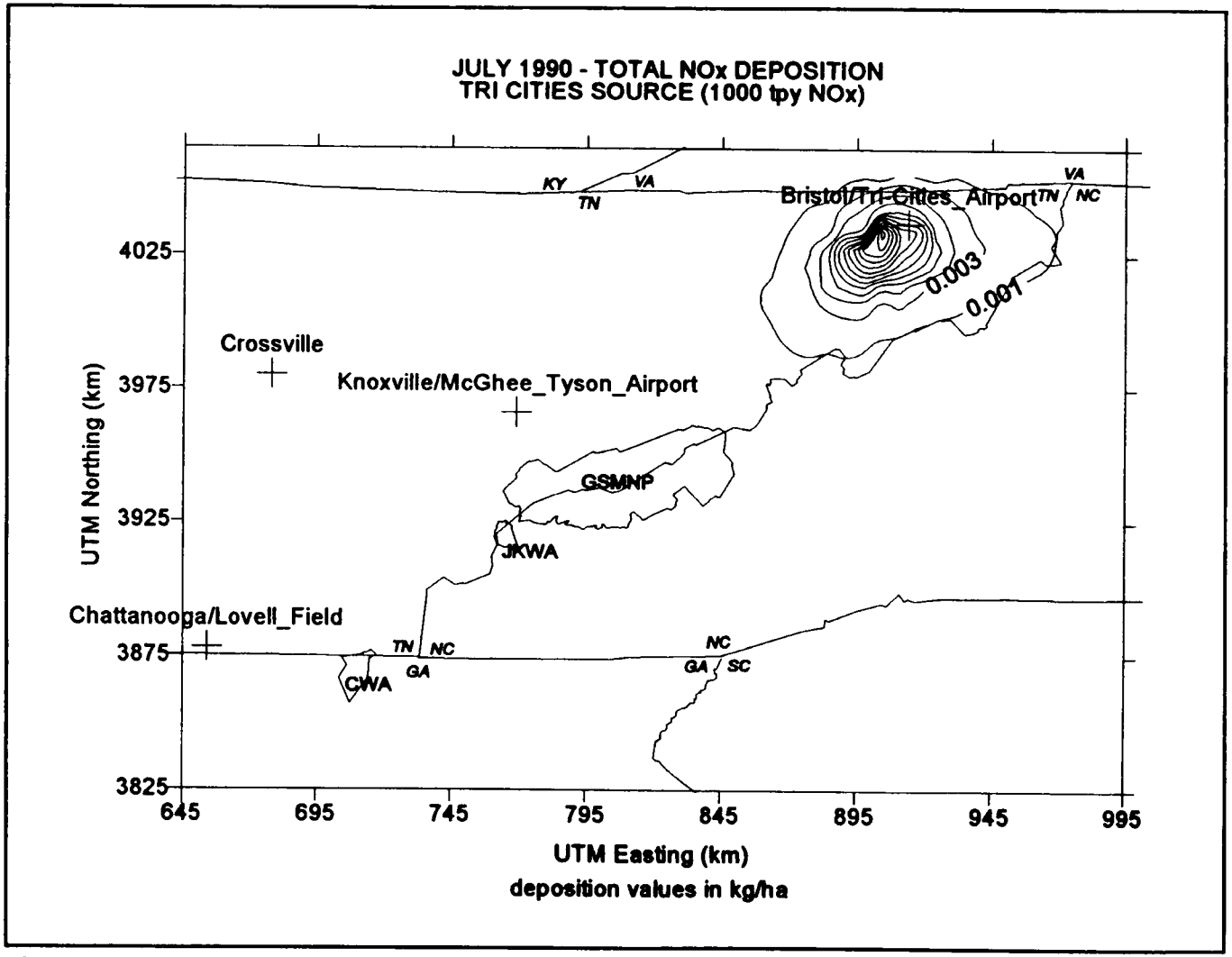

Fig. E.27. Total (wet+dry) NO_x deposition estimated for July 1990 resulting from a 28.8 g/s (1000 tpy) hypothetical NO_x emission source located at Bristol/Tri Cities Airport.

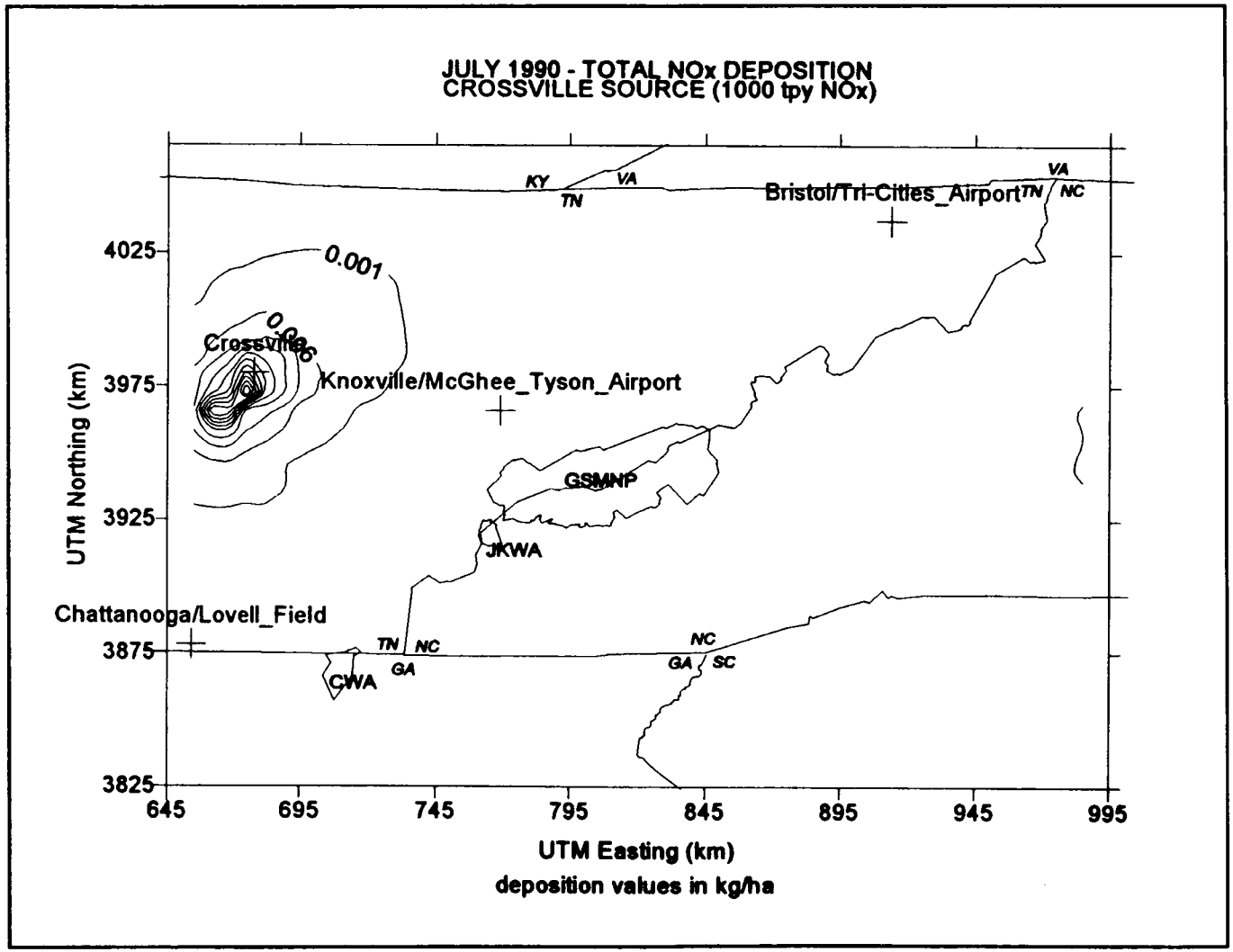

Fig. E.28. Total (wet+dry) NO_x deposition estimated for July 1990 resulting from a 28.8 g/s (1000 tpy) hypothetical NO_x emission source located in Crossville.

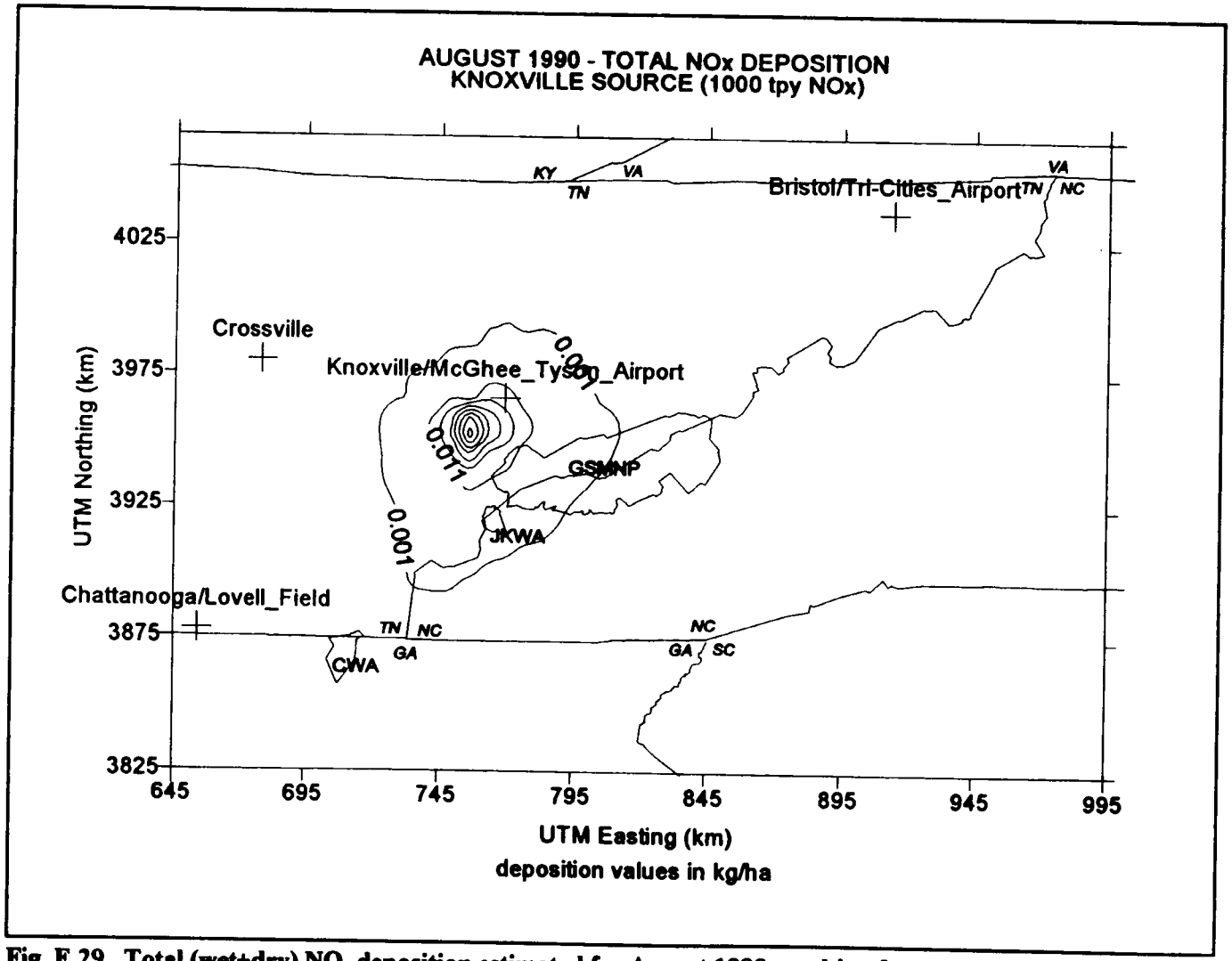

Fig. E.29. Total (wet+dry) NO_x deposition estimated for August 1990 resulting from a 28.8 g/s (1000 tpy) hypothetical NO_x emission source located at Knoxville /McGhee Tyson Airport.

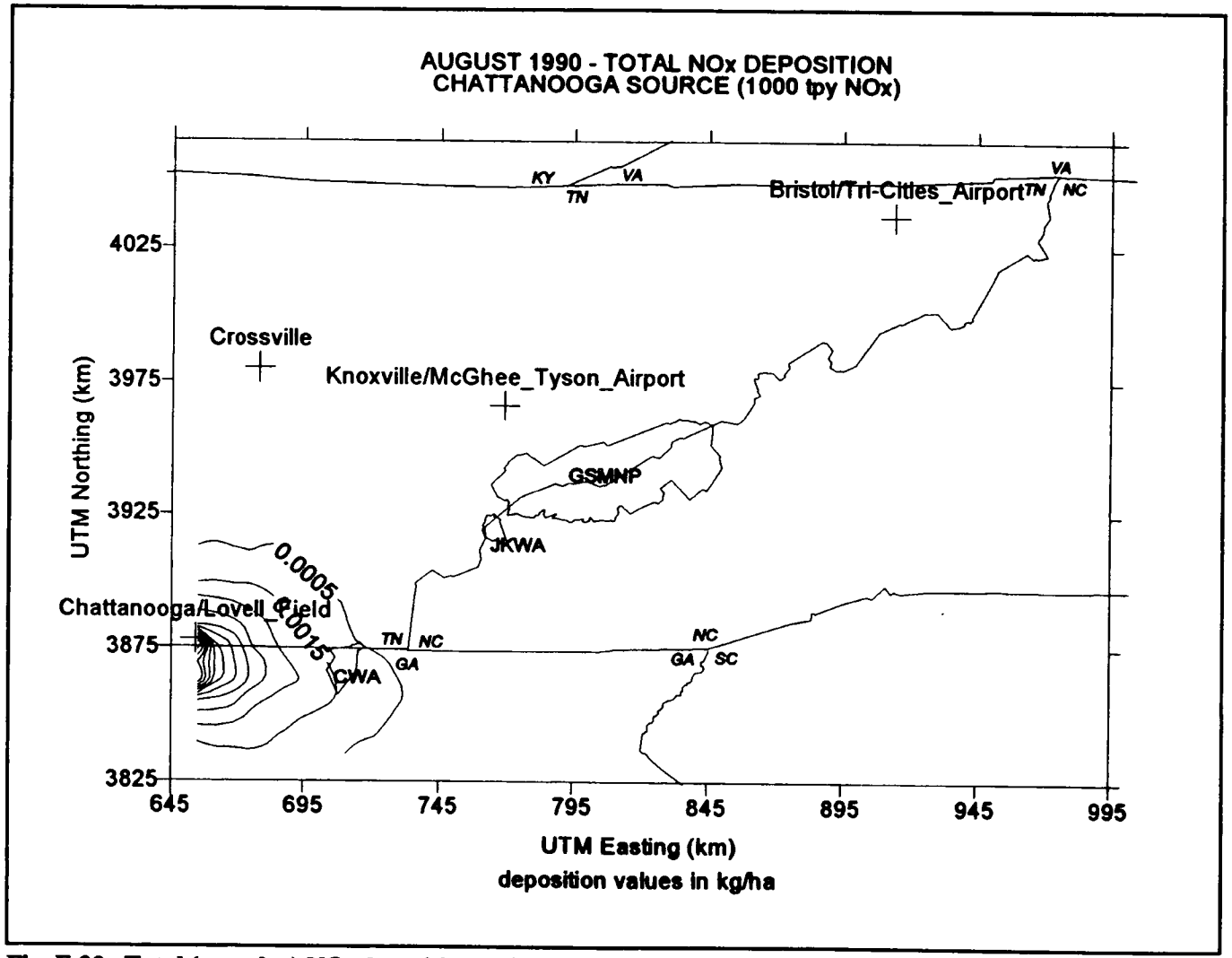

Fig. E.30. Total (wet+dry) NO_x deposition estimated for August 1990 resulting from a 28.8 g/s (1000 tpy) hypothetical NO_x emission source located at Chattanooga/Lovell Field.

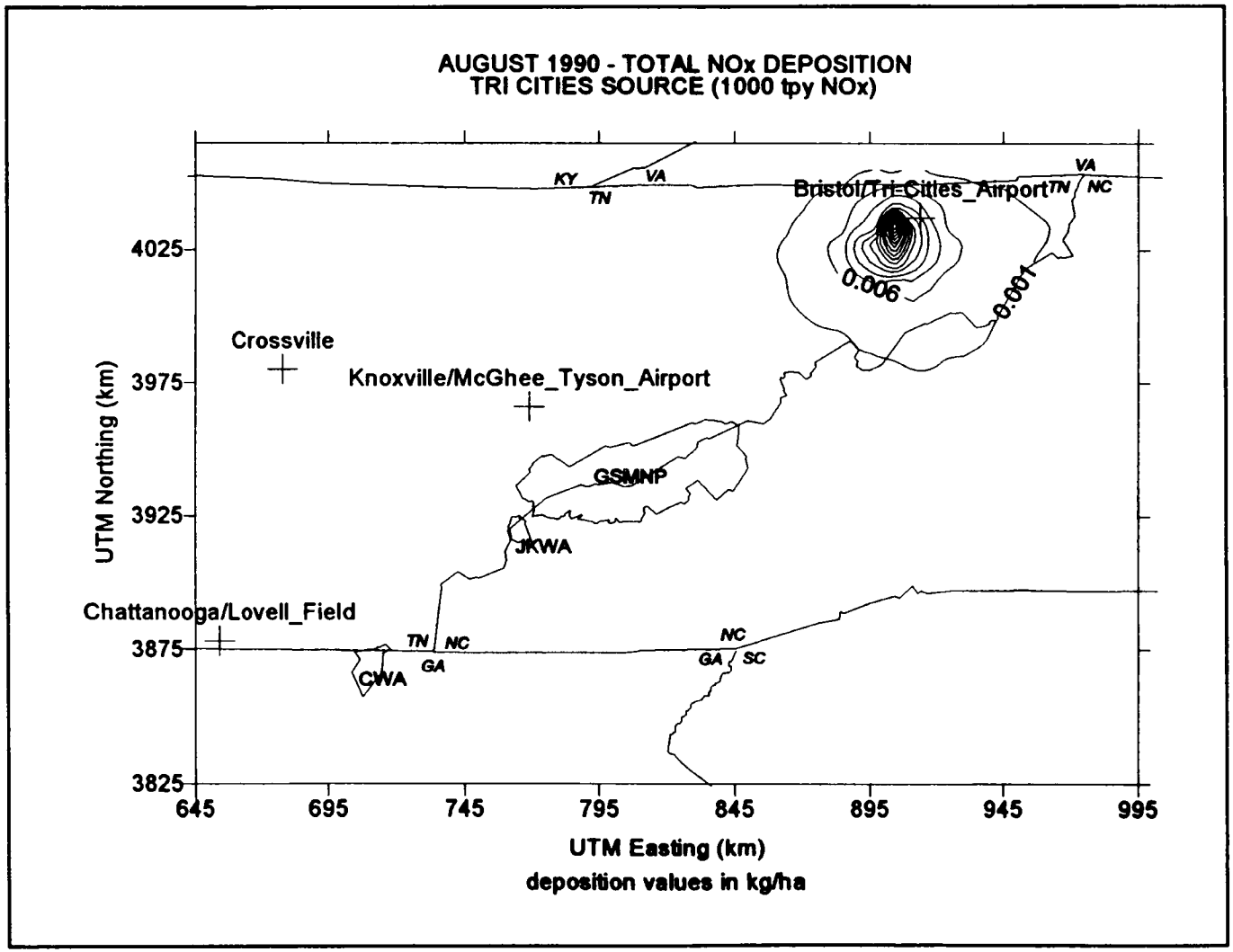

Fig. E.31. Total (wet+dry) NO_x deposition estimated for August 1990 resulting from a 28.8 g/s (1000 tpy) hypothetical NO_x emission source located at Bristol/Tri Cities Airport.

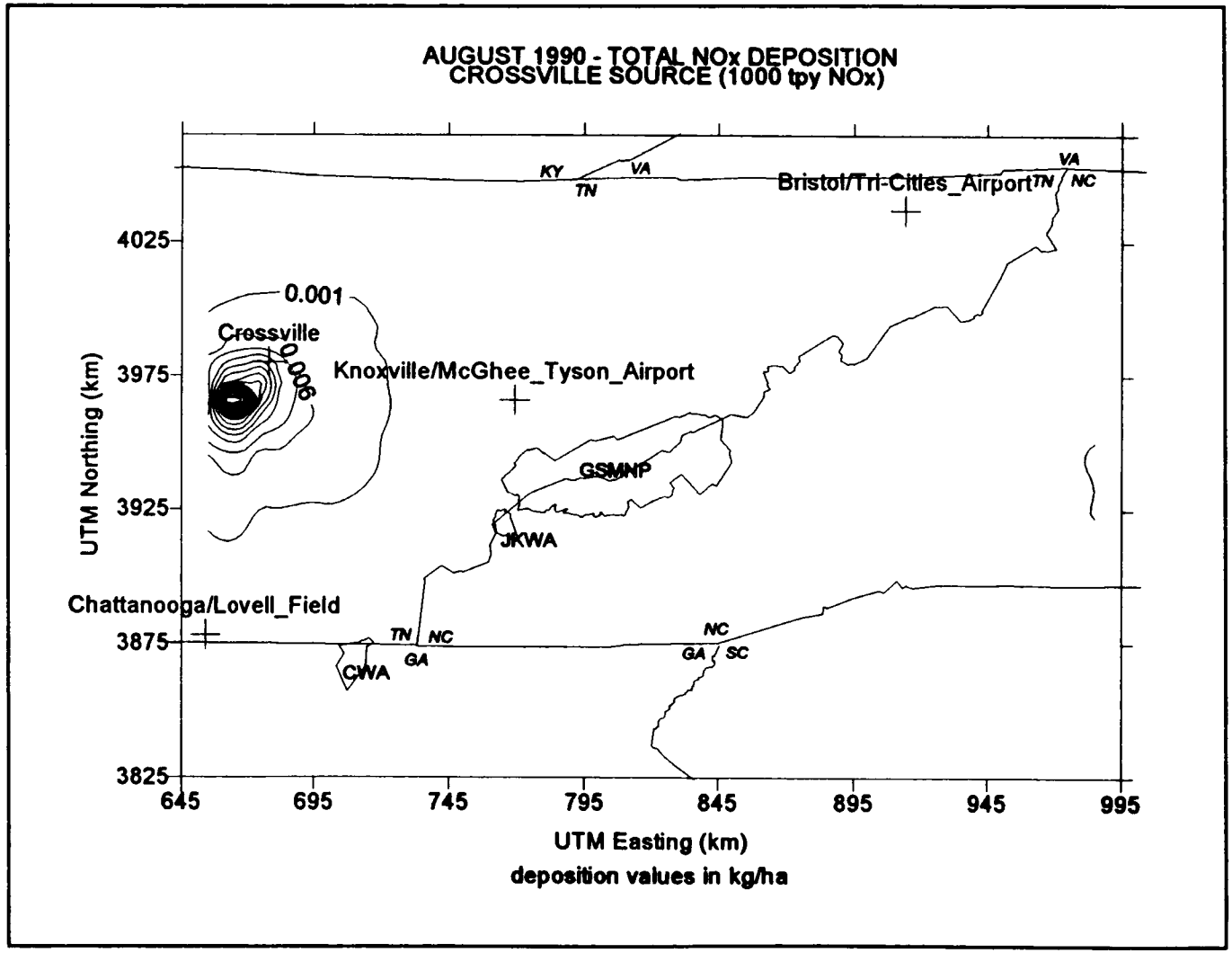

Fig. E.32. Total (wet+dry) NO_x deposition estimated for August 1990 resulting from a 28.8 g/s (1000 tpy) hypothetical NO_x emission source located in Crossville.

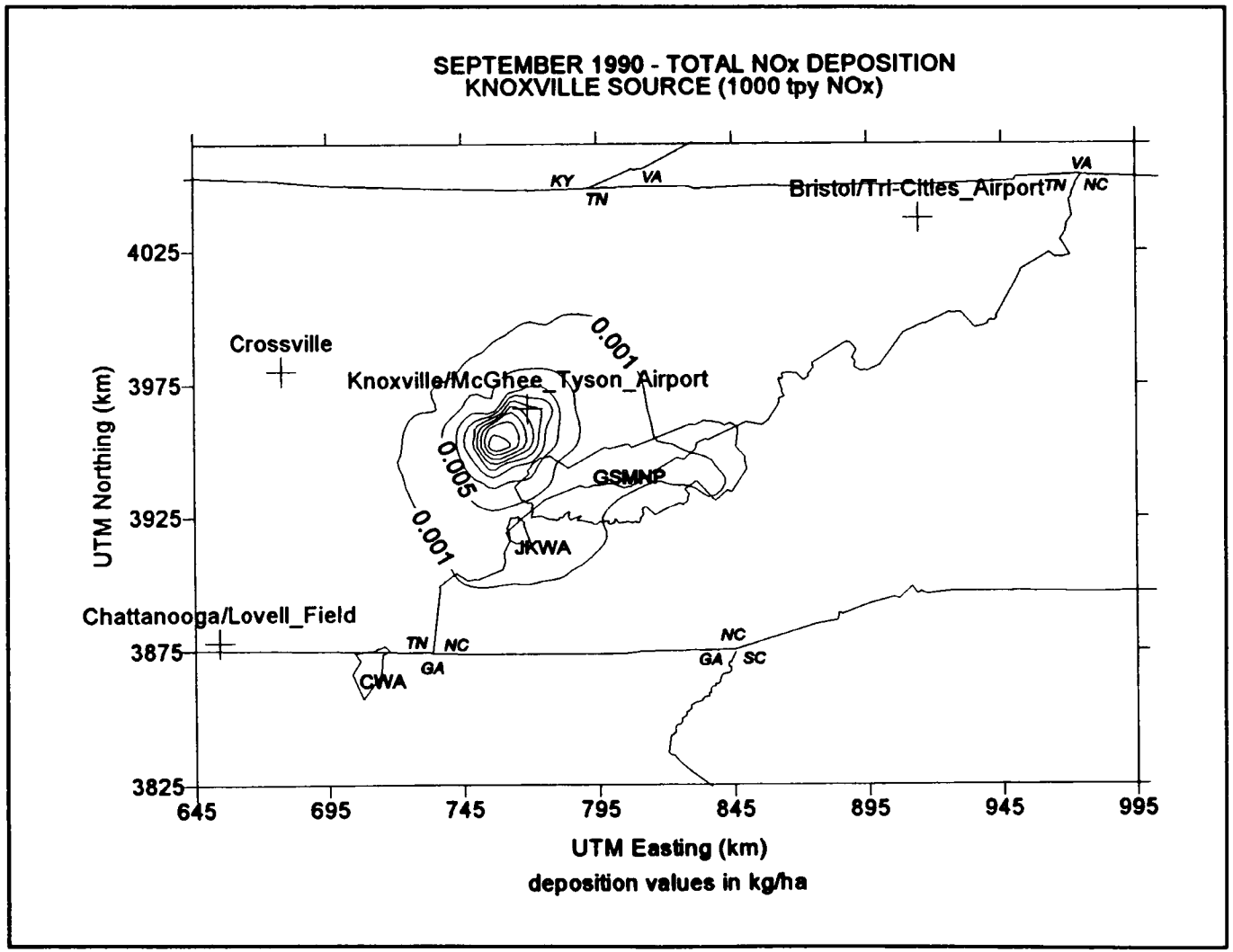

Fig. E.33. Total (wet+dry) NO_x deposition estimated for September 1990 resulting from a 28.8 g/s (1000 tpy) hypothetical NO_x emission source located at Knoxville /McGhee Tyson Airport.

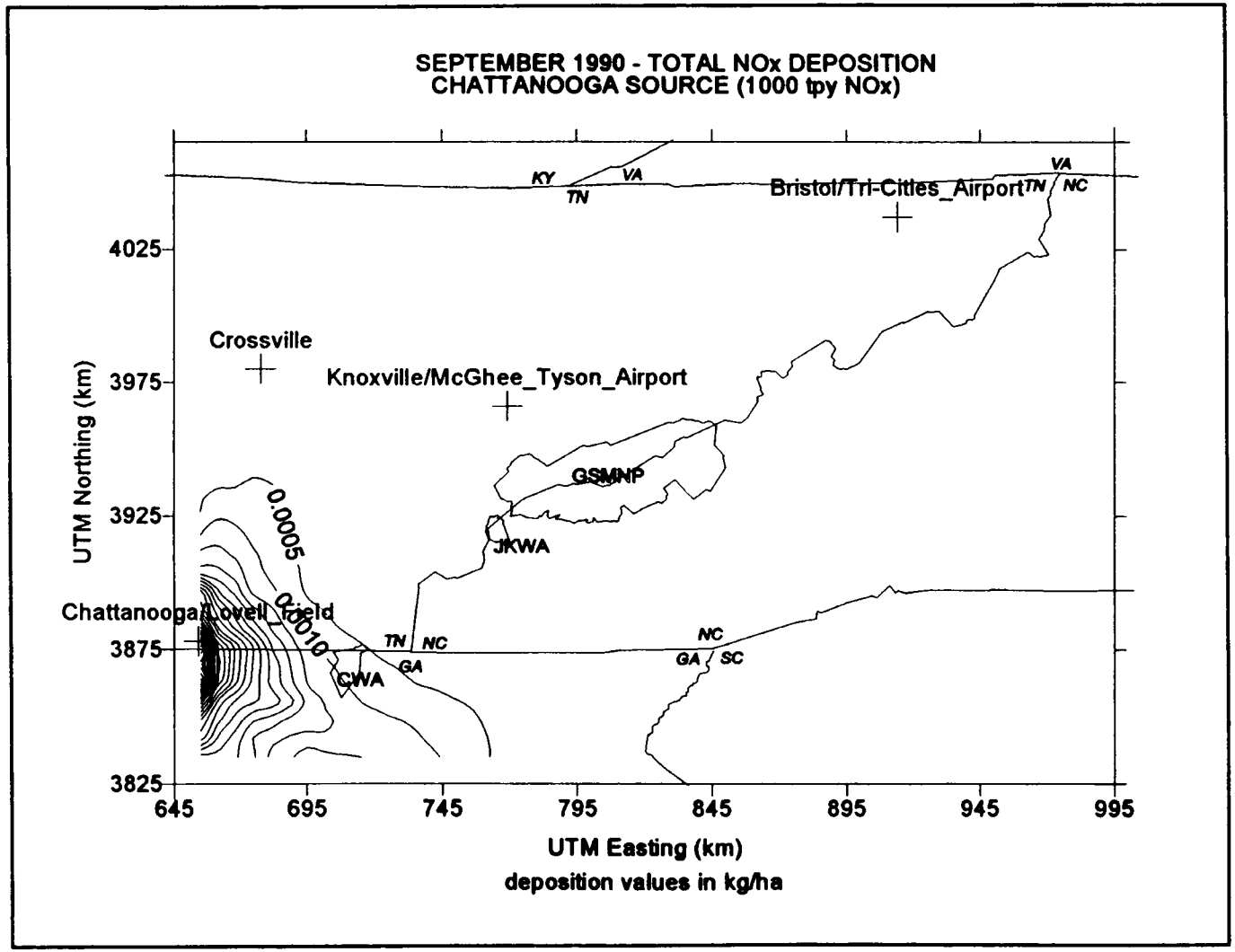

Fig. E.34. Total (wet+dry) NO_x deposition estimated for September 1990 resulting from a 28.8 g/s (1000 tpy) hypothetical NO_x emission source located at Chattanooga/Lovell Field.

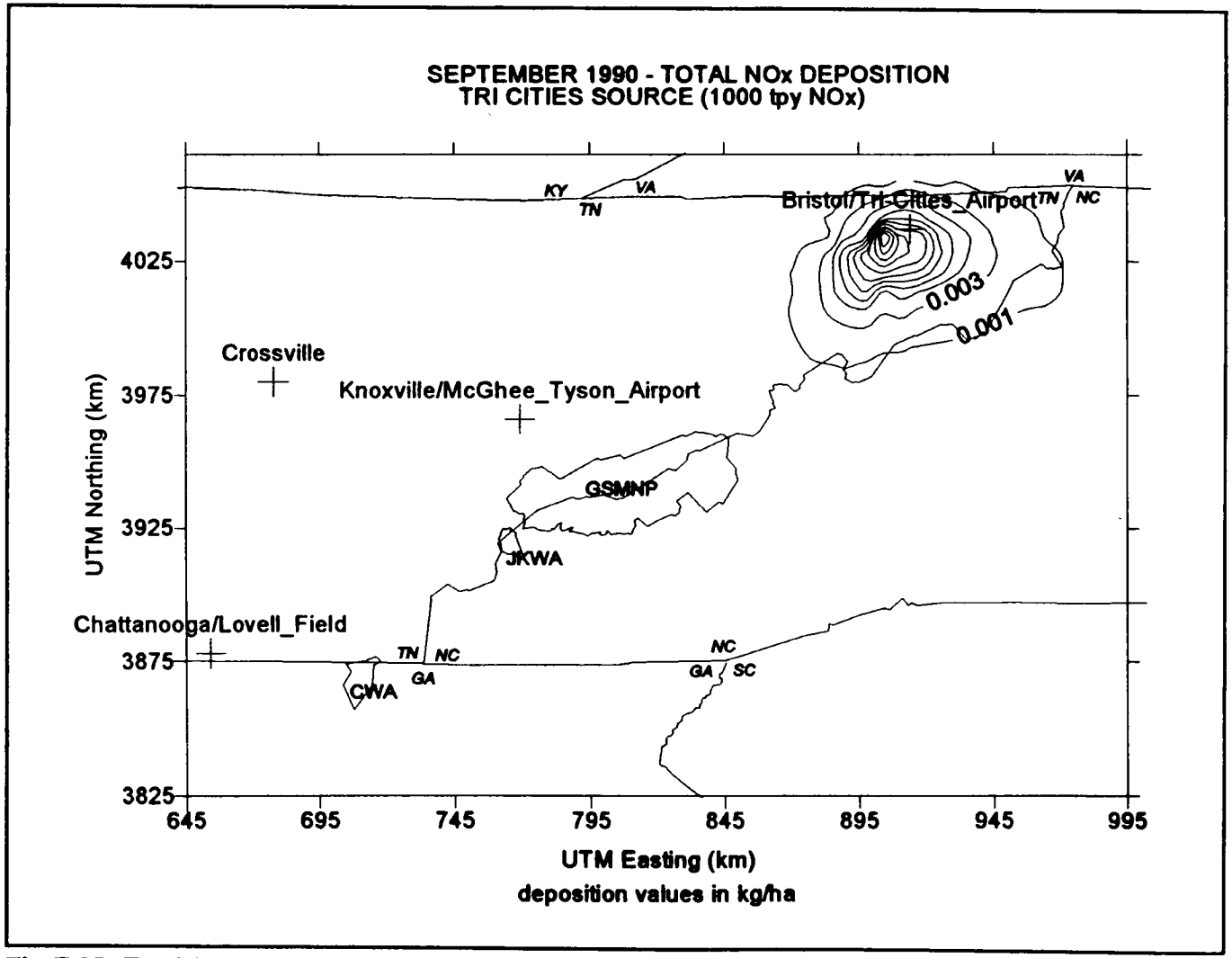

Fig. E.35. Total (wet+dry) NO_x deposition estimated for September 1990 resulting from a 28.8 g/s (1000 tpy) hypothetical NO_x emission source located at Bristol/Tri Cities Airport.

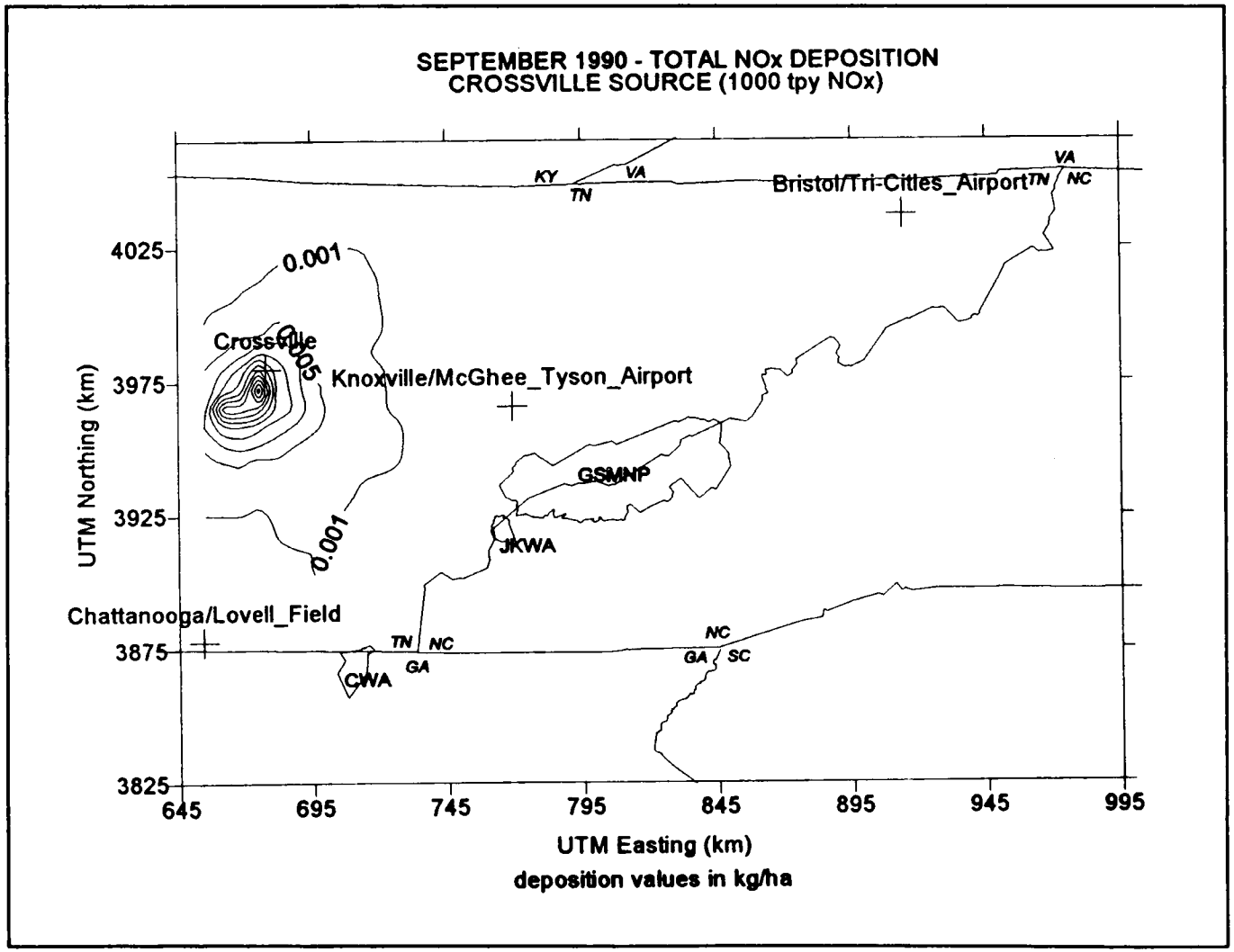

Fig. E.36. Total (wet+dry) NO_x deposition estimated for September 1990 resulting from a 28.8 g/s (1000 tpy) hypothetical NO_x emission source located in Crossville.

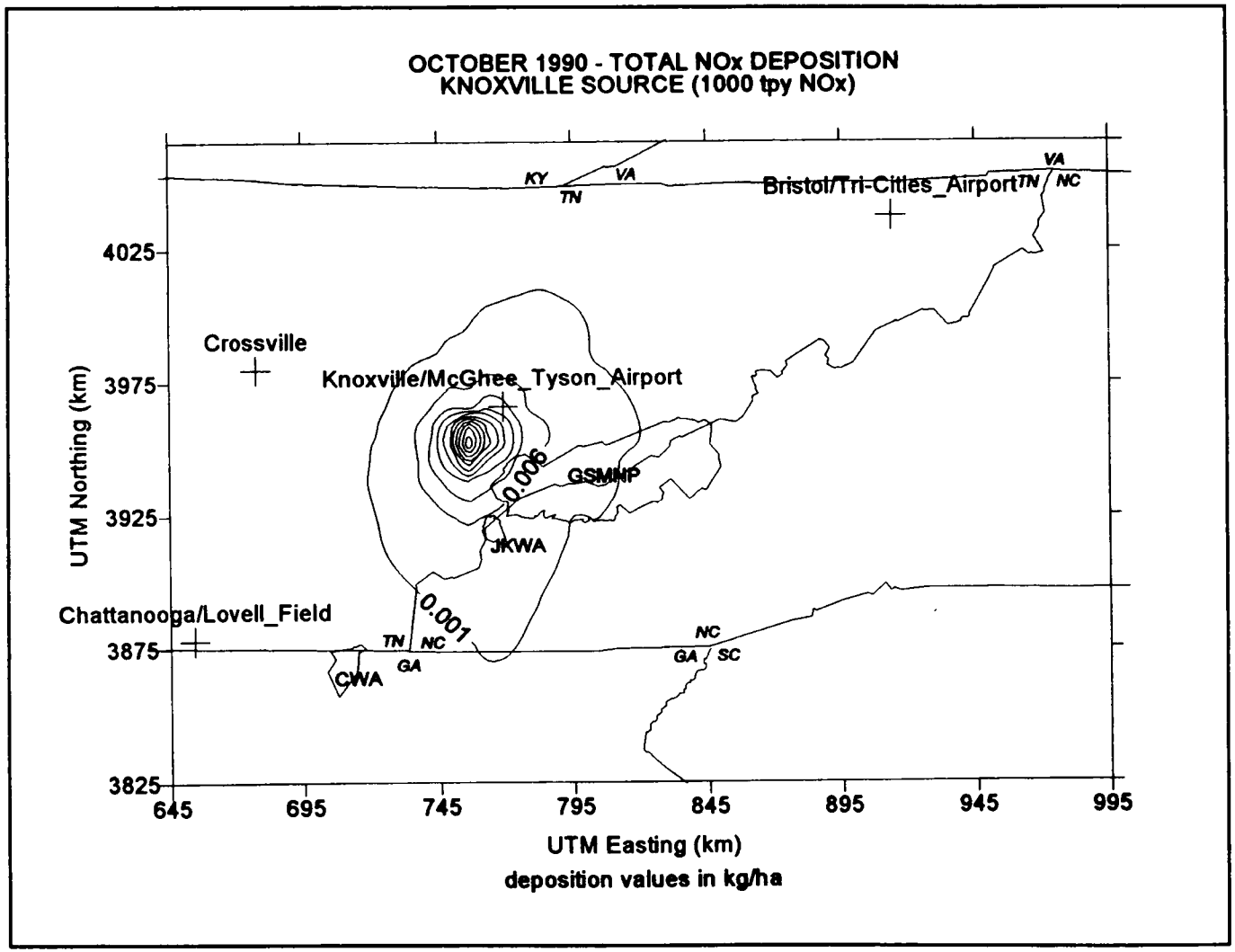

Fig. E.37. Total (wet+dry) NO_x deposition estimated for October 1990 resulting from a 28.8 g/s (1000 tpy) hypothetical NO_x emission source located at Knoxville /McGhee Tyson Airport.

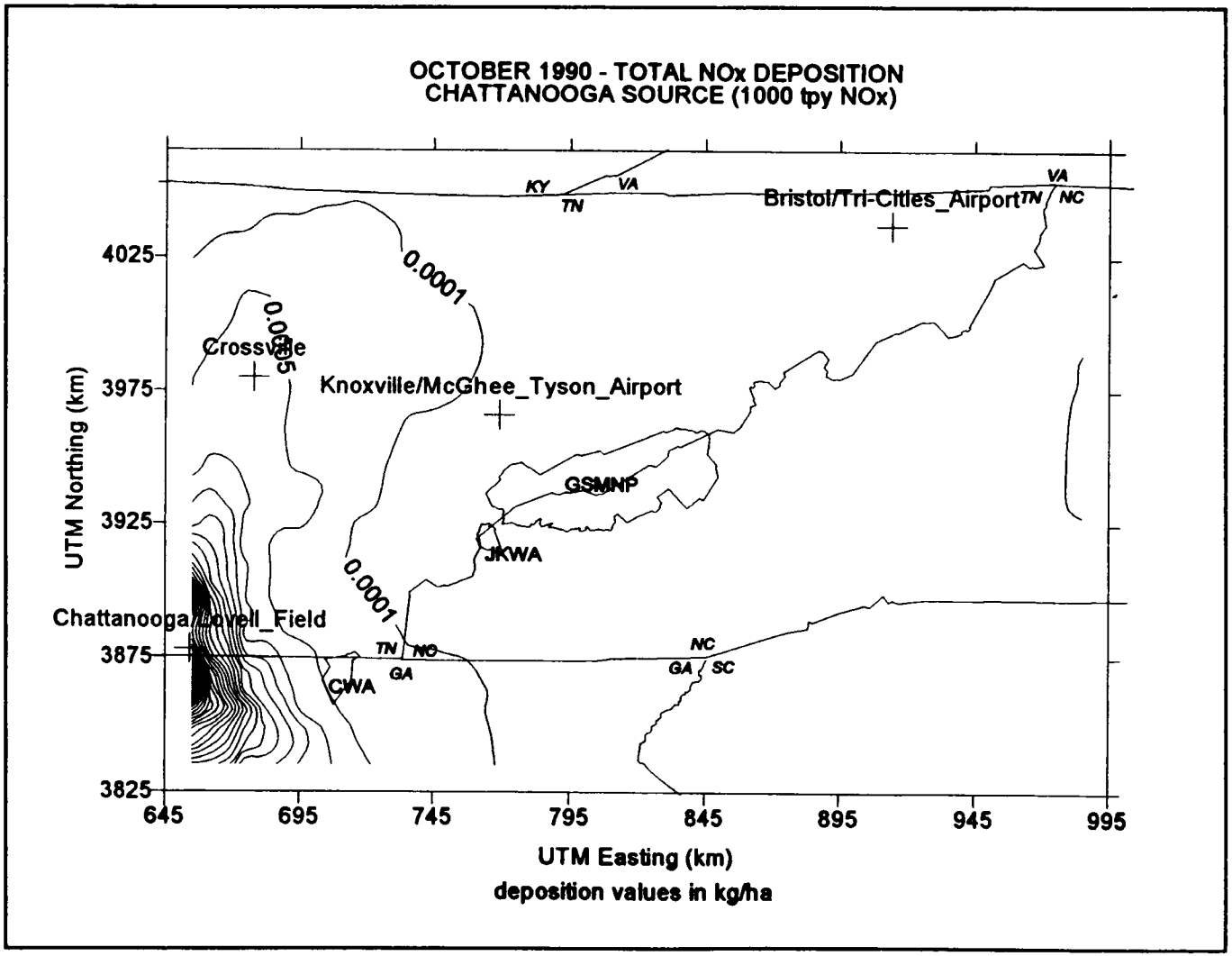

Fig. E.38. Total (wet+dry) NO_x deposition estimated for October 1990 resulting from a 28.8 g/s (1000 tpy) hypothetical NO_x emission source located at Chattanooga/Lovell Field.

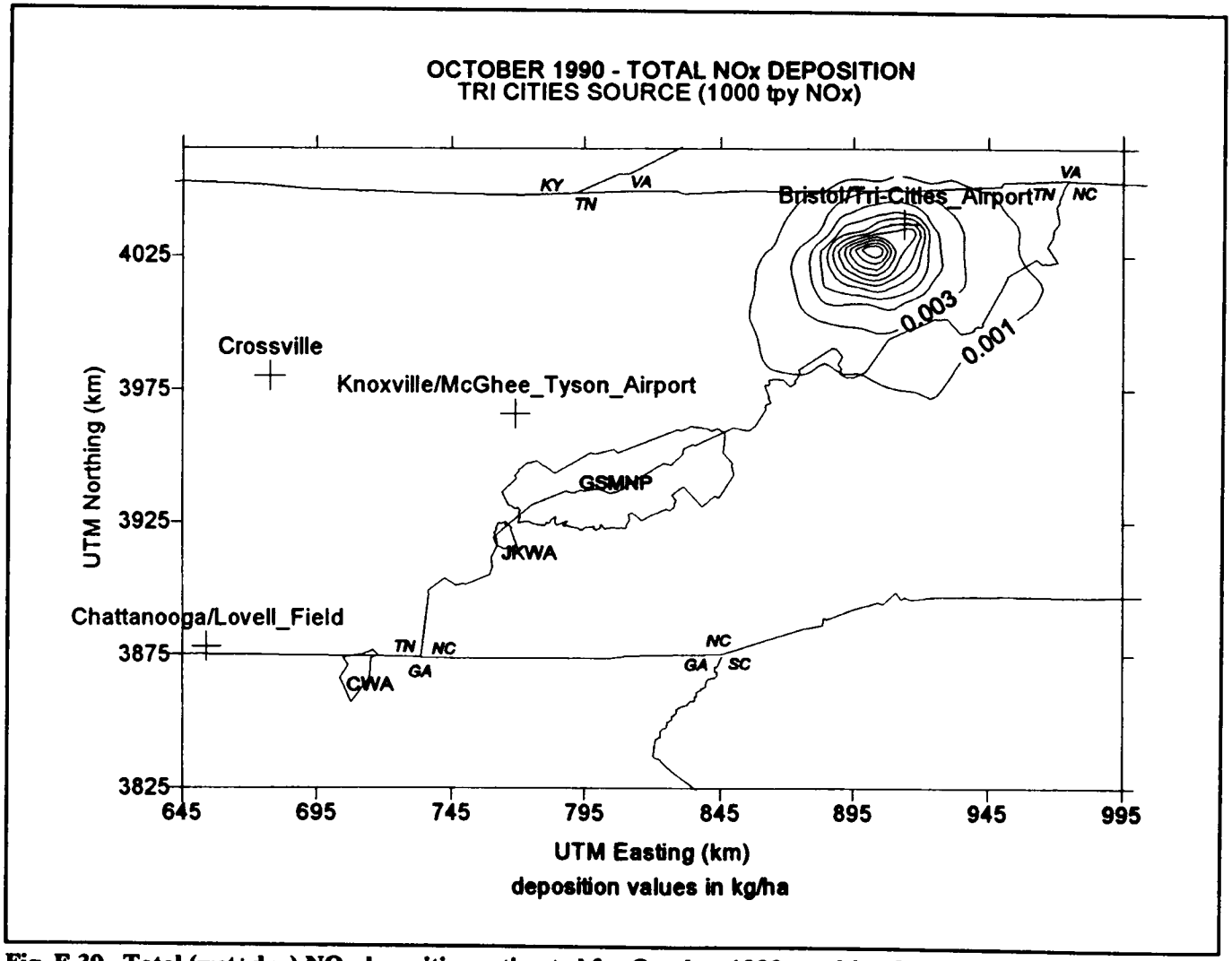

Fig. E.39. Total (wet+dry) NO_x deposition estimated for October 1990 resulting from a 28.8 g/s (1000 tpy) hypothetical NO_x emission source located at Bristol/Tri Cities Airport.

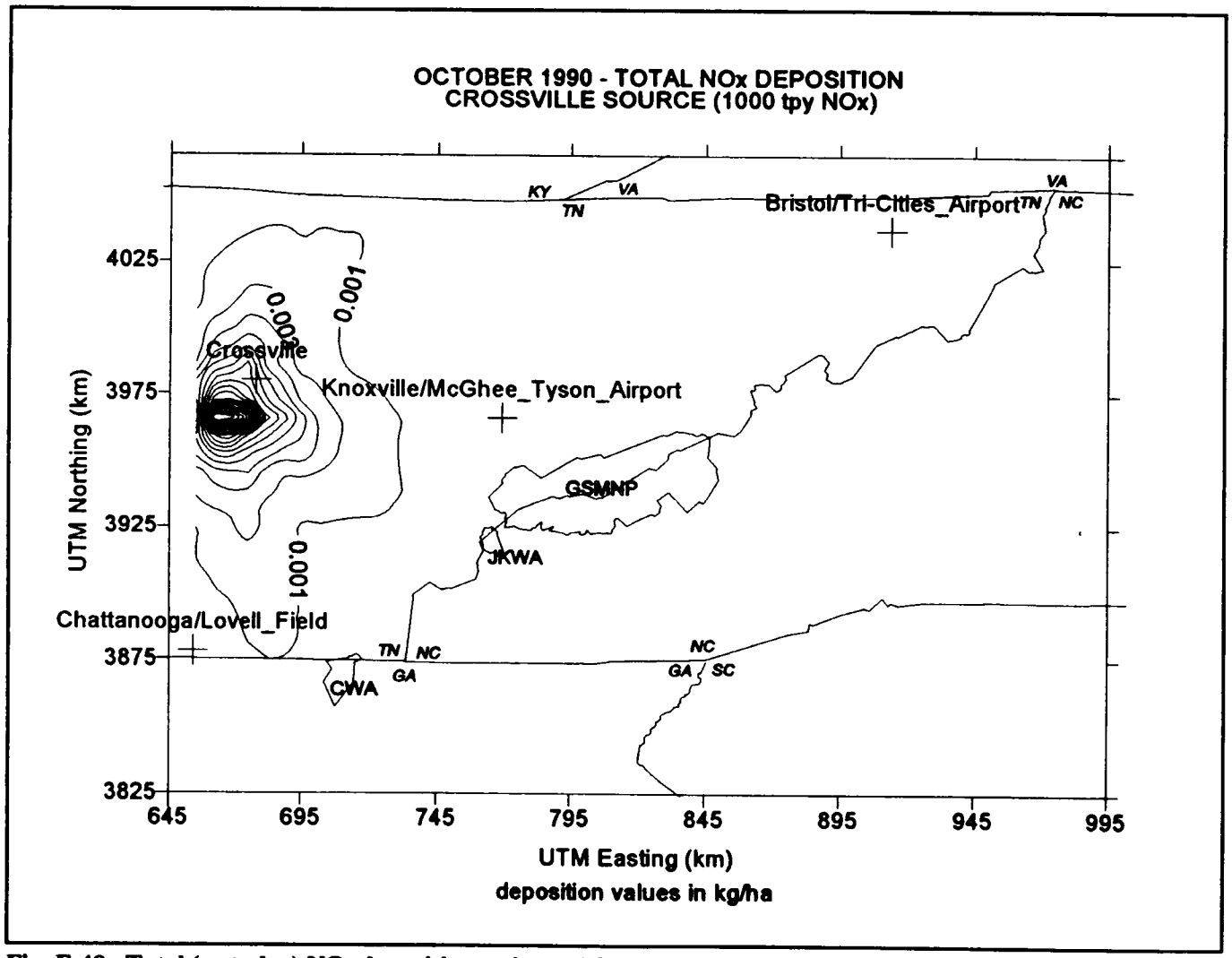

Fig. E.40. Total (wet+dry) NO_x deposition estimated for October 1990 resulting from a 28.8 g/s (1000 tpy) hypothetical NO_x emission source located in Crossville.

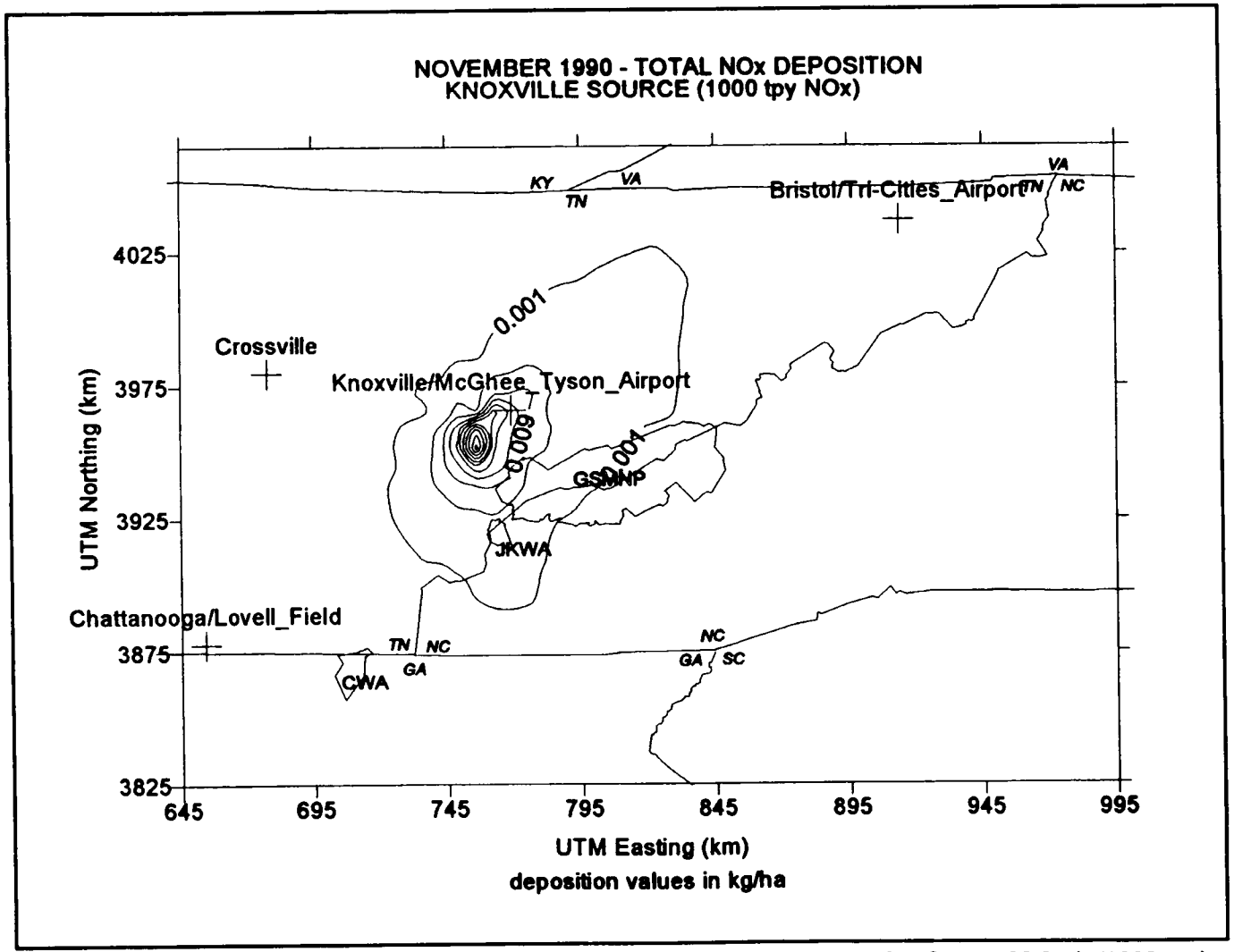

Fig. E.41. Total (wet+dry) NO_x deposition estimated for November 1990 resulting from a 28.8 g/s (1000 tpy) hypothetical NO_x emission source located at Knoxville /McGhee Tyson Airport.

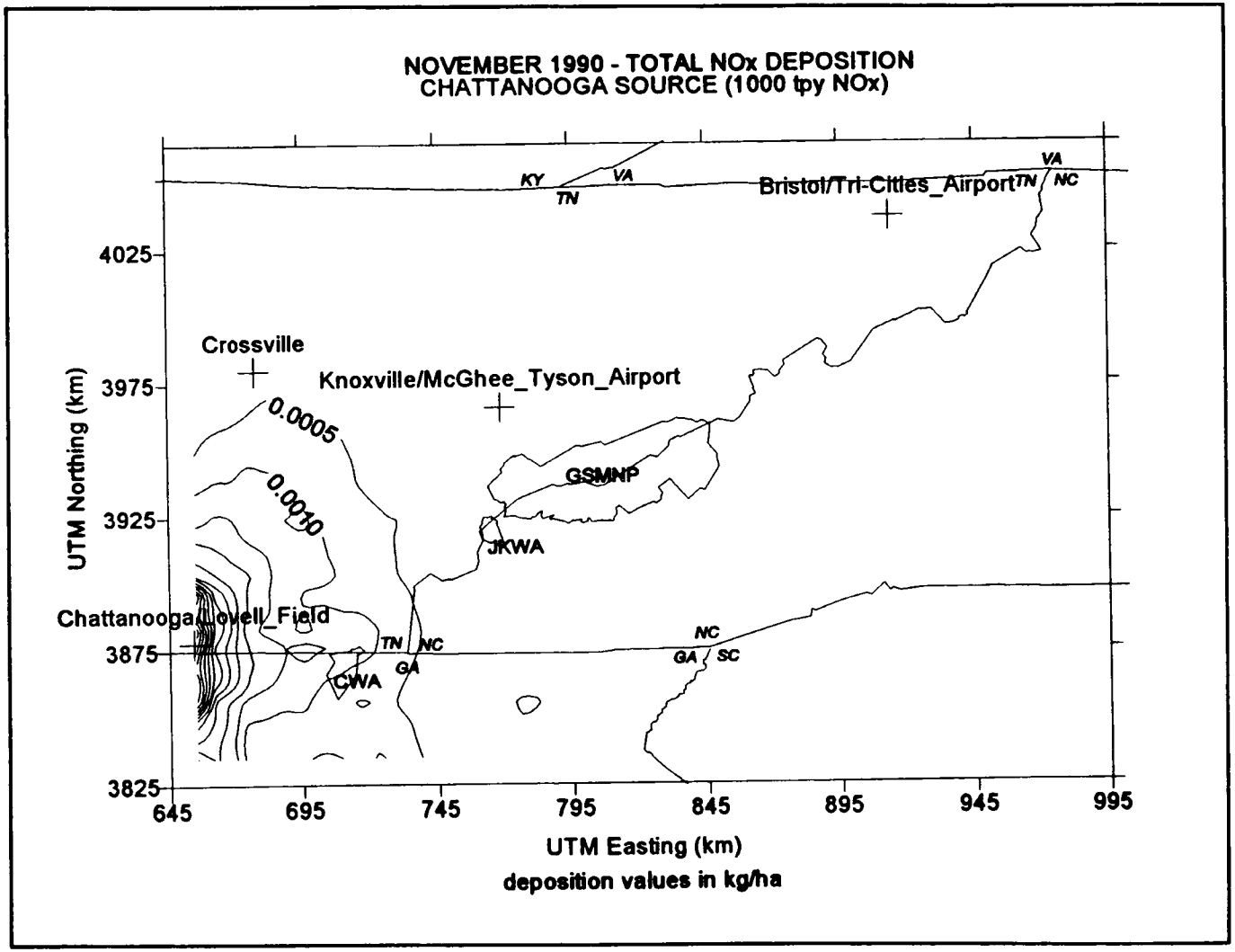

Fig. E.42. Total (wet+dry) NO_x deposition estimated for November 1990 resulting from a 28.8 g/s (1000 tpy) hypothetical NO_x emission source located at Chattanooga/Lovell Field.

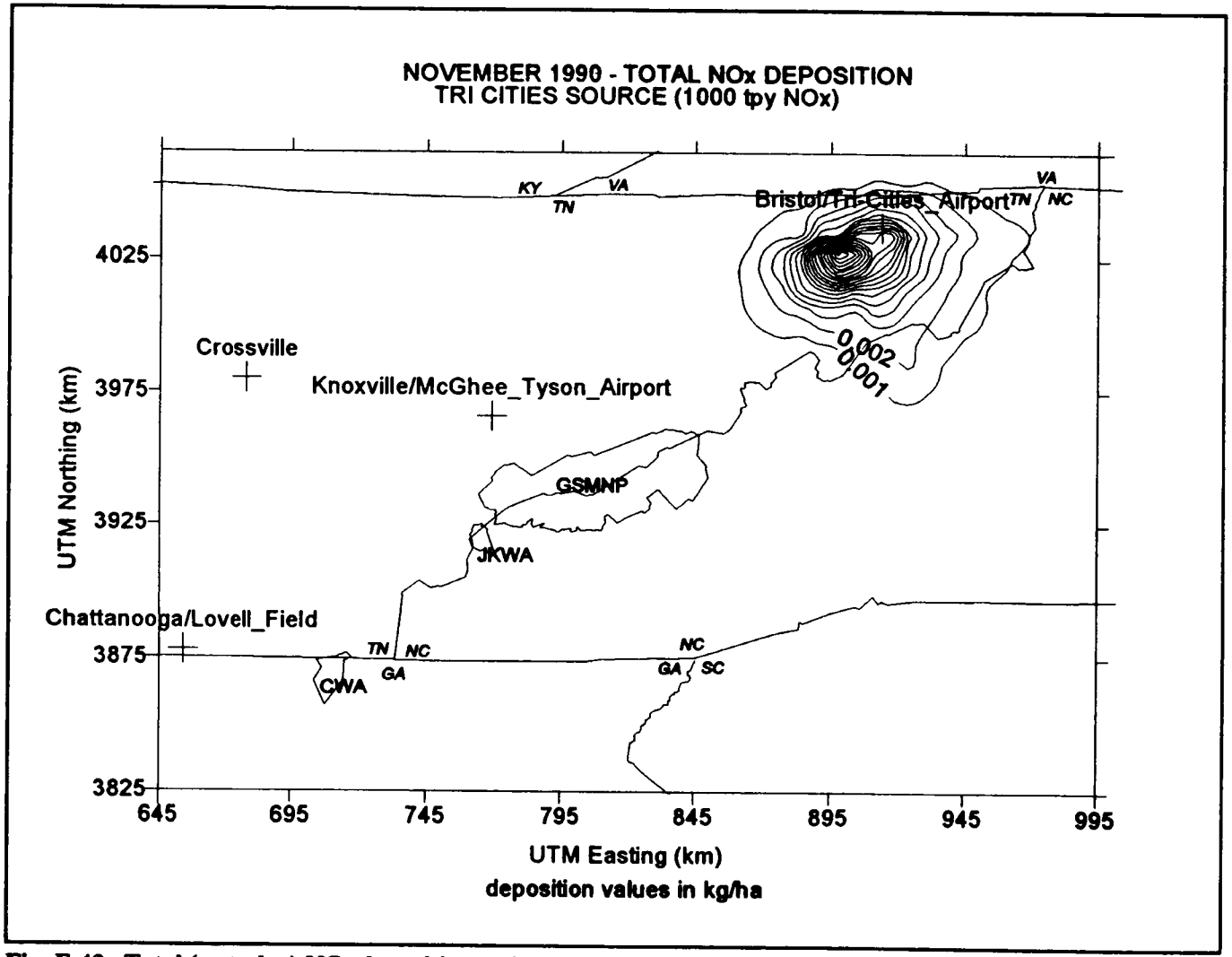

Fig. E.43. Total (wet+dry) NO_x deposition estimated for November 1990 resulting from a 28.8 g/s (1000 tpy) hypothetical NO_x emission source located at Bristol/Tri Cities Airport.

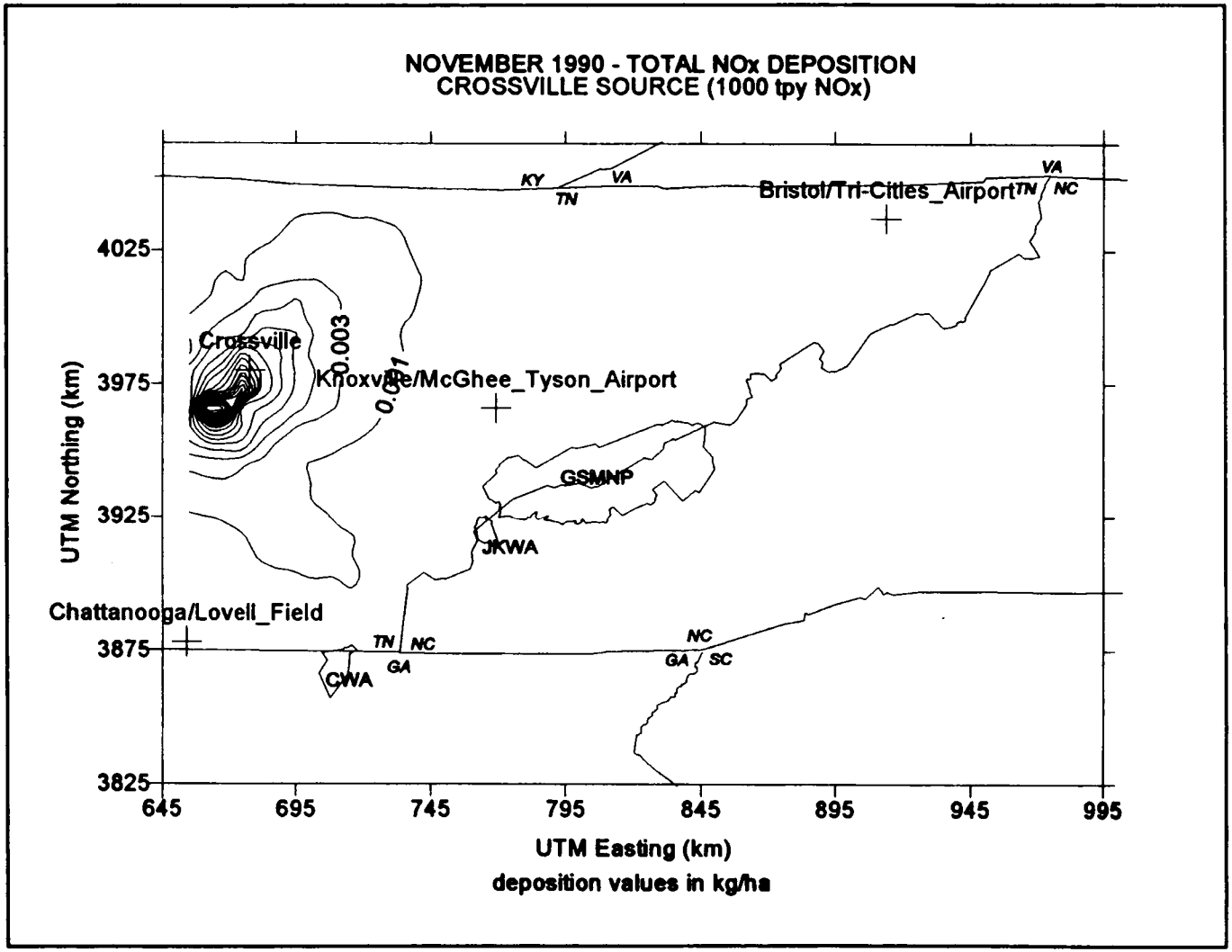

Fig. E.44. Total (wet+dry) NO_x deposition estimated for November 1990 resulting from a 28.8 g/s (1000 tpy) hypothetical NO_x emission source located in Crossville.

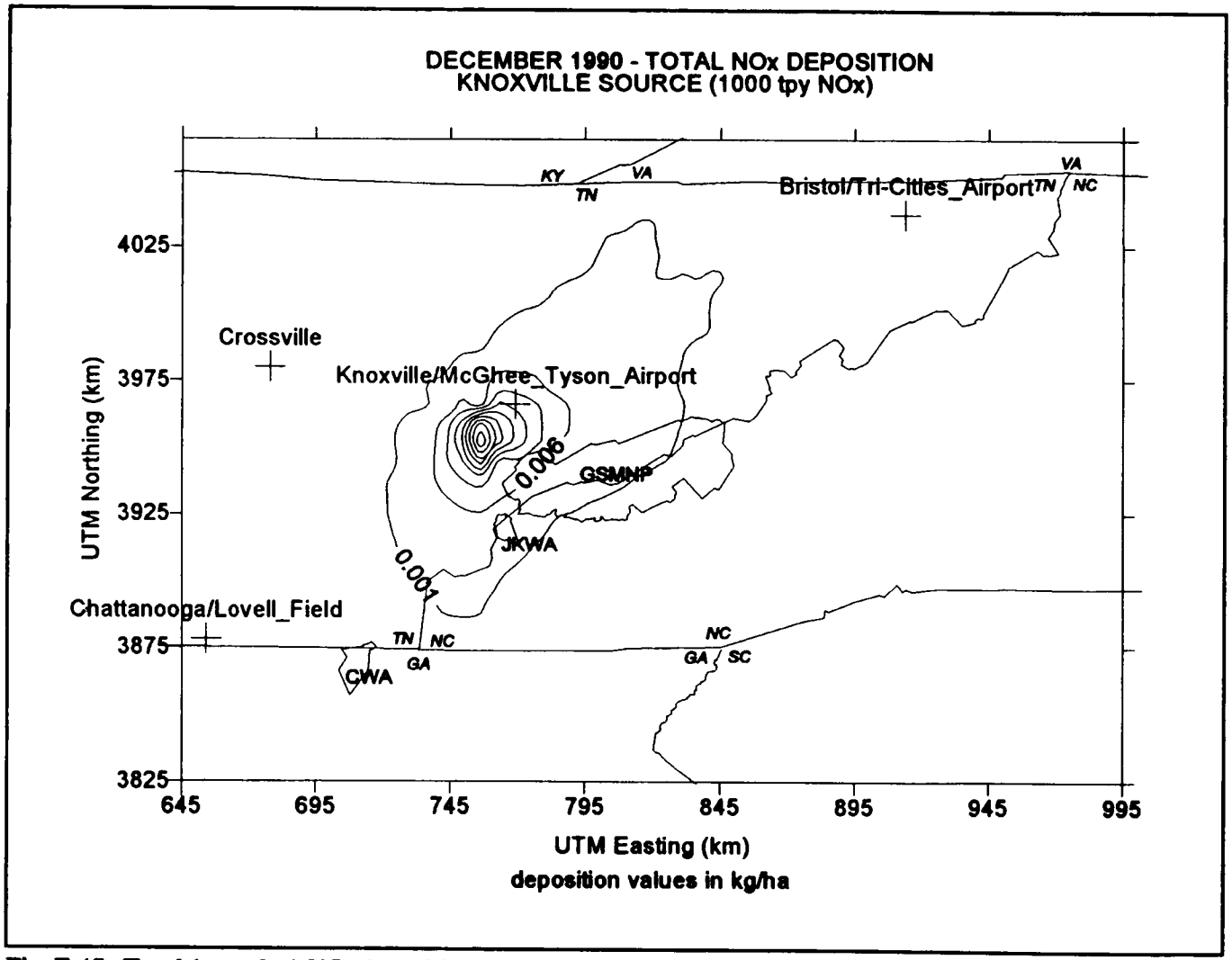

Fig. E.45. Total (wet+dry) NO_x deposition estimated for December 1990 resulting from a 28.8 g/s (1000 tpy) hypothetical NO_x emission source located at Knoxville /McGhee Tyson Airport.

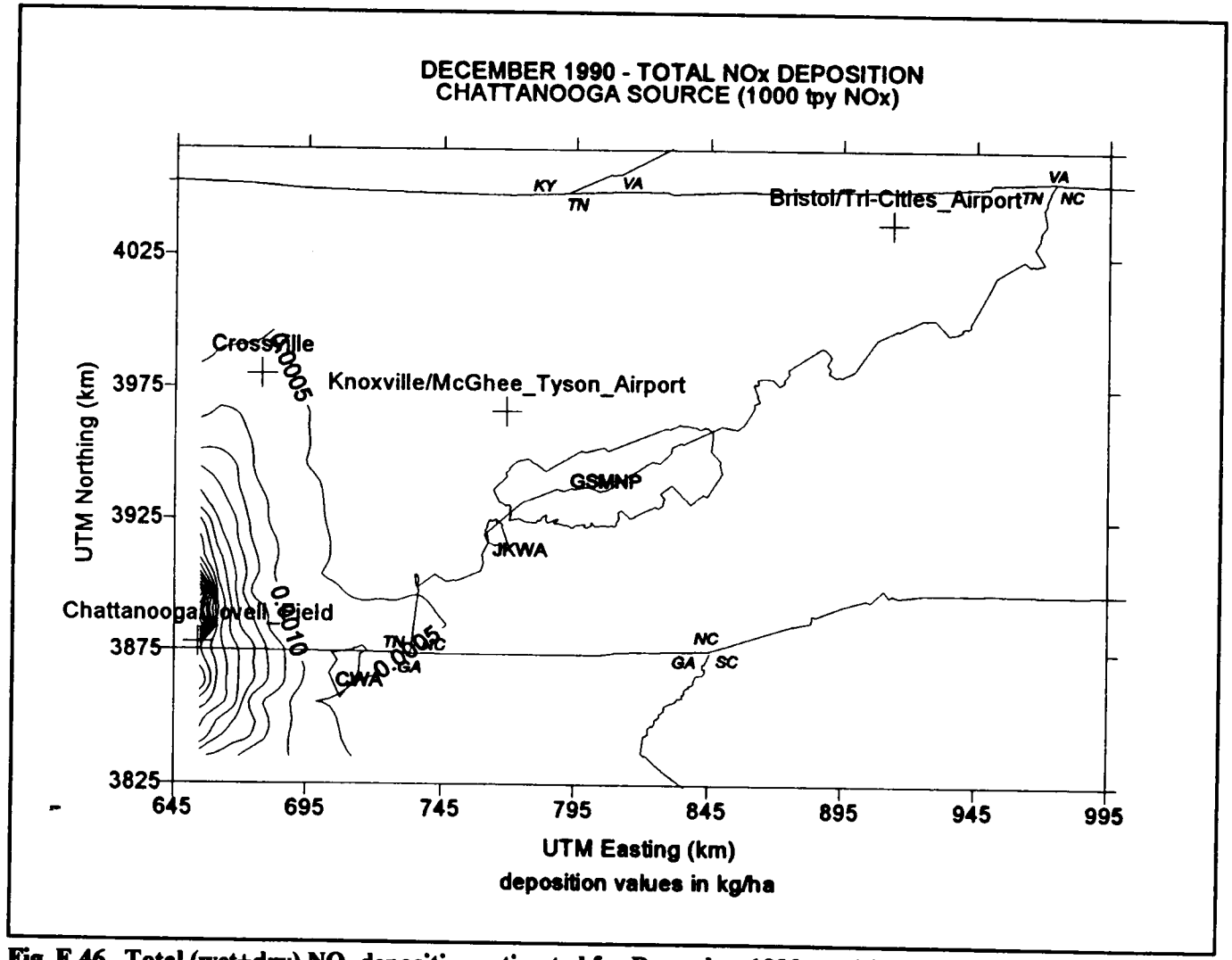

Fig. E.46. Total (wet+dry) NO_x deposition estimated for December 1990 resulting from a 28.8 g/s (1000 tpy) hypothetical NO_x emission source located at Chattanooga/Lovell Field.

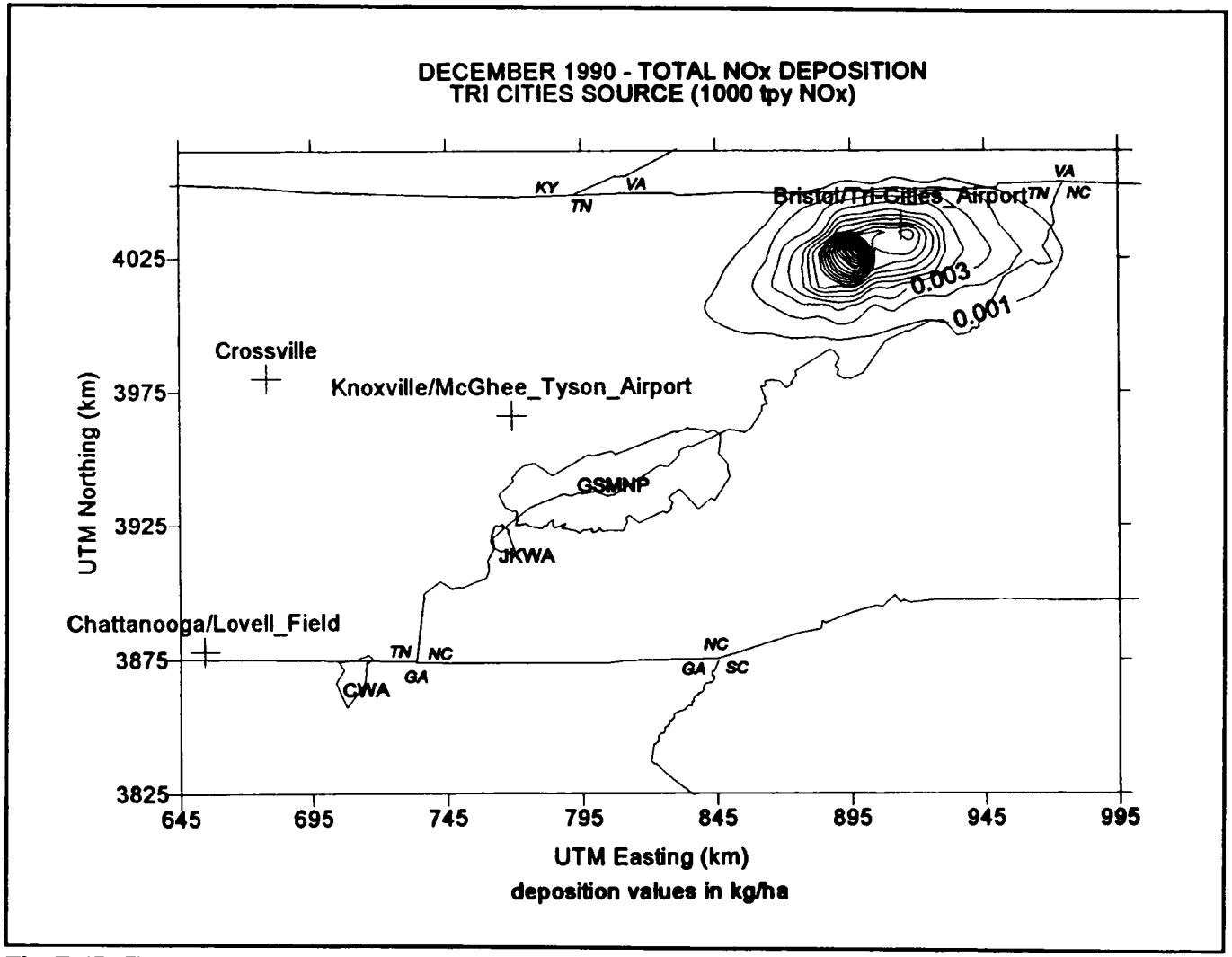

Fig. E.47. Total (wet+dry) NO_x deposition estimated for December 1990 resulting from a 28.8 g/s (1000 tpy) hypothetical NO_x emission source located at Bristol/Tri Cities Airport.

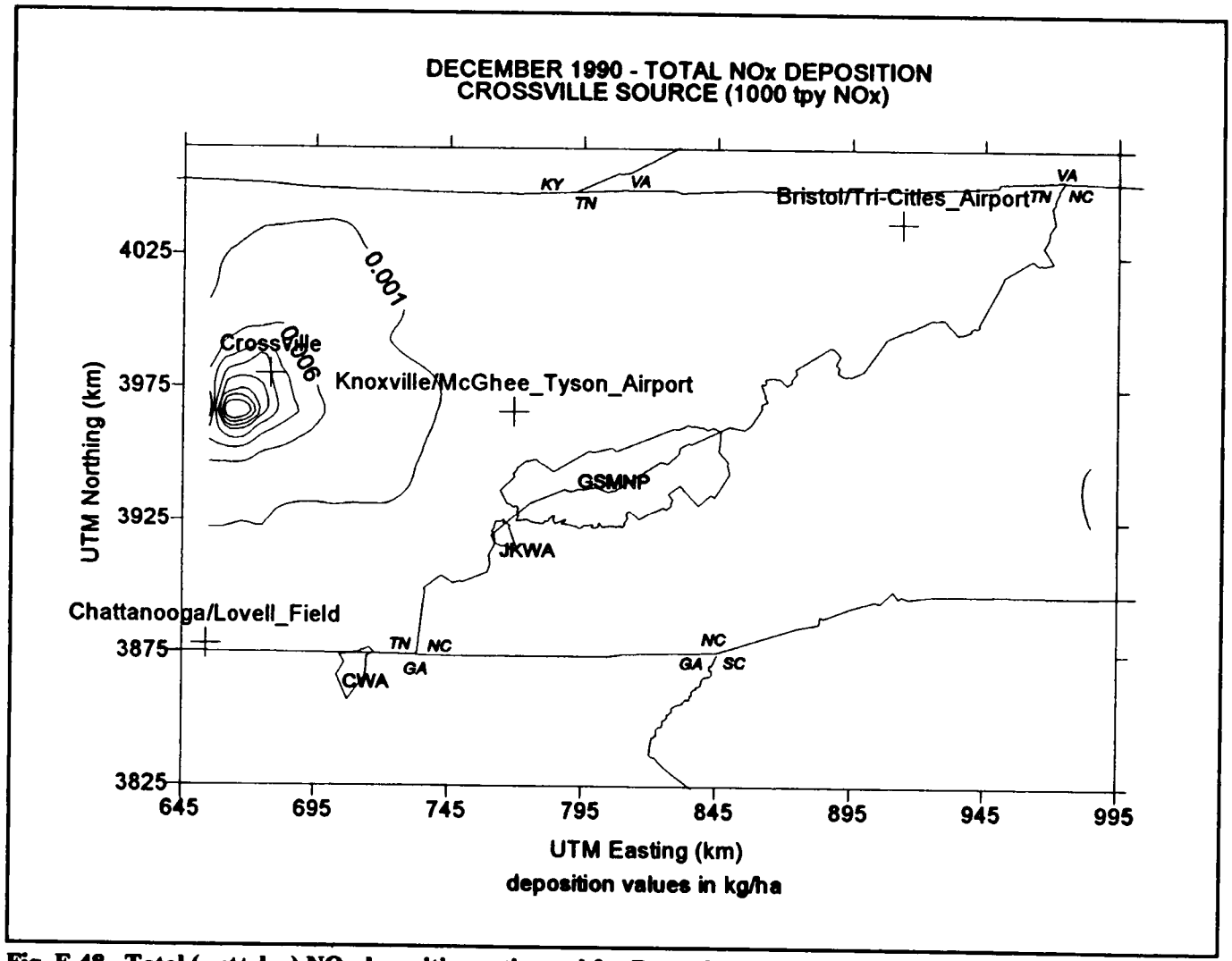

Fig. E.48. Total (wet+dry) NO_x deposition estimated for December 1990 resulting from a 28.8 g/s (1000 tpy) hypothetical NO_x emission source located in Crossville.

APPENDIX F
MONTHLY HNO_3 DEPOSITION CONTOUR MAPS

The following figures are contour maps of monthly total (wet + dry) HNO_3 deposition in the East Tennessee modeling domain. One contour map per month has been generated for each of the four hypothetical source locations.

The following abbreviations are used on the contour maps:

GSMNP	=	The Great Smoky Mountains National Park
JKWA	=	Joyce Kilmer Wilderness Area
CWA	=	Cohutta Wilderness Area
TN	=	Tennessee
NC	=	North Carolina
GA	=	Georgia
VA	=	Virginia
KY	=	Kentucky
UTM	=	Universal Transverse Mercator

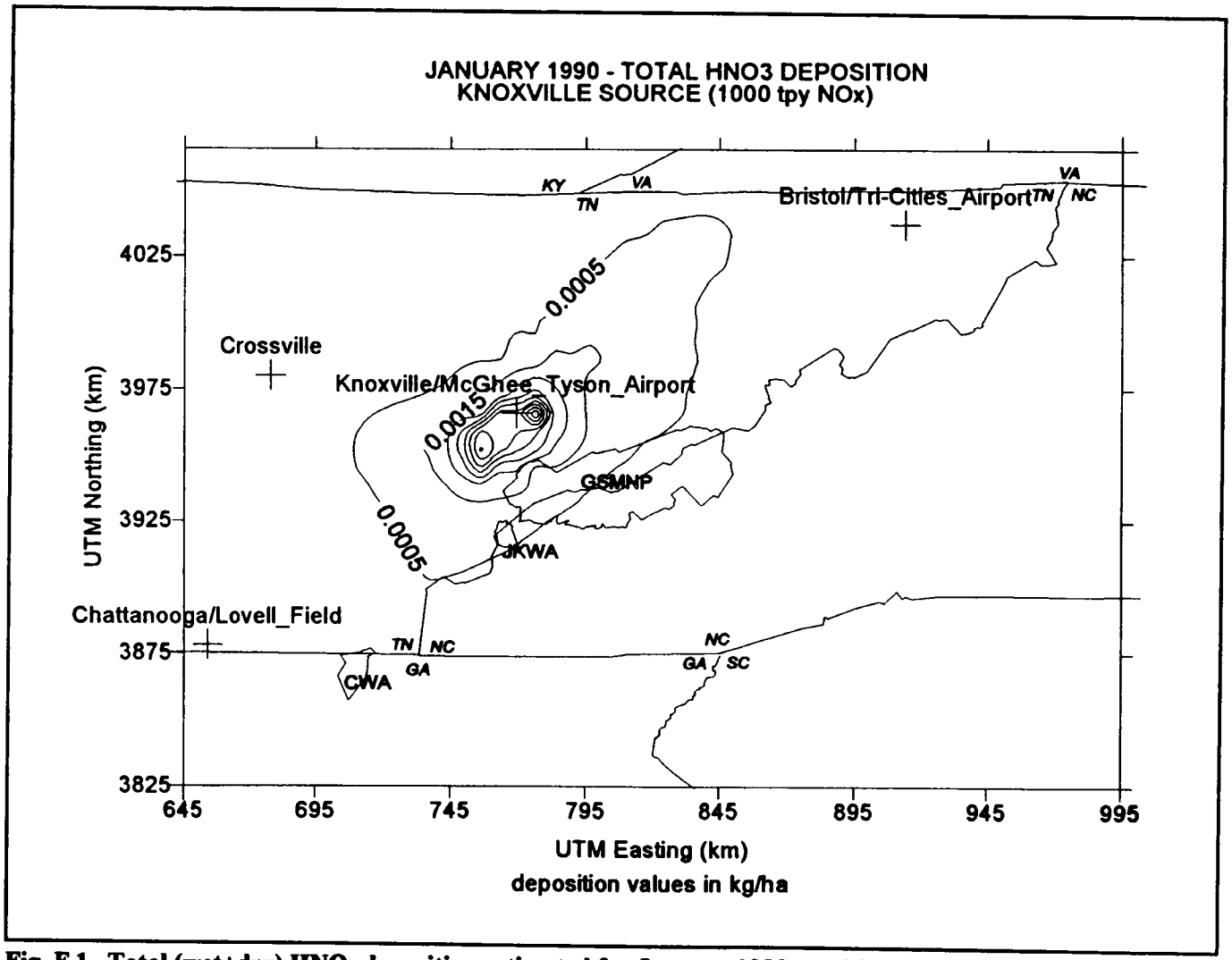

Fig. F.1. Total (wet+dry) HNO_3 deposition estimated for January 1990 resulting from a 28.8 g/s (1000 tpy) hypothetical NO_x emission source located at Knoxville /McGhee Tyson Airport.

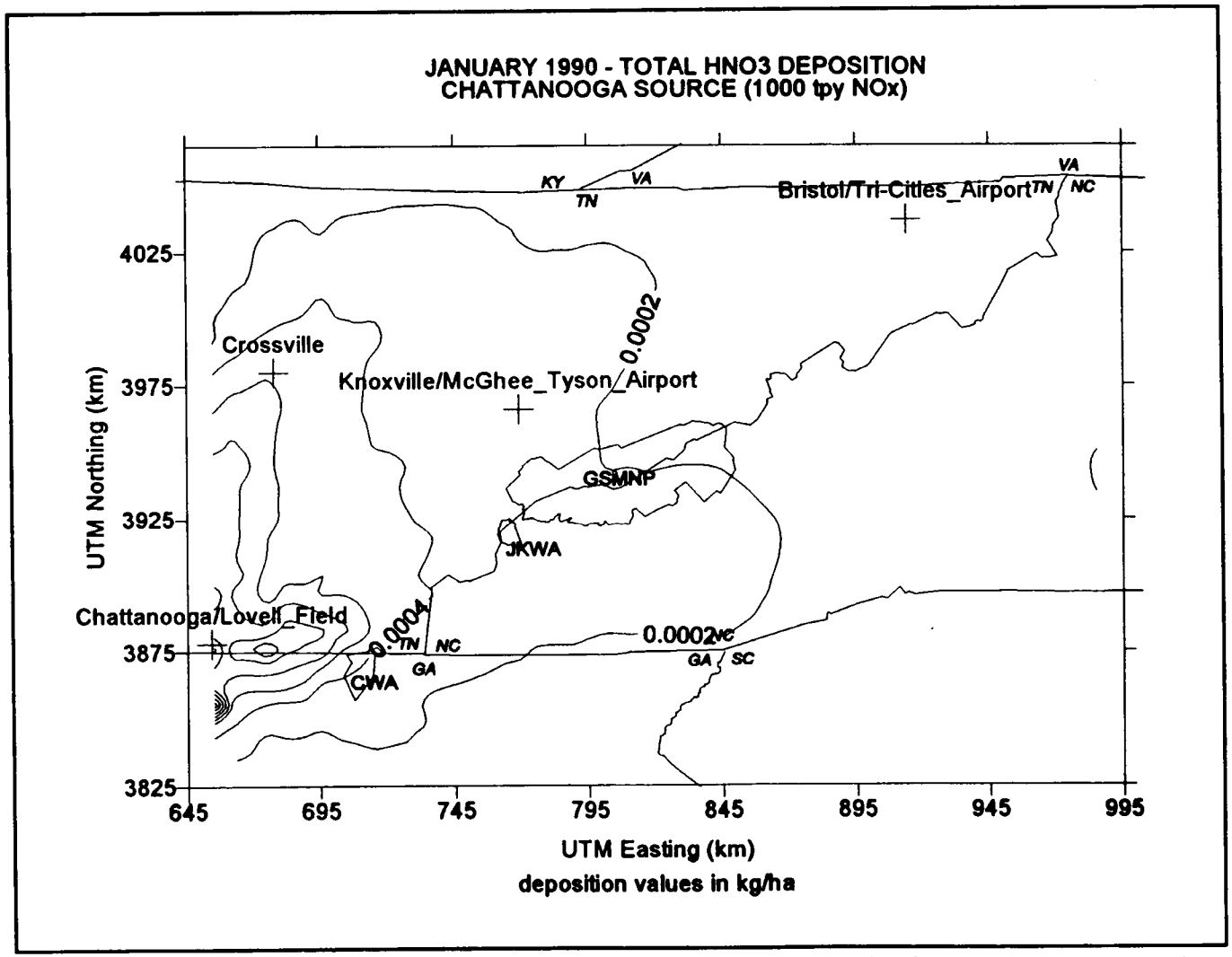

Fig. F.2. Total (wet+dry) HNO_3 deposition estimated for January 1990 resulting from a 28.8 g/s (1000 tpy) hypothetical NO_x emission source located at Chattanooga/Lovell Field.

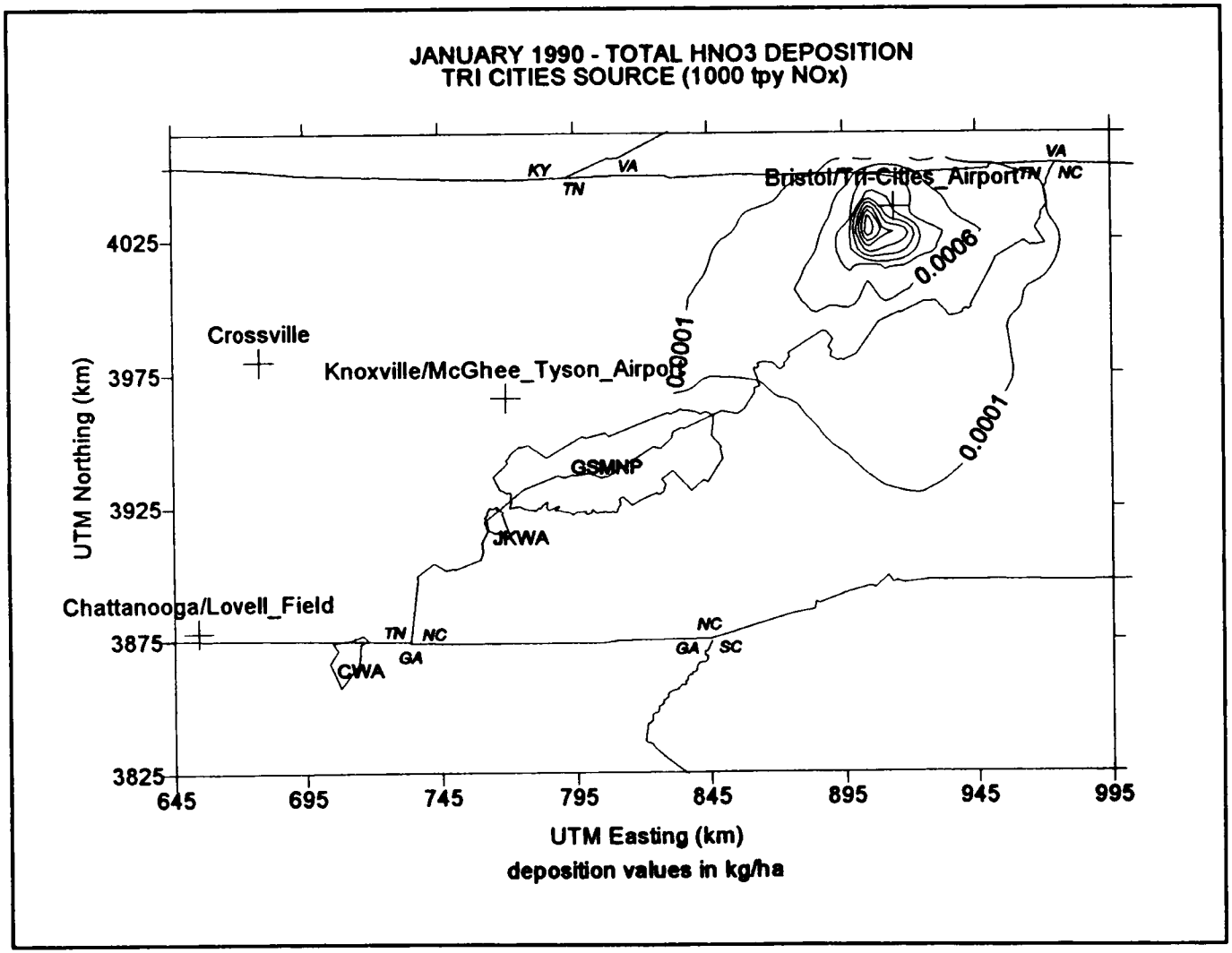

Fig. F.3. Total (wet+dry) HNO_3 deposition estimated for January 1990 resulting from a 28.8 g/s (1000 tpy) hypothetical NO_x emission source located at Bristol/Tri Cities Airport.

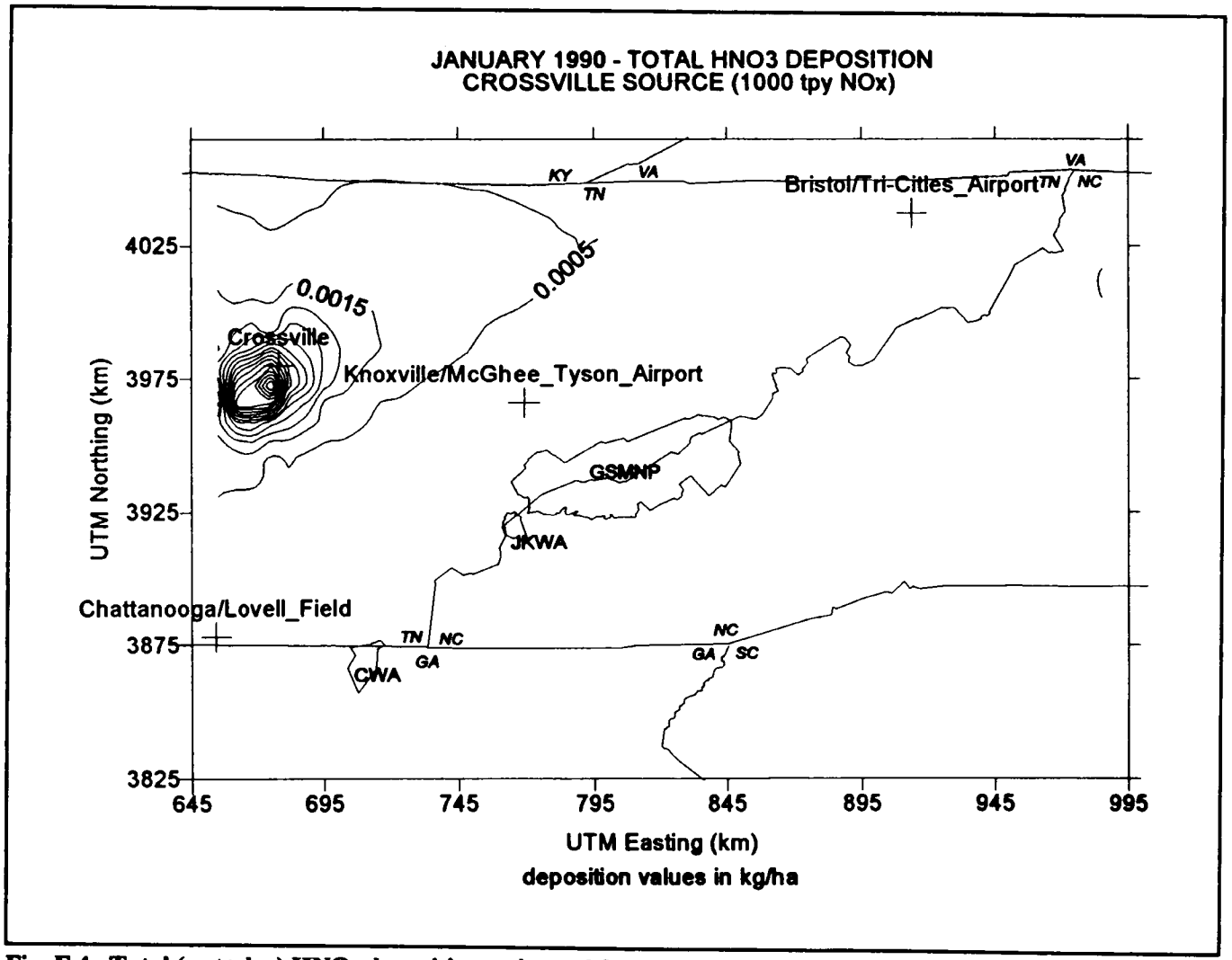

Fig. F.4. Total (wet+dry) HNO_3 deposition estimated for January 1990 resulting from a 28.8 g/s (1000 tpy) hypothetical NO_x emission source located in Crossville.

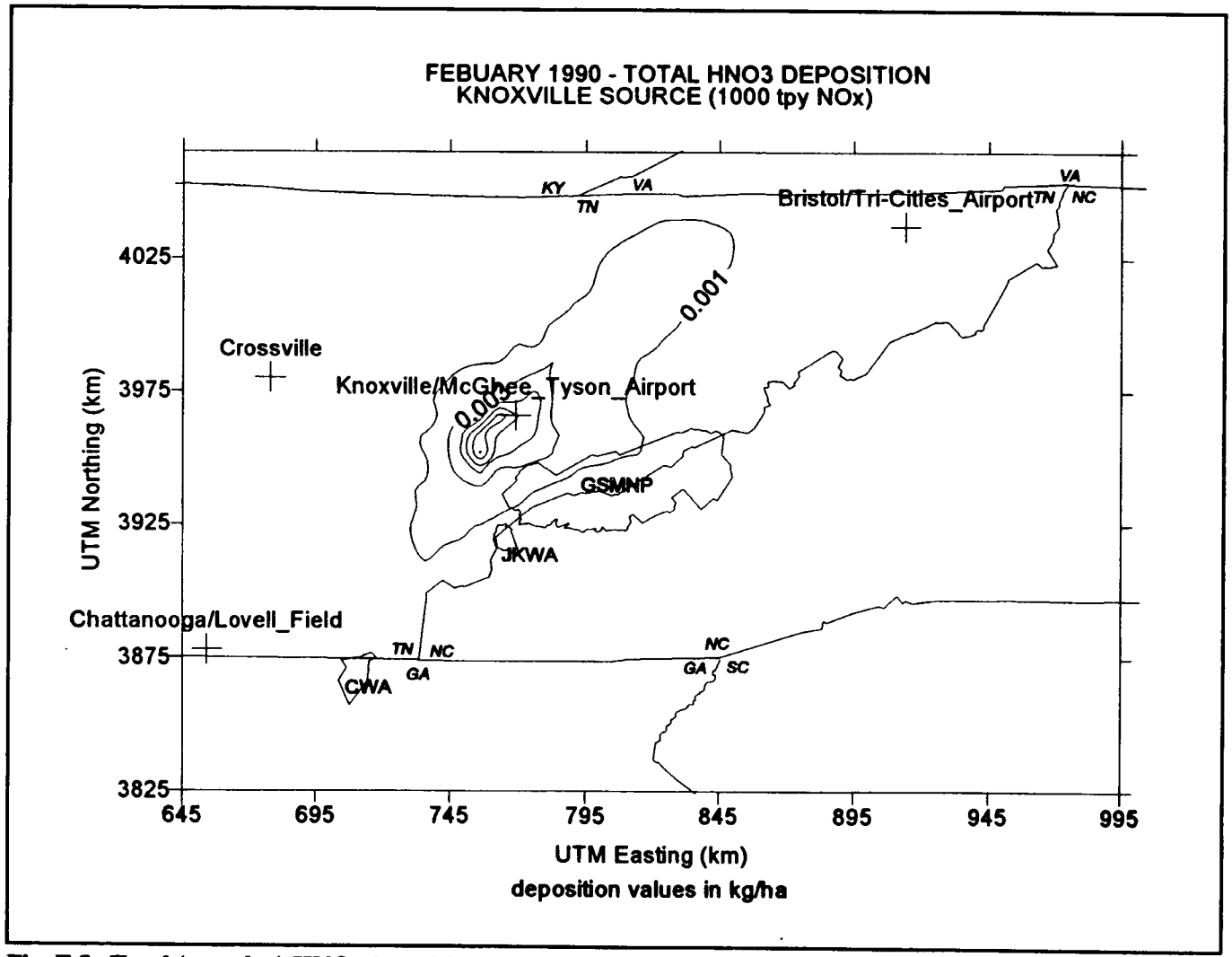

Fig. F.5. Total (wet+dry) HNO_3 deposition estimated for February 1990 resulting from a 28.8 g/s (1000 tpy) hypothetical NO_x emission source located at Knoxville /McGhee Tyson Airport.

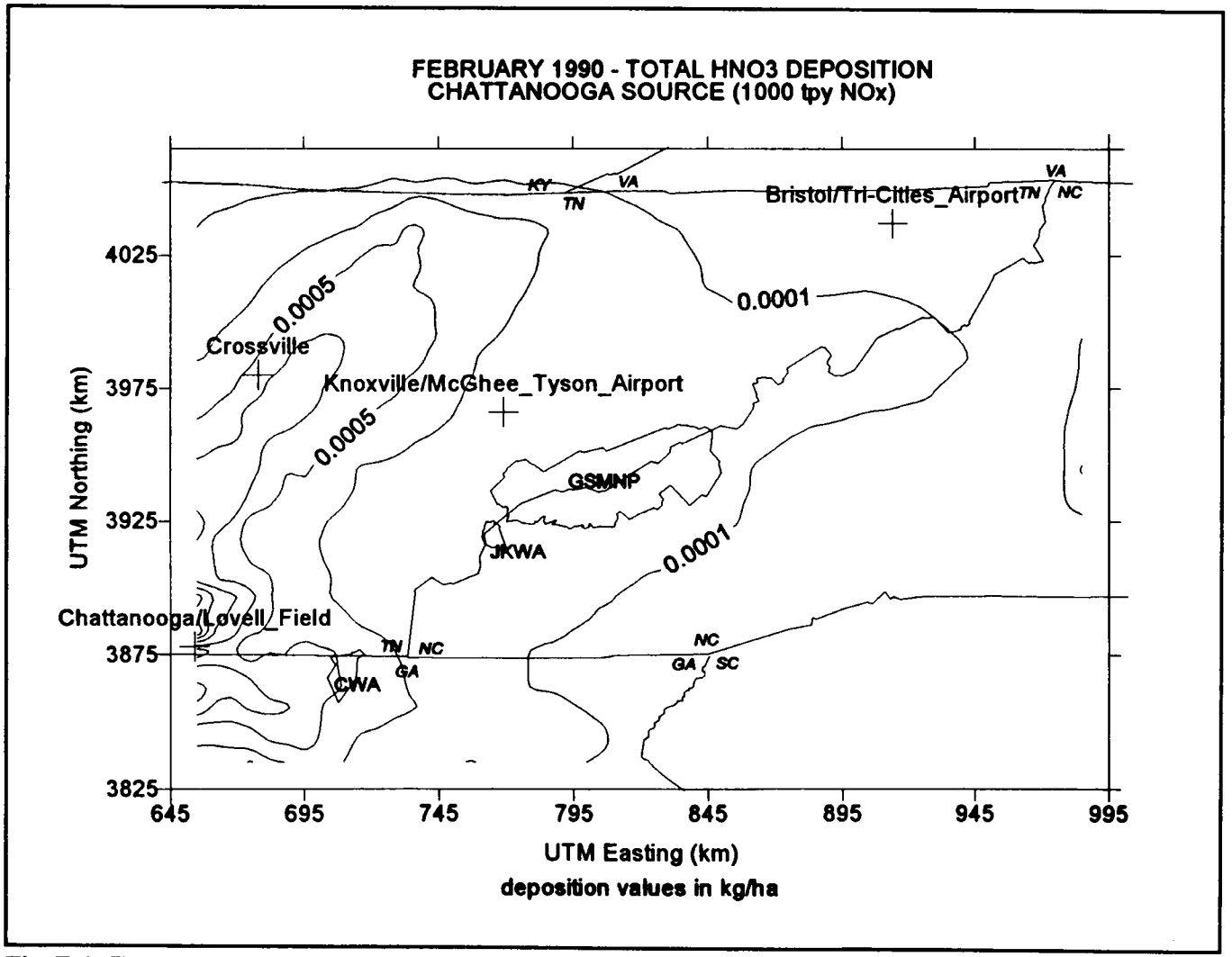

Fig. F.6. Total (wet+dry) HNO_3 deposition estimated for February 1990 resulting from a 28.8 g/s (1000 tpy) hypothetical NO_x emission source located at Chattanooga/Lovell Field.

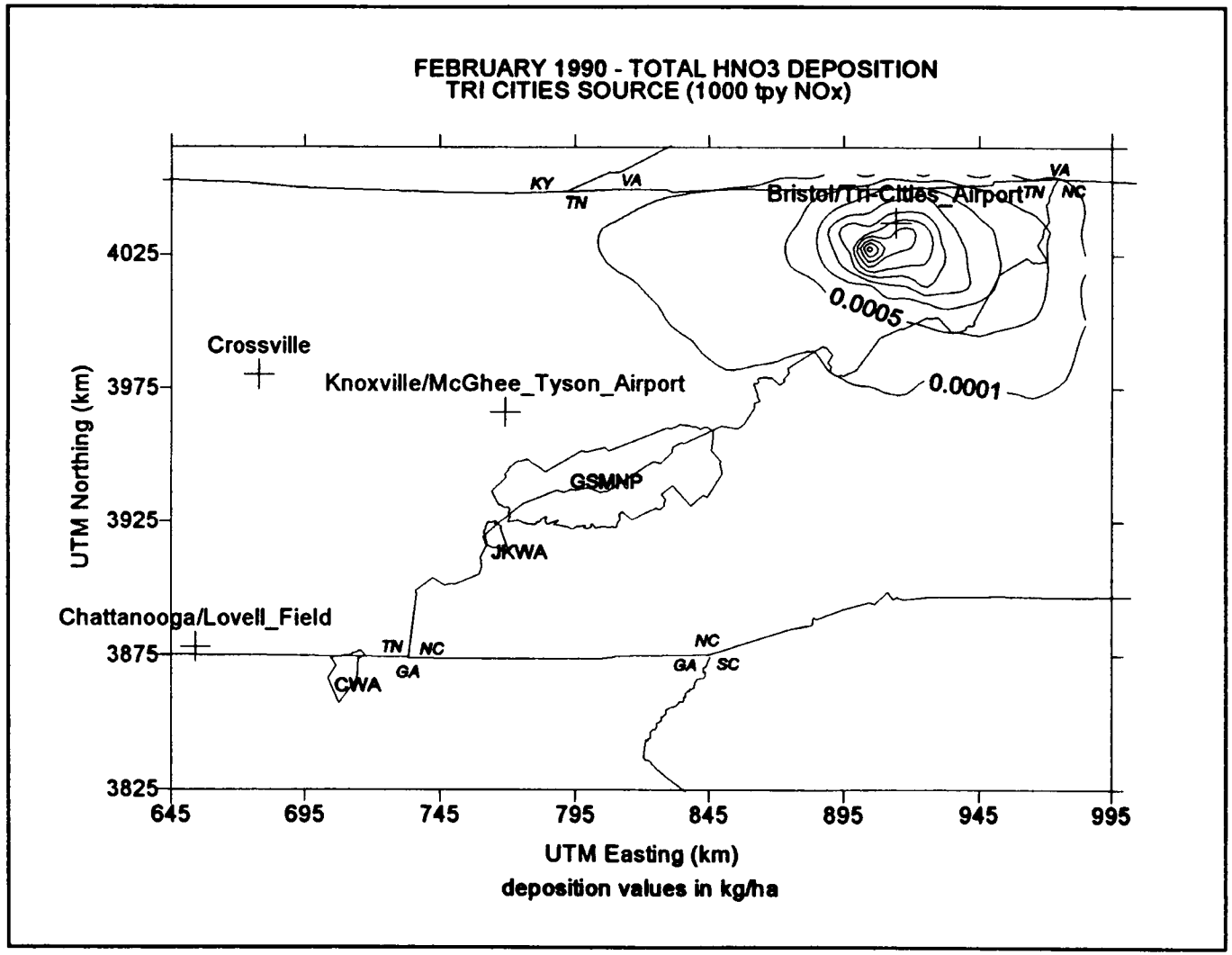

Fig. F.7. Total (wet+dry) HNO_3 deposition estimated for February 1990 resulting from a 28.8 g/s (1000 tpy) hypothetical NO_x emission source located at Bristol/Tri Cities Airport.

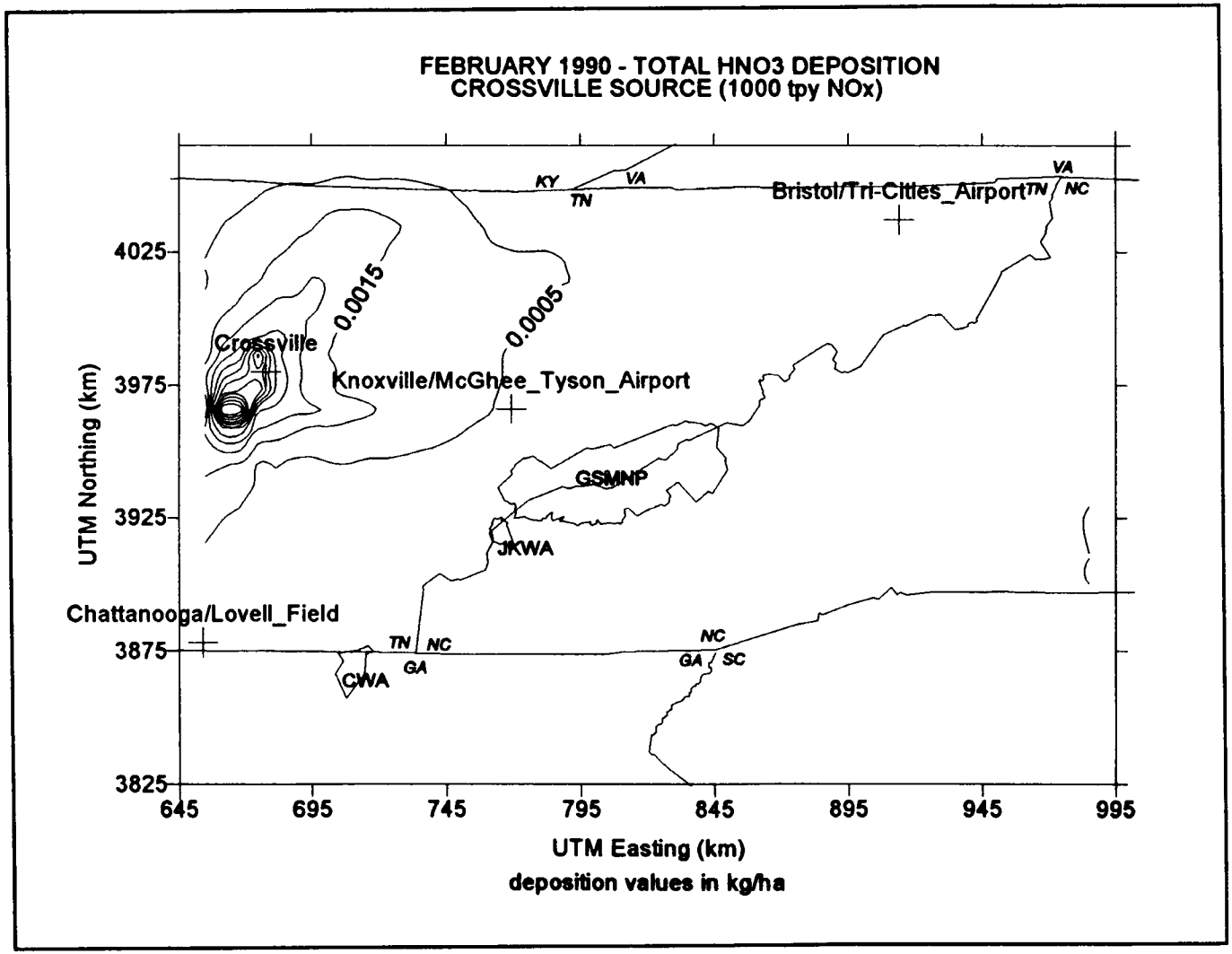

Fig. F.8. Total (wet+dry) HNO_3 deposition estimated for February 1990 resulting from a 28.8 g/s (1000 tpy) hypothetical NO_x emission source located in Crossville.

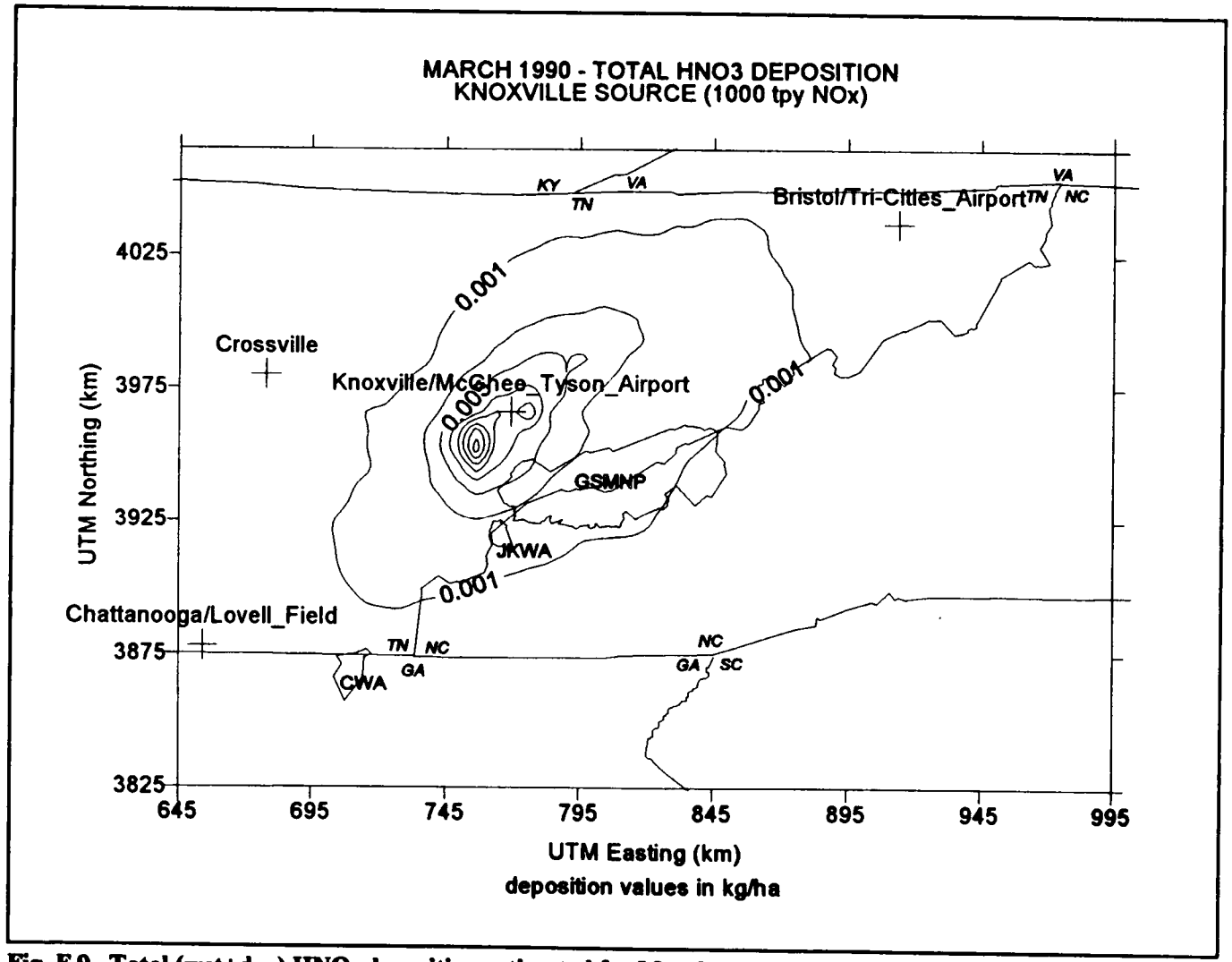

Fig. F.9. Total (wet+dry) HNO_3 deposition estimated for March 1990 resulting from a 28.8 g/s (1000 tpy) hypothetical NO_x emission source located at Knoxville /McGhee Tyson Airport.

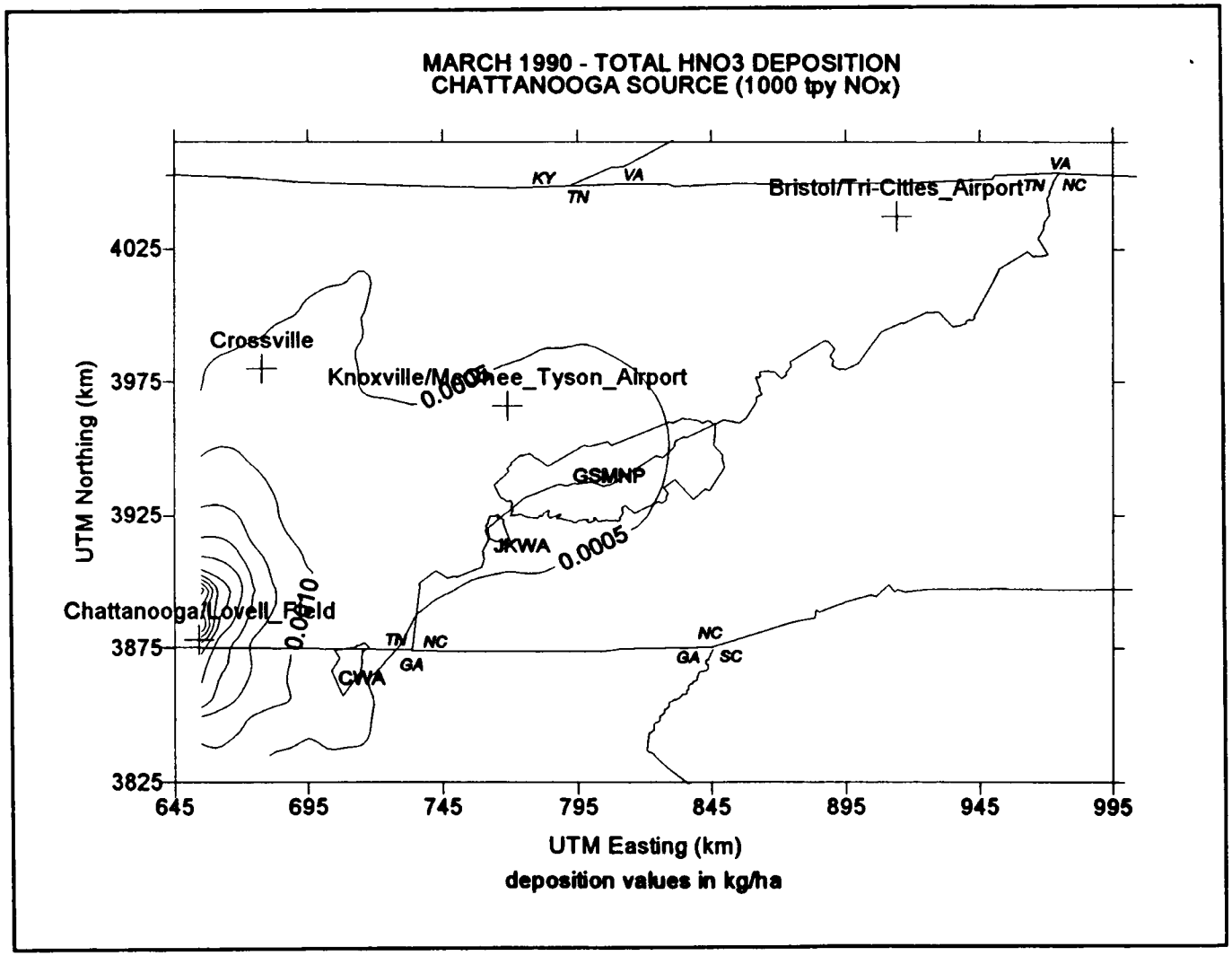

Fig. F.10. Total (wet+dry) HNO_3 deposition estimated for March 1990 resulting from a 28.8 g/s (1000 tpy) hypothetical NO_x emission source located at Chattanooga/Lovell Field.

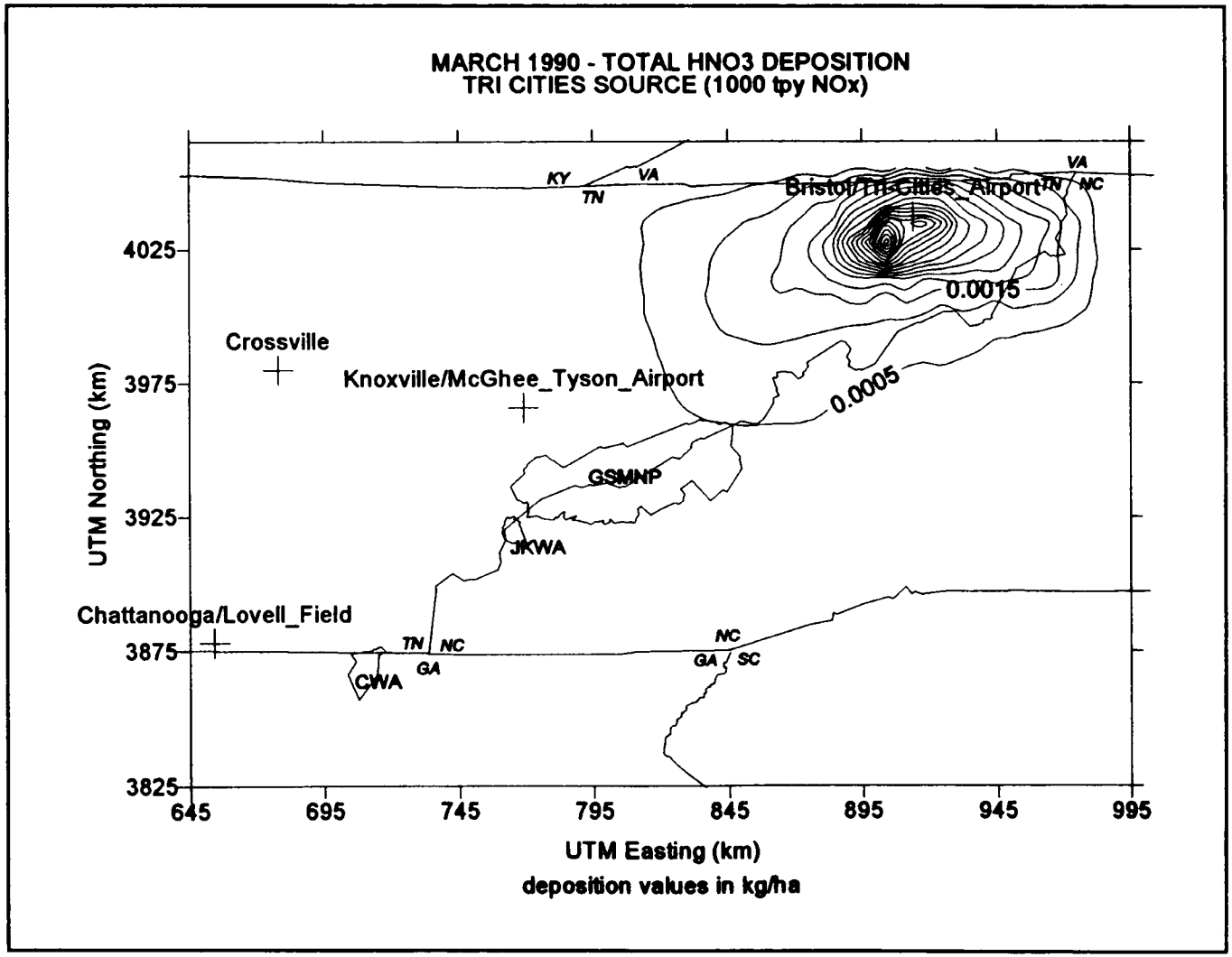

Fig. F.11. Total (wet+dry) HNO_3 deposition estimated for March 1990 resulting from a 28.8 g/s (1000 tpy) hypothetical NO_x emission source located at Bristol/Tri Cities Airport.

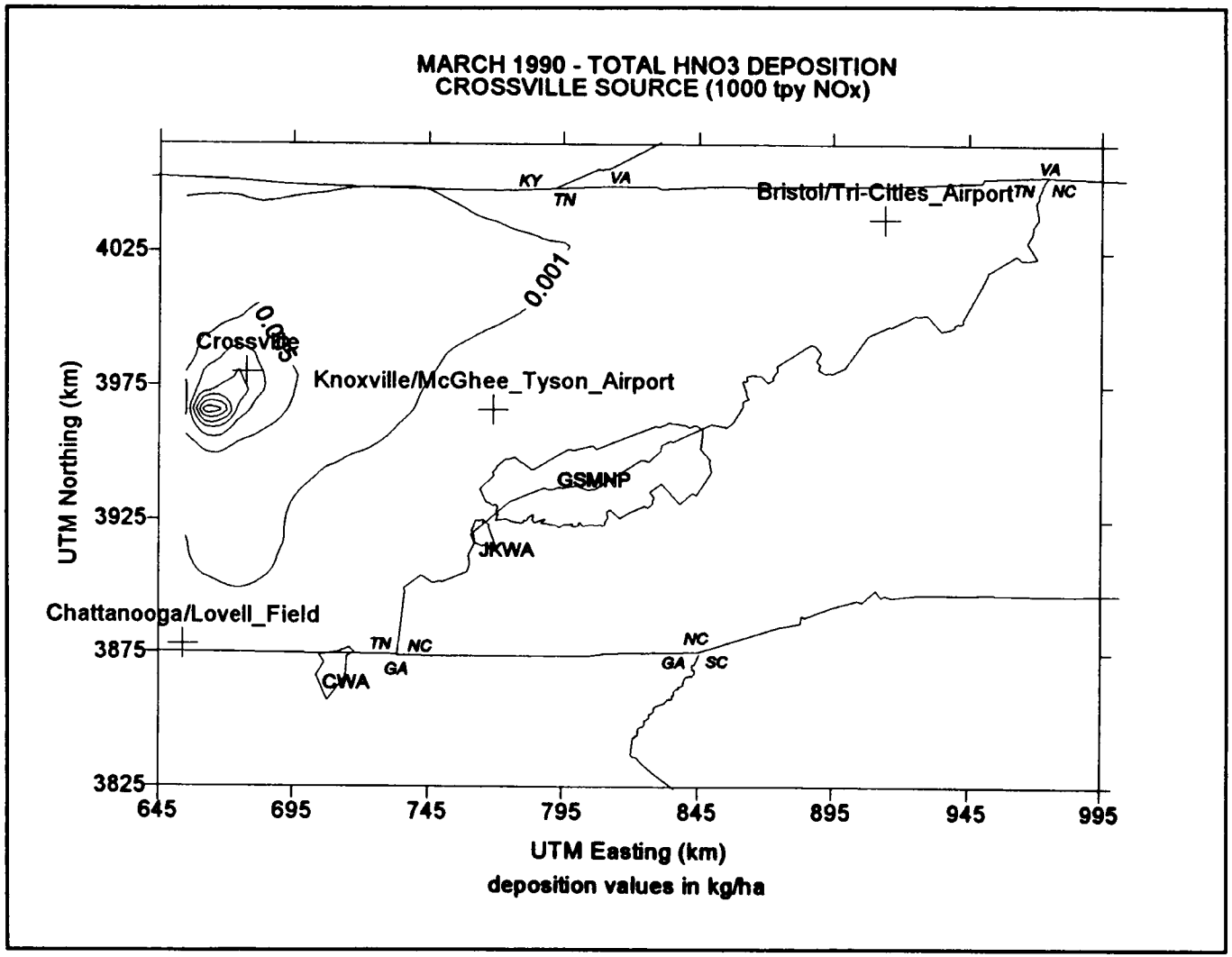

Fig. F.12. Total (wet+dry) HNO_3 deposition estimated for March 1990 resulting from a 28.8 g/s (1000 tpy) hypothetical NO_x emission source located in Crossville.

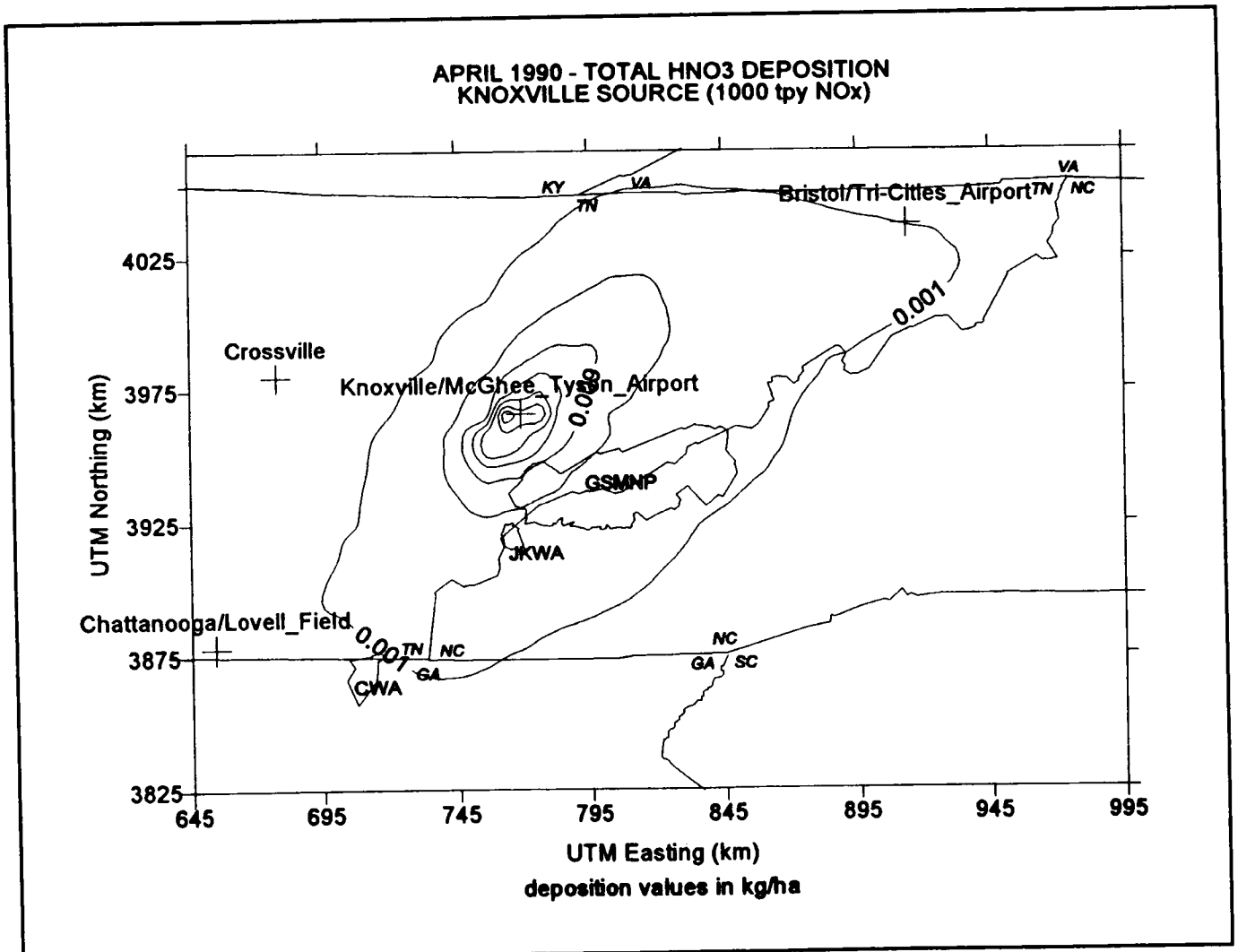

Fig. F.13. Total (wet+dry) HNO_3 deposition estimated for April 1990 resulting from a 28.8 g/s (1000 tpy) hypothetical NO_x emission source located at Knoxville /McGhee Tyson Airport.

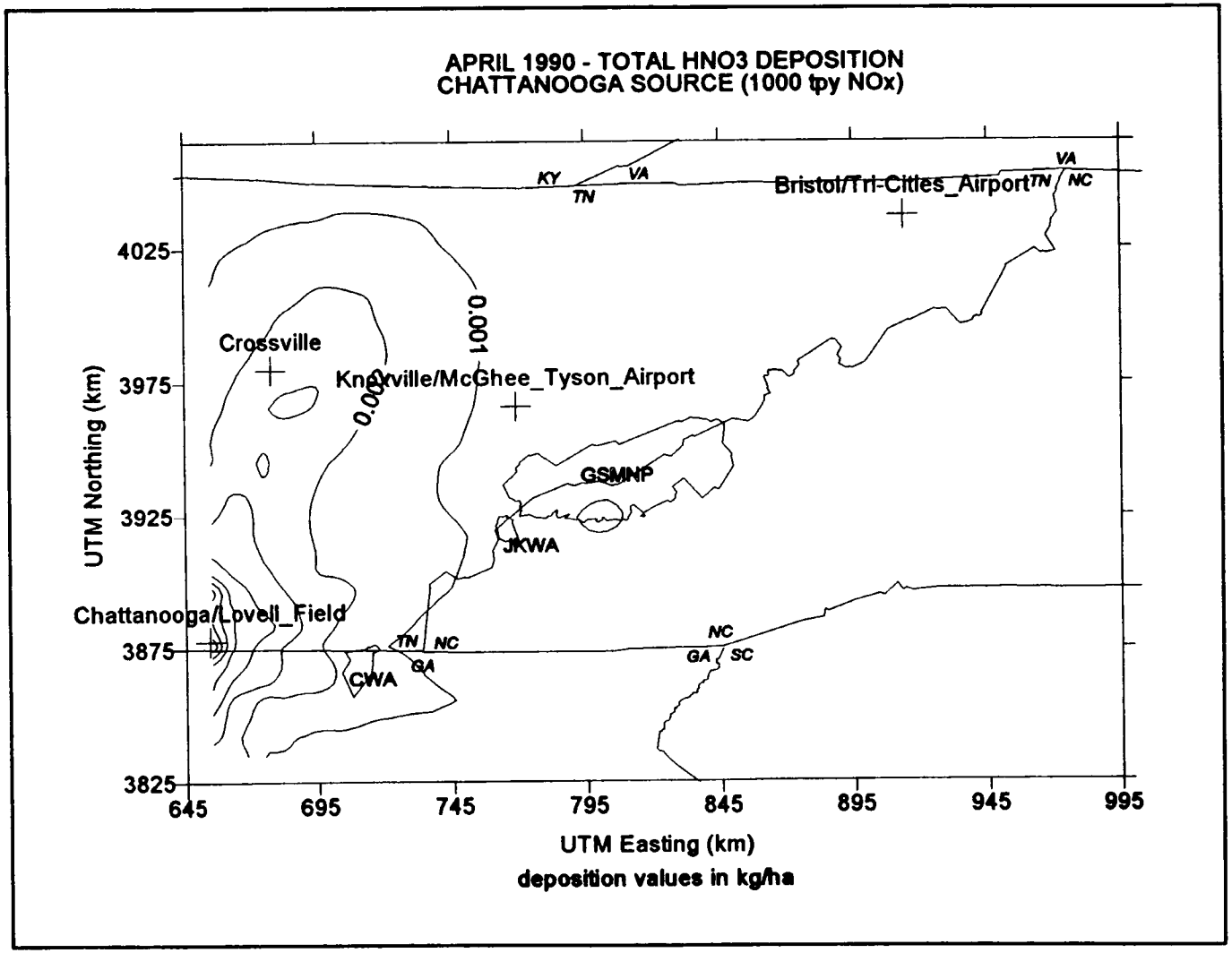

Fig. F.14. Total (wet+dry) HNO_3 deposition estimated for April 1990 resulting from a 28.8 g/s (1000 tpy) hypothetical NO_x emission source located at Chattanooga/Lovell Field.

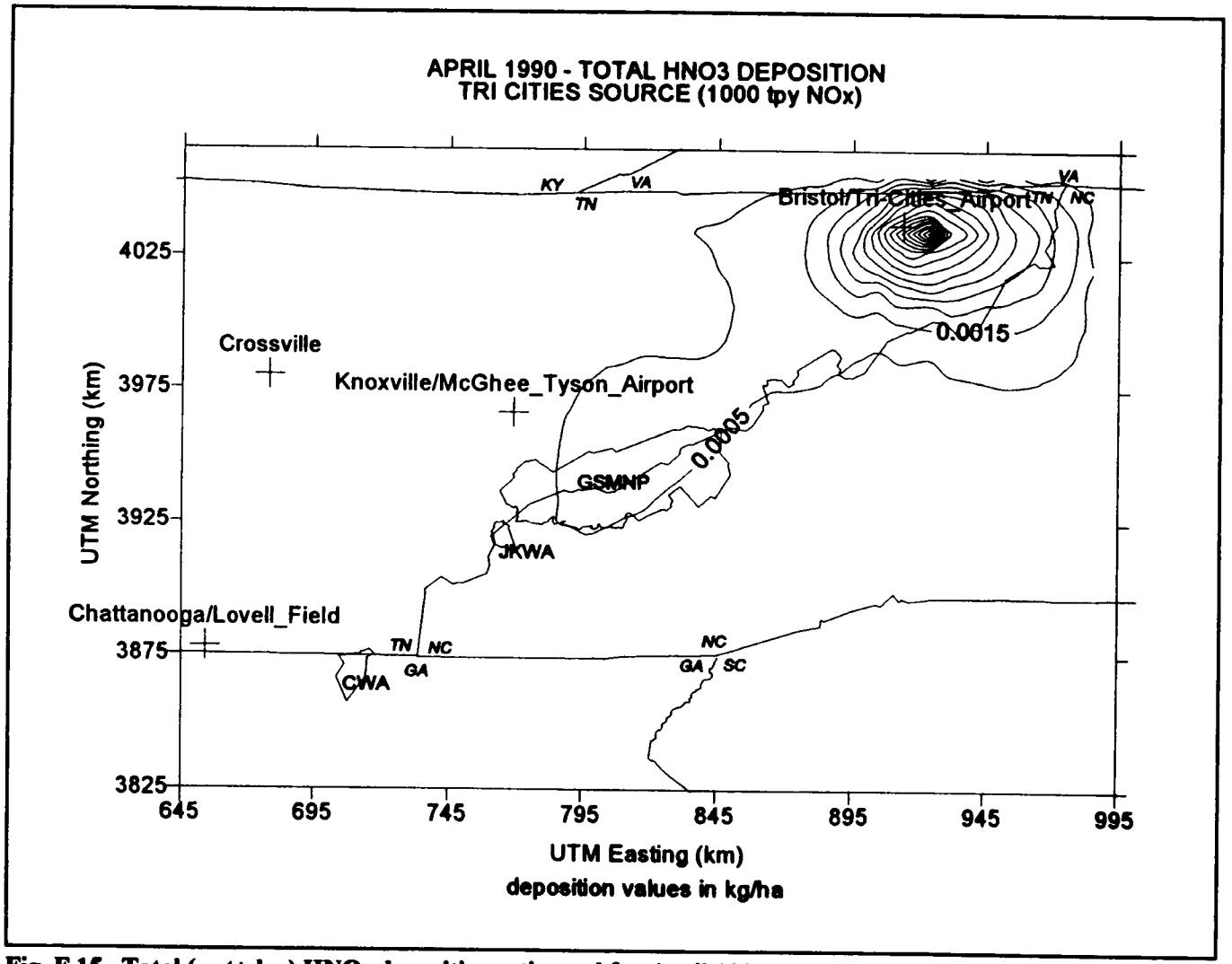

Fig. F.15. Total (wet+dry) HNO_3 deposition estimated for April 1990 resulting from a 28.8 g/s (1000 tpy) hypothetical NO_x emission source located at Bristol/Tri Cities Airport.

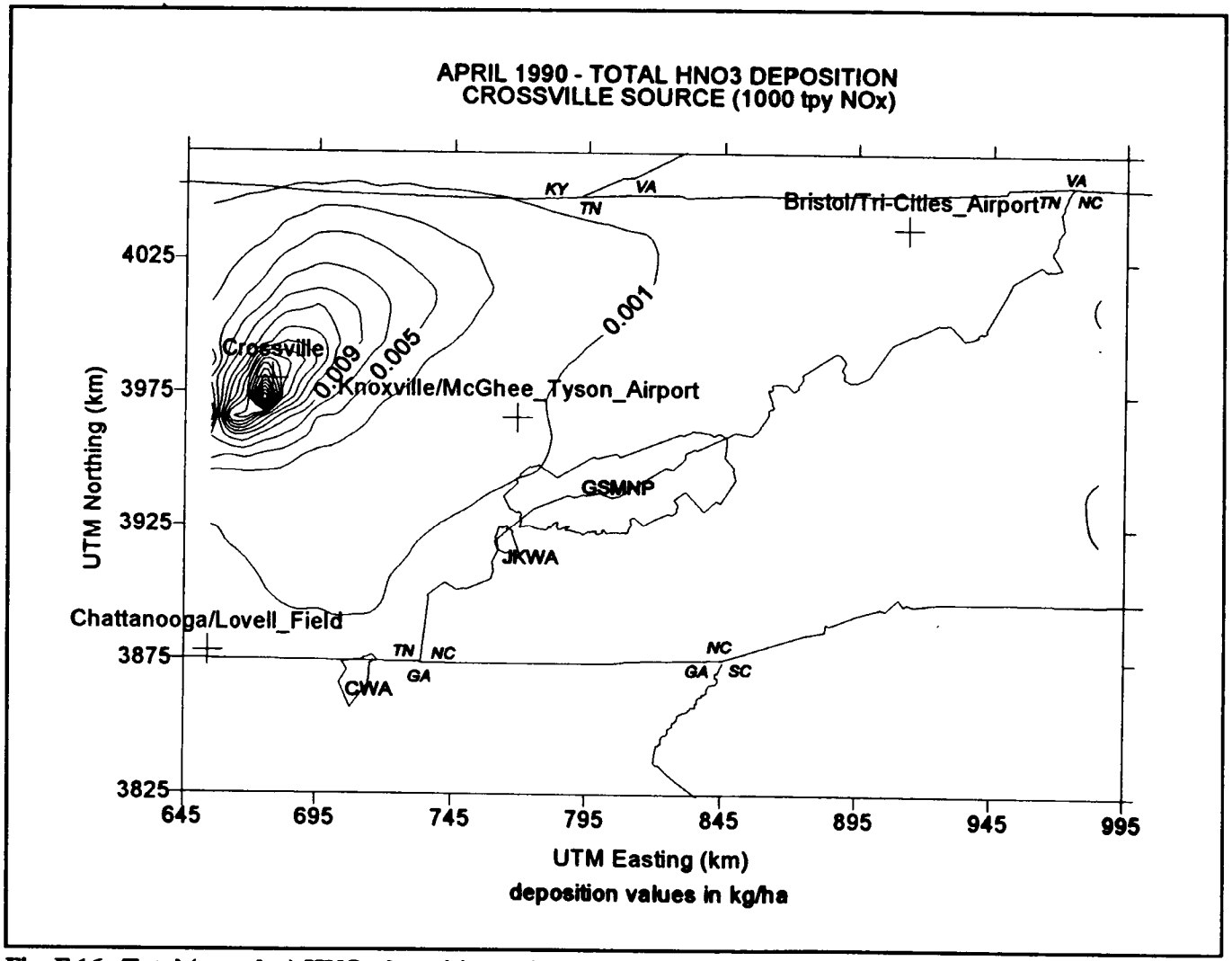

Fig. F.16. Total (wet+dry) HNO_3 deposition estimated for April 1990 resulting from a 28.8 g/s (1000 tpy) hypothetical NO_x emission source located in Crossville.

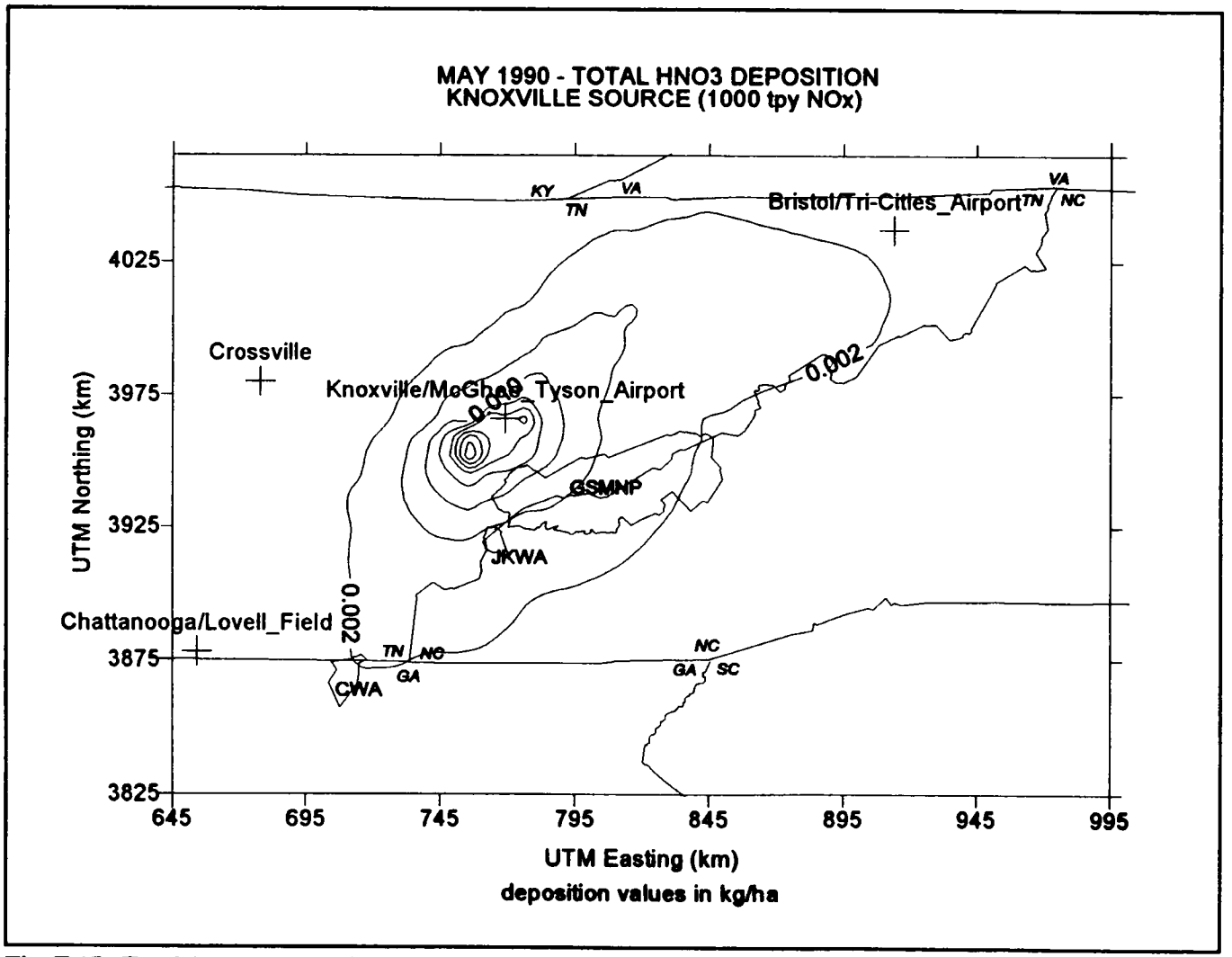

Fig. F.17. Total (wet+dry) HNO_3 deposition estimated for May 1990 resulting from a 28.8 g/s (1000 tpy) hypothetical NO_x emission source located at Knoxville /McGhee Tyson Airport.

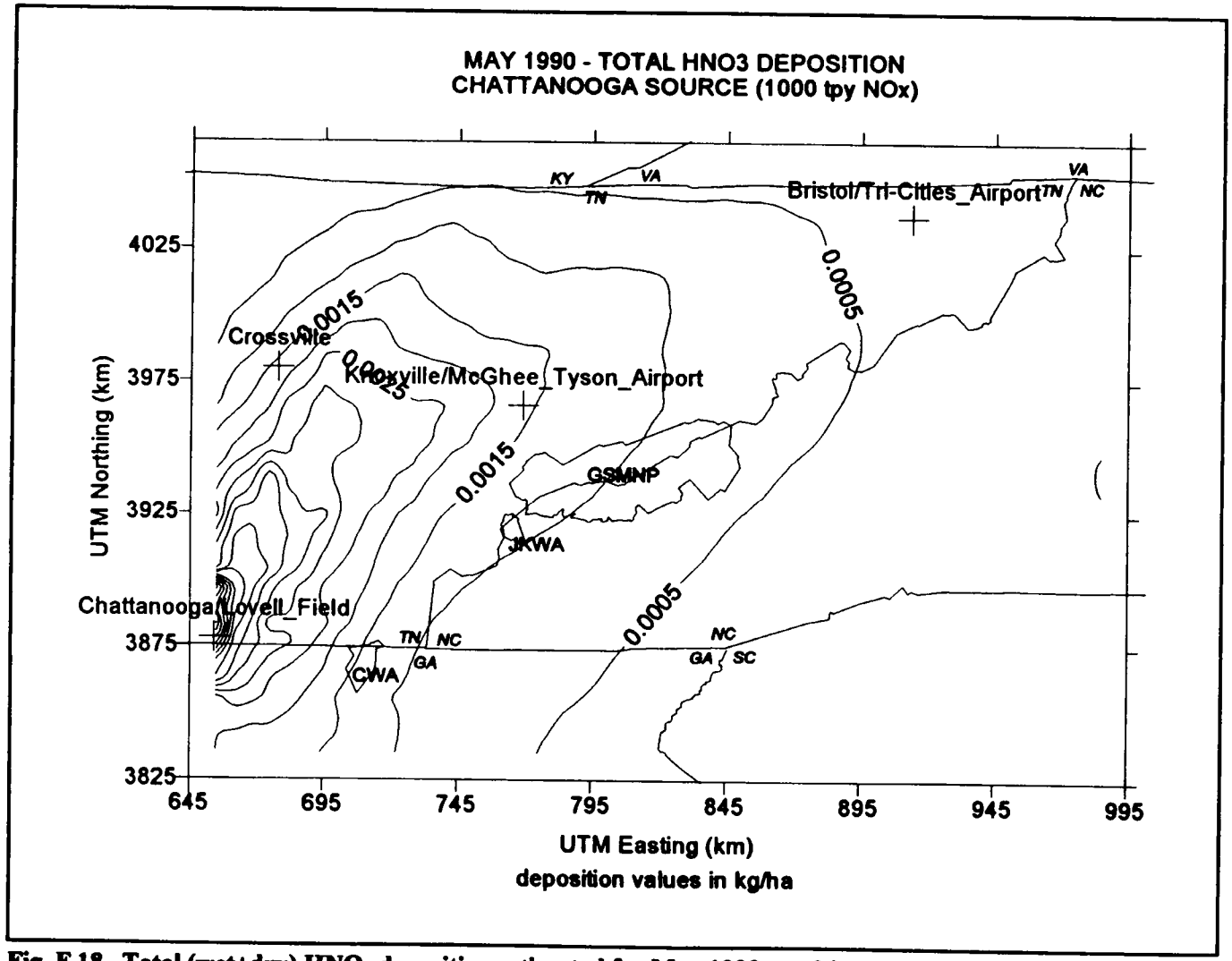

Fig. F.18. Total (wet+dry) HNO_3 deposition estimated for May 1990 resulting from a 28.8 g/s (1000 tpy) hypothetical NO_x emission source located at Chattanooga/Lovell Field.

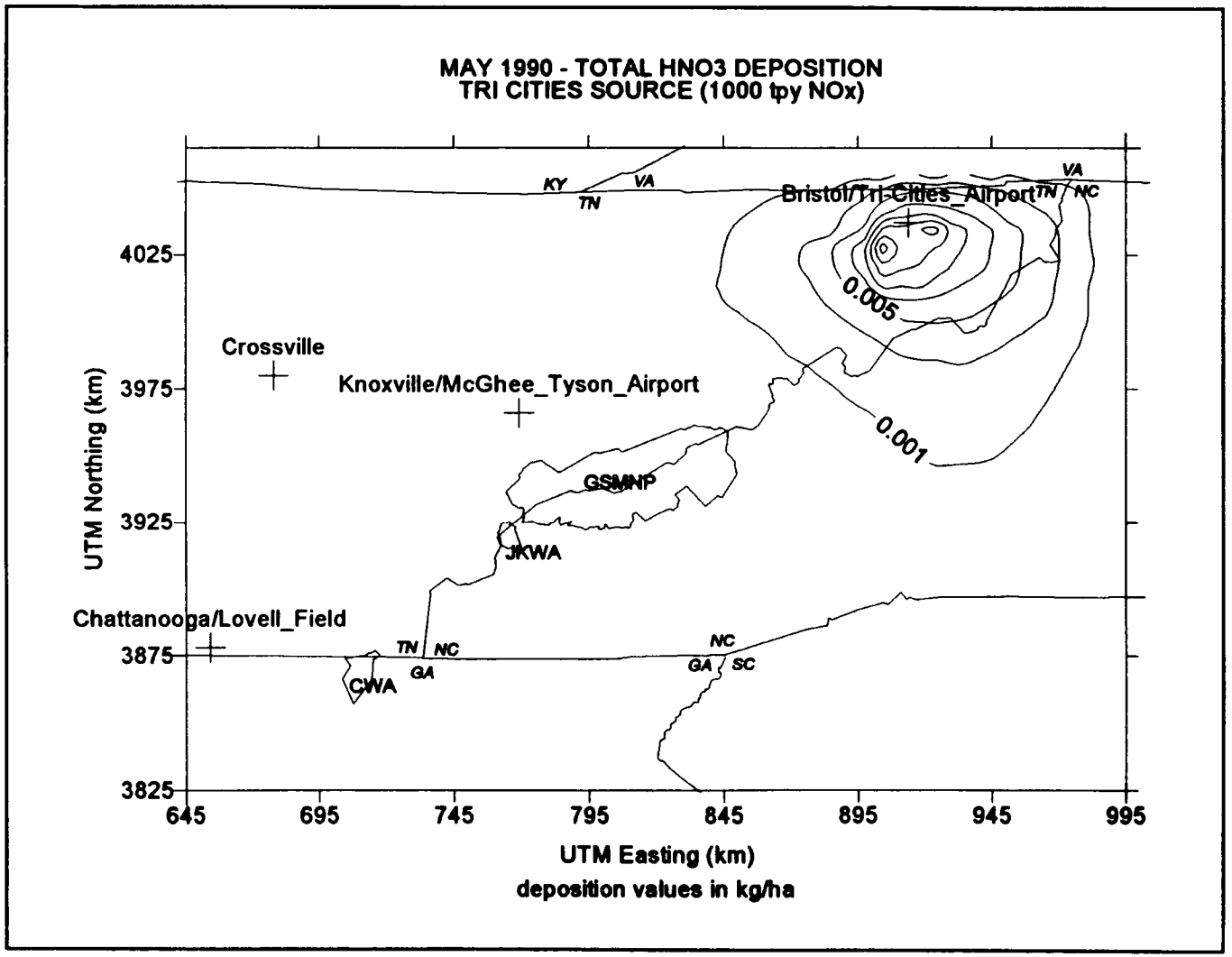

Fig. F.19. Total (wet+dry) HNO_3 deposition estimated for May 1990 resulting from a 28.8 g/s (1000 tpy) hypothetical NO_x emission source located at Bristol/Tri Cities Airport.

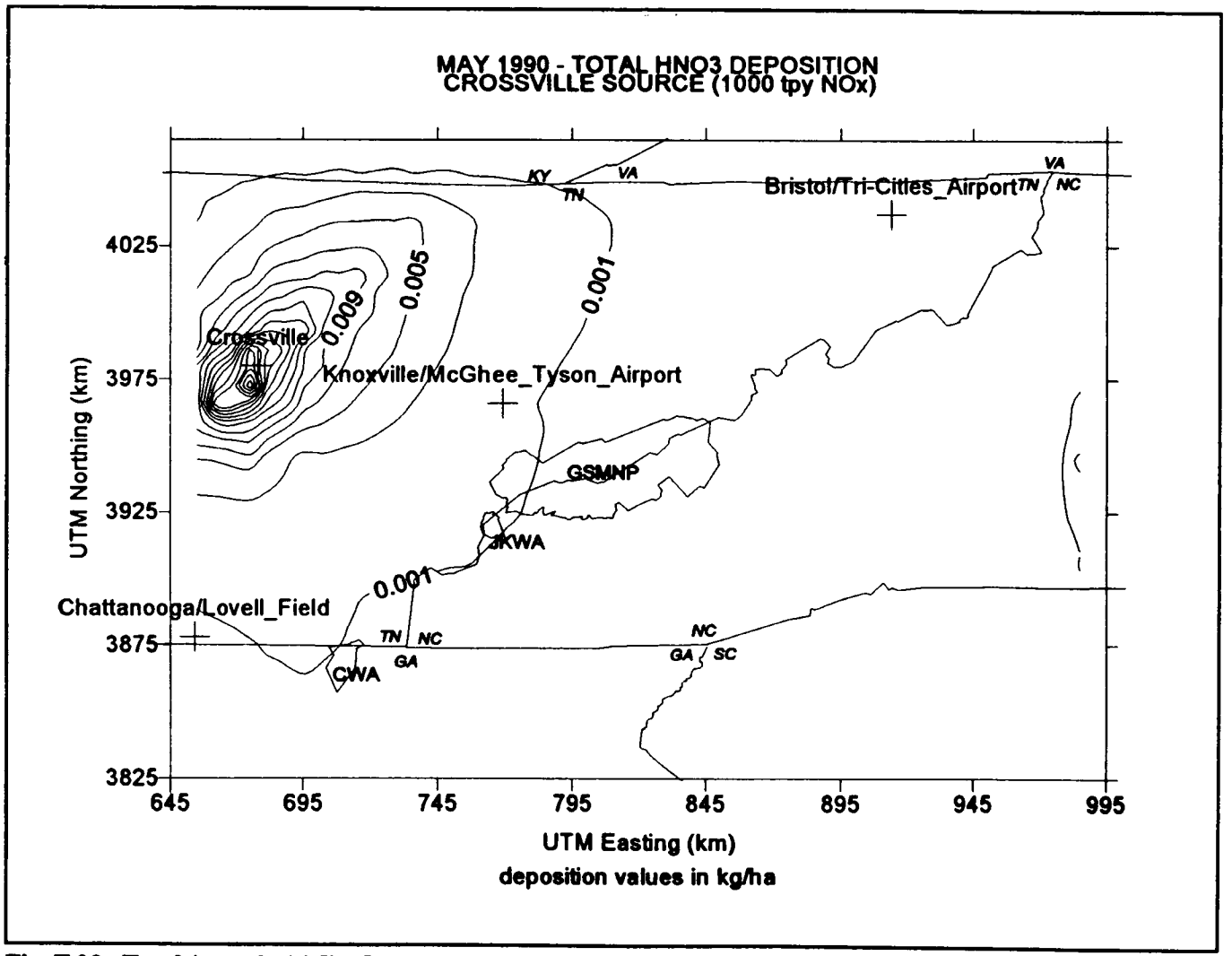

Fig. F.20. Total (wet+dry)) HNO_3 deposition estimated for May 1990 resulting from a 28.8 g/s (1000 tpy) hypothetical NO_x emission source located in Crossville.

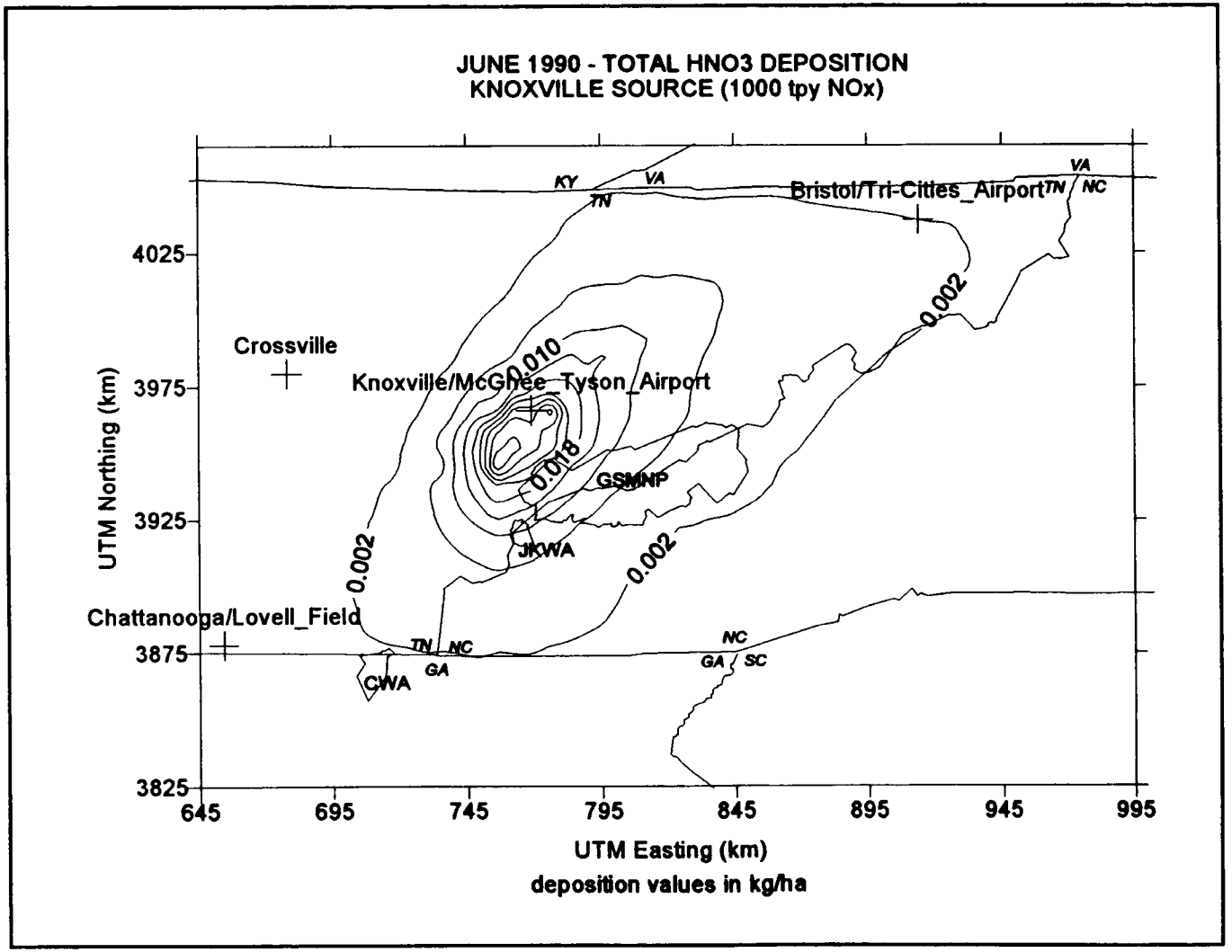

Fig. F.21. Total (wet+dry) HNO_3 deposition estimated for June 1990 resulting from a 28.8 g/s (1000 tpy) hypothetical NO_x emission source located at Knoxville /McGhee Tyson Airport.

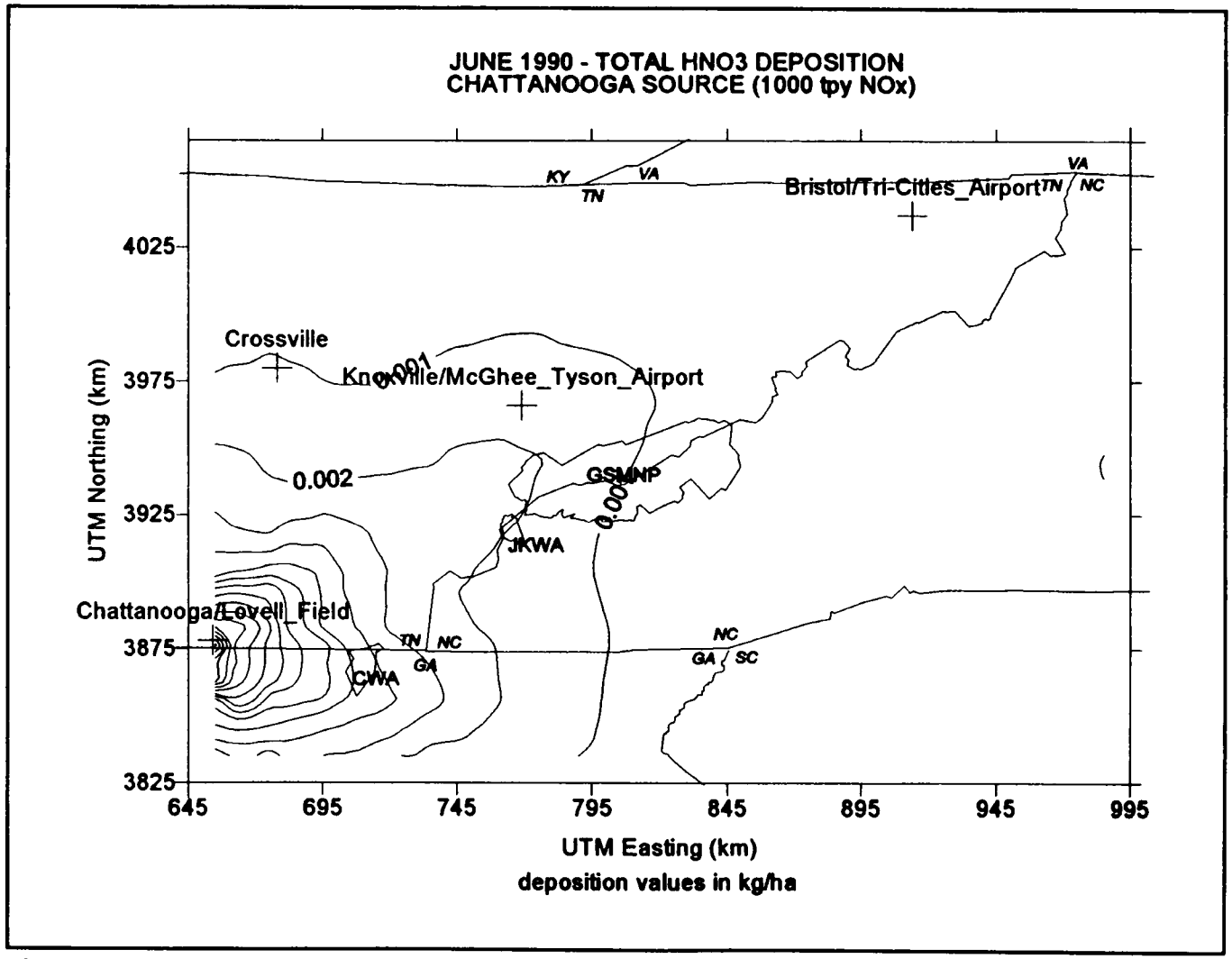

Fig. F.22. Total (wet+dry) HNO_3 deposition estimated for June 1990 resulting from a 28.8 g/s (1000 tpy) hypothetical NO_x emission source located at Chattanooga/Lovell Field.

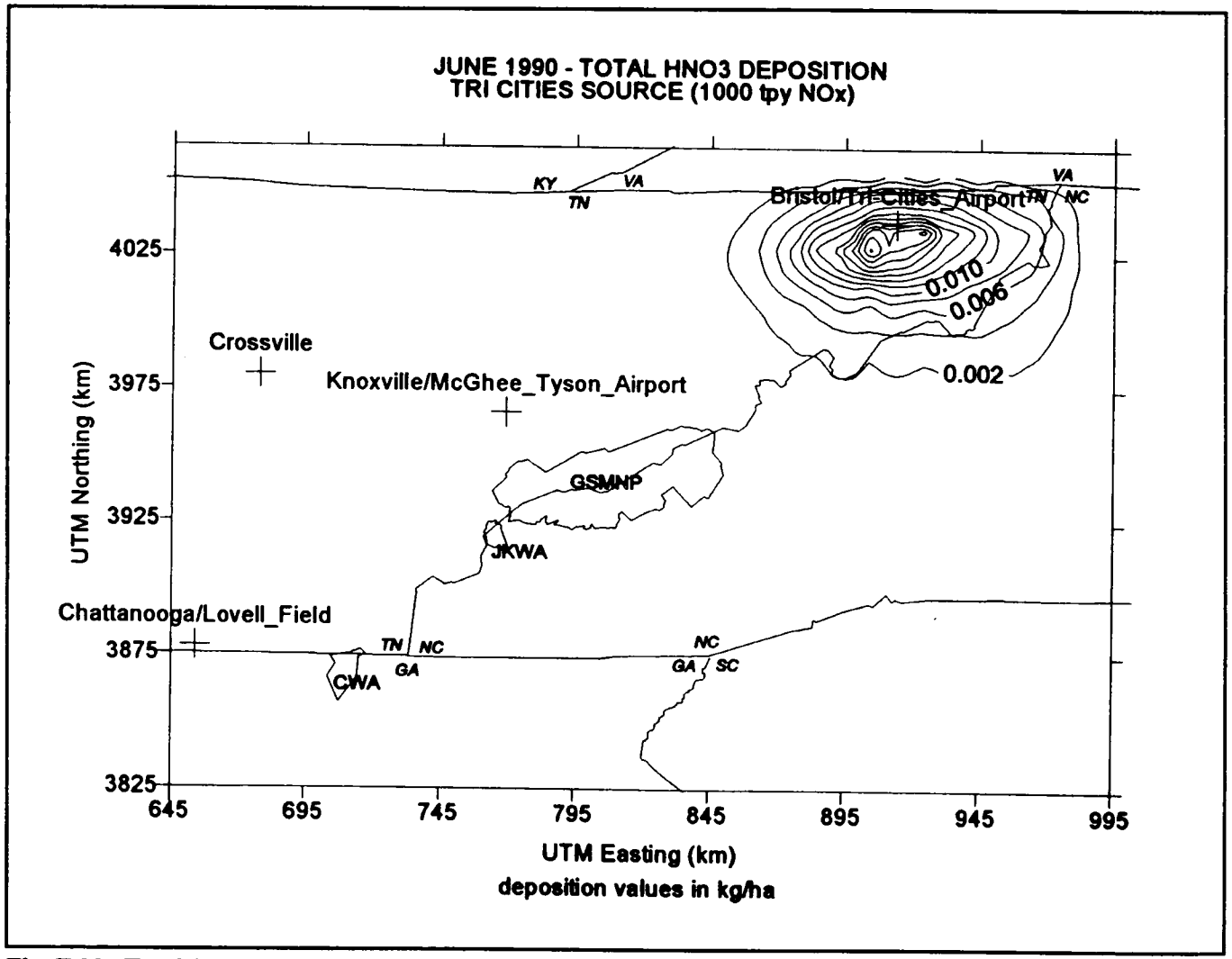

Fig. F.23. Total (wet+dry) HNO_3 deposition estimated for June 1990 resulting from a 28.8 g/s (1000 tpy) hypothetical NO_x emission source located at Bristol/Tri Cities Airport.

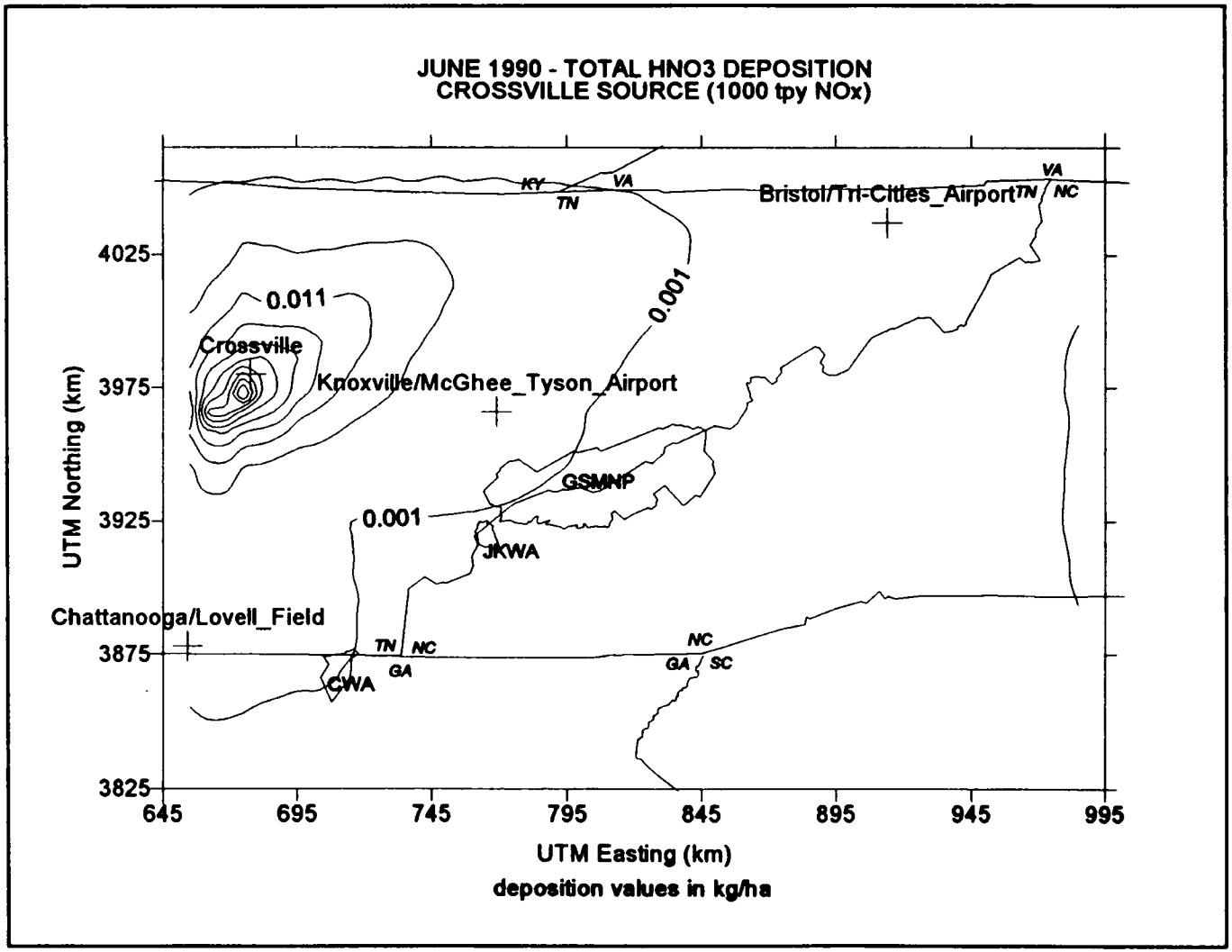

Fig. F.24. Total (wet+dry) HNO_3 deposition estimated for June 1990 resulting from a 28.8 g/s (1000 tpy) hypothetical NO_x emission source located in Crossville.

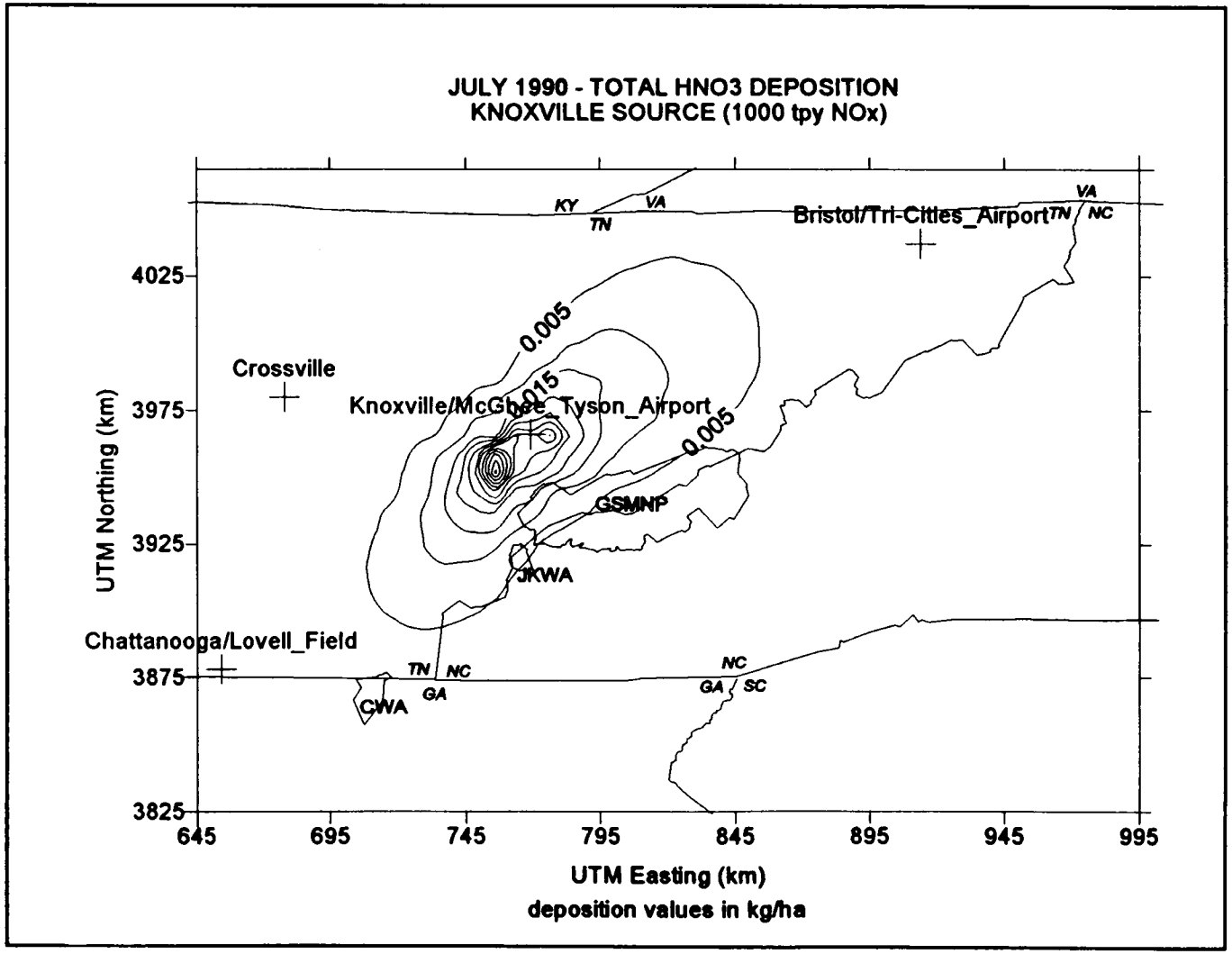

Fig. F.25. Total (wet+dry) HNO_3 deposition estimated for July 1990 resulting from a 28.8 g/s (1000 tpy) hypothetical NO_x emission source located at Knoxville /McGhee Tyson Airport.

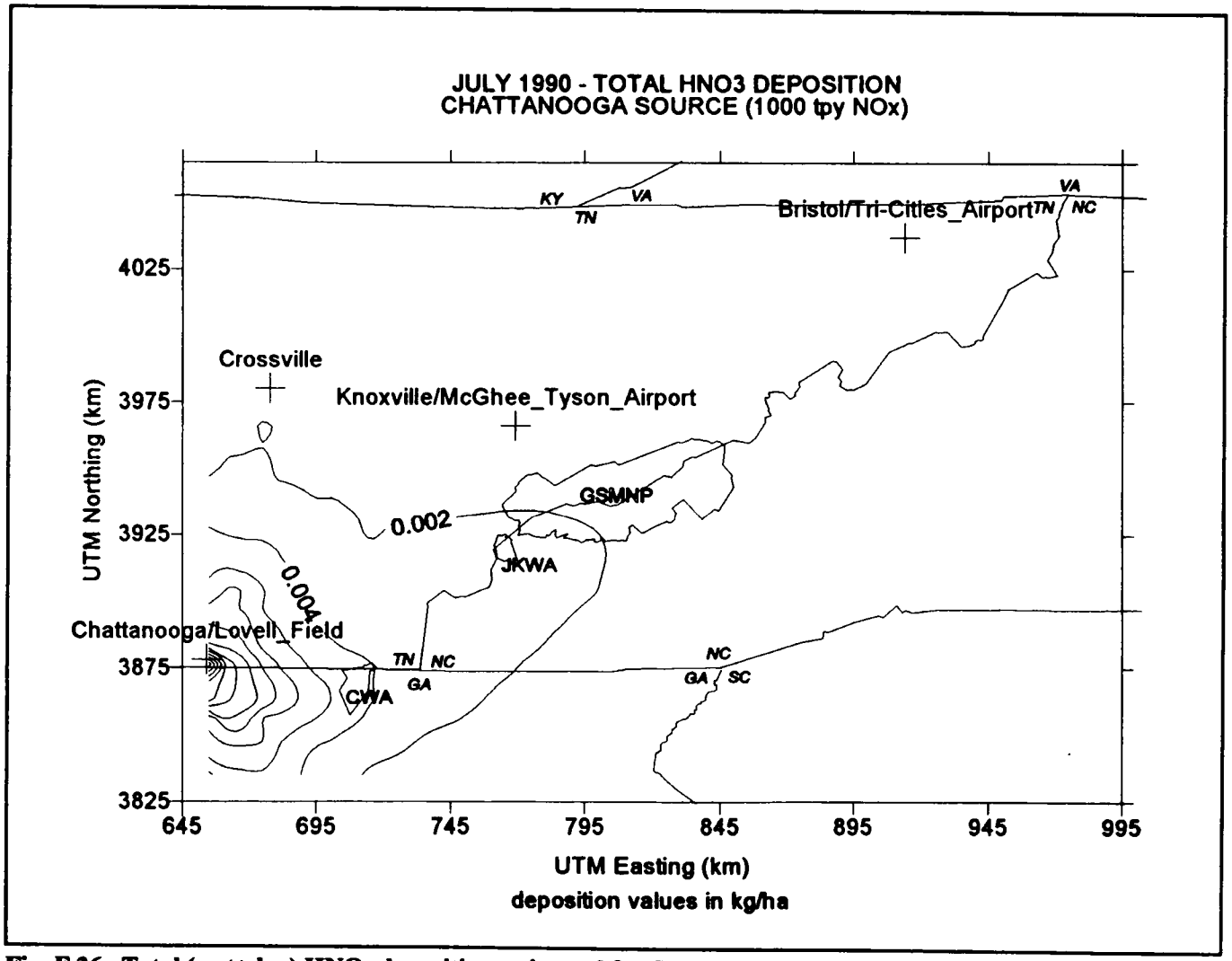

Fig. F.26. Total (wet+dry) HNO_3 deposition estimated for July 1990 resulting from a 28.8 g/s (1000 tpy) hypothetical NO_x emission source located at Chattanooga/Lovell Field.

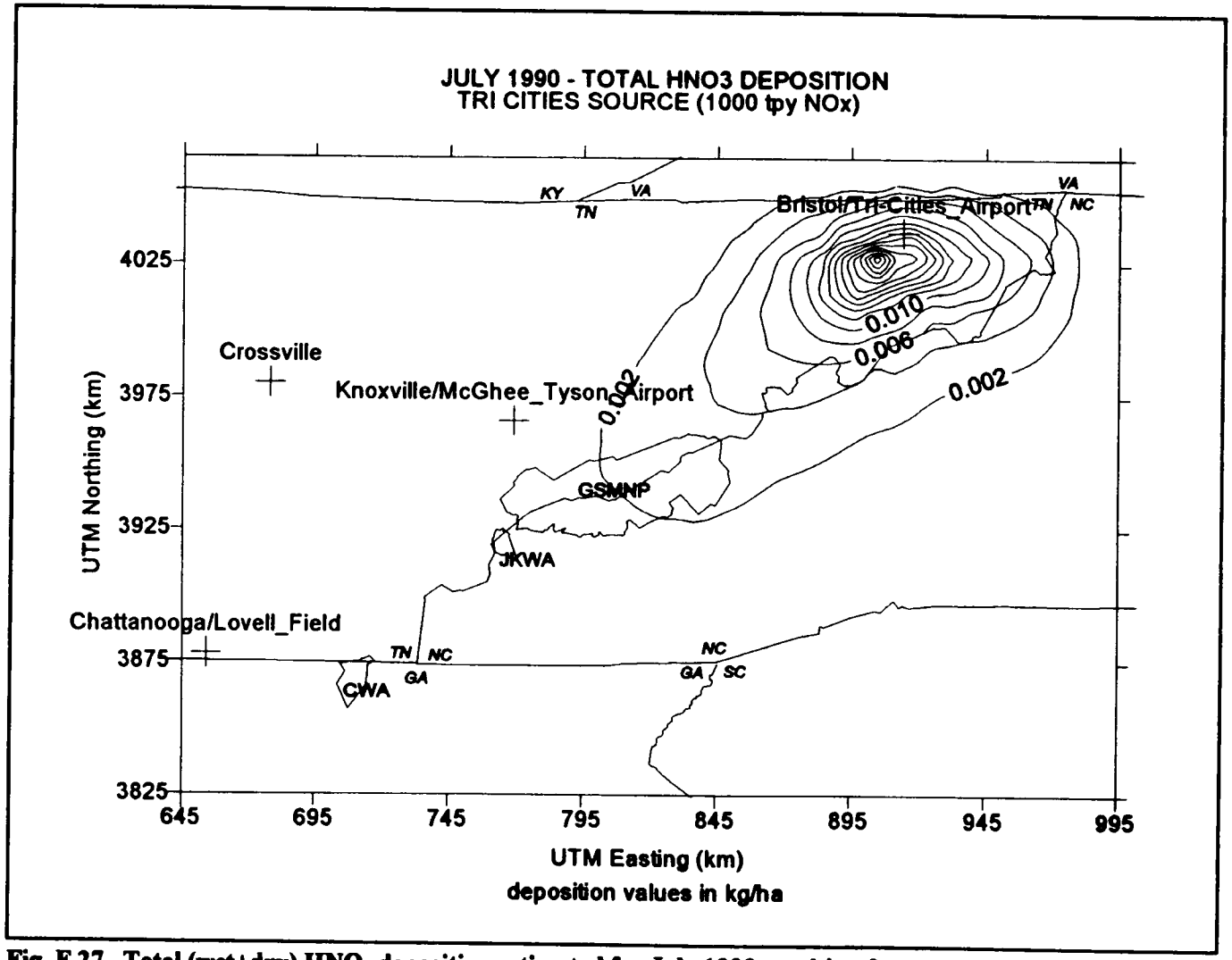

Fig. F.27. Total (wet+dry) HNO_3 deposition estimated for July 1990 resulting from a 28.8 g/s (1000 tpy) hypothetical NO_x emission source located at Bristol/Tri Cities Airport.

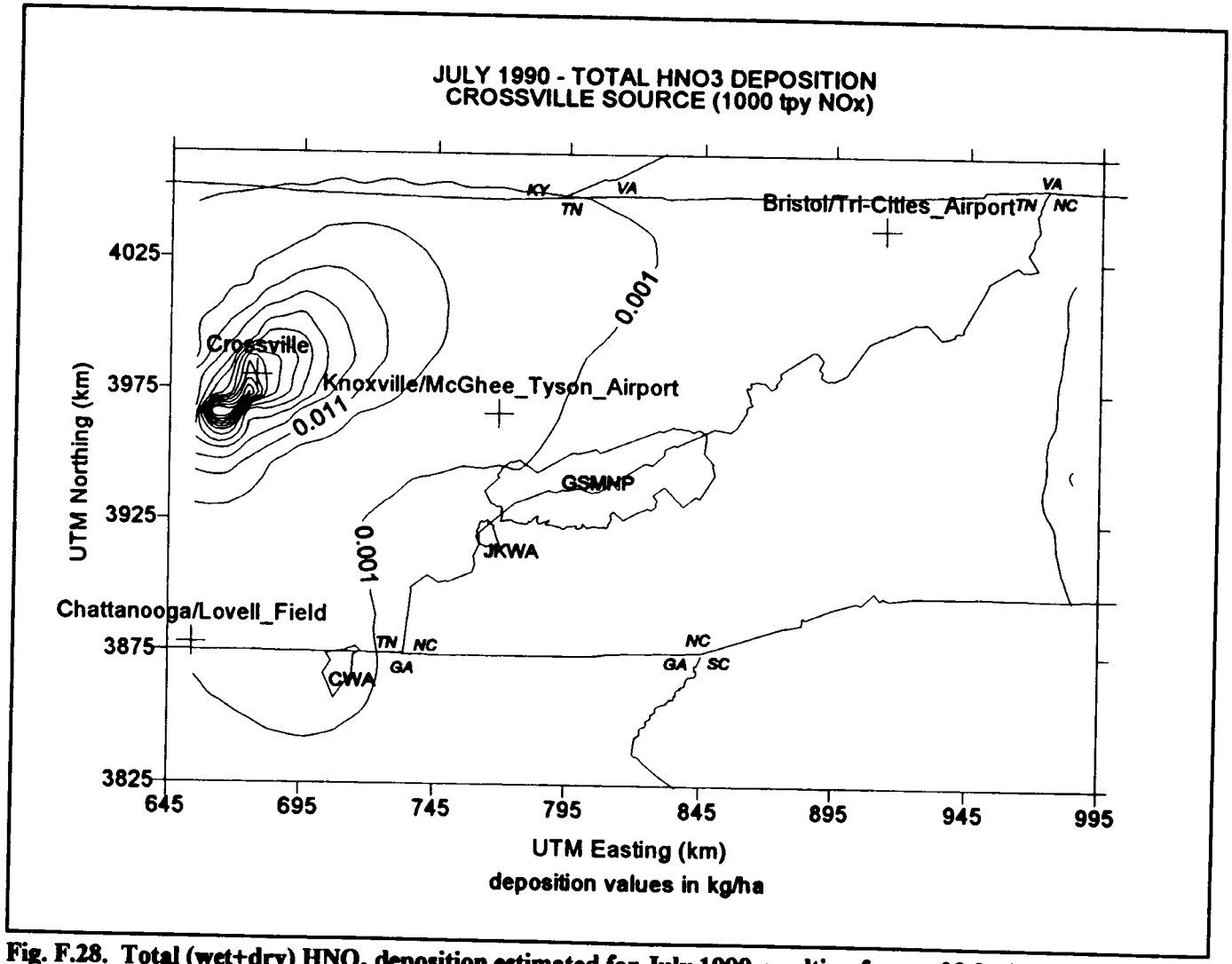

Fig. F.28. Total (wet+dry) HNO_3 deposition estimated for July 1990 resulting from a 28.8 g/s (1000 tpy) hypothetical NO_x emission source located in Crossville.

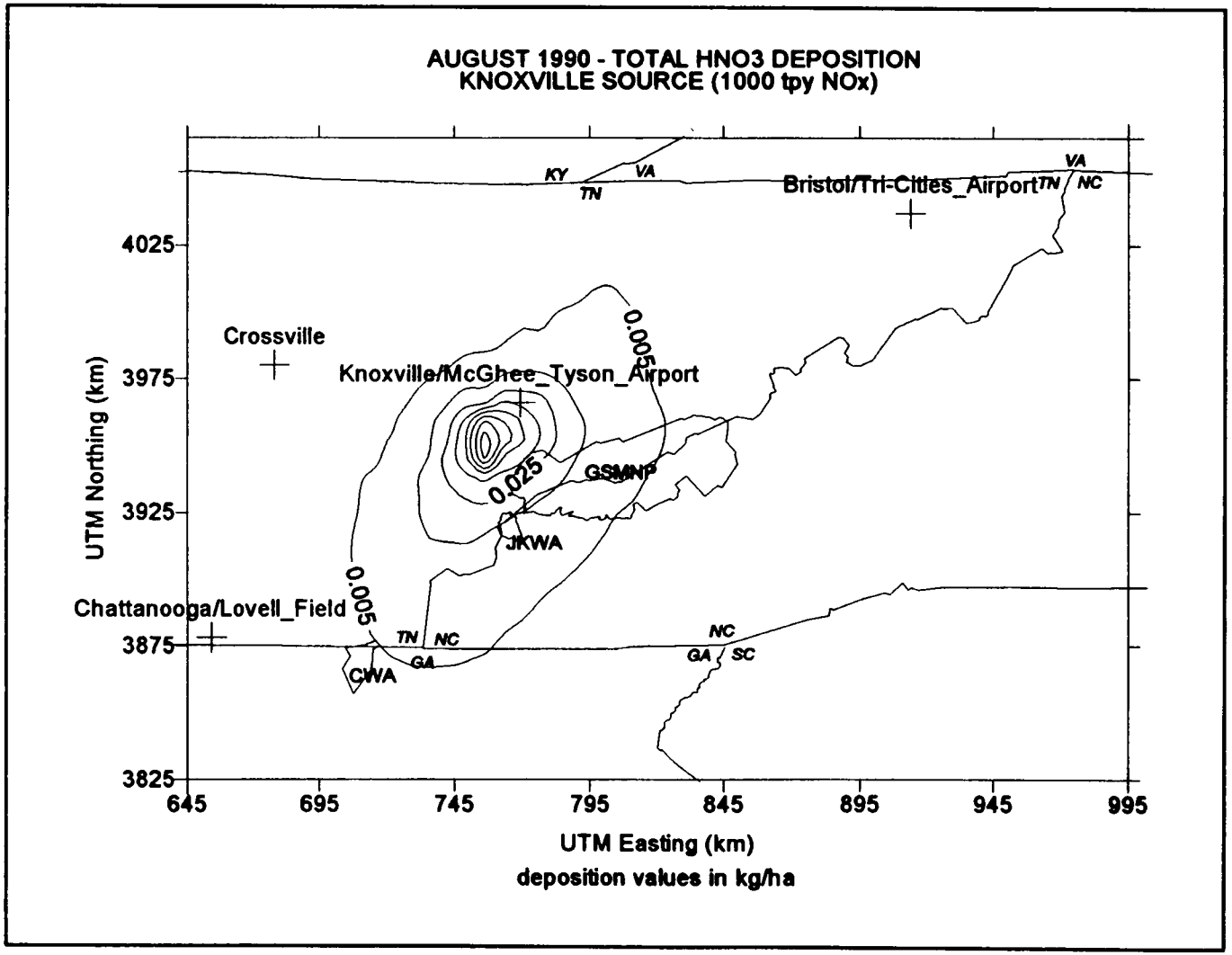

Fig. F.29. Total (wet+dry) HNO_3 deposition estimated for August 1990 resulting from a 28.8 g/s (1000 tpy) hypothetical NO_x emission source located at Knoxville /McGhee Tyson Airport.

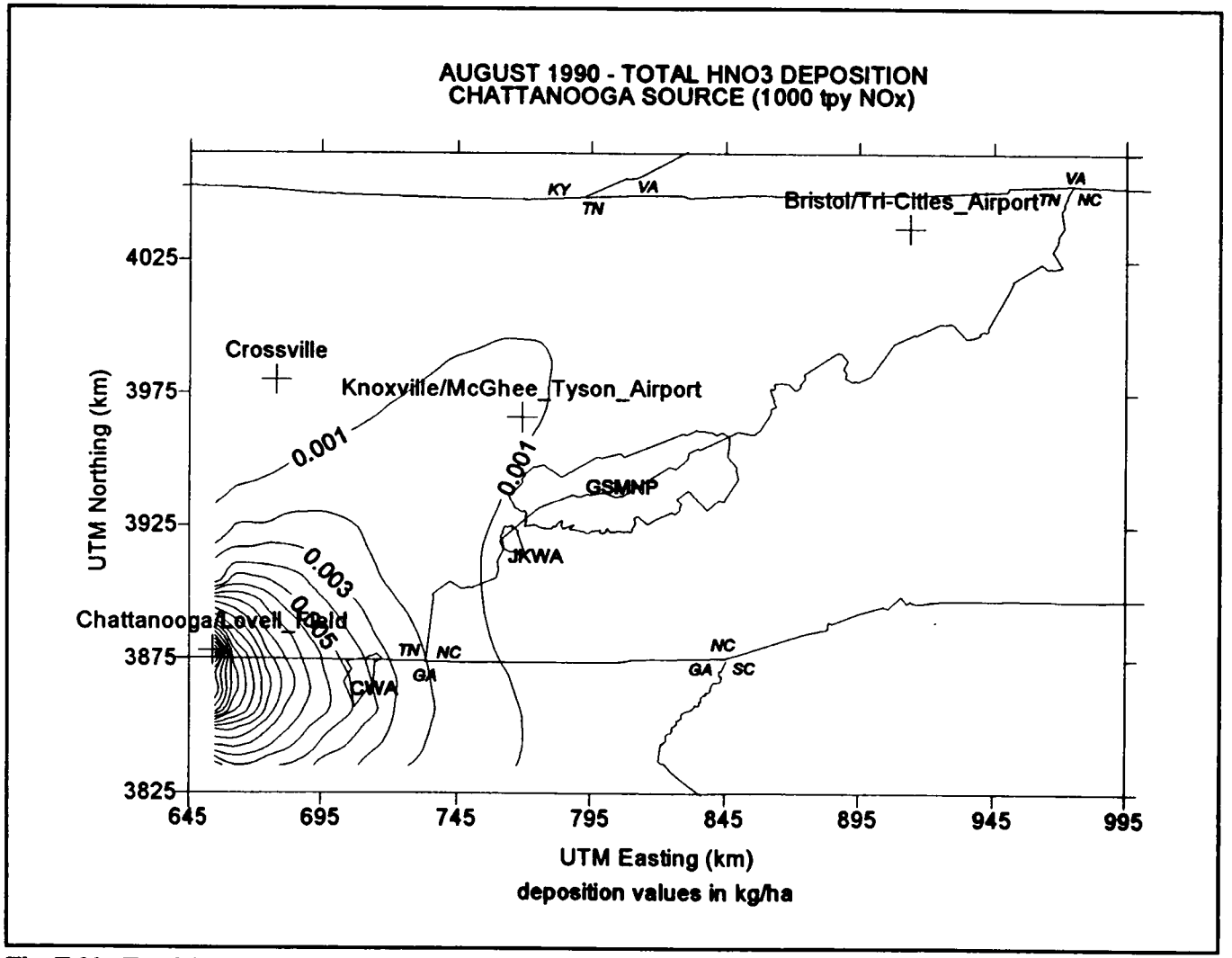

Fig. F.30. Total (wet+dry) HNO_3 deposition estimated for August 1990 resulting from a 28.8 g/s (1000 tpy) hypothetical NO_x emission source located at Chattanooga/Lovell Field.

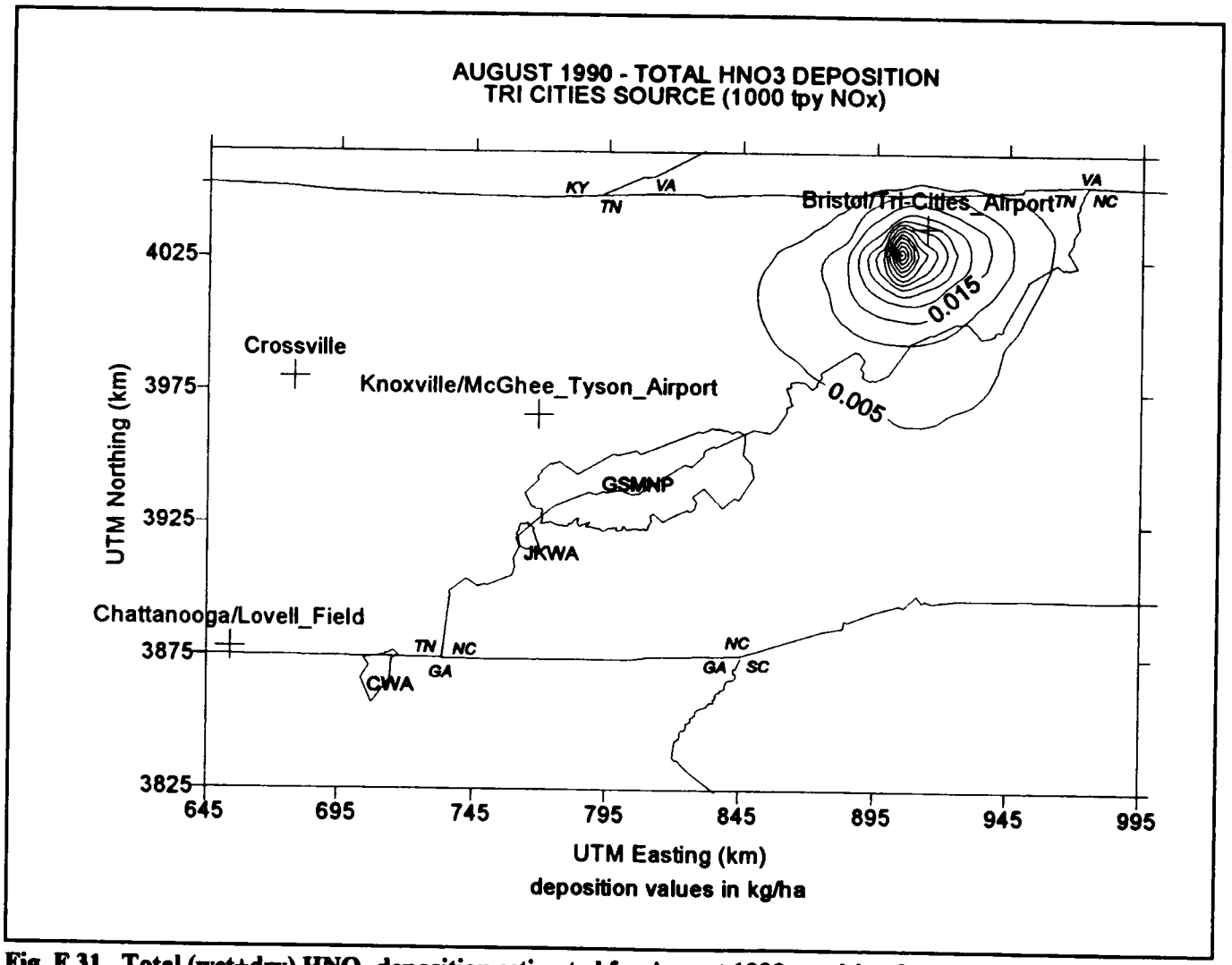

Fig. F.31. Total (wet+dry) HNO_3 deposition estimated for August 1990 resulting from a 28.8 g/s (1000 tpy) hypothetical NO_x emission source located at Bristol/Tri Cities Airport.

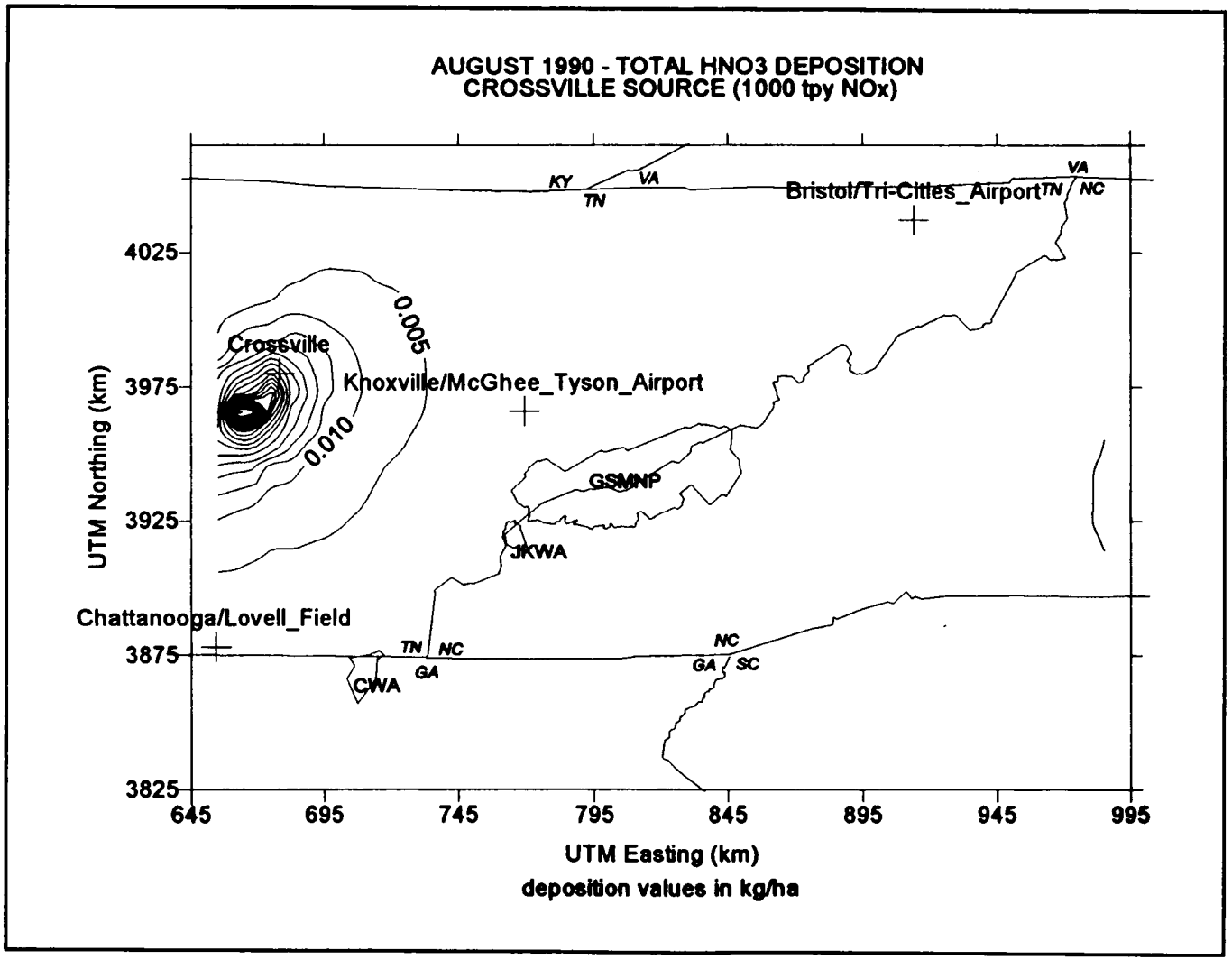

Fig. F.32. Total (wet+dry) HNO_3 deposition estimated for August 1990 resulting from a 28.8 g/s (1000 tpy) hypothetical NO_x emission source located in Crossville.

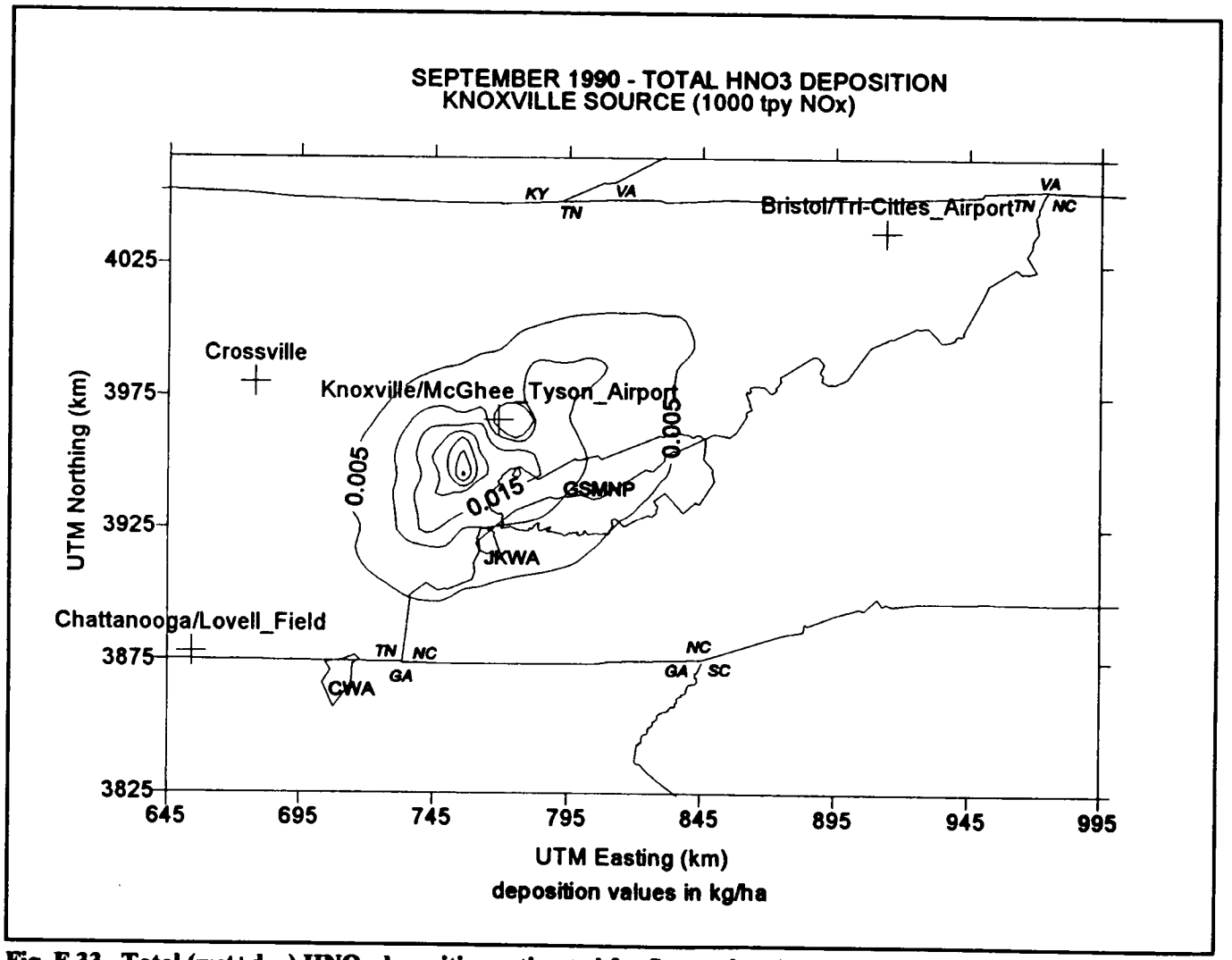

Fig. F.33. Total (wet+dry) HNO_3 deposition estimated for September 1990 resulting from a 28.8 g/s (1000 tpy) hypothetical NO_x emission source located at Knoxville /McGhee Tyson Airport.

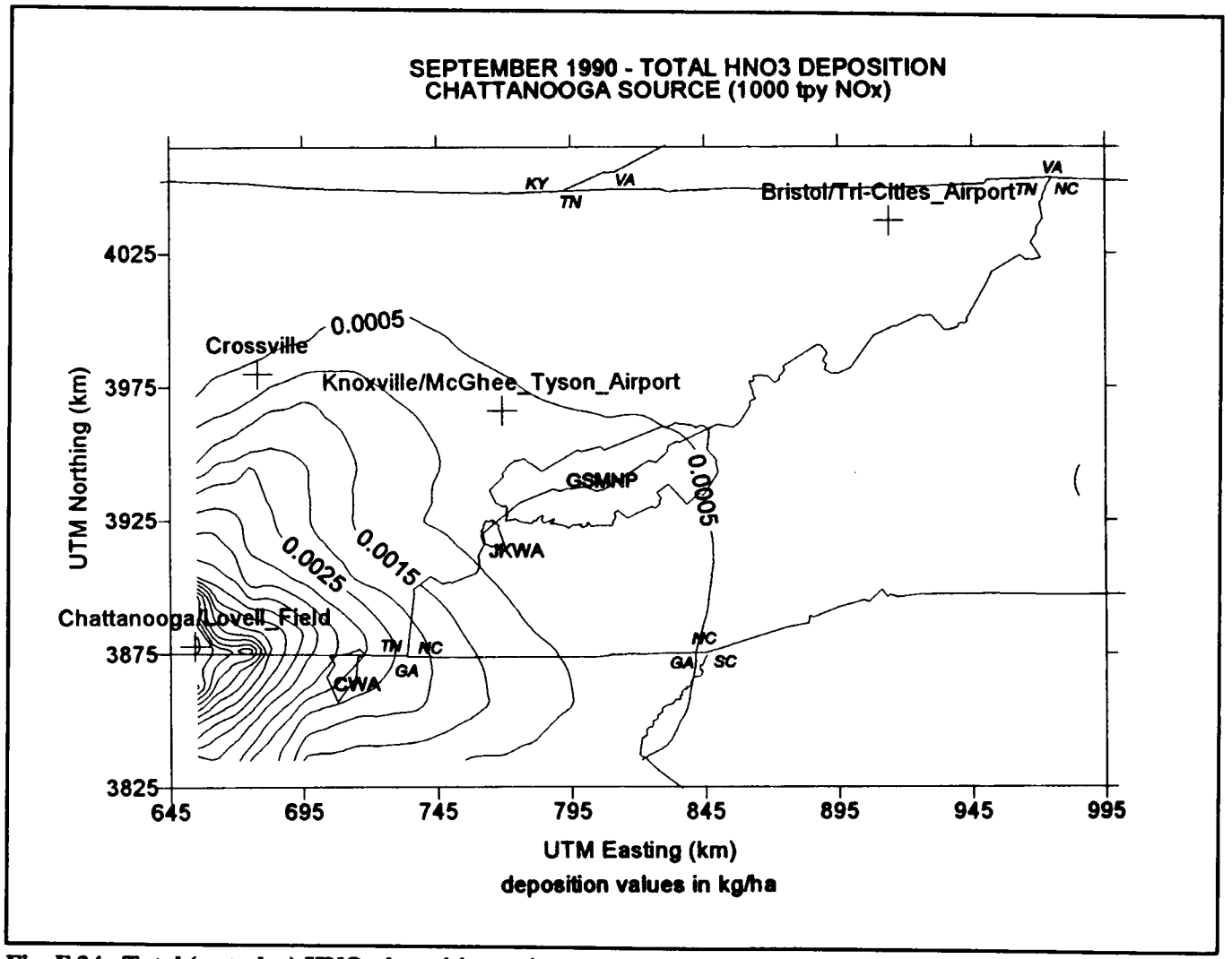

Fig. F.34. Total (wet+dry) HNO_3 deposition estimated for September 1990 resulting from a 28.8 g/s (1000 tpy) hypothetical NO_x emission source located at Chattanooga/Lovell Field.

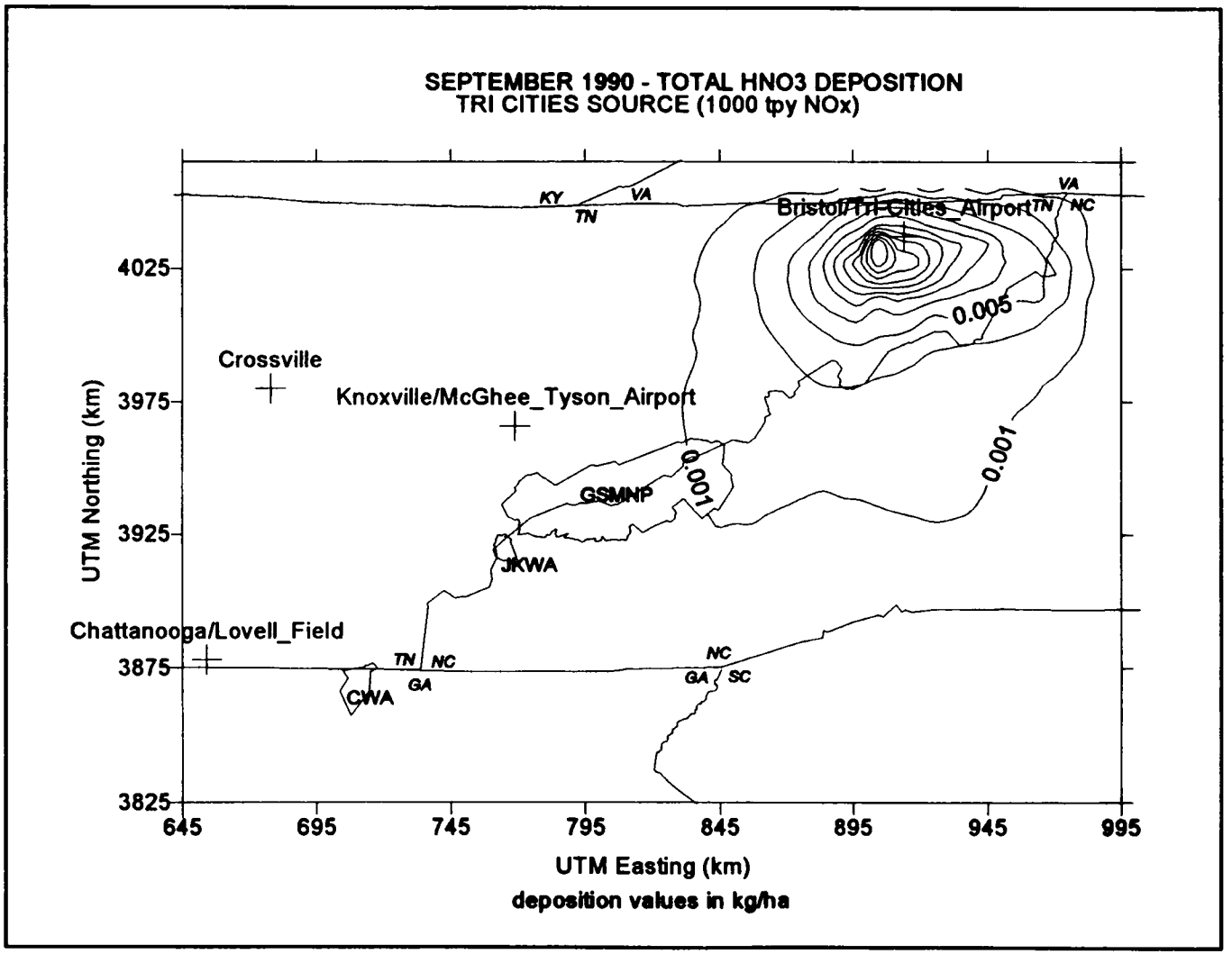

Fig. F.35. Total (wet+dry) HNO_3 deposition estimated for September 1990 resulting from a 28.8 g/s (1000 tpy) hypothetical NO_x emission source located at Bristol/Tri Cities Airport.

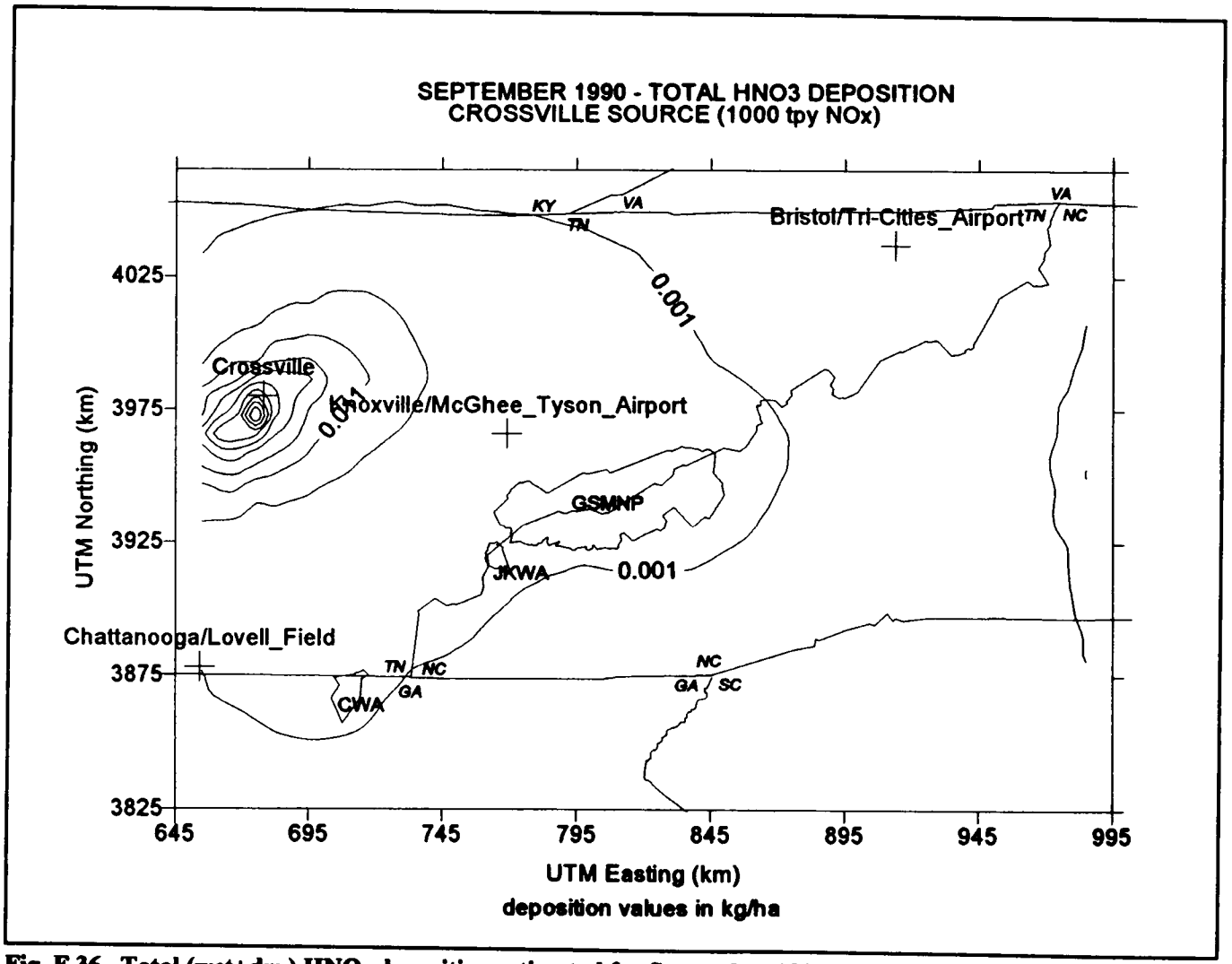

Fig. F.36. Total (wet+dry) HNO_3 deposition estimated for September 1990 resulting from a 28.8 g/s (1000 tpy) hypothetical NO_x emission source located in Crossville.

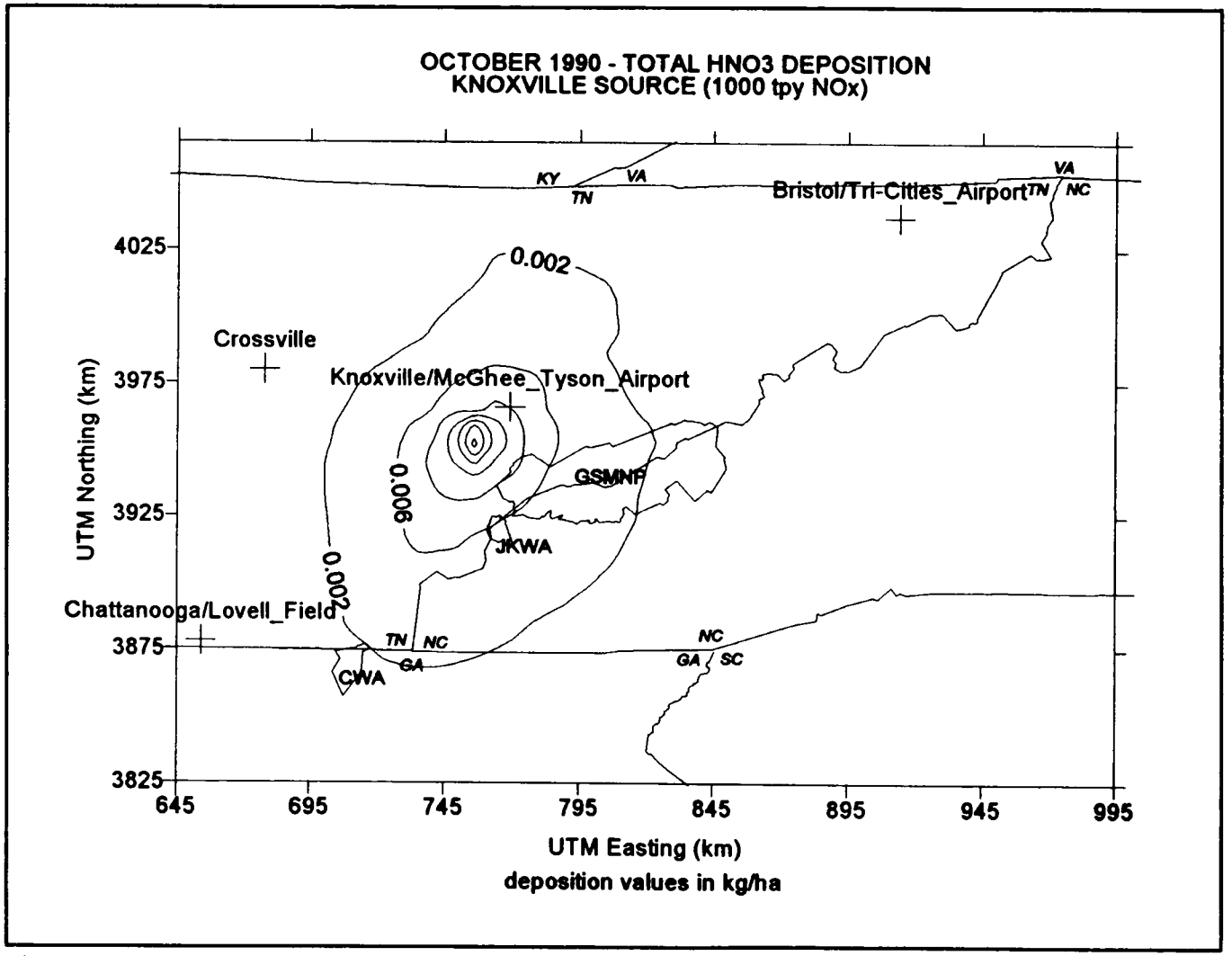

Fig. F.37. Total (wet+dry) HNO_3 deposition estimated for October 1990 resulting from a 28.8 g/s (1000 tpy) hypothetical NO_x emission source located at Knoxville /McGhee Tyson Airport.

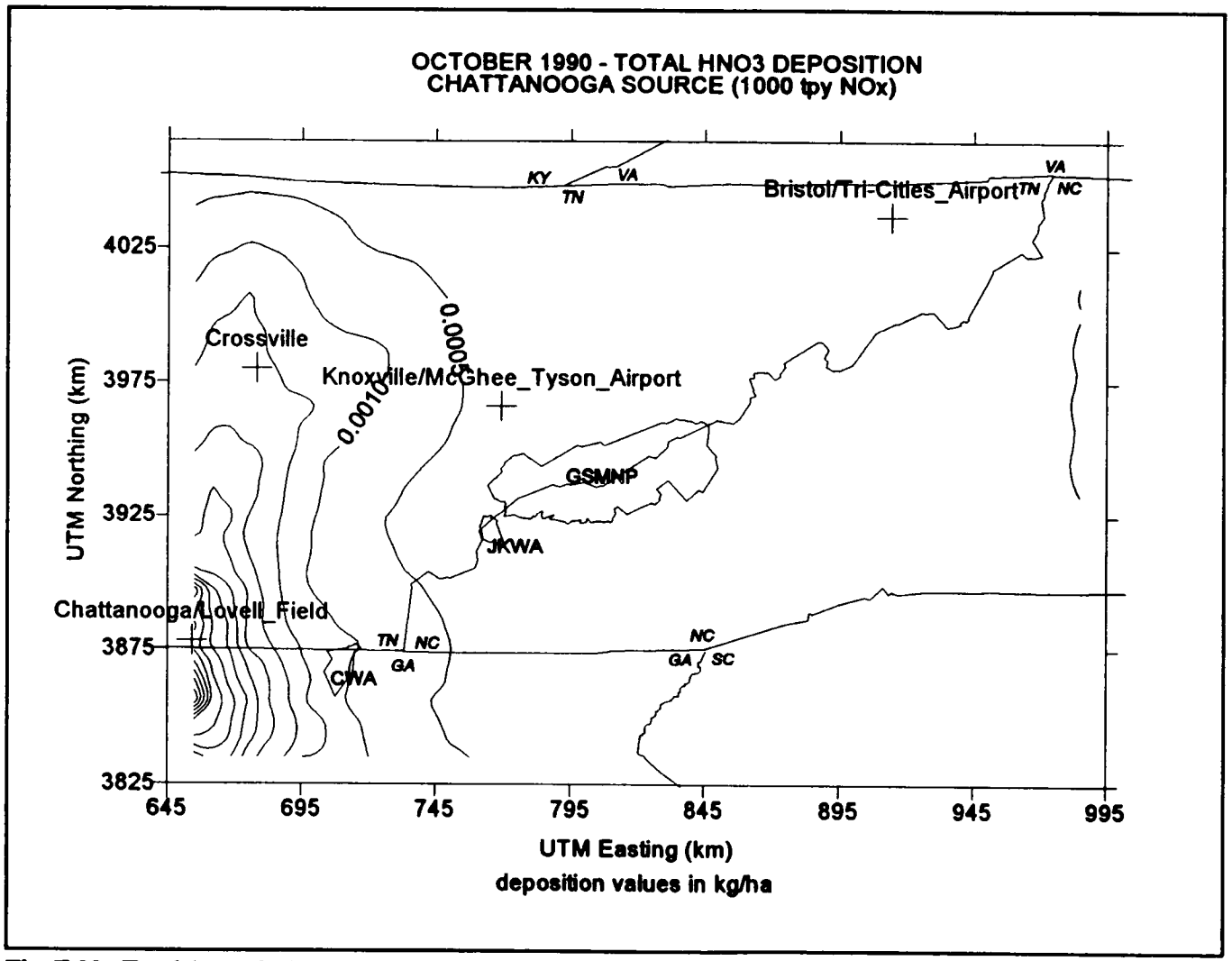

Fig. F.38. Total (wet+dry) HNO_3 deposition estimated for October 1990 resulting from a 28.8 g/s (1000 tpy) hypothetical NO_x emission source located at Chattanooga/Lovell Field.

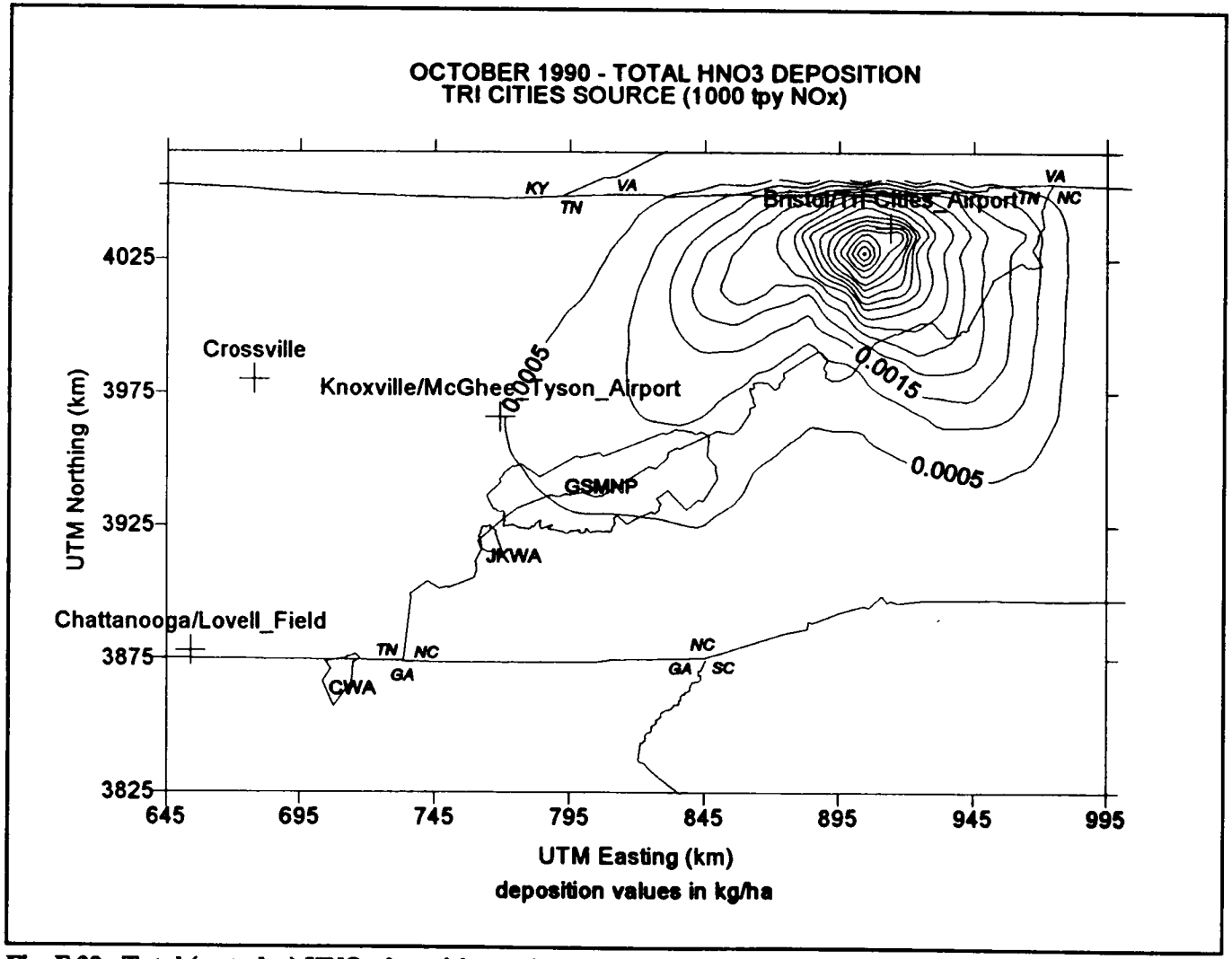

Fig. F.39. Total (wet+dry) HNO_3 deposition estimated for October 1990 resulting from a 28.8 g/s (1000 tpy) hypothetical NO_x emission source located at Bristol/Tri Cities Airport.

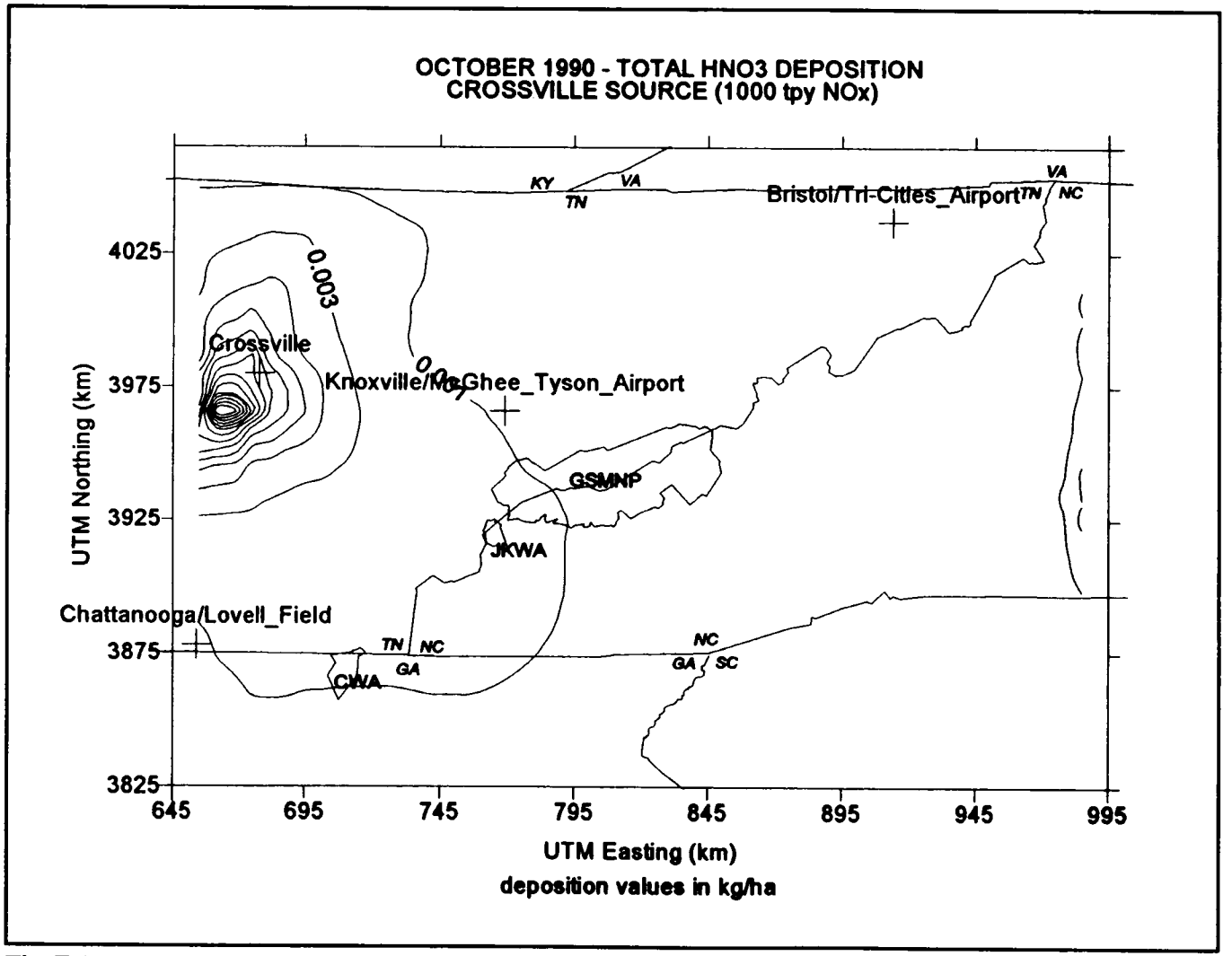

Fig. F.40. Total (wet+dry) HNO_3 deposition estimated for October 1990 resulting from a 28.8 g/s (1000 tpy) hypothetical NO_x emission source located in Crossville.

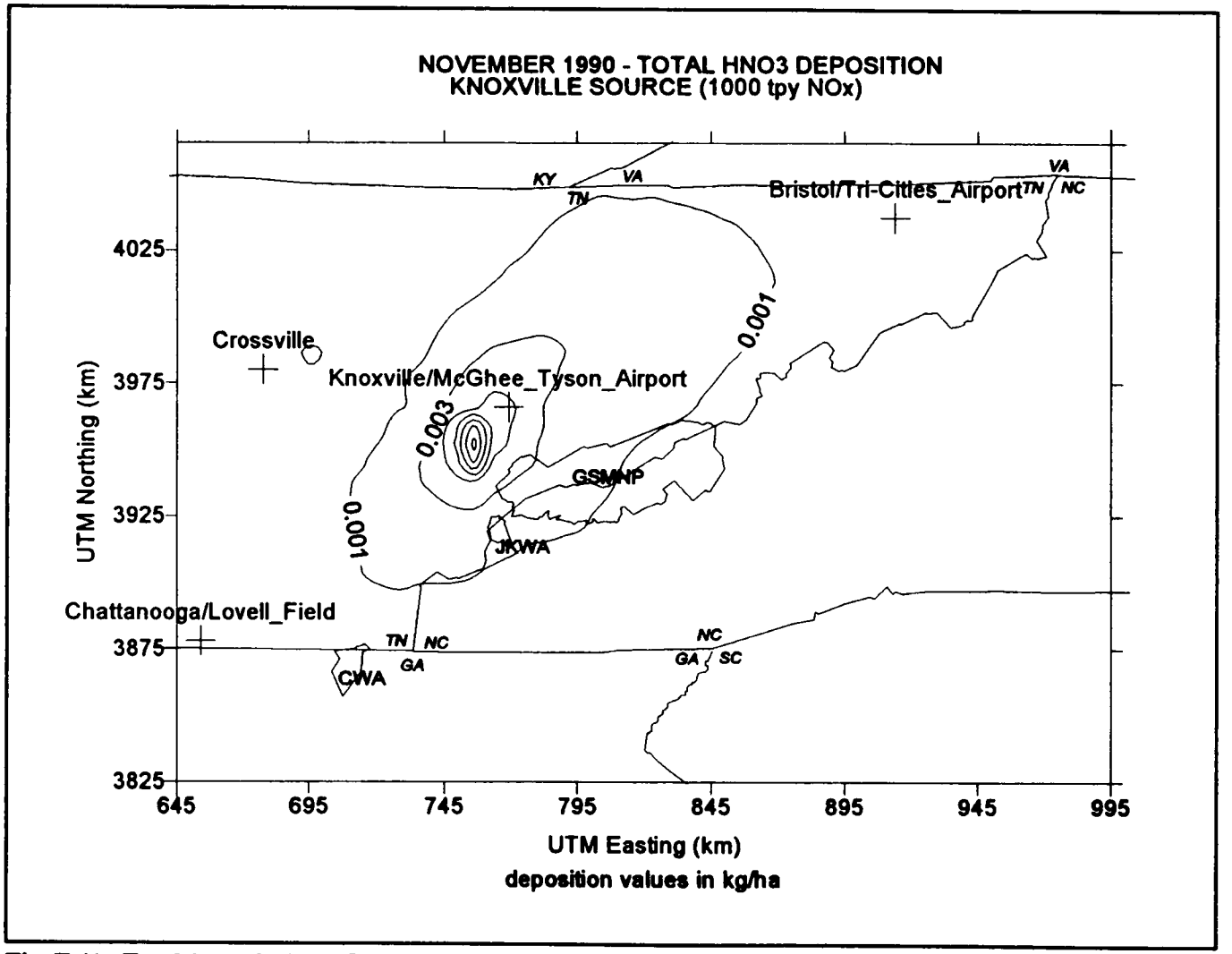

Fig. F.41. Total (wet+dry) HNO_3 deposition estimated for November 1990 resulting from a 28.8 g/s (1000 tpy) hypothetical NO_x emission source located at Knoxville /McGhee Tyson Airport.

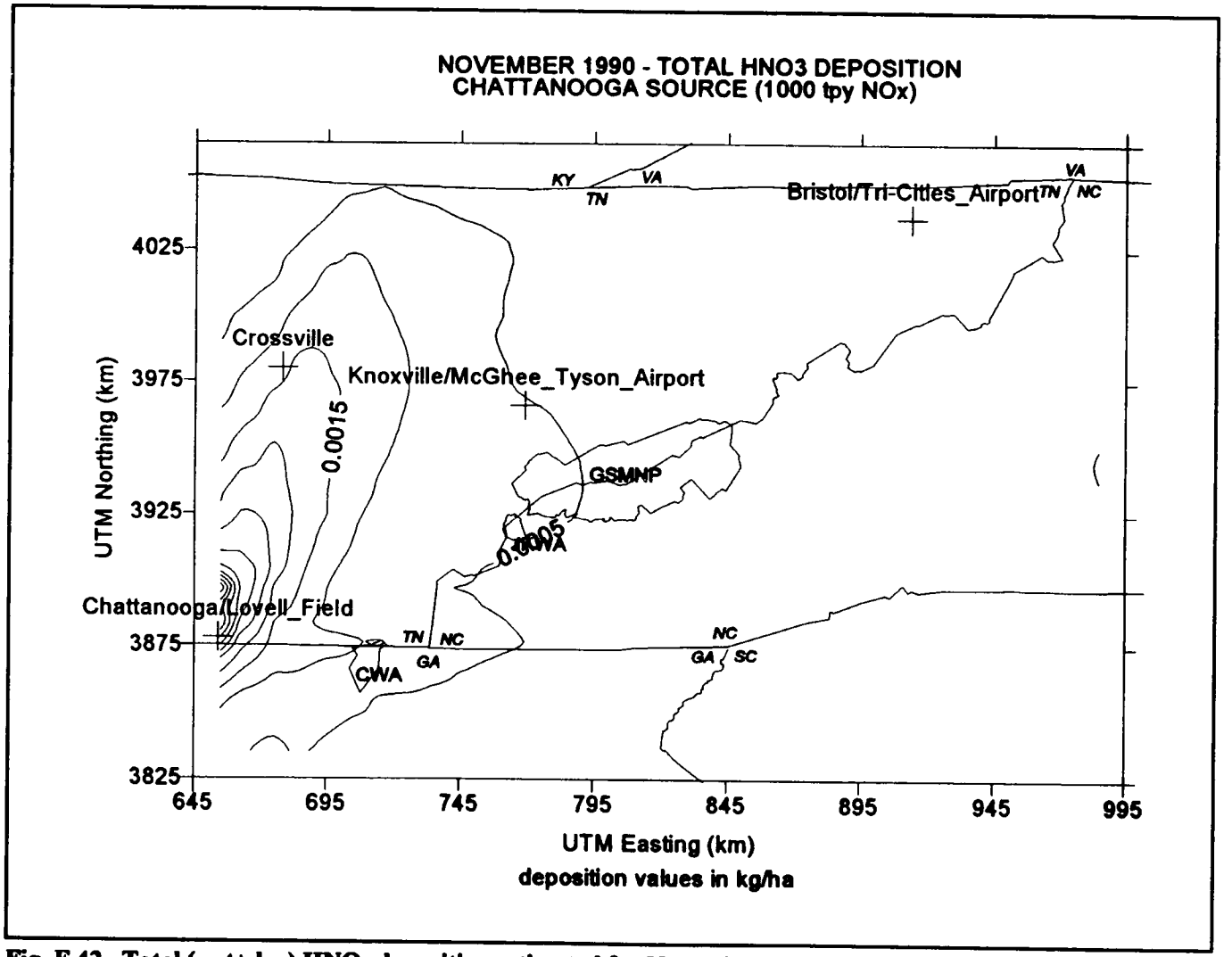

Fig. F.42. Total (wet+dry) HNO_3 deposition estimated for November 1990 resulting from a 28.8 g/s (1000 tpy) hypothetical NO_x emission source located at Chattanooga/Lovell Field.

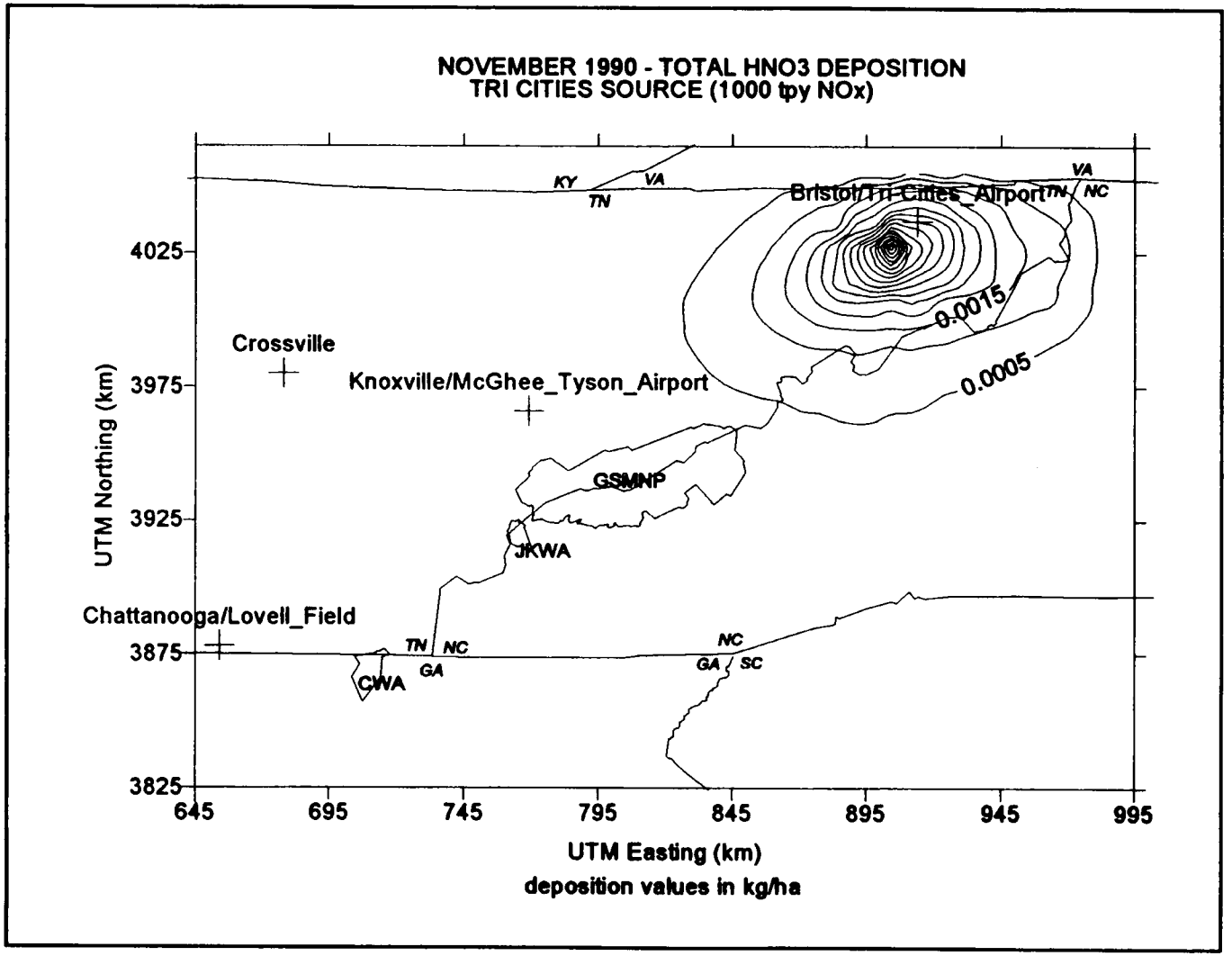

Fig. F.43. Total (wet+dry) HNO_3 deposition estimated for November 1990 resulting from a 28.8 g/s (1000 tpy) hypothetical NO_x emission source located at Bristol/Tri Cities Airport.

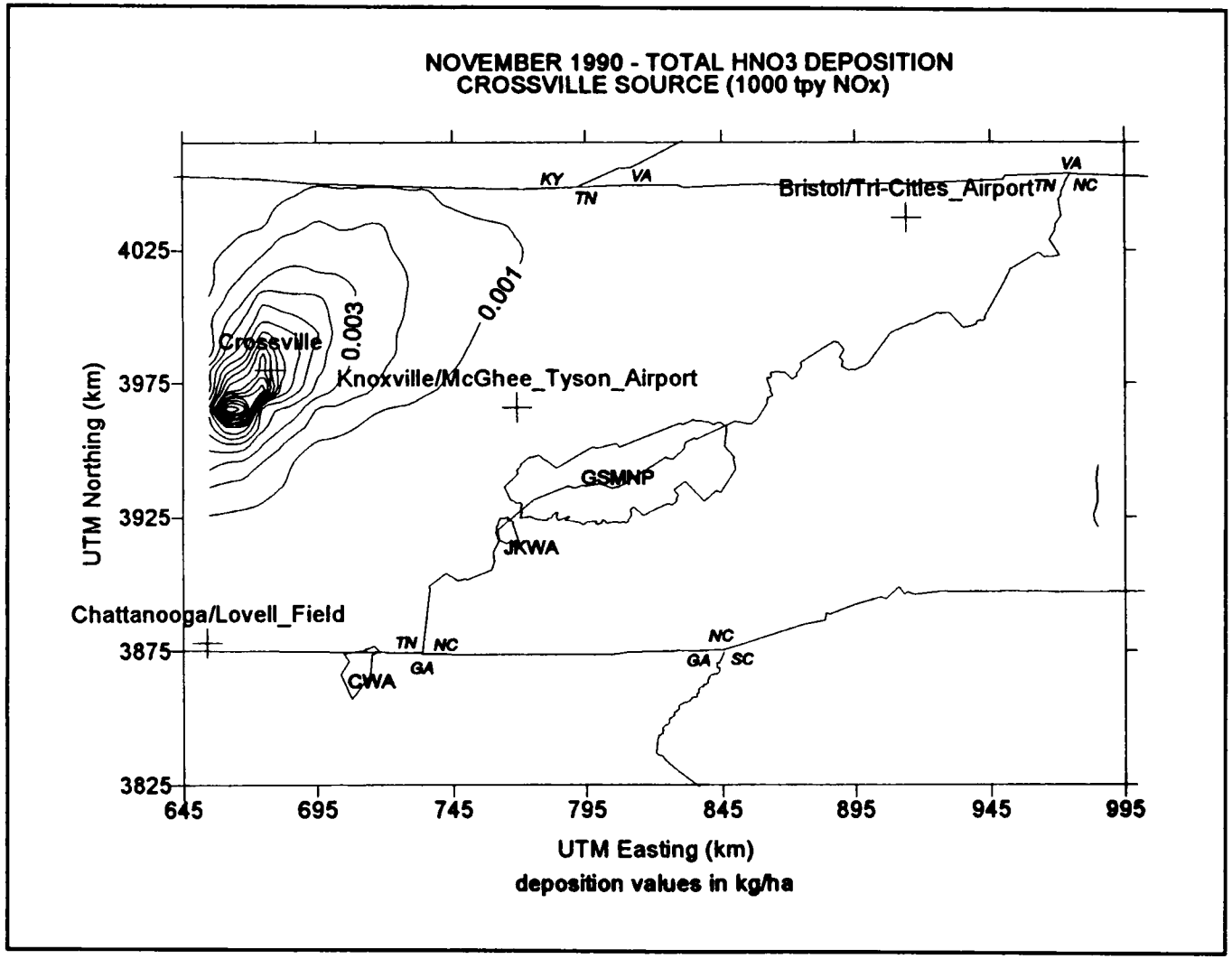

Fig. F.44. Total (wet+dry) HNO_3 deposition estimated for November 1990 resulting from a 28.8 g/s (1000 tpy) hypothetical NO_x emission source located in Crossville.

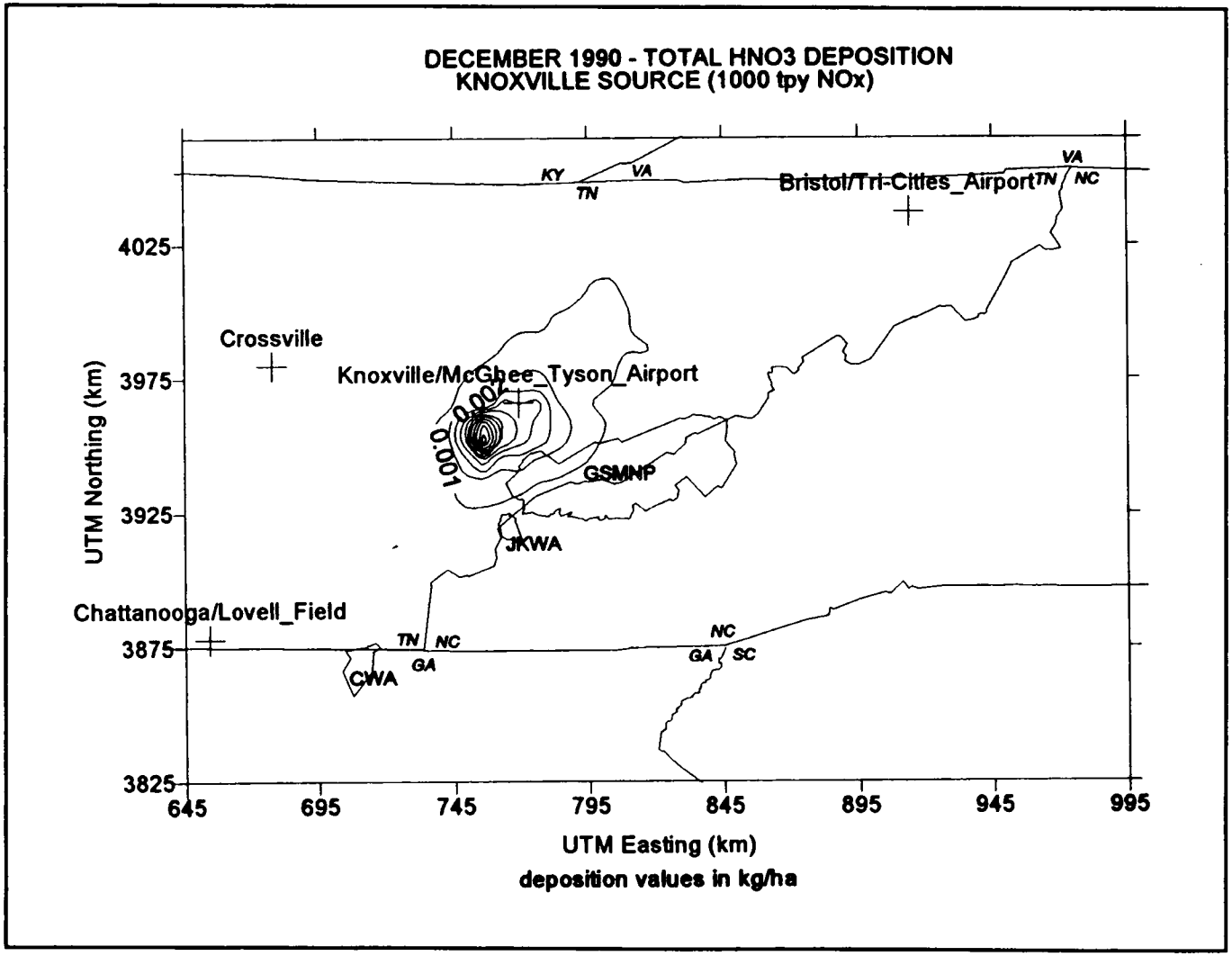

Fig. F.45. Total (wet+dry) HNO_3 deposition estimated for December 1990 resulting from a 28.8 g/s (1000 tpy) hypothetical NO_x emission source located at Knoxville /McGhee Tyson Airport.

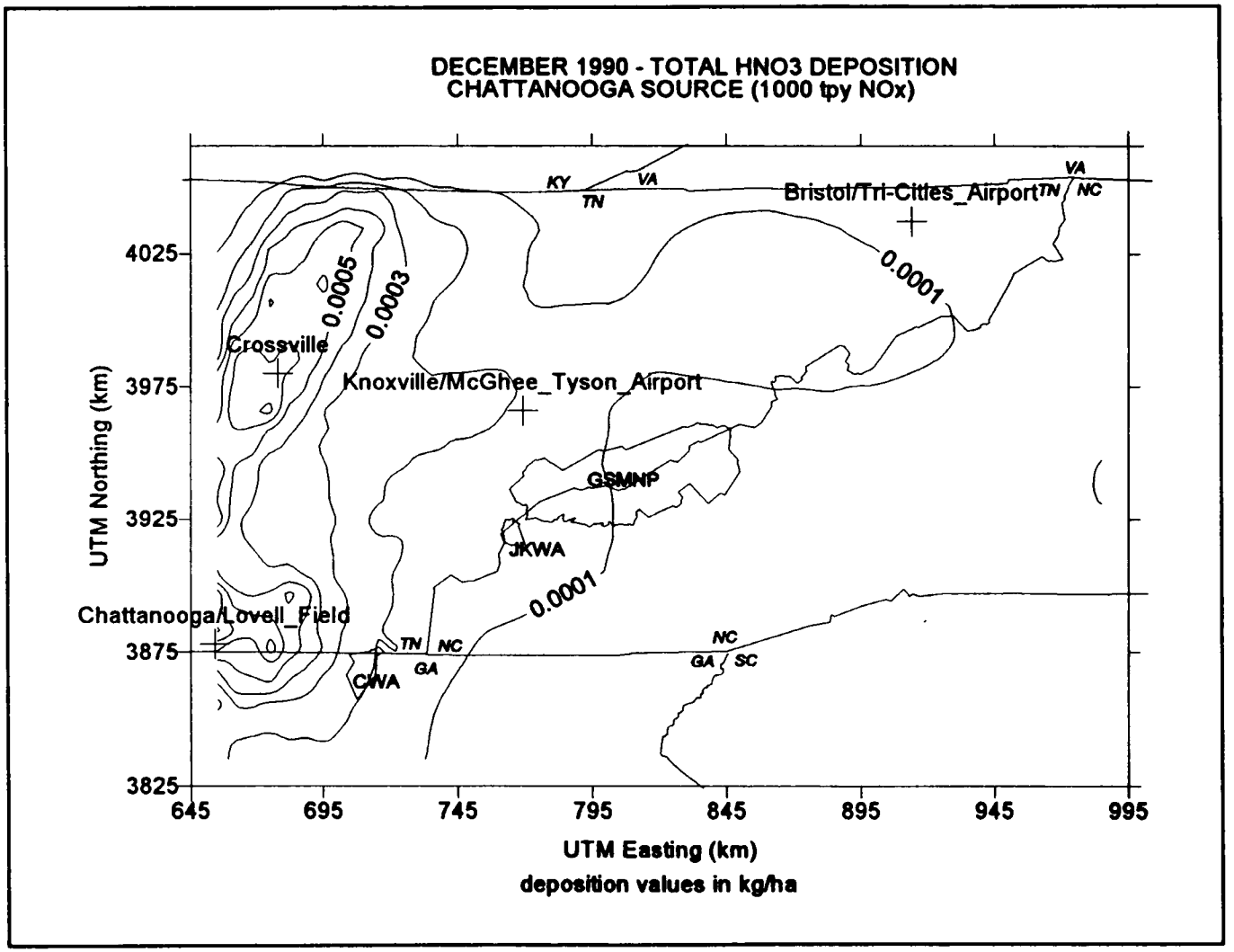

Fig. F.46. Total (wet+dry) HNO_3 deposition estimated for December 1990 resulting from a 28.8 g/s (1000 tpy) hypothetical NO_x emission source located at Chattanooga/Lovell Field.

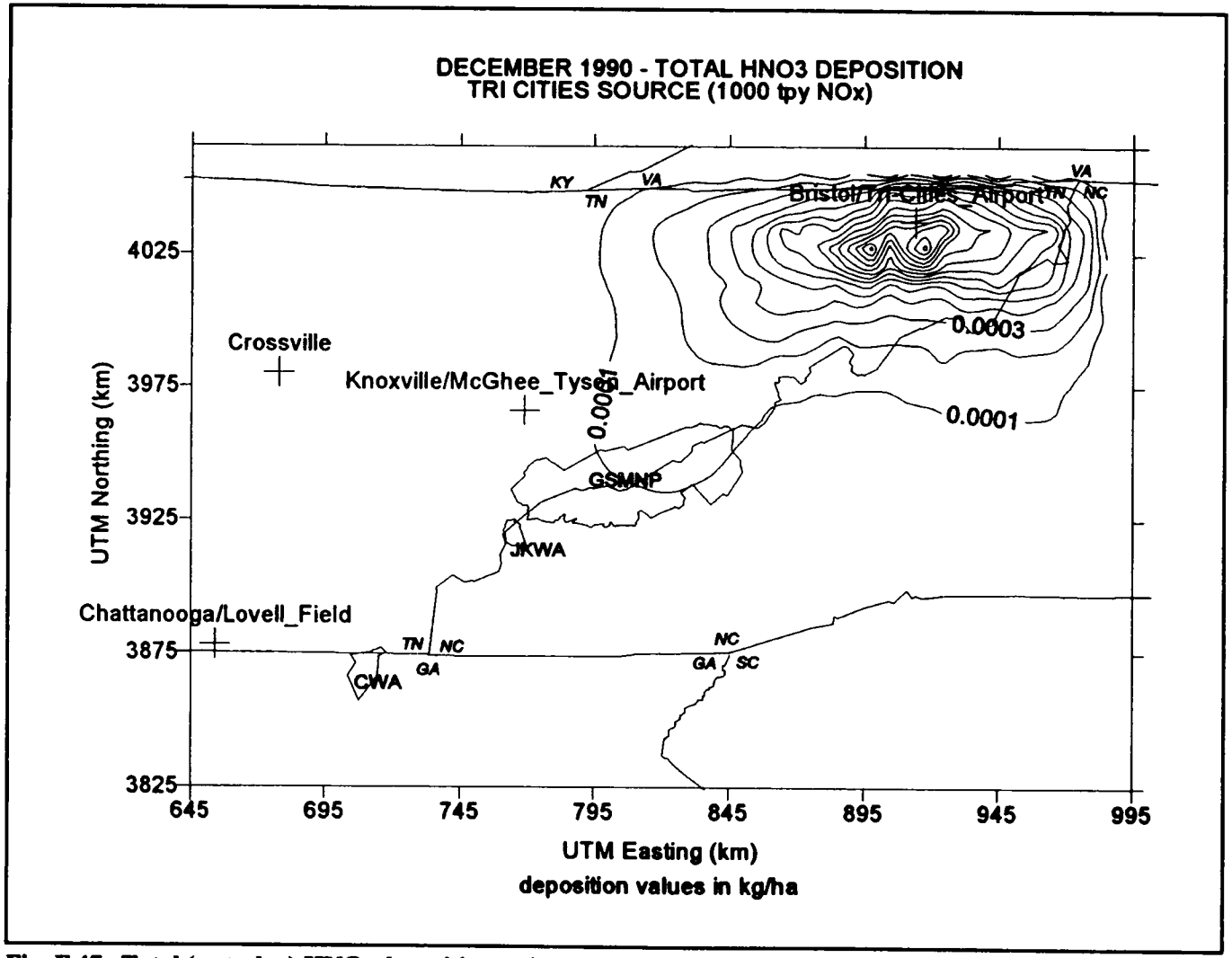

Fig. F.47. Total (wet+dry) HNO_3 deposition estimated for December 1990 resulting from a 28.8 g/s (1000 tpy) hypothetical NO_x emission source located at Bristol/Tri Cities Airport.

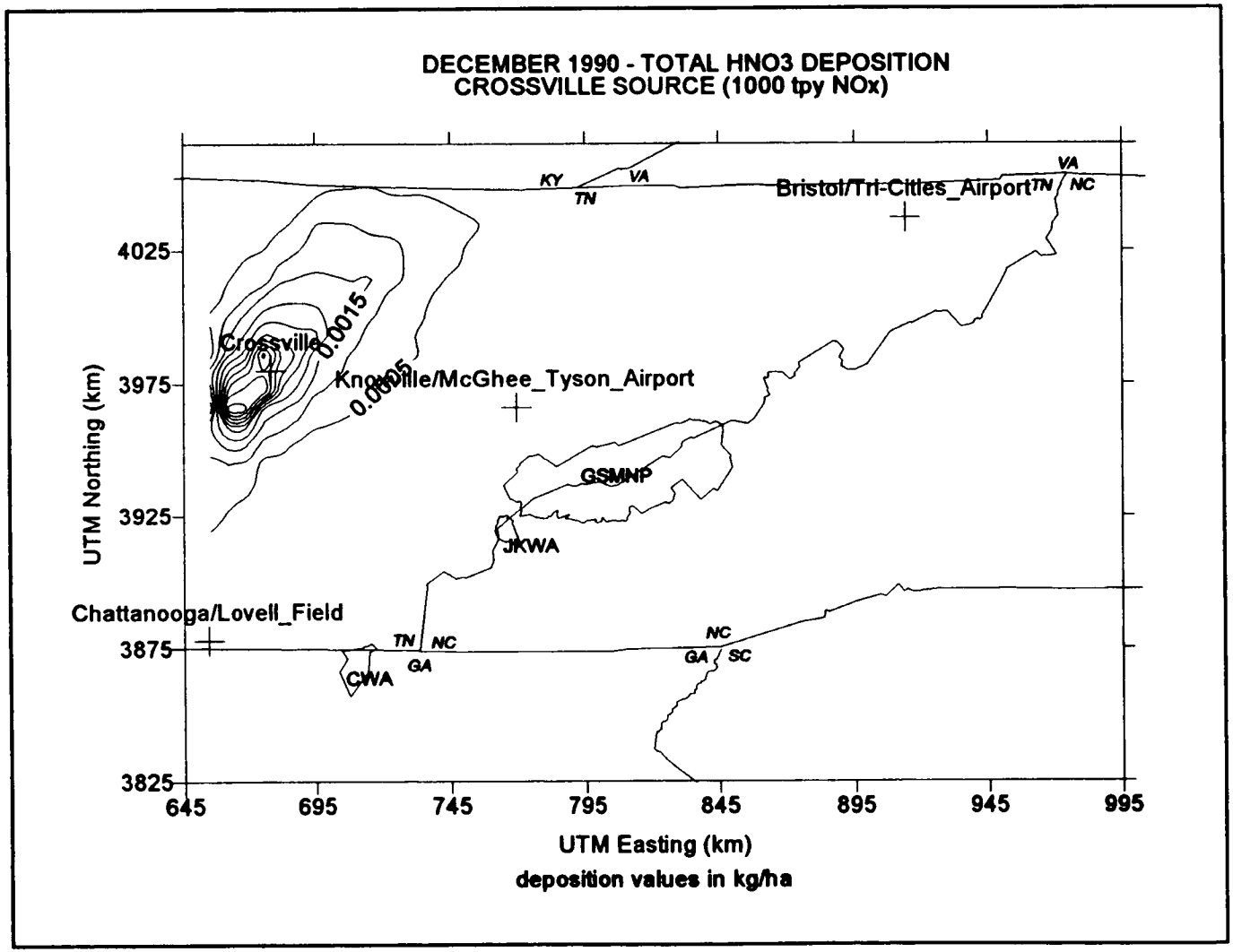

Fig. F.48. Total (wet+dry) HNO_3 deposition estimated for December 1990 resulting from a 28.8 g/s (1000 tpy) hypothetical NO_x emission source located in Crossville.

APPENDIX G
MONTHLY NO_3^- DEPOSITION CONTOUR MAPS

The following figures are contour maps of monthly total (wet + dry) NO_3^- deposition in the East Tennessee modeling domain. One contour map per month has been generated for each of the four hypothetical source locations.

The following abbreviations are used on the contour maps:

GSMNP	=	The Great Smoky Mountains National Park
JKWA	=	Joyce Kilmer Wilderness Area
CWA	=	Cohutta Wilderness Area
TN	=	Tennessee
NC	=	North Carolina
GA	=	Georgia
VA	=	Virginia
KY	=	Kentucky
UTM	=	Universal Transverse Mercator

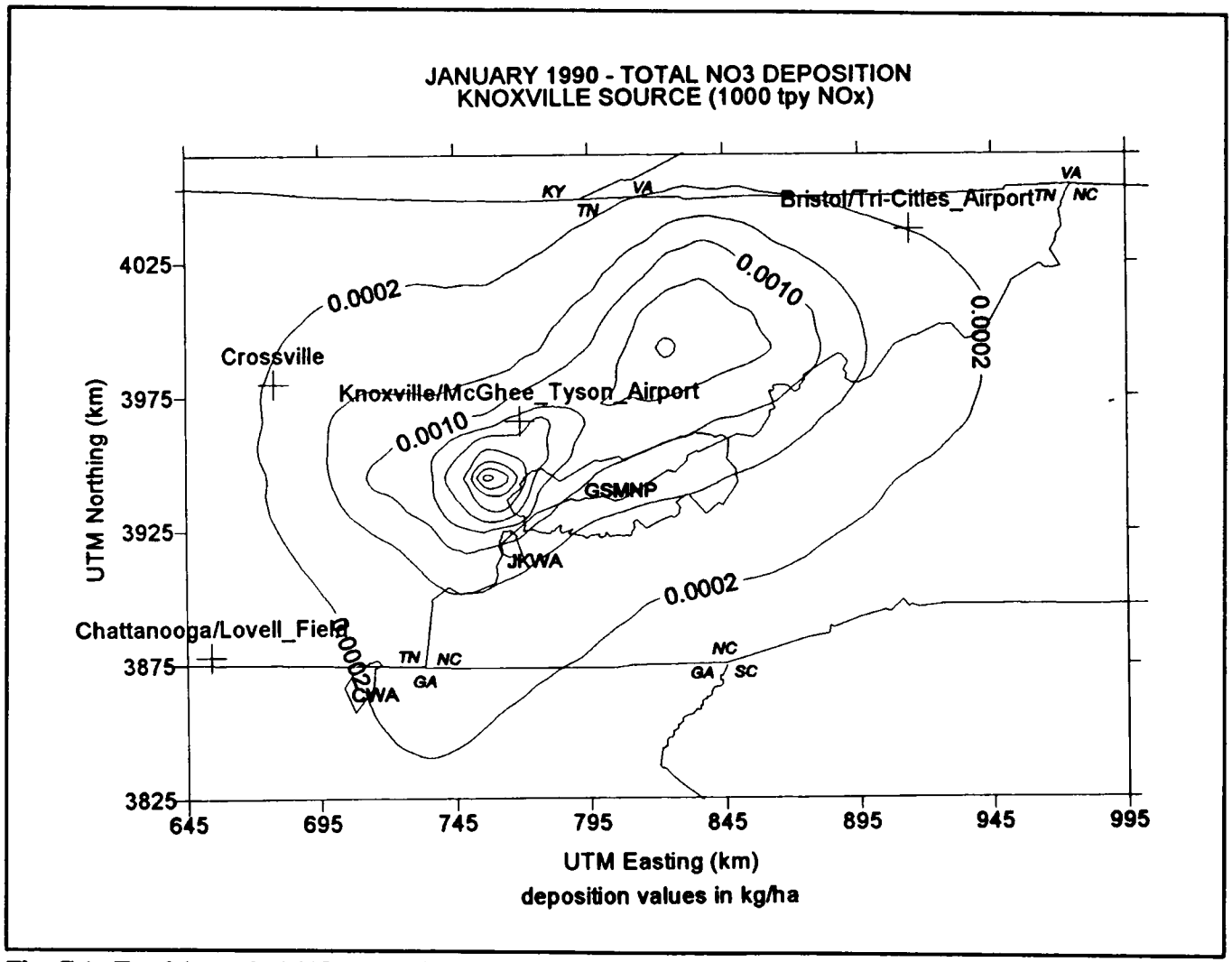

Fig. G.1. Total (wet+dry) NO_3^- deposition estimated for January 1990 resulting from a 28.8 g/s (1000 tpy) hypothetical NO_x emission source located at Knoxville /McGhee Tyson Airport.

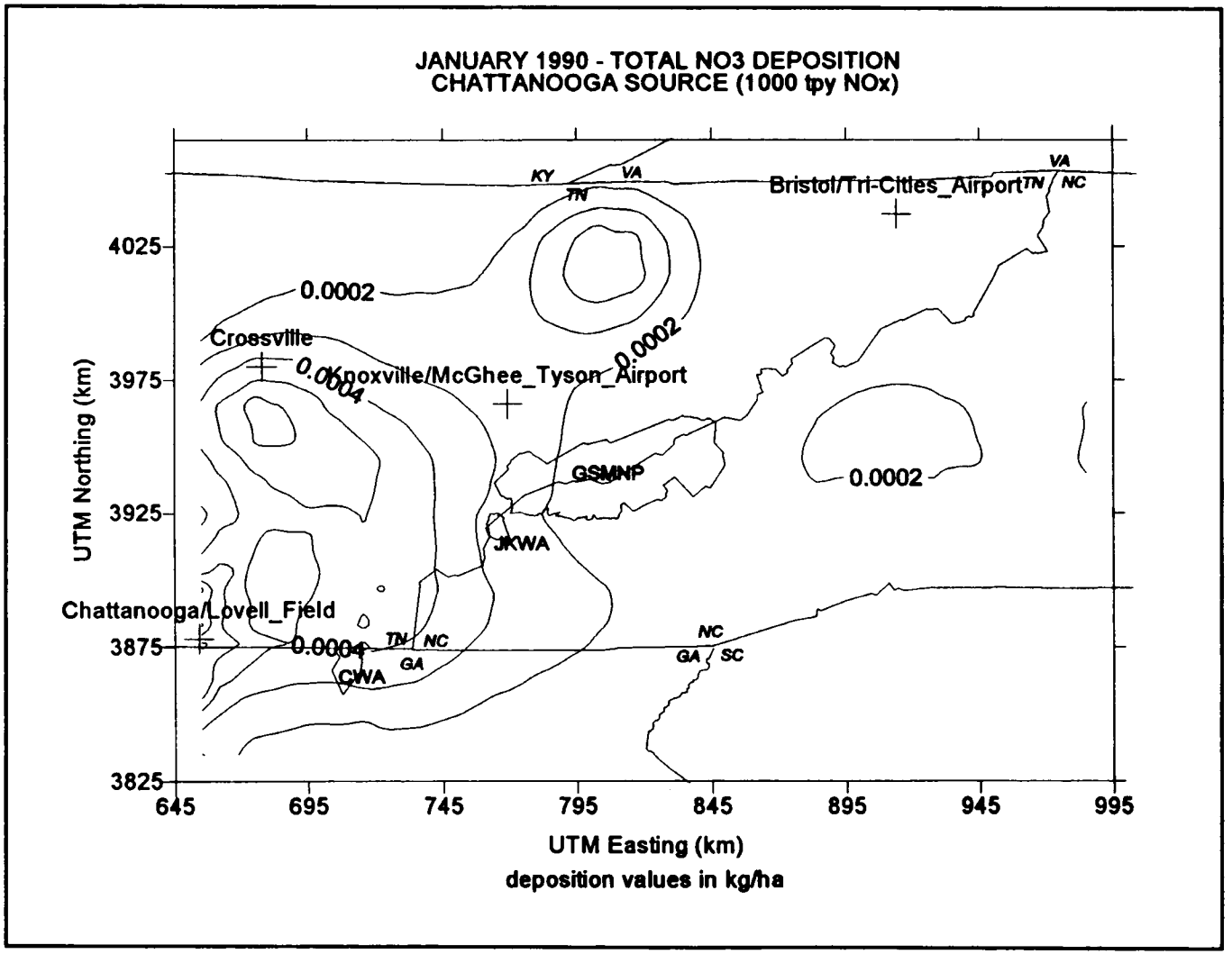

Fig. G.2. Total (wet+dry) NO_3^- deposition estimated for January 1990 resulting from a 28.8 g/s (1000 tpy) hypothetical NO_x emission source located at Chattanooga/Lovell Field.

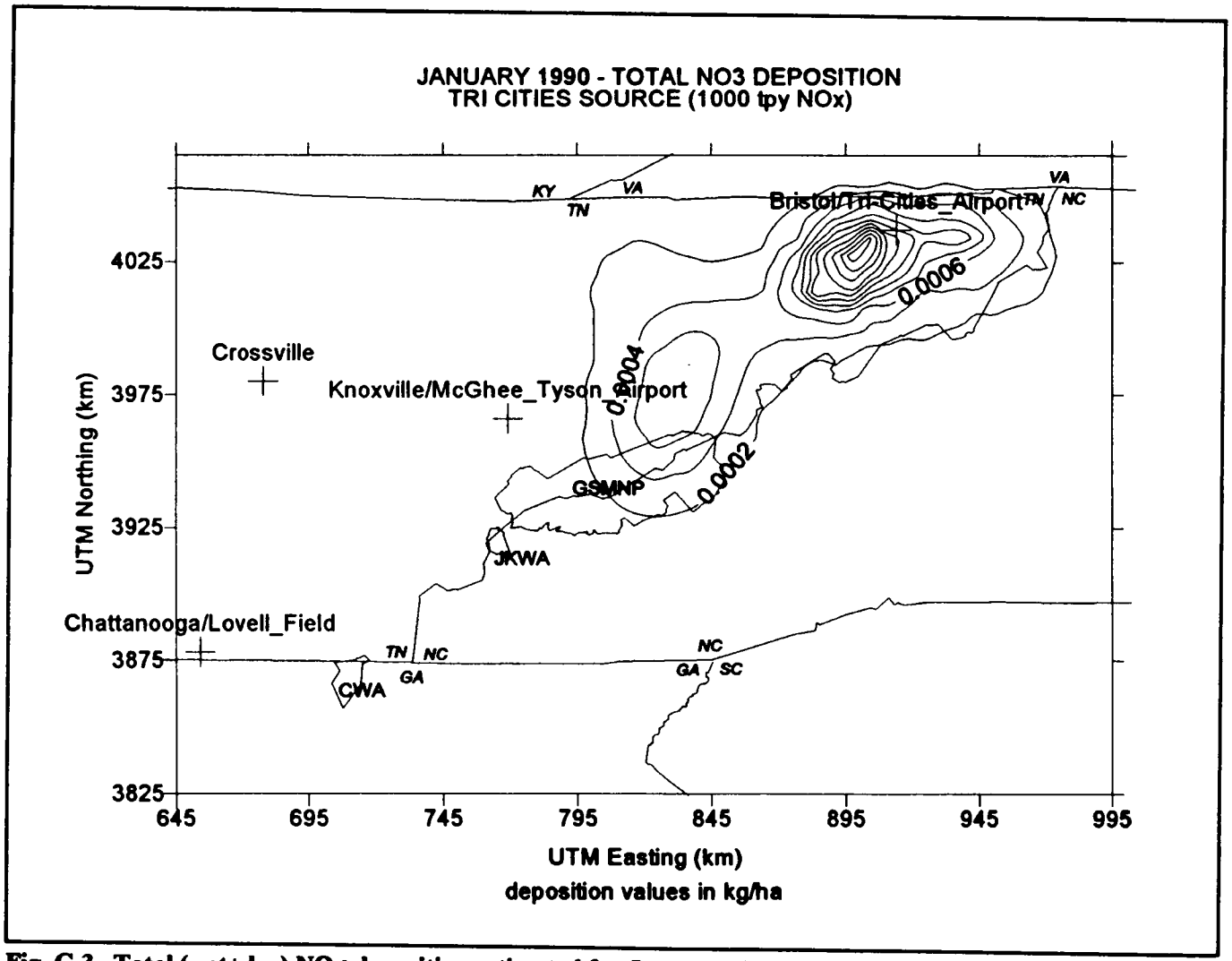

Fig. G.3. Total (wet+dry) NO_3^- deposition estimated for January 1990 resulting from a 28.8 g/s (1000 tpy) hypothetical NO_x emission source located at Bristol/Tri Cities Airport.

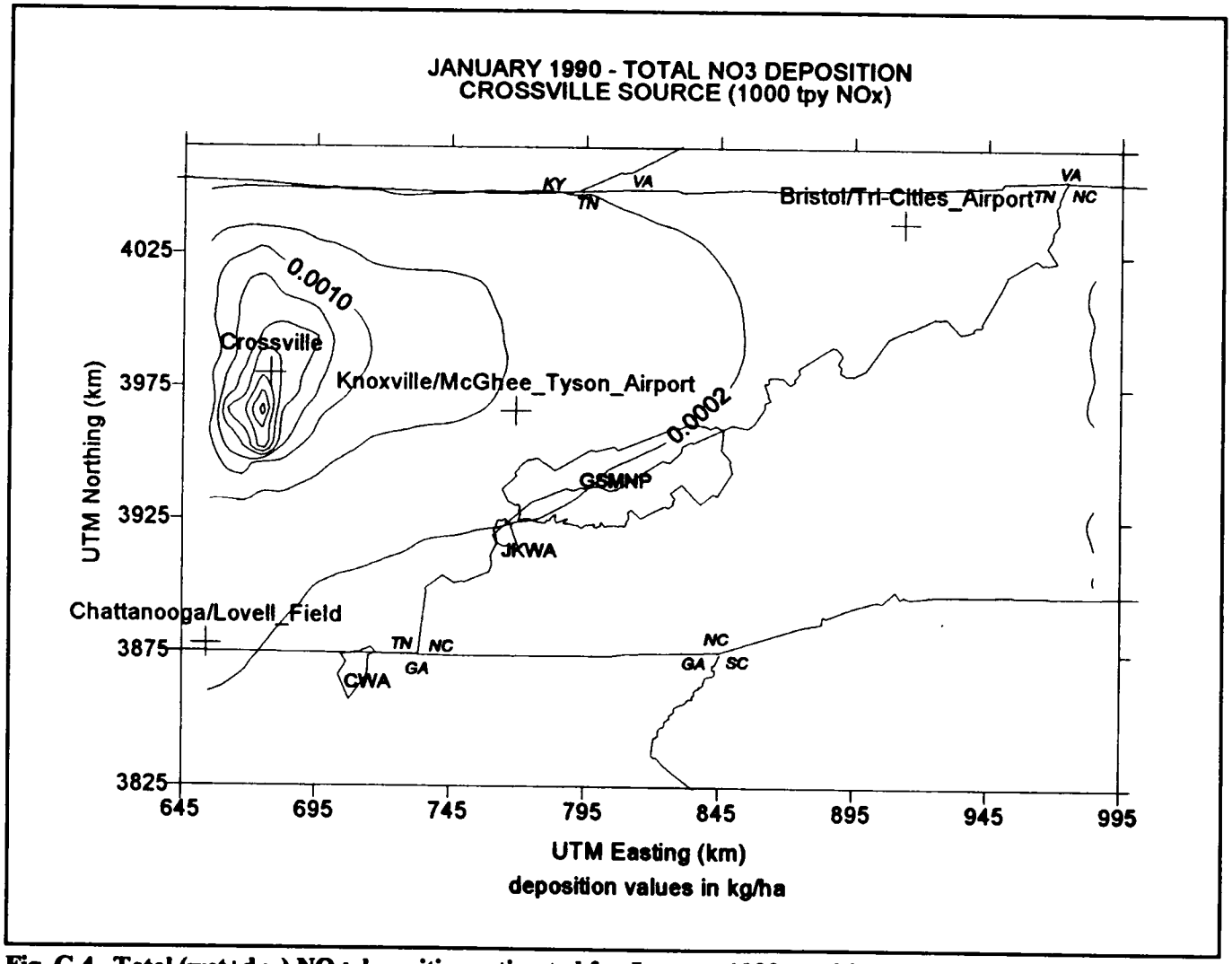

Fig. G.4. Total (wet+dry) NO_3^- deposition estimated for January 1990 resulting from a 28.8 g/s (1000 tpy) hypothetical NO_x emission source located in Crossville.

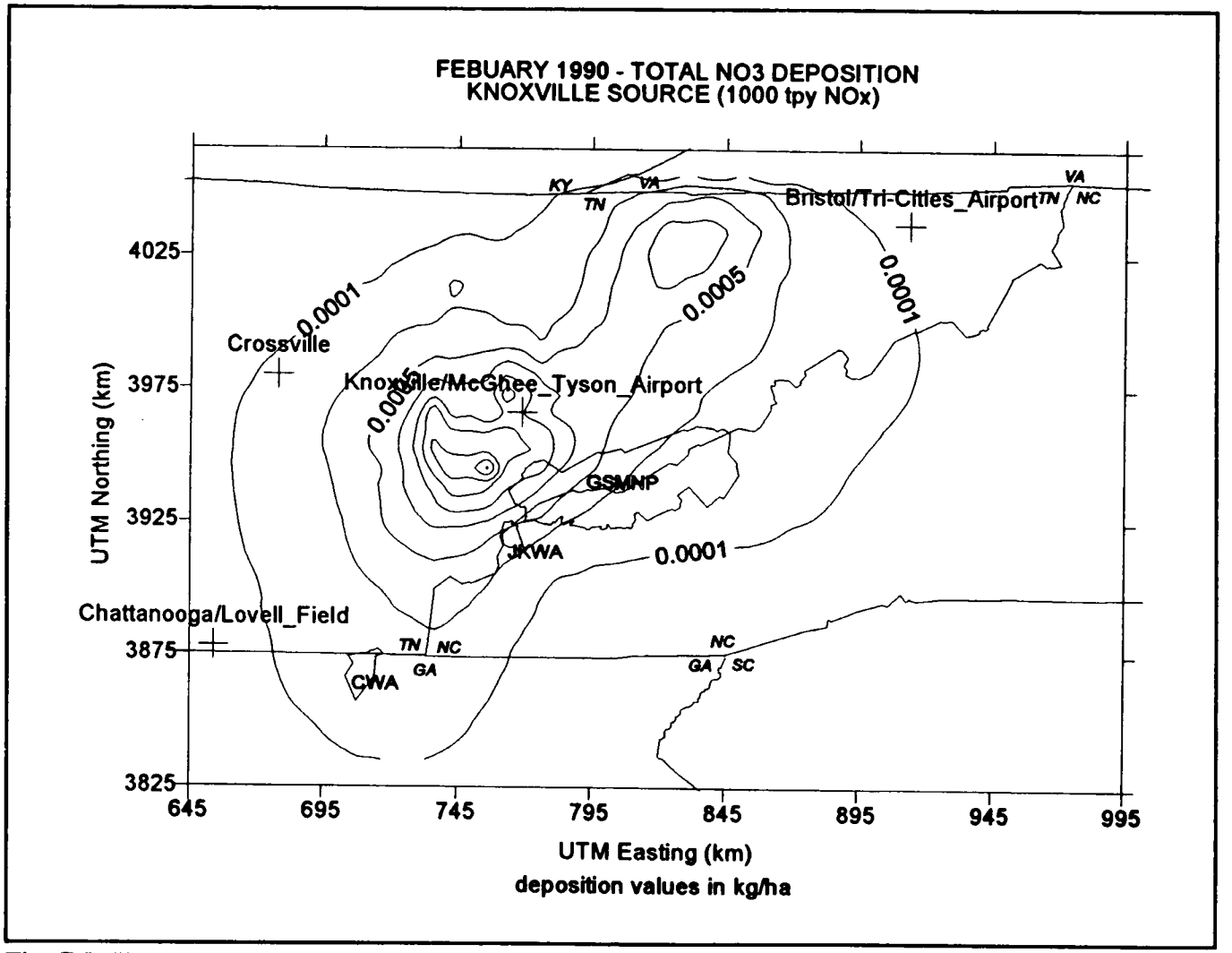

Fig. G.5. Total (wet+dry) NO_3^- deposition estimated for February 1990 resulting from a 28.8 g/s (1000 tpy) hypothetical NO_x emission source located at Knoxville /McGhee Tyson Airport.

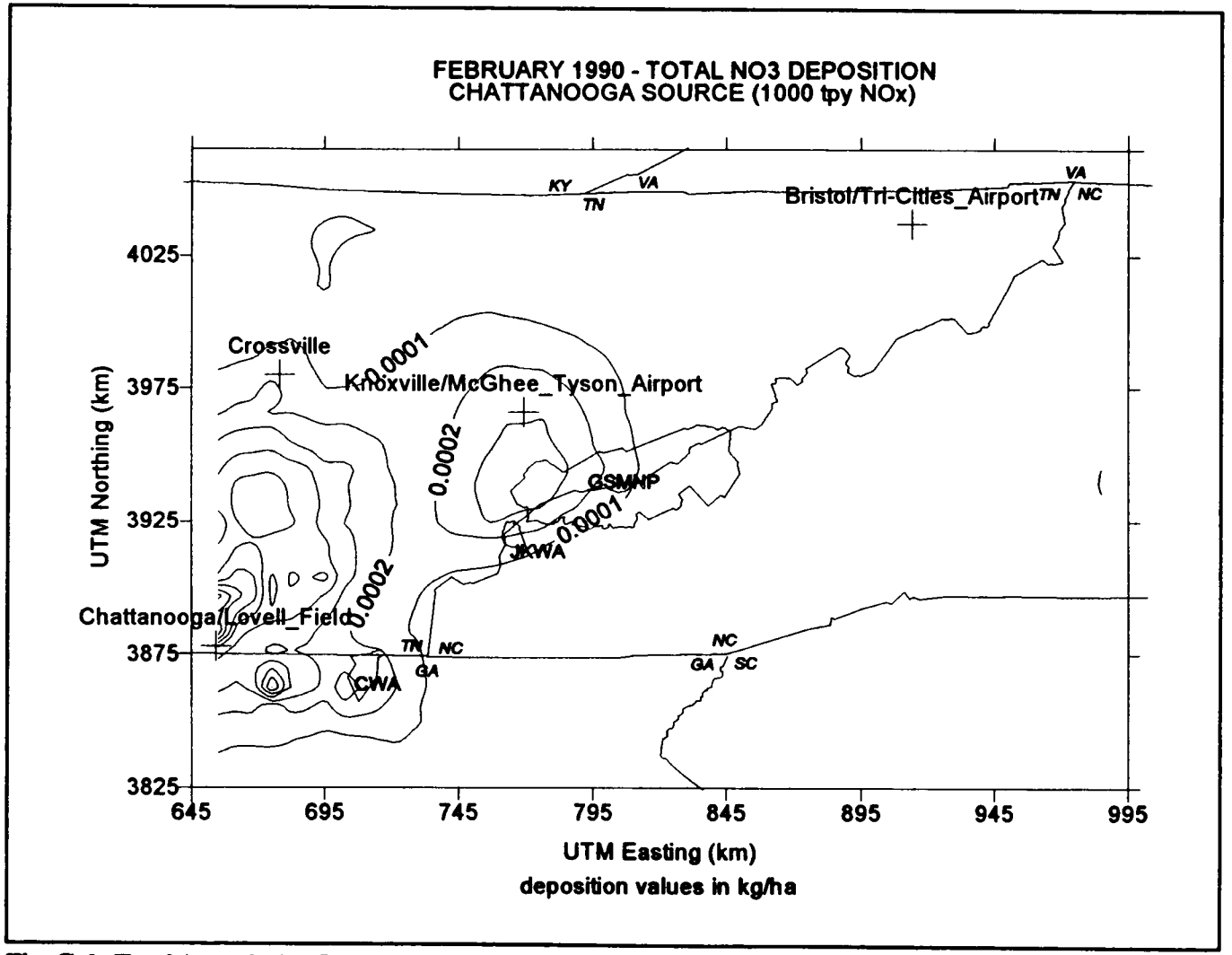

Fig. G.6. Total (wet+dry) NO_3^- deposition estimated for February 1990 resulting from a 28.8 g/s (1000 tpy) hypothetical NO_x emission source located at Chattanooga/Lovell Field.

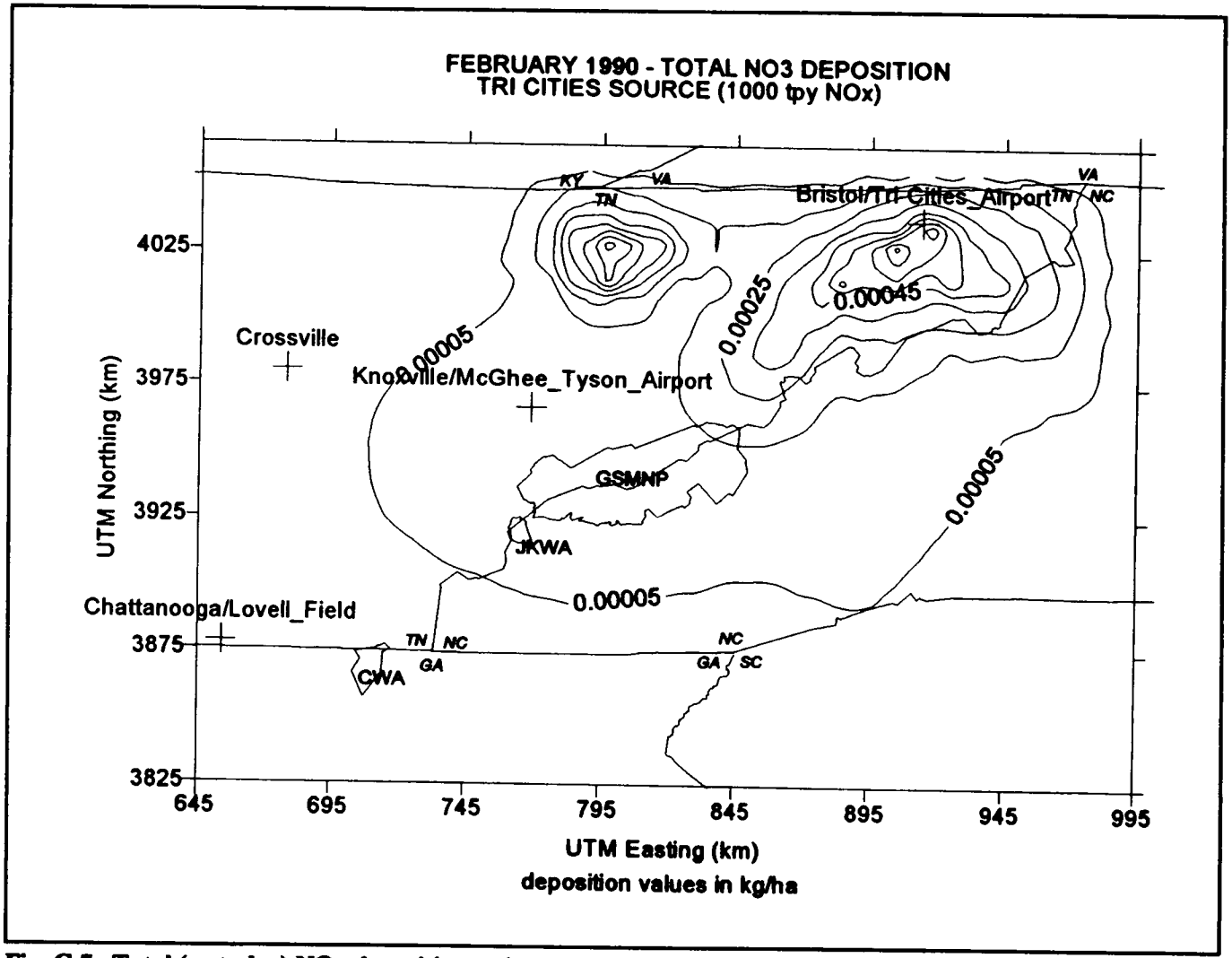

Fig. G.7. Total (wet+dry) NO_3^- deposition estimated for February 1990 resulting from a 28.8 g/s (1000 tpy) hypothetical NO_x emission source located at Bristol/Tri Cities Airport.

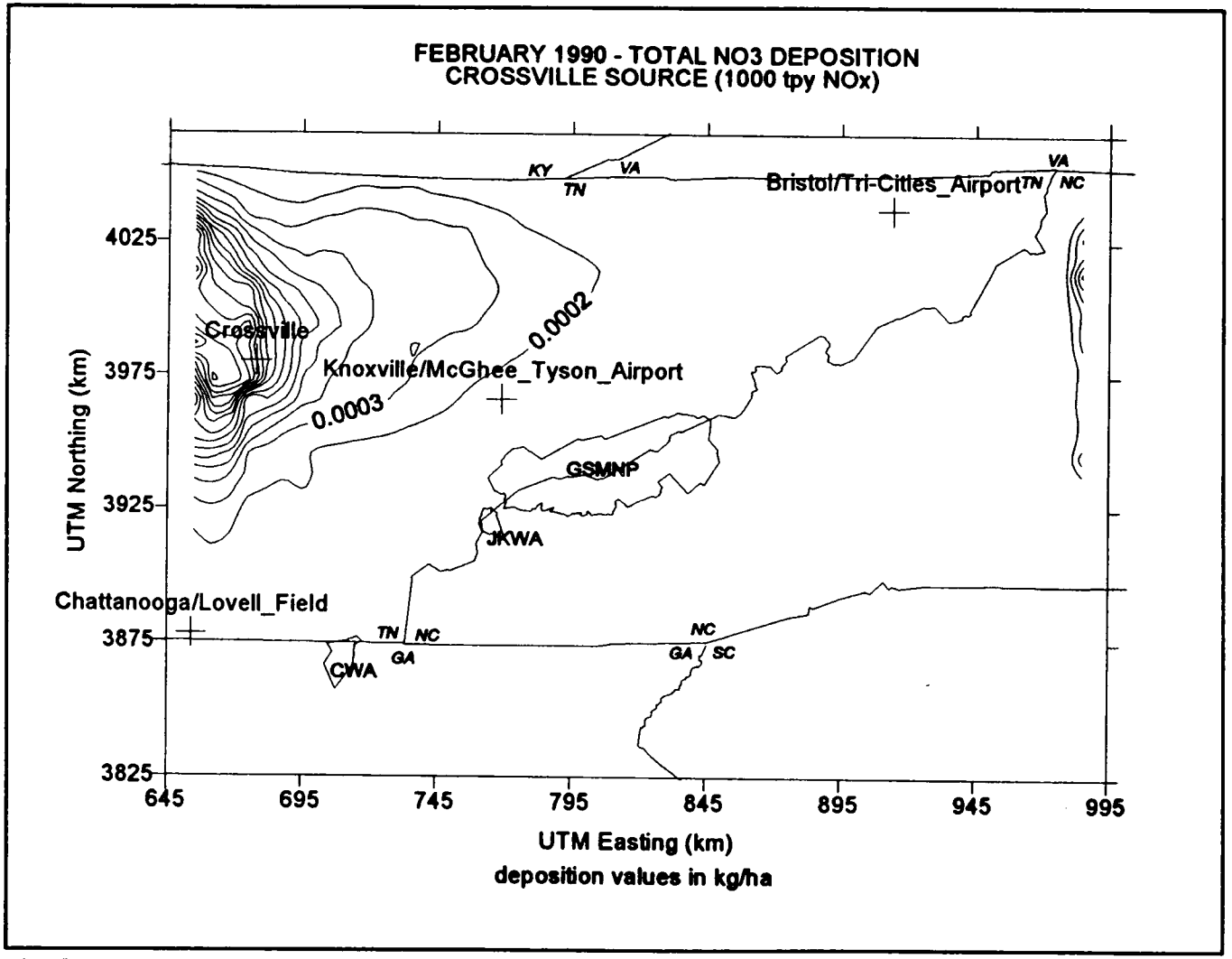

Fig. G.8. Total (wet+dry) NO_3^- deposition estimated for February 1990 resulting from a 28.8 g/s (1000 tpy) hypothetical NO_x emission source located in Crossville.

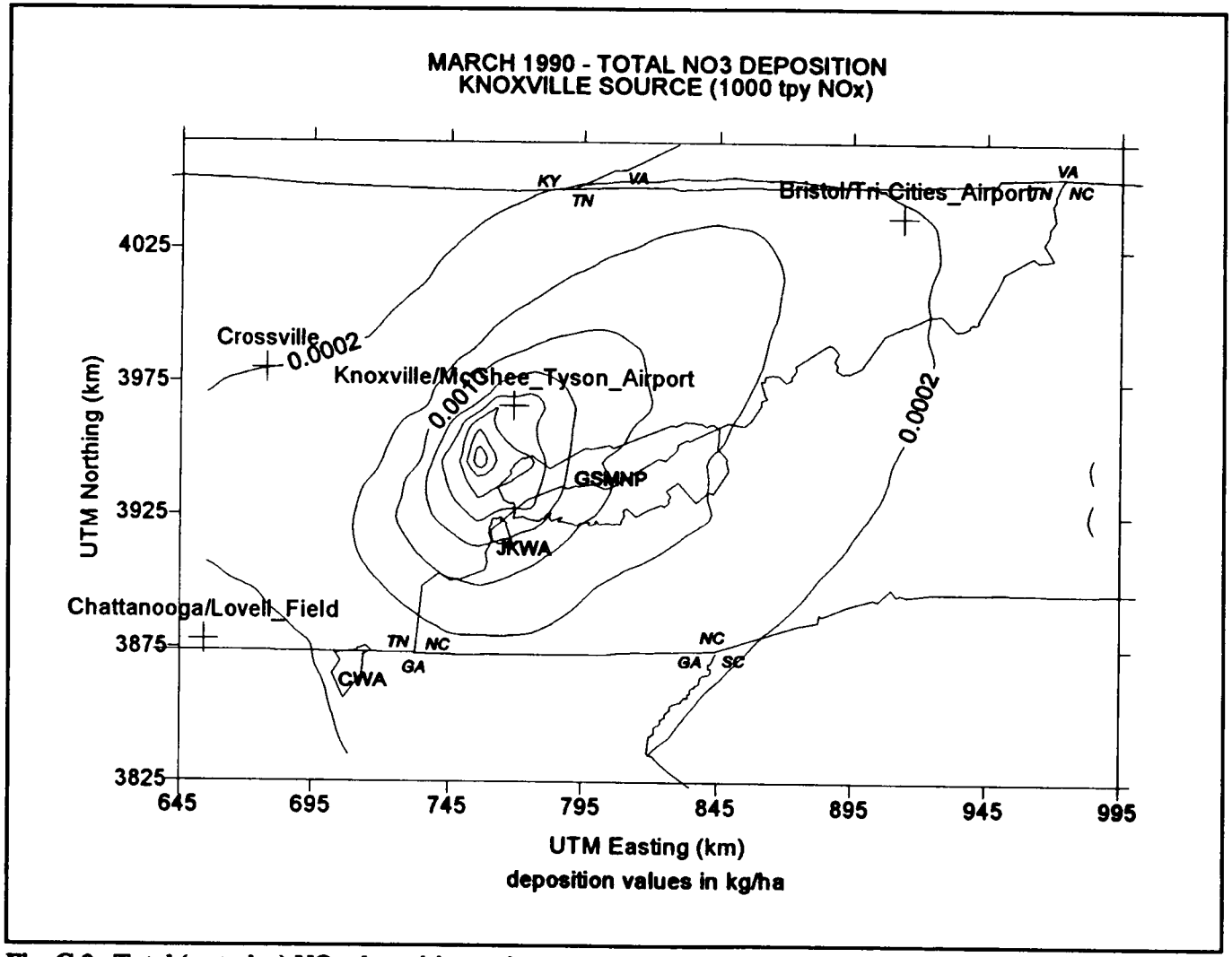

Fig. G.9. Total (wet+dry) NO_3^- deposition estimated for March 1990 resulting from a 28.8 g/s (1000 tpy) hypothetical NO_x emission source located at Knoxville /McGhee Tyson Airport.

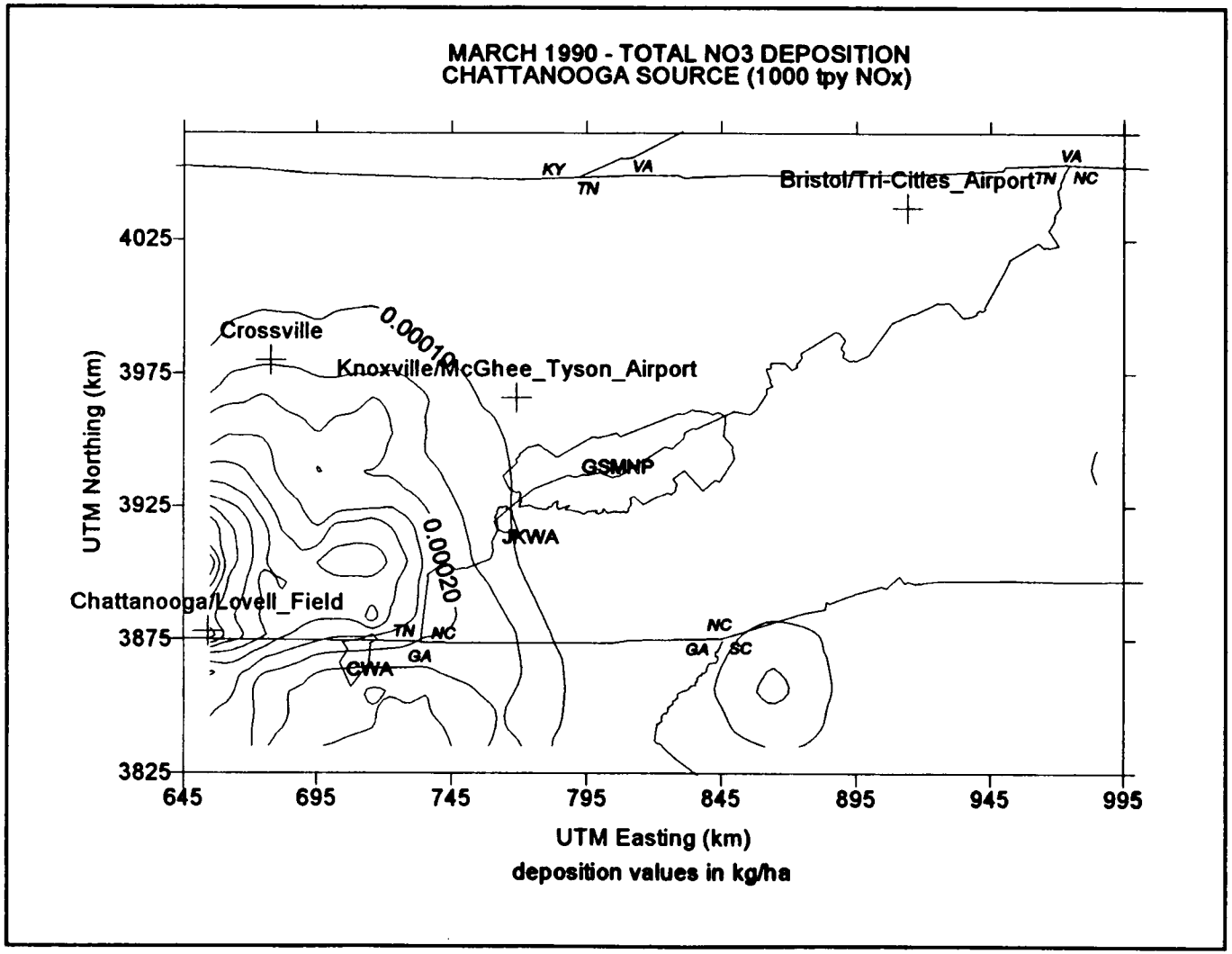

Fig. G.10. Total (wet+dry) NO_3^- deposition estimated for March 1990 resulting from a 28.8 g/s (1000 tpy) hypothetical NO_x emission source located at Chattanooga/Lovell Field.

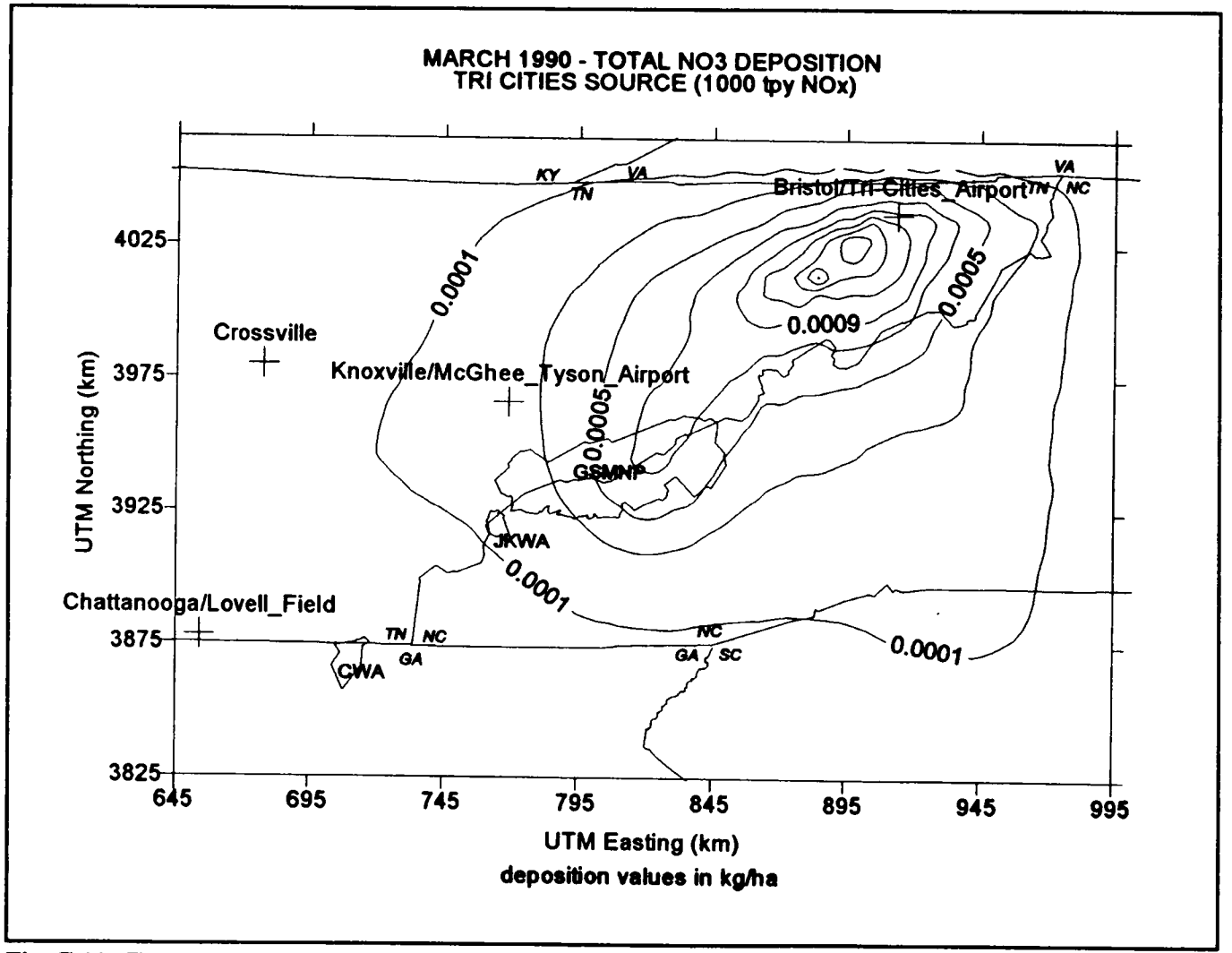

Fig. G.11. Total (wet+dry) NO_3^- deposition estimated for March 1990 resulting from a 28.8 g/s (1000 tpy) hypothetical NO_x emission source located at Bristol/Tri Cities Airport.

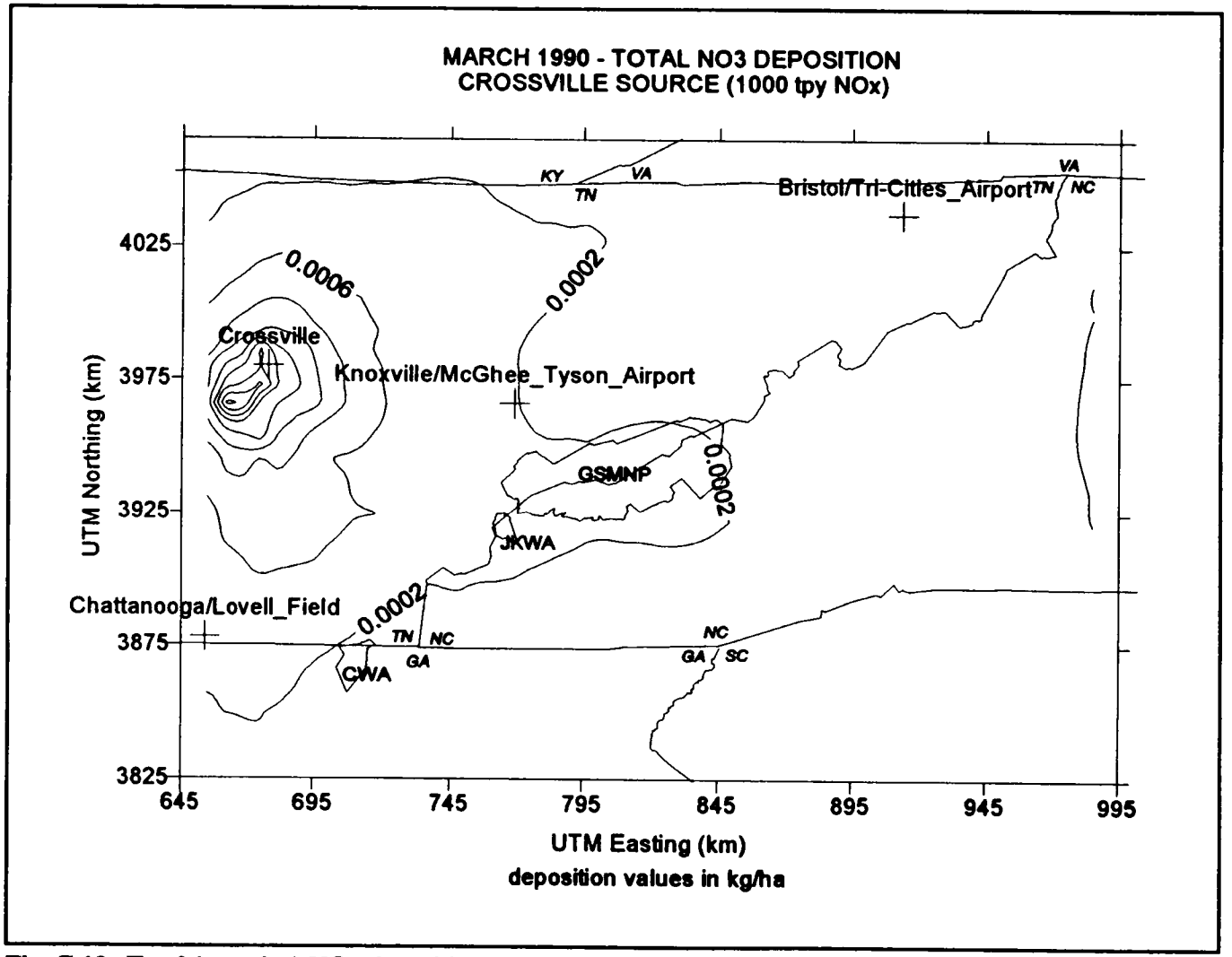

Fig. G.12. Total (wet+dry) NO_3^- deposition estimated for March 1990 resulting from a 28.8 g/s (1000 tpy) hypothetical NO_x emission source located in Crossville.

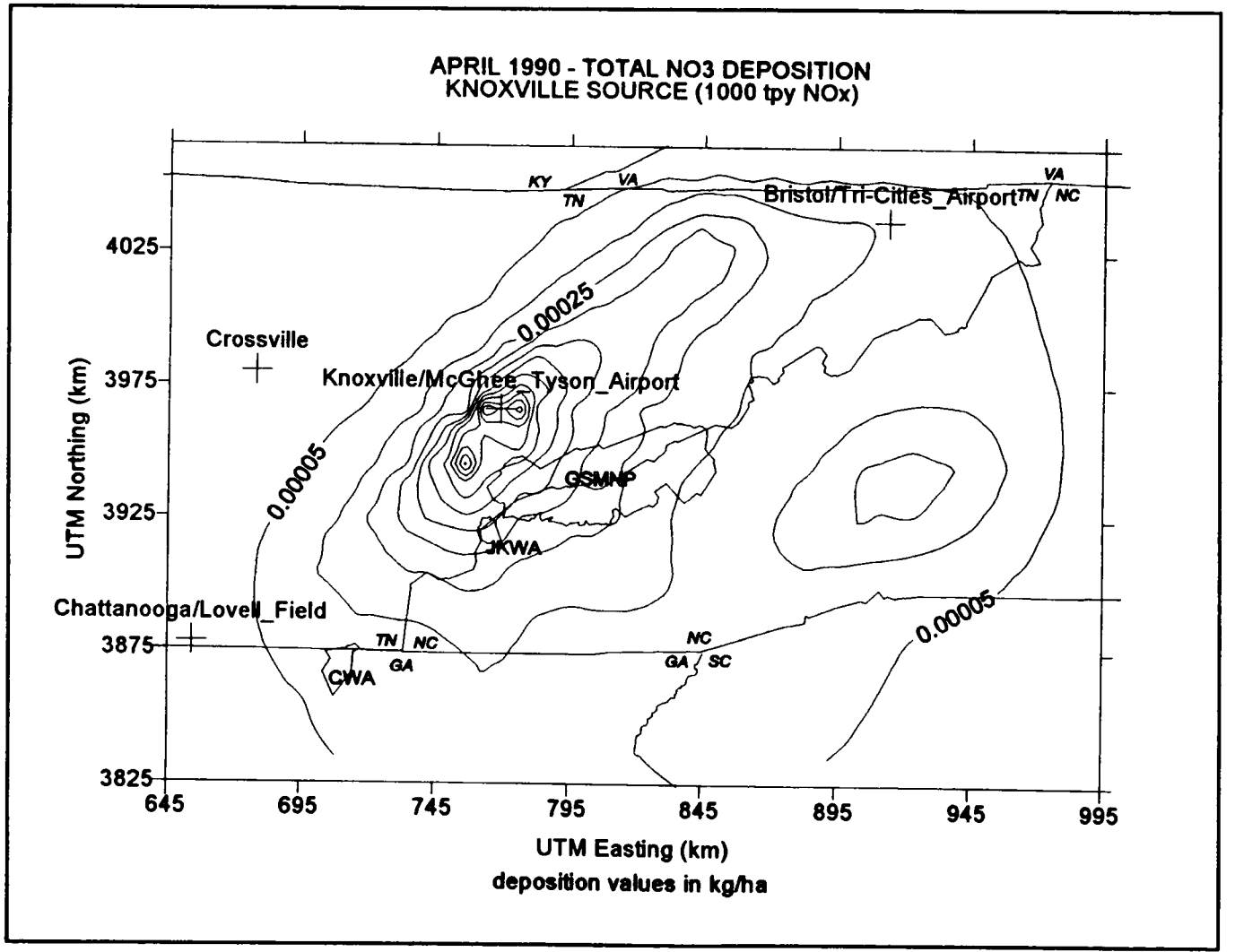

Fig. G.13. Total (wet+dry) NO_3^- deposition estimated for April 1990 resulting from a 28.8 g/s (1000 tpy) hypothetical NO_x emission source located at Knoxville /McGhee Tyson Airport.

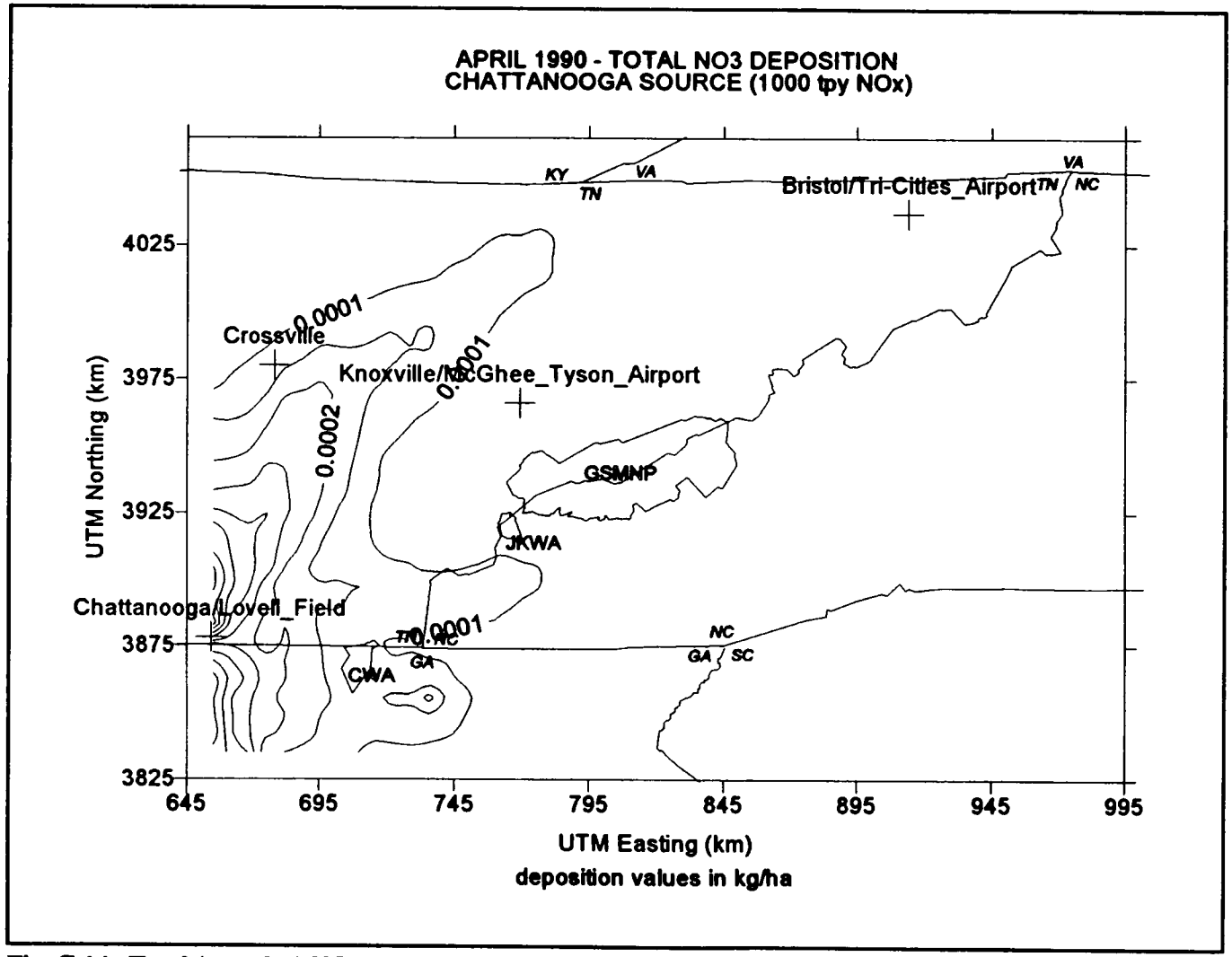

Fig. G.14. Total (wet+dry) NO_3^- deposition estimated for April 1990 resulting from a 28.8 g/s (1000 tpy) hypothetical NO_x emission source located at Chattanooga/Lovell Field.

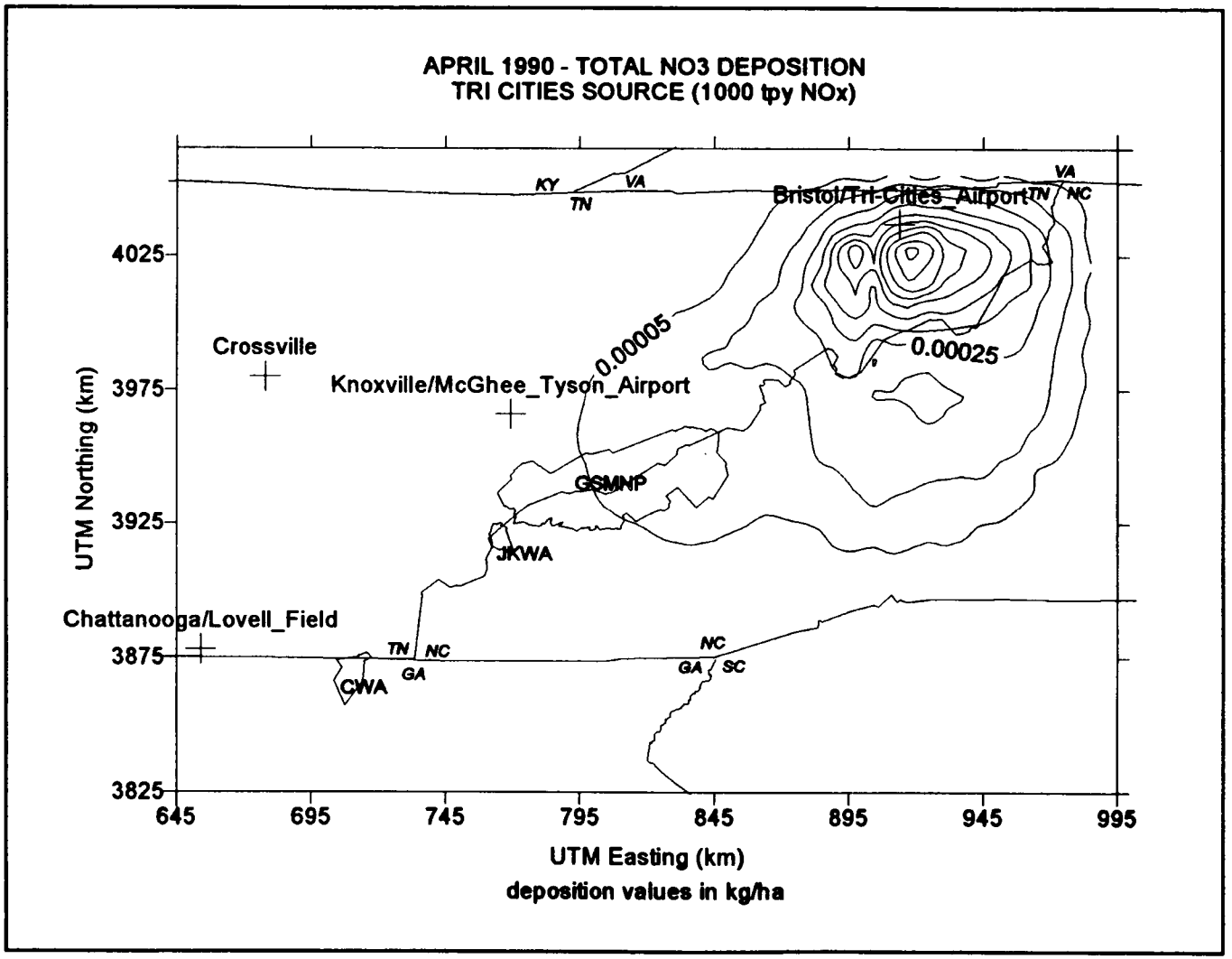

Fig. G.15. Total (wet+dry) NO_3^- deposition estimated for April 1990 resulting from a 28.8 g/s (1000 tpy) hypothetical NO_x emission source located at Bristol/Tri Cities Airport.

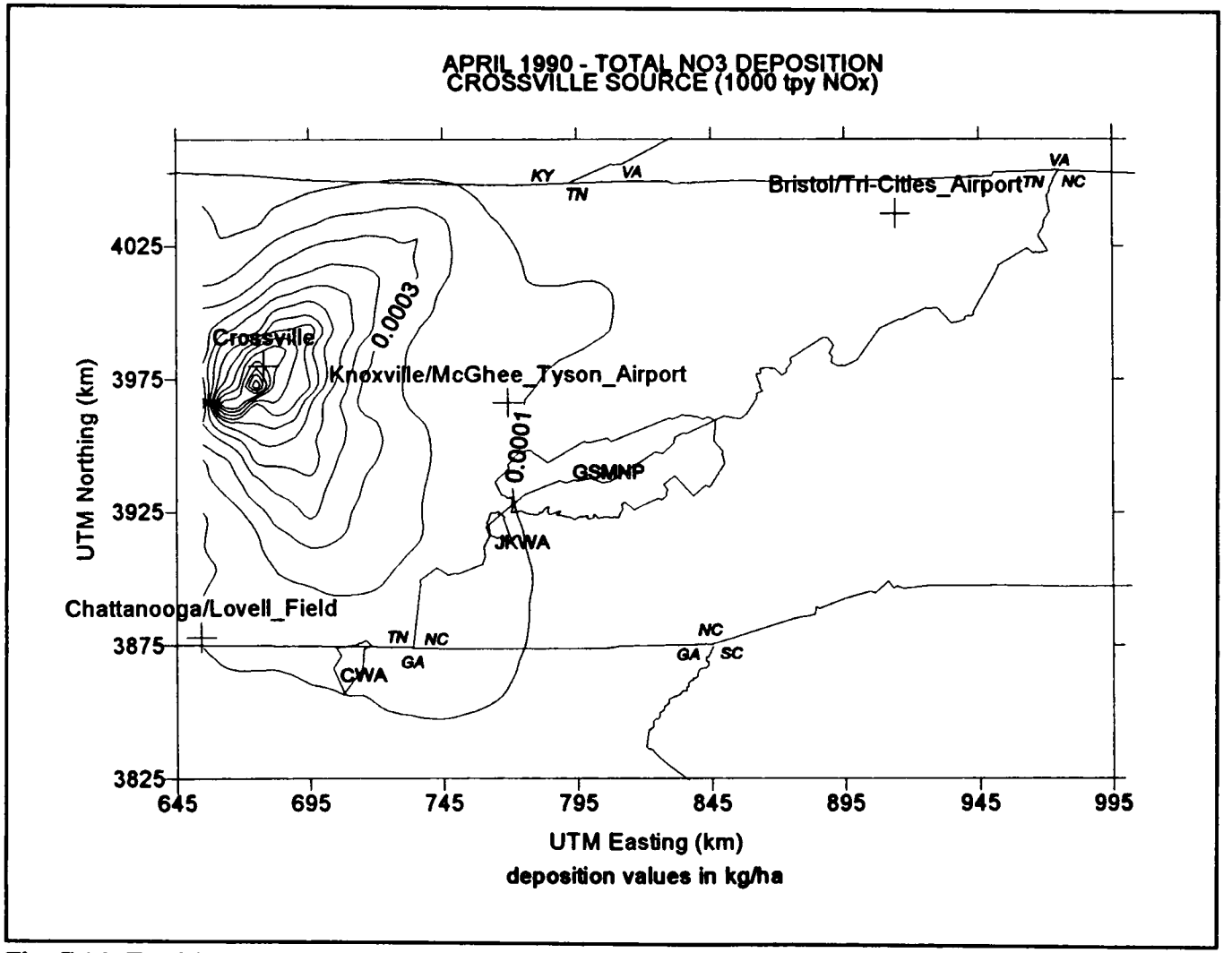

Fig. G.16. Total (wet+dry) NO_3^- deposition estimated for April 1990 resulting from a 28.8 g/s (1000 tpy) hypothetical NO_x emission source located in Crossville.

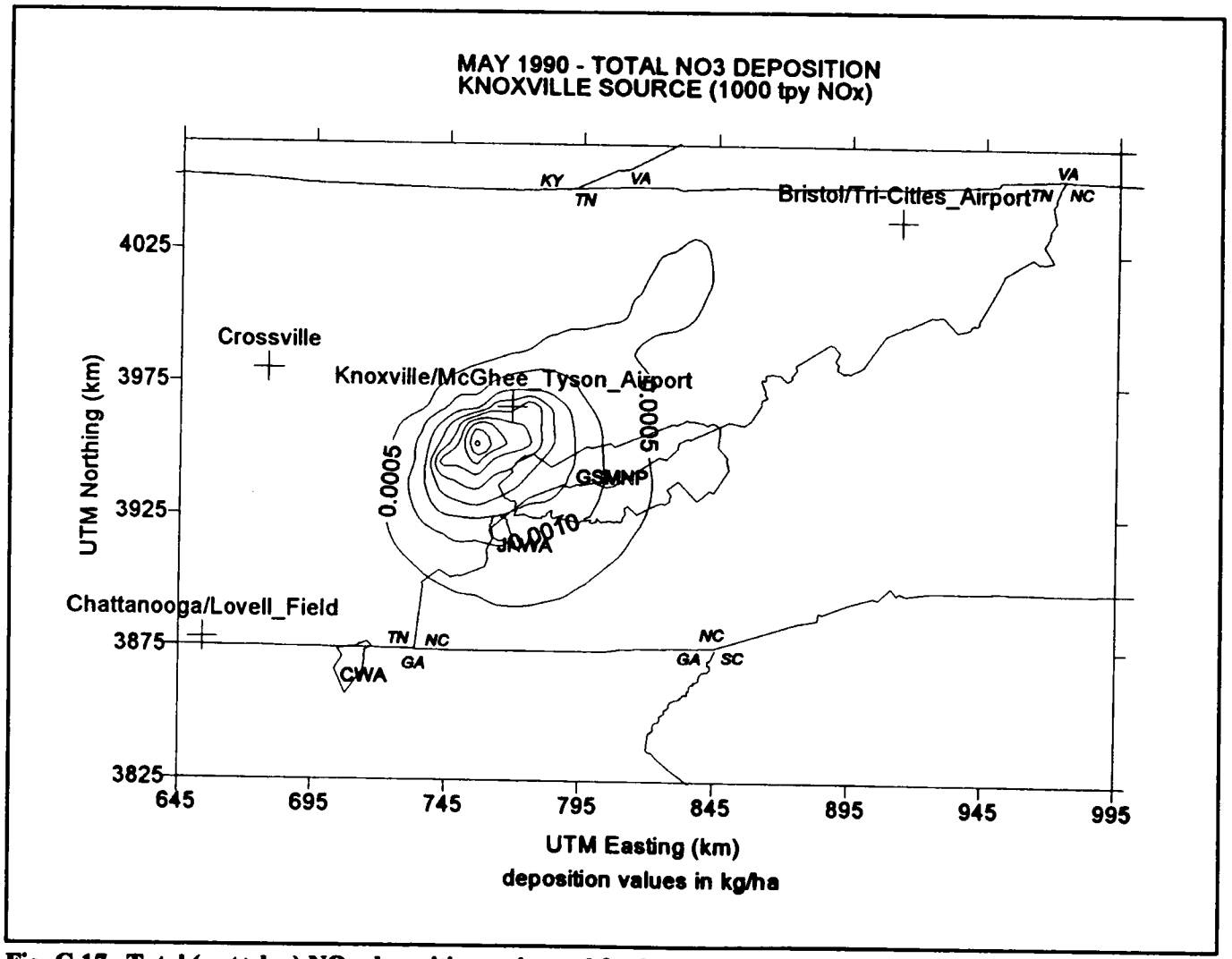

Fig. G.17. Total (wet+dry) NO_3^- deposition estimated for May 1990 resulting from a 28.8 g/s (1000 tpy) hypothetical NO_x emission source located at Knoxville /McGhee Tyson Airport.

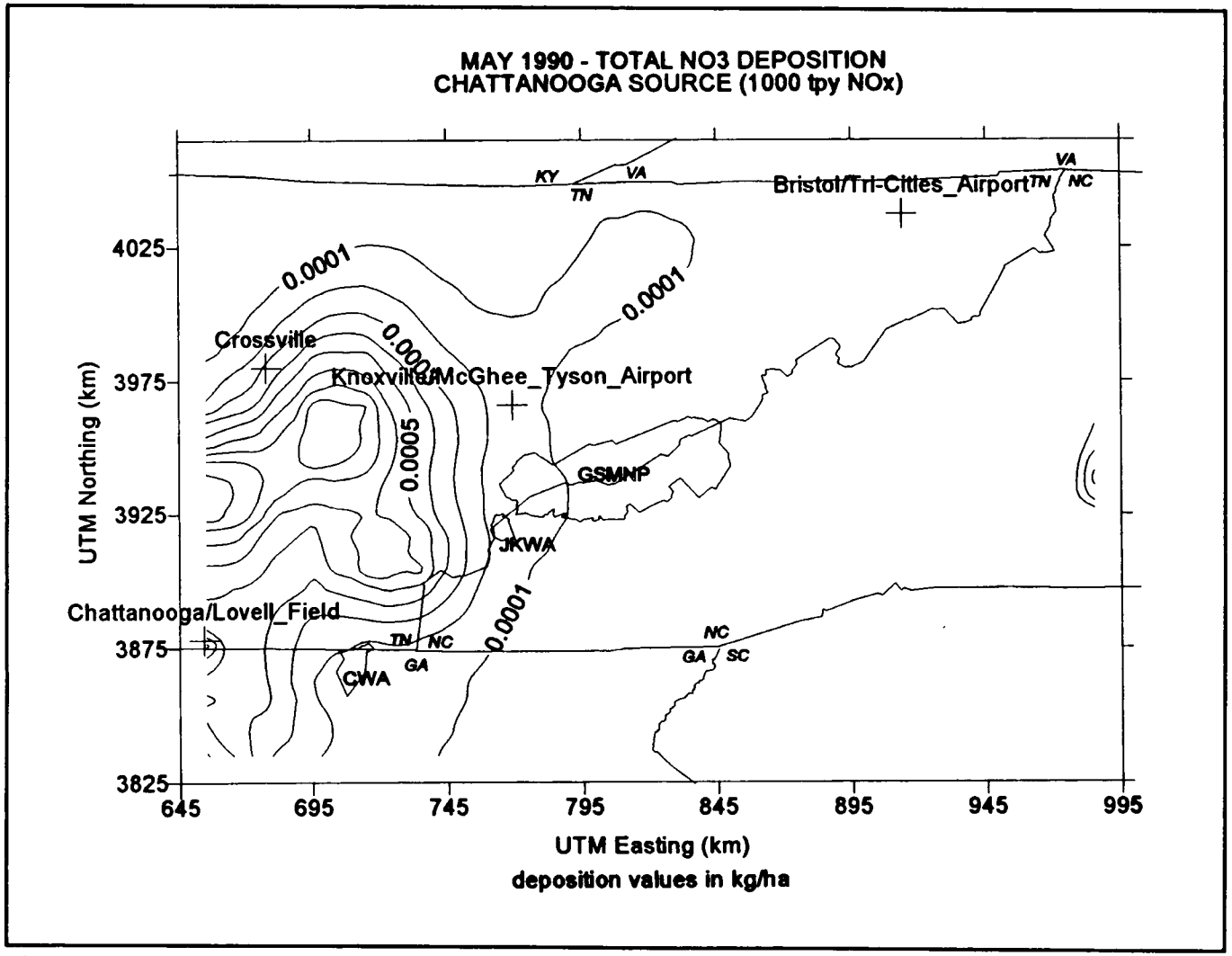

Fig. G.18. Total (wet+dry) NO_3^- deposition estimated for May 1990 resulting from a 28.8 g/s (1000 tpy) hypothetical NO_x emission source located at Chattanooga/Lovell Field.

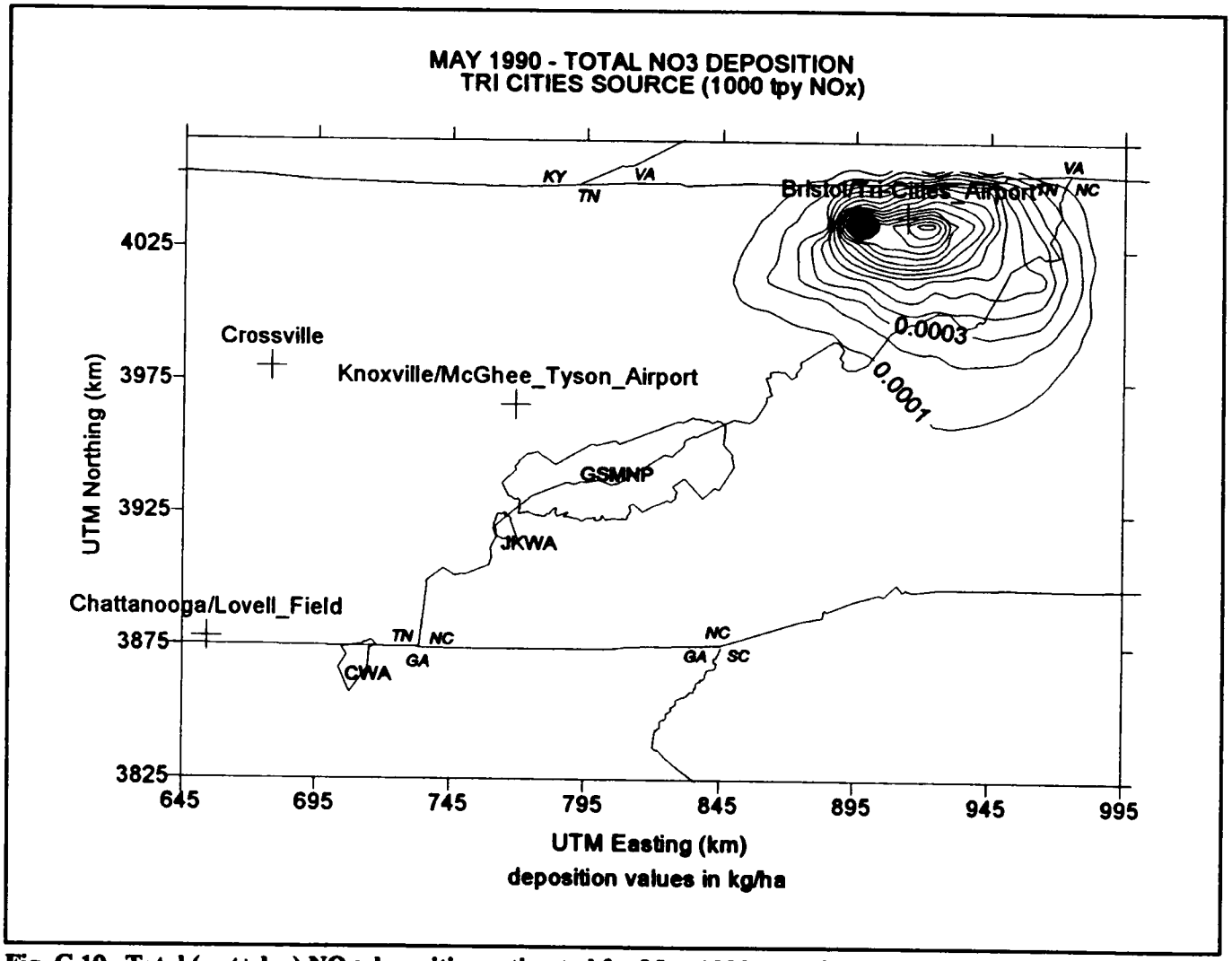

Fig. G.19. Total (wet+dry) NO_3^- deposition estimated for May 1990 resulting from a 28.8 g/s (1000 tpy) hypothetical NO_x emission source located at Bristol/Tri Cities Airport.

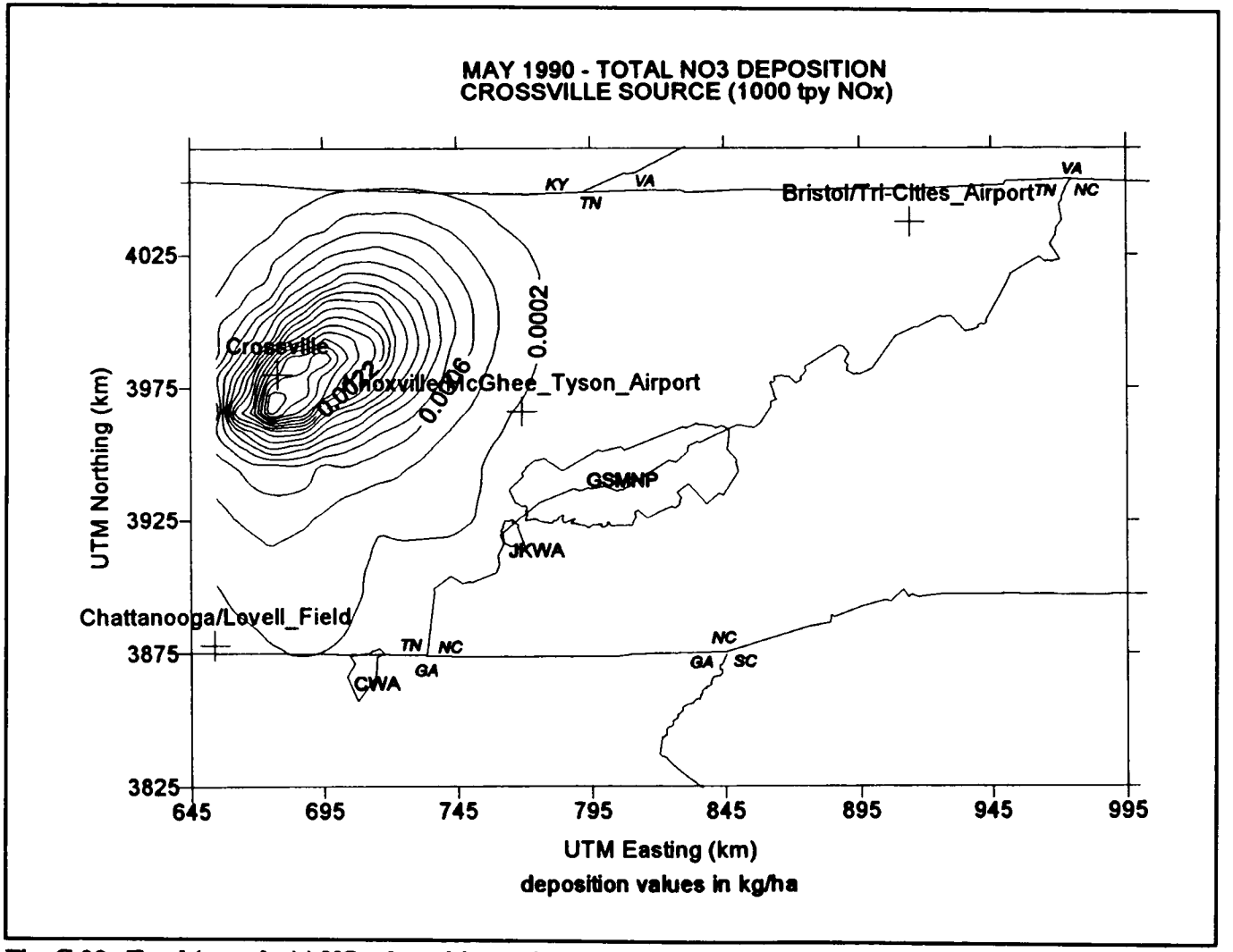

Fig. G.20. Total (wet+dry)) NO_3^- deposition estimated for May 1990 resulting from a 28.8 g/s (1000 tpy) hypothetical NO_x emission source located in Crossville.

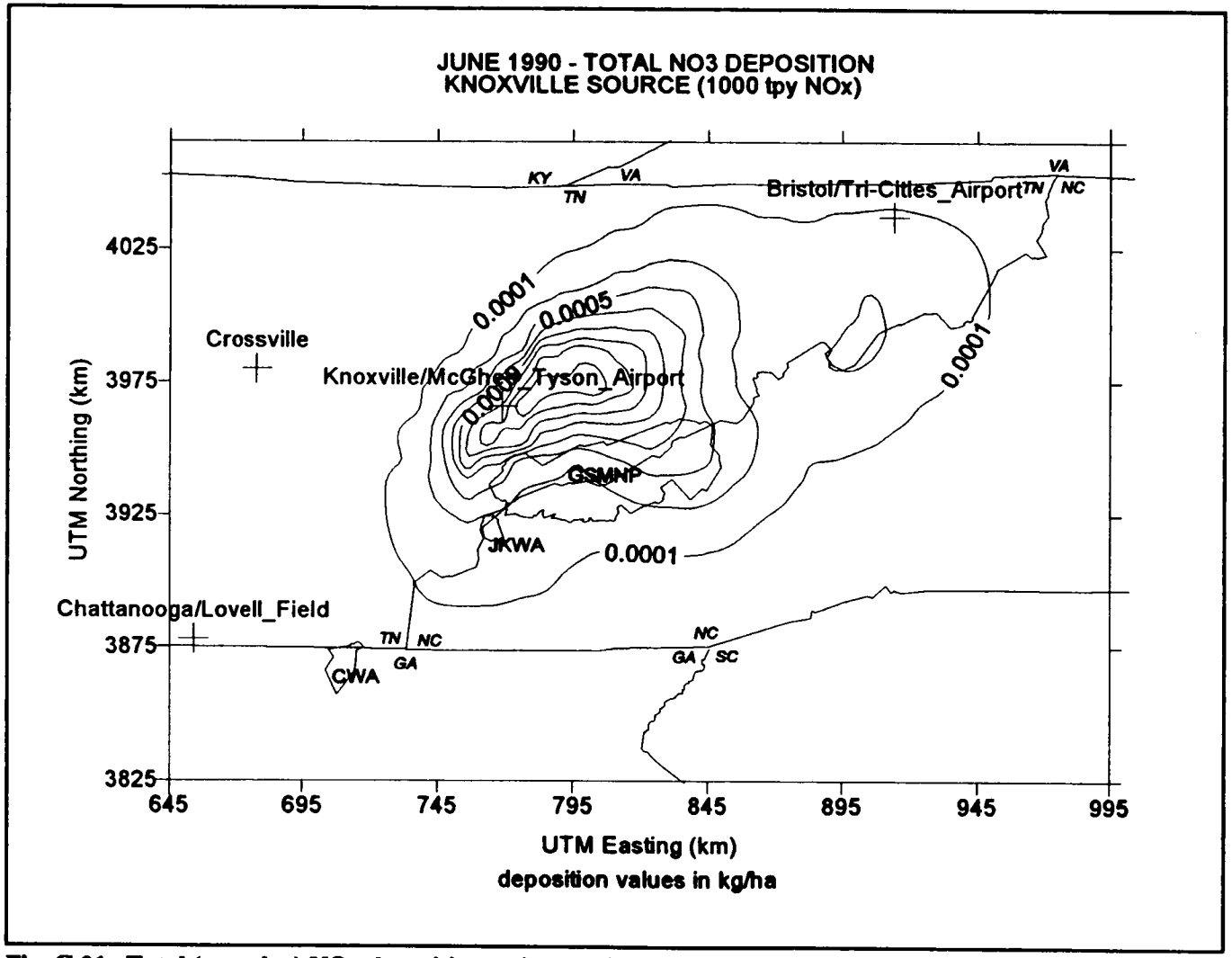

Fig. G.21. Total (wet+dry) NO_3^- deposition estimated for June 1990 resulting from a 28.8 g/s (1000 tpy) hypothetical NO_x emission source located at Knoxville /McGhee Tyson Airport.

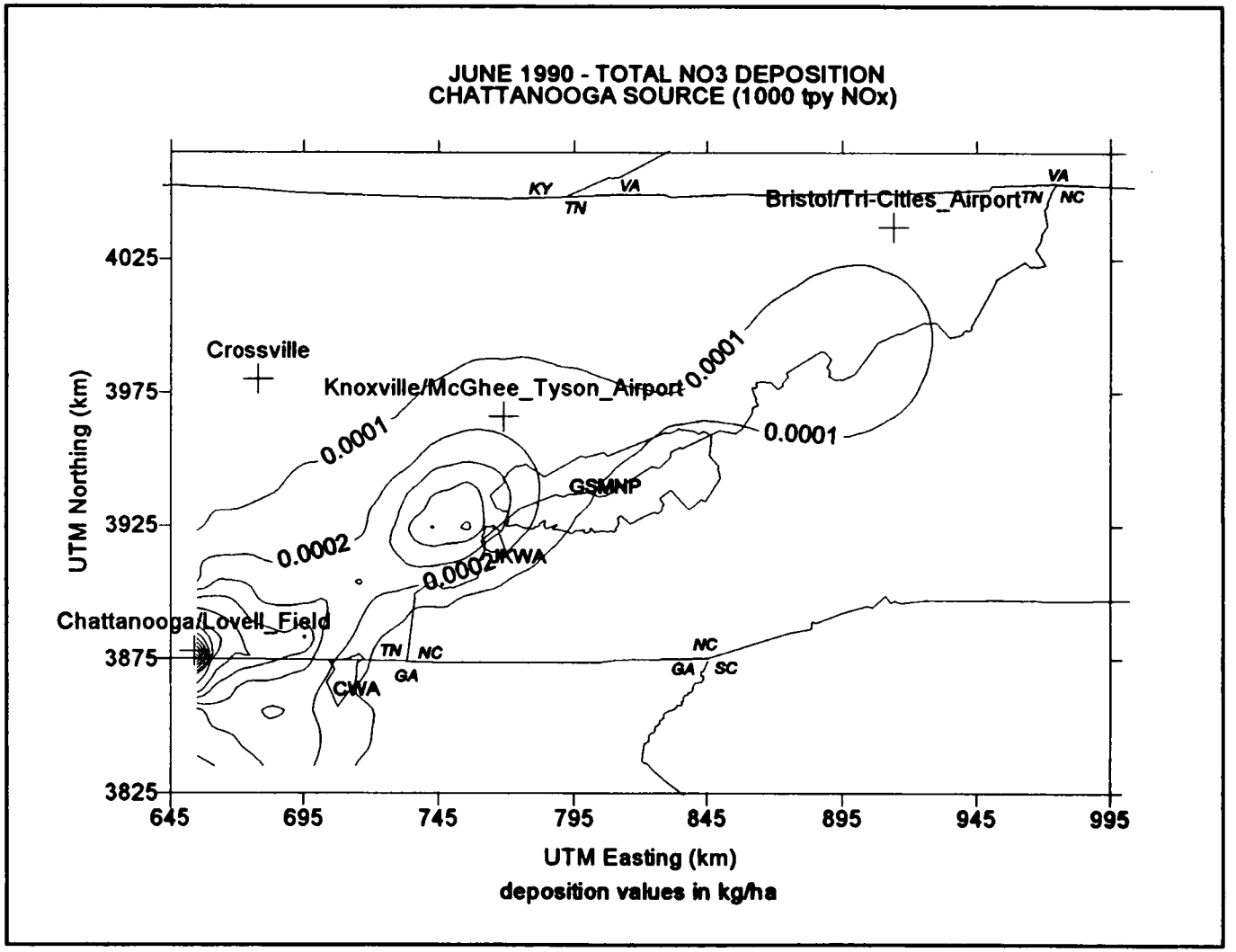

Fig. G.22. Total (wet+dry) NO_3^- deposition estimated for June 1990 resulting from a 28.8 g/s (1000 tpy) hypothetical NO_x emission source located at Chattanooga/Lovell Field.

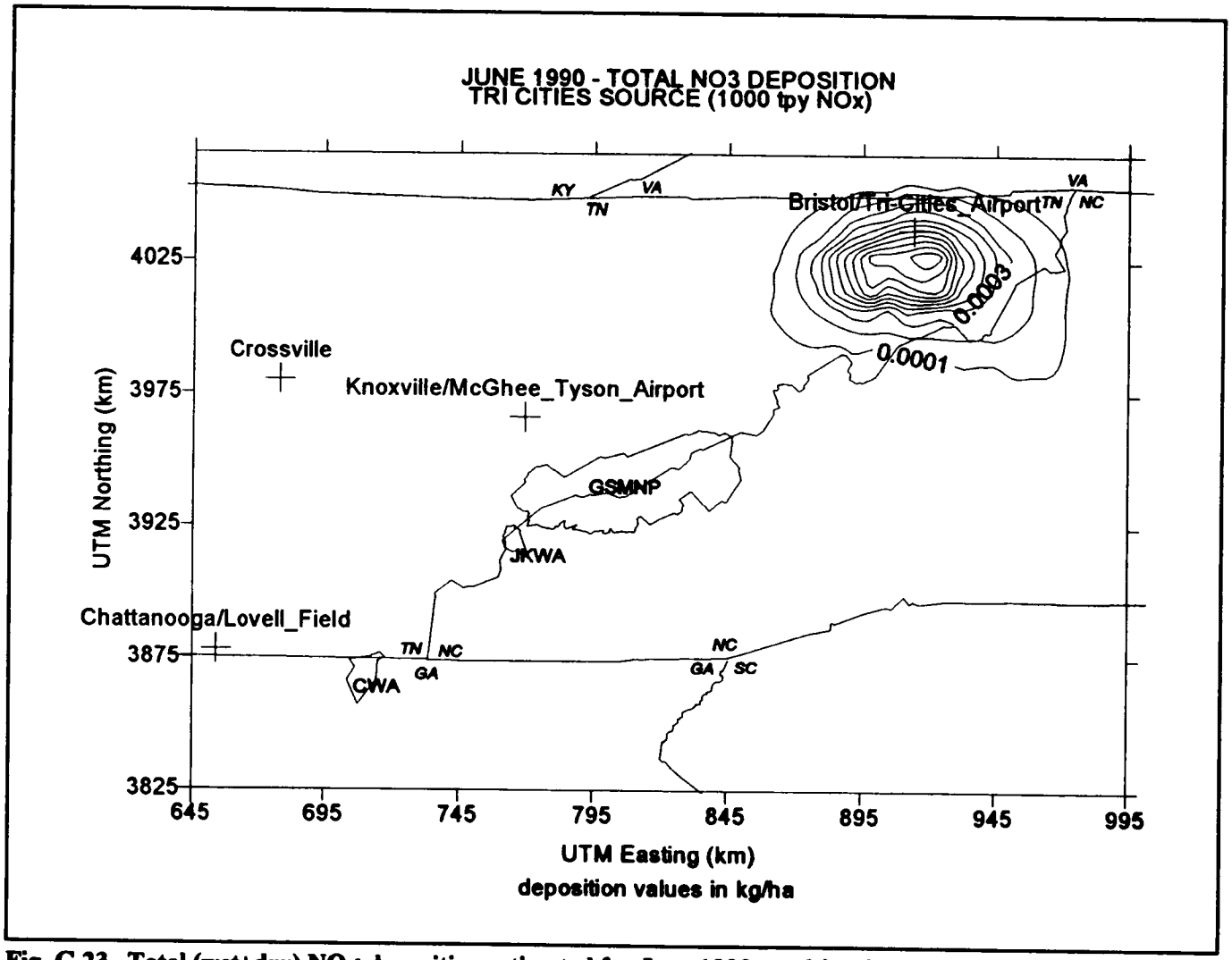

Fig. G.23. Total (wet+dry) NO_3^- deposition estimated for June 1990 resulting from a 28.8 g/s (1000 tpy) hypothetical NO_x emission source located at Bristol/Tri Cities Airport.

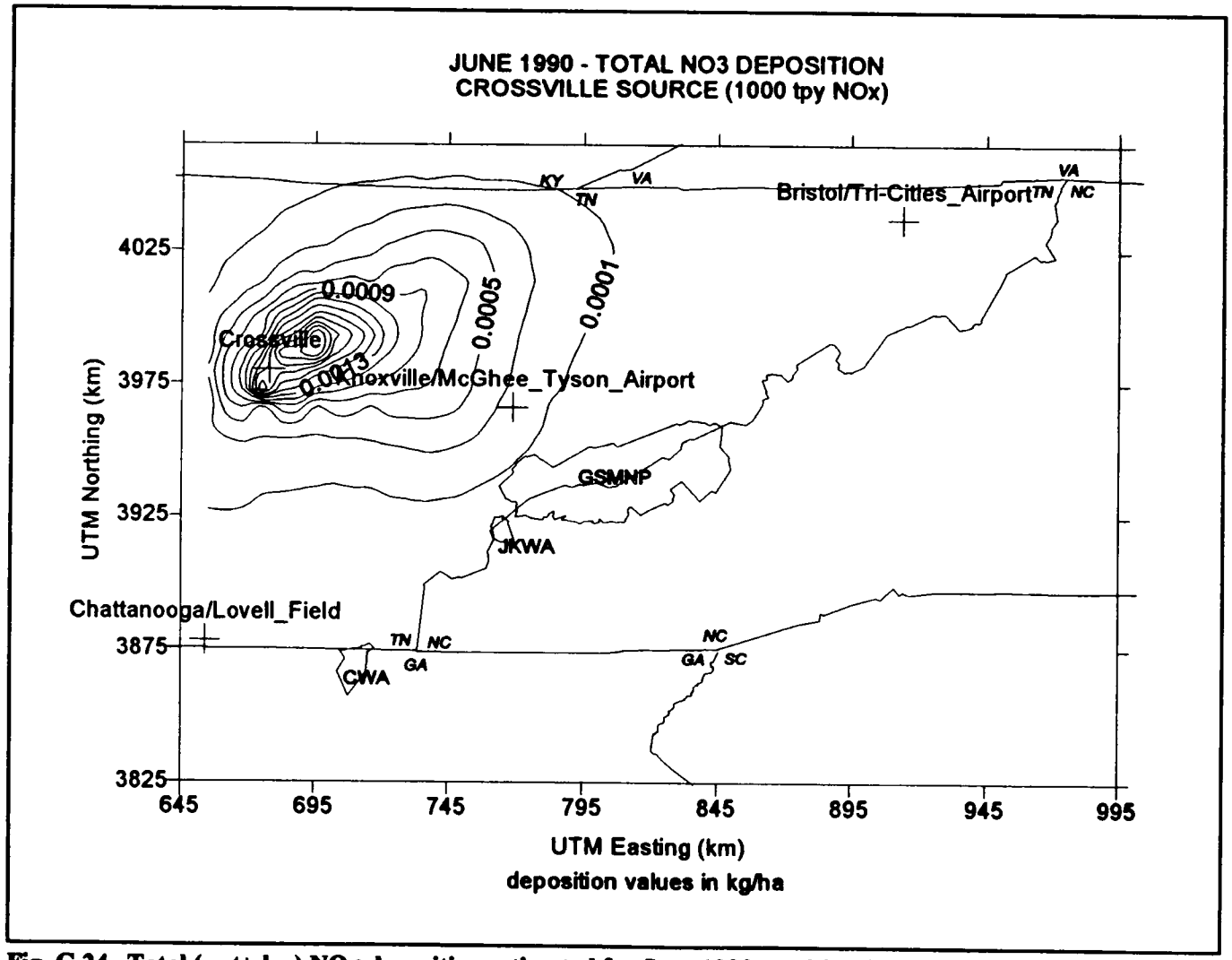

Fig. G.24. Total (wet+dry) NO_3^- deposition estimated for June 1990 resulting from a 28.8 g/s (1000 tpy) hypothetical NO_x emission source located in Crossville.

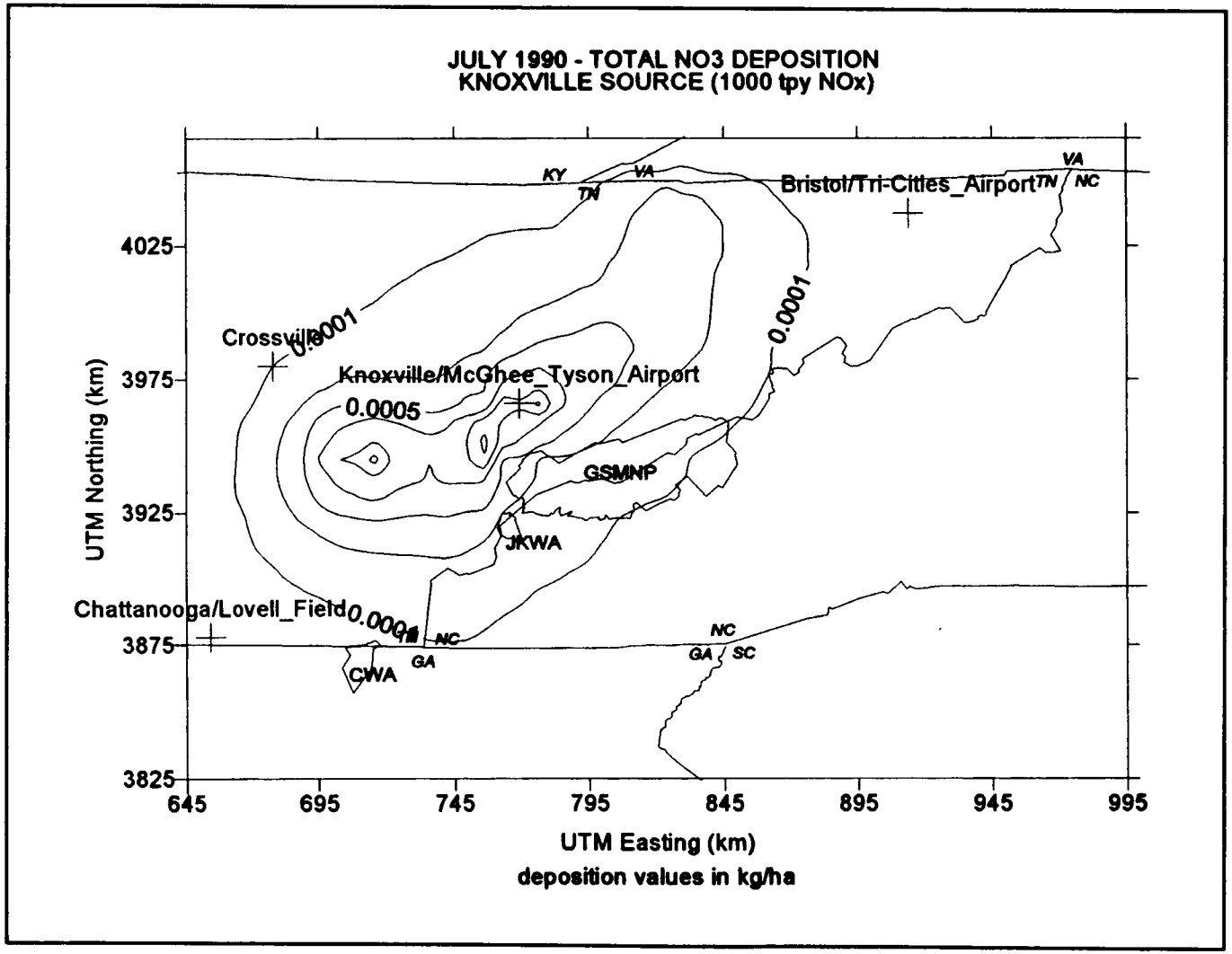

Fig. G.25. Total (wet+dry) NO_3^- deposition estimated for July 1990 resulting from a 28.8 g/s (1000 tpy) hypothetical NO_x emission source located at Knoxville /McGhee Tyson Airport.

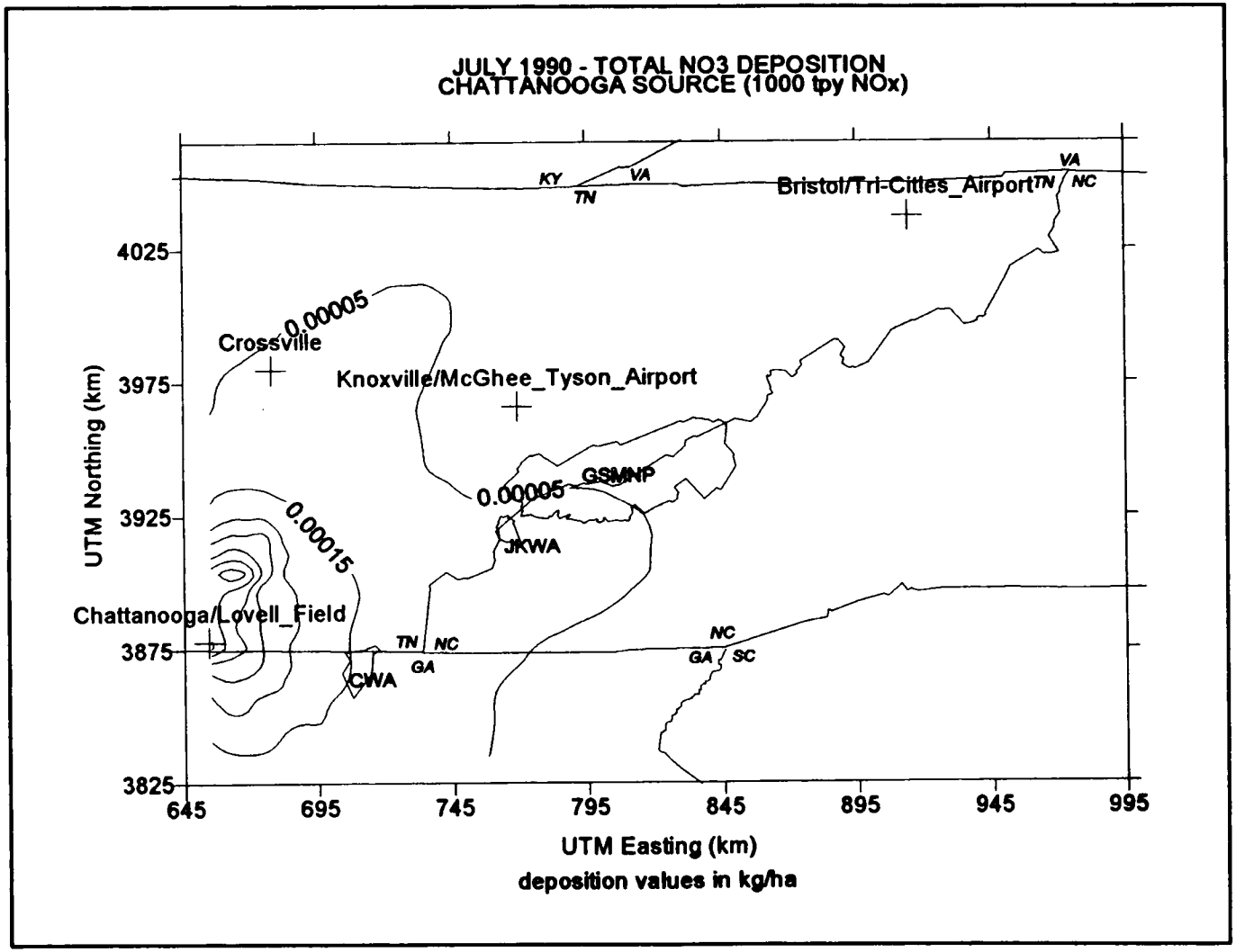

Fig. G.26. Total (wet+dry) NO_3^- deposition estimated for July 1990 resulting from a 28.8 g/s (1000 tpy) hypothetical NO_x emission source located at Chattanooga/Lovell Field.

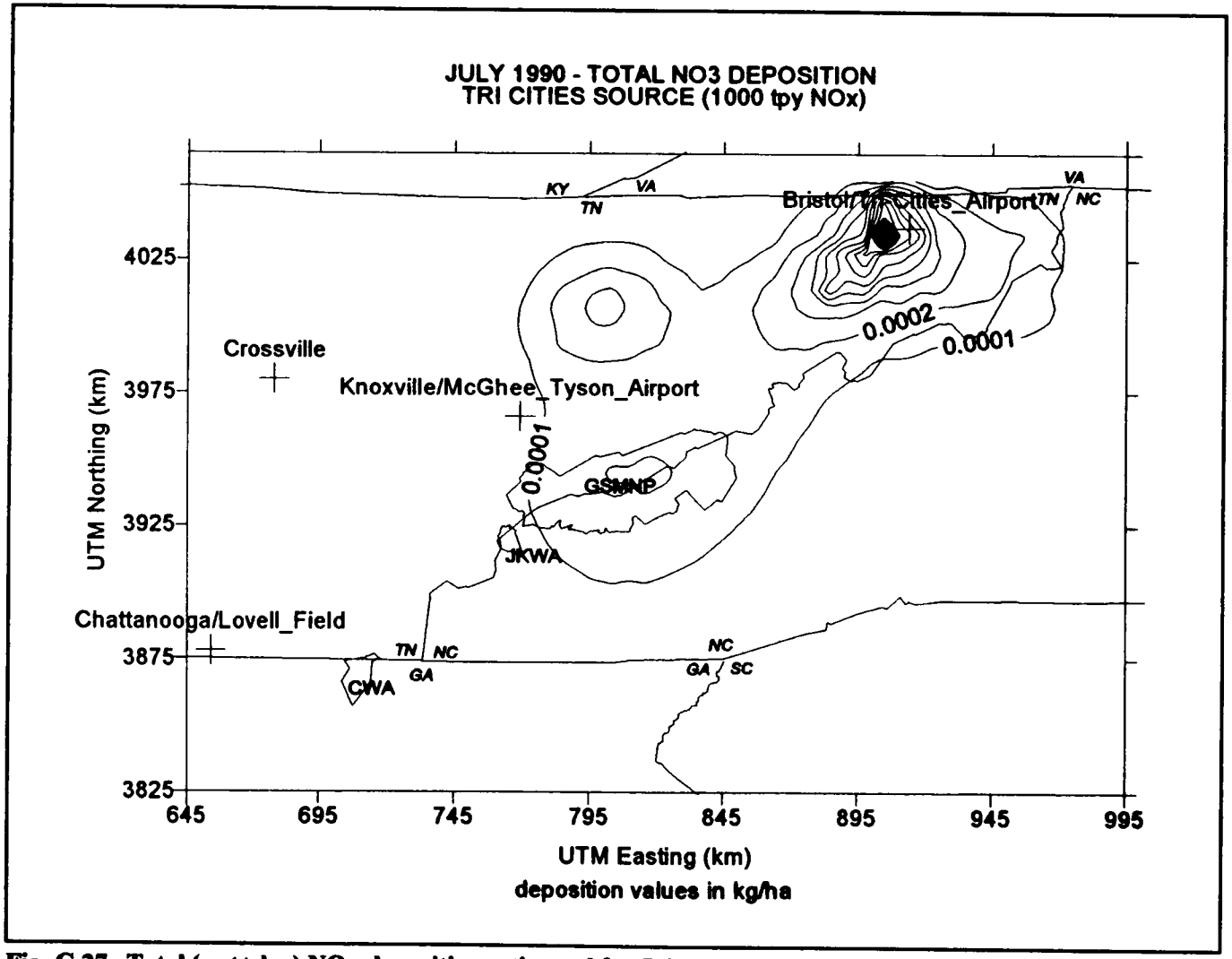

Fig. G.27. Total (wet+dry) NO_3^- deposition estimated for July 1990 resulting from a 28.8 g/s (1000 tpy) hypothetical NO_x emission source located at Bristol/Tri Cities Airport.

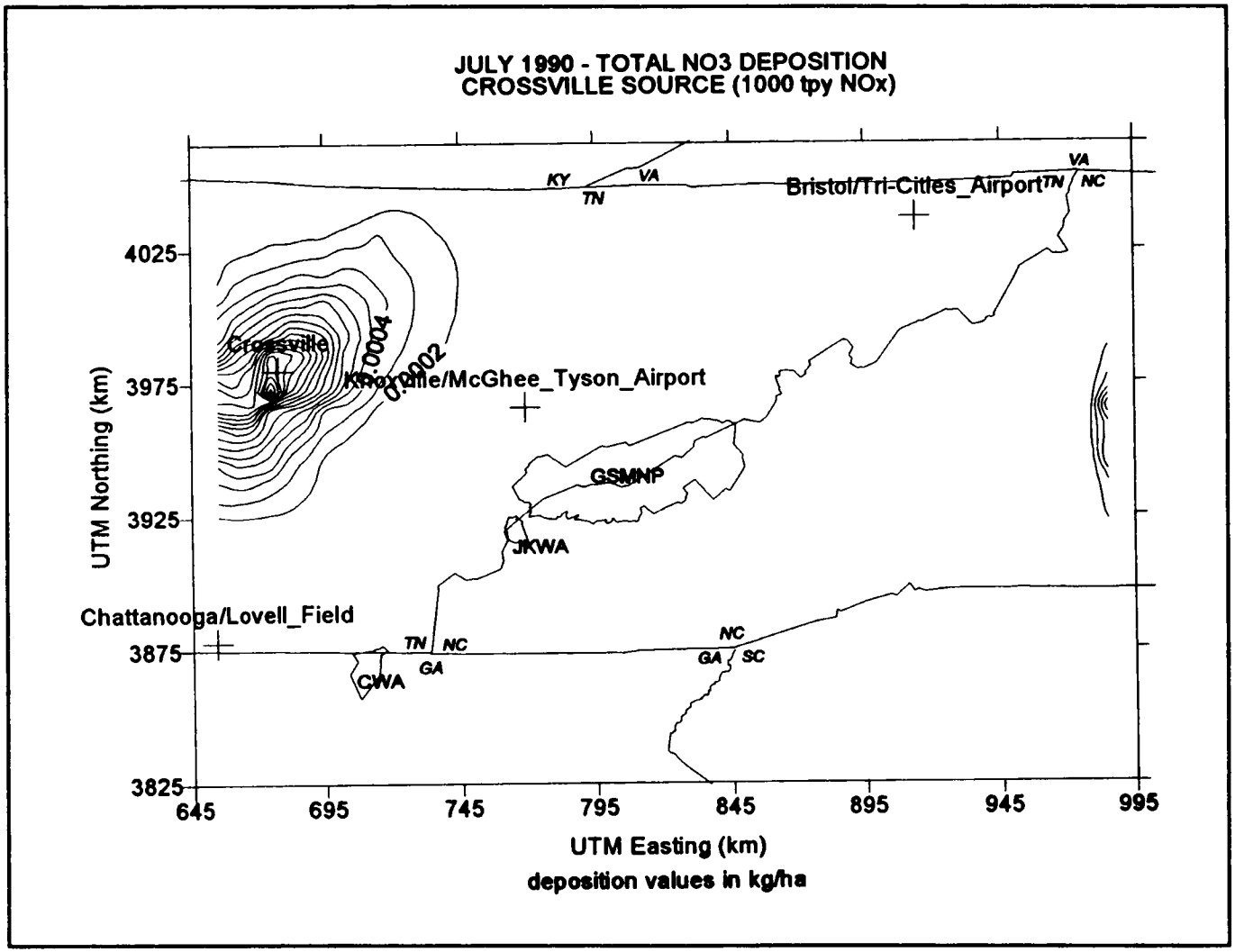

Fig. G.28. Total (wet+dry) NO_3^- deposition estimated for July 1990 resulting from a 28.8 g/s (1000 tpy) hypothetical NO_x emission source located in Crossville.

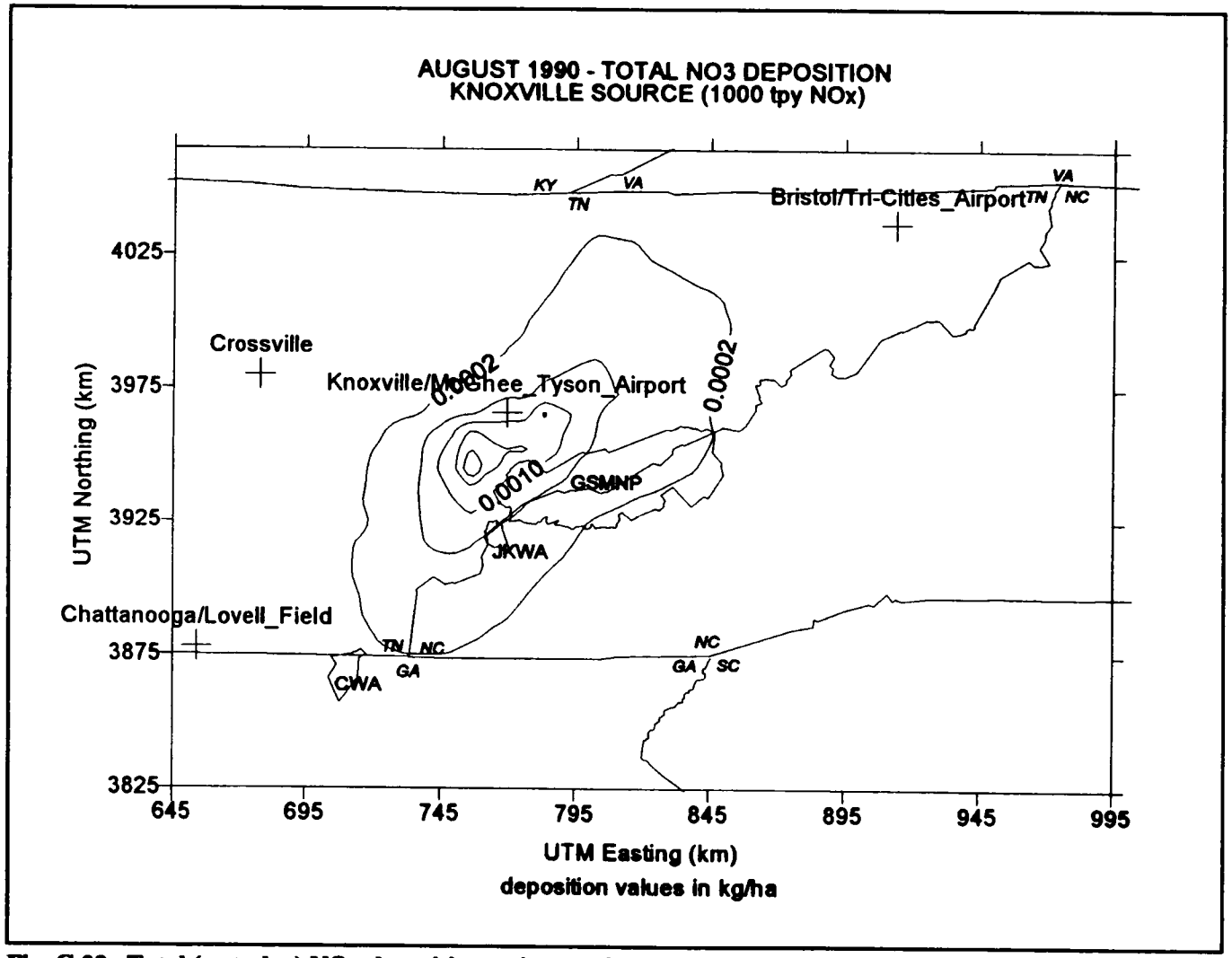

Fig. G.29. Total (wet+dry) NO_3^- deposition estimated for August 1990 resulting from a 28.8 g/s (1000 tpy) hypothetical NO_x emission source located at Knoxville /McGhee Tyson Airport.

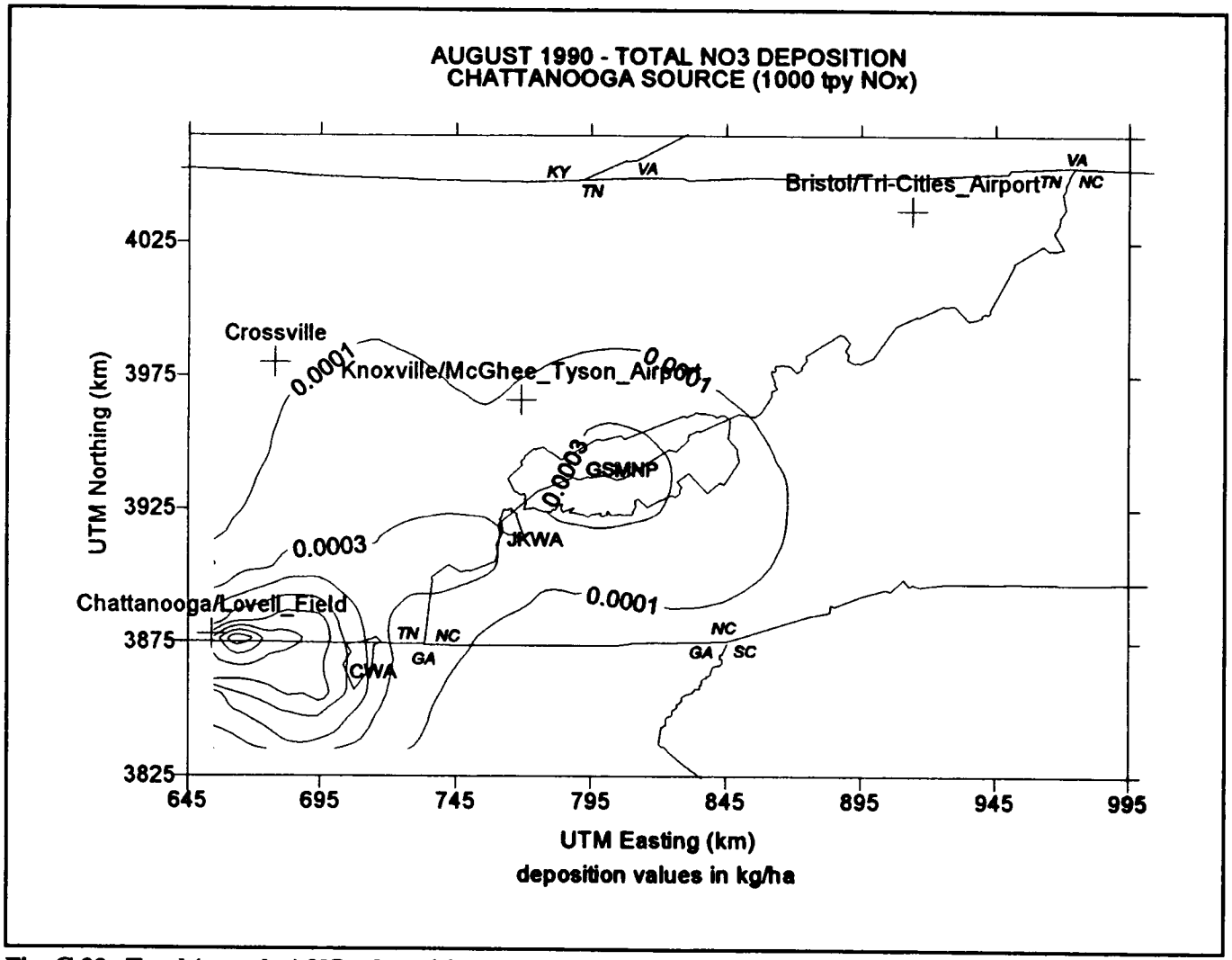

Fig. G.30. Total (wet+dry) NO_3^- deposition estimated for August 1990 resulting from a 28.8 g/s (1000 tpy) hypothetical NO_x emission source located at Chattanooga/Lovell Field.

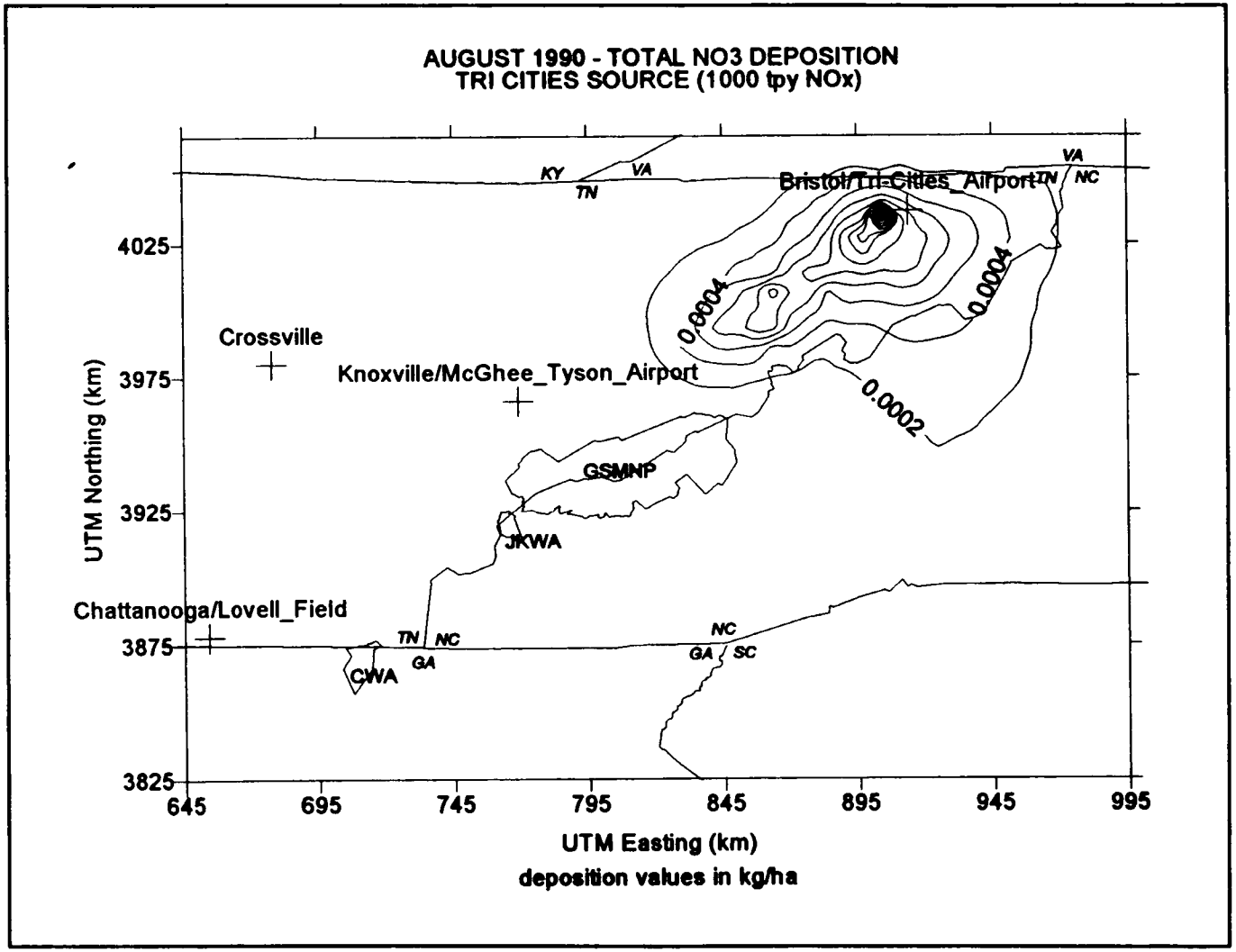

Fig. G.31. Total (wet+dry) NO_3^- deposition estimated for August 1990 resulting from a 28.8 g/s (1000 tpy) hypothetical NO_x emission source located at Bristol/Tri Cities Airport.

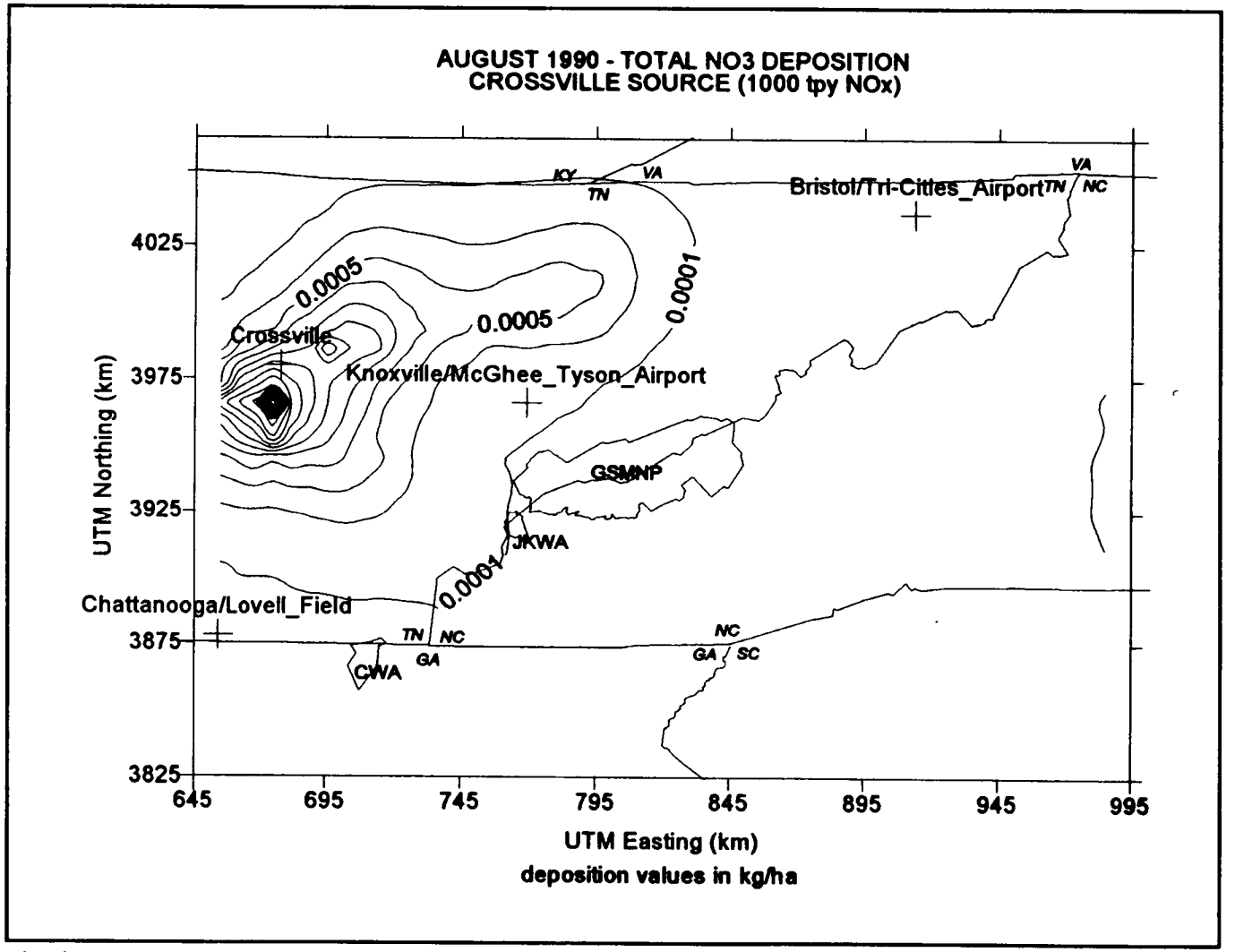

Fig. G.32. Total (wet+dry) NO_3^- deposition estimated for August 1990 resulting from a 28.8 g/s (1000 tpy) hypothetical NO_x emission source located in Crossville.

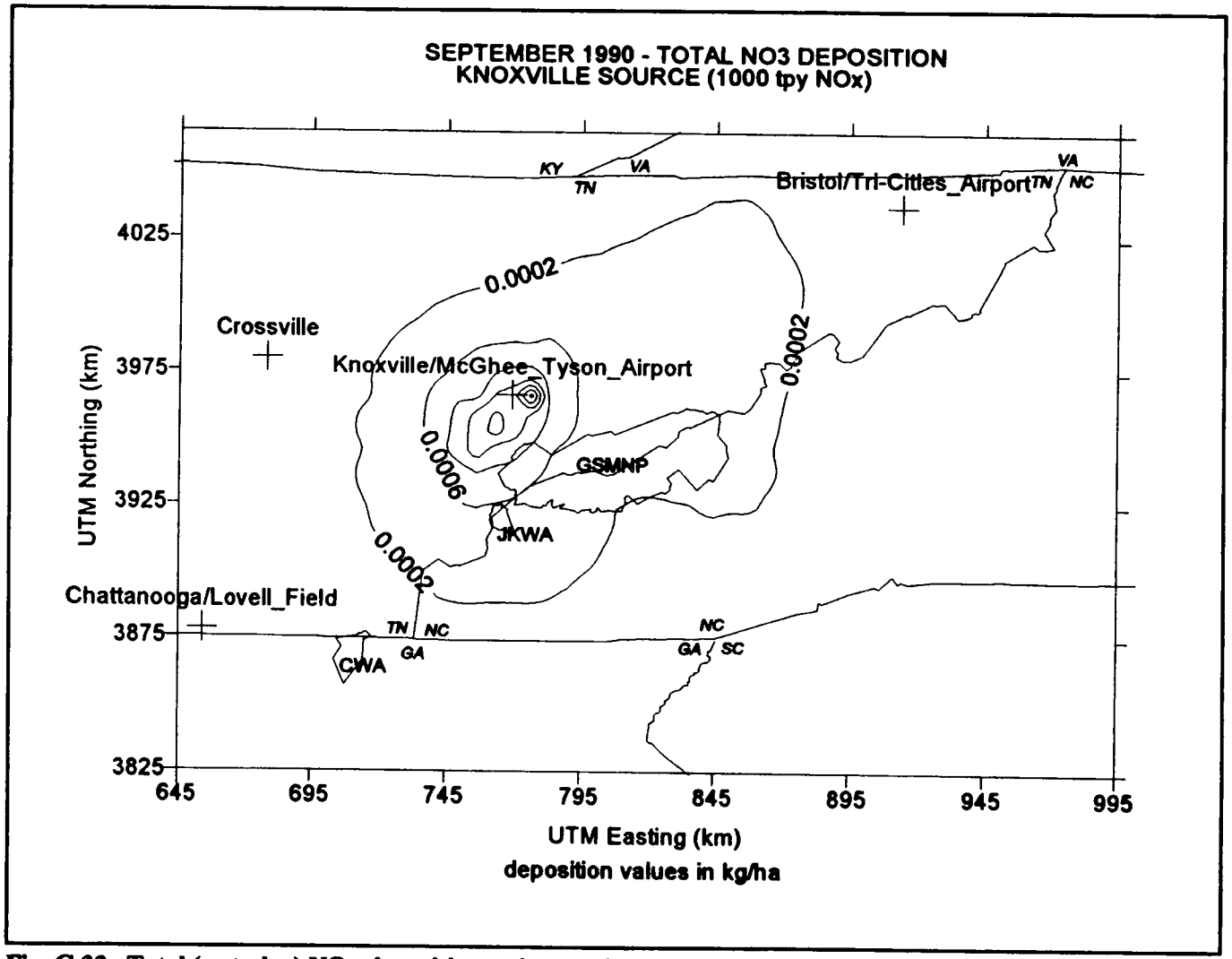

Fig. G.33. Total (wet+dry) NO_3^- deposition estimated for September 1990 resulting from a 28.8 g/s (1000 tpy) hypothetical NO_x emission source located at Knoxville /McGhee Tyson Airport.

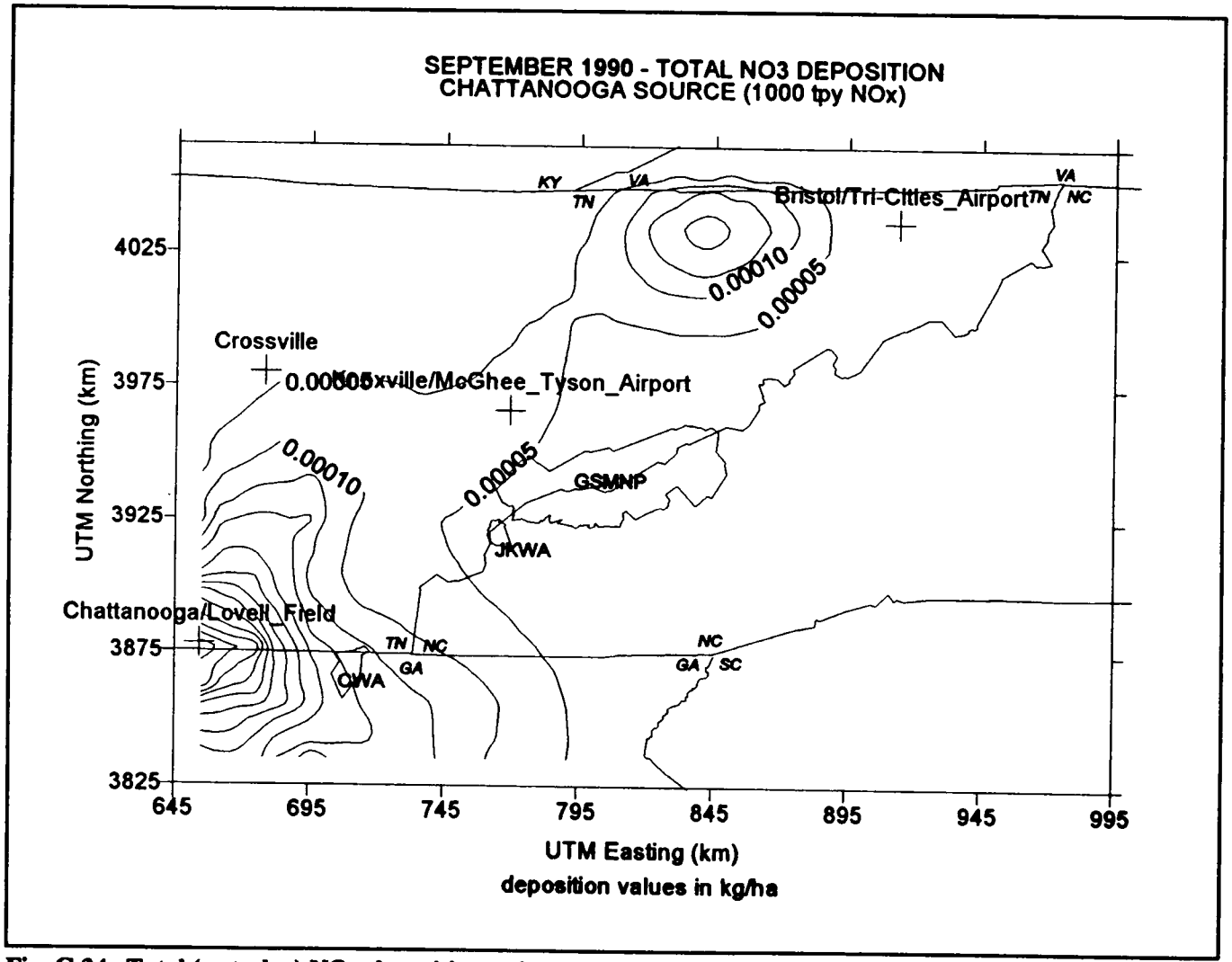

Fig. G.34. Total (wet+dry) NO_3^- deposition estimated for September 1990 resulting from a 28.8 g/s (1000 tpy) hypothetical NO_x emission source located at Chattanooga/Lovell Field.

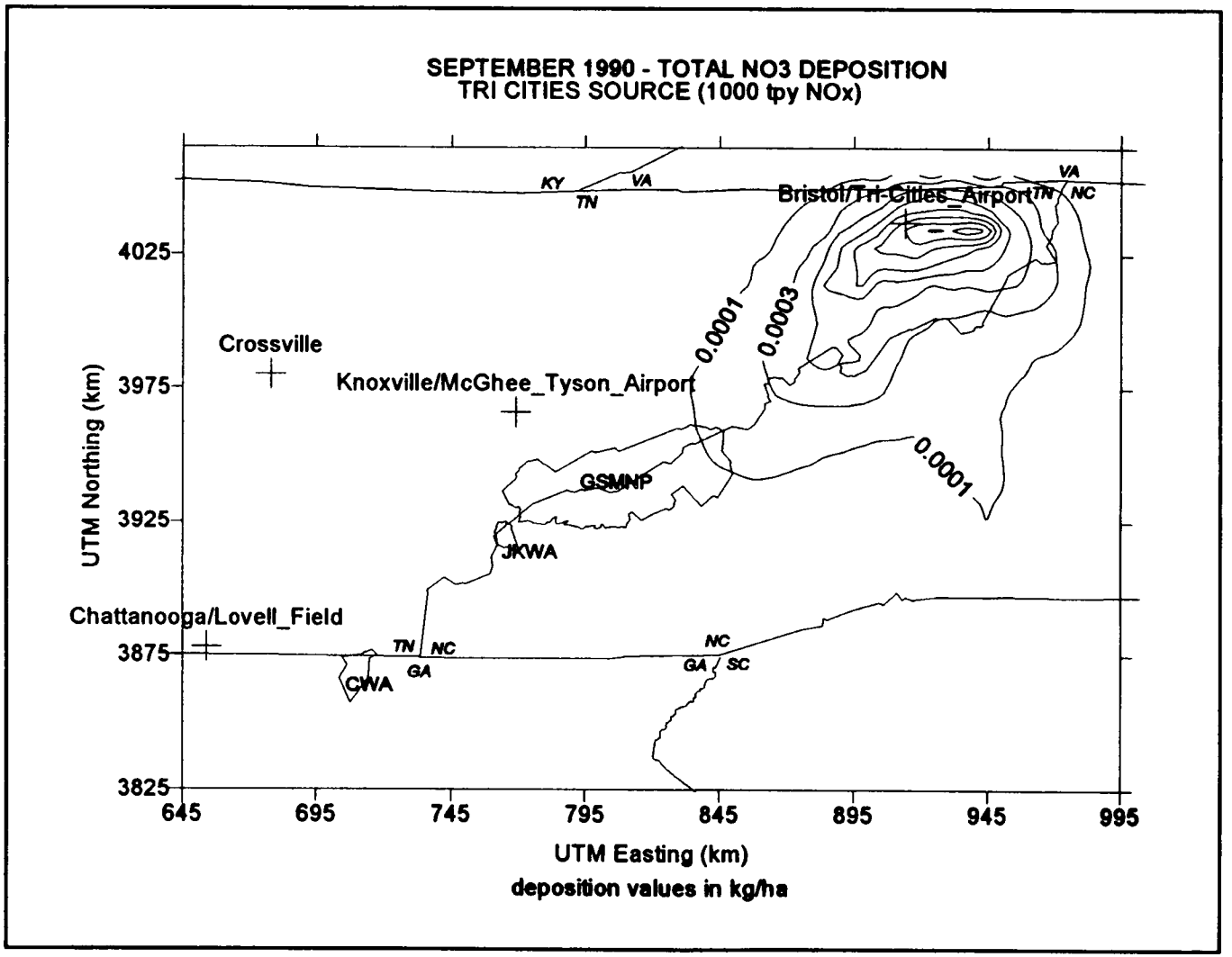

Fig. G.35. Total (wet+dry) NO_3^- deposition estimated for September 1990 resulting from a 28.8 g/s (1000 tpy) hypothetical NO_x emission source located at Bristol/Tri Cities Airport.

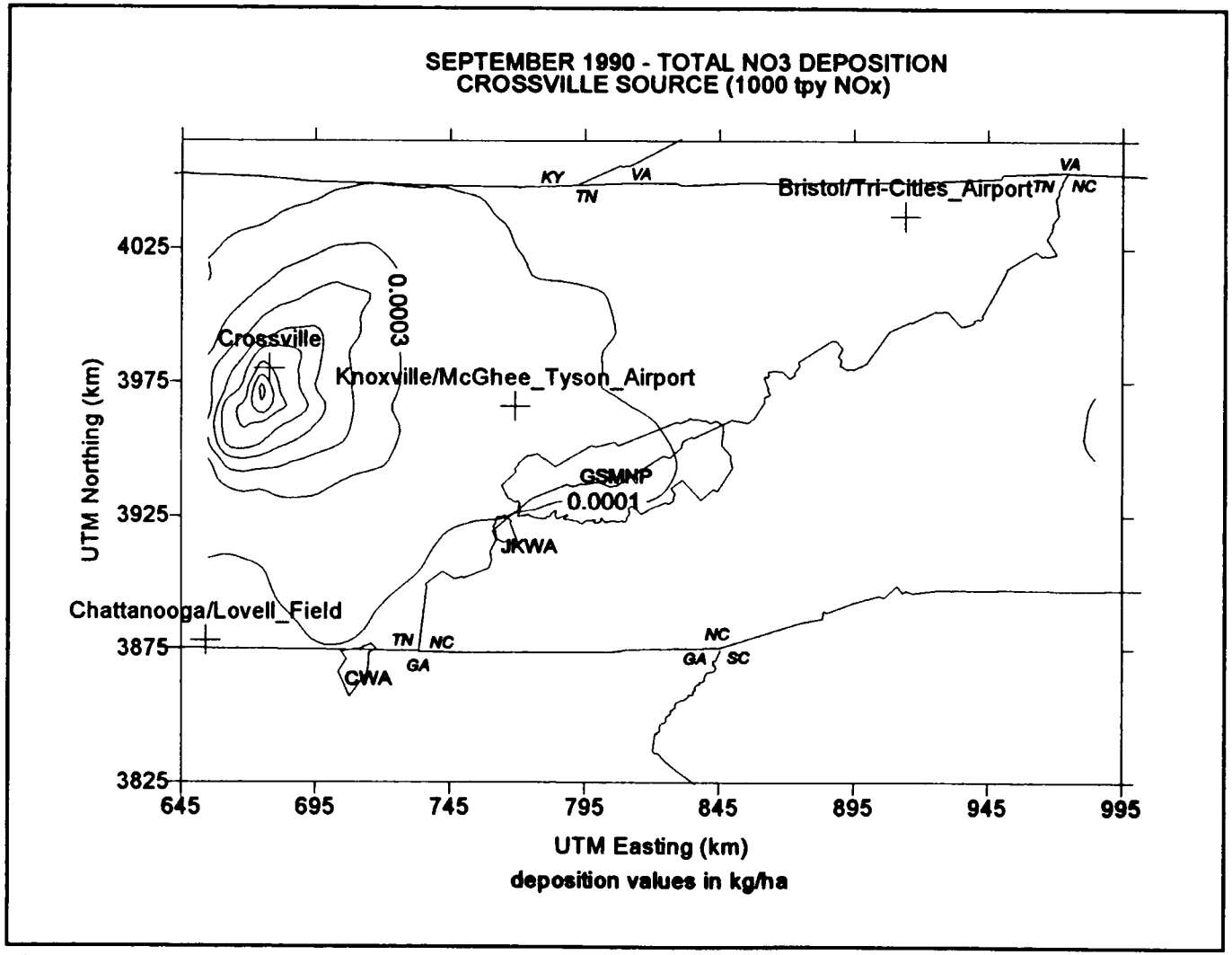

Fig. G.36. Total (wet+dry) NO_3^- deposition estimated for September 1990 resulting from a 28.8 g/s (1000 tpy) hypothetical NO_x emission source located in Crossville.

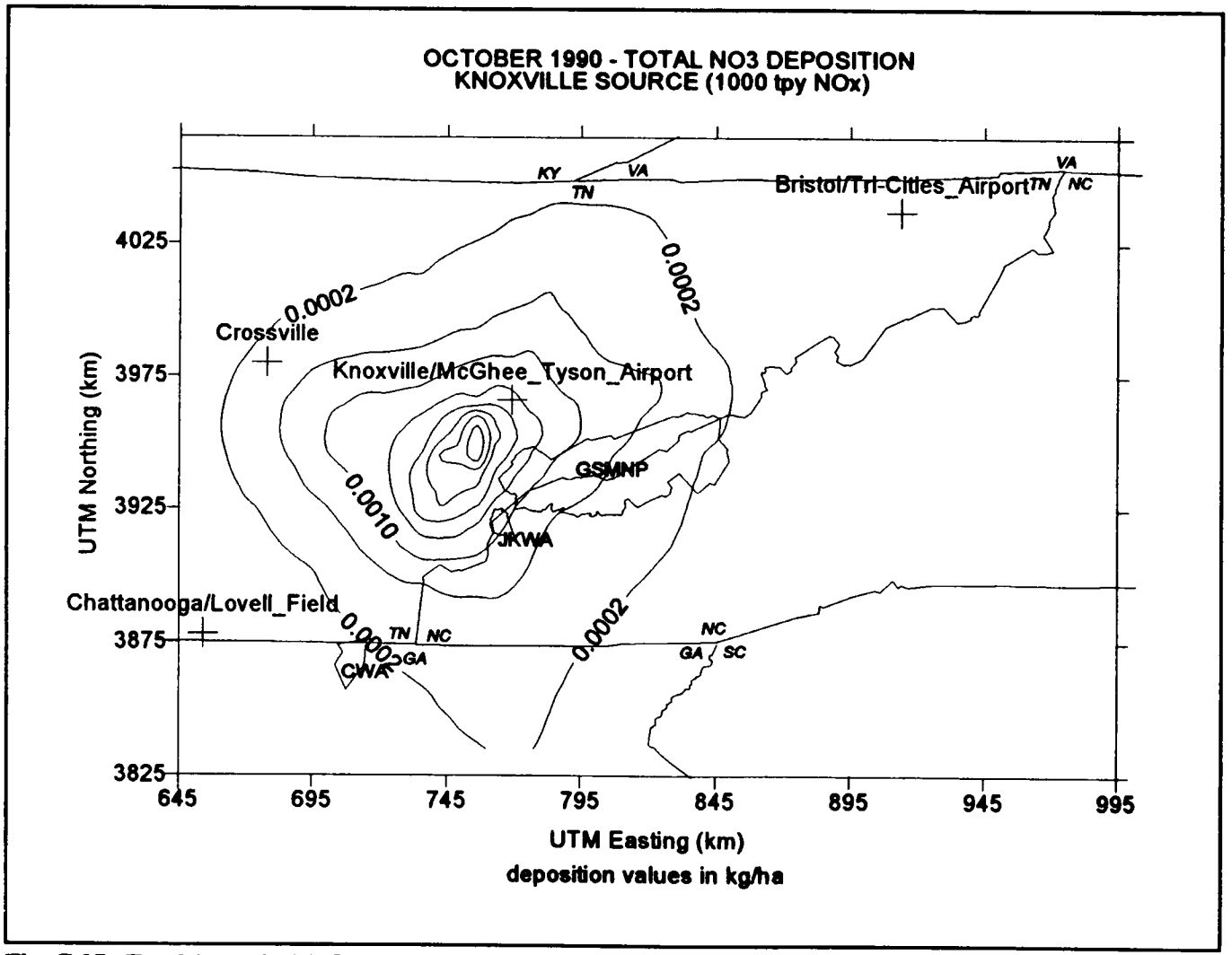

Fig. G.37. Total (wet+dry) NO_3^- deposition estimated for October 1990 resulting from a 28.8 g/s (1000 tpy) hypothetical NO_x emission source located at Knoxville /McGhee Tyson Airport.

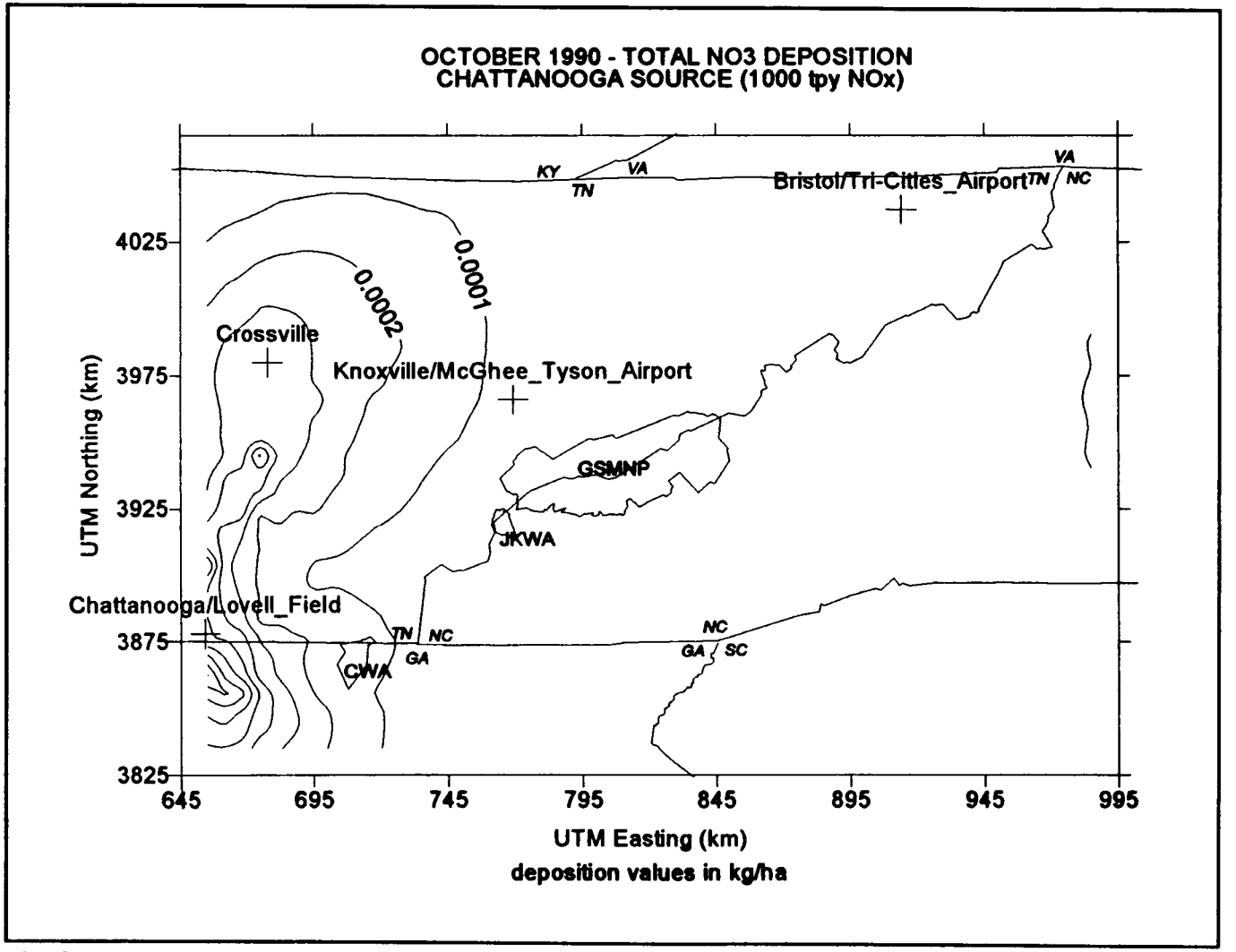

Fig. G.38. Total (wet+dry) NO_3^- deposition estimated for October 1990 resulting from a 28.8 g/s (1000 tpy) hypothetical NO_x emission source located at Chattanooga/Lovell Field.

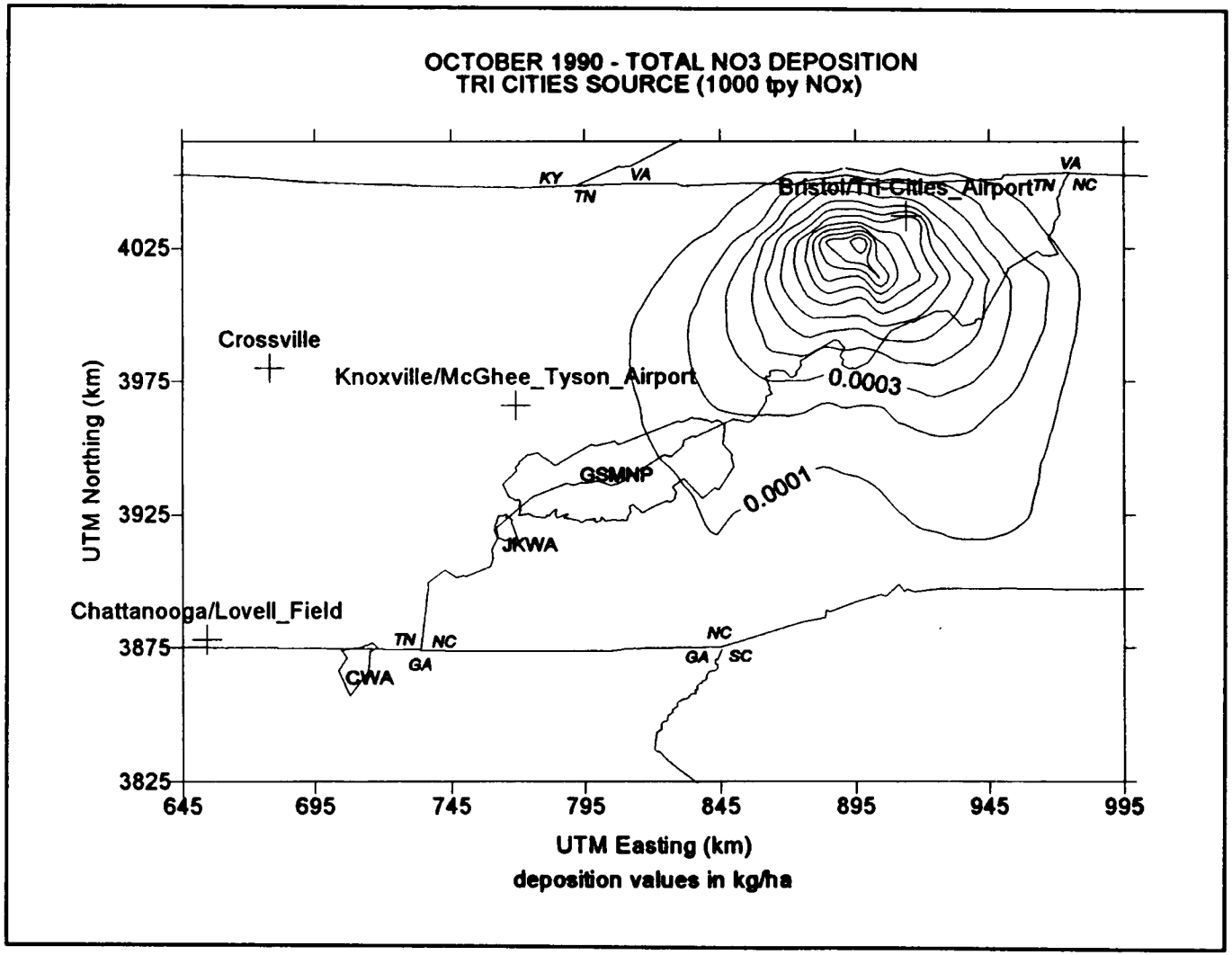

Fig. G.39. Total (wet+dry) NO_3^- deposition estimated for October 1990 resulting from a 28.8 g/s (1000 tpy) hypothetical NO_x emission source located at Bristol/Tri Cities Airport.

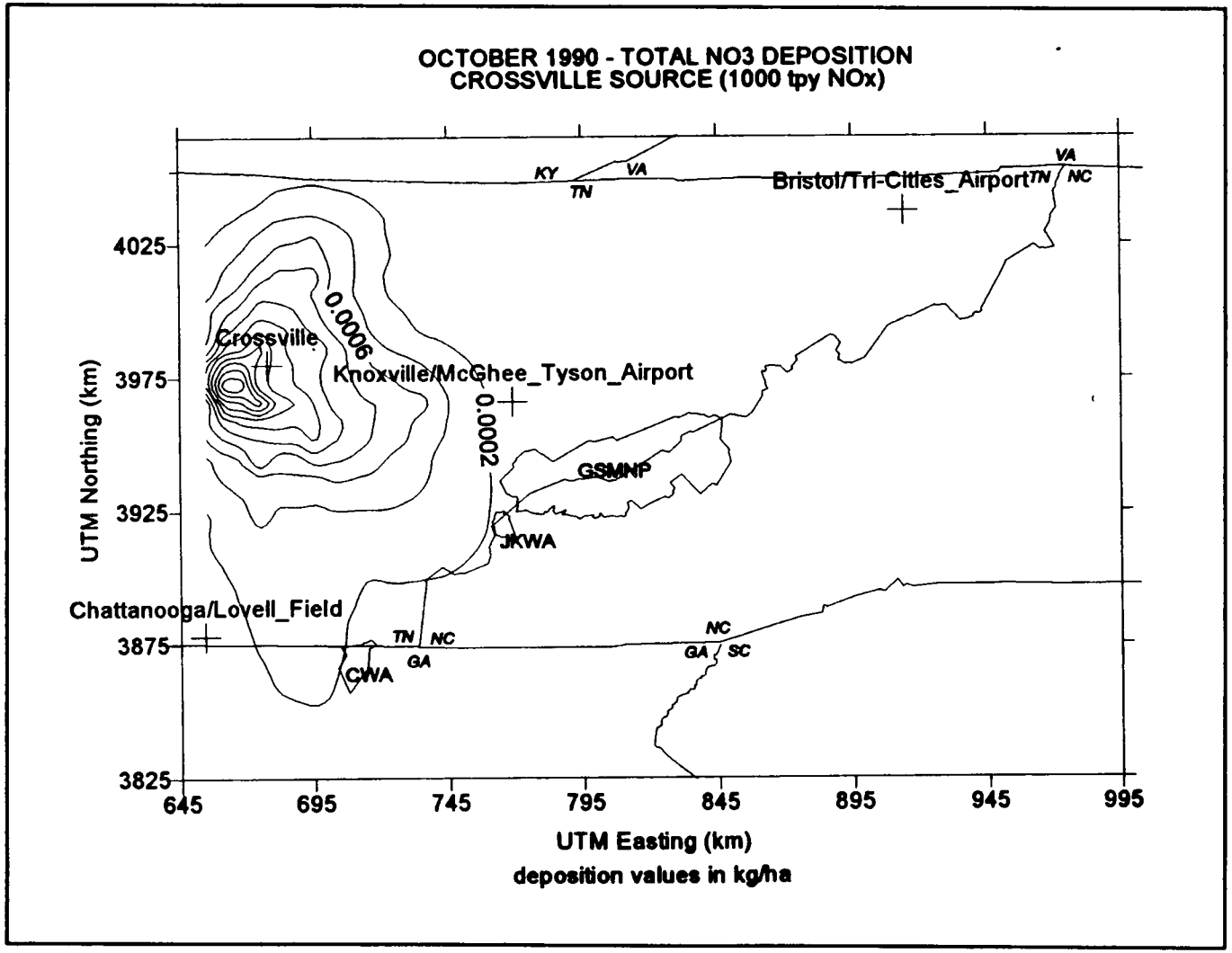

Fig. G.40. Total (wet+dry) NO_3^- deposition estimated for October 1990 resulting from a 28.8 g/s (1000 tpy) hypothetical NO_x emission source located in Crossville.

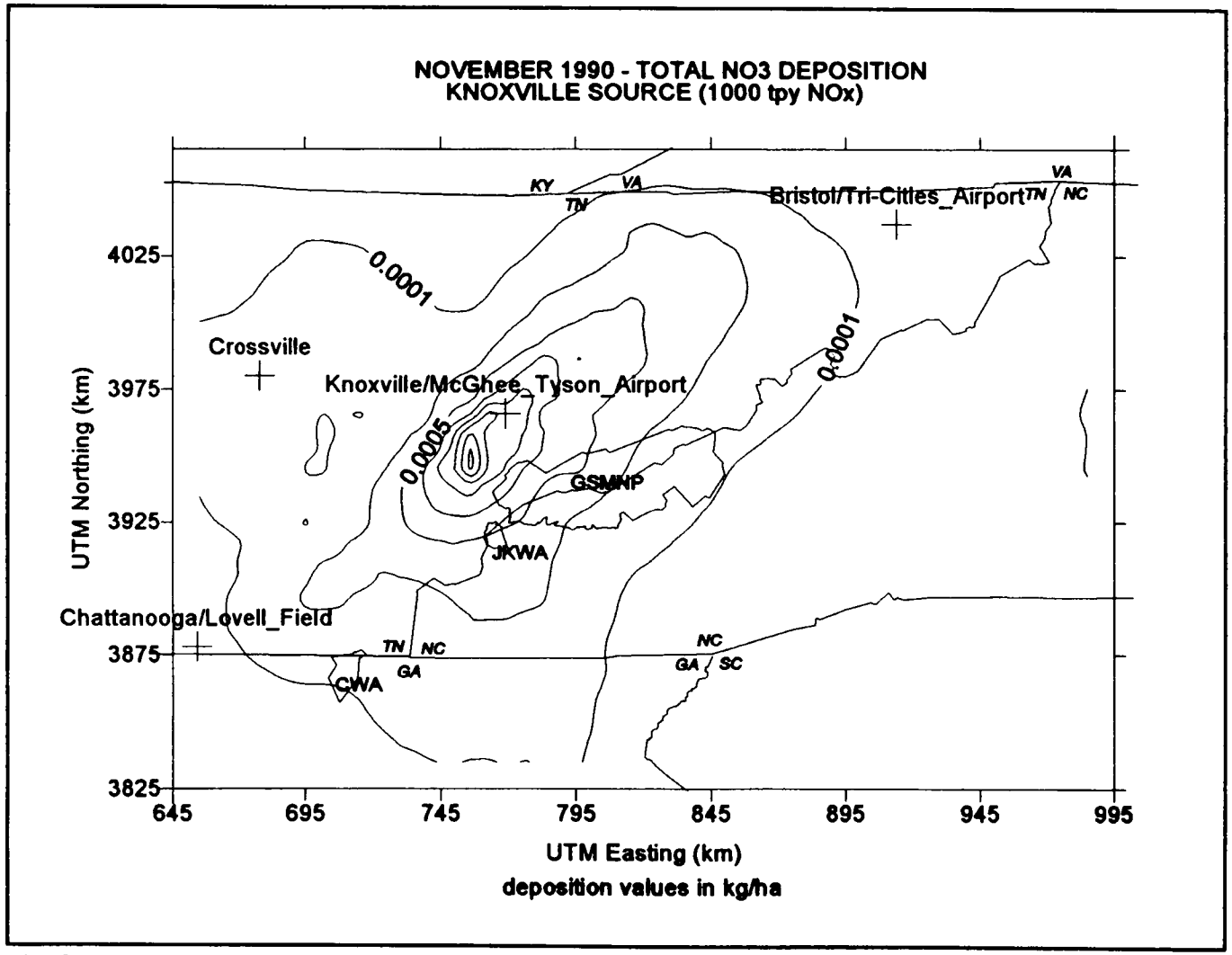

Fig. G.41. Total (wet+dry) NO_3^- deposition estimated for November 1990 resulting from a 28.8 g/s (1000 tpy) hypothetical NO_x emission source located at Knoxville /McGhee Tyson Airport.

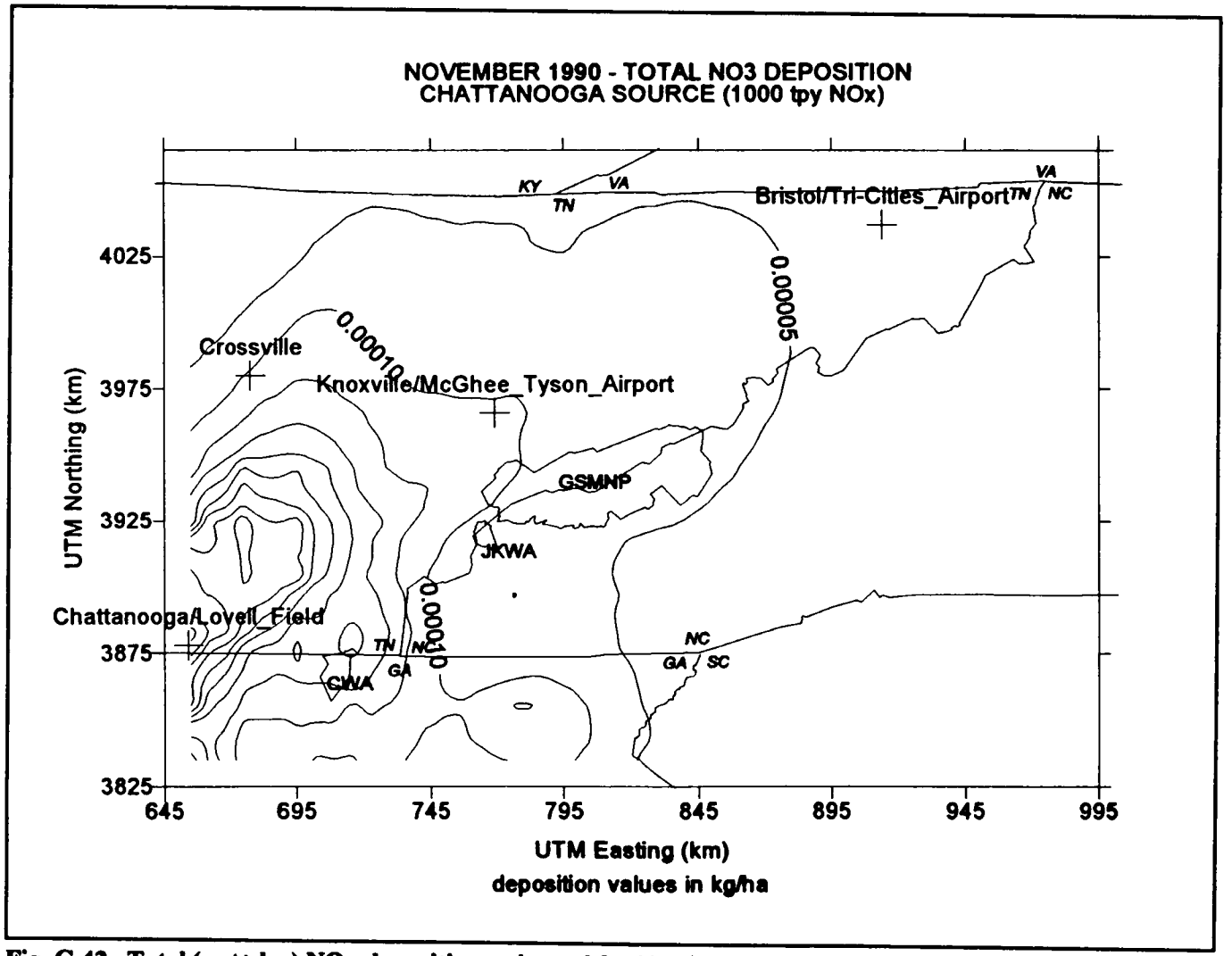

Fig. G.42. Total (wet+dry) NO_3^- deposition estimated for November 1990 resulting from a 28.8 g/s (1000 tpy) hypothetical NO_x emission source located at Chattanooga/Lovell Field.

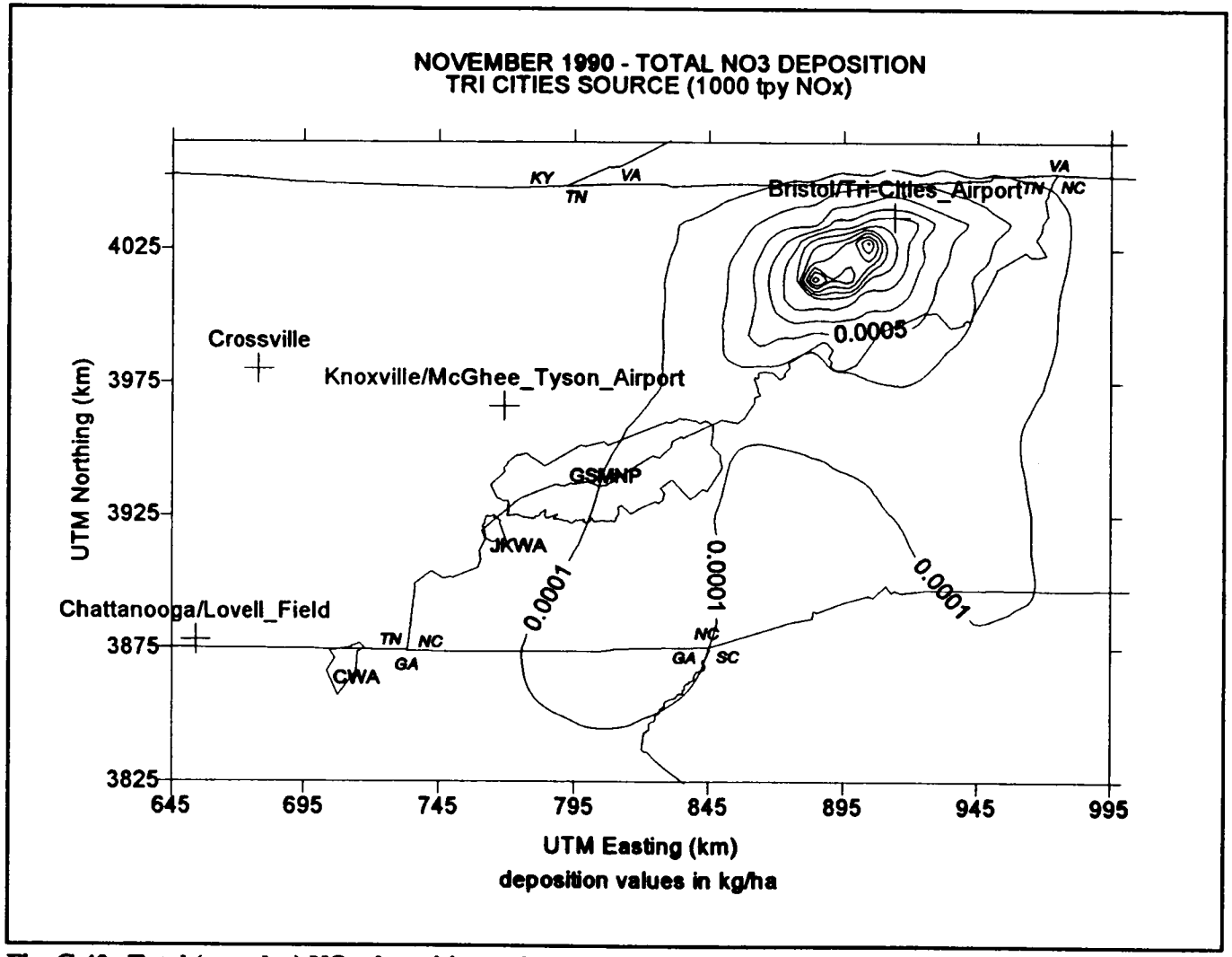

Fig. G.43. Total (wet+dry) NO_3^- deposition estimated for November 1990 resulting from a 28.8 g/s (1000 tpy) hypothetical NO_x emission source located at Bristol/Tri Cities Airport.

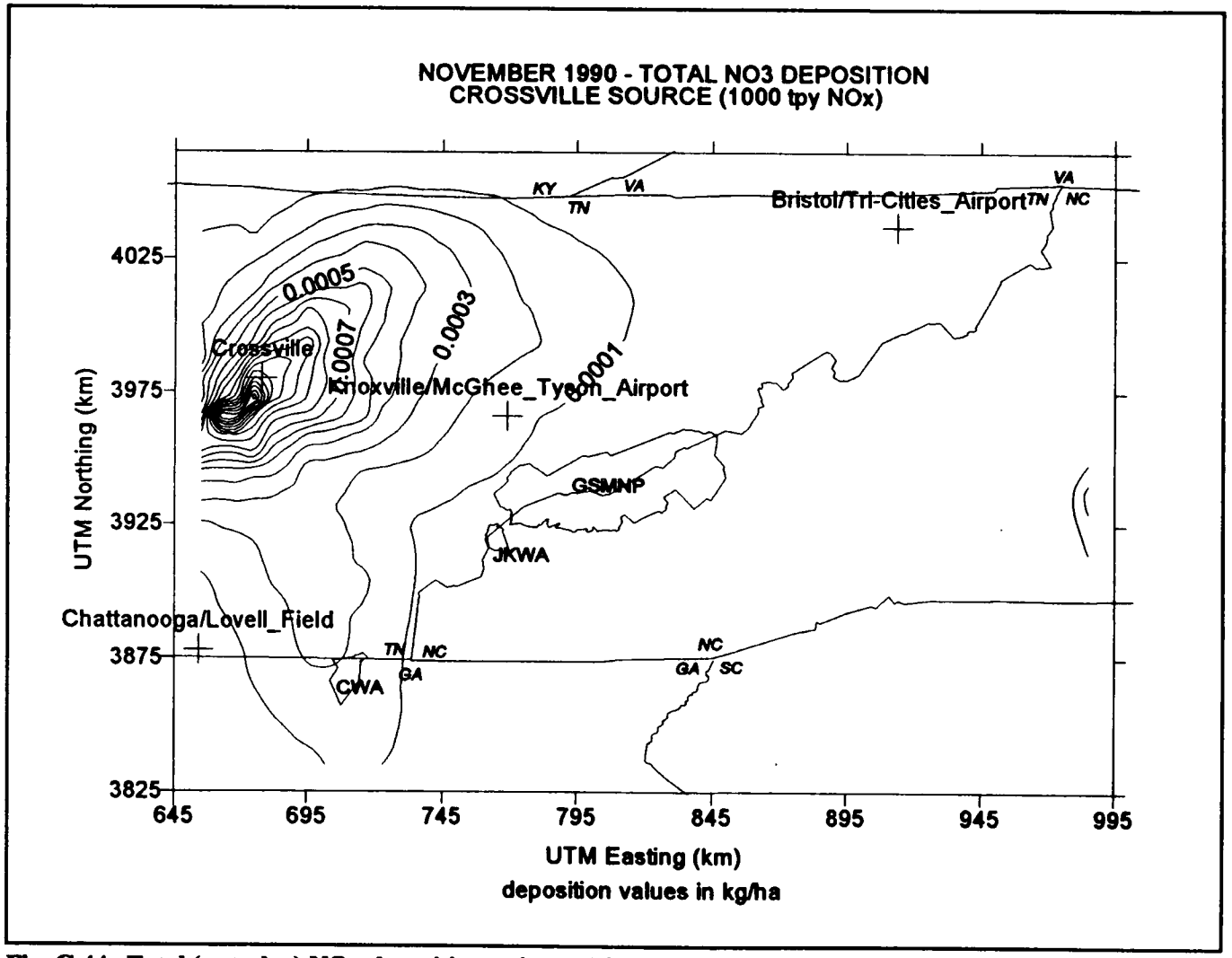

Fig. G.44. Total (wet+dry) NO_3^- deposition estimated for November 1990 resulting from a 28.8 g/s (1000 tpy) hypothetical NO_x emission source located in Crossville.

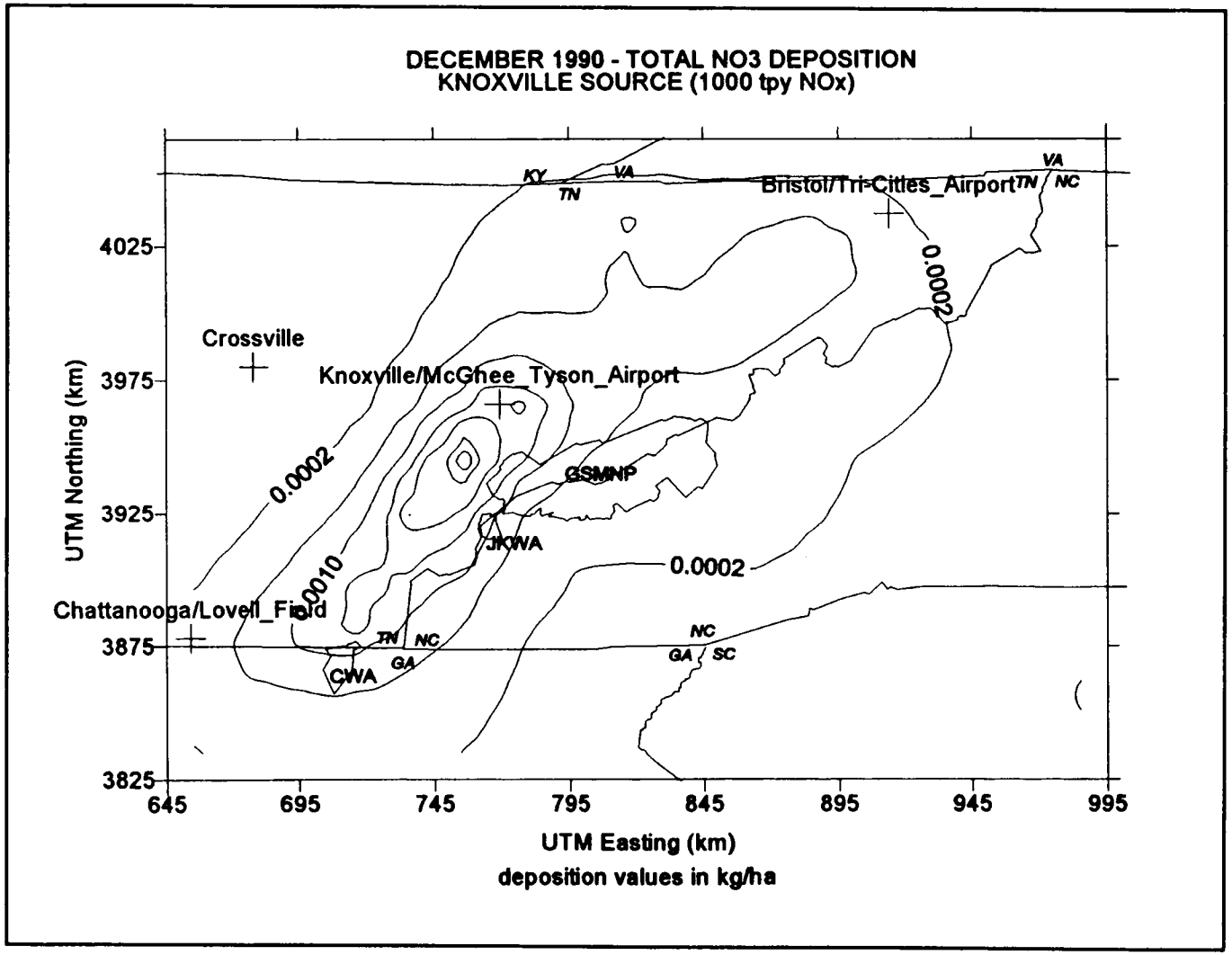

Fig. G.45. Total (wet+dry) NO_3^- deposition estimated for December 1990 resulting from a 28.8 g/s (1000 tpy) hypothetical NO_x emission source located at Knoxville /McGhee Tyson Airport.

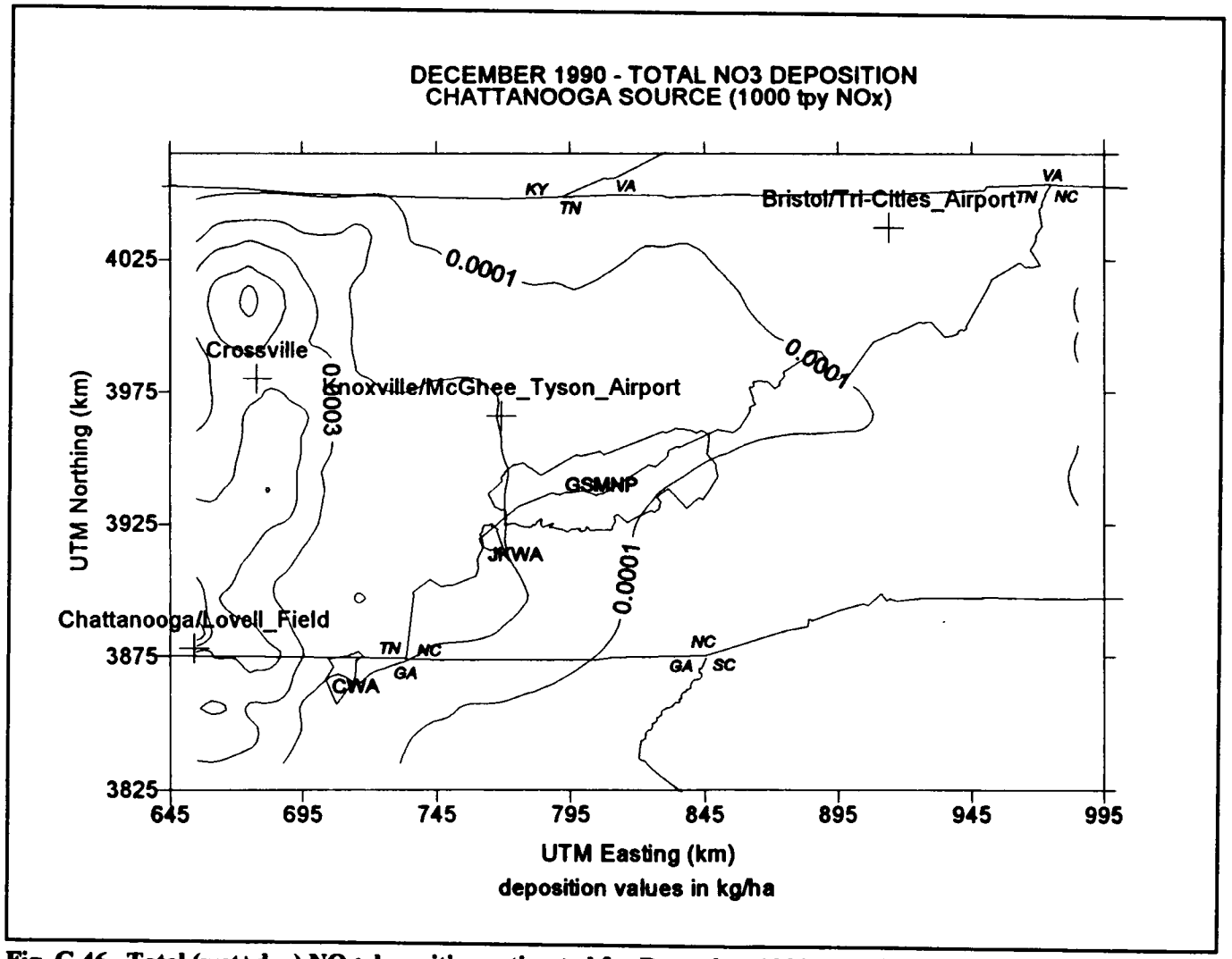

Fig. G.46. Total (wet+dry) NO_3^- deposition estimated for December 1990 resulting from a 28.8 g/s (1000 tpy) hypothetical NO_x emission source located at Chattanooga/Lovell Field.

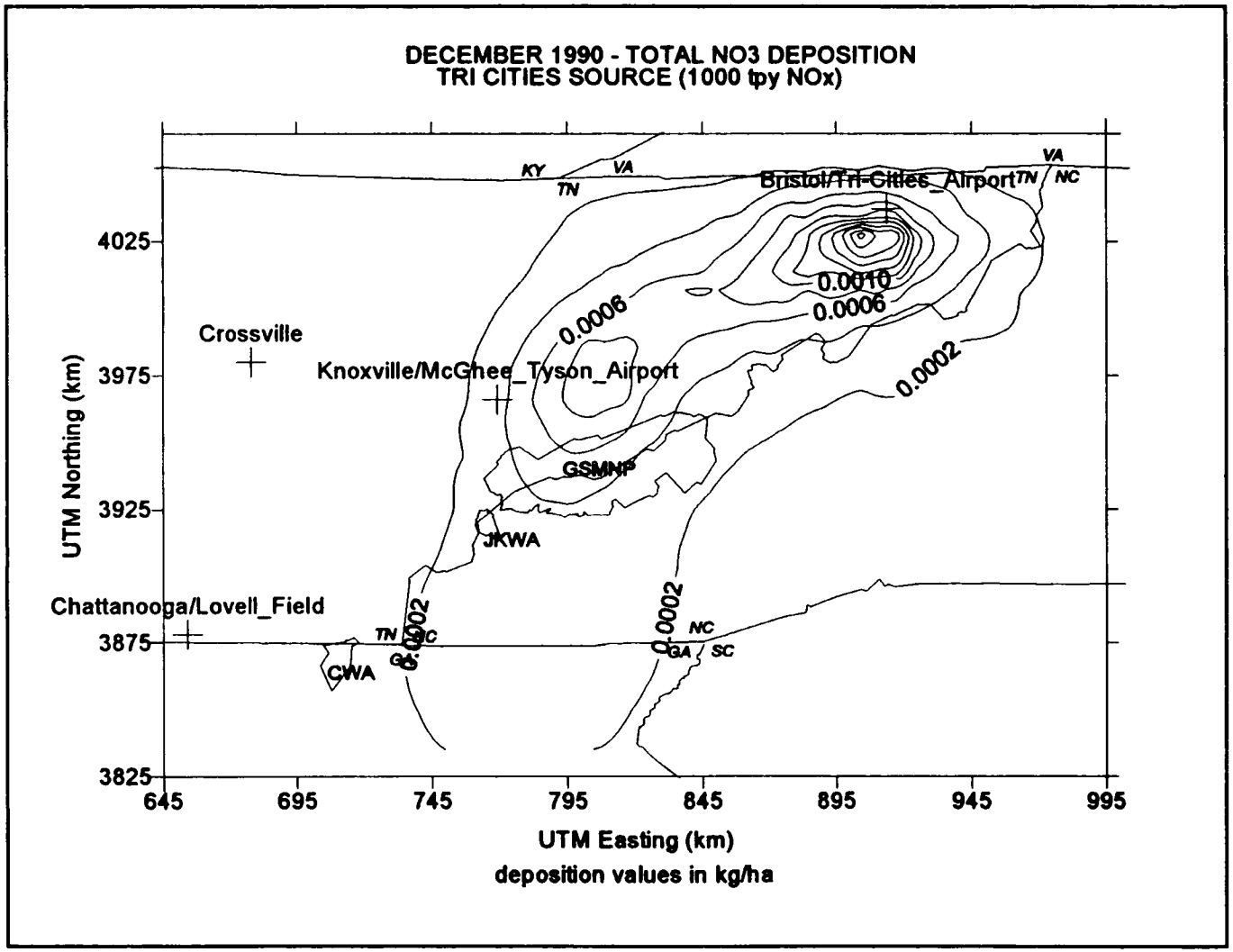

Fig. G.47. Total (wet+dry) NO_3^- deposition estimated for December 1990 resulting from a 28.8 g/s (1000 tpy) hypothetical NO_x emission source located at Bristol/Tri Cities Airport.

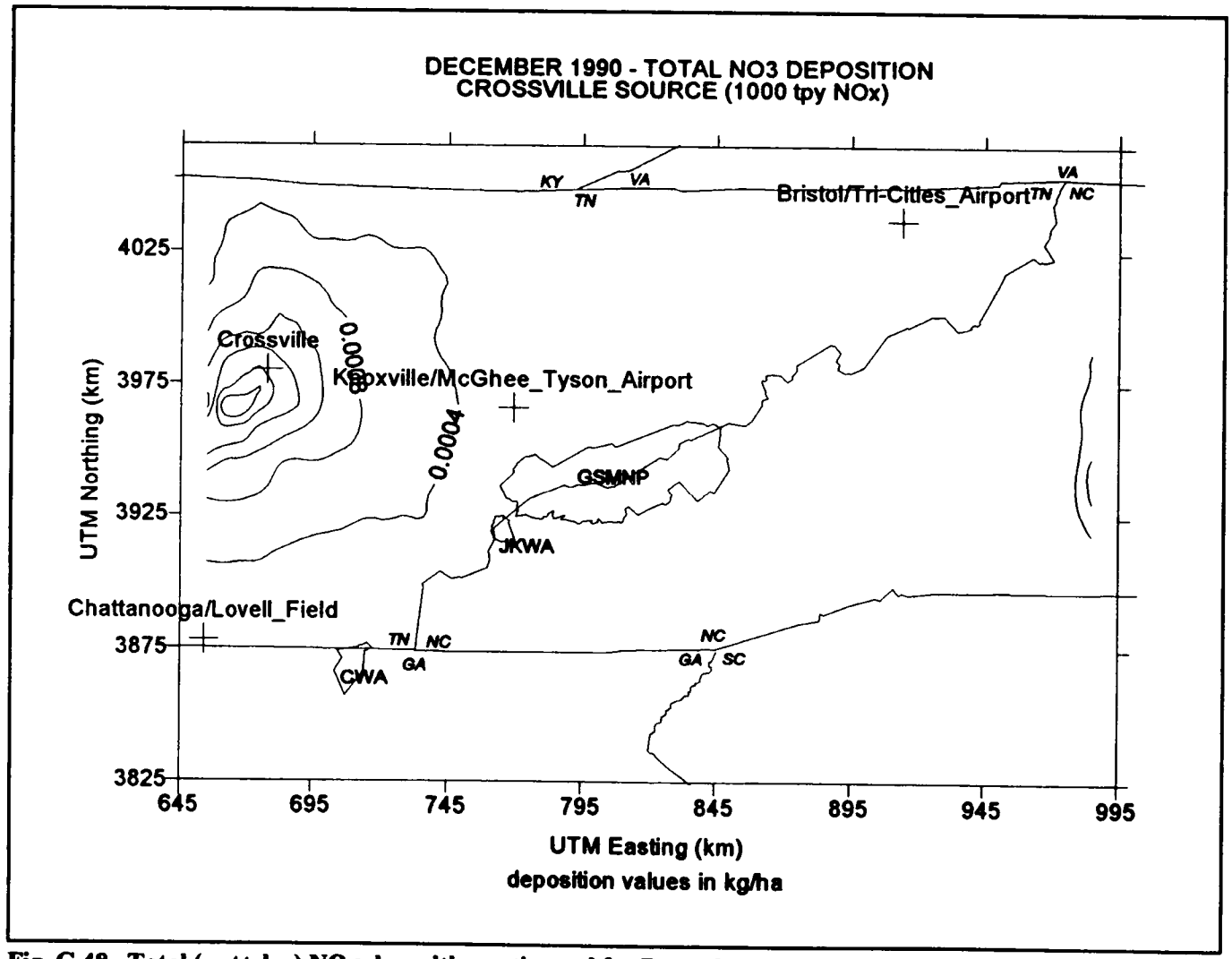

Fig. G.48. Total (wet+dry) NO_3^- deposition estimated for December 1990 resulting from a 28.8 g/s (1000 tpy) hypothetical NO_x emission source located in Crossville.

APPENDIX H
MAXIMUM AND ANNUAL CONCENTRATION CONTOUR MAPS

The following figures are contour maps of maximum and annual concentrations in the East Tennessee modeling domain. One contour map for each of the four hypothetical source locations has been generated for each of the pollutant forms as follows: (1) maximum 3-h SO_2 concentrations (Figs. H.1 through H.4) , (2) maximum 24-h SO_2 concentrations (Figs. H.5 through H.8), (3) annual average SO_2 concentrations (Figs. H.9 through H.12) and (4) annual average NO_x concentrations (Figs. H.13 through H.16).

The following abbreviations are used on the contour maps:

GSMNP	=	The Great Smoky Mountains National Park
JKWA	=	Joyce Kilmer Wilderness Area
CWA	=	Cohutta Wilderness Area
TN	=	Tennessee
NC	=	North Carolina
GA	=	Georgia
VA	=	Virginia
KY	=	Kentucky
UTM	=	Universal Transverse Mercator

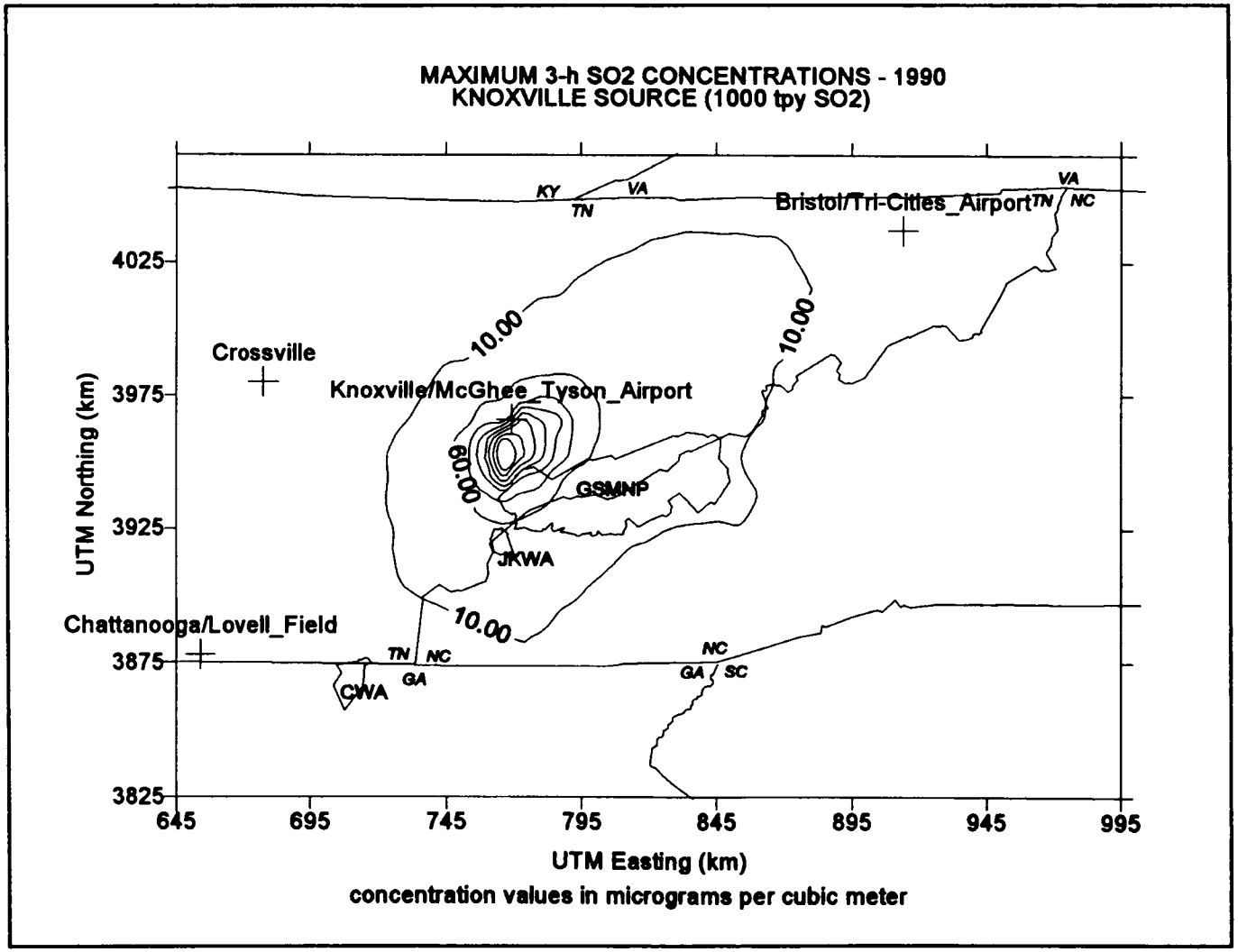

Fig. H.1. Maximum 3-h average SO_2 concentrations estimated for 1990 resulting from a 28.8 g/s (1000 tpy) hypothetical SO_2 emission source located at Knoxville /McGhee Tyson Airport.

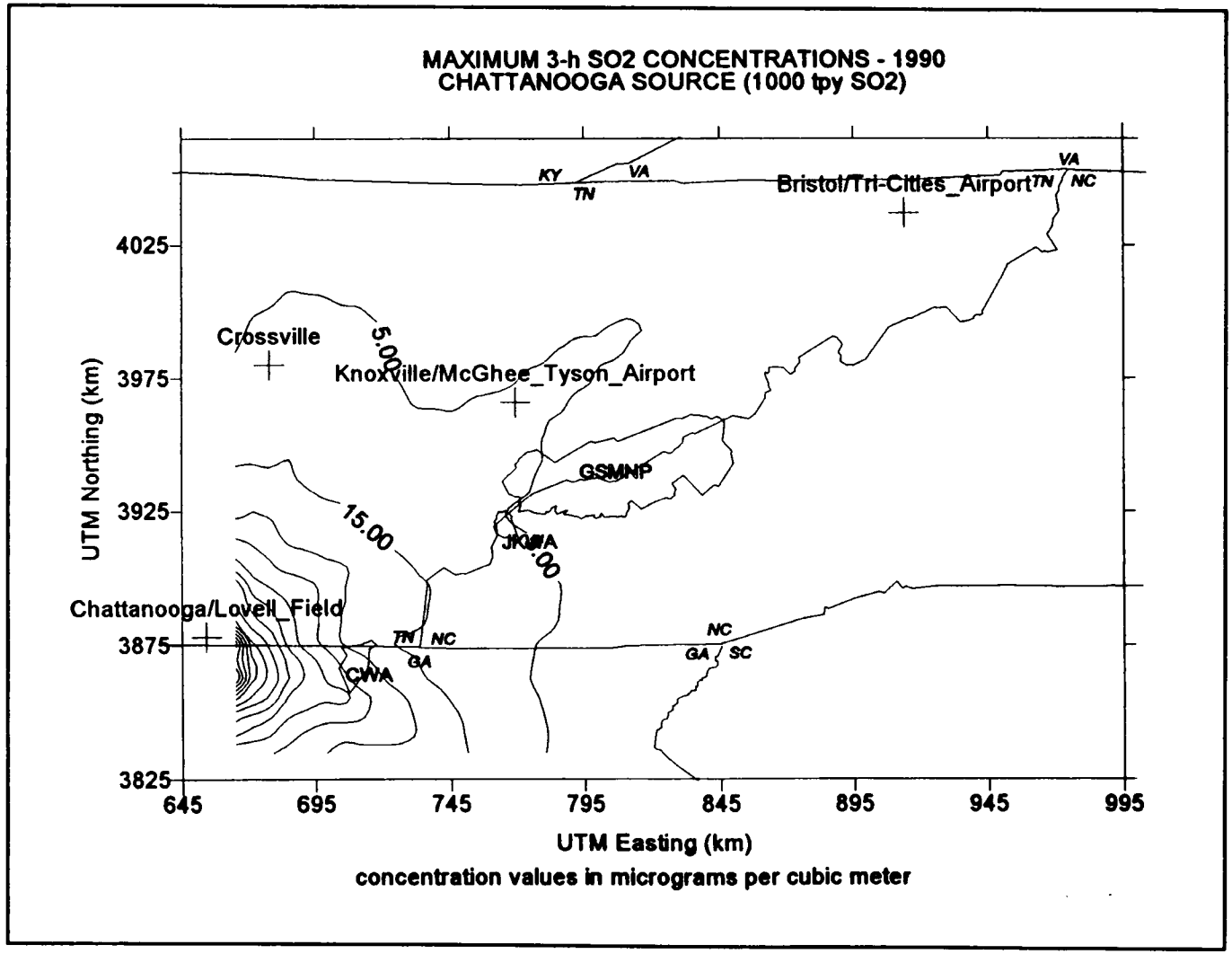

Fig. H.2. Maximum 3-h average SO_2 concentrations estimated for 1990 resulting from a 28.8 g/s (1000 tpy) hypothetical SO_2 emission source located at Chattanooga/Lovell Field.

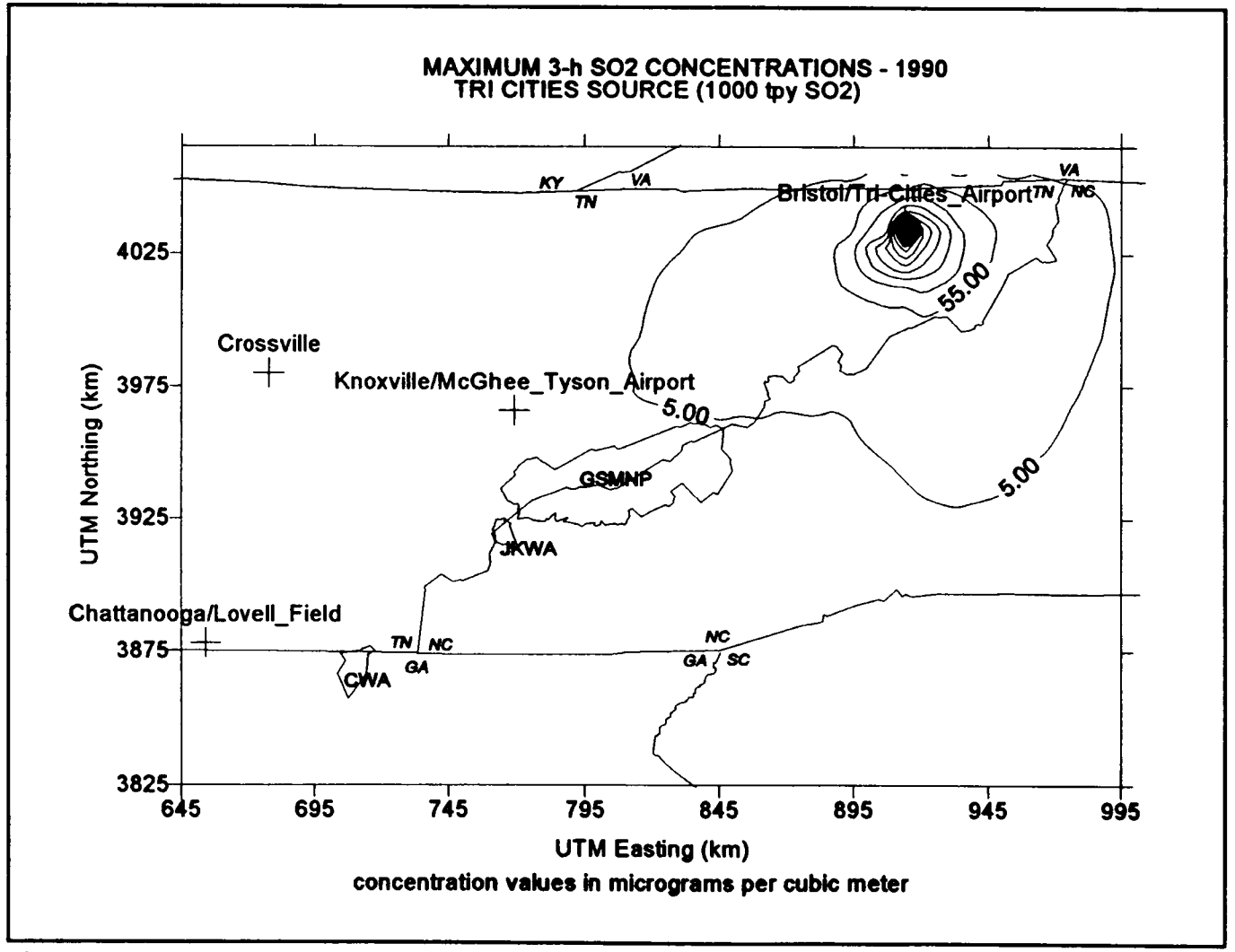

Fig. H.3. Maximum 3-h average SO_2 concentrations estimated for 1990 resulting from a 28.8 g/s (1000 tpy) hypothetical SO_2 emission source located at Bristol/Tri Cities Airport.

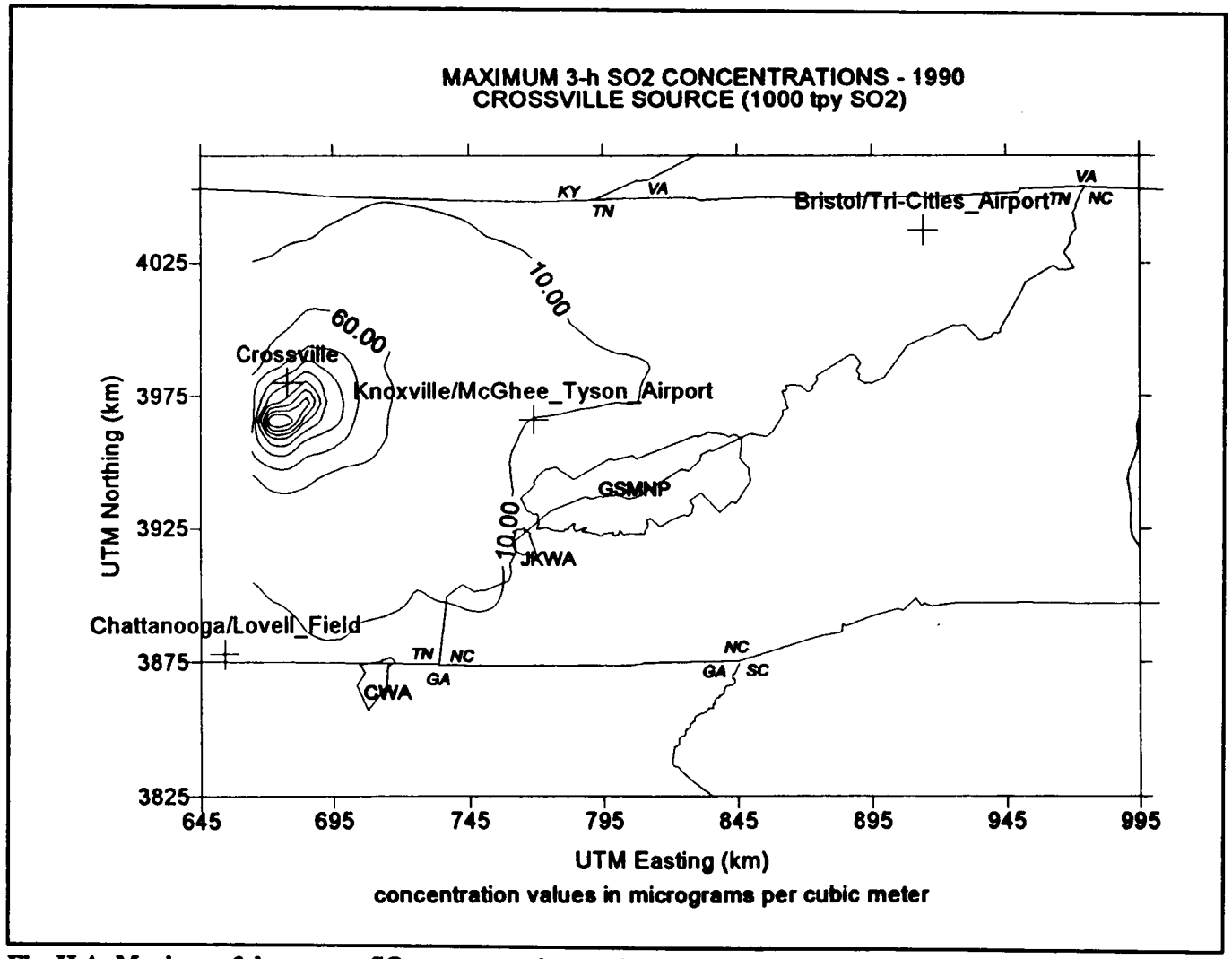

Fig. H.4. Maximum 3-h average SO_2 concentrations estimated for 1990 resulting from a 28.8 g/s (1000 tpy) hypothetical SO_2 emission source located in Crossville.

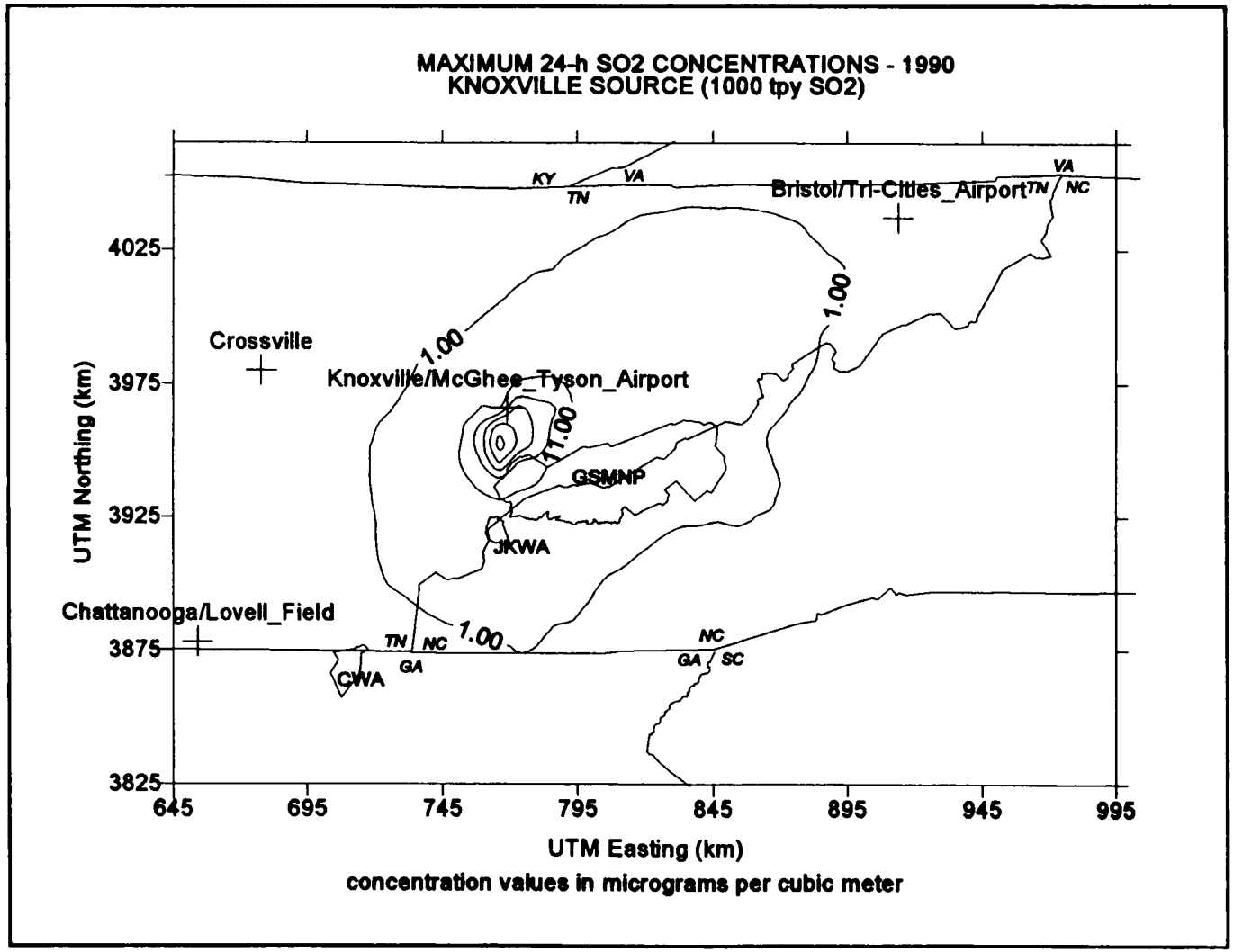

Fig. H.5. Maximum 24-h average SO_2 concentrations estimated for 1990 resulting from a 28.8 g/s (1000 tpy) hypothetical SO_2 emission source located at Knoxville /McGhee Tyson Airport.

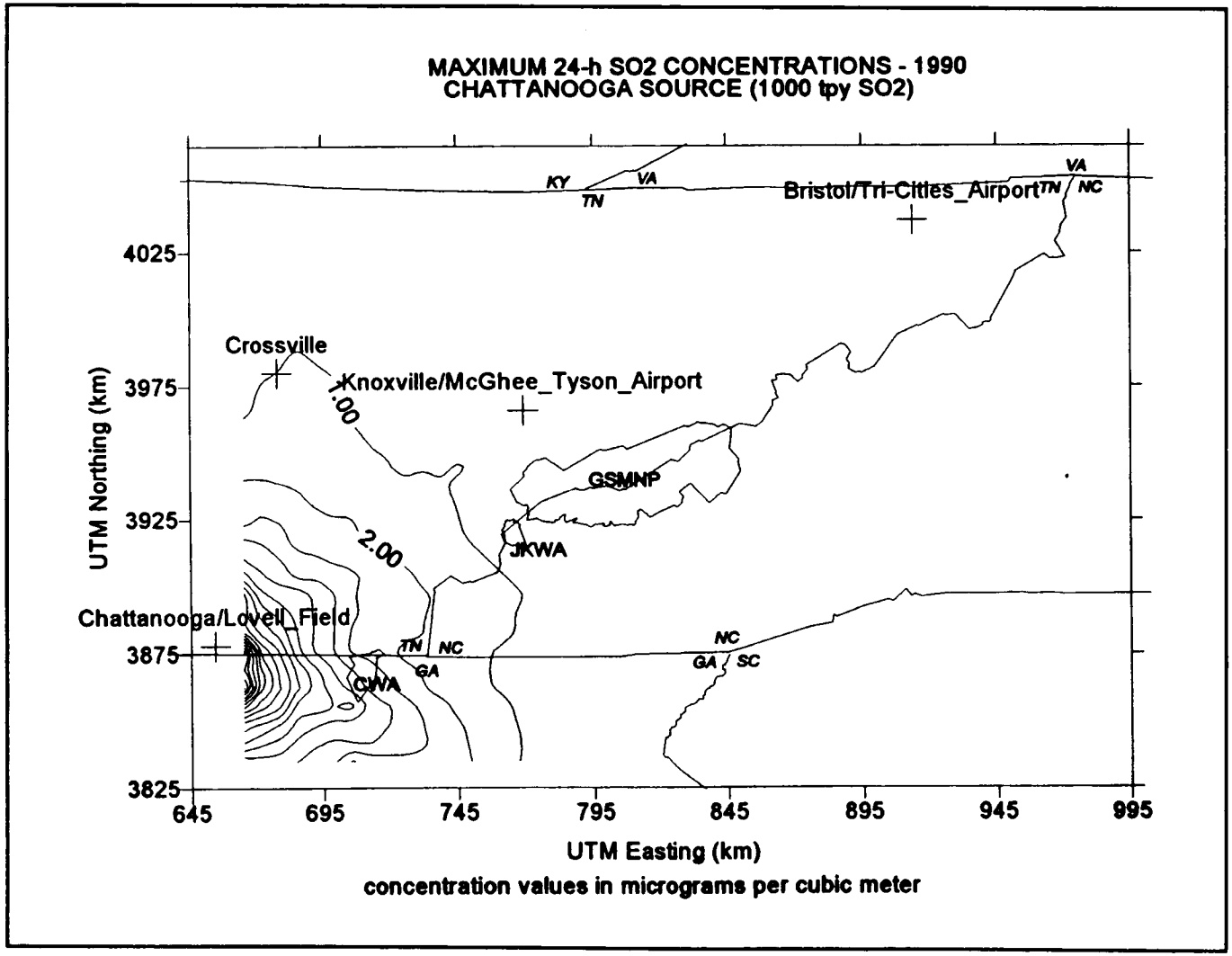

Fig. H.6. Maximum 24-h average SO_2 concentrations estimated for 1990 resulting from a 28.8 g/s (1000 tpy) hypothetical SO_2 emission source located at Chattanooga/Lovell Field.

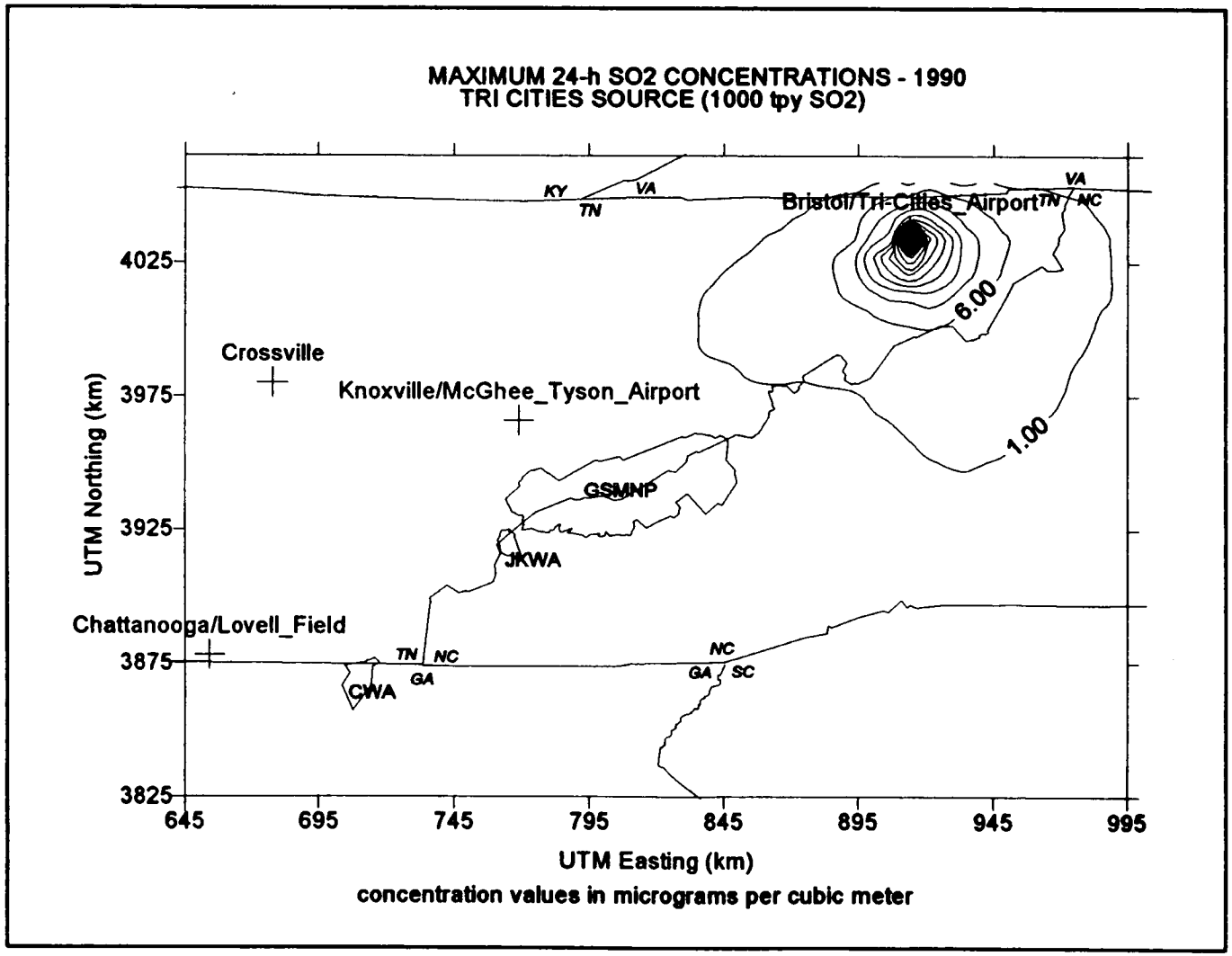

Fig. H.7. Maximum 24-h average SO_2 concentrations estimated for 1990 resulting from a 28.8 g/s (1000 tpy) hypothetical SO_2 emission source located at Bristol/Tri Cities Airport.

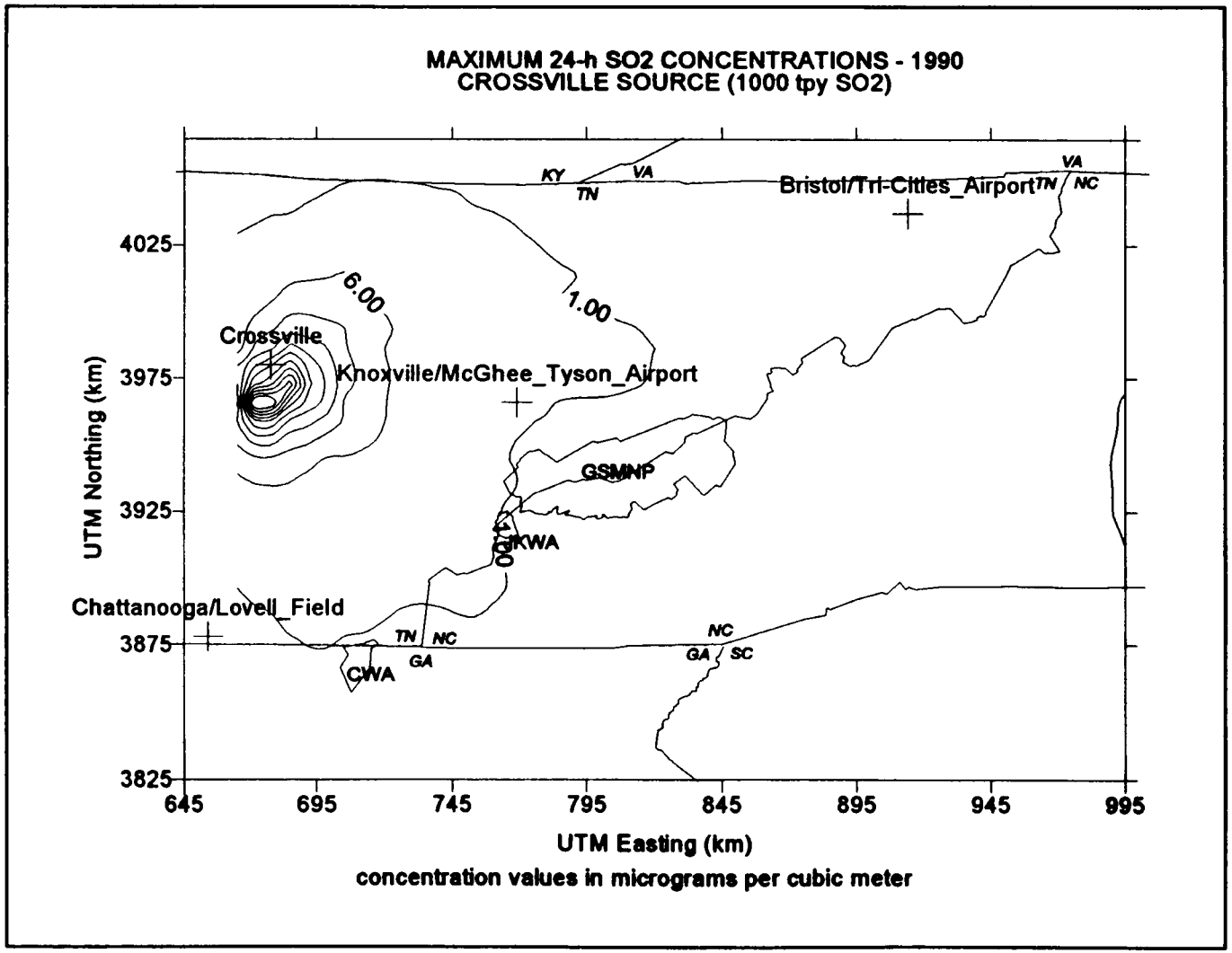

Fig. H.8. Maximum 24-h average SO_2 concentrations estimated for 1990 resulting from a 28.8 g/s (1000 tpy) hypothetical SO_2 emission source located in Crossville.

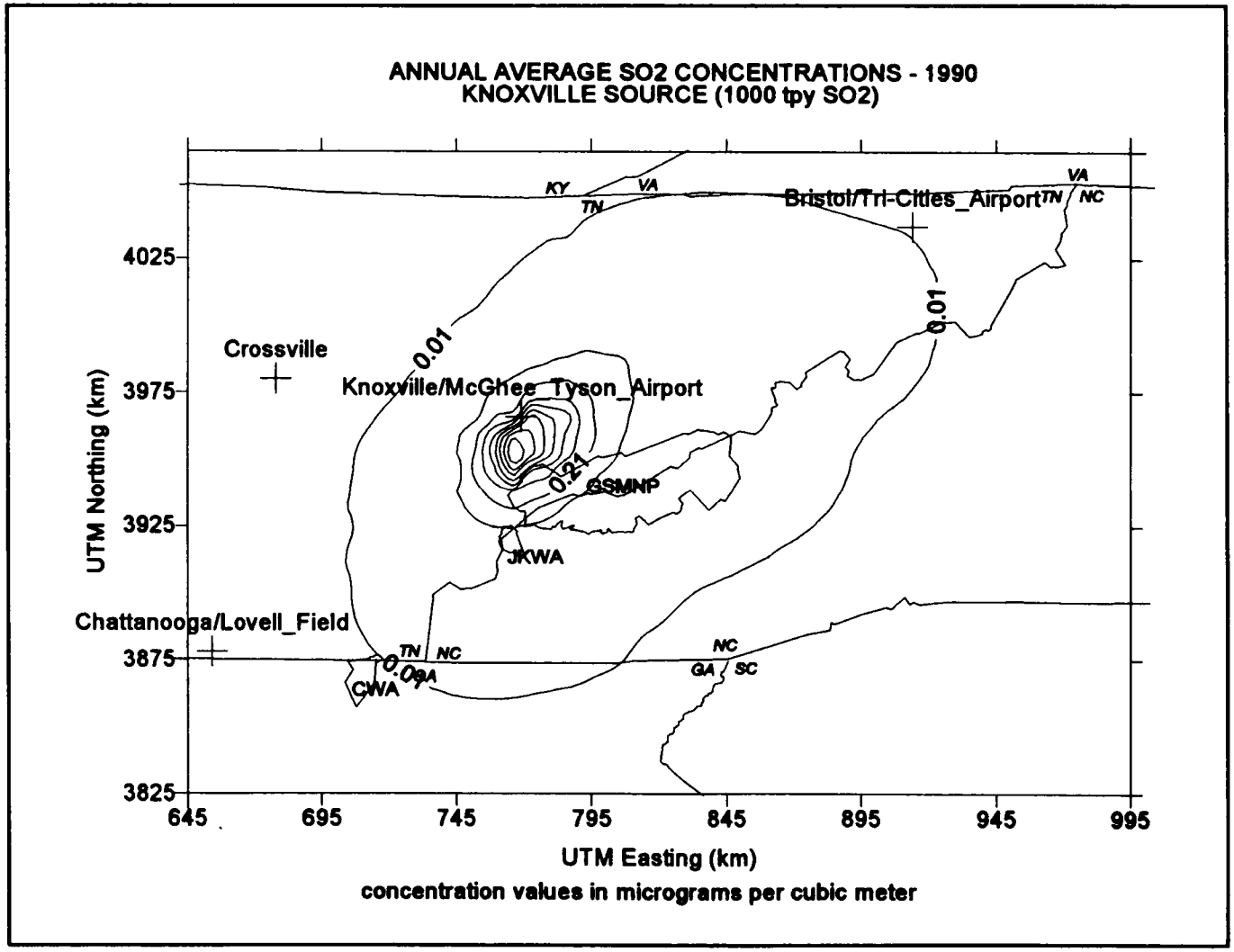

Fig. H.9. Annual average SO_2 concentrations estimated for 1990 resulting from a 28.8 g/s (1000 tpy) hypothetical SO_2 emission source located at Knoxville /McGhee Tyson Airport.

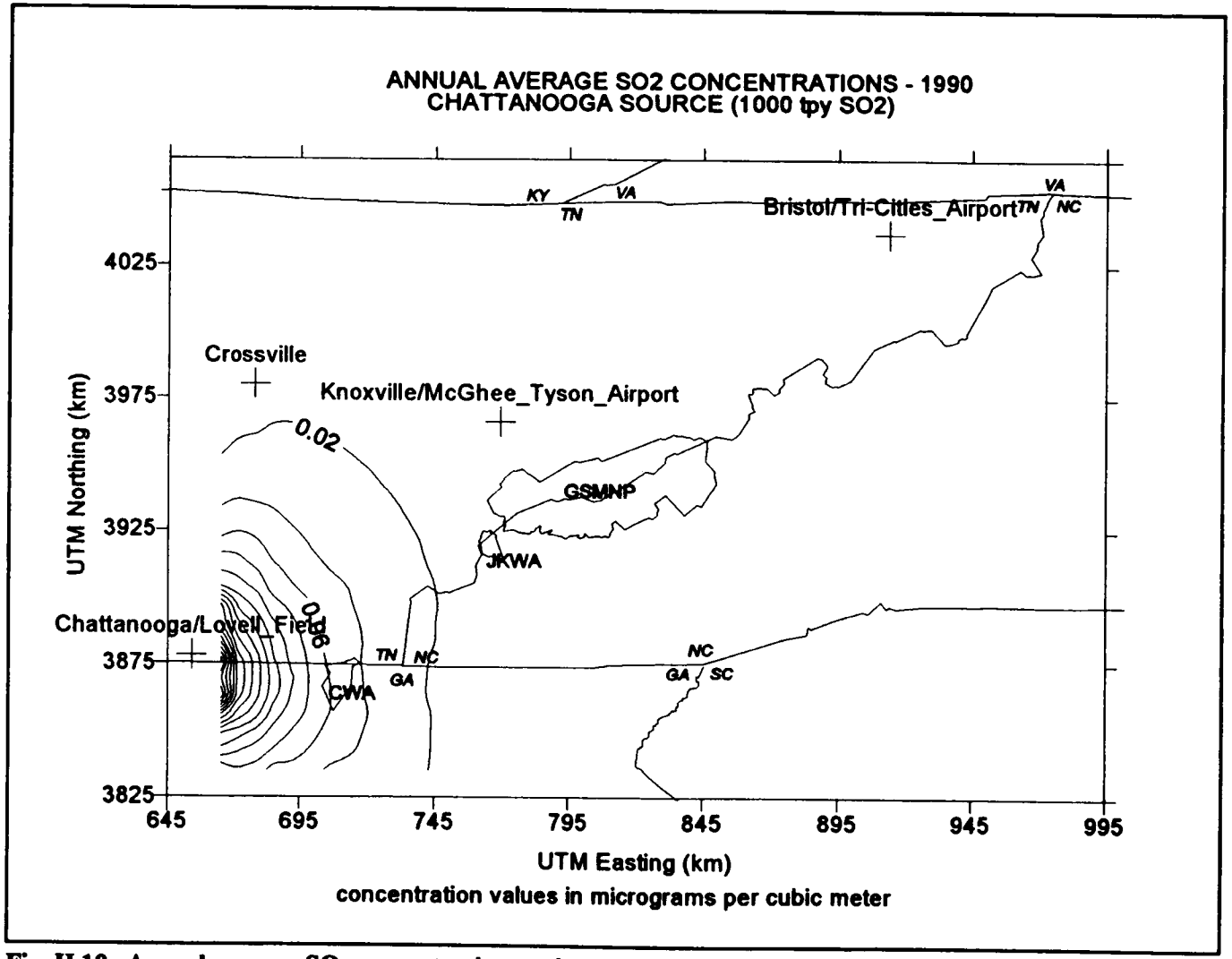

Fig. H.10. Annual average SO_2 concentrations estimated for 1990 resulting from a 28.8 g/s (1000 tpy) hypothetical SO_2 emission source located at Chattanooga/Lovell Field.

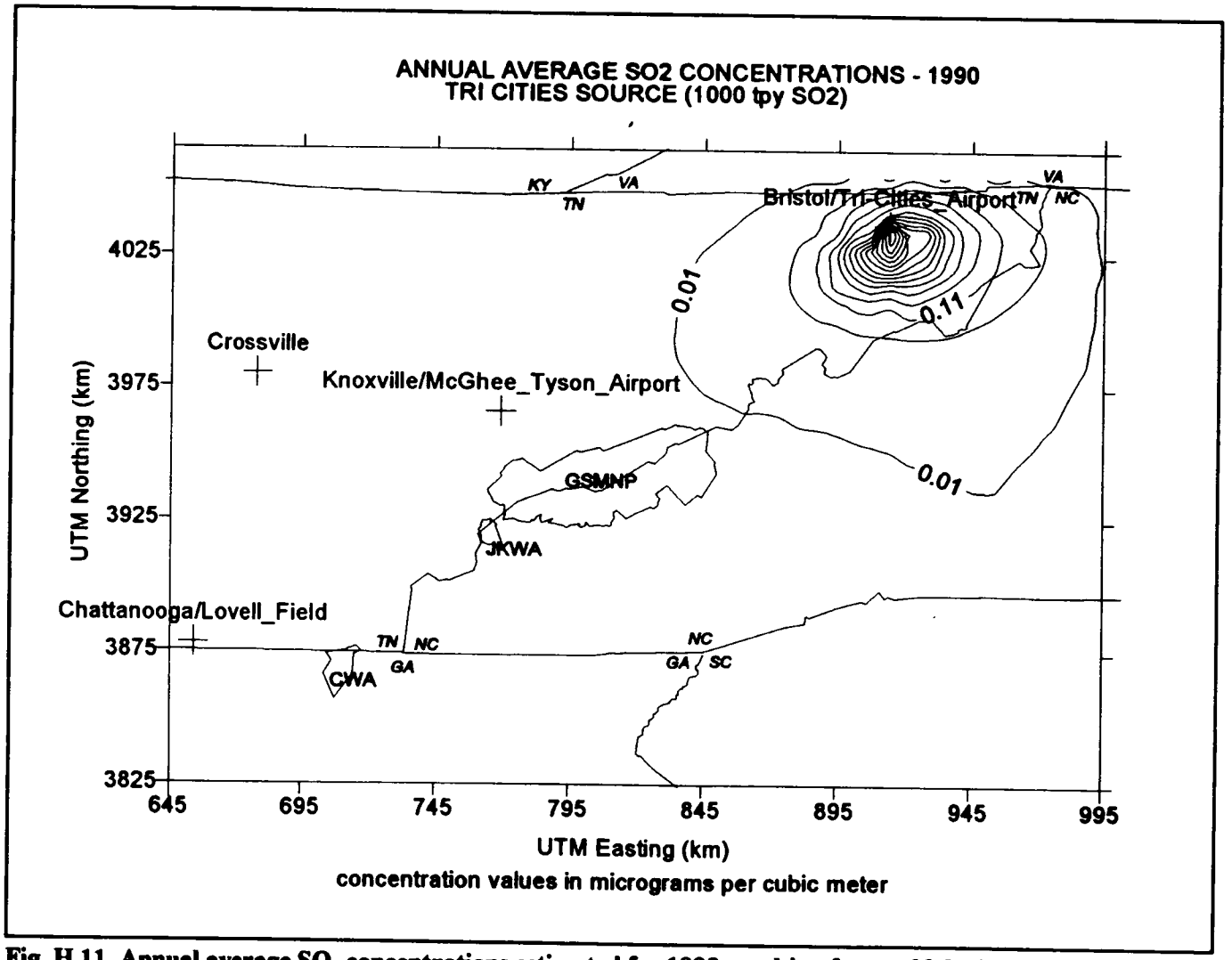

Fig. H.11. Annual average SO_2 concentrations estimated for 1990 resulting from a 28.8 g/s (1000 tpy) hypothetical SO_2 emission source located at Bristol/Tri Cities Airport.

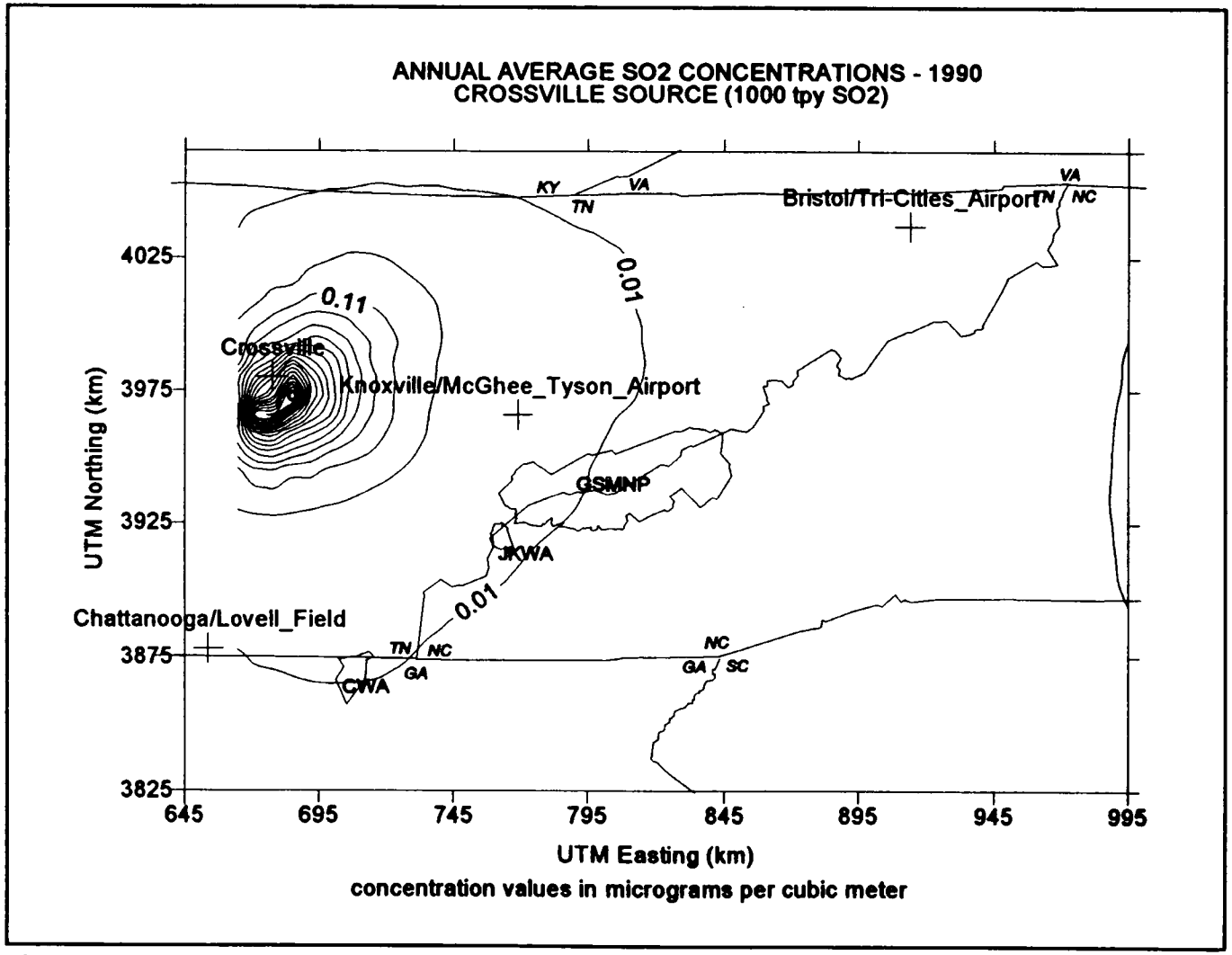

Fig. H.12. Annual average SO_2 concentrations estimated for 1990 resulting from a 28.8 g/s (1000 tpy) hypothetical SO_2 emission source located in Crossville.

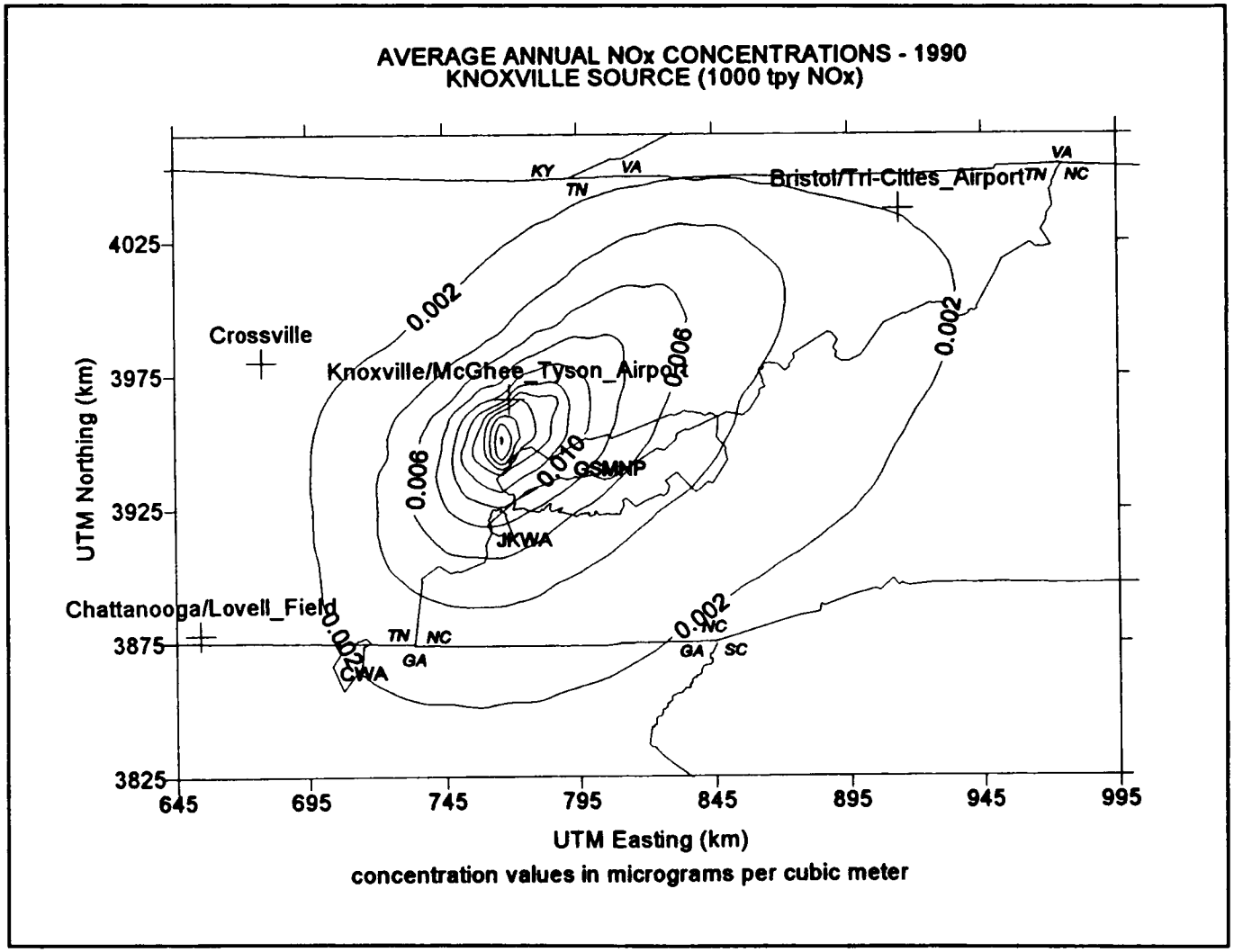

Fig. H.13. Annual average NO_x concentrations estimated for 1990 resulting from a 28.8 g/s (1000 tpy) hypothetical NO_x emission source located at Knoxville /McGhee Tyson Airport.

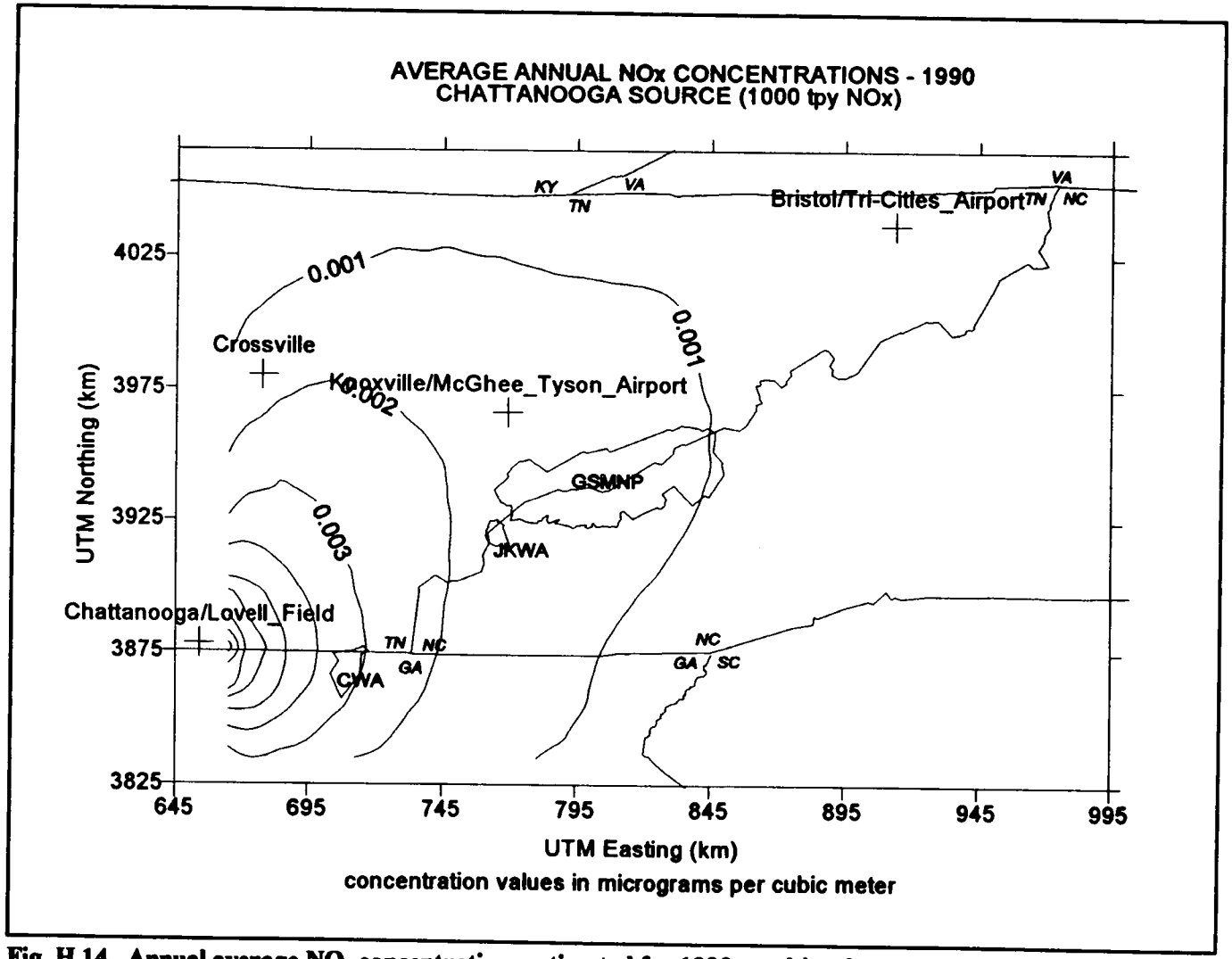

Fig. H.14. Annual average NO_x concentrations estimated for 1990 resulting from a 28.8 g/s (1000 tpy) hypothetical NO_x emission source located at Chattanooga/Lovell Field.

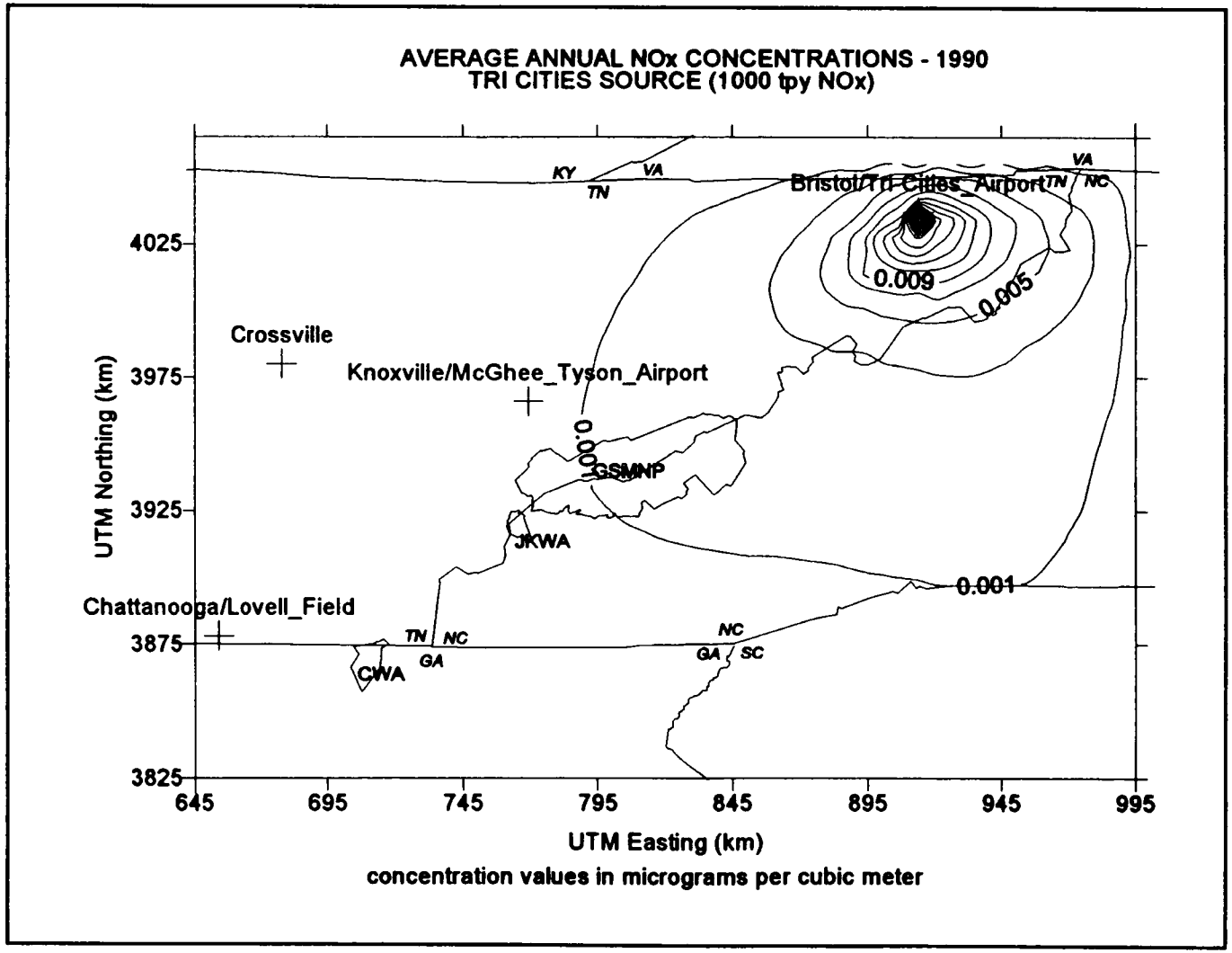

Fig. H.15. Annual average NO_x concentrations estimated for 1990 resulting from a 28.8 g/s (1000 tpy) hypothetical NO_x emission source located at Bristol/Tri Cities Airport.

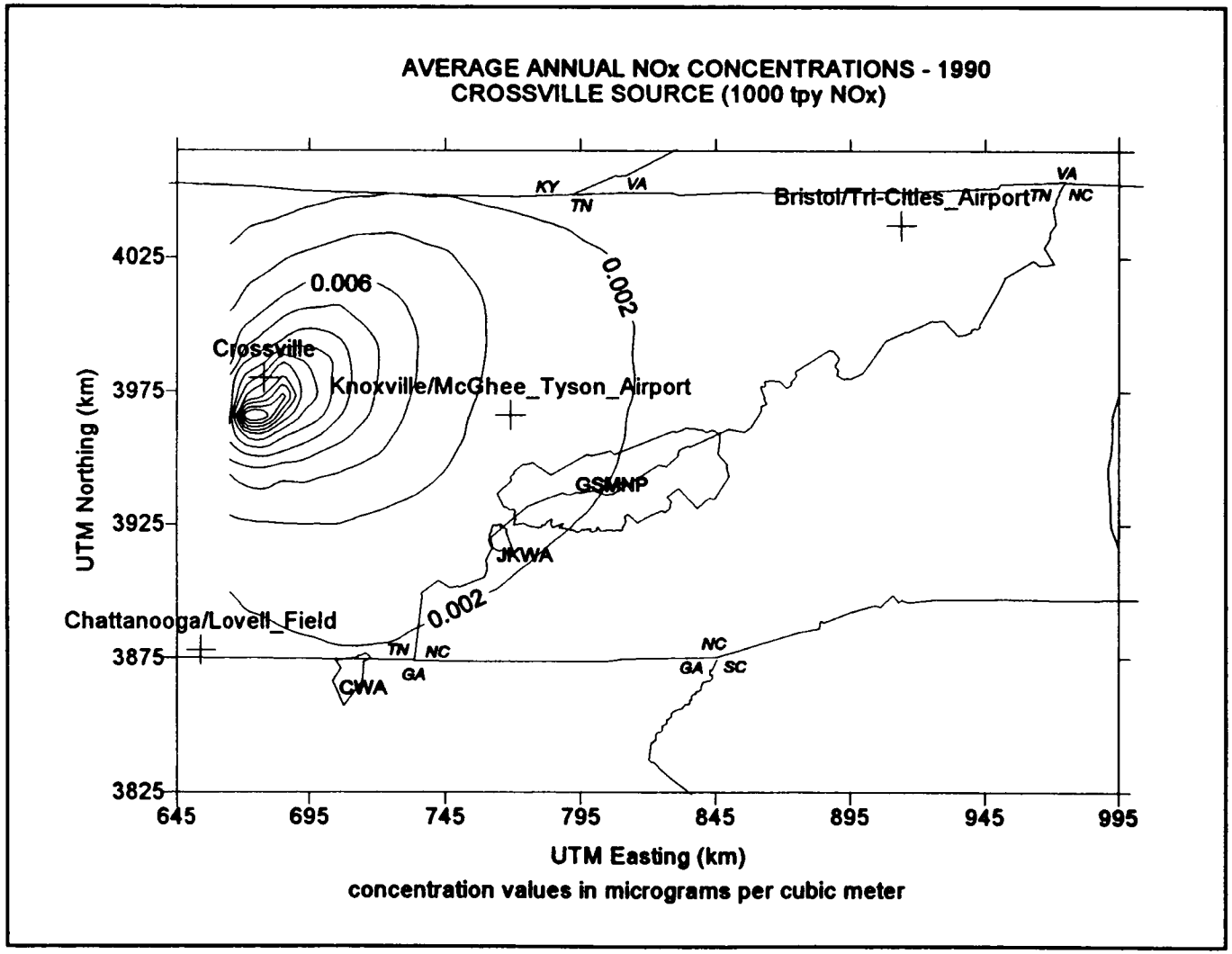

Fig. H.16. Annual average NO_x concentrations estimated for 1990 resulting from a 28.8 g/s (1000 tpy) hypothetical NO_x emission source located in Crossville.

APPENDIX I

READDEP CODE LISTING

```
1     c
2     ************************************************************************
3     c
4     c  READDEP   Version 1.0                          Last modified:  12/15/95
5     c                                                 First created:  11/03/95
6     c  Douglas A. Lombardi
7     c  Oak Ridge National Laboratory
8     c  Building 4500N, Mailstop 6200
9     c  Oak Ridge, Tennessee 37831-6200
10    c  (423) 576-9231
11    c  e-mail: d76@ornl.gov
12    c
13    c
14    c  Purpose:  This program reads unformatted deposition
15    c            output files created by MESOPUFF II and outputs the
16    c            total monthly deposition for each species at
17    c            each grid point in the East Tennessee
18    c            modeling domain
19    c
20    c  Warning:   This postprocessor only works for MESOPUFF II runs
21    c             made in the East Tennessee modeling domain.
22    c
23    ************************************************************************
24    c
25          REAL DSO2(34,23),DNOX(34,23),DSO4(34,23),DHNO3(34,23),DNO3(34,23)
26          REAL WSO2(34,23),WNOX(34,23),WSO4(34,23),WHNO3(34,23),WNO3(34,23)
27          REAL TSO2(34,23),TNOX(34,23),TSO4(34,23),THNO3(34,23),TNO3(34,23)
28          REAL ROUTD(34,23),ROUTW (34,23)
29          REAL X(36,25), Y(36,25)
30          REAL VERSION,DGRID,WSAMP
31          LOGICAL LGAUSS,LCHEM,LDRY,LWET,LPRINT,L3VL,LVSAMP,LSGRID
32          LOGICAL LWETG,LWETNG,LDRYG,LDRYNG,LPRFLX
33          INTEGER IDPOL(4)
34          CHARACTER*12 FNAME5,FNAME6,FNAME7,FNAME8,FNAME9
35          CHARACTER*12 FNAME10,FNAME11,FNAME12,FNAME13,FNAME14
36          OPEN(1,FILE='READDEP.IN',STATUS='old')
37    C **
38    C **  READ INPUT FILE
39    C **  WHERE
40    C **  WHERE: FNAME5 IS THE DRY FLUX OUTPUT FILE (e.g., FLUXDRY.DAT)
41    C **  WHERE: FNAME6 IS THE WET FLUX OUTPUT FILE (e.g., FLUXWET.DAT)
42    C **  WHERE: FNAME7 IS THE DRY DEPOSITION OUTPUT FILE
43    C **  WHERE: FNAME8 IS THE WET DEPOSITION OUTPUT FILE
44    C **  WHERE: FNAME9 IS THE TOTAL DEPOSITION OUTPUT FILE
45    C **  WHERE: FNAME10 IS THE TOTAL SO2 DEPOSITION DATA FILE
46    C **  WHERE: FNAME11 IS THE TOTAL SO4 DEPOSITION DATA FILE
47    C **  WHERE: FNAME12 IS THE TOTAL NOX DEPOSITION DATA FILE
48    C **  WHERE: FNAME13 IS THE TOTAL HNO3 DEPOSITION DATA FILE
49    C **  WHERE: FNAME14 IS THE TOTAL NO3 DEPOSITION DATA FILE
50    C **
51          READ(1,10)FNAME5,FNAME6,FNAME7,FNAME8,FNAME9
52          READ(1,10)FNAME10,FNAME11,FNAME12,FNAME13,FNAME14
53          OPEN(5,FILE=FNAME5,STATUS='old',FORM='unformatted')
54          OPEN(6,FILE=FNAME6,STATUS='old',FORM='unformatted')
55          OPEN(7,FILE=FNAME7,STATUS='new')
56          OPEN(8,FILE=FNAME8,STATUS='new')
57          OPEN(9,FILE=FNAME9,STATUS='new')
58          OPEN(10,FILE=FNAME10,STATUS='new')
59          OPEN(11,FILE=FNAME11,STATUS='new')
60          OPEN(12,FILE=FNAME12,STATUS='new')
61          OPEN(13,FILE=FNAME13,STATUS='new')
62          OPEN(14,FILE=FNAME14,STATUS='new')
63    C **
64    C **  READ HEADER FROM DRYFLUX AND WETFLUX FILES
65    C **
```

```
      READ(6)VERSION,LEVEL,NSTY,NSDAY,NSHR,NADVTS,IAVG,NPUF,NSAMAD,
     1       IELMET,JELMET,DGRID,IASTAR,IASTOP,JASTAR,JASTOP,ISASTR,
     2       ISASTP,JSASTR,JSASTP,MESHDN,NPTS,NAREAS,NREC,IPRINF,
     3       LGAUSS,LCHEM,LDRY,LWET,LPRINT,L3VL,LVSAMP,WSAMP,LSGRID,
     4       NSPEC,LWETG,LWETNG,LDRYG,LDRYNG,LPRFLX
      READ(5)VERSION,LEVEL,NSTY,NSDAY,NSHR,NADVTS,IAVG,NPUF,NSAMAD,
     1       IELMET,JELMET,DGRID,IASTAR,IASTOP,JASTAR,JASTOP,ISASTR,
     2       ISASTP,JSASTR,JSASTP,MESHDN,NPTS,NAREAS,NREC,IPRINF,
     3       LGAUSS,LCHEM,LDRY,LWET,LPRINT,L3VL,LVSAMP,WSAMP,LSGRID,
     4       NSPEC,LWETG,LWETNG,LDRYG,LDRYNG,LPRFLX
C **
C **  READ HOURLY RECORDS
C **  WHERE: NADVTS = NUMBER OF HOURS IN THE RUN
C **         ROUTD  = GRIDDED RECEPTOR DRY FLUX (g/m2/s)
C **         ROUTW  = GRIDDED RECEPTOR WET FLUX (g/m2/s)
C **
      DO 1000 K=1,NADVTS
      WRITE(*,*)K
      DO 1500 L=1,5
      READ(5)IDPOL,ROUTD
      READ(6)IDPOL,ROUTW
C **
C **  COMPUTING DEPOSITION
C **
C      IYR=IDPOL(1)
C      JDAY=IDPOL(2)
C      IHR=IDPOL(3)
C      IPOL=IDPOL(4)
C      WRITE(7,*)'YR = ',IYR,'JDAY = ',JDAY,'HR = ',IHR,'IPOL = ',IPOL
      IF(L.EQ.1)THEN
      DO 100 I=2,35
         DO 150 J=2,24
C **
C **  DETERMINE HOURLY FLUX IN kg/ha
C **
                  ROUTD(I,J)=ROUTD(I,J)*3600.*(10000./1000.)
                  ROUTW(I,J)=ROUTW(I,J)*3600.*(10000./1000.)
C **
C **  ADD HOURLY FLUX TO PREVIOUS TOTAL
C **
                  DSO2(I,J)=DSO2(I,J)+ROUTD(I,J)
                  WSO2(I,J)=WSO2(I,J)+ROUTW(I,J)
                  TSO2(I,J)=TSO2(I,J)+ROUTD(I,J)+ROUTW(I,J)
  150     CONTINUE
  100 CONTINUE
      ELSEIF(L.EQ.2)THEN
      DO 200 I=2,35
         DO 250 J=2,24
C **
C **  DETERMINE HOURLY FLUX IN kg/ha
C **
                  ROUTD(I,J)=ROUTD(I,J)*3600.*(10000./1000.)
                  ROUTW(I,J)=ROUTW(I,J)*3600.*(10000./1000.)
C **
C **  ADD HOURLY FLUX TO PREVIOUS TOTAL
C **
                  DSO4(I,J)=DSO4(I,J)+ROUTD(I,J)
                  WSO4(I,J)=WSO4(I,J)+ROUTW(I,J)
                  TSO4(I,J)=TSO4(I,J)+ROUTD(I,J)+ROUTW(I,J)
  250     CONTINUE
  200 CONTINUE
      ELSEIF(L.EQ.3)THEN
      DO 300 I=2,35
         DO 350 J=2,24
C **
```

```
C **  DETERMINE HOURLY FLUX IN kg/ha
C **
                  ROUTD(I,J)=ROUTD(I,J)*3600.*(10000./1000.)
                  ROUTW(I,J)=ROUTW(I,J)*3600.*(10000./1000.)
C **
C **  ADD HOURLY FLUX TO PREVIOUS TOTAL
C **
                  DNOX(I,J)=DNOX(I,J)+ROUTD(I,J)
                  WNOX(I,J)=WNOX(I,J)+ROUTW(I,J)
                  TNOX(I,J)=TNOX(I,J)+ROUTD(I,J)+ROUTW(I,J)
  350     CONTINUE
  300 CONTINUE
      ELSEIF(L.EQ.4)THEN
      DO 400 I=2,35
         DO 450 J=2,24
C **
C **  DETERMINE HOURLY FLUX IN kg/ha
C **
                  ROUTD(I,J)=ROUTD(I,J)*3600.*(10000./1000.)
                  ROUTW(I,J)=ROUTW(I,J)*3600.*(10000./1000.)
C **
C **  ADD HOURLY FLUX TO PREVIOUS TOTAL
C **
                  DHNO3(I,J)=DHNO3(I,J)+ROUTD(I,J)
                  WHNO3(I,J)=WHNO3(I,J)+ROUTW(I,J)
                  THNO3(I,J)=THNO3(I,J)+ROUTD(I,J)+ROUTW(I,J)
  450     CONTINUE
  400 CONTINUE
      ELSE
      DO 500 I=2,35
         DO 550 J=2,24
C **
C **  DETERMINE HOURLY FLUX IN kg/ha
C **
                  ROUTD(I,J)=ROUTD(I,J)*3600.*(10000./1000.)
                  ROUTW(I,J)=ROUTW(I,J)*3600.*(10000./1000.)
C **
C **  ADD HOURLY FLUX TO PREVIOUS TOTAL
C **
                  DNO3(I,J)=DNO3(I,J)+ROUTD(I,J)
                  WNO3(I,J)=WNO3(I,J)+ROUTW(I,J)
                  TNO3(I,J)=TNO3(I,J)+ROUTD(I,J)+ROUTW(I,J)
  550     CONTINUE
  500 CONTINUE
      ENDIF
 1500 CONTINUE
 1000 CONTINUE
C **
C **  WRITING OUTPUT FILES **
C **
      WRITE(*,*)'Writing output files. . . '
      WRITE(7,*)
      WRITE(7,*)'SO2 DRY DEPOSITION'
      WRITE(7,*)
      WRITE(7,15)'UTM COORDINATES'
      WRITE(7,17)'EASTING (m)','NORTHING (m)',
     1           '    DEPOSITION (kg/ha)    '
      WRITE(7,*)'-------------------------------------------------------
     1--------'
      WRITE(8,*)
      WRITE(8,*)'SO2 WET DEPOSITION'
      WRITE(8,*)
      WRITE(8,15)'UTM COORDINATES'
      WRITE(8,17)'EASTING (m)','NORTHING (m)',
     1           '    DEPOSITION (kg/ha)    '
```

```
196          WRITE(8,*)'-------------------------------------------------------
197         1--------'
198          WRITE(9,*)
199          WRITE(9,*)'SO2 TOTAL (WET + DRY) DEPOSITION'
200          WRITE(9,*)
201          WRITE(9,15)'UTM COORDINATES'
202          WRITE(9,17)'EASTING (m)','NORTHING (m)',
203         1           '    DEPOSITION (kg/ha)    '
204          WRITE(9,*)'-------------------------------------------------------
205         1--------'
206          DO 2000 I=2,35
207             DO 2500 J=2,24
208                     X(I,J)=((I-1)*10.)+645.
209                     Y(I,J)=((J-1)*10.)+3825.
210                     WRITE(7,20)X(I,J),Y(I,J),DSO2(I,J)
211                     WRITE(8,20)X(I,J),Y(I,J),WSO2(I,J)
212                     WRITE(9,20)X(I,J),Y(I,J),TSO2(I,J)
213                     WRITE(10,20)X(I,J),Y(I,J),TSO2(I,J)
214      2500 CONTINUE
215      2000 CONTINUE
216          WRITE(7,*)
217          WRITE(7,*)'SO4 DRY DEPOSITION'
218          WRITE(7,*)
219          WRITE(7,15)'UTM COORDINATES'
220          WRITE(7,17)'EASTING (m)','NORTHING (m)',
221         1           '    DEPOSITION (kg/ha)    '
222          WRITE(7,*)'-------------------------------------------------------
223         1--------'
224          WRITE(8,*)
225          WRITE(8,*)'SO4 WET DEPOSITION'
226          WRITE(8,*)
227          WRITE(8,15)'UTM COORDINATES'
228          WRITE(8,17)'EASTING (m)','NORTHING (m)',
229         1           '    DEPOSITION (kg/ha)    '
230          WRITE(8,*)'-------------------------------------------------------
231         1--------'
232          WRITE(9,*)
233          WRITE(9,*)'SO4 TOTAL (WET + DRY) DEPOSITION'
234          WRITE(9,*)
235          WRITE(9,15)'UTM COORDINATES'
236          WRITE(9,17)'EASTING (m)','NORTHING (m)',
237         1           '    DEPOSITION (kg/ha)    '
238          WRITE(9,*)'-------------------------------------------------------
239         1--------'
240          DO 3000 I=2,35
241             DO 3500 J=2,24
242                     X(I,J)=((I-1)*10.)+645.
243                     Y(I,J)=((J-1)*10.)+3825.
244                     WRITE(7,20)X(I,J),Y(I,J),DSO4(I,J)
245                     WRITE(8,20)X(I,J),Y(I,J),WSO4(I,J)
246                     WRITE(9,20)X(I,J),Y(I,J),TSO4(I,J)
247                     WRITE(11,20)X(I,J),Y(I,J),TSO4(I,J)
248      3500 CONTINUE
249      3000 CONTINUE
250          WRITE(7,*)
251          WRITE(7,*)'NOX DRY DEPOSITION'
252          WRITE(7,*)
253          WRITE(7,15)'UTM COORDINATES'
254          WRITE(7,17)'EASTING (m)','NORTHING (m)',
255         1           '    DEPOSITION (kg/ha)    '
256          WRITE(7,*)'-------------------------------------------------------
257         1--------'
258          WRITE(8,*)
259          WRITE(8,*)'NOX WET DEPOSITION'
260          WRITE(8,*)
```

```
      WRITE(8,15)'UTM COORDINATES'
      WRITE(8,17)'EASTING (m)','NORTHING (m)',
     1           '    DEPOSITION (kg/ha)    '
      WRITE(8,*)'-------------------------------------------------------
     1--------'
      WRITE(9,*)
      WRITE(9,*)'NOX TOTAL (WET + DRY) DEPOSITION'
      WRITE(9,*)
      WRITE(9,15)'UTM COORDINATES'
      WRITE(9,17)'EASTING (m)','NORTHING (m)',
     1           '    DEPOSITION (kg/ha)    '
      WRITE(9,*)'-------------------------------------------------------
     1--------'
      DO 4000 I=2,35
         DO 4500 J=2,24
                 X(I,J)=((I-1)*10.)+645.
                 Y(I,J)=((J-1)*10.)+3825.
                 WRITE(7,20)X(I,J),Y(I,J),DNOX(I,J)
                 WRITE(8,20)X(I,J),Y(I,J),WNOX(I,J)
                 WRITE(9,20)X(I,J),Y(I,J),TNOX(I,J)
                 WRITE(12,20)X(I,J),Y(I,J),TNOX(I,J)
 4500 CONTINUE
 4000 CONTINUE
      WRITE(7,*)
      WRITE(7,*)'HNO3 DRY DEPOSITION'
      WRITE(7,*)
      WRITE(7,15)'UTM COORDINATES'
      WRITE(7,17)'EASTING (m)','NORTHING (m)',
     1           '    DEPOSITION (kg/ha)    '
      WRITE(7,*)'-------------------------------------------------------
     1--------'
      WRITE(8,*)
      WRITE(8,*)'HNO3 WET DEPOSITION'
      WRITE(8,*)
      WRITE(8,15)'UTM COORDINATES'
      WRITE(8,17)'EASTING (m)','NORTHING (m)',
     1           '    DEPOSITION (kg/ha)    '
      WRITE(8,*)'-------------------------------------------------------
     1--------'
      WRITE(9,*)
      WRITE(9,*)'HNO3 TOTAL (WET + DRY) DEPOSITION'
      WRITE(9,*)
      WRITE(9,15)'UTM COORDINATES'
      WRITE(9,17)'EASTING (m)','NORTHING (m)',
     1           '    DEPOSITION (kg/ha)    '
      WRITE(9,*)'-------------------------------------------------------
     1--------'
      DO 5000 I=2,35
         DO 5500 J=2,24
                 X(I,J)=((I-1)*10.)+645.
                 Y(I,J)=((J-1)*10.)+3825.
                 WRITE(7,20)X(I,J),Y(I,J),DHNO3(I,J)
                 WRITE(8,20)X(I,J),Y(I,J),WHNO3(I,J)
                 WRITE(9,20)X(I,J),Y(I,J),THNO3(I,J)
                 WRITE(13,20)X(I,J),Y(I,J),THNO3(I,J)
 5500 CONTINUE
 5000 CONTINUE
      WRITE(7,*)
      WRITE(7,*)'NO3 DRY DEPOSITION'
      WRITE(7,*)
      WRITE(7,15)'UTM COORDINATES'
      WRITE(7,17)'EASTING (m)','NORTHING (m)',
     1           '    DEPOSITION (kg/ha)    '
      WRITE(7,*)'-------------------------------------------------------
     1--------'
```

```
      WRITE(8,*)
      WRITE(8,*)'NO3 WET DEPOSITION'
      WRITE(8,*)
      WRITE(8,15)'UTM COORDINATES'
      WRITE(8,17)'EASTING (m)','NORTHING (m)',
     1           '    DEPOSITION (kg/ha)    '
      WRITE(8,*)'-----------------------------------------------------
     1--------'
      WRITE(9,*)
      WRITE(9,*)'NO3 TOTAL (WET + DRY) DEPOSITION'
      WRITE(9,*)
      WRITE(9,15)'UTM COORDINATES'
      WRITE(9,17)'EASTING (m)','NORTHING (m)',
     1           '    DEPOSITION (kg/ha)    '
      WRITE(9,*)'-----------------------------------------------------
     1--------'
      DO 6000 I=2,35
         DO 6500 J=2,24
                 X(I,J)=((I-1)*10.)+645.
                 Y(I,J)=((J-1)*10.)+3825.
                 WRITE(7,20)X(I,J),Y(I,J),DNO3(I,J)
                 WRITE(8,20)X(I,J),Y(I,J),WNO3(I,J)
                 WRITE(9,20)X(I,J),Y(I,J),TNO3(I,J)
                 WRITE(14,20)X(I,J),Y(I,J),TNO3(I,J)
 6500 CONTINUE
 6000 CONTINUE
   10 FORMAT(1X,A12,1X,A12,1X,A12,1X,A12,1X,A12)
   15 FORMAT(12X,A16)
   17 FORMAT(7X,A11,4X,A12,3X,A26)
   20 FORMAT(2F15.2,7X,F20.15)
      STOP
      END
```

APPENDIX J

READCON CODE LISTING

```
c
*************************************************************************
c
c  READCON   Version 1.0                          Last modified:  12/15/95
c                                                 First created:  11/04/95
c  Douglas A. Lombardi
c  Oak Ridge National Laboratory
c  Building 4500N, Mailstop 6200
c  Oak Ridge, Tennessee 37831-6200
c  (423) 576-9231
c  e-mail: d76@ornl.gov
c
c
c  Purpose:  This program reads unformatted concentration
c            output files created by MESOPUFF II and outputs the
c            total maximum 3-h and 24-h and average period
c            SO2 concentrations and the maximum 1-h and average
c            period concentrations for the other four species
c            at all grid points in the East Tennessee modeling domain.
c
c  Warning:   This postprocessor only works for MESOPUFF II runs
c             made in the East Tennessee modeling domain.
c
*************************************************************************
c
      REAL ASO2(34,23),ANOX(34,23),ASO4(34,23),AHNO3(34,23),ANO3(34,23)
      REAL            MNOX(34,23),MSO4(34,23),MHNO3(34,23),MNO3(34,23)
      REAL TASO2(34,23),TANOX(34,23),TASO4(34,23),TAHNO3(34,23),
     1     TANO3(34,23)
      REAL A3SO2(34,23),MA3SO2(34,23),T3SO2(34,23)
      REAL A4SO2(34,23),MA4SO2(34,23),T4SO2(34,23)
      REAL ROUT2(34,23)
      REAL X(36,25), Y(36,25)
      REAL VERSION,DGRID,WSAMP
      LOGICAL LGAUSS,LCHEM,LDRY,LWET,LPRINT,L3VL,LVSAMP,LSGRID
      LOGICAL LWETG,LWETNG,LDRYG,LDRYNG,LPRFLX
      INTEGER IDPOL(4)
      CHARACTER*12 FNAME5,FNAME6,FNAME7,FNAME8,FNAME9
      CHARACTER*12 FNAME10,FNAME11,FNAME12,FNAME13,FNAME14
      CHARACTER*12 FNAME15,FNAME16,FNAME17
      OPEN(1,FILE='READCON.IN',STATUS='old')
C **
C **  READ INPUT FILE
C **  WHERE
C **  WHERE: FNAME5 IS THE CONCENTRATION OUTPUT FILE (e.g., PUFFOUT.DAT)
C **  WHERE: FNAME6 IS THE CONCENTRATION OUTPUT FILE FOR ALL POLLUTANTS
C **  WHERE: FNAME7 IS THE MAXIMUM 3-H SO2 CONCENTRATION OUTPUT FILE
C **  WHERE: FNAME8 IS THE MAXIMUM 24-H SO2 CONCENTRATION OUTPUT FILE
C **  WHERE: FNAME9 IS THE AVERAGE PERIOD SO2 CONCENTRATION OUTPUT FILE
C **  WHERE: FNAME10 IS THE MAXIMUM 1-H SO4 CONCENTRATION OUTPUT FILE
C **  WHERE: FNAME11 IS THE AVERAGE PERIOD SO4 CONCENTRATION OUTPUT FILE
C **  WHERE: FNAME12 IS THE MAXIMUM 1-H NOX CONCENTRATION OUTPUT FILE
C **  WHERE: FNAME13 IS THE AVERAGE PERIOD NOX CONCENTRATION OUTPUT FILE
C **  WHERE: FNAME14 IS THE MAXIMUM 1-H HNO3 CONCENTRATION OUTPUT FILE
C **  WHERE: FNAME15 IS THE AVERAGE PERIOD HNO3 CONCENTRATION OUTPUT FILE
C **  WHERE: FNAME16 IS THE MAXIMUM 1-H NO3 CONCENTRATION OUTPUT FILE
C **  WHERE: FNAME17 IS THE AVERAGE PERIOD NO3 CONCENTRATION OUTPUT FILE
C **
      READ(1,10)FNAME5,FNAME6
      READ(1,11)FNAME7,FNAME8,FNAME9
      READ(1,10)FNAME10,FNAME11
      READ(1,10)FNAME12,FNAME13
      READ(1,10)FNAME14,FNAME15
      READ(1,10)FNAME16,FNAME17
      OPEN(5,FILE=FNAME5,STATUS='old',FORM='unformatted')
```

```
      OPEN(6,FILE=FNAME6,STATUS='new')
      OPEN(7,FILE=FNAME7,STATUS='new')
      OPEN(8,FILE=FNAME8,STATUS='new')
      OPEN(9,FILE=FNAME9,STATUS='new')
      OPEN(10,FILE=FNAME10,STATUS='new')
      OPEN(11,FILE=FNAME11,STATUS='new')
      OPEN(12,FILE=FNAME12,STATUS='new')
      OPEN(13,FILE=FNAME13,STATUS='new')
      OPEN(14,FILE=FNAME14,STATUS='new')
      OPEN(15,FILE=FNAME15,STATUS='new')
      OPEN(16,FILE=FNAME16,STATUS='new')
      OPEN(17,FILE=FNAME17,STATUS='new')
C **
C **  READ HEADER FROM CONCENTRATION FILE
C **
      READ(5)VERSION,LEVEL,NSTY,NSDAY,NSHR,NADVTS,IAVG,NPUF,NSAMAD,
     1       IELMET,JELMET,DGRID,IASTAR,IASTOP,JASTAR,JASTOP,ISASTR,
     2       ISASTP,JSASTR,JSASTP,MESHDN,NPTS,NAREAS,NREC,IPRINF,
     3       LGAUSS,LCHEM,LDRY,LWET,LPRINT,L3VL,LVSAMP,WSAMP,LSGRID,
     4       NSPEC,LWETG,LWETNG,LDRYG,LDRYNG,LPRFLX
C **
C **  READ HOURLY RECORDS
C **  WHERE: NADVTS = NUMBER OF HOURS IN THE RUN
C **         ROUT2  = GRIDDED RECEPTOR CONCENTRATION (g/m3)
C **
      IDAY=NADVTS/24
      WRITE(*,*)'NO. OF DAYS = ',IDAY
      DO 1000 K=1,IDAY
         WRITE(*,*)'PROCESSING DAY NO. ',K
         DO 1100 IHR=1,8
            DO 1200 M=1,3
               DO 1500 L=1,5
                  READ(5)IDPOL,ROUT2
C **
C **  COMPUTING CONCENTRATIONS
C **
                  IF(L.EQ.1)THEN
                    DO 100 I=2,35
                       DO 150 J=2,24
                          T3SO2(I,J)=T3SO2(I,J)+ROUT2(I,J)
                          T4SO2(I,J)=T4SO2(I,J)+ROUT2(I,J)
                          TASO2(I,J)=TASO2(I,J)+ROUT2(I,J)
  150                  CONTINUE
  100               CONTINUE
                  ELSEIF(L.EQ.2)THEN
                    DO 200 I=2,35
                       DO 250 J=2,24
                          TASO4(I,J)=TASO4(I,J)+ROUT2(I,J)
                          IF(ROUT2(I,J).GT.MSO4(I,J))THEN
                             MSO4(I,J)=ROUT2(I,J)
                          ENDIF
  250                  CONTINUE
  200               CONTINUE
                  ELSEIF(L.EQ.3)THEN
                    DO 300 I=2,35
                       DO 350 J=2,24
                          TANOX(I,J)=TANOX(I,J)+ROUT2(I,J)
                          IF(ROUT2(I,J).GT.MNOX(I,J))THEN
                             MNOX(I,J)=ROUT2(I,J)
                          ENDIF
  350                  CONTINUE
  300               CONTINUE
                  ELSEIF(L.EQ.4)THEN
                    DO 400 I=2,35
                       DO 450 J=2,24
```

```
131                                TAHNO3(I,J)=TAHNO3(I,J)+ROUT2(I,J)
132                                IF(ROUT2(I,J).GT.MHNO3(I,J))THEN
133                                   MHNO3(I,J)=ROUT2(I,J)
134                                ENDIF
135      450                    CONTINUE
136      400                  CONTINUE
137                         ELSE
138                           DO 500 I=2,35
139                              DO 550 J=2,24
140                                 TANO3(I,J)=TANO3(I,J)+ROUT2(I,J)
141                                 IF(ROUT2(I,J).GT.MNO3(I,J))THEN
142                                    MNO3(I,J)=ROUT2(I,J)
143                                 ENDIF
144      550                    CONTINUE
145      500                  CONTINUE
146                         ENDIF
147     1500              CONTINUE
148     1200              CONTINUE
149                       DO 1210 I=2,35
150                          DO 1220 J=2,24
151                             A3SO2(I,J)=T3SO2(I,J)/3.0
152                             IF(A3SO2(I,J).GT.MA3SO2(I,J))THEN
153                               MA3SO2(I,J)=A3SO2(I,J)
154                             ENDIF
155     1220                 CONTINUE
156     1210              CONTINUE
157     1100     CONTINUE
158              DO 1110 I=2,35
159                 DO 1120 J=2,24
160                    A4SO2(I,J)=T4SO2(I,J)/24.0
161                    IF(A4SO2(I,J).GT.MA4SO2(I,J))THEN
162                      MA4SO2(I,J)=A4SO2(I,J)
163                    ENDIF
164     1120        CONTINUE
165     1110     CONTINUE
166     1000 CONTINUE
167          DO 900 I=2,35
168             DO 950 J=2,24
169                ASO2(I,J)  =TASO2(I,J)/NADVTS
170                ASO4(I,J)  =TASO4(I,J)/NADVTS
171                ANOX(I,J)  =TANOX(I,J)/NADVTS
172                AHNO3(I,J)=TAHNO3(I,J)/NADVTS
173                ANO3(I,J)  =TANO3(I,J)/NADVTS
174
175      950     CONTINUE
176      900 CONTINUE
177     C **
178     C **  WRITING OUTPUT FILES **
179     C **
180          WRITE(*,*)'Writing output files. . . '
181          WRITE(6,*)
182          WRITE(6,*)'MAXIMUM 3-H SO2 CONCENTRATIONS'
183          WRITE(6,*)
184          WRITE(6,15)'UTM COORDINATES           CONCENTRATION'
185          WRITE(6,17)'EASTING (m)','NORTHING (m)','(micrograms per m**3)'
186          WRITE(6,*)'-------------------------------------------------------
187         1--------'
188          DO 2000 I=2,35
189             DO 2100 J=2,24
190                     X(I,J)=((I-1)*10.)+645.
191                     Y(I,J)=((J-1)*10.)+3825.
192                     MA3SO2(I,J)=MA3SO2(I,J)*1000000.
193                     WRITE(6,20)X(I,J),Y(I,J),MA3SO2(I,J)
194                     WRITE(7,20)X(I,J),Y(I,J),MA3SO2(I,J)
195     2100     CONTINUE
```

```
196     2000 CONTINUE
197          WRITE(6,*)
198          WRITE(6,*)'MAXIMUM 24-H SO2 CONCENTRATIONS'
199          WRITE(6,*)
200          WRITE(6,15)'UTM COORDINATES           CONCENTRATION'
201          WRITE(6,17)'EASTING (m)','NORTHING (m)','(micrograms per m**3)'
202          WRITE(6,*)'-------------------------------------------------------
203         1--------'
204          DO 2200 I=2,35
205             DO 2300 J=2,24
206                     X(I,J)=((I-1)*10.)+645.
207                     Y(I,J)=((J-1)*10.)+3825.
208                     MA4SO2(I,J)=MA4SO2(I,J)*1000000.
209                     WRITE(6,20)X(I,J),Y(I,J),MA4SO2(I,J)
210                     WRITE(8,20)X(I,J),Y(I,J),MA4SO2(I,J)
211     2300    CONTINUE
212     2200 CONTINUE
213          WRITE(6,*)
214          WRITE(6,*)'AVERAGE PERIOD SO2 CONCENTRATIONS'
215          WRITE(6,*)
216          WRITE(6,15)'UTM COORDINATES           CONCENTRATION'
217          WRITE(6,17)'EASTING (m)','NORTHING (m)','(micrograms per m**3)'
218          WRITE(6,*)'-------------------------------------------------------
219         1--------'
220          DO 2400 I=2,35
221             DO 2500 J=2,24
222                     X(I,J)=((I-1)*10.)+645.
223                     Y(I,J)=((J-1)*10.)+3825.
224                     ASO2(I,J)=ASO2(I,J)*1000000.
225                     WRITE(6,20)X(I,J),Y(I,J),ASO2(I,J)
226                     WRITE(9,20)X(I,J),Y(I,J),ASO2(I,J)
227     2500    CONTINUE
228     2400 CONTINUE
229          WRITE(6,*)
230          WRITE(6,*)'MAXIMUM 1-H SO4 CONCENTRATIONS'
231          WRITE(6,*)
232          WRITE(6,15)'UTM COORDINATES           CONCENTRATION'
233          WRITE(6,17)'EASTING (m)','NORTHING (m)','(micrograms per m**3)'
234          WRITE(6,*)'-------------------------------------------------------
235         1--------'
236          DO 3000 I=2,35
237             DO 3100 J=2,24
238                     X(I,J)=((I-1)*10.)+645.
239                     Y(I,J)=((J-1)*10.)+3825.
240                     MSO4(I,J)=MSO4(I,J)*1000000.
241                     WRITE(6,20)X(I,J),Y(I,J),MSO4(I,J)
242                     WRITE(10,20)X(I,J),Y(I,J),MSO4(I,J)
243     3100    CONTINUE
244     3000 CONTINUE
245          WRITE(6,*)
246          WRITE(6,*)'AVERAGE PERIOD SO4 CONCENTRATIONS'
247          WRITE(6,*)
248          WRITE(6,15)'UTM COORDINATES           CONCENTRATION'
249          WRITE(6,17)'EASTING (m)','NORTHING (m)','(micrograms per m**3)'
250          WRITE(6,*)'-------------------------------------------------------
251         1--------'
252          DO 3500 I=2,35
253             DO 3600 J=2,24
254                     X(I,J)=((I-1)*10.)+645.
255                     Y(I,J)=((J-1)*10.)+3825.
256                     ASO4(I,J)=ASO4(I,J)*1000000.
257                     WRITE(6,20)X(I,J),Y(I,J),ASO4(I,J)
258                     WRITE(11,20)X(I,J),Y(I,J),ASO4(I,J)
259     3600    CONTINUE
260     3500 CONTINUE
```

```
      WRITE(6,*)
      WRITE(6,*)'MAXIMUM 1-H NOX CONCENTRATIONS'
      WRITE(6,*)
      WRITE(6,15)'UTM COORDINATES           CONCENTRATION'
      WRITE(6,17)'EASTING (m)','NORTHING (m)','(micrograms per m**3)'
      WRITE(6,*)'-------------------------------------------------------
     1--------'
      DO 4000 I=2,35
         DO 4100 J=2,24
                X(I,J)=((I-1)*10.)+645.
                Y(I,J)=((J-1)*10.)+3825.
                MNOX(I,J)=MNOX(I,J)*1000000.
                WRITE(6,20)X(I,J),Y(I,J),MNOX(I,J)
                WRITE(12,20)X(I,J),Y(I,J),MNOX(I,J)
4100     CONTINUE
4000  CONTINUE
      WRITE(6,*)
      WRITE(6,*)'AVERAGE PERIOD NOX CONCENTRATIONS'
      WRITE(6,*)
      WRITE(6,15)'UTM COORDINATES            CONCENTRATION'
      WRITE(6,17)'EASTING (m)','NORTHING (m)','(micrograms per m**3)'
      WRITE(6,*)'-------------------------------------------------------
     1--------'
      DO 4500 I=2,35
         DO 4600 J=2,24
                X(I,J)=((I-1)*10.)+645.
                Y(I,J)=((J-1)*10.)+3825.
                ANOX(I,J)=ANOX(I,J)*1000000.
                WRITE(6,20)X(I,J),Y(I,J),ANOX(I,J)
                WRITE(13,20)X(I,J),Y(I,J),ANOX(I,J)
4600     CONTINUE
4500  CONTINUE
      WRITE(6,*)
      WRITE(6,*)'MAXIMUM 1-H HNO3 CONCENTRATIONS'
      WRITE(6,*)
      WRITE(6,15)'UTM COORDINATES           CONCENTRATION'
      WRITE(6,17)'EASTING (m)','NORTHING (m)','(micrograms per m**3)'
      WRITE(6,*)'-------------------------------------------------------
     1--------'
      DO 5000 I=2,35
         DO 5100 J=2,24
                X(I,J)=((I-1)*10.)+645.
                Y(I,J)=((J-1)*10.)+3825.
                MHNO3(I,J)=MHNO3(I,J)*1000000.
                WRITE(6,20)X(I,J),Y(I,J),MHNO3(I,J)
                WRITE(14,20)X(I,J),Y(I,J),MHNO3(I,J)
5100     CONTINUE
5000  CONTINUE
      WRITE(6,*)
      WRITE(6,*)'AVERAGE PERIOD HNO3 CONCENTRATIONS'
      WRITE(6,*)
      WRITE(6,15)'UTM COORDINATES           CONCENTRATION'
      WRITE(6,17)'EASTING (m)','NORTHING (m)','(micrograms per m**3)'
      WRITE(6,*)'-------------------------------------------------------
     1--------'
      DO 5500 I=2,35
         DO 5600 J=2,24
                X(I,J)=((I-1)*10.)+645.
                Y(I,J)=((J-1)*10.)+3825.
                AHNO3(I,J)=AHNO3(I,J)*1000000.
                WRITE(6,20)X(I,J),Y(I,J),AHNO3(I,J)
                WRITE(15,20)X(I,J),Y(I,J),AHNO3(I,J)
5600     CONTINUE
5500  CONTINUE
      WRITE(6,*)
```

```
      WRITE(6,*)'MAXIMUM 1-H NO3 CONCENTRATIONS'
      WRITE(6,*)
      WRITE(6,15)'UTM COORDINATES           CONCENTRATION'
      WRITE(6,17)'EASTING (m)','NORTHING (m)','(micrograms per m**3)'
      WRITE(6,*)'-----------------------------------------------------
     1--------'
      DO 6000 I=2,35
         DO 6100 J=2,24
                X(I,J)=((I-1)*10.)+645.
                Y(I,J)=((J-1)*10.)+3825.
                MNO3(I,J)=MNO3(I,J)*1000000.
                WRITE(6,20)X(I,J),Y(I,J),MNO3(I,J)
                WRITE(16,20)X(I,J),Y(I,J),MNO3(I,J)
6100     CONTINUE
6000  CONTINUE
      WRITE(6,*)
      WRITE(6,*)'AVERAGE PERIOD NO3 CONCENTRATIONS'
      WRITE(6,*)
      WRITE(6,15)'UTM COORDINATES           CONCENTRATION'
      WRITE(6,17)'EASTING (m)','NORTHING (m)','(micrograms per m**3)'
      WRITE(6,*)'-----------------------------------------------------
     1--------'
      DO 6500 I=2,35
         DO 6600 J=2,24
                X(I,J)=((I-1)*10.)+645.
                Y(I,J)=((J-1)*10.)+3825.
                ANO3(I,J)=ANO3(I,J)*1000000.
                WRITE(6,20)X(I,J),Y(I,J),ANO3(I,J)
                WRITE(17,20)X(I,J),Y(I,J),ANO3(I,J)
6600     CONTINUE
6500  CONTINUE
  10  FORMAT(1X,A12,1X,A12)
  11  FORMAT(1X,A12,1X,A12,1X,A12)
  15  FORMAT(12X,A39)
  17  FORMAT(7X,A11,4X,A12,A22)
  20  FORMAT(2F15.2,7X,F11.5)
      STOP
      END
```

APPENDIX K

MAXPARK CODE LISTING

```
c
*************************************************************************
c
c  MAXPARK   Version 1.0                          Last modified:  12/13/95
c                                                 First created:  11/18/95
c  Douglas A. Lombardi
c  Oak Ridge National Laboratory
c  Building 4500N, Mailstop 6200
c  Oak Ridge, Tennessee 37831-6200
c  (423) 576-9231
c  e-mail: d76@ornl.gov
c
c
c  Purpose:  This program reads concentration and deposition
c            output files created by the READDEP and READCON
c            postprocessors and outputs concentration or deposition
c            values at the Class I areas in the East Tennessee
c            modeling domain
c
c  Variables:
c  ----------
c   x        real array          UTM Coordinate Easting (km)
c   y        real array          UTM Coordinate Northing (km)
c   val      real array          Concentration or deposition value
c   maxgsm   real                Maximum value in the Great Smoky
c                                Mountains National Park
c   maxjk    real                Maximum value in Joyce Kilmer
c                                Wilderness Area
c   maxco    real.               Maximum value in Cohutta Wilderness
c                                Area
c
c
*************************************************************************
c
      REAL X(36,25), Y(36,25), VAL(36,25)
      REAL MAXGSM,MAXJK,MAXCO
c
c  read concentration or deposition values
c
      DO 100 I=2,35
         DO 150 J=2,24
             READ(1,20)X(I,J),Y(I,J),VAL(I,J)
  150   CONTINUE
  100 CONTINUE
c
c  write concentration or deposition values in the Great Smoky Mountains
National Park
c
      WRITE(2,*)'GREAT SMOKY MOUNTAINS NATIONAL PARK'
      WRITE(2,20)X(13,12),Y(13,12),VAL(13,12)
      MAXGSM=VAL(13,12)
      DO 200 I=14,17
         DO 250 J=11,13
            WRITE(2,20)X(I,J),Y(I,J),VAL(I,J)
            IF(VAL(I,J).GT.MAXGSM)THEN
              MAXGSM=VAL(I,J)
            ENDIF
  250    CONTINUE
  200 CONTINUE
      DO 300 I=18,19
         DO 350 J=11,14
            WRITE(2,20)X(I,J),Y(I,J),VAL(I,J)
            IF(VAL(I,J).GT.MAXGSM)THEN
              MAXGSM=VAL(I,J)
            ENDIF
```

```
 66      350    CONTINUE
 67      300 CONTINUE
 68          DO 400 I=20,21
 69             DO 450 J=12,14
 70                WRITE(2,20)X(I,J),Y(I,J),VAL(I,J)
 71                IF(VAL(I,J).GT.MAXGSM)THEN
 72                  MAXGSM=VAL(I,J)
 73                ENDIF
 74      450    CONTINUE
 75      400 CONTINUE
 76          WRITE(2,20)X(22,13),Y(22,13),VAL(22,13)
 77          IF(VAL(22,13).GT.MAXGSM)THEN
 78             MAXGSM=VAL(I,J)
 79          ENDIF
 80    c
 81    c  write maximum value in the Great Smoky Mountains National Park
 82    c
 83          WRITE(2,*)'MAX DEP IN GSMNP = ',MAXGSM
 84          WRITE(2,*)
 85    c
 86    c  write concentration or deposition values in Cohutta Wilderness Area
 87    c
 88          WRITE(2,*)'COHUTTA WILDERNESS AREA'
 89          I=7
 90          J=4
 91          MAXCO=0.
 92          DO 500 I=7
 93             DO 550 J=4,6
 94                WRITE(2,20)X(I,J),Y(I,J),VAL(I,J)
 95                IF(VAL(I,J).GT.MAXCO)THEN
 96                  MAXCO=VAL(I,J)
 97                ENDIF
 98      550    CONTINUE
 99      500 CONTINUE
100          I=8
101          J=5
102          DO 600 I=8
103             DO 650 J=5,6
104                WRITE(2,20)X(I,J),Y(I,J),VAL(I,J)
105                IF(VAL(I,J).GT.MAXCO)THEN
106                  MAXCO=VAL(I,J)
107                ENDIF
108      650    CONTINUE
109      600 CONTINUE
110   c
111   c  write maximum value in Cohutta Wilderness Area
112   c
113         WRITE(2,*)'MAX DEP IN COHUTTA = ',MAXCO
114         WRITE(2,*)
115   c
116   c  write concentration or deposition values in Joyce Kilmer Wilderness
117   Area
118   c
119         WRITE(2,*)'JOYCE KILMER WILDERNESS AREA'
120         I=13
121         J=10
122         MAXJK=0.
123         DO 700 I=13
124            DO 750 J=10,11
125               WRITE(2,20)X(I,J),Y(I,J),VAL(I,J)
126               IF(VAL(I,J).GT.MAXJK)THEN
127                 MAXJK=VAL(I,J)
128               ENDIF
129      750    CONTINUE
130      700 CONTINUE
```

```
131           I=14
132           J=9
133           DO 800 I=14
134              DO 850 J=9,10
135                 WRITE(2,20)X(I,J),Y(I,J),VAL(I,J)
136                 IF(VAL(I,J).GT.MAXJK)THEN
137                   MAXJK=VAL(I,J)
138                 ENDIF
139        850    CONTINUE
140        800 CONTINUE
141     c
142     c  write maximum value in Cohutta Wilderness Area
143     c
144           WRITE(2,*)'MAX DEP IN JOYCE KILMER = ',MAXJK
145        20 FORMAT(2F15.2,7X,F20.15)
146           STOP
147           END
148     c
149     c  end of program
150     c
151
```

APPENDIX L

CODE MODIFICATIONS MADE TO MESOPAC II SUBROUTINE VERTAV

```
c**********************************************************************
      SUBROUTINE VERTAV(NEARU,LDB1,UFLD,VFLD)
c
C      MESOPAC II   VERSION 2.4   LEVEL 921025   VERTAV     ERT
C**********************************************************************
C     This subroutine is part of:
C
C     MESOPAC II METEOROLOGICAL PREPROCESSOR PROGRAM
c
C         VERSION 2.4   LEVEL 930430
c
C     WRITTEN BY: J. SCIRE
C                 SIGMA RESEARCH CORPORATION
C                 196 BAKER AVENUE, CONCORD, MA  01742
C
C**********************************************************************
c  This subroutine has been modified by:
c
c  Douglas A. Lombardi
c  Oak Ridge National Laboratory
c  Building 4500N, Mailstop 6200
c  Oak Ridge, Tennessee 37831-6200
c  (423) 576-9231
c  e-mail: d76@ornl.gov
c
c
c  Purpose of
c  modification:     This subroutine has been modified to smooth out
c                   discontinuities in the lower-layer wind fields.
c                   Additionally, the wind direction is only
c                    determined by surface stations to better reflect
c                    up- and down-valley flow in the East Tennessee
c                    modeling domain.
c
c  All modifications are indicated by the initials: dal
c
c**********************************************************************
c
c --- Include parameters
      INCLUDE 'params.pac'
c
      REAL U(79),V(79),Z(79),UFLD(mxnx,mxny),VFLD(mxnx,mxny)
      REAL RATSPD(mxus),DDIR(mxus)
cdal
      REAL XR(mxus),WGT(mxus)
      REAL TOTXR,XSQ,YSQ,DSTN,WTRAT,SUBRAT
cdal
cdal  09/22/95
cdal  The following variables have been added to the subroutine:
      REAL TOTRAT,AVRAT
cdal  where:  TOTRAT is the sum of wind speed ratios from the
cdal                 rawindsonde stations
cdal          AVRAT is the average wind speed ratio from the
cdal                 rawindsonde stations
cdal  end of added variables
cdal
      INTEGER NEARU(mxnx,mxny)
      LOGICAL LDB1
      COMMON /METP/ IMAX,JMAX,NSSTA,NUSTA,DGRID
      COMMON/UPPER/P00(mxus,79),ZL00(mxus,79),TZ00(mxus,79),
     1 DIRU00(mxus,79),WSV00(mxus,79),P12(mxus,79),ZL12(mxus,79),
     2 TZ12(mxus,79),DIRU12(mxus,79),WSV12(mxus,79),NL00(mxus),
     3 NL12(mxus),NEARI(mxus),NEARJ(mxus)
      COMMON/MET/US(mxnx,mxny),VS(mxnx,mxny),UL(mxnx,mxny),
     1 VL(mxnx,mxny),UUP(mxnx,mxny),VUP(mxnx,mxny),WT(mxnx,mxny),
```

```
      2 USTAR(mxnx,mxny),WSTAR(mxnx,mxny),CAPL(mxnx,mxny),ZI(mxnx,mxny),
      3 IPGT(mxnx,mxny)
       COMMON/DATE/NYR,NMO,NDAY,NJULDY,NARRHR,NHR
       COMMON/IOUNIT/IN5,IOUT6,IN7,IOUT8,ISUNIT(mxss),IUUNIT(mxus)
cdal
       COMMON/COORD/SLAT(mxss),SLONG(mxss),SZONE(mxss),XSCOOR(mxss),
     1 YSCOOR(mxss),ULAT(mxus),ULONG(mxus),UZONE(mxus),XUCOOR(mxus),
     2 YUCOOR(mxus)
C
C      FIND MIXED-LAYER AVERAGED WIND FIELDS AT EACH GRID POINT
C
C      CALCULATE (LAYER AVE WS)/(SURF WS) & (LAYER AVE WD)-(SURF WD)
C      AT UPPER AIR STATIONS USING MIXING HT AT NEAREST GRID PT
       DO 10 I=1,NUSTA
       IG=NEARI(I)
       JG=NEARJ(I)
       HTMIX=ZI(IG,JG)
       ISTAB=IPGT(IG,JG)
       IF(ISTAB.LE.4)GO TO 50
C
C      IF STABLE, USE 12Z SOUNDING TO CALCULATE MIXED-LAYER AVE. WINDS
       NLEV=NL12(I)
C      ADD 100. TO U, V TO MAKE ALL NUMBERS POSITIVE
       DO 15 K=1,NLEV
       U(K)=DIRU12(I,K)+100.
       V(K)=WSV12(I,K)+100.
       Z(K)=ZL12(I,K)
15     CONTINUE
       GO TO 76
C
C      IF NEUTRAL OR UNSTABLE, USE 00Z SOUNDING TO CALCULATE MIXED-LAYER
C      AVERAGED WINDS
50     CONTINUE
       NLEV=NL00(I)
C      ADD 100 TO U, V TO MAKE ALL NUMBERS POSITIVE
       DO 75 K=1,NLEV
       U(K)=DIRU00(I,K)+100.
       V(K)=WSV00(I,K)+100.
       Z(K)=ZL00(I,K)
75     CONTINUE
76     CONTINUE
C      FIND THE  LEVEL (NMIX) JUST BELOW THE MIXING HT
       DO 70 J=2,NLEV
       IF(Z(J).LT.HTMIX)GO TO 70
       NMIX=J-1
       GO TO 72
70     CONTINUE
       WRITE(6,11)I,HTMIX,NJULDY,NHR,ISTAB
11     FORMAT(//1x,'EXECUTION TERMINATING -- MIXING HT EXCEEDS ',
     1 'HIGHEST RAWINSONDE OBSERVATIONS'//1x,'RAWINSONDE STATION: ',
     2 I2,3X,'HTMIX: ',F10.1,5X,'JULIAN DAY: ',I3,3X,'HOUR: ',I2,3X,
     3 'STABILITY CLASS: ',I1)
       STOP
72     CONTINUE
C
C      CALCULATE SURFACE WIND SPEED AND (VECTOR) DIRECTION
       USF=U(1)-100.
       VSF=V(1)-100.
       IF(ABS(USF).LT.0.01.AND.ABS(VSF).LT.0.01)GO TO 77
       SURFDR=ATAN2(USF,VSF)
C      0 LE SURFDR LE 2*PI
       IF(SURFDR.LT.0.0)SURFDR=6.2831853+SURFDR
       SURFSP=SQRT(USF**2+VSF**2)
       SURFSP=AMAX1(SURFSP,1.0)
       GO TO 78
```

```
131     77    CONTINUE
132     C     SURFACE WS IS ZERO -- SET SURFACE WS = 1.0 M/S; FLAG SURFACE WD
133           SURFSP=1.0
134           SURFDR=999.
135     78    CONTINUE
136     C
137     C     CALCULATE MIXED-LAYER AVERAGED WS, WD
138           SUMU=0.0
139           SUMV=0.0
140           IF(NMIX.EQ.1)GO TO 81
141           DO 80 N=2,NMIX
142           NM1=N-1
143           UMIN=AMIN1(U(NM1),U(N))
144           VMIN=AMIN1(V(NM1),V(N))
145           DZ=Z(N)-Z(NM1)
146           SUMU=SUMU+(UMIN+0.5*ABS(U(N)-U(NM1)))*DZ
147           SUMV=SUMV+(VMIN+0.5*ABS(V(N)-V(NM1)))*DZ
148     80    CONTINUE
149     81    CONTINUE
150           NMIXP1=NMIX+1
151           RAT1=(Z(NMIXP1)-HTMIX)/(Z(NMIXP1)-Z(NMIX))
152           UHTMIX=U(NMIXP1)-(U(NMIXP1)-U(NMIX))*RAT1
153           VHTMIX=V(NMIXP1)-(V(NMIXP1)-V(NMIX))*RAT1
154           UMIN=AMIN1(U(NMIX),UHTMIX)
155           VMIN=AMIN1(V(NMIX),VHTMIX)
156           DZ=HTMIX-Z(NMIX)
157           SUMU=SUMU+(UMIN+0.5*ABS(UHTMIX-U(NMIX)))*DZ
158           SUMV=SUMV+(VMIN+0.5*ABS(VHTMIX-V(NMIX)))*DZ
159     C     SUMU/HTMIX IS THE MIXED LAYER AVERAGED U
160           UAVE=SUMU/HTMIX
161           VAVE=SUMV/HTMIX
162     95    CONTINUE
163           UAVE=UAVE-100.
164           VAVE=VAVE-100.
165     C     to prevent error during calm conditions
166           if (uave.eq.0.0.and.vave.eq.0.0) vave=1.0e-6
167           AVEDR=ATAN2(UAVE,VAVE)
168     C     Do if 0 IS LESS THAN AVEDR LE 2*PI
169           IF(AVEDR.LT.0.0)AVEDR=6.2831853+AVEDR
170           AVESP=SQRT(UAVE*UAVE+VAVE*VAVE)
171           AVESP=AMAX1(AVESP,1.0)
172     C
173     C     CALCULATE THE RATIO OF LAYER-AVE. WS TO SURF WS & DELTA WD VECTOR
174     C
175     C     RATSPD=(AVE. WS)/(SURF. WS) -- DDIR=AVE. WD - SURF. WD
176           RATSPD(I)=AVESP/SURFSP
177           DDIR(I)=AVEDR-SURFDR
178           IF(SURFDR.GE.999.)DDIR(I)=0.0
179     10    CONTINUE
180     C*****
181           IF(.NOT.LDB1)GO TO 2004
182           WRITE(IOUT6,2001)NYR,NJULDY,NHR
183     2001  FORMAT(/1x,'CALCULATION TO AVERAGE WIND THROUGH MIXED LAYER - ',
184          1 'YEAR:',I2,2X,'JULIAN DAY:',I3,2X,'HR:',I2/1X,'UPPER AIR ',
185          2 'STATION',5X,'RATSPD',5X,'DDIR (RADIANS)'/)
186           DO 2003 N=1,NUSTA
187           WRITE(IOUT6,2002)N,RATSPD(N),DDIR(N)
188     2002  FORMAT(8X,I3,13X,F6.2,6X,F6.2)
189     2003  CONTINUE
190     2004  CONTINUE
191     C*****
192     C     CALCULATE MIXED-LAYER AVERAGED WS, WD
193           DO 200 IG=1,IMAX
194           DO 100 JG=1,JMAX
195     C     'I' IS THE NEAREST RAWINSONDE STATION TO THE CURRENT GRID POINT
```

```
196           I=NEARU(IG,JG)
197           SPD=SQRT(US(IG,JG)**2+VS(IG,JG)**2)
198           IF(SPD.EQ.0.)GO TO 98
199           DIR=ATAN2(US(IG,JG),VS(IG,JG))
200     C     0 LE DIR LE 2*PI
201           IF(DIR.LT.0.0)DIR=6.2831853+DIR
202     cdal
203           TOTXR=0.0
204           DO 225 LR=1,NUSTA
205              XSQ=(IG-XUCOOR(LR))**2.
206              YSQ=(JG-YUCOOR(LR))**2.
207              DSTN=SQRT(XSQ+YSQ)
208              XR(LR)=1/(DSTN**2.)
209              TOTXR=TOTXR+XR(LR)
210      225  CONTINUE
211           DO 226 LR=1,NUSTA
212              WGT(LR)=XR(LR)/TOTXR
213      226  CONTINUE
214           WTRAT=0.0
215           DO 227 KT=1,NUSTA
216              SUBRAT=(WGT(KT)*RATSPD(KT))
217              WTRAT=WTRAT+SUBRAT
218      227  CONTINUE
219           SPD=WTRAT*SPD
220     cdal
221     cdal  09/22/95
222     cdal  The following lines have been altered to change the ratio
223     cdal  by which surface wind speed is varied to get the mixed layer
224     cdal  average wind speed:
225     cdal      SPD=RATSPD(I)*SPD
226     c      TOTRAT=0.0
227     c      DO 227 KOUNT=1,NUSTA
228     c         TOTRAT = TOTRAT + RATSPD(KOUNT)
229     c 227  CONTINUE
230     c      AVRAT = TOTRAT/NUSTA
231     c      SPD=AVRAT*SPD
232     cdal
233     cdal  09/06/95
234     cdal  The following line has been changed:
235     cdal      DIR=DIR+DDIR(I)
236     cdal  to:
237           DIR=DIR
238     C     DIR IS VECTOR WD
239     C     CONVERT TO U,V COMPONENTS
240           UFLD(IG,JG)=SPD*SIN(DIR)
241           VFLD(IG,JG)=SPD*COS(DIR)
242           GO TO 100
243     98    CONTINUE
244           UFLD(IG,JG)=0.0
245           VFLD(IG,JG)=0.0
246     100   CONTINUE
247     200   CONTINUE
248           RETURN
249           END
```

VITA

Douglas Adler Lombardi was born in Tacoma, Washington and raised in Littleton, Colorado. He graduated in May 1987 from the University of Colorado, Boulder, with a Bachelor of Science degree in Mechanical Engineering and was commissioned a Second Lieutenant in the United States Air Force as a distinguished graduate. Before entering active duty, he worked for a short time with Canon Virginia, Inc. as a manufacturing engineer. His first year of active duty was spent at Texas A&M University in the Basic Meteorology Program in which he graduated in December 1988. His second assignment was to serve as the Staff Weather Officer for the United States Army's 75th Ranger Regiment. In November 1991, he left active duty to join the staff of Oak Ridge National Laboratory, where he currently works in the Energy Division. His work at Oak Ridge National Laboratory includes environmental impact analysis and atmospheric dispersion modeling.